Synthesis and Characterization of Functional Amphiphilic Gradient Copolymers by Atom Transfer Radical Polymerization

Inaugural–Dissertation

zur Erlangung des Grades eines Doktors der Naturwissenschaften der Universität Osnabrück Fachbereich Biologie/Chemie

vorgelegt von

Sandra Schwitke

Osnabrück

28. July 2014

1. Gutachter: Prof. Dr. U. Beginn,
Universität Osnabrück, Fachbereich Biologie/Chemie
Organische Materialchemie

2. Gutachter: Prof. Dr. H.-J. Steinhoff
Universität Osnabrück, Fachbereich Physik
Makromolekülstruktur

"In der Welt von heute hat die Chemie Einfluss auf alles."

Linus Pauling

Die vorliegende Arbeit wurde in der Zeit von Juli 2008 bis Juli 2014 am Institut für Chemie neuer Materialien der Universität Osnabrück unter der Leitung von Prof. Dr. U. Beginn durchgeführt.

Erklärung

Hiermit erkläre ich an Eides statt, dass ich die vorliegende Arbeit selbständig angefertigt und keine anderen als die von mir angegebenen Quellen und Hilfsmittel verwendet habe. Ein früherer Promotionsversuch hat nicht stattgefunden.

Osnabrück, der 28. Juli 2014

_____

Sandra Schwitke

Danksagung

Für das interessante Thema und die damit verbundenen Aufgabenstellungen, sowie für seine intensive Betreuung während meiner Arbeit, möchte ich mich als erstes bei Herrn Prof. Dr. Beginn bedanken. Bei Herrn Prof. Dr. Steinhoff möchte ich mich bedanken, dass er das Korefferat meiner Arbeit übernommen hat.

Desweitern möchte ich mich bei den Technischen Assistentinnen der Arbeitsgruppe Organische Materialchemie für ihre Unterstützung bedanken: Petra Bösel für ihre Hilfe bei der gesamten Laborarbeit, ihrer tollen Laborорganisation, der Unterstützung bei der Wartung der GPC–Anlage, die Einweisung in die DSC und insbesondere für die Hilfe bei den Hydrolysen; Marianne Gather für die vielen gemessenen "Blumensträuße"; Iris Helms für die IR–Messungen; Elisabeth Michalek für die Versuche mit dem MALDI–TOF und ihre Hilfe bei der Laborорganisation und Anja Schuster, aus der ACII, für die Elementar–Analysen.

Ich möchte meinen Kollegen Marina Zorn, Ralph Beckmann, Enfeng Song, Marius Ciobanu, Ana–Maria Lepadatu, Miriam Brand, Xihomara Casallas Cruz und Eduard Belke für die tolle Zusammenarbeit danken. Carina Ellermann möchte ich für ihre Unterstützung bei den Synthesen danken. Traute Stunk danke ich für ihre Hilfe durch den Bürokratismus.

Besonderer Dank gilt meinem Freund Martin, der mir viel Verständnis und Hilfe entgegen gebracht hat.

Meinen Eltern und meinem Bruder danke ich für ihre Unterstützung und dass sie mir Rückhalt gegeben haben, damit ich es bis hierhin schaffen konnte.

Contents

1. Introduction

Since the research and discovery of *Staudinger* [1] at the beginning of the last century the field of polymer science has developed with increasing rate. Today neither industry or daily life can renounce synthetic polymers. [2] Free radical polymerization (FRP) is used very often in industry because of the broad spectrum of monomers that can be used and the comparative easy experimental setup and reaction control. [3] With the advancement of controlled radical polymerization (CRP), first reported by *Otsu* and *Yoshida* in 1982 [4], involving the suppress of termination reactions, it is possible to overcome the disadvantages of the FRP like broad molar mass distribution and weak control over the structure of the polymer chains. [5, 6, 7, 8] CRP allows the preparation of telomers, end– and side–group functional polymers, as well as block–copolymers. One type of CRP is the Atom Transfer Radical Polymerization (ATRP) which was developed by the working groups of *Kato* et al. [9] and *Matyjaszewski* et al. [10] nearly at the same time in 1995. Block–copolymers are used e. g. as emulsifiers in polymer blends and ink–jet inks. [11, 12] A structural relative to block copolymers, accessible by CRP, are the gradient copolymers. [13, 14, 15]

The aim of this work is to synthesize functional amphiphilic copolymers with a well defined gradient structure along the polymer chains, consisting of two monomers that have nearly the same reaction kinetic parameters. For this purpose the kinetic parameters of the two investigated monomer pairs, *tert*–butyl and *n*–butyl methacrylate as well as *tert*–butyl and benzyl methacrylate, were determined by batch ATRP. Then the data were used for the calculation of a monomer feeding program, to prepare gradient copolymers by means of semibatch ATRP. In a second step the resulting copolymers were hydrolyzed to obtain functional amphiphilic gradient copolymers. Three different kinds of hydrolysis were investigated to find the most effective strategy. Moreover di–block copolymers with the same monomer–units were synthesized and compared with the statistical and gradient copolymers. In a cooperation with the working group of *Prof. Dr. H.–U. Moritz* from the University of Hamburg gradient copolymers were polymerized by a semibatch ATRP with online IR–spectroscopy observation to control the monomer feed during the synthesis. The resulting statistical, gradient and di–block copolymers were compared due to their physical properties by ^{1}H–NMR–spectroscopy, elementary analysis, ATR–FTIR spectroscopy, size exclusion chromatography and differential scanning calorimetry.

This thesis consists of twelve chapters. *Chapter 2* contains an overview of the state of the literature about polymer architecture and synthesis, the properties and applications of block copolymers and the comparison of them with gradient copolymers together with a short review of the molar mass determination by light scattering.

In *Chapter 3* the batch ATRP of *tert*–butyl and *n*–butyl methacrylate is described. Different monomer compositions were examined by ^{1}H–NMR–spectroscopy to find their kinetic parameters. These values were needed for semibatch synthesis of the gradient copolymers. Moreover samples of the resulting statistical copolymers from different polymerization times were investigated in respect to the structure of the resulting copolymers, the molar mass development of the copolymers with reaction time, the polymerization control and the polymers thermal behavior and the changes with increase of polymerization time.

Chapter 4 details the three different kinds of hydrolysis that were investigated. The target copolymers are amphiphilic bearing carboxylic acid side–groups. Since acrylic acid containing monomers can not be used with ATRP [16], the *tert*–butyl–ester groups protected acids were used. The ester groups were cleaved and replaced by OH–groups. Two acidic hydrolysis, one with trifluoroacetic acid (TFA) and one with methanesulfonic acid (MSA) and a hydrolysis under neutral conditions, with trimethylsilyl iodide (TMSI), were performed. The resulting copolymers were investigated for complete conversion of the *tert*–butyl–ester groups, the progress of the molar mass and thermal behavior of the amphiphilic products.

Chapter 5 describes the synthesis of four gradient copolymers with different compositions of *tert*–butyl and *n*–butyl methacrylate by semibatch ATRP. The kinetic parameters as determined in *Chapter 3*, were incorporated into the monomer addition programs. The monomer feeding curves were calculated to control the addition of feed–solution into the stock–solution. The development of the cumulative and the instantaneous compositions of the copolymers were determined from data obtained from ^{1}H–NMR–spectra of samples that were taken periodically during the reaction. Moreover precipitated samples taken at different polymerization times were examined by the same methods and under the same conditions as the statistical copolymers before. The differences and the similarities between the gradient and the statistical copolymers were worked out as well as the differences and the similarities between the different compositions of the gradient copolymers.

The hydrolysis of the P[tBMA–grad–nBMA] is given in *Chapter 6*. The hydrolysis strategy that have been determined in *Chapter 4* as the most effective one was used for the cleavage of the the *tert*–butyl groups on the chain of the gradient copolymers to receive the intended amphiphilic gradient copolymers. The hydrolysis products were analyzed as before with ^{1}H–NMR, EA, ATR–FTIR, SEC and DSC.

Chapter 7 contains the batch copolymerization of *tert*–butyl and benzyl methacrylate. Similar to the monomer system of tBMA and nBMA seven different mixtures of tBMA and BzMA were polymerized by ATRP. Samples which were taken at different polymerization times were investigated by ^{1}H–NMR–spectroscopy to determine the kinetic parameters of the system. Additionally precipitated samples were studied with the same methods and under the same conditions as it was done with the P[tBMA–co–nBMA] products to determine the structure, the molar masses and the thermal behavior of the samples. The resulting data of the P[tBMA–co–nBMA] and P[tBMA–co–BzMA] were compared.

In *Chapter 8* the semibatch synthesis of the gradient copolymer from tBMA and BzMA is described. The kinetic parameters resulting from the batch copolymerization of the two monomers were introduced into the monomer addition program to calculate the monomer feeding program for the ATRP as it was done for the gradient copolymers with tBMA– and nBMA–units in *Chapter 5* before. Also the cumulative and the instantaneous compositions of samples taken during the synthesis were calculated from data resulting from ^{1}H–NMR–spectroscopy and even more precipitated samples taken at different polymerization times were analyzed with elementary analysis, ATR–FTIR–spectroscopy to investigate the structure of samples, SEC for determination of molar mass changes and DSC for examination of the thermal behavior. The results were compared with the results of the gradient copolymers with tBMA– and nBMA–units.

Chapter 9 describes the hydrolysis of a statistical and the gradient copolymer with tBMA– and BzMA–units. The same hydrolysis reagent and the same experimental procedure that was used for the hydrolysis in *Chapter 6* was used to ensure the comparability of the results. Hence, the resulting amphiphilic statistical and gradient copolymer were examined with the same methods (^{1}H–NMR, ATR–FTIR, SEC, DSC) under the same conditions. The resulting data were compared with the data of the amphiphilic copolymers with tBMA– and nBMA–units.

Chapter 10 contains the synthesis of di–block copolymers by ATRP. The influence of the structure of the copolymer and the physical behavior were examined by the comparison of the di–block copolymers P[tBMA]–b–P[nBMA] and P[tBMA]–b–P[BzMA] with the previous synthesized and analyzed statistical and gradient copolymers. First a macroinitiator from *tert*–butyl methacrylate was polymerized. Then a second block of *n*–butyl methacrylate, respectively benzyl methacrylate was added. ATRP with the same initiator system and under the same experimental conditions was used for all three experiments to ensure the compatibility of the product with the other copolymers of this thesis. On this account also the analysis methods and conditions were used to characterize the polymer products.

In cooperation with the working group of *Prof. Dr. H.–U. Moritz* from the University of

Hamburg gradient copolymers were polymerized using online infrared–spectroscopy observation to control the monomer feed during the synthesis. This is given in *Chapter 11*. The resulting copolymers were analyzed in the same way as the statistical an gradient copolymers with tBMA– and BzMA–units before and then they were compared.

The summary of this thesis is the content of *Chapter 12*. It gives a short overview of the results of the experiments and analyzes that were realized.

2. Literature Review

In this chapter the current state of the scientific literature on the architecture and the synthesis of copolymers is given. Special attention is payed to the block– and gradient–copolymers and the controlled radical polymerization technique of Atom Transfer Radical Polymerization.

2.1. Polymer Architecture

Polymers can be described in different ways. A basis of the description is the overall structure of the polymer. Such structure–based characterization are: [17, 18]

- homo–chain and hetero–chain polymer
- monodisperse and polydisperse
- regular and irregular

The backbone of homo–chain polymers consist of only one kind of element, for example the carbon–backbone chain of poly(acrylonitrile) or poly(methacrylate). Hetero–chain polymers contain at the minimum two different elements, for example poly(urethane) which contains carbon and oxygen on the backbone chain. When the macromolecules e. g. in a solution have all the same molecular weight, the molecules are monodisperse. An example here are enzymes. For the synthesis of monodisperse macromolecules matrices are necessary. In contrast, a typical solution with synthetic polymer is polydisperse. That means they are non–uniform with respect to the molar mass. A homopolymer is called regular when it contains units that repeat uniformly (ABCABCABC...) and with the same sense of direction (head–to–tail). Diketo– or peroxide–groups along the polymer backbone distribute the regularity as well as head–to–head and tail–to–tail conjunctions. Then the macromolecule is irregular. [17]

The process based description of polymer chains reflects the order of the monomer–units along the polymer chain. In *Figure 2.1* are listed different types of sequences of monomer–units on a linear polymer chain. A first distinction is the number of different monomers which were used during the polymerization. A polymer chain that contains only one kind of monomer–units is called a homopolymer, see *Figure 2.1 A*. When two or more different monomers are used at the polymerization, the resulting polymers is called copolymer. When just one monomer is used for the synthesis but isomers of the monomer rise during the reaction the product is called pseudo–copolymer. An example is the polymerization of 1,3–butadiene. The resulting

product contains mainly cis–1,4–, but also trans–1,4– and 1,2–units which originate from the same monomer. [17]

Fig. 2.1.: Overview of linear copolymer architectures; (A) homopolymer P[A], (B) di–block copolymer P[A]–b–P[B], (C) tri–block copolymer P[A]–b–P[B]–b–P[C], (D) tri–block copolymer P[A]–b–P[B]–b–P[A], (E) alternating copolymer P[A–alt–B], (F) gradient copolymer P[A–grad–B], (G) statistical copolymer P[A–co–B], following [14]

Block copolymers consist of two or more sequences of homopolymers which are covalently joined together, see *Figure 2.1 B, C* and *D*. The monomer units of the polymer chain of an alternating copolymer (c. f. *Figure 2.1 E*) change totally regular in alternating fashion. The composition of the polymer chain of a gradient copolymer changes continuously, for example from a begin that is rich of monomer unit A to an end of the polymer chain which is rich of monomer unit B, see *Figure 2.1 F.* [13, 14, 15] A statistical copolymer contains no structure in with respect to the sequence of the monomer units along the polymer chain (c. f. *Figure 2.1 G*) [17, 19]. In the following text only binary copolymers containing two monomers A and B are described. With polymerization reactions the sequence of the monomer units depend on the reactivity ratios of a pair of monomers r_A and r_B. These ratios describe the ability of the growing polymer chain M_x^*, terminated with growth–active side derived from monomer x (x = A, B), to react with either the same monomer or the other monomer during a polymerization. [20, 21]

$$M_A^* + M_A \xrightarrow{k_{AA}} M_A^* \tag{2.1.1}$$

$$M_A^* + M_B \xrightarrow{k_{AB}} M_B^* \tag{2.1.2}$$

$$M_B^* + M_A \xrightarrow{k_{BA}} M_A^* \tag{2.1.3}$$

$$M_B^* + M_B \xrightarrow{k_{BB}} M_B^* \tag{2.1.4}$$

with * as the reactive species, k_{AA} representing the rate constant for the propagation end of a polymer chain ending on A adding monomer A and k_{AB} denoting the rate constant of the propagation end of a polymer chain ending in A adding monomer B and vice versa. [3]

When a monomer was incorporated into the polymer chain, it disappeared from the monomer solution. This is described by *Equations 2.1.5* and *2.1.6*.

$$-\frac{d[M_A]}{dt} = k_{AA}[M_A^*][M_A] + k_{BA}[M_B^*][M_A] \tag{2.1.5}$$

$$-\frac{d[M_B]}{dt} = k_{AB}[M_A^*][M_B] + k_{BB}[M_B^*][M_B] \tag{2.1.6}$$

It is conveniently assumed that the reaction rates of the reactions *2.1.2* and *2.1.3* are equal and two reactivity parameters r_A and r_B are defined from the reactions *2.1.1* and *2.1.2*, as well as reactions *2.1.3* and *2.1.4*.

$$k_{BA}[M_B^*][M_A] = k_{AB}[M_A^*][M_B] \tag{2.1.7}$$

$$r_A = \frac{k_{AA}}{k_{AB}} \tag{2.1.8}$$

$$r_B = \frac{k_{BB}}{k_{BA}} \tag{2.1.9}$$

The instantaneous quotient of monomer A– and B–consumption $d[M_A]/d[M_B]$ is obtained by dividing *Equation 2.1.5* by *Equation 2.1.6*. On subsequent insertion of condition *2.1.7*, as well as the definitions of the reactivity parameters (*Equations 2.1.8* and *2.1.9*) one obtains the *Lewis–Mayo* or *Copolymerization–Equation 2.1.10* that relates the instantaneous polymer composition to the actual monomer concentration in the reaction mixture.

$$\frac{d[M_A]}{d[M_B]} = \frac{[M_A](r_A[M_A] + [M_B])}{[M_B]([M_A] + r_B[M_B])} \tag{2.1.10}$$

Another way to describe the conversion of the monomers is the use of mole fractions instead of the concentrations, c. f. *Equations 2.1.5* and *2.1.6*.

$$f_A = 1 - f_B = \frac{[M_A]}{[M_A] + [M_B]} \tag{2.1.11}$$

$$F_A = 1 - F_B = \frac{[M_A]}{[M_A] + [M_B]} \tag{2.1.12}$$

with f_x = mole fraction of the monomers and F_x = mole fraction of the monomer–units inside the polymer chain

For the determination of the composition of a copolymer the *Equations 2.1.10*, *2.1.11* and *2.1.12* are combined. [3]

$$F_A = \frac{r_A f_A^2 + f_A f_B}{r_A f_A^2 + 2 f_A f_B + r_B f_B^2} \tag{2.1.13}$$

The plot of the molar fraction copolymer composition F_A versus the monomer compositions f_A of a pair of monomers is called a copolymerization diagram of these monomers. *Figure 2.2* shows copolymerization diagrams from monomer pairs with different couples of reactivity ratios. Only when the reactivity ratios of both monomers are equal to one, the resulting copolymer has the same composition as the monomer mixture. When the r–values of the monomer pair differ from one in the final copolymer chain the amount of one monomer unit is different from the amount of this monomer in the monomer mixture. The reactivity ratios of a pair of monomers also influence the sequence of two monomer units on the copolymer chain.

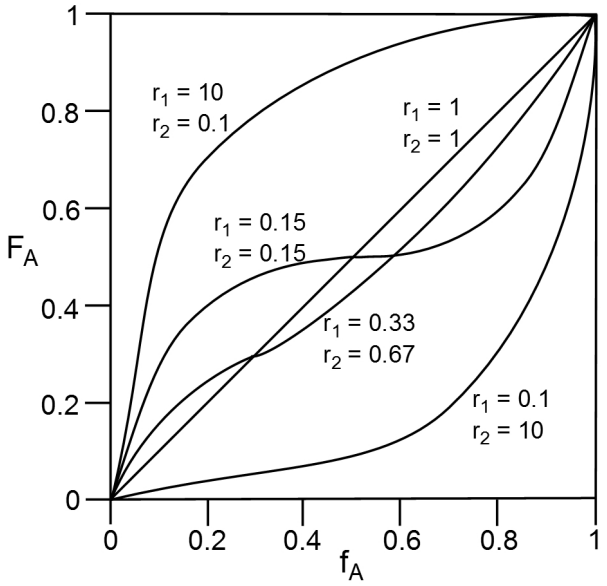

Fig. 2.2.: Copolymerization Diagram of monomer pairs with different reactivity ratios [19]

In an alternating copolymerization monomer A may only react with monomer B. Hence, the reactivity ratios of both monomers must be zero. An ideal random or ideal statistical copolymer is the result when both reactivity ratios are one. Hence, active chain A reacts with monomer A and monomer B in the same way. The structure of a block–like copolymer results from monomer pairs with the reactive ratios that are both obviously greater than one. That means that one kind of monomer reacts preferentially with themself and parts of the copolymer (the blocks) contains almost only monomer A and the other part monomer B. Note that well defined di– or tri–block copolymers cannot be made by means of random copolymerization reactions that include termination steps. [19]

Beside the different compositions of the monomer units on the polymer chain also the arrangement of linked polymer chains lead to different polymer architectures. In *Figure 2.3* different kinds of branched copolymers are depicted. "Three or more polymer chain originate from a branching point of branched copolymers. According to the relative arrangement of the part of the chains to each other one distinguish further star–shaped, dendritic, statistical (hyper–branched) and comb–liked branched molecules."[17][a] In this thesis only linear polymer chains are investigated, in particular block, gradient and statistical copolymers.

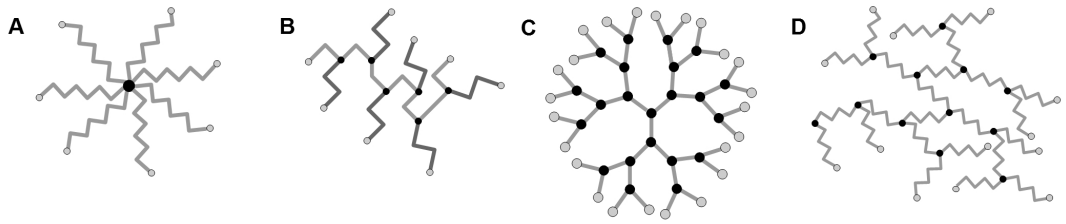

Fig. 2.3.: Overview of branched copolymer architectures; (A) star polymer, (B) graft polymer, (C) dendrimer, (D) hyper–branched polymer; • branching point, • end group; following [17]

It is a well known characteristic of high–molar weight polymers to be mutually "incompatible", i. e. mixtures of homopolymers are unstable and separate into different phases. [22] This is also observable between the different blocks of block copolymers. Four factors influence the phase behavior of polymer mixtures and block copolymers: the architecture of the polymer (chains), the kind of monomer–units, their composition on the polymer chains and finally the degree of polymerization which is the number of repeating units on the polymer chains. The energy of the mixture is characterized by the *Flory–Huggins* segment–segment interaction parameter χ with *Equation 2.1.14*. [22, 23]

$$\chi = \frac{1}{k_B T}\left[\epsilon_{AB} - \frac{1}{2}(\epsilon_{AA} + \epsilon_{BB})\right] \tag{2.1.14}$$

$$\epsilon_{ij} = \sum_{ij} \frac{3}{4}\frac{I_i I_j}{I_i + I_j}\frac{\alpha_i \alpha_j}{r_{ij}^6} \tag{2.1.15}$$

with ϵ_{ij} = contact energy between i and j segments, k_B = Boltzmann constant, r_{ij} = segment–segment separation, α = segment polarizability, I = ionization potential

χ is one parameter to estimate the miscibility of a polymer blend. Miscibility can be expected if χ has a negative value, hence, the energy between A–B–segment contact is lower than the sum of the A–A and B–B contracts. An example of such favorable interactions are hydrogen–bonds. In a polymer mixture the value of χ is typically positive, that means the energy of the system increases with the number of A–B contacts in the mixture. [22, 23]

[a] "Bei verzweigten Polymeren (E: branched polymers) gehen von den Verzweigungspunkten drei oder mehr Ketten aus. Je nach der relativen Anordung dieser Kettenteile zueinander unterscheidet man weiter sternförmig, dendritisch, statistisch (baumähnlich) und kammförmige verzweigte Moleküle."[17]

Two different treatments exist for the description of the behavior of the phase separation of block copolymers. The strong segregation limit (SSL) treat a polymer mixture with $\chi N >> 10$ and the weak segregation limit (WSL) a mixture with $\chi N \approx 10$. The SSL approach was developed in the 1960s by *D. J. Meier* [24] and a further development by *E. Helfand* and *Z. R. Wasserman* [25, 26, 27, 28] For both treatments various approaches were developed. The SSL investigates block copolymers that show sharp borderlines between the phases. The borderline between the phases of block copolymers that are diffuse and broad are described by the WSL, developed by *L. Leibler*. [29] A second approach came from *G. H. Fredrickson* and *E. Helfand*. [30] The SSL and the WSL were brought together by *M. W. Matsen* and *F. S. Bates*. [31] The strong and weak segregation limits explain the different phases that occur at different compositions of a block copolymer.

The meso–phases that can be exhibited by a SSL–di–block copolymer of different compositions are depicted in *Figure 2.4*. The length scale of the phases is around 5 to 100 nm [22].

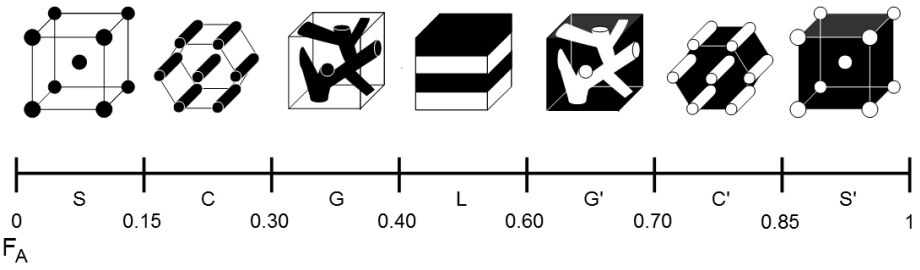

Fig. 2.4.: Structures of di–block copolymer mesophases at different copolymer compositions F_A; S/S' – body–centered spherical micelles, C/C' – hexagonally packed cylindrical micelles, G/G' – bicontinuous gyroid, L – lamella [19, 22]

A lamella structure of the phases occurs at a composition of around $F_A = 0.5$. There layers of PA and PB alternate regularly. When the amount of PA decrease, between $F_A = 0.30$ and $F_A = 0.40$, the structure of the phase change to the gyroid structure. Here a labyrinth of PA permeates a matrix of PB. The PA–channels connect all sides of the sample consistently. When the amount of PA is between $F_A = 0.60$ and $F_A = 0.70$ the inverse gyroid structure with a labyrinth of PB in a PA matrix occurs. Another notation for the gyroid structure is ordered bicontinuous double diamond. [22] That the gyroid structure is a stable phase was first shown by *E. L. Thomas et al.* in 1994. [32] Hexagonally packed cylindrical micelles of PA in a PB matrix are observed between $F_A = 0.15$ and $F_A = 0.30$ and the inverse structure between $F_A = 0.70$ and $F_A = 0.85$. Microspheres of PA in a body–centered cubic PB Matrix are regarded for di–block copolymers with less than $F_A = 0.15$ and with more than $F_A = 0.85$ PB microspheres in a PA matrix. [22, 23] The different compositions and the corresponding phase structures of the di–block copolymers are associated with a change of χN. When the χN–values of the different structures are plotted against the respective compositions the result is the phase diagram that is depicted in *Figure 2.5*. The transfer from the disordered state to the ordered phases is called ordered–disordered–transition (ODT). [22, 31]

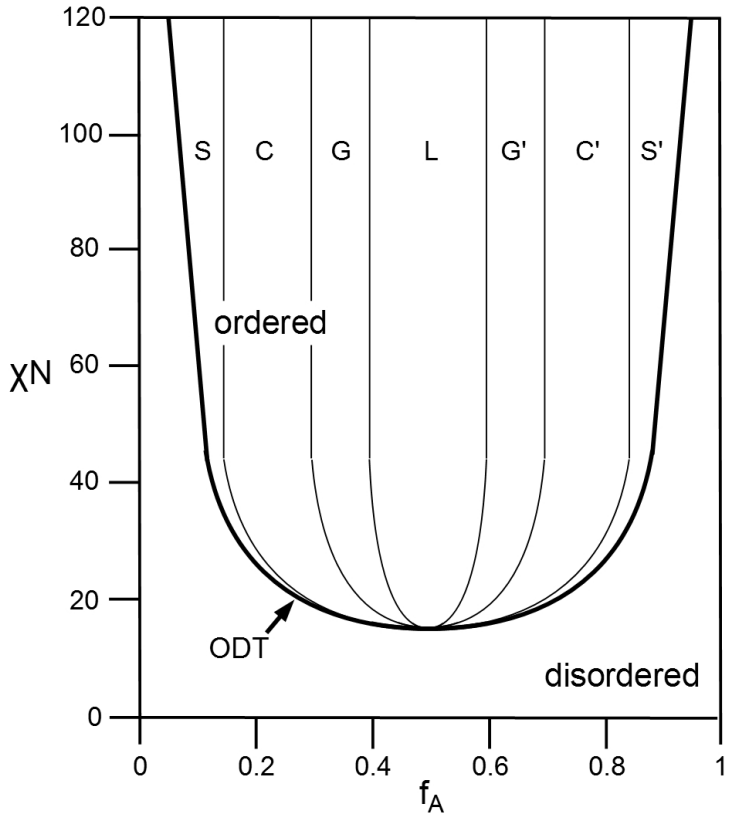

Fig. 2.5.: Phase diagram of A–B–di–block copolymer; ODT – ordered–disordered–transition, S/S' – body–centered spherical micelles, C/C' – hexagonally packed cylindrical micelles, G/G' – bicontinuous gyroid, L – lamellae [31]

Phase segregation is not only observed for block copolymers. Even gradient copolymers may show this behavior. [33, 34, 35] *Lefebvre* et al. figure out "that a gradient in composition along the chain makes phase separation more difficult than for a block copolymer" [33] *Mok* et al. compare the phase behavior of a styrene/*n*–butly acrylate block copolymer and the corresponding gradient copolymer. Both copolymers show phase separation but the calculated phase diagram of the gradient copolymer is much more complex than the one of the block copolymer. [35]

2.2. Polymer Synthesis

A survey on the different kinds of polymer reactions is given in *Table 2.6.* There are three types of polymer reactions, the build–up of polymers, their decomposition and polymer–analogous reactions. The latter are reactions of functional groups on the polymer chain which change the chemical properties of the macromolecules without alternating the degree of polymerization, for examples the hydrolysis of *tert*–butyl–ester–groups to COOH–groups. In principal these reactions are the same as with low–molecular–weight molecules but because the polymer chains are present as statistical coils the functional groups are not perfectly homogeneously distributed in the reaction solution. Furthermore frequent neighbor–group effects, as well as the fact that side products can not be removed from the polymeric products, result in a

different reaction kinetics, and request specialized synthesis techniques. The decomposition of polymer chains can occur in two ways: by depolymerization ($P_{m+1} \rightarrow P_m + M$) or by divide of the polymer chain ($P_{m+n} \rightarrow P_m + P_n$). [18]

The two main types of polymerization reactions are step–growth and chain–growth reactions. In a step–growth reaction two molecules with at least two functional groups react. At the beginning of the reaction dimers, trimers and then oligomers are built. Long macromolecules are only reached with high conversion and even then oligomers and unconverted monomers are in the mixture. The growth of the polymers is a random process at step–growth reactions. At a polyaddition two functional groups react and at a polycondensation beside the covalent bond a byproduct, c. f. H_2O, is generated. [18]

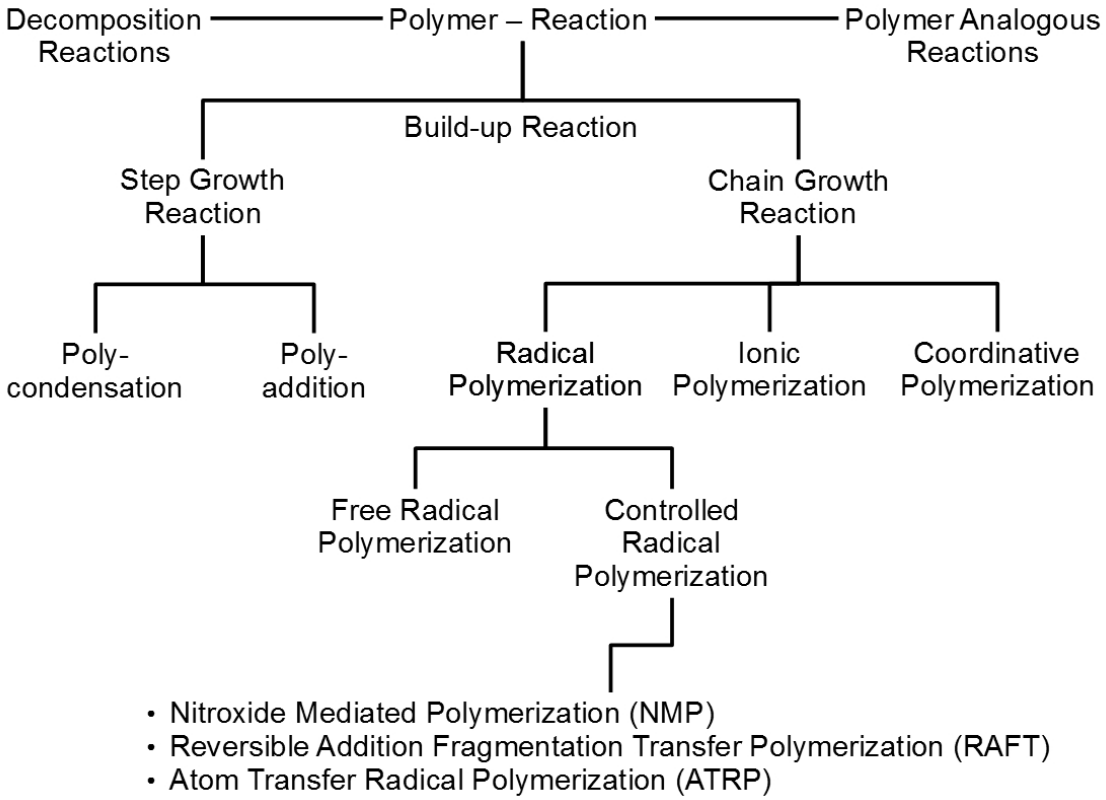

Fig. 2.6.: Overview on polymer reaction (following [18])

Beside the step growth reaction the chain growth reaction is the second way for synthesis of polymer chains. Polymerization are reactions, involving active species such as radicals, cations, anions or metal–organic species. With coordinative polymerizations the addition of monomer units is controlled by catalysts, for example the *Ziegler–Natta*–Polymerization where different catalyst–components like $TiCl_4$ and $AlEt_3$ are used, or enzymes. With this polymerization technique the tacticity of the monomer units on the polymer chain can be controlled. Here the monomer is inserted between the catalyst and the last added monomer unit. [17]

The active species of the ionic polymerization is an anion $[R(M_i)^{\ominus} \rightarrow R(M_{i+1})^{\ominus} \rightarrow R(M_{i+2})^{\ominus}]$ or a cation $[R(M_i)^{\oplus} \rightarrow R(M_{i+1})^{\oplus} \rightarrow R(M_{i+2})^{\oplus}]$. [17] Various initiators are used here. To start cationic polymerizations *Brønsted* and *Lewis* acids, halogens and salts like aryldiazonium and tetrafluoroborate can be used. [36, 37] For a anionic polymerization initiators like alkyllithium compounds or naphthalene radical–anions are used. [36, 38] The main problem with carbon–cationic polymerizations is the high termination rate because of the instability of the cations. The anionic polymerization is very sensitive against oxygen and water. In addition the monomers must have certain properties. Monomers with electron–releasing substituents are needed for a cationic polymerization, like alkoxy–, phenyl–, vinyl– or 1,1–dialkyl–groups. The monomers for a anionic polymerization must possess electron– withdrawing groups, like nitrile–, carbonyl–, phenyl– or vinyl–groups. However, the initiator and the monomer have to be adjusted. The amount of suitable couples is severely limited. More over polar solvents can not be used because they can react with the ions, destroy of build up stable complexes with them. [3] The method that is used here is the radical polymerization, so this is discussed more intensive here.

The chain–growth polymerization mechanism consists of three steps. The initiation is followed of the propagation of the chain. The polymerization of an individual growing radical ends with the termination reaction. The reactions are given in the *Equations 2.2.1* to *2.2.6*. [3] Initiator decomposition:

$$I \xrightarrow{k_d} 2\,R\bullet \tag{2.2.1}$$

Initiation:

$$R\bullet \xrightarrow{k_i} RM_1\bullet \tag{2.2.2}$$

Chain growth:

$$RM_1\bullet + M \xrightarrow{k_p} RM_2\bullet \tag{2.2.3}$$

$$RM_n\bullet + M \xrightarrow{k_p} RM_{n+1}\bullet \tag{2.2.4}$$

Termination:

$$RM_n\bullet + RM_m\bullet \xrightarrow{k_{t,c}} RM_{n+m} \tag{2.2.5}$$

$$RM_n\bullet + RM_m\bullet \xrightarrow{k_{t,d}} RM_n + RM_m \tag{2.2.6}$$

with I = initiator molecule, R• = radical, M = monomer molecule, k_d = rate constant of initiator dissociation, k_i = rate constant of first monomer adding, k_p = rate constant of propagation, $k_{t,c}$ = rate constant of termination by coupling, $k_{t,d}$ = rate constant of termination by disproportionation

Equation 2.2.1 shows the homolytic dissociation of the initiator into two radicals i. e. the generation of the active species. The radicals can be produced with different ways. *Figure 2.7* depicts different initiators as examples.

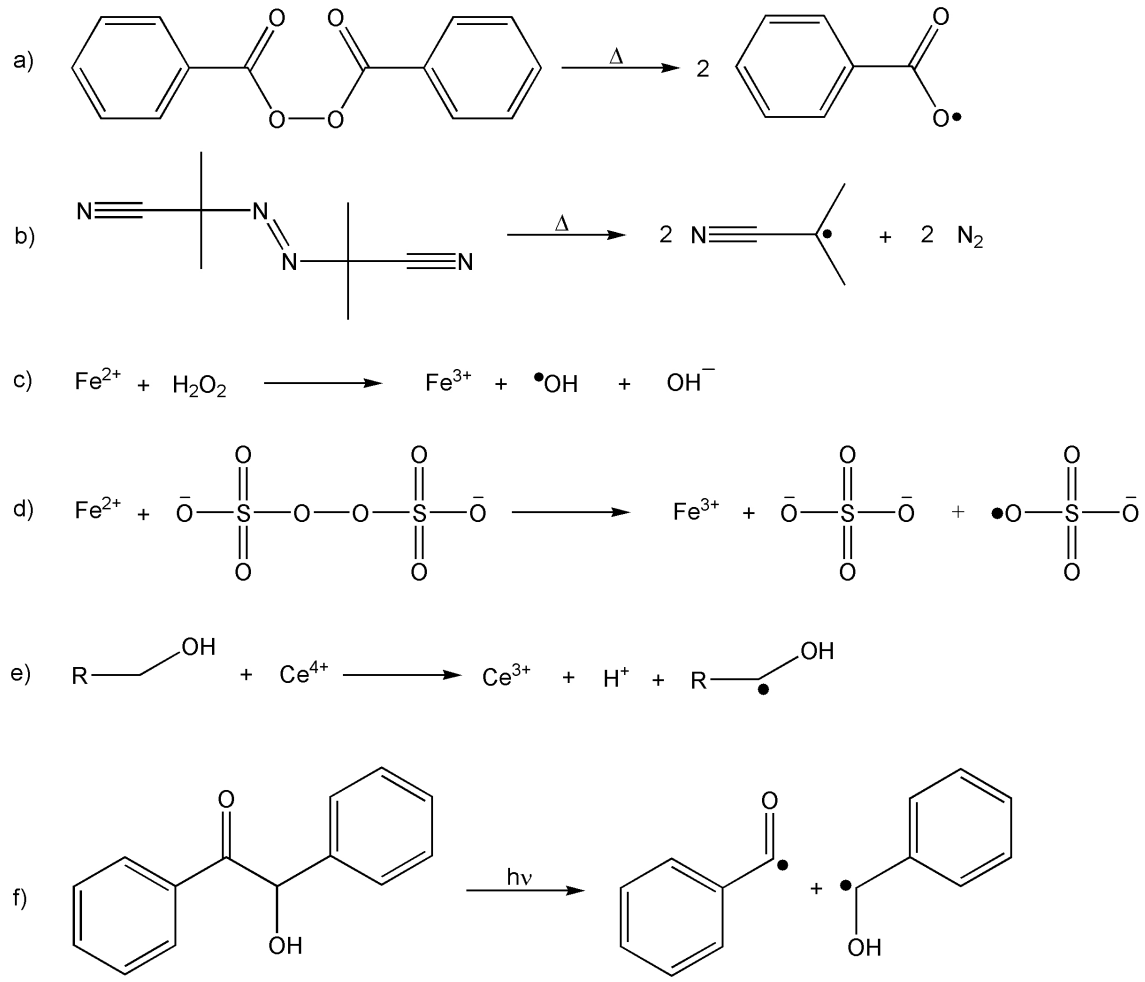

Fig. 2.7.: Homolytic dissociation of different initiators; a) benzyl peroxide (BPO), b) azobisisobutyronitrile (AIBN), c) hydrogen peroxide with iron ions, d) peroxodisulfate with iron ions, e) alcohol and cesium ions, f) benzoin (following [3, 19])

The most common way is the thermal decomposition of the initiator which are peroxy–, azo–, disulfid– or tetrazene– compounds. [36, 39] The two most frequently applied thermal initiators are benzyl peroxide (BPO) and azobisisobutyronitrile (AIBN), see *Figure 2.7a,b.* A limitation for the use of a substance as thermal initiator is the dissociation energy of the substance that must be between 100 and 170 $kJ \cdot mol^{-1}$. The thermal initiators have different dissociation temperatures where the half–life time ranges from 6 to 8 h, e. g. AIBN in a range from 50 to 70 °C and BPO from 80 to 95 °C. "The differences in the rates of decomposition of the various initiators are related to differences in the structures of the initiators and of the radicals produced." [3] An other way of producing of radicals is by means of redox reactions, for example the reaction of hydrogen peroxide with iron ions, see *Figure 2.7c.* Other kinds of redox initiators are a mixture inorganic oxidant and reductant, for instance peroxodisulfate and a metal ion, a organic–inorganic redox pairs and monomers that are a part of the redox pair itself. The third way of homolytic dissociation which is used at radical polymerization is

the photoinitiated one. [36, 40] "In general, light absorption results in radical production by either of two pathways: 1. Some compounds in the system undergoes excitation by energy absorption and subsequent decomposition into radicals. 2. Some compounds undergoes excitation and the excited species interacts with a second compound by either energy transfer or redox reaction to from radicals derived from the latter and/or former compound(s)." [3]

Equation 2.2.2 shows the addition of the first monomer. This reaction is the second step of the initiation of a radical chain polymerization. It is much faster than the dissociation step, hence, the dissociation of the initiator molecule is the rate–determining step of the initiation. [3] The addition of the subsequent monomer to the active radical is called "propagation step". The propagation rate constant k_p is independent of the viscosity of the reaction mixture and on the conversion of the monomer. The ratio between propagation and termination is stable up to a conversion of $\leq 80\,\%$. [41] The value of k_p of the most monomers is in a range of 10^2 to $10^4\,l \cdot mol^{-1} \cdot s^{-1}$. [3] Monomers with similar structure have similar propagation rates, for example methyl acrylate and methyl methacrylate. The solvent which is used at the polymerization has just little influence on the propagation rate constant. [41]

The termination of the polymerization can occur by two reactions. During a coupling reaction, see *Equation 2.2.5*, two active ends of polymer chains react to one long polymer chain and a disproportionation reaction, see *Equation 2.2.6*, means a hydrogen atom is transferred from one polymer chain to a second polymer chain. That leads to two polymer chains without active ends, one with a double bond at the end. The rate constant of the two termination reactions is in the same range for both types, in an order of 10^6 to $10^8\,l \cdot mol^{-1} \cdot s^{-1}$. A coupling termination is more frequent at lower temperature, while at higher temperature the disproportionation termination is preferred. "It is generally accepted that the termination rate coefficient depends on the following factors and experimental parameters: (1) the system viscosity, (2) the chain length of the terminating free macroradicals, (3) the temperature, (4) the pressure, and the (5) monomer conversion." [41] "The much greater values of k_t (whether $k_{t,c}$ or $k_{t,d}$) compared to k_p does not prevent propagation because the radical species are present in very low concentrations and because the polymerization rate is dependent on only the one–half power of k_t." [3]

For the determination of the rate of propagation R_p the total concentration of the radicals is needed.

$$-\frac{d[M]}{dt} = R_p = k_p[M][RM\bullet] \tag{2.2.7}$$

The concentration of the radicals in the polymerization is very low and because of this it is difficult to determine. Hence, for the solution of *Equation 2.2.7* it is assumed that their concentration is constant during the "steady–state" regime. [3]

$$R_i = R_t = k_t[RM\bullet]^2 \tag{2.2.8}$$

$$[RM\bullet] = \left(\frac{R_i}{k_t}\right)^{\frac{1}{2}} \tag{2.2.9}$$

Equation 2.2.9 is introduced into *Equation 2.2.7*. [3]

$$R_p = k_p[M]\left(\frac{R_i}{2k_t}\right)^{\frac{1}{2}} \tag{2.2.10}$$

The rate of polymerization can be determined experimentally by measuring the decrease of the monomer concentration, respectively the increase of the polymer concentration in the reaction mixture against the polymerization time. Different kind of techniques are available here: infra–red, ultra–violet or nuclear magnetic resonance spectroscopy or even gravimetric analysis. In this work, the presence of the monomers and the polymers will be monitored by ^{1}H–NMR–spectroscopy. Another technique is the analysis of unreacted monomer functional groups, like the titration of the carboxyl group at polyesterification. But this is more often used for step–growth polymerization. Dilatometry is the measurement of the volume change which occurs during the polymerization. [3]

The kinetic chain length $\bar{\nu}$ of a polymer is defined by the ratio of the rate of polymerization R_p and the rate of initiation R_i, respectively the rate of termination R_t, see *Equation 2.2.11*. It is the average number of monomer units that are added to one radical.

$$\bar{\nu} = \frac{R_p}{R_i} = \frac{R_p}{R_t} \tag{2.2.11}$$

When a polymerization is terminated by a disproportionation reaction the number of polymer chains remains constant, see *Equation 2.2.6*, and the kinetic chain length equals to the number average degree of polymerization X_n. A termination by coupling or combination, see *Equation 2.2.5*, reduces the number of polymerchains by half. [3, 19]

$$\bar{\nu_d} = X_n \tag{2.2.12}$$

$$\bar{\nu_c} = \frac{X_n}{2} \tag{2.2.13}$$

The time interval between the initiation and the termination of a chain is the radical life–time τ. For example, in a radical polymerization with the initiator AIBN at a concentration of $10^{-3}\,\mathrm{mol}\cdot\mathrm{l}^{-1}$ the radicals have an average lifetime τ of around one second. τ is influenced by the kind of initiator, monomer and solvent, their concentration and the reaction temper-

ature. [19]

$$\tau = \frac{X_n}{k_p[M]} \tag{2.2.14}$$

The average radical life–time τ is short which leads to high termination rates. Hence, polymer chains appear, add some monomers and is disabled during the free radical polymerization in a random process. The result is a mixture of polymer chains with most different molar masses and the termination reactions results in a large molar mass distribution or polydispersity (PDI). [3] Hence, the termination reactions must be prevented or at least suppressed and all polymer chains must growth simultaneously and consistently when a polymer mixture with a narrow polydispersity and a linear increase of the average molar mass over the increase of the conversion are aspired. That are the characteristics of a "living" polymerization. [3, 18] The first living polymerization was the anionic living polymerization, developed by *M. Szwarc* in the 1950s. [5] A radical polymerization with suppressed termination was first reported by *Otsu* and *Yoshida* in 1982. [4] The term "living" means the lack of any termination at all. But since the termination reactions were only suppressed to a very low level, the better term is "controlled" radical polymerization (CRP). There are different kinds of CRP. They have in common that the radical which is build up from the initiator is stabilized by a second radical. The two radicals combine to from a dormant species. The dormant species reversible decomposes to the propagation radical (= active species) and the stable radical. The monomers are added to the propagation radical and then the radical compose to the dormant species again. The equilibrium between active and dormant species lays on the side of the dormant species and only a small number of radicals is active at each moment. The radical is protected by the dormant species and so termination reactions are suppressed to a minimum. Another important point is that all propagation radicals are created simultaneously at the start of the reaction and that the polymer chains growth in parallel. The different methods of controlled radical polymerization are the Nitroxide Mediated Polymerization (NMP), the Reversible Addition Fragmentation Transfer Polymerization (RAFT) and the Atom Transfer Radical Polymerization (ATRP), see *Figure 2.6*. At a NMP the initiator is an alkoxy amine which dissociate to a reactive alkyl radical and a stable nitroxide radical. [42] The stabilization at a RAFT is given by a dithio benzoate. [43] The Atom Transfer Radical Polymerization is the technique that is used for this thesis, and will be described more detailed.

The ATRP was developed in the mid 1990s parallel in the working groups of *Kato* et al. [9] and *Matyjaszewski* et al. [10]. This technique is established well in the organic material science by this time. [44] The general reaction mechanism of an Atom Transfer Radical Polymerization is depicted in *Figure 2.8*. The initiator system consists of the initiator molecule R–X, the activator catalyst M^m–X and the ligand L. Moreover monomers and the solvent are involved in the reaction, see *Figure 2.8*.

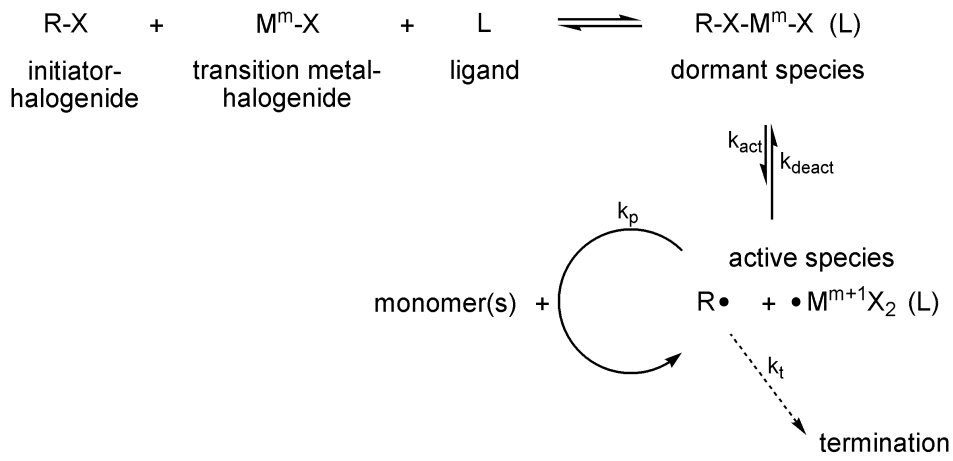

Fig. 2.8.: General reaction mechanism of Atom Transfer Radical Polymerization (following [16, 18])

The advantage of a radical polymerization towards the anionic polymerization is the large number of monomers that can be used. Styrenes, (meth)acrylates, (meth)acrylamides and acetonitril are possible monomers for an ATRP. [45] "Even under the same conditions using the same catalyst, each monomer has its own unique atom transfer equilibrium constant for its active ans dormant species." [16] As initiator every kind of alkyl halide is useable. Bromides and chlorides are mostly used. Iodines just work in the ATRP of a acrylate with copper and styrene with ruthenium or rhenium. Fluorines can only be used limited because the bond between carbon and fluoride is too strong for homolytic cleavage. [3, 16] As a general guideline the structure of the initiator should be similar to the structure of the used monomer. Beside molecules with bonds between a halogen and a carbon, other initiators with weak R–X bonds, like N–X, S–X and O–X can be used. Molecules with several halogens attached to one carbon atom, like e. g. CCl_4 or $CHCl_3$, can also be used. The initiator concentration influences the degree of polymerization (DP), see *Equation 2.2.15.* [16]

$$\mathrm{DP} = \frac{[\mathrm{M}]_0}{[\mathrm{I}]_0} \cdot \mathrm{p} \tag{2.2.15}$$

with $[\mathrm{M}]_0$ = initial monomer concentration, $[\mathrm{I}]_0$ = initial initiator concentration, p = conversion

The concentration of the initiator determines the number of growing chains which is a constant when termination reactions are suppressed by the initiator system of the ATRP. [3, 16] A catalyst must have two oxidation states which are separated by one electron, affinity of the transition metal to the halogen, the possibility of the coordination sphere to expand when the second halogen is incorporated by the oxidation of the catalyst and affinity of building of a complex of the catalyst with the ligand. [16] The transition metals which have been used for ATRP are, for example, molybdenum, rhenium, iron, rhodium, nickel, copper. [16] Copper is the most often used transition metal of Atom Transfer Radical Polymerizations. For an ATRP with copper as transition metal a multidentate nitrogen ligand stabilizes the initiator complex

best. In this work the initiator complex is made from of copper chloride and PMDETA, for example. The selection criteria of a nitrogen–containing ligand are the electronic and steric properties of the molecules. These criteria are influenced as follows: [41]

1. the coordination of the nitrogen
   with rise of the denticity of the ligand the activity increases; N1 << N2 < N3 < N4

2. the number of linked carbon atoms
   with rise of the linked C–atoms the activity increases; C2 > C3 >> C4

3. the linked functional groups
   the activiy of the ligand increase with change of the linked functional group in this order: R_2N- ~ Pyr− > R – N = > Ph – N = > Ph – NR−

4. bridged systems are more active than cyclic systems

When iron is used, the ligand should be a monodentate or bidentate nitrogen ligand. [46] Initiator systems with rhenium, nickel and palladium need phosphorus–based ligands. [16] There is a large amount of different solvents that are used at an ATRP, like "benzene, toluene, anisole, diphenyl ether, ethyl acetate, acetone, dimethyl formamide, ethylene carbonate, alcohol, water, carbon dioxide and many others". [16] Moreover an ATRP can be performed in bulk or with a solvent in a homogenous solution, but also in suspensions [47], emulsions [48, 49] and dispersions [50]. A solvent can influence the ATRP considerably, i. e. by influencing the structure of the catalyst–ligand–complex which may alter the the reaction rate. [51] A solvent can also poison the catalyst or leads to side reactions. [52, 53] A positive effect of a solvent is to improve the solubility of the catalyst. [54] Beside the solvent also the temperature influences the reaction rate. With a higher temperature the radical propagation rate constant and the atom transfer equilibrium constant increase which causes a better control over the reaction. Moreover, the termination reaction rates also increase with higher temperature. [53] The solubility of the catalyst becomes better with higher temperature. On the other side it is possible that the catalyst decomposes at higher temperatures. [55]

The polymerization rate R_p of an ATRP is described by *Equation 2.2.16* for a copper–mediated ATRP as example. [16]

$$R_p = k_p[M][P\bullet] = k_p K_{eq}[M][I]_0 \cdot [Cu^I]/[X - Cu^{II}] \tag{2.2.16}$$

$$K_{eq} = \frac{k_{act}}{k_{deact}} \tag{2.2.17}$$

with k_p = rate constant of propagation, [M] = monomer concentration, [P•] = radical concentration, k_{act} = rate constant of activation of the dormant species, k_{deact} = rate constant of deactivation of the active species

The conversion–time–curve and the semi–logarithmic representation of the conversion against the reaction time are depicted in *Figure 2.9a*. The curves base on *Equation 2.2.16*. The linear progression of ln(1-p) is a result of the constant radical concentration and, hence, the reaction is of pseudo–first–order with respect to the concentrations of monomer(s), initiator and catalyst. The ratio of ligand to catalyst also influences the kinetic of the ATRP. Every change of monomer, of any part of the initiator system, of the solvent or the reaction temperature leads to another rate. [55, 56, 57]

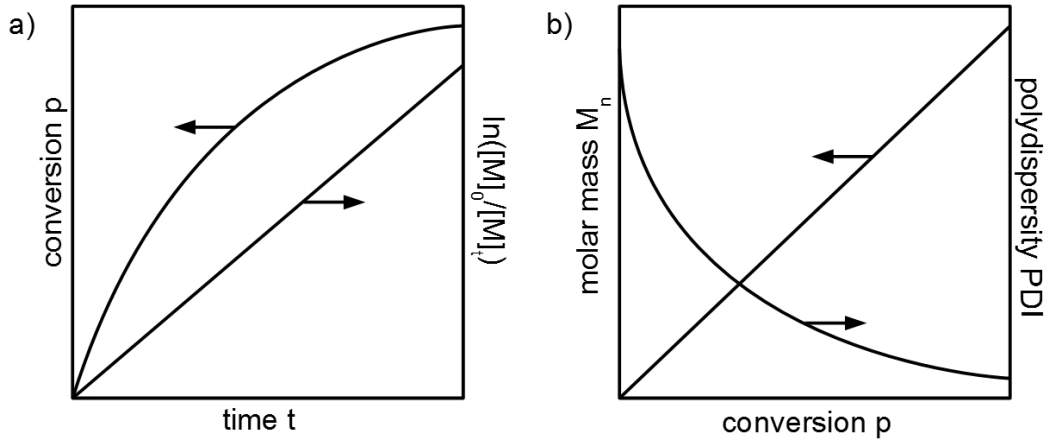

Fig. 2.9.: Schematic representation of a) the dependence of conversion and semi–logarithmic plot of conversion against time, b) the evolution of molar mass and polydispersity against conversion (following [16])

The typical development of the molar mass of a polymer during an ATRP is given in *Figure 2.9b*. Due to the good control of the polymerization the molar mass increases linear with the conversion. This is effected by the constant radical concentration and the suppression of termination reactions. The molar mass of the resulting polymer can be modulated between 1000 and 150000 $g \cdot mol^{-1}$. [53, 58] The polydispersity decreases with the increase of the conversion because at the beginning of the reaction the propagation rate is high and at each propagation step several monomer–units are added. With progression of the polymerization the polymer chain become more uniform as stated by *Equation 2.2.18*. [16]

$$\frac{M_w}{M_n} = 1 + \left(\frac{[RX]_0 k_p}{k_{deact}[D]}\right)\left(\frac{2}{p} - 1\right) \tag{2.2.18}$$

with $[RX]_0$ = initial initiator concentration, $[D]$ = deactivator concentration

The slow, but controlled, reaction leads to polydispersities less than 1.5. The value of the polydispersity is influenced by the catalyst reactivity. With a fast deactivation of the active species the polydispersity of the resulting polymer decreases, for example by an increase of the deactivator concentration. But this also means a decrease of the polymerization rate. [58]

In this PhD–thesis the initiator system was applied as depicted in *Figure 2.10*. The ini-

tiator R–X is *para*–toluenesulfonyl chloride (pTSC), the catalyst M_mX is copper chloride (CuCl) and the ligand L is N,N,N',N',N"–pentamethyldiethylenetriamine (PMDETA). The used monomers are *tert*–butyl methacrylate (tBMA), *n*–butyl methacrylate (nBMA) and benzyl methacrylate (BzMA). The initiator pTSC is common used in ATRP for the polymerization of methyl methacrylate (MMA) and mostly with a bipyridine–derivative as ligand and CuBr or CuCl as catalyst. [59, 60] MMA was also copolymerized by using an ATRP–initiator system with pTSC/ PMDETA/ CuBr [61] or pTSC/ PMDETA/ CuCl [62, 63].

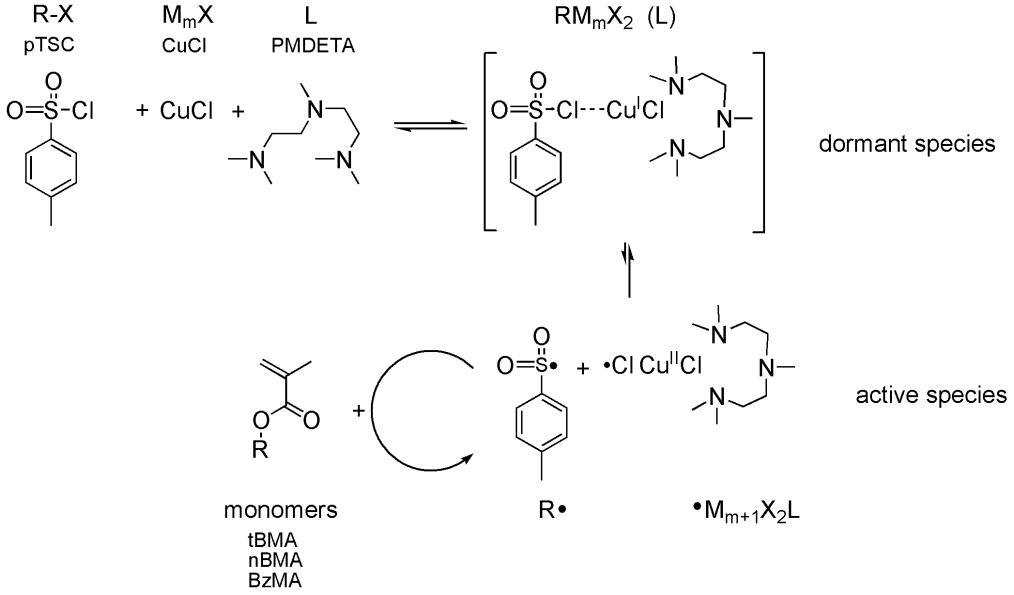

Fig. 2.10.: Reaction mechanism of the Atom Transfer Radical Polymerization as used in this work

2.3. Properties and Applications of Block Copolymers

One has tried to mix up polymers with different properties, to create materials with combined or even new features. Moreover the intensity of the features should be adjusted by the ratio of the different parts of the mixture like it is done with metals at alloys. The problem is that most polymers are not mixable among each other and the different polymers separate into different phases. Hence, an unity of the properties is not possible because there is no connection between the phases. The solution of this problem is a bridge between the two phases which is done by block copolymers. Hence, the block copolymer is used as surfactant or polymer soap. [11, 12] For example a mixture of poly(styrene) and poly(2–vinylpyridine) can be stabilized by P(S)–b–P(VP). [64] *Figure 2.11* shows the effect of a block copolymer for the stabilization of a polymer blend. Spheres of homopolymer B are enclosed in the matrix of homopolymer A. The upper images of *Figure 2.11* show the electron–microscopical recordings of the freeze fractures of the polymer blend. *Figure 2.11a* displays the blend without additives. The lack of connections between the two phases is obviously because the line of break follows the borders of the spheres. *Figure 2.11b* exhibits the blend with added block copolymer. The break goes consistently through both parts of the blend because the block copolymer connects the homopolymers steadily.

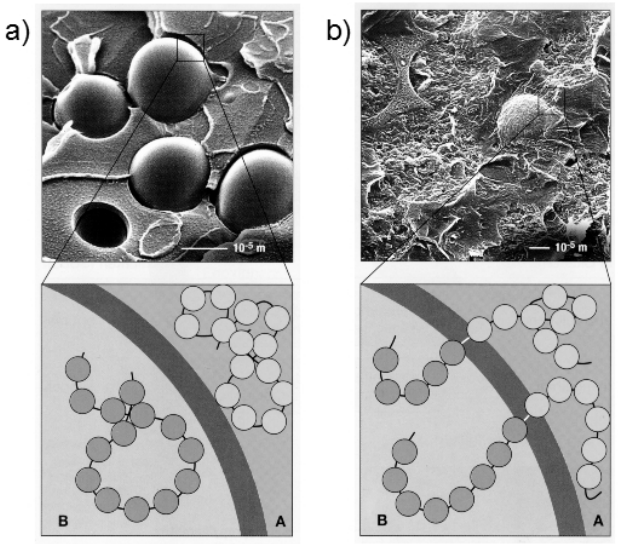

Fig. 2.11.: Effect of block copolymer in polymer blend; a) shell break – interface without molecular bridging, b) force break – interface bridged with A–B–diblock copolymer [65]

One method to describe a block copolymer is the critical micelle concentration (CMC). This is the point of concentration at which a surfactant does not decrease the surface tension any more and micelles are builded in the emulsion. Literature studies indicate that gradient copolymers can be more effective surfactants than block copolymers. [66] When a gradient copolymer is used as compatibilizer in a polymer blend "the success of this strategy depends significantly on the overall composition of the gradient copolymer as well as details regarding the inherent incompatibility of the blends." [67]

Polymers are also used for noise isolation. [68] This is possible because of the ability of polymers to quieten sonic. This ability is coupled to the glass transition of macromolecules as it is described by the *Williams–Landel–Ferry–Equation*. [69, 70]

$$\log\frac{\nu_1}{\nu_2} = \frac{a\Delta T}{b + \Delta T} \tag{2.3.1}$$

Here a and b are constants with values between 9 and 100. [69]

The composition of a copolymer influences the thermal behavior. [71, 72, 73] The theoretical thermograms of copolymers with different monomer sequences along the polymer chain are depicted in *Figure 2.12*. A statistical copolymer P[A–co–B] and also a gradient copolymer P[A–grad–B] show one glass transition step, while the AB–diblock copolymer P[A]–b–P[B] exhibits two steps. The first T_g–step of the block copolymer is related to the first block A of the copolymer and at the same temperature as the homopolymer A, respectively the second step is related to the second block B and at the same temperature as the homopolymer B. The glass transition step of the statistical copolymer lie between the steps of the homopolymers, respectively the two steps of the block copolymer. The slope of the step of the statistical copolymer is similar to the slope of the steps of the homopolymers. [74, 75] The glass transition

step of the gradient copolymer starts at the T_{onset} temperature of the T_g–step of homopolymer A and ends at the T_{offset} temperature of the T_g–step of homopolymer B. Hence, the slope of the glass transition step of the gradient copolymer is lower and its temperature range is wider than the one of the statistical copolymer. [14, 75, 76]

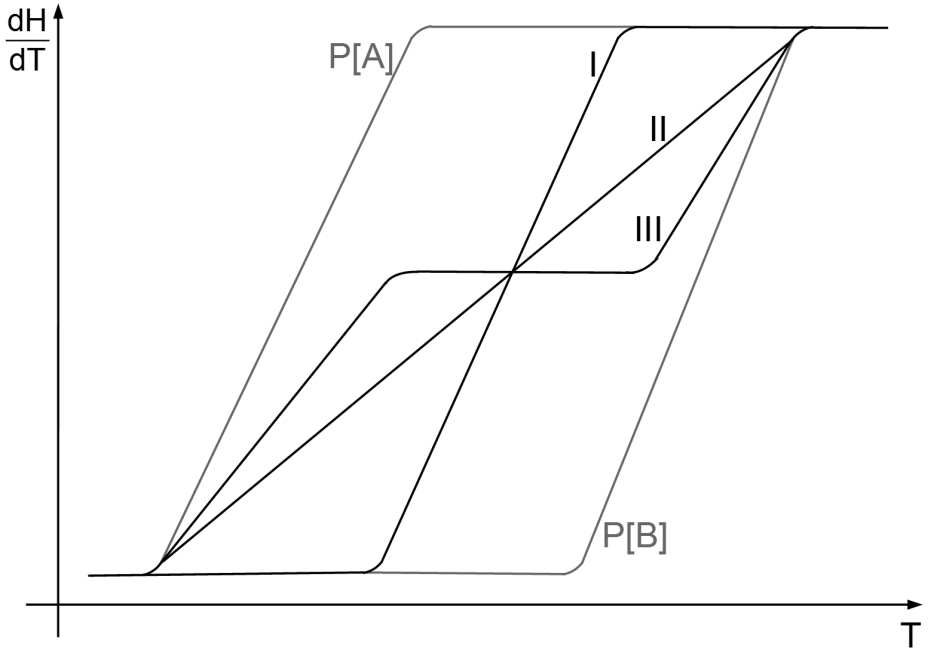

Fig. 2.12.: Scheme of theoretical DSC thermograms in the vicinity of glass transitions of different copolymer structures (black lines) in relation to homopolymers A and B (grey lines); (I) statistical copolymer P[A–co–B], (II) gradient copolymer P[A–grad–B], (III) AB–diblock copolymer P[A]–b–P[B]

Therewith a statistical copolymer quietens the sonic of one small band of frequencies and a di–block copolymer the sonic of two small band. The glass transition region of a gradient copolymer is extremely broad. Hence, gradient copolymers can dampen the sonic of a very broad band of frequencies. [68]

2.4. Molar Mass Determination by Light Scattering

The molar mass of a polymer can be determined by light scattering (LS) of the molecules in solution. The basis of this measurement method originated from the studies of Rayleigh explaining the scattering of light by small molecules ($d < \lambda/20$). [77, 78] Small molecules scatters uniformly in all directions, see *Figure 2.13*, and are called isotropic scatterer. This specific kind of light scattering is described with the Rayleigh ratio R_θ. [79]

$$R_\theta = \frac{i_\theta r^2}{I_0(1+\cos^2\theta)} \tag{2.4.1}$$

with I_0 = intensity of the incident laser beam, i_θ = intensity of the scattered light, r = distance of the center from the observer, θ = scattering angle

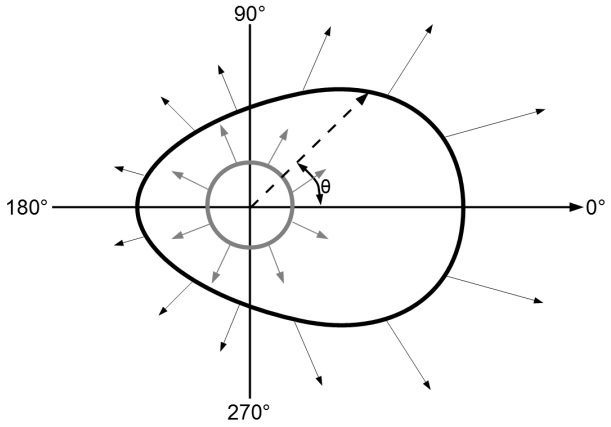

Fig. 2.13.: Intensity of light scattering of small molecules ($d < \lambda/20$, grey line) and large molecules ($d > \lambda/20$, black line) (following [80])

Debye extended the work of Rayleigh to large molecules. [81, 82] Large particles like polymer molecules ($d > \lambda/20$) are anisotropic scatterers. They scatter stronger in forward direction than in backward direction. [79, 80] The comparison of the scattering of small and large molecules is illustrated in *Figure 2.13*. The complex equations of Rayleigh and Debye and their implementation on large molecules is given in literature. [79] The solution of this equations for large molecules is *Equation 2.4.2*. [79, 80]

$$\frac{K\,c}{R_\theta} = \frac{1}{M_w}\left(1 + \frac{Q^2\left\langle \bar{S}^2\right\rangle}{3}\right) + 2A_2c + 3A_3c_2^2 + \ldots \tag{2.4.2}$$

with c = concentration, S = radius of gyration, A_2 = second virial coefficient, A_3 = third virial coefficient

In *Equation 2.4.2* K denotes the optical constant, see *Equation 2.4.3*, which include the refractive index increment (dn/dc). This is depended among others on the structure and the composition of the molecule and the measuring temperature and is measured prior to the molecular weight determination. Q is the scattering vector or angle ratio, see *Equation 2.4.4*.

$$K = \frac{2\pi^2 n_0^2}{\lambda^4 N_A}\left(\frac{dn}{dc}\right)^2 \tag{2.4.3}$$

$$Q = \frac{4\pi}{\lambda'}\sin\left(\frac{\theta}{2}\right) \tag{2.4.4}$$

For the determination of the molar mass from *Equation 2.4.2* the values of Q and c are extrapolated to 0, see *Figure 2.14*. The intersection of the resulting straight line with the ordinate is M_w^{-1}. The slope of $c \to 0$ is the values of the second virial coefficient and the slope of $\theta \to 0$ is the values of the average radius of gyration. Due to the fact that the sample fractions are extremely diluted when the light scattering detection is coupled with size exclusion chromatography, the part of *Equation 2.4.2* after the second virial coefficent

can be negligible.

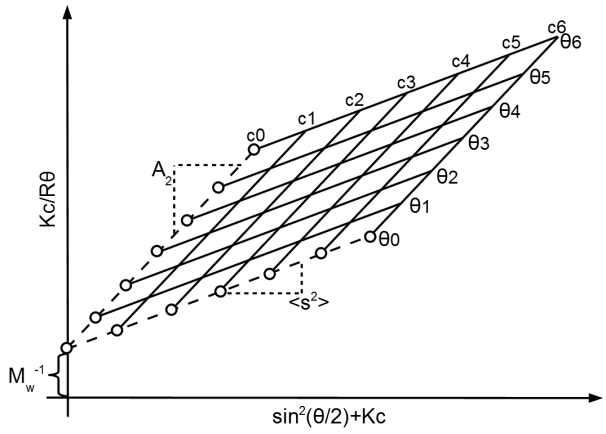

Fig. 2.14.: Zimm–plot for the analysis of light scattering data [79]

The concentration of the investigated fraction of the whole polymer sample is measured by a concentration detector. This can be a viscometer or a refractive index (RI) detector. For the measurements of the molar mass in this work the light scattering detector is linked with a RI–detector. The used LS–detector measures the light scattering at 18 different angles. Hence, for each sample fraction a Debye–plot of 18 angles θ is evaluated and solved form the analysis–software. The resulting values are the molar mass M_w, the radius of gyration S and the second virial coefficient A_2 of each sample fraction. With the molar mass of each fraction the molar mass distribution of the whole polymer sample can be determined.

3. Synthesis of Statistic Copolymers from n– and tert–Butyl Methacrylate by means of Batch Polymerization

The aim of this part of this PhD thesis is the preparation of statistical copolymers of *n*–butyl methacrylate (nBMA) and *tert*–butyl methacrylate (tBMA) by means of Atom Transfer Radical Polymerization (ATRP). [16] Batch experiments were carried out to measure (i) the rate of polymerization of the two monomers, (ii) the composition of the copolymers, as well as (iii) the molecular weights of the products in dependence of the monomer–educt mixture and the reaction time. The evaluated data are used to calculate the respective rate constants and to construct the copolymerization diagram of the system tBMA/nBMA.

3.1. Materials and Methods

3.1.1. Materials

N–Butyl methacrylate (nBMA, 99 %, *Sigma–Aldrich*) and *tert*–butyl methacrylate (tBMA, 98 %, *Alfa Aesar*) were purified via filtration over 1.5 g per 1 g monomer basic Al_2O_3 (*Sigma–Aldrich*) to remove the inhibitor 4–methoxyphenol. 2–Butanone (MEK, *BDH Prolabo*, chromasol.) was dried with boron oxide B_2O_3 (99.9 %, *Sigma–Aldrich*) as described in literature. [83] Copper(I) chloride (97 %, *Sigma–Aldrich*) was given into a tenfold amount of glacial acetic acid and heated under reflux for five hours. Subsequently the grey powder was washed with 100 ml ethanol and 100 ml acetone and then dried in vacuo at 60 °C over night (following [84]). N,N,N',N',N"–Pentamethyldiethylenetriamine (PMDETA, 99 %, *Sigma–Aldrich*) and *para*–toluenesulfonyl chloride (pTSC, 98 %, *Sigma–Aldrich*) were used as received.

3.1.2. Batch Copolymerization of Statistical Copolymers

Two series of batch experiments were made. *Series A* (experiments V11 to V19, *Table 3.1*) consists of preparative synthesis without sampling and *Series B* (experiments V21 to V29, *Table 3.2*) consists of analytical copolymerizations with samples taken for ATR–FTIR–, EA–, SEC– and DSC–analysis.

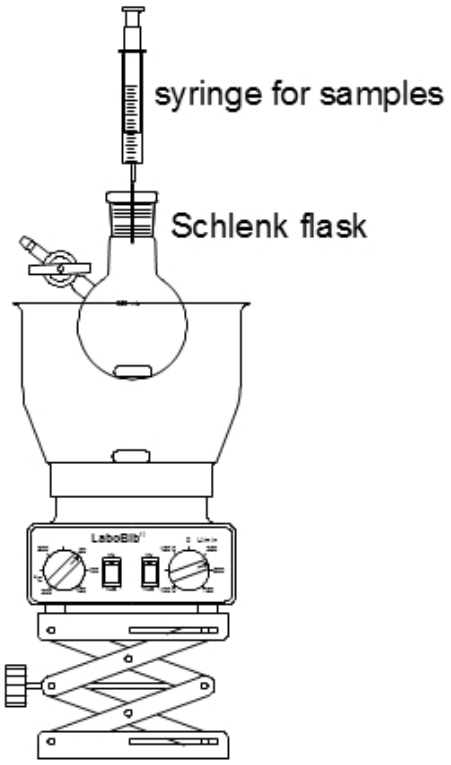

Fig. 3.1.: Experimental setup for batch copolymerization

Series A was performed in analogy to reference [63]. The experimental setup is depicted in *Figure 3.1.* A 25 ml Schlenk flask was heated out with a hot gun (air temperature ≈ 400 °C) under vacuum for five minutes and then flushed with nitrogen. The chemicals were weighted in a screw–cap glass in a specific order: First 0.0313 g ($1.81 \cdot 10^{-4}$ mol) pTSC was weighted, followed by the respective amounts of the two monomers, e.g. 2.2468 g (0.0158 mol) nBMA and 2.2468 g (0.0158 mol) tBMA (cf. *Table 3.1*). When the pTSC was dissolved, 0.0344 g ($1.81 \cdot 10^{-4}$ mol) PMDETA, and 0.0179 g ($1.81 \cdot 10^{-4}$ mol) CuCl were added. The mixture was rinsed into the Schlenk flask with 4.4935 g of the solvent MEK under nitrogen flow. Then the flask was sealed with a rubber septum. Subsequently the solution was degassed by means of 5 freeze–melt–cycles, flooded with nitrogen and then heated up to 80 °C for 3 hours. During the reaction time 0.05 ml samples were taken periodically by means of a syringe through the sealed septum at 0, 15, 30, 45, 60, 90, 120, 150 and 180 min for ^{1}H–NMR analysis. The 0.05 ml of aliquot–sample were given into 0.5 ml cold $CDCl_3$ without further purification.

After 3 hours the Schlenk flask was removed from the oil bath. The reactions mixture was cooled to 20 °C with a mixture of ice and water. Afterward the solution was diluted with 20 ml of MEK, filtered over 30 g Al_2O_3 and two-thirds of the solvent was removed by vacuum distillation. The residual mixture of polymer, monomers, initiator components and remaining solvent was slowly dropped into 500 ml of an ice cooled water:methanol (1:1 vol:vol) mixture. The precipitated polymer was filtered over a P4 glass filter and dried at 45 °C under vacuum over night. This technique is denoted as *"work–up A"* in the text throughout. The yields of the polymerizations are listed in *Table 3.1.*

For *Series B* 0.0689 g ($3.61 \cdot 10^{-4}$ mol) pTSC, 0.0626 g ($3.61 \cdot 10^{-4}$ mol) PMDETA, 0.0357 g ($3.61 \cdot 10^{-4}$ mol) CuCl and 8.986 g MEK were mixed with the corresponding amount of the monomers (cf. *Table 3.2*). The preparation of the Schlenk flask, the mixture and the transfer of the chemicals were performed as described with *Series A* but using a 50 ml Schlenk flask. The same holds true with the synthesis temperature, the reaction time as well as the working up procedure. Reaction conditions and yields are summarized in *Table 3.2*. In *Series B* 1 ml aliquot samples were taken, at 0, 60, 90, 120, 150, 180 min for SEC analysis and another 0.05 ml sample were treated as described with *Series A* and used for ^{1}H–NMR analysis.

SEC–samples were worked up differently from the final polymer. SEC–sample–work–up is denoted as *"work–up B"*. 1 ml of the solution was dropped into 20 ml of a ice cooled water:methanol = 1:1 vol:vol mixture. The precipitated polymer was separated by centrifugation and dried at 45 °C under vacuum over night. The precipitated was dissolved in 5 ml CH_2Cl_2 and transferred into a separatory funnel. 5 ml H_2O were added and thoroughly shaken. The organic phase was separated and given into a round–bottom flask. The water phase was extracted two times more, each with 2 ml CH_2Cl_2. All organic phased were combined. The solvent was removed by vacuum evaporation. The polymer yields of the copolymers isolated from the samples are listed in *Table 3.2*.

All the precipitated, cleaned and dried copolymers were examined with elemental analysis, ATR–FTIR, SEC and DSC. The respective composition data of all performed test polymerizations are summarized in *Tables 3.1 and 3.2*.

Tab. 3.1.: Monomer compositions and final yields of nBMA–tBMA batch copolymerization experiments – *Series A*

Entry	nBMA [mol]	tBMA [mol]	nBMA:tBMA	f_{nBMA}	m_{nBMA} [g]	m_{tBMA} [g]	yield [g]	yield [%]
V11	0.0158	0.0158	1:1	0.50	2.2468	2.2468	2.35	51.82
V12	0.0105	0.0211	1:2	0.33	1.4931	3.0004	2.21	48.80
V13	0.0211	0.0105	2:1	0.66	3.0004	1.4931	2.42	53.51
V14	0.0079	0.0237	1:3	0.25	1.1234	3.3701	3.04	67.08
V15	0.0237	0.0079	3:1	0.75	3.3701	1.1234	2.78	61.40
V16	0.0063	0.0253	1:4	0.20	0.8987	3.5948	2.67	59.02
V17	0.0253	0.0063	4:1	0.80	3.5948	0.8987	2.59	57.24
V18	–	0.0316	0:1	0.00	–	4.4935	2.94	64.84
V19	0.0316	–	1:0	1.00	4.4935	–	2.90	64.01

Tab. 3.2.: Monomer compositions and final yields of nBMA–tBMA batch copolymerization experiments – *Series B*

Entry	nBMA [mol]	tBMA [mol]	nBMA:tBMA	f_{nBMA}	m_{nBMA} [g]	m_{tBMA} [g]	yield [g]	yield [%]
V21	0.0316	0.0316	1:1	0.50	4.4935	4.4935	5.02	55.47
V22	0.0211	0.0421	1:2	0.33	3.0004	5.9866	4.85	53.53
V23	0.0421	0.0211	2:1	0.66	5.9866	3.0004	5.43	59.92
V24	0.0158	0.0474	1:3	0.25	2.2468	6.7403	5.25	57.92
V25	0.0474	0.0158	3:1	0.75	6.7403	2.2468	5.69	62.82
V26	0.0126	0.0506	1:4	0.20	1.7917	7.1953	5.38	59.60
V27	0.0506	0.0126	4:1	0.80	7.1953	1.7917	5.86	64.69
V28	–	0.0632	0:1	0.00	–	8.9870	5.71	63.10
V29	0.0632	–	1:0	1.00	4.4935	–	5.79	63.24

Tab. 3.3.: Time–conversion data obtained from samples taken during the batch copolymerization reactions of nBMA and tBMA (*Series B*)

time [min]	Entry	yield [g]	yield [%]	Entry	yield [g]	yield [%]	Entry	yield [g]	yield [%]
60	V21	0.17	39.15	V22	0.20	46.81	V23	0.24	57.71
90		0.26	60.56		0.26	61.82		0.19	44.51
120		0.28	67.12		0.27	63.31		0.27	63.71
150		0.29	69.56		0.30	71.46		0.31	74.67
180		0.36	84.91		0.35	82.17		0.32	77.95
60	V24	0.22	51.98	V25	0.22	53.30	V26	0.18	42.16
90		0.24	55.55		0.27	63.41		0.34	79.33
120		0.24	58.78		0.37	86.78		0.30	70.10
150		0.29	68.94		0.32	77.02		0.32	74.35
180		0.33	76.85		0.36	85.38		0.35	82.57
60	V27	0.23	55.08	V28	0.19	45.88	V29	0.27	63.23
90		0.31	73.50		0.28	66.53		0.32	76.12
120		0.37	87.95		0.32	75.27		0.33	79.43
150		0.37	88.50		0.35	82.78		0.34	79.93
180		0.38	89.92		0.39	92.60		0.34	80.14

T = 80 °C, [M] = $1.436\,\mathrm{mol}\cdot\mathrm{l}^{-1}$, I:M = 1:175

Experiment V18 (PtBMA):

^{1}***H–NMR:*** 1.25–1.45 ppm (broad peak, –C(CH_3)$_3$, P[tBMA]); 1.42 ppm (s, –C(CH_3)$_3$, tBMA); 1.7–1.9 ppm (broad peak, –CH_3, P[tBMA]); 1.9 ppm (s, –CH_3, tBMA); 5.3 ppm (t, CH_2=C–, cis, tBMA); 5.9 ppm (s, CH_2=C–, trans, tBMA)

EA: 66.54 % C, 9.59 % H, (23.87 % O_{calc})

ATR–FTIR: 3100–2800 cm^{-1} (=CH_2, –CH_2–, –CH_3); 1719 cm^{-1} (–C=O); 1475 cm^{-1} (–CH_2–, –CH_3); 1457 cm^{-1} (–CH_2–, –CH_3); 1392 cm^{-1}; 1366 cm^{-1} (tBu); 1331 cm^{-1}; 1248 cm^{-1} (tBu); 1133 cm^{-1} (–C–O–C–); 1036 cm^{-1}; 969 cm^{-1}; 875 cm^{-1} (tBu); 847 cm^{-1}; 752 cm^{-1}; 516 cm^{-1}; 502 cm^{-1}; 471 cm^{-1}

SEC: dn/dc = 0.0612 ml $\cdot$ g^{-1}; M_n = 21420 g $\cdot$ mol^{-1}; M_w = 28820 g $\cdot$ mol^{-1}; M_z = 32910 g $\cdot$ mol^{-1}

DSC: T_{onset} = 96.0 °C; T_{midpt} = 103.0 °C; T_g = 107.5 °C; T_{offset} = 111.0 °C; ΔC_p = 0.223 J $\cdot$ g^{-1} $\cdot$ K^{-1}

Experiment V19 (PnBMA):

^{1}***H–NMR:*** 0.6–0.8 ppm (broad peak, –CH_3, nBMA and P[nBMA]); 1.25–1.45 ppm (broad peak, –CH_2–, nBMA and P[nBMA]); 1.5–1.6 ppm (broad peak, –CH_2–, nBMA and P[nBMA]); 1.7–1.9 ppm (broad peak, –CH_3, P[nBMA]); 1.8 ppm (s, –CH_3, nBMA); 3.8–3.95 ppm (broad peak, –OCH_2R, P[nBMA]); 4.0 ppm (t, OCH_2R, nBMA); 5.4 ppm (t, CH_2=C–, cis, nBMA); 6.0 ppm (s, CH_2=C–, trans, nBMA)

EA: 67.13 % C, 9.68 % H, (23.20 % O_{calc})

ATR–FTIR: 3050–2800 cm^{-1} (=CH_2, –CH_2–, –CH_3); 1723 cm^{-1} (–C=O); 1466 cm^{-1} (–CH_2–, –CH_3); 1450 cm^{-1} (–CH_2–, –CH_3); 1381 cm^{-1}; 1323 cm^{-1}; 1304 cm^{-1}; 1269 cm^{-1}; 1240 cm^{-1} (nBu); 1143 cm^{-1} (–C–O–C–); 1063 cm^{-1} (nBu); 1020 cm^{-1}; 999 cm^{-1}; 965 cm^{-1} (nBu); 945 cm^{-1}; 881 cm^{-1}; 844 cm^{-1}; 748 cm^{-1}; 517 cm^{-1}; 490 cm^{-1}

SEC: dn/dc = 0.988 ml $\cdot$ g^{-1}; M_n = 25110 g $\cdot$ mol^{-1}; M_w = 26790 g $\cdot$ mol^{-1}; M_z = 30990 g $\cdot$ mol^{-1}

DSC: T_{onset} = 16.5 °C; T_{midpt} = 29.0 °C; T_g = 27.5 °C; T_{offset} = 38.0 °C; ΔC_p = 0.230 J $\cdot$ g^{-1} $\cdot$ K^{-1}

Experiment V11 (P[nBMA–co–tBMA], f_{BzMA} = 0.5, F_{BzMA} = 0.32):

^{1}***H–NMR:*** 0.6–0.8 ppm (broad peak, –CH_3, nBMA and P[nBMA]); 1.25–1.45 ppm (broad peak, –C(CH_3)$_3$, P[tBMA], –CH_2–, nBMA and P[nBMA]); 1.42 ppm (s, –C(CH_3)$_3$, tBMA);

1.5–1.6 ppm (broad peak, –CH_2–, nBMA and P[nBMA]); 1.7–1.9 ppm (broad peak, –CH_3, P[tBMA] and P[nBMA]); 1.9 ppm (s, –CH_3, tBMA); 1.8 ppm (s, –CH_3, nBMA); 3.8–3.95 ppm (broad peak, –OCH_2R, P[nBMA]); 4.0 ppm (t, OCH_2R, nBMA); 5.3 ppm (t, CH_2=C–, cis, tBMA); 5.4 ppm (t, CH_2=C–, cis, nBMA); 5.9 ppm (s, CH_2=C–, trans, tBMA); 6.0 ppm (s, CH_2=C–, trans, nBMA)

EA: 67.15 % C, 9.76 % H, (23.09 % O_{calc})

ATR–FTIR: 3050–2800 cm^{-1} (=CH_2, –CH_2–, –CH_3); 1720 cm^{-1} (–C=O); 1473 cm^{-1} (–CH_2–, –CH_3); 1456 cm^{-1} (–CH_2–, –CH_3); 1392 cm^{-1}; 1366 cm^{-1} (tBu); 1327 cm^{-1}; 1270 cm^{-1} (tBu); 1247 cm^{-1} (nBu); 1136 cm^{-1} (–C–O–C–); 1065 cm^{-1} (nBu); 1035 cm^{-1}; 1020 cm^{-1}; 1000 cm^{-1}; 967 cm^{-1} (nBu); 945 cm^{-1}; 876 cm^{-1} (tBu)

SEC: $dn/dc = 0.0799\,ml \cdot g^{-1}$; $M_n = 23510\,g \cdot mol^{-1}$; $M_w = 25390\,g \cdot mol^{-1}$; $M_z = 26700\,g \cdot mol^{-1}$

DSC: $T_{onset} = 55.5\,°C$; $T_{midpt} = 64.5\,°C$; $T_g = 63.0\,°C$; $T_{offset} = 72.0\,°C$; $\Delta C_p = 0.249\,J \cdot g^{-1} \cdot K^{-1}$

Experiment V12 – V17 (P[nBMA–co–tBMA]):

The ^1H– and IR–spectra of the compounds V12 to V17 exhibited the same signals, i. e. band positions as observed in the analogous copolymer V11. The integral intensities of important NMR signals are detailed in *Table 3.5* (cf. *Section 3.3*), the elemental analysis results are stated in *Table 3.7*. The band intensities of the ATR–FTIR–spectra are listed in *Table 3.9*. The SEC–data are summarized in *Table 3.11* and the DSC–data in *Table 3.14*.

3.2. Characterization

In this paragraph the different characterization methods are described together with the used analysis–software.

3.2.1. Nuclear Magnetic Resonance Spectroscopy

^{1}H–NMR measurements were carried out on a Bruker Avance III 500 MHz spectrometer with 32 scans in deuterated chloroform ($CDCl_3$), respectively DMSO–d_6, as solvent, using approx. 100 mg analyte $\cdot$ ml^{-1}. Data acquisition was controlled and data evaluation was performed with the "Bruker Topspin" software.

3.2.2. Elementary Analysis

The samples contents of carbon, hydrogen and nitrogen were analyzed by means of an elemental analyzer the vario MICRO Cube from Elementar. Each sample was measured three times, and for each measurement around 2.5 mg of analyte were used. An average–values was calculated from the results for each sample.

For the determination of the elements a sample was burned with oxygen to get the oxidation products CO_2, H_2O, N_2 and NO_x. The burning column was filled with quartz wool, WO_3–granule and corundum pellets. The nitrous gases were reduced to N_2 subsequently. The reduction column were filled with quartz wool, copper wool, corundum pellets and silver wool. The obtained gases were absorbed on an absorption column, were released one after another at the corresponding desorption temperatures and passed a thermal conductivity detector. From the integral values of the measured peaks, the exact weight of the sample, and with the respective calibration factor the absolute content of the elements in the sample was calculated. Data acquisition and evaluation was performed with the vario MICRO Software.

The amount of oxygen in the samples was calculated from the from the difference to 100 %.

3.2.3. Infra Red Spectroscopy

The ATR–FTIR–spectra were detected with a "Spectrum Two" FT–IR Spectrometer from Perkin Elmer with a resolution of 4 cm^{-1}. The samples were homogenized in an agate–mortar and then the amount of a micro spatula was pressed on the ATR–crystal. The measured spectral range was 4000 to 450 cm^{-1}. Data acquisition and evaluation was performed with the software "Spectrum" from Perkin Elmer.

3.2.4. Size Exclusion Chromatography

Size exclusion chromatography (SEC) was performed by gel permeation chromatography (GPC) with multi angle light scattering (MALS) and refractive index (RI) detection. A solution with $4\,\mathrm{mg \cdot ml^{-1}}$ of a sample in tetrahydrofuran was filtered over a $0.45\,\mu$m PTFE membrane and then was injected into the chromatography system by a Waters 2695 alliance auto–sampler with a flow rate of $1\,\mathrm{ml \cdot min^{-1}}$. The GPC columns were filled with a styrene-divinylbenzene copolymer network (SDV) with a particle size of $5\,\mu$m and three different nominal pore sizes of 1 000 Å, 100 000 Å and 1 000 000 Å. The MALS detector was a Wyatt Dawn Heleos II and the added RI detector for concentration determination was a Wyatt Optilab rex. Each online measurement lasted 45 min.

For the determination of the molar mass with SEC the refractive index increment (dn/dc) of the compound is needed. This value depends on the composition and the molar mass of the polymer chain and also on the measurement temperature, λ and the solvent. The required dn/dc values were measured with the Wyatt Optilab rex in batch operation mode. The used sample concentrations were $0.1\,\mathrm{mg \cdot ml^{-1}}$, $0.2\,\mathrm{mg \cdot ml^{-1}}$, $0.5\,\mathrm{mg \cdot ml^{-1}}$, $1.0\,\mathrm{mg \cdot ml^{-1}}$ and $2.0\,\mathrm{mg \cdot ml^{-1}}$. Data acquisition and evaluation of the online and batch measurements was performed with Waters Empower and Wyatt Astra V.

3.2.5. Differential Scanning Calorimetry

For the measurement of the thermal behavior of the polymers a Netzsch DSC 204 F1 dynamic differential calorimeter was used. The device was calibrated against Bi, Hg, In, Sn and Zn standards. Samples of approximately 10 mg were sealed in $25\,\mu$g aluminium pans, containing a small hole in their lids. The DSC-thermogram was measured in a temperature range from −80 °C to 150 °C, at a heating rate of $10\,\mathrm{°C \cdot min^{-1}}$. Data acquisition and evaluation was performed with the "Netzsch Proteus" software.

3.3. Results and Discussion

In following paragraph the results of the analyzes from the different statistical copolymers from *n*–butyl and *tert*–butyl methacrylate P[nBMA–co–tBMA] and also their discussion is given.

The ATRP–co–polymerizations of *n*–butyl and *tert*–butyl methacrylate P[nBMA–co–tBMA] were carried out in analogy to [63], using *para*–toluenesulfonyl chloride (pTSC) as the initiator, $Cu^{I}Cl$ as the catalyst and N,N,N',N',N"–pentamethyldiethylenetriamine (PMDETA) as the ligand. The initial ratio of the substances was $pTSC : CuCl : PMDETA : Mon = 1 : 1 : 1 : 175$. The reactions were carried out in 2–butanone (MEK) as solvent at 80 °C. The ratio of monomer to solvent was wt : wt 1 : 1 (cf. experimental part *Section 3.1.2*). Two series of copolymerization were performed. *Series A*, see *Table 3.1*, were preparative syntheses series with sampling for ^{1}H–NMR–analysis, and *Series B* (see *Table 3.2*), were preparative syntheses series with sampling for ^{1}H–NMR–, ATR–FTIR–, SEC– and DSC–analysis. The resulting copolymers were filtered over Al_2O_3 to remove the CuCl, subsequently precipitated in an ice–cooled mixture of water:methanol vol:vol 1:1, filtered over a P4 glass filter and dried at 45 °C under vacuum over night. This technique was called *"work–up A"*. The samples for ^{1}H–NMR were used without further purification. The other samples were precipitated also in an ice–cooled mixture of water and methanol with vol:vol 1:1, then the precipitated polymers were separated from the liquid phase by centrifugation and dried over night at 45 °C under vacuum. The polymers were re–dissolved in dichloromethane and transferred in a separation funnel. Water was added and the CuCl was extracted. The polymer–dichloromethane solution was clear and green. After the extraction the organic phase was clear and colorless and the water phase was clear and blue. The organic phase was separated and the solvent was removed by vacuum evaporation. This technique was called *"work–up B"*. The consistence of the resulting polymers varies with the amount of tBMA inside the polymer. Experiments V14, V16 and V18 resulted in fine white powders. The resulting polymer of V11, V12, V13 and V15 were also white powders but not so fine as the three polymers before. The experiments V17 and V19 resulted in white amorphous substances.

3.3.1. Kinetic Studies

In a first series of copolymerization experiments (*Series A*) preparative batch synthesis were performed to measure the rate of copolymerization as well as the resulting copolymer compositions. Aliquot samples were taken after 0, 15, 30, 45, 60, 90, 120, 150 and 180 min and analyzed by means of ^{1}H–NMR–spectroscopy. The ^{1}H–NMR–spectra were evaluated regarding the conversion p of the monomers which was the basis for the calculation of the reaction rates. The signals in the resulting spectra were assigned to the structure elements of the monomers and the copolymer as shown in *Table 3.4*. The position of the peaks were largely taken from literature [63], and for the cis– and trans–conformation calculated by [85].

Tab. 3.4.: Position and assignments of the signals in the obtained ^{1}H–NMR–spectra of P[nBMA–co–tBMA] polymers

δ [ppm]	Multiplicity	No. of carbons	Carbon No.*	Structure element
0.6–0.8	broad peak	3H	9,9'	–CH_3, nBMA and P[nBMA] side chain
1.25–1.45	broad peak	9H	3'	–$C(CH_3)_3$, P[tBMA]
		2H	7,7'	–CH_2–, nBMA and P[nBMA] side chain
1.42	s	9H	3	–$C(CH_3)_3$, tBMA
1.5–1.6	broad peak	2H	8,8'	–CH_2–, nBMA and P[nBMA] side chain
1.7–1.9	broad peak	6H	10',11'	–CH_3 backbone, P[nBMA] and P[tBMA]
1.8	s	3H	10	–CH_3, tBMA
1.9	s	3H	11	–CH_3, nBMA
3.8–3.95	broad peak	2H	6'	–OCH_2R, P[nBMA]
4.0	t	2H	6	–OCH_2R, nBMA
5.3	t	1H	2	CH_2=C–, cis, tBMA
5.4	t	1H	5	CH_2=C–, cis, nBMA
5.9	s	1H	1	CH_2=C–, trans, tBMA
6.0	s	1H	4	CH_2=C–, trans, nBMA

* cf. *Figure 3.2*

The structures of the monomers and the copolymer are depicted in *Figure 3.2* together with the numbering of the carbon–atoms for the assignment of the peaks in the ^{1}H–NMR–spectra. *Figure 3.3* shows the ^{1}H–NMR–spectrum of experiment V11, taken after 180 min, as an example for the obtained spectra, in comparison to the ^{1}H–NMR–spectra of the two monomers. In this figure the signals are assigned to the corresponding carbon–atoms of the monomers and the polymer chain.

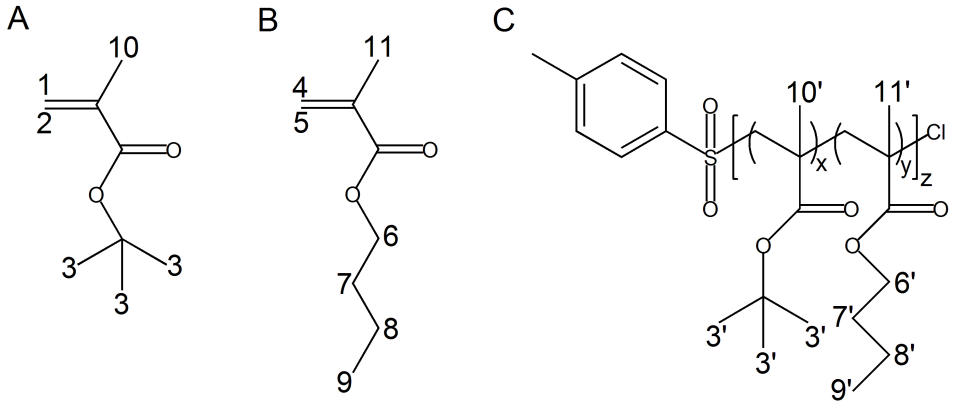

Fig. 3.2.: Molecular structures of the monomers (A) tBMA and (B) nBMA and (C) the resulting copolymer of *Series A* and *Series B* with carbon–atom labels (z = x + y = 1)

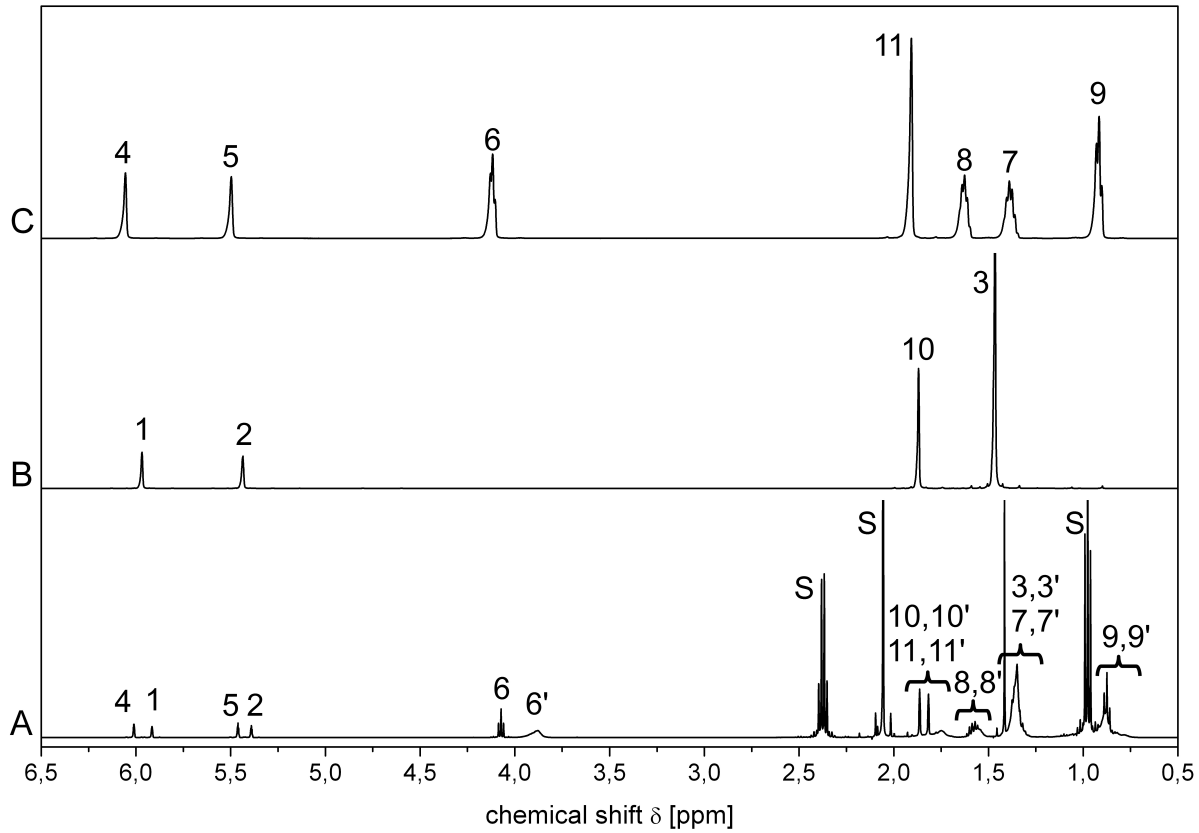

Fig. 3.3.: ^{1}H–NMR–spectra of (A) reaction mixture V11 ($f_{nBMA} = 0.5$) after 180 min reaction time (nBMA:tBMA = 1:1, I:M = 1:175, T = 80 °C), (B) tBMA and (C) nBMA (S = solvent signals: MEK)

Within the subsequent text the numbers of the appropriate carbons from the chemical structure, that is shown in *Figure 3.3*, are given in the brackets. The nBMA–monomer showed a singlet signal at 6.0 ppm and a triplet at 5.4 ppm originating from the vinyl–group (4 and 5) and a singlet at 1.8 ppm caused by the methyl–group (11) of the methacrylate part. The *n*–butyl chain exhibited signals of the α–proton (6) at 4.0 ppm, the β–proton (7) at 1.3 to 1.45 ppm, the γ–proton (8) at 1.5 to 1.6 ppm and the δ–proton (9) at 0.6 to 0.8 ppm. The nBMA–ester chain of the polymer is represented in the spectra with broad peaks at around 3.8 to 3.95 ppm of the α–proton (6'), 1.5 to 1.6 ppm from the γ–proton (8'), 1.3 to 1.45 ppm caused by the β–proton (7') and 0.6 to 0.8 ppm originating from the δ–proton (9'). Hence the monomer– and polymer–peaks of the β–, γ– and δ–protons appear in the same chemical shift region and become mutually overlapped. The methacrylate–part of the tBMA monomer shows a singlet at 5.9 ppm, a triplet at 5.3 ppm and a singlet at 1.9 ppm (1, 2, 10) and the *tert*–butyl group gives raise to a sharp singlet at 1.42 ppm (3). The broad signal between circa 1.25 to 1.45 ppm is caused by the *tert*–butyl group of PtBMA (3'). The CH_2–signals of the polymer–backbone (10', 11') are present in form of a broad peak ranging from 1.7 to 1.9 ppm. The signals at circa 2.4 ppm (quartet), 2.1 ppm (singlet) and 1.0 ppm (triplet) ppm belong to MEK.

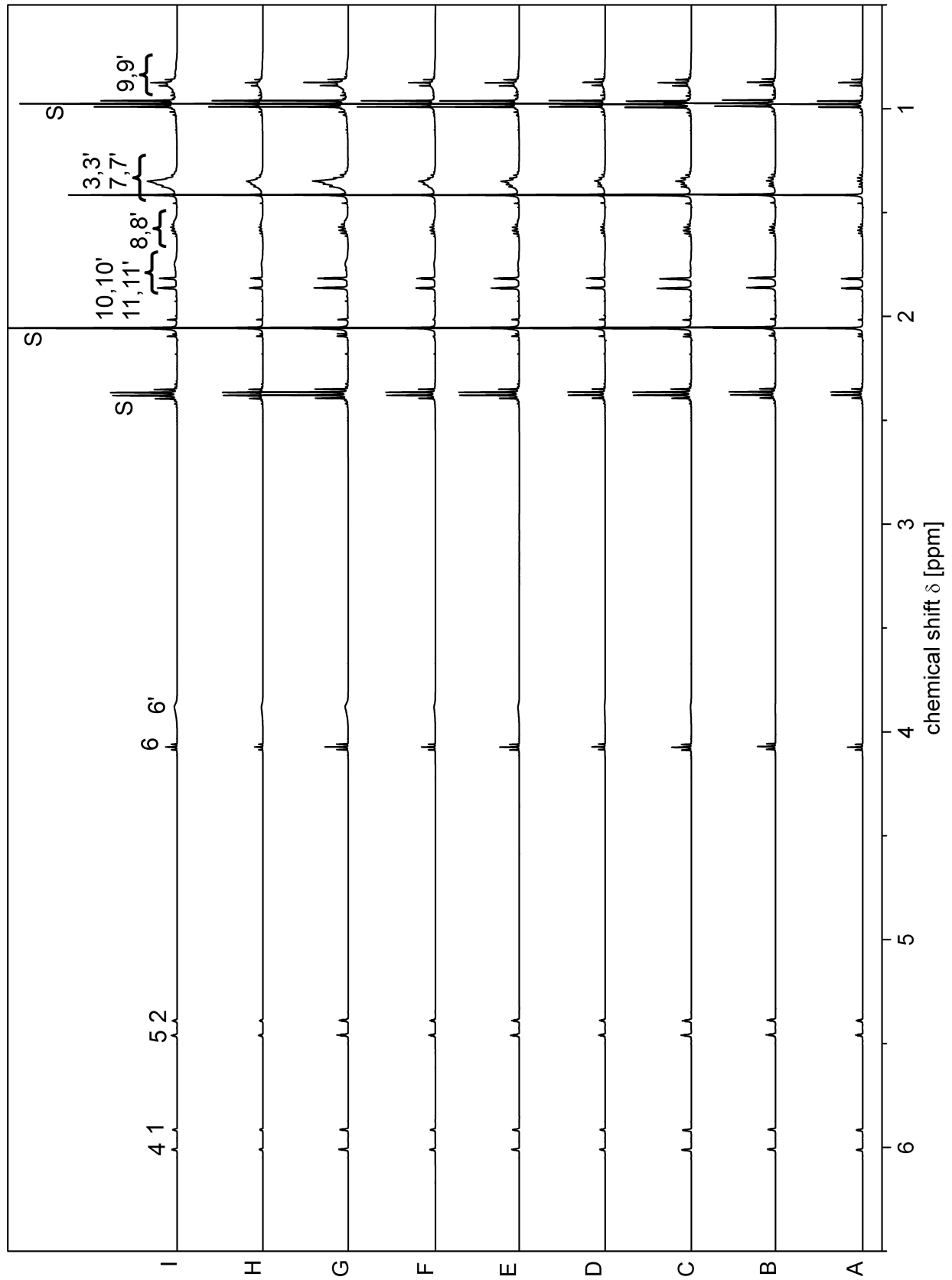

Fig. 3.4.: ^{1}H–NMR–spectra of samples, taken from the copolymerization mixture V11 (f_{nBMA} = 0.5), at different polymerization times; A – 0 min, B – 15 min, C – 30 min, D – 45 min, E – 60 min, F – 90 min, G – 120 min, H – 150 min and I – 180 min

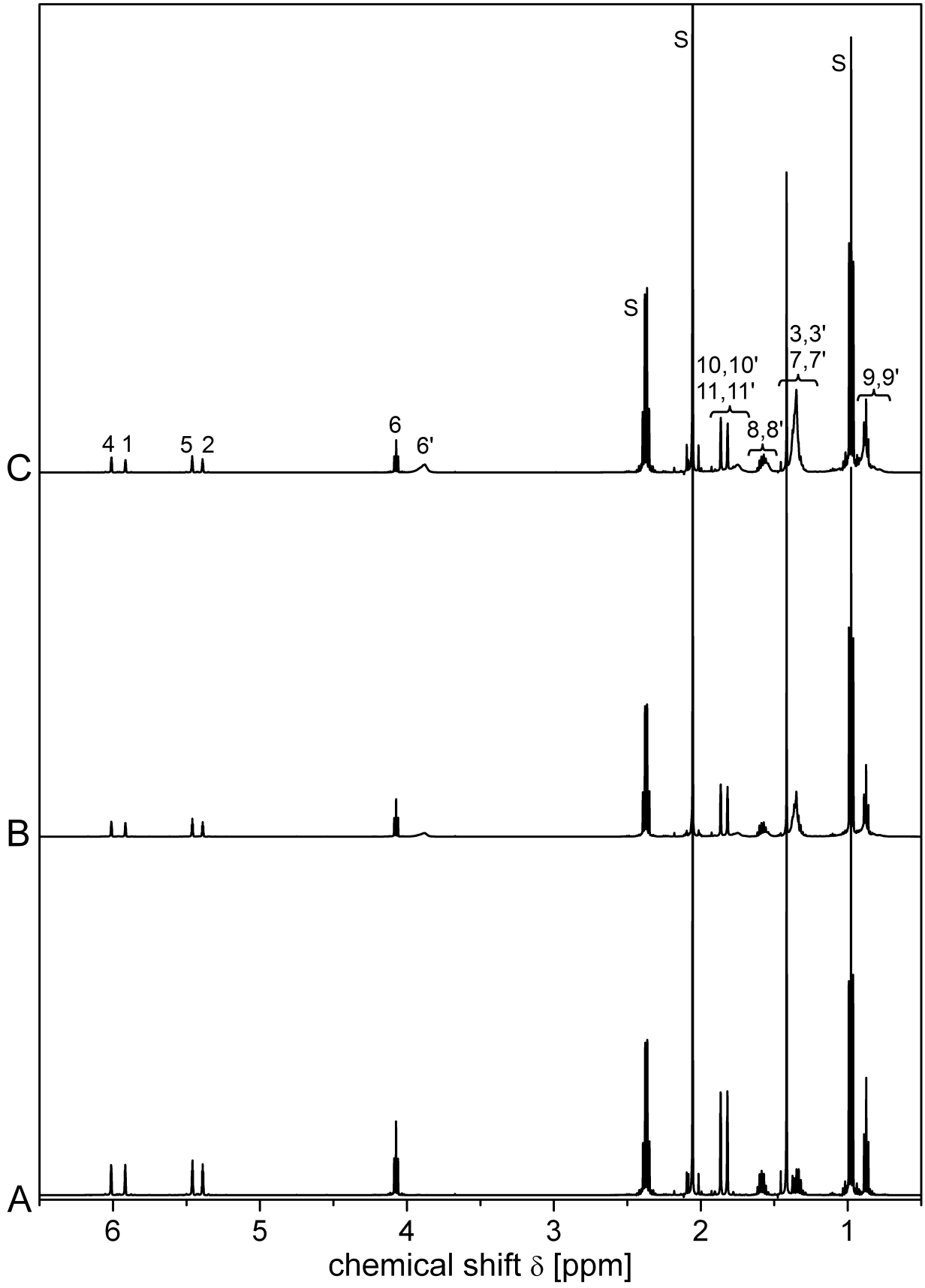

Fig. 3.5.: ^{1}H–NMR–spectra of samples, taken from the copolymerization mixture V11 (f_{nBMA} = 0.5), at A – 0 min, B – 90 min and C – 180 min

The changes of the ^{1}H-NMR-spectra during the polymerization are shown in *Figure 3.4* and in *Figure 3.5*. In *Figure 3.5* only the spectra of three samples, taken at 0, 90 and 180 min, were depicted to point out the differences more in detail. The intensities of the different monomer–signals decrease in relation to the solvent peaks which remain constant during the polymerization. The signal 6' of the α–proton of PnBMA appears and increases over time as a very broad peak around 3.8 ppm. The signals 7 and 7' from nBMA and PnBMA (β–proton) overlap just as 8 and 8' (γ–proton) and 9 and 9' (δ–proton). One can see an increase of the three peaks. Especially for the broad peak around 1.3 to 1.45 ppm this is very obvious, because there is also the signal for the PtBMA – *tert*–butyl group – which rises. In the region between 1.7 to 1.9 ppm the CH_2–signal of the polymer–backbone (10', 11') gets up in comparison with the solvent–signals directly next to the corresponding monomer peaks (10, 11) and they overlap.

The peak areas of the signals 1, 2, 3, 3', 6, 6', 7, 7', 8 and 8' were measured (see *Table 3.5*) and the molar ratios of monomers to polymer were calculated by means of *Equations 3.3.1 to 3.3.5*, taken from the PhD thesis of *C. Schmitz* [63]. To determine of the conversion of nBMA p_{nBMA} the integrals of the *n*–butyl chains α–protons (6, 6') of the monomer (A_6) and the polymer ($A_{6'}$) respectively were set into a ratio (cf. *Equation 3.3.1*).

$$p_{nBMA} = \frac{A_{6'}}{A_6 + A_{6'}} \tag{3.3.1}$$

with A_6 = integral intensity at 4.0 to 4.1 ppm; $A_{6'}$ = integral intensity at 3.8 to 3.95 ppm

For *tert*–butyl methacrylate the signals of the CH_3–groups of the *tert*–butyl group of the monomer (A_3) and the polymer ($A_{3'}$) were taken (cf. *Equation 3.3.5*) to calculate the conversion of the monomer p_{tBMA}. But these signals partially overlap, perturbing each other, as well with the signals of the β–protons of the *n*–butyl chain do (A_7, $A_{7'}$). These integrals had to be subtracted from the mixed signal, here labeled as A_x (cf. *Equation 3.3.2*). For this purpose A_3 was replaced by 3/2 A_1, with A_1 representing the signal intensity of the monomers vinylic CH_2=–protons (cf. signals 1 and 2 in *Figure 3.5*) of the tBMA monomer. The signal intensity of the β–methylene group of the *n*–butyl methacrylate, A_7 and $A_{7'}$, equals that of the γ–CH_2 group, A_8 and $A_{8'}$, of the same monomer. Since the latter signal forms an isolated and well integratable signal between 1.5 to 1.6 ppm. The relation of the β– and the γ–proton signals were determined for t = 0 min. The result is the value *y* (see *Equation 3.3.3*). The signal intensity of the γ–proton, multiplied by *y* was subtracted from the mixed signal A_x.

The subtraction result A_{tBMA} was used to calculate the conversion of tBMA by means of *Equation 3.3.5.*

$$A_{tBMA} = \frac{A_x - y \cdot A_8}{z} - A_1 \tag{3.3.2}$$

$$y = \frac{A_{7,0}}{A_{8,0}} \tag{3.3.3}$$

$$z = \frac{A_{x,0} - A_{7,0}}{A_{1,0}} \tag{3.3.4}$$

$$p_{tBMA} = \frac{A_{tBMA}}{A_1 + A_{tBMA}} \tag{3.3.5}$$

with A_x = integral intensity at 1.25 to 1.45 ppm from different parts of the monomers and the polymer; $A_{x,0}$ = integral intensity at 1.35 to 1.45 ppm at t = 0 min; A_1 = integral intensity at 5.9 to 5.95 ppm; $A_{1,0}$ = integral intensity at 5.9 to 5.95 ppm at t = 0 min; A_8 = integral intensity at 1.5 to 1.6 ppm; $A_{8,0}$ = integral intensity at 1.5 to 1.6 ppm at t = 0 min; $A_{7,0}$ = integral intensity at 1.3 to 1.38 ppm at t = 0 min; A_{tBMA} = integral intensity at 1.25 to 1.45 ppm only from the *tert*–butyl group of the polymer; y = signal intensity ratios of β– and γ– protons of the *n*–butyl chain at t = 0 min; z = signal intensity ratio of the *tert*–butyl group to the monomers vinylic CH_2=–protons at t = 0 min

The values of the integrals that were needed for the calculations of the conversions as well as the results of the *Equations 3.3.1* and *3.3.5* and the total conversions of the ^{1}H–NMR–samples taken from the experiments of *Series A* are listed in *Table 3.5.*

Figure 3.6a depicts a representative time conversion curve as obtained with reaction V11 (*Table 3.1,* $f_{nBMA} = 0.5$). The conversion of both monomers increased steadily, however, the initial slope of the curves was larger than that of the later stages of the reaction. Note that both monomers were consumed with similar rate in the present example. In the absence of side reactions the reaction kinetic of an ATRP homopolymerization is of pseudo–first–order. [16] As long as the monomer composition of the reaction mixture is not altered during the course of a copolymerization this kinetic law should be valid, too.

Tab. 3.5.: Values of integrated ^{1}H–NMR signals and calculated conversions of *Series A*

Entry	time	Integral							conversion p		
f_{nBMA}	[min]	A1	A6	A6'	A8,8'	A_x	A_7	A_{tBMA}	BzMA	tBMA	total
V11	0	0.9614	1.9603	0.0000	2.3145	12.1823	2.7980	0.0000	0.0000	0.0000	0.0000
0.50	15	0.9401	1.9814	0.3337	2.6763	13.8661		0.1490	0.1368	0.1441	0.1405
	30	0.9287	1.9958	0.7094	2.3018	16.1957		0.4454	0.3242	0.2622	0.2932
	45	0.9092	1.9993	1.1215	3.5670	18.2433		0.5180	0.3630	0.3594	0.3612
	60	0.9179	2.0127	1.4430	3.8872	20.3477		0.6853	0.4274	0.4176	0.4225
	90	0.8968	1.9895	2.0506	4.5088	23.6085		0.9634	0.5179	0.5076	0.5127
	120	0.8887	2.0298	2.8266	5.4700	27.8109		1.2830	0.5908	0.5820	0.5864
	150	0.8606	2.0141	3.4344	5.9811	31.7980		1.6563	0.6581	0.6303	0.6442
	180	0.8562	2.0290	4.2754	7.0193	36.2377		1.9869	0.6989	0.6782	0.6885
V12	0	1.9413	1.9910	0.0000	2.4045	21.9696	3.0627	0.0000	0.0000	0.0000	0.0000
0.33	15	1.9163	1.9738	0.0897	2.4109	23.0358		0.1337	0.0652	0.0435	0.0580
	30	1.8981	1.9719	0.3026	2.6547	25.0173		0.3234	0.1456	0.1330	0.1414
	45	1.9070	2.0010	0.5803	3.0088	27.5974		0.5331	0.2185	0.2248	0.2206
	60	1.8951	1.9994	0.7899	3.2710	30.0176		0.7592	0.2860	0.2832	0.2851
	90	1.8686	2.0100	1.2650	3.9086	34.4535		1.1578	0.3826	0.3863	0.3838
	120	1.8419	2.0099	1.7578	4.5355	39.6678		1.6379	0.4707	0.4665	0.4693
	150	1.8205	2.0127	2.3121	5.1293	45.4791		2.1783	0.5447	0.5346	0.5414
	180	1.7840	2.0127	2.8796	5.8751	51.1888		2.7036	0.6025	0.5886	0.5979
V13	0	0.4860	2.0027	0.0000	2.2451	6.9899	2.3092	0.0000	0.0000	0.0000	0.0000
0.66	15	0.4676	1.9884	0.4530	2.6053	8.3513		0.0492	0.0951	0.1855	0.1548

Continuation on next page ...

Entry	time	Integral							conversion p		
f_{nBMA}	[min]	A1	A6	A6'	A8,8'	A_x	A_7	A_{tBMA}	BzMA	tBMA	total
	30	0.4556	2.0090	0.8606	3.0886	9.9814		0.1653	0.2663	0.2999	0.2885
	45	0.4584	1.9957	1.2826	3.4953	11.1668		0.2311	0.3351	0.3912	0.3722
	60	0.4478	1.9910	1.5832	3.7640	12.3329		0.3263	0.4215	0.4430	0.4357
	90	0.4479	2.0107	2.3088	4.6635	14.5626		0.4375	0.4941	0.5345	0.5208
	120	0.4370	1.9888	2.7597	4.9585	16.4766		0.6063	0.5811	0.5812	0.5812
	150	0.4368	2.0023	2.9938	5.3032	17.0460		0.6199	0.5866	0.5992	0.5949
	180	0.4334	2.0047	3.4443	5.8032	18.6352		0.7211	0.6246	0.6321	0.6295
V14	0	2.8587	2.0044	0.0000	2.2469	29.7631	2.5556	0.0000	0.0000	0.0000	0.0000
0.25	15	2.8845	2.0018	0.0069	2.2607	30.3668		0.0360	0.0123	0.0034	0.0101
	30	2.8638	1.9930	0.0525	2.3114	31.1212		0.1299	0.0434	0.0257	0.0390
	45	2.9018	2.0284	0.1372	2.5988	31.0675		0.0519	0.0176	0.0634	0.0290
	60	2.8535	2.0183	0.2645	2.6704	33.7548		0.3740	0.1159	0.1159	0.1159
	90	2.7521	1.9970	1.0802	3.5579	45.1544		1.5671	0.3628	0.3510	0.3599
	120	2.6267	1.9978	2.1345	4.7879	60.9455		3.2047	0.5496	0.5165	0.5413
	150	2.5460	1.9636	3.4786	6.2730	83.4249		5.4698	0.6824	0.6392	0.6716
	180	2.4655	1.9705	5.2595	7.6173	109.3715		8.1159	0.7670	0.7275	0.7571
V15	0	0.3237	2.0096	0.0000	2.0777	5.1651	2.1218	0.0000	0.0000	0.0000	0.0000
0.75	15	0.3114	2.0081	0.3150	2.4287	6.1090		0.0746	0.1932	0.1356	0.1500
	30	0.3060	2.0354	0.8440	2.9864	7.3940		0.1561	0.3378	0.2931	0.3043
	45	0.3060	2.0130	1.3195	3.4411	8.5940		0.2343	0.4337	0.3959	0.4054
	60	0.3041	2.0202	1.7360	3.9589	9.7396		0.3018	0.4981	0.4622	0.4712

Continuation on next page ...

Entry	time	Integral							conversion p		
f_{nBMA}	[min]	A1	A6	A6'	A8,8'	A_x	A_7	A_{tBMA}	BzMA	tBMA	total
	90	0.2959	2.0242	2.5475	4.7501	11.9857		0.4630	0.6101	0.5572	0.5704
	120	0.2897	2.0208	3.3382	5.5661	14.0473		0.5999	0.6743	0.6229	0.6358
	150	0.2892	2.0347	4.2456	6.5112	16.4046		0.7484	0.7213	0.6760	0.6873
	180	0.2820	2.0404	5.2009	7.5726	18.9665		0.9128	0.7640	0.7182	0.7297
V16	0	3.8767	2.0049	0.0000	2.3822	38.8312	2.3788	0.0000	0.0000	0.0000	0.0000
0.20	15	3.8650	2.0153	0.1770	2.6243	42.9300		0.4219	0.0984	0.0807	0.0949
	30	3.7966	2.0033	0.5179	2.9323	49.5963		1.1666	0.2350	0.2054	0.2291
	45	3.8039	2.0147	0.7534	3.1586	58.2782		2.0586	0.3511	0.2722	0.3353
	60	3.7719	2.0610	1.2031	4.0691	63.6674		2.5670	0.4050	0.3686	0.3977
	90	3.6259	2.0218	1.8178	4.6417	74.5945		3.8143	0.5127	0.4734	0.5048
	120	3.6050	2.0381	2.4701	5.3132	87.6047		5.1475	0.5881	0.5479	0.5801
	150	3.5386	2.0319	3.0874	6.2831	98.8949		6.3116	0.6408	0.6031	0.6332
	180	3.4761	2.0147	3.7342	6.6630	111.4444		7.6684	0.6881	0.6496	0.6804
V17	0	0.2363	2.0116	0.0000	2.1018	4.3832	2.0962	0.0000	0.0000	0.0000	0.0000
0.80	15	0.2382	2.0233	0.3128	2.4245	5.1084		0.0398	0.1431	0.1339	0.1357
	30	0.2325	2.0154	0.7379	2.8615	6.0371		0.0964	0.2931	0.2680	0.2730
	45	0.2314	2.0173	1.1433	3.3319	6.9517		0.1435	0.3828	0.3617	0.3660
	60	0.2266	2.0195	1.5280	3.7320	7.8521		0.2001	0.4690	0.4307	0.4384
	90	0.2211	2.0310	2.3653	4.5971	9.7265		0.3102	0.5838	0.5380	0.5472
	120	0.2199	2.0344	3.2524	5.4792	11.7290		0.4274	0.6603	0.6152	0.6242
	150	0.2109	2.0403	4.1881	6.4989	13.8780		0.5533	0.7240	0.6724	0.6827

Continuation on next page ...

Entry	time	Integral							conversion p		
f_{nBMA}	[min]	A1	A6	A6'	A8,8'	A_x	A_7	A_{tBMA}	BzMA	tBMA	total
	180	0.2077	2.0331	5.0599	7.3760	15.9194		0.6771	0.7653	0.7134	0.7237
V18	0	1.0000	–	–	–	10.5056		0.0000	0.0000		0.0000
0.00	15	1.0000	–	–	–	11.2915		0.2310	0.1876		0.1876
	30	1.0000	–	–	–	14.5431		1.8461	0.6486		0.6486
	45	1.0000	–	–	–	15.5065		2.3364	0.7003		0.7003
	60	1.0000	–	–	–	17.5861		3.4418	0.7749		0.7749
	90	1.0000	–	–	–	22.2706		5.6720	0.8501		0.8501
	120	1.0000	–	–	–	24.3656		6.8268	0.8722		0.8722
	150	1.0000	–	–	–	28.3900		8.8411	0.8984		0.8984
	180	1.0000	–	–	–	32.6596		10.9706	0.9165		0.9165
V19	0	–	2.0252	0.0000	2.0556	2.0526		--		0.0000	0.0000
1.00	15	–	2.0229	0.2987	2.3766	2.3765		--		0.1287	0.1287
	30	–	2.0339	0.8210	2.9333	2.9805		--		0.2876	0.2876
	45	–	2.0334	1.2871	3.4118	3.5032		--		0.3876	0.3876
	60	–	2.0332	1.6922	3.8416	3.9693		--		0.4542	0.4542
	90	–	2.0394	2.7158	4.9173	5.0735		--		0.5711	0.5711
	120	–	2.0411	3.4060	5.6364	5.8696		--		0.6253	0.6253
	150	–	2.0446	4.3964	6.6391	6.9221		--		0.6826	0.6826
	180	–	2.0622	5.5151	7.7963	8.1689		--		0.7278	0.7278

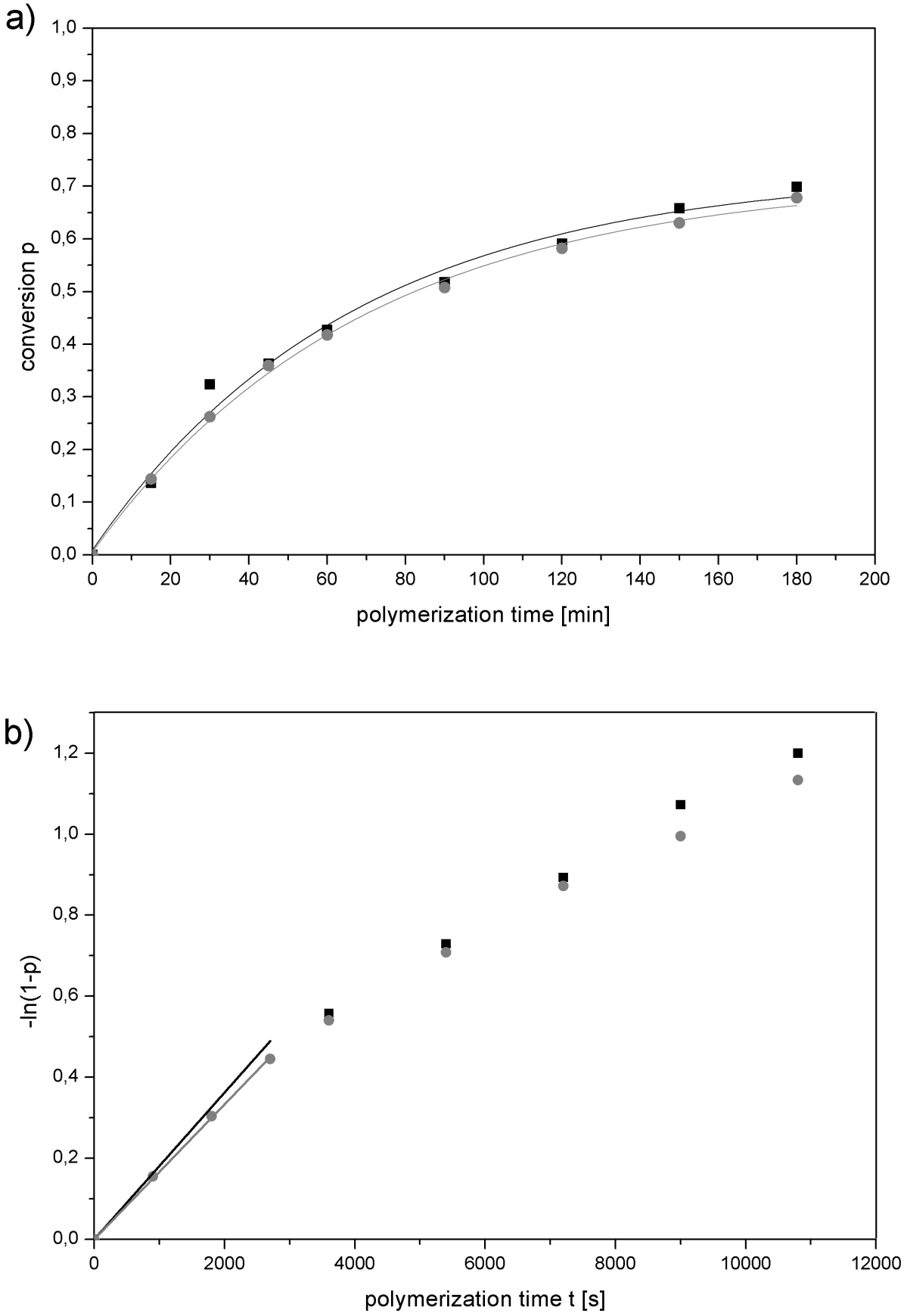

Fig. 3.6.: Monomer conversion and first order kinetic plot based on the ^{1}H–NMR–evaluation of experiment V11 (f_{nBMA} = 0.5); a) conversion p versus time [min]; b) first order kinetic parameters versus time [s]; ■ tBMA, ● nBMA

Note that the effective rate constant k may depend on the monomer composition.

$$\frac{d[M]}{dt} = -k_{eff} \cdot [M] \qquad \text{with } [M] = [M]_1 + [M]_2 \tag{3.3.6}$$

with [M] = total monomer concentration, $[M]_i$ = concentration of monomer i, k_{eff} = effective rate constant of copolymerization

At least the low conversion, initial stages of a copolymerization reaction can be described by *Equation 3.3.6*. Hence, a first order kinetic plot of $(-\ln(1-p))$ can be set up. The calculated conversions of the samples were inserted into *Equation 3.3.6* and the results were also plotted in *Figure 3.6b*. The rate constants of the monomers (k_{nBMA} and k_{tBMA}) were determined from the slope of a regression line in the range of small conversions of the kinetic plots. The first four data points (up to a reaction time of 45 min) of all members of *Series A* were used and became located on straight lines (cf. *Figure 3.6*) up to conversion of about 35 %. The continuity during all the polymerizations and over all the monomer compositions was a signal for the very well control over the reaction by ATRP. Note that the time–unit was changed from minutes to seconds, because in the literature rate constants are given in s^{-1} by default. The resulting kinetic plot with the two regression lines for experiment V11 is given in *Figure 3.6b* exemplarily.

The rate constants $k_{nBMA}(f_{nBMA})$ and $k_{tBMA}(f_{nBMA})$ as obtained from the experiments using the monomer ratios f_{nBMA} = 0, 0.2, 0.25, 0.33, 0.5, 0.66, 0.75, 0.8 and 1 were plotted against the monomer molar fraction of nBMA and a regression line was calculated for the data points (see *Figure 3.7*). In a binary ATRP–copolymerization the consumption of each monomer obeys a pseudo first order–reaction kinetics, as long as the monomer–mixture composition does not change. Hence, one can describe the initial stages of the copolymerization by means of *Equation 3.3.7 and 3.3.8*.

$$-\ln(1-p_{nBMA}) = k_{nBMA}(f_{nBMA}) \cdot t \tag{3.3.7}$$

$$-\ln(1-p_{tBMA}) = k_{tBMA}(f_{nBMA}) \cdot t \tag{3.3.8}$$

In these equations $k_i(f_{nBMA})$ represent the composition–dependent rate constants of the monomers. *Figure 3.6b* depicts the respective kinetic plot obtained from the data of experiment V11. An analogous analysis was performed with all obtained time conversion data of reactions V12 to 19. The measured individual rate constants $k_i(f_i)$ are summarized in *Table 3.6*. *Figure 3.7* depicts a plot of the individual monomer rate constant $k_i(f_{nBMA})$ (i = nBMA, tBMA) versus the initial molar fraction of nBMA in the monomer mixture, f_{nBMA}. tBMA ($k_{tBMA} = 9.45 \cdot 10^{-5}\,s^{-1}$) polymerized about half as fast as nBMA ($k_{nBMA} = 22.2 \cdot 10^{-5}\,s^{-1}$). The measured effective rate constants of the copolymerizations lay within this range. Between f_{nBMA} = 0.2 and 0.8 the values were of similar level ($1.2 \ldots 2.0 \cdot 10^{-4}$) and close to

$k_{nBMA}(f_{nBMA} = 1)$; i. e. the constant of the homopolymerization of nBMA. In the interval $f_{nBMA} \in [0.2, 0.8]$ the rate constants were approximated by straight lines, their low slopes ($m_t = \frac{dk_{tBMA}}{df_{tBMA}} = 8.97 \cdot 10^{-5} \pm 6.58 \cdot 10^{-5}$, $m_n = \frac{dk_{nBMA}}{df_{nBMA}} = 10.6 \cdot 10^{-5} \pm 5.36 \cdot 10^{-5}$) indicating a very weak dependence of the copolymerization rate on the monomer mixture composition.

Tab. 3.6.: Kinetic rate constants and copolymer compositions of the different copolymer compositions of *Series A* (ATRP, I:M = 1:175, T = 80 °C)

Entry	f_{nBMA}	k_{nBMA} $[s^{-1}]$	$k_{eff\,nBMA}$ $^{(a)}$ $[s^{-1}]$	k_{tBMA} $[s^{-1}]$	$k_{eff\,tBMA}$ $^{(b)}$ $[s^{-1}]$	k_{eff} $[s^{-1}]$	F_{nBMA}
V18	0.00	–	$1.17 \cdot 10^{-4}$	$4.40 \cdot 10^{-4}$	$1.30 \cdot 10^{-4}$	$1.38 \cdot 10^{-4}$	0.00
V16	0.20	$1.21 \cdot 10^{-4}$	$1.32 \cdot 10^{-4}$	$1.54 \cdot 10^{-4}$	$1.53 \cdot 10^{-4}$	$1.48 \cdot 10^{-4}$	0.10
V14	0.25	$1.66 \cdot 10^{-4}$	$1.35 \cdot 10^{-4}$	$1.82 \cdot 10^{-4}$	$1.56 \cdot 10^{-4}$	$1.51 \cdot 10^{-4}$	0.14
V12	0.33	$8.98 \cdot 10^{-5}$	$1.41 \cdot 10^{-4}$	$9.14 \cdot 10^{-5}$	$1.62 \cdot 10^{-4}$	$1.55 \cdot 10^{-4}$	0.20
V11	0.50	$1.66 \cdot 10^{-4}$	$1.53 \cdot 10^{-4}$	$1.81 \cdot 10^{-4}$	$1.74 \cdot 10^{-4}$	$1.64 \cdot 10^{-4}$	0.32
V13	0.66	$2.04 \cdot 10^{-4}$	$1.65 \cdot 10^{-4}$	$1.59 \cdot 10^{-4}$	$1.85 \cdot 10^{-4}$	$1.72 \cdot 10^{-4}$	0.52
V15	0.75	$1.87 \cdot 10^{-4}$	$1.72 \cdot 10^{-4}$	$2.13 \cdot 10^{-4}$	$1.91 \cdot 10^{-4}$	$1.77 \cdot 10^{-4}$	0.57
V17	0.80	$1.67 \cdot 10^{-4}$	$1.75 \cdot 10^{-4}$	$1.82 \cdot 10^{-4}$	$1.95 \cdot 10^{-4}$	$1.79 \cdot 10^{-4}$	0.66
V19	1.00	$1.74 \cdot 10^{-4}$	$1.90 \cdot 10^{-4}$	–	$2.09 \cdot 10^{-4}$	$1.90 \cdot 10^{-4}$	1.00

(a) calculated from *Equation 3.3.11*; (b) calculated from *Equation 3.3.12*

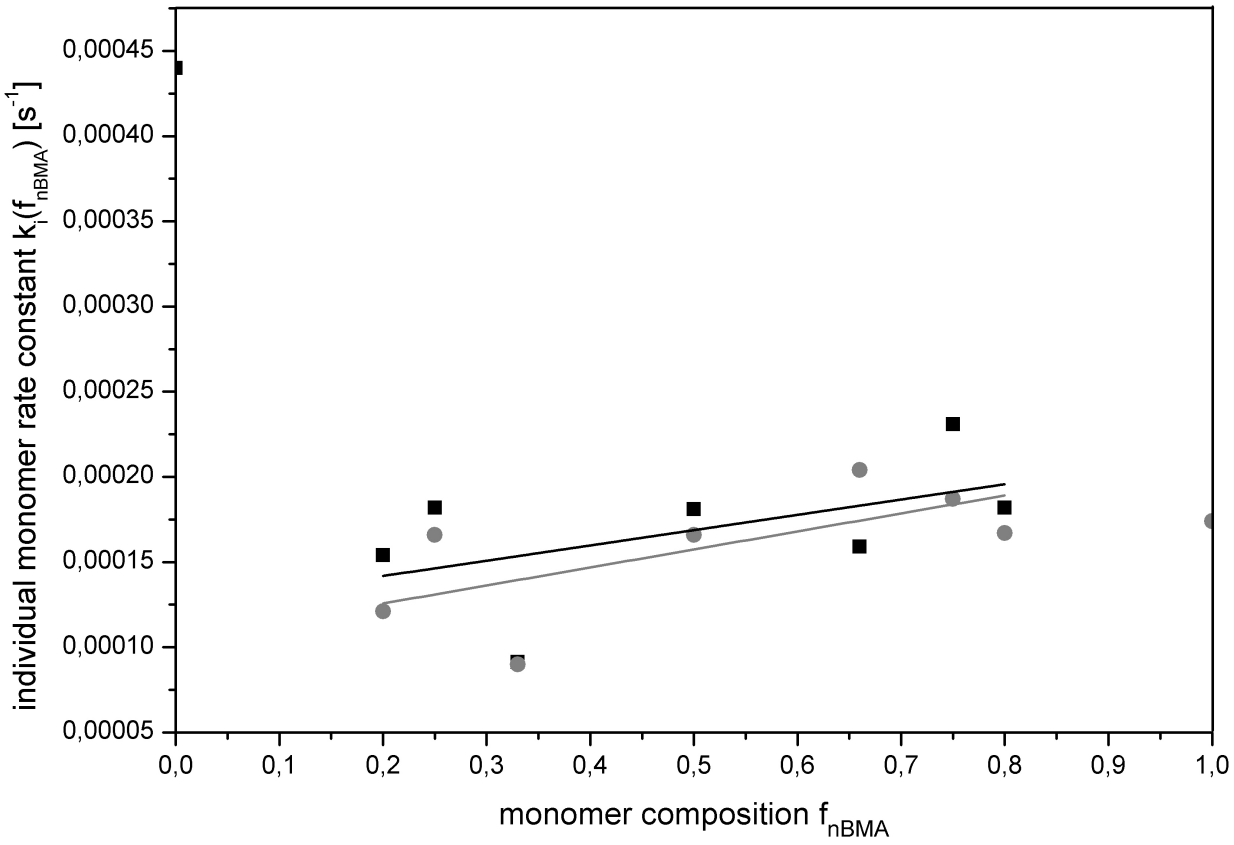

Fig. 3.7.: Plot of the individual monomer rate constants k_{nBMA} and k_{tBMA} versus the nBMA–content of the monomer feed ratio; ■ tBMA, ● nBMA

Both fitted lines are shown in *Figure 3.8* without the measured data. The rate constant of the homopolymerizations of tBMA was almost twice as fast as the nBMA/tBMA mixtures. It hence seems that even small quantities of nBMA substantially perturb the polymerization of tBMA.

If both monomers are consumed according to a first–order kinetics, the sum of both monomer concentrations $[M] = [M_{nBMA}] + [M_{tBMA}]$ must follow the same law. Hence, the total rate of copolymerization will follow *Equation 3.3.6*, with k_{eff} representing the monomer mixture dependence effective rate constant. It can be shown that k_{eff} is related to the monomer composition f_{nBMA} and the individual rate constant according to *Equation 3.3.13*.

With the equations of the regression lines from the rate constants and the monomer composition of the different feed ratios the effective rate constants of the monomers ($k_{eff,nBMA}$ and $k_{eff,tBMA}$) were calculated, see *Equations 3.3.9 and 3.3.10*.

$$k_{eff,nBMA} = a_{k_{nBMA}} + b_{k_{nBMA}} \cdot f_{nBMA} \tag{3.3.9}$$

$$k_{eff,tBMA} = a_{k_{tBMA}} + b_{k_{tBMA}} \cdot f_{tBMA} \tag{3.3.10}$$

The fit of *Equations 3.3.9* and *3.3.10* to the experimental data of *Table 3.6* gave the resulted in *Equations 3.3.11* and *3.3.12*.

$$k_{eff,nBMA} = (1.17 \cdot 10^{-4})\,s^{-1} + (7.29 \cdot 10^{-5})\,s^{-1} \cdot f_{nBMA} \tag{3.3.11}$$

$$k_{eff,tBMA} = (1.38 \cdot 10^{-4})\,s^{-1} + (7.06 \cdot 10^{-5})\,s^{-1} \cdot f_{nBMA} \tag{3.3.12}$$

The data points here lied on straight lines for both monomers (*Figure 3.8*). The values of the effective rate constants were used to determine the copolymerizations total effective rate constant (k_{eff}) with *Equation 3.3.13*.

$$k_{eff} = f_1 \cdot k_1 + f_2 \cdot k_2 \tag{3.3.13}$$

The total rate constant was expressed either in terms of the molar fraction of nBMA in the reaction mixture (f_{nBMA}, cf. *Equation 3.3.14*) or in dependence of f_{tBMA} (cf. *Equation 3.3.15*).

$$k_{eff}(f_{nBMA}) = (1.38 \cdot 10^{-4})\,s^{-1} + (5.15 \cdot 10^{-5})\,s^{-1} \cdot f_{nBMA} \tag{3.3.14}$$

$$k_{eff}(f_{tBMA}) = (1.89 \cdot 10^{-4})\,s^{-1} - (5.15 \cdot 10^{-5})\,s^{-1} \cdot f_{tBMA} \tag{3.3.15}$$

The results are depicted in *Figure 3.8b*, to demonstrate the linear relation. All the results of the previous calculations are summarized in *Table 3.6*.

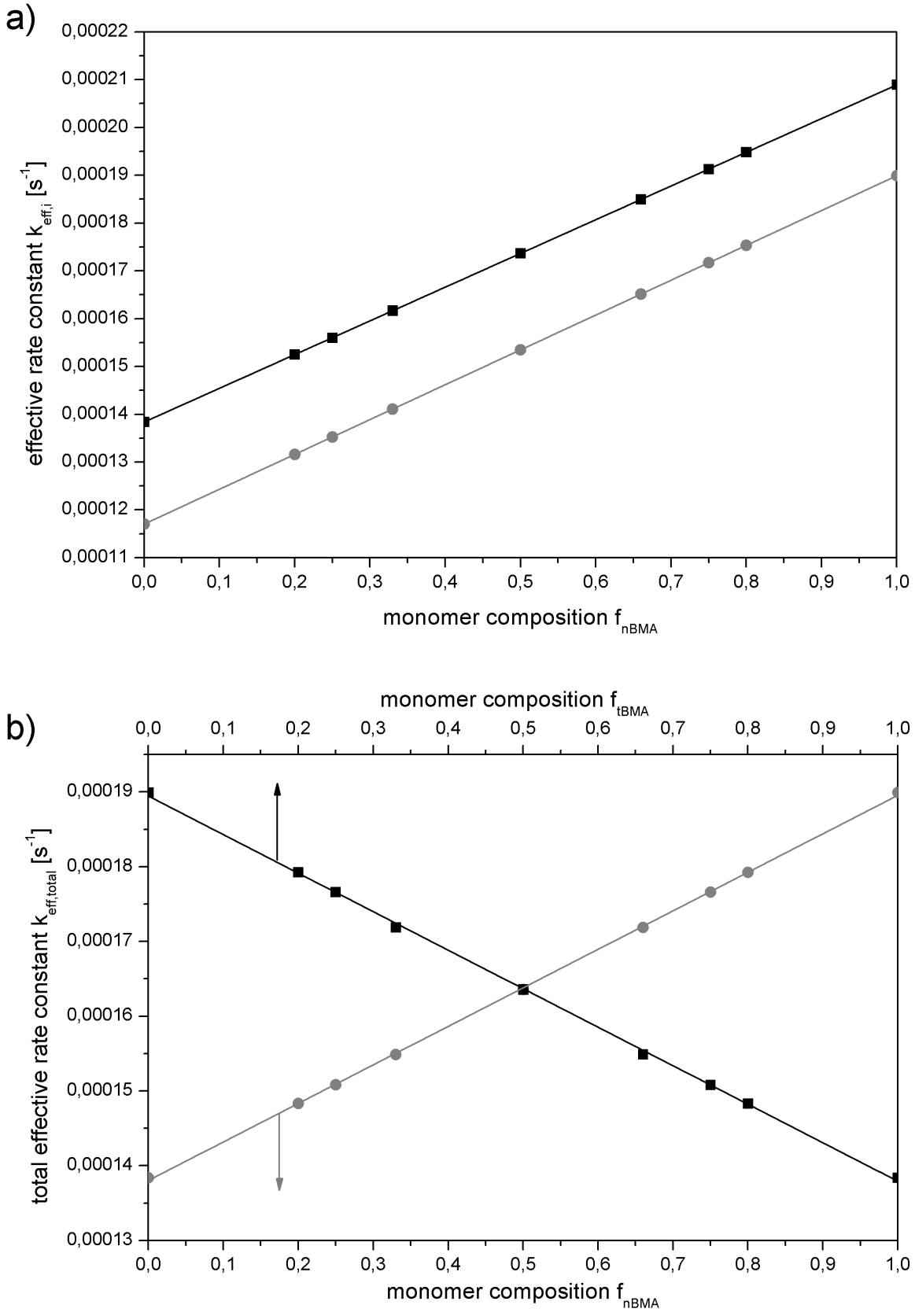

Fig. 3.8.: Effective rate constants of the individual monomer consumptions $k_{eff,i}$ and total effective rate constants $k_{eff,total}$ of the total reaction for the different monomer feed ratios of *Series A*; a) effective rate monomer constants $k_{eff,nBMA}$ (●) (*Eq. 3.3.11*) and $k_{eff,tBMA}$ (■) (*Eq. 3.3.12*); b) total effective rate constant $k_{eff}(f_{nBMA})$ (●) (*Eq. 3.3.14*) and $k_{eff}(f_{tBMA})$ (■) (*Eq. 3.3.15*)

The measured rates constants were also used to determine the instantaneous polymer composition $\frac{d[nBMA]}{d[tBMA]}$ of the resulting copolymers by means of *Equation 3.3.16*.

$$F_{nBMA} = \frac{R_{nBMA}}{R_{nBMA} + R_{tBMA}} = \frac{f_{nBMA} \cdot k_{nBMA}}{k_{nBMA} + f_{tBMA} \cdot k_{tBMA}} \tag{3.3.16}$$

with R_i= rate of copolymerization of monomer i, k_i= effective, composition dependent individual rate constant of monomer i, f_i= molar fraction of monomer i in the reaction mixture

The copolymerization diagram of *n–* and *tert–*butylmethacrylate as obtained from *Equation 3.3.16* is shown in *Figure 3.9*. The compositions of the resulting copolymers from *Series A* were summarized in *Table 3.6*. At any monomer composition f_{nBMA} the monomer tBMA copolymerized faster than nBMA, resulting in copolymers that contained less nBMA than was initially present in the monomer mixture.

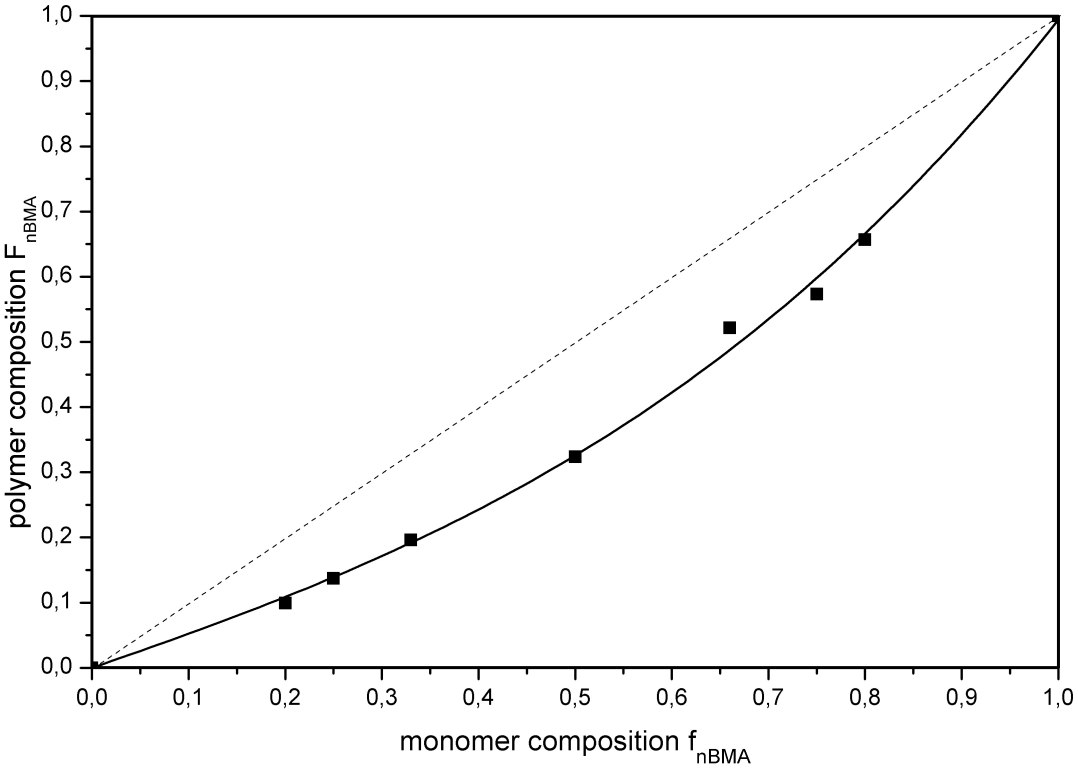

Fig. 3.9.: Copolymerization diagram of *n–* and *tert–*butylmethacrylate; dashed line for ideal random copolymerization, solid line for line of fit: $r_{nBMA} = 0.475$, $r_{tBMA} = 0.886$

Such a copolymerization diagram is described in the terminal–model by means of the *Lewis–Mayo–Equation* with one reactivity ratio larger and one reactivity ratio smaller than one. [20, 86]

$$F_1 = \frac{d[M_1]}{d[M_1] + d[M_2]} = \frac{r_1 f_1^2 + f_1 f_2}{r_1 f_1^2 + 2 f_1 f_2 + r_2 f_2^2} \tag{3.3.17}$$

with r_i= reactivity ratio, i. e. copolymerization parameter of monomer i, f_i= molar fraction

of monomer i in the reaction mixture, F_i= instantaneous molar fraction of monomer i incorporated on the copolymer, $d[M_i]$= different change of the concentration of monomer i due to a differential conversion, (1) = nBMA and (2) = tBMA

The monomer reactivity ratios were determined by a least–square fit of *Equation 3.3.17* to the data points of *Figure 3.9* to yield $r_{nBMA} = 0.475 \pm 0.05$ and $r_{tBMA} = 0.886 \pm 0.05$. A comparison of the values with literature data was not possible, since copolymerization reactivity ratios of this system have not yet been published.

3.3.2. Structural Analysis

The next investigations referred to the compositional analysis of the copolymers. First the elementary analysis of all resulting copolymers of *Series A* and *Series B* is detailed. The purity and the composition of the resulting copolymers were controlled with elementary analysis. The molecular formula of the monomers, which are isomers, is $C_8H_{14}O_2$. Therefore the amounts are 67.57 % of C, 9.92 % of H and 22.50 % of O. With the analysis method described in *Section 3.2.2* the content of only C and H can be measured, while the amount of O had to be calculated from the difference to 100 %. The results of the elementary analyze and as well as the results from the calculations are listed in the *Tables 3.7* and *3.8*. Furthermore the differences between the theoretical values and the analysis results are given. As part of the initiator–molecule pTSC in each polymer–chain one sulfur–atom occurs, however, its amount was below the detection limit of the elementary analysis device of around 2 %.

Tab. 3.7.: Results of the elementary analysis of the different copolymer compositions of *Series A* with divergence from the set value

Entry	F_{nBMA}	C [%]	ΔC	H [%]	ΔH	O [%]	ΔO
theory		67.57		9.92		22.50	
V18	0.00	66.54	-1.03	9.59	-0.34	23.87	1.37
V16	0.10	67.23	-0.34	9.67	-0.26	23.10	0.60
V14	0.14	66.74	-0.83	9.64	-0.28	23.62	1.11
V12	0.20	67.30	-0.27	9.76	-0.17	22.94	0.44
V11	0.32	67.15	-0.42	9.76	-0.16	23.09	0.58
V13	0.52	67.01	-0.56	9.63	-0.29	23.36	0.85
V15	0.57	67.13	-0.44	9.67	-0.26	23.20	0.70
V17	0.66	67.29	-0.28	9.67	-0.25	23.04	0.54
V19	1.00	67.13	-0.44	9.68	-0.25	23.20	0.69

Tab. 3.8.: Results of the elementary analysis of the different copolymer compositions of *Series B* with divergence from the set value

Entry f_{nBMA}	time [min]	C [%]	ΔC	H [%]	ΔH	O [%]	ΔO
theory		67.57		9.92		22.50	
V28	60	66.97	-0.60	9.46	-0.46	23.57	1.07
0.0	90	67.13	-0.44	9.72	-0.20	23.15	0.64
	120	67.07	-0.50	9.42	-0.50	23.51	1.01
	150	67.13	-0.44	9.37	-0.56	23.50	1.00
	180	66.97	-0.60	9.45	-0.47	23.58	1.07
V26	60	67.34	-0.23	9.41	-0.51	23.25	0.75
0.2	90	67.28	-0.29	9.38	-0.54	23.34	0.83
	120	67.40	-0.17	9.32	-0.60	23.28	0.77
	150	67.38	-0.19	9.41	-0.52	23.21	0.71
	180	67.41	-0.16	9.43	-0.50	23.17	0.66
V24	60	67.22	-0.35	9.39	-0.53	23.39	0.89
0.25	90	67.34	-0.23	9.56	-0.36	23.10	0.60
	120	67.35	-0.22	9.71	-0.22	22.95	0.44
	150	67.29	-0.28	9.61	-0.31	23.10	0.59
	180	67.35	-0.22	9.62	-0.30	23.03	0.53
V22	60	67.34	-0.23	9.37	-0.56	23.29	0.79
0.33	90	67.39	-0.18	9.53	-0.40	23.09	0.58
	120	67.22	-0.35	9.27	-0.65	23.51	1.01
	150	67.36	-0.21	9.46	-0.47	23.18	0.68
	180	67.35	-0.22	9.41	-0.52	23.24	0.74
V21	60	67.29	-0.28	9.45	-0.47	23.26	0.76
0.5	90	67.19	-0.38	9.11	-0.81	23.70	1.19
	120	67.31	-0.26	9.55	-0.38	23.15	0.64
	150	67.41	-0.16	9.60	-0.32	22.99	0.49
	180	67.93	0.36	9.64	-0.28	22.43	-0.07
V23	60	67.37	-0.20	9.08	-0.85	23.56	1.05
0.66	90	67.48	-0.09	9.06	-0.86	23.46	0.95
	120	67.29	-0.28	9.19	-0.74	23.52	1.02
	150	67.31	-0.26	9.49	-0.44	23.21	0.70
	180	67.30	-0.27	9.34	-0.58	23.36	0.86

Continuation on next page ...

Entry f_{nBMA}	time [min]	C [%]	ΔC	H [%]	ΔH	O [%]	ΔO
V25	60	67.41	-0.16	9.77	-0.15	22.82	0.32
0.75	90	67.22	-0.35	9.66	-0.26	23.12	0.62
	120	67.44	-0.13	9.77	-0.16	22.79	0.29
	150	67.40	-0.17	9.55	-0.37	23.05	0.54
	180	67.43	-0.14	9.62	-0.31	22.95	0.45
V27	60	67.13	-0.44	9.45	-0.47	23.42	0.91
0.8	90	67.97	0.40	10.37	0.44	21.66	-0.84
	120	67.79	0.22	10.26	0.33	21.95	-0.55
	150	67.68	0.11	10.30	0.38	22.02	-0.48
	180	67.53	-0.04	10.06	0.14	22.41	-0.09
V29	60	66.94	-0.63	9.43	-0.49	23.63	1.13
1.0	90	66.98	-0.59	9.50	-0.42	23.52	1.01
	120	67.03	-0.54	9.50	-0.43	23.47	0.97
	150	66.95	-0.62	9.53	-0.39	23.52	1.01
	180	67.05	-0.52	9.69	-0.23	23.26	0.76

The elementary analysis yielded two results. In all measurements the differences to the theoretical values were small. That implied that all samples were free of pollution from solvents etc. When all the samples were compared all the values were very similar. That means that all the reactions worked in the same way independent from the monomer composition. That was a good requirement for the semibatch polymerization were the monomer composition will change continuously during the reaction.

Another way to characterize the copolymer compositions is ATR–FTIR–spectroscopy. Before the IR–spectra of the polymers were measured, the spectra of the monomers were gathered to find the characteristic vibration bands that can be used to distinguish monomers and polymer units. These spectra of nBMA and tBMA are shown in *Figure 3.10*. Note that the ATR–FTIR is a reflection measurement technique. The intensity of an IR–band depends on the penetration depth of the IR radiation ($\approx 0.1 \ldots 1.0 \cdot \lambda$), but not on the sample thickness as long as the measurement film in much thicker than the longest measured wavelength. [87] For the comparison purpose the spectra were normalized by setting the adsorption intensity of the vibrational band at $1136\,\mathrm{cm}^{-1}$ to one by dividing all intensities A_x by A_1. In the spectra the peaks were equal for both the monomers that belonged to the methacrylate–part of the molecules.

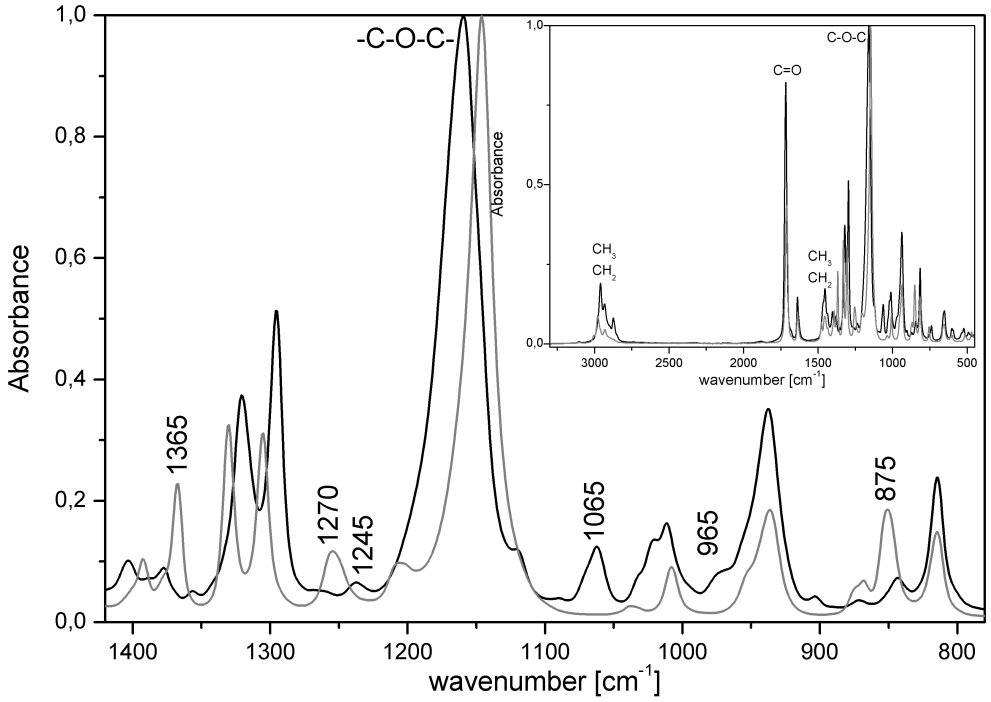

Fig. 3.10.: Finger print region of the ATR–FTIR–spectra of nBMA and tBMA (black line – nBMA, grey line – tBMA). Insert: full MIR–spectra (Spectra normalized to $A_{1136} = 1$)

The vibrational bands of $=CH_2$, $–CH_2-$ and $–CH_3$ was found between 3050 to 2800 cm^{-1}, but the one for $=CH_2$ which was located higher than 3000 cm^{-1} was merely weak and imperceptible. The vibrational band of C=O was located at 1720 cm^{-1}, for $–CH_2-$ and $–CH_3$ at 1473 cm^{-1} and 1450 cm^{-1} and for C–O–C at 1136 cm^{-1}.

The differences between the two spectra resulted from the two different ester–groups of the monomers, the *n*–butyl–chain and the *tert*–butyl–group, that became particularly visible between 600 and 1400 cm^{-1}. tBMA showed distinct bands at 1366 cm^{-1}, 1270 cm^{-1} and 876 cm^{-1}. The characteristic bands for nBMA laid at 1247 cm^{-1}, 1065cm^{-1} and 967cm^{-1}. Because these bands are within the finger print region it was not possible to assign the vibrational bands to specific vibrations of the functional groups of the molecules.

The IR–spectrum of the statistic copolymer of experiment V11 ($F_{nBMA} = 0.32$) from *Series A*, containing both the *n*–butyl– and the *tert*–butyl–ester groups, is given in *Figure 3.11* together with the spectra of the two monomers to work out the differences between the copolymers and the two monomers. The three vibrational bands that were characteristic for nBMA and also the three bands for tBMA were marked there in the spectra of the polymer and the corresponding monomer–spectra. However, two bands in each monomer spectra did not have corresponding bands in the polymer spectrum. They were at 1295 cm^{-1} and 1321 cm^{-1} in the nBMA spectrum and at 1305 cm^{-1} and 1330 cm^{-1} in the tBMA spectrum. In the polymer spectrum were no bands in the region between 1290 cm^{-1} and 1350 cm^{-1}. Hence that bands resulted from the vibration of $=CH_2$. [87]

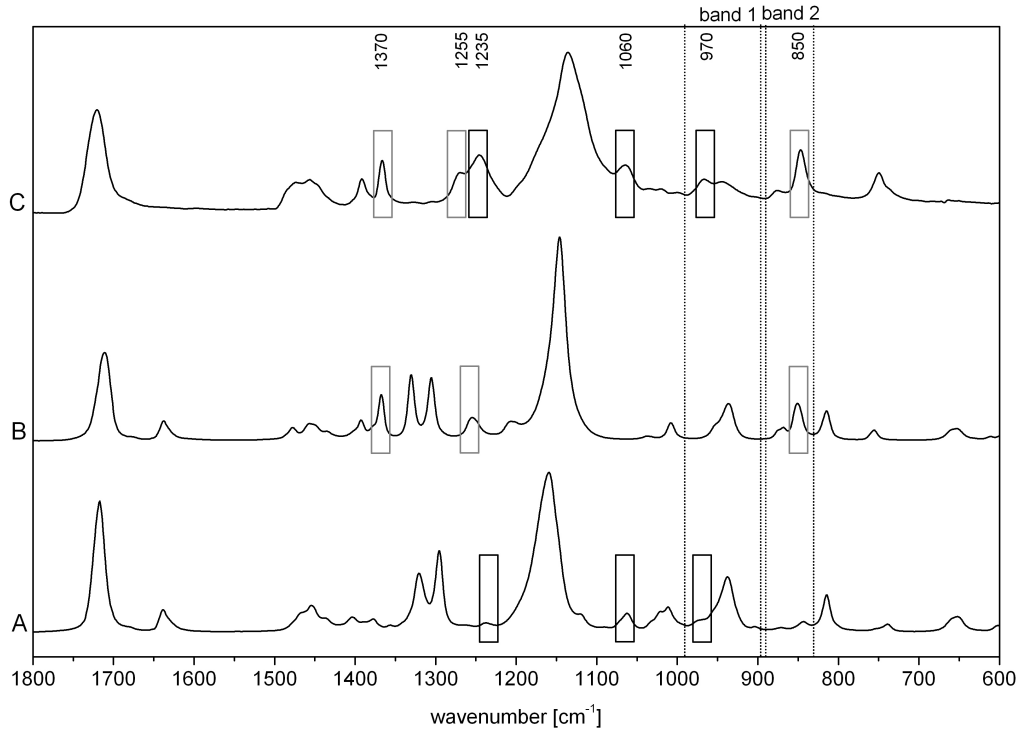

Fig. 3.11.: Comparison of the finger print region of the ATR–FTIR–spectra of A – nBMA, B – tBMA and C – experiment V11 (F_nBMA = 0.32); □ – nBMA specific bands, □ – tBMA specific bands; analyzed bands were marked with dashed lines (Spectra normalized to $A_{1136} = 1$)

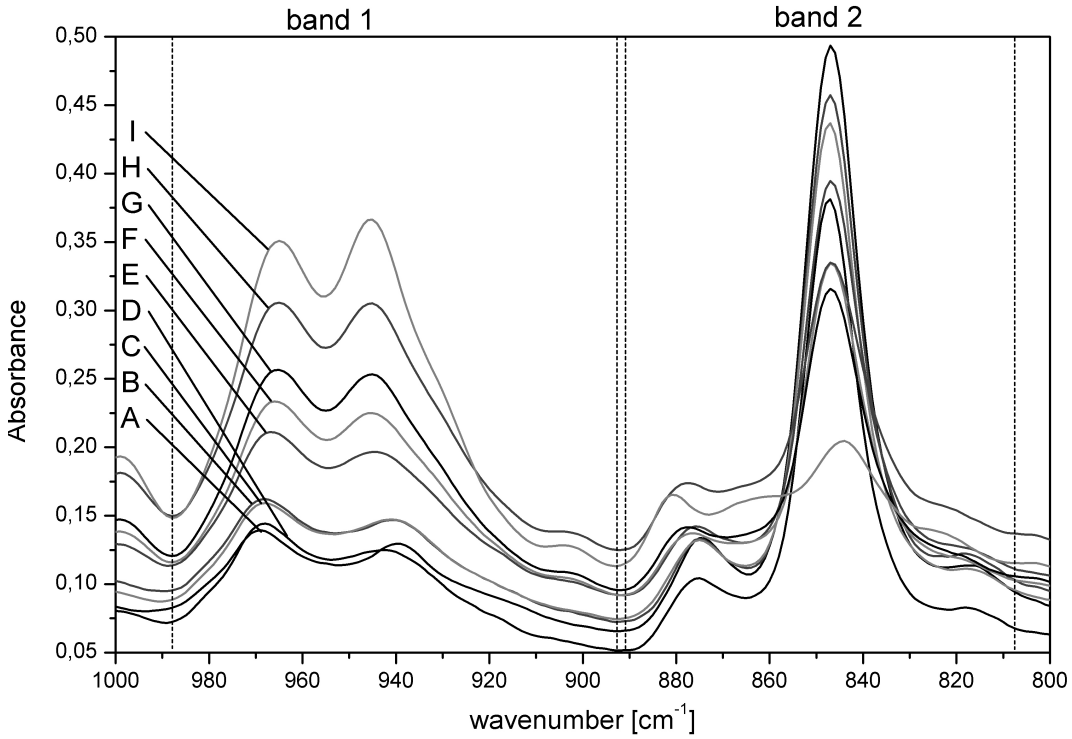

Fig. 3.12.: Analyzed section of the ATR–FTIR–spectra of the different copolymer compositions of P[tBMA–co–nBMA]; A – F_{nBMA} = 0.00, B – F_{nBMA} = 0.10, C – F_{nBMA} = 0.14, D – F_{nBMA} = 0.20, E – F_{nBMA} = 0.32, F – F_{nBMA} = 0.52, G – F_{nBMA} = 0.57, H – F_{nBMA} = 0.66, I – F_{nBMA} = 1.00 (normalized on the band at 1136 cm^{-1})

The band at 850 cm^{-1} (*band 2*) characteristic for tBMA and the one at 970 cm^{-1} (*band 1*) caused by nBMA were most suited for the investigation of the copolymer compositions. They were clearly separated and could be investigated well in view to peak area (PA) and peak height (PH). In *Figure 3.12* these two vibrational bands of the IR–spectra of the different copolymers from *Series A* are compared. It was recognizable that with the change in copolymer composition the peak area and the peak height changed. *Band 1* is a characteristic band from nBMA and with the rise of the amount of *n*–butyl–chain in the copolymer chain also the band intensity increased. Conversely, the intensity of *band 2* which is characteristic for the *tert*–butyl–group decreased. To show that behaviors more precisely the peak area and the peak height of the two bands were determined and then the composition of the samples, taken from analysis of ^{1}H–NMR–spectra, was plotted against the peak area and the peak height. This is depicted in *Figure 3.13* and further the values are listed in *Table 3.9*.

Tab. 3.9.: Peak area and peak height of the analyzed ATR–FTIR–bands of *Series A*

		band 1		*band 2*	
Entry	F_{nBMA}[a]	peak area [cm^{-1}]	peak height [A]	peak area [cm^{-1}]	peak height [A]
V18	0.00	2.98	0.063	8.68	0.423
V16	0.10	3.40	0.072	7.80	0.378
V14	0.14	3.60	0.075	7.54	0.360
V12	0.20	3.64	0.077	6.77	0.328
V11	0.32	4.86	0.103	6.79	0.302
V13	0.52	5.86	0.123	5.79	0.245
V15	0.57	6.74	0.142	5.77	0.223
V17	0.66	7.59	0.162	5.81	0.213
V19	1.00	9.86	0.234	4.33	0.010

[a] calculated from ^{1}H–NMR–spectra

All values, peak area and peak height of both vibrational bands, changed with the change of copolymer composition F_{nBMA}. The aforementioned increase of *band 1* and decrease of *band 2* proceeded the equations, that are given in the *Equations 3.3.18* to *3.3.21*.

$$\begin{aligned} F_{nBMA}(PA_1) &= (-0.453 \pm 0.108)\,cm^{-1} \\ &\quad + (0.175 \pm 0.039)\,cm^{-1} \cdot PA_1 - (0.003 \pm 0.003)\,cm^{-1} \cdot PA_1^2 \end{aligned} \tag{3.3.18}$$

$$\begin{aligned} F_{nBMA}(PA_2) &= (3.169 \pm 0.531)\,cm^{-1} \\ &\quad - (0.622 \pm 0.165)\,cm^{-1} \cdot PA_2 + (0.029 \pm 0.013)\,cm^{-1} \cdot PA_2^2 \end{aligned} \tag{3.3.19}$$

$$\begin{aligned} F_{nBMA}(PH_1) &= (-0.524 \pm 0.081) \\ &\quad + (9.862 \pm 1.278) \cdot PH_1 - (14.471 \pm 4.374) \cdot PH_1^2 \end{aligned} \tag{3.3.20}$$

$$\begin{aligned} F_{nBMA}(PH_2) &= (1.405 \pm 0.070) \\ &\quad - (4.067 \pm 0.556) \cdot PH_2 + (1.622 \pm 1.030) \cdot PH_2^2 \end{aligned} \tag{3.3.21}$$

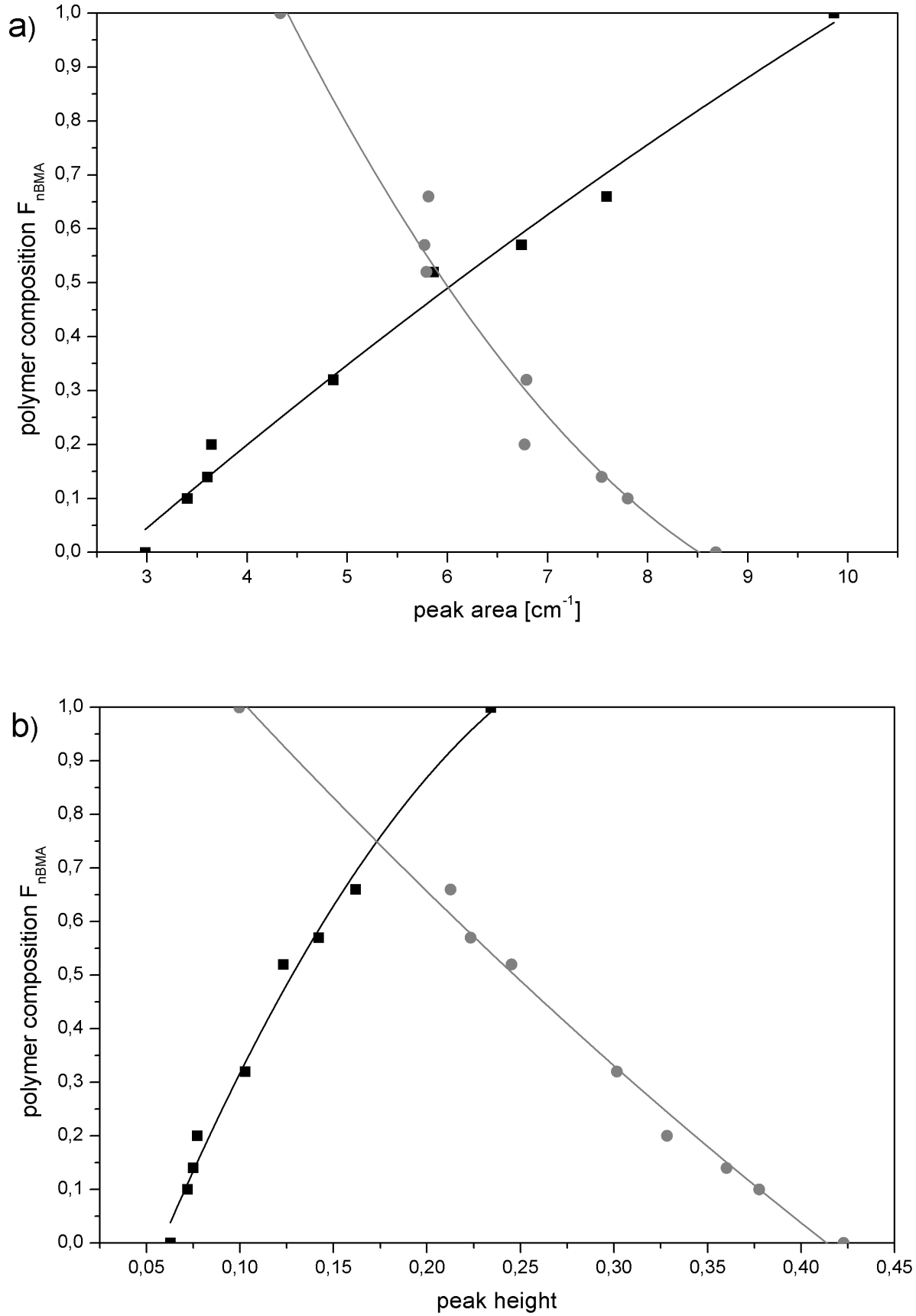

Fig. 3.13.: ATR–FTIR calibration curves, relating to the composition of the copolymers of *Series A* to a) peak area and b) peak height of *band 1* (970 cm^{-1}, ■) and *band 2* (850 cm^{-1}, ●)

The fitting of the the peak height of both vibrational bands worked better than the ones of the peak area as can be seen in *Figure 3.13*. The reason to perform the fittings was that either the peak area or the peak height should be applied for the determination of the composition of the gradient copolymers, hence, the ATR–FTIR–spectra of the copolymers could be analyzed not only quantitatively but also qualitatively. Because of the quality of the fittings the peak heights of the samples of *Series A*, will be used for the calibration curve. Moreover this is the classical values of IR–analysis. [87]

3.3.3. Molecular Weight Characterization

Beside the investigation of the kinetic and the structure, the resulting polymers were also investigated with size exclusion chromatography. For this purpose the experiments of *Series A* were repeated in larger batches *Series B*, cf. *Section 3.1.2*, to allow for sampling of sufficient larger quantities to obtain enough polymer per sample for a SEC analysis. On the one hand that was done for the verification of the polymerization control and on the other hand to find out how the molar mass growth during the polymerization via the samples from *Series B*. The control of the polymerization can be judged by the polydispersity of the polymer, because the lower the PDI the better the control. With a perfect control over the reaction the PDI would be $1 + \frac{1}{x_1}$. [41] During the polymerization the first sample was taken after one hour because at earlier times the conversion was not sufficiently high to support the analysis. Other samples were taken every 30 min up to 3 hours.

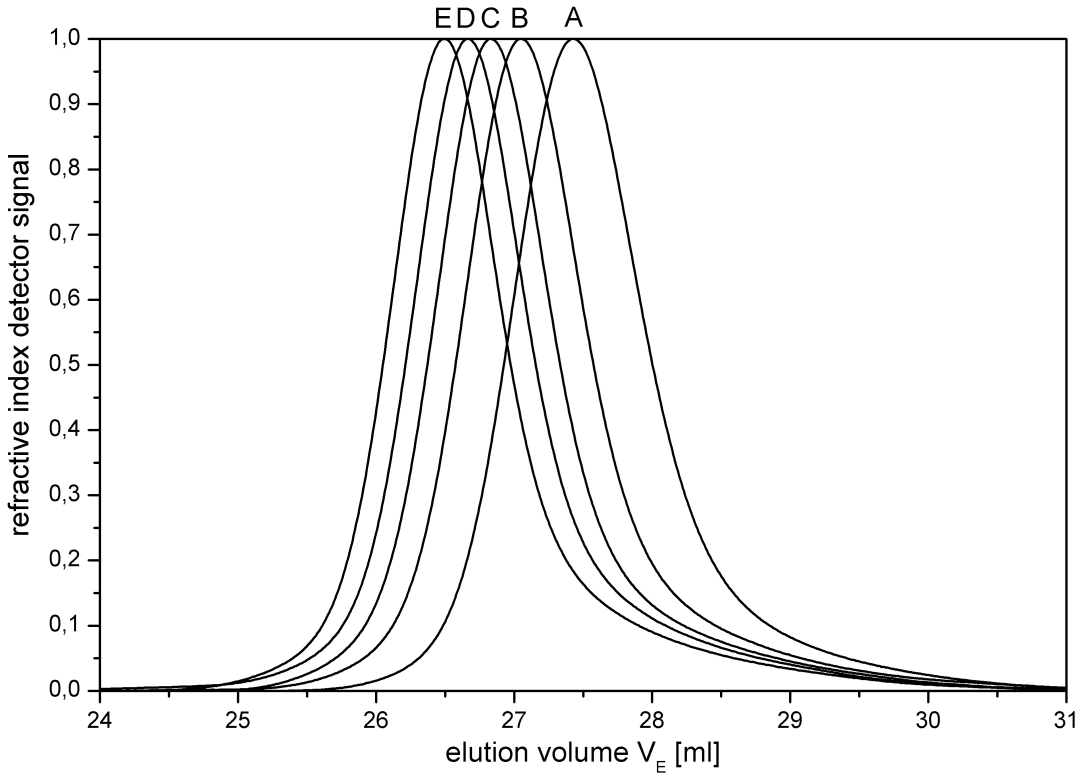

Fig. 3.14.: SEC elution diagrams of the samples of batch copolymerization V23 (f nBMA = 0.66) at reaction times of A – 60 min, B – 90 min, C – 120 min, D – 150 min, E – 180 min

Figure 3.14 shows the elution diagrams (RI–signals) of the samples from batch copolymerization V23. With growing reaction time the peaks of the elution diagrams became shifted to lower elution volumes, from 27.4 to 26.5 ml. Hence, the molar mass of the copolymers became larger during the course of the reaction. All the GPC–analysis of the samples of *Series B* showed this behavior. In view to the growth of the molar mass all the entries of *Series B* worked well. The RI–signals also demonstrated the absence of side reactions over the course of reaction, due to the lack of multimodality and front– or back–tailing effects. The signals are monomodal and with a narrow distribution. This observation is valid for all samples of *Series A* and *B*.

From the elution volume of the peak–maximum of the RI–peak the relative molar mass of the samples with respect to polystyrene standards was determined. For this purpose a calibration curve was constructed from SEC measurements of polymer standards. Narrow distributed polystyrene with molar masses of $1920\,g \cdot mol^{-1}$, $5610\,g \cdot mol^{-1}$ and $27500\,g \cdot mol^{-1}$ were used. Their molar masses were plotted logarithmic against their maximum elution volume. The result was a linear calibration curve, see *Figure 3.15*.

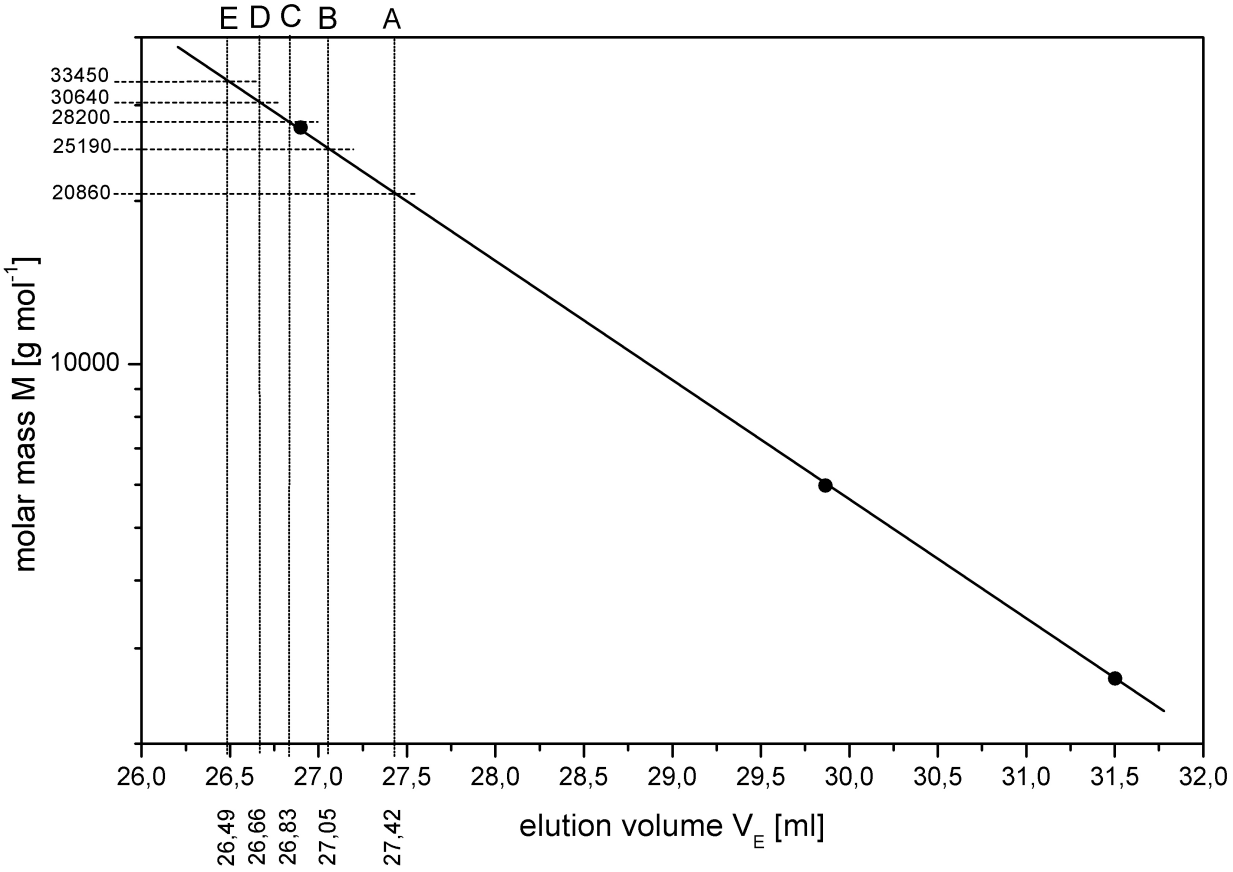

Fig. 3.15.: SEC calibration curve based on narrow distributed polystyrene standards (PS–Standard) and determination of the relative peak molecular weights of P[nBMA–co–tBMA] (batch copolymerization V23 (f_{nBMA} = 0.66), A – 60 min, B – 90 min, C – 120 min, D – 150 min, E – 180 min)

The equation of the curve was given in *Equation 3.3.22*.

$$\ln(M) = (23.884 \pm 0.095) - (0.508 \pm 0.003) \cdot V_E \tag{3.3.22}$$

From this curve the relative molar mass of the samples can be read off and also calculated with the maximum elution–volume V_E of the samples and *Equation 3.3.22*. The molar masses rose linear from 20860 to 33450 $g \cdot mol^{-1}$ during the polymerization. The results of the calculations are listed in *Table 3.13*. Because of the fact that only the one point of the RI–peak the maximum elution–volume was used for the determination of the relative molar mass the results only reflected a small part of the sample. Therefore the absolute molar masses of the samples were also determined.

For the determination of the absolute molar masses of the samples by means of static light scattering first the differential refractive index increment (dn/dc) of the resulting polymers from *Series A* must be measured, see *Section 2.4*. Moreover a correlation between polymer composition and dn/dc in THF as solvent at 25 °C was investigated. Five different concentrations of each copolymer (*Series A*) were injected one after another; before and after the polymer solution pure THF was injected. Then the gathered diagram was analyzed. First a baseline between the solvent levels was drawn and the regions of the different concentrations were marked. An example of such a time/n–diagram obtained from the copolymer V12 is depicted in *Figure 3.16a*. The five obtains refractive indices $n(c_i)$ of the concentration series were plotted against the concentrations c_i,see *Figure 3.16b*.

The measured refractive indices of the polymer solutions fairly laid on a straight line of positive slope. The slope of the fitted linear function is the differential refractive index increment dn/dc of copolymer V12 in THF at 25 °C. The other copolymers of *Series A* were investigated in an analogous way. The measured differential refractive index increments of the copolymers are summarized in *Table 3.10* while *Figure 3.17* depicts a plot of the dn/dc versus the molar fraction of nBMA (F_{nBMA}) in the respective substance.

Tab. 3.10.: Differential refractive index increments dn/dc of P[nBMA–co–tBMA] (*Series A*) copolymers in THF at 25 °C

Entry	F_{nBMA}	dn/dc [$ml \cdot g^{-1}$]
V18	0.00	0.0612 ± 0.0019
V16	0.10	0.0701 ± 0.0008
V14	0.14	0.0654 ± 0.0006
V12	0.20	0.0806 ± 0.0034
V11	0.32	0.0799 ± 0.0033
V13	0.52	0.0774 ± 0.0012
V15	0.57	0.0779 ± 0.0039
V17	0.66	0.0730 ± 0.0034
V19	1.00	0.0988 ± 0.0178

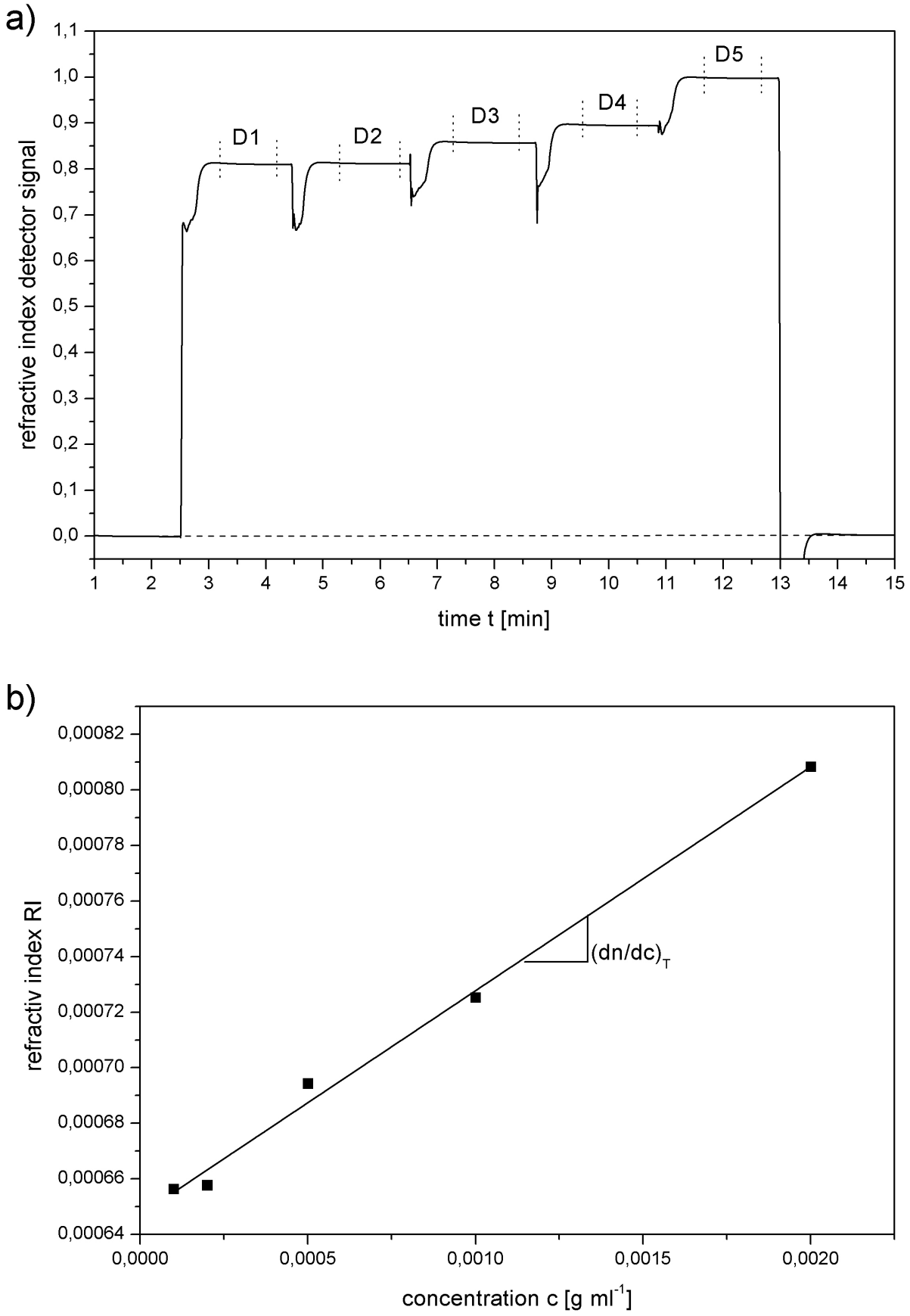

Fig. 3.16.: Refractive index increment of experiment V12 ($F_{nBMA} = 0.2$); a) elution diagram of solutions D1 – 0.1 mg · ml^{-1}, D2 – 0.2 mg · ml^{-1}, D3 – 0.5 mg · ml^{-1}, D4 – 1.0 mg · ml^{-1}, D5 – 2.0 mg · ml^{-1} (dashed vertical lines) and THF – baseline (dashed horizontal line); b) determination of dn/dc – concentrations against refractive index (dn/dc = 0.081 ± 0.003 g · mol^{-1}); in THF at 25 °C

A simple relation between dn/dc and F_{nBMA} cannot be stated, however, between F_{nBMA} 0.1 to 0.6 the dependence of the refractive index increment on the copolymer composition is low ($d[dn/dc]/dF_{nBMA} < 0.009$). Above $F_{nBMA} = 0.7$ the refractive index increment seems to inverse stronger, since dn/dc of the PnBMA– homopolymer was 0.099. Literature values of the dn/dc for PnBMA or PtBMA in THF at 25 °C were not available.

The measured dn/dc values of P[nBMA–co–tBMA] copolymers in THF were used to analyze the molecular weight distributions and to determine the absolute molar masses of the nBMA/ tBMA copolymers of *Series A* and *B* (batch copolymerization, cf. *Section 3.1.2*) by means of online MALS during SEC characterization.

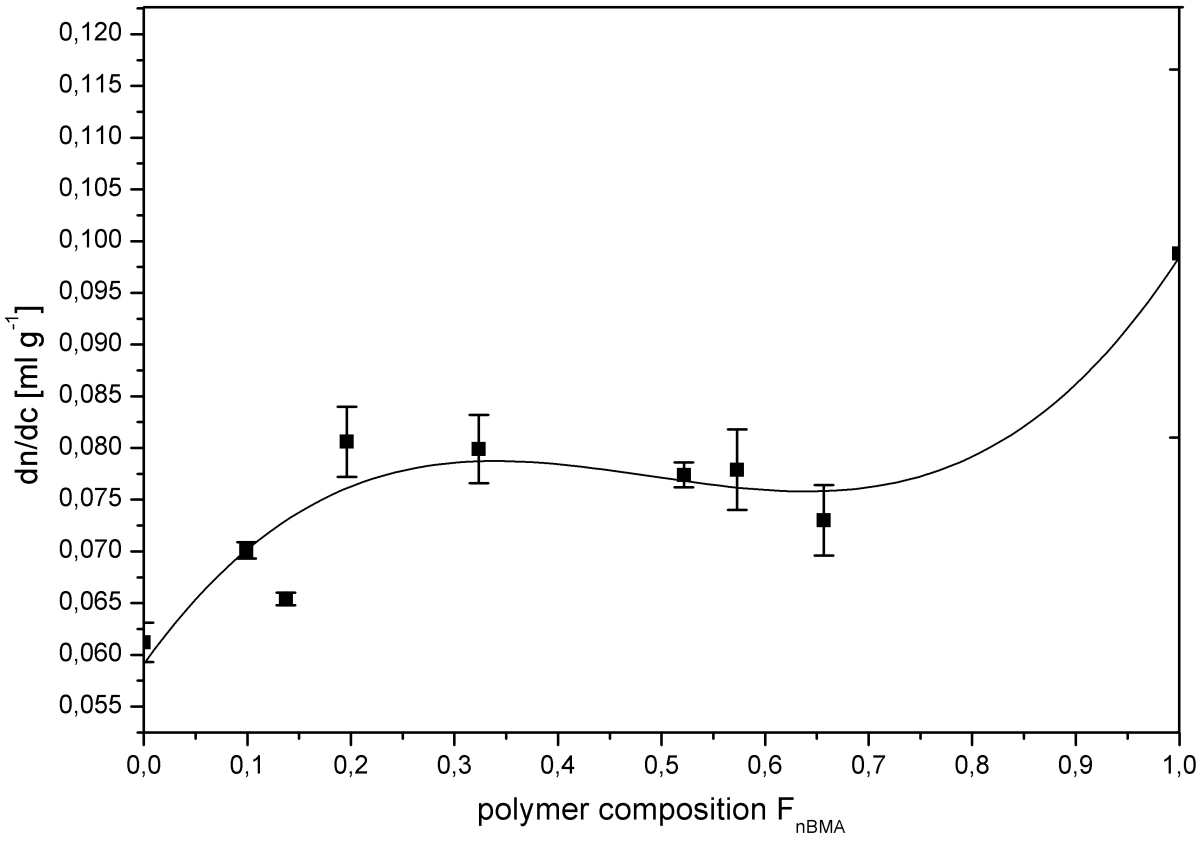

Fig. 3.17.: Plot of the measured differential refractive index increments dn/dc of the solutions of P[nBMA–co–tBMA] copolymers (Polymers of *Series A*, cf. *Table 3.1*, THF, 25 °C)

Figure 3.18 depicts the RI– and the 90°–MALS–detector signals of the elution–diagram of P[nBMA-co-tBMA] copolymer V13 ($F_{nBMA} = 0.52$). From the angle dependence of the scattered light intensity and the known dn/dc–value of $dn/dc = 0.0774\,ml \cdot g^{-1}$ (cf. *Table 3.10*) the absolute molecular weight of a fraction at a given elution volume can be derived, see *Section 2.4*. The calculated molecular weights are shown in *Figure 3.18* (right axis). Since the RI–signal is proportional to the weight fraction of the eluted polymer, the complete molecular weight distribution (MWD) of the measured polymer can be obtained. Both detector signals were also monomodal without fronting and tailing. From these MWD the molecular weight

averages (M_n, M_w, M_z) and the polydispersity indices M_w/M_n, and respectively M_z/M_n were calculated. The obtained values are detailed in *Table 3.11* for *Series A* and in *Table 3.12* for *Series B*.

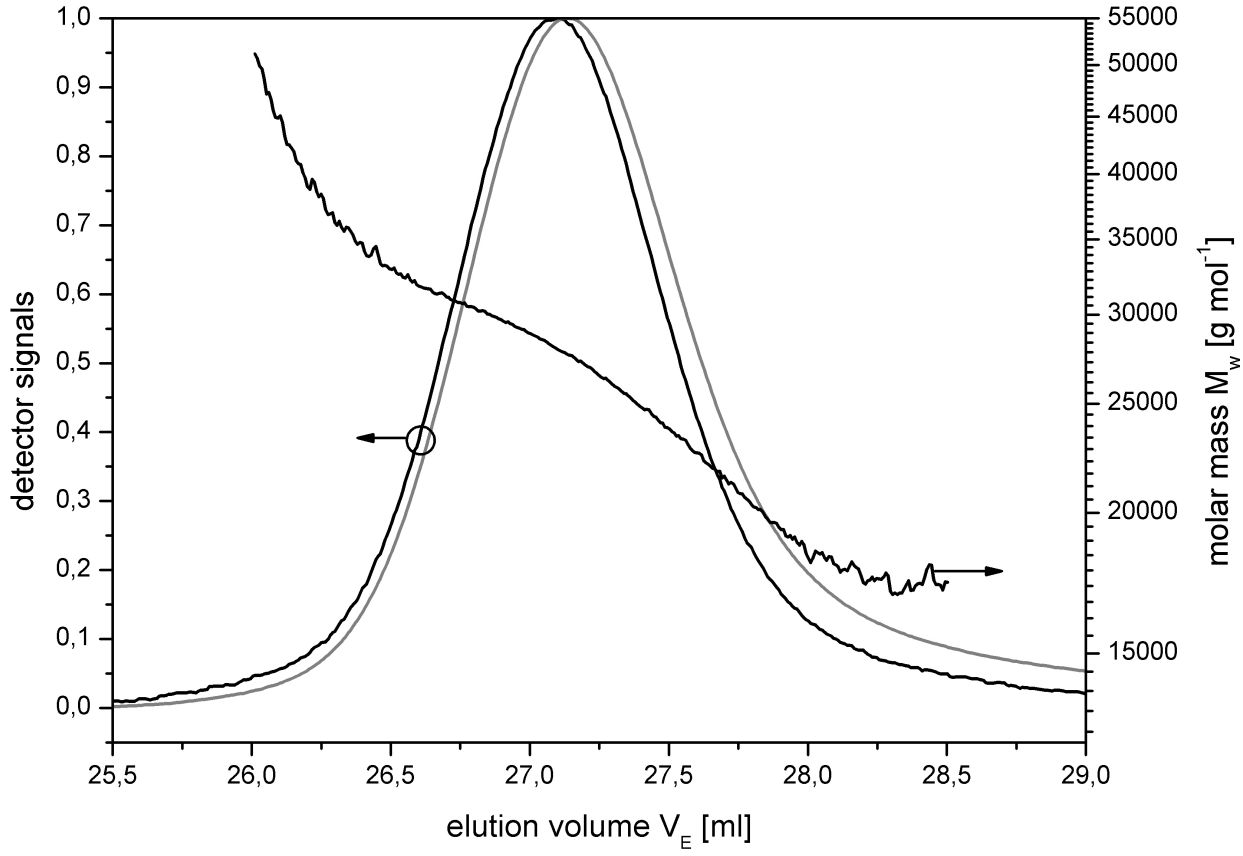

Fig. 3.18.: SEC elution diagrams and molar masses of experiment V13 (F_{nBMA} = 0.52); black curve – light scattering signal, grey curve – refractive index signal

Tab. 3.11.: SEC results of the different copolymer–compositions of *Series A*

Entry	F_{nBMA}	M_n [g · mol^{-1}]	M_w [g · mol^{-1}]	M_z [g · mol^{-1}]	M_w/M_n	M_z/M_n
V18	0.00	21420 ±1071	28820 ±288	32910 ±658	1.345 ±0.0673	1.536 ±0.0768
V16	0.10	27580 ±276	29660 ±267	31640 ±949	1.075 ±0.0215	1.147 ±0.0459
V14	0.14	23630 ±473	28850 ±288	35590 ±4627	1.221 ±0.0366	1.506 ±0.1958
V12	0.20	19500 ±195	19950 ±200	20500 ±820	1.023 ±0.0205	1.051 ±0.0315
V11	0.32	23510 ±470	25390 ±229	26700 ±534	1.080 ±0.0216	1.135 ±0.0227
V13	0.52	25320 ±253	26380 ±211	27950 ±559	1.042 ±0.0104	1.104 ±0.0331
V15	0.57	31990 ±960	33520 ±670	37210 ±3349	1.048 ±0.0419	1.163 ±0.1047
V17	0.66	34520 ±276	37420 ±150	39570 ±356	1.084 ±0.0098	1.146 ±0.0115
V19	1.00	25110 ±201	26790 ±187	30990 ±620	1.067 ±0.0107	1.234 ±0.0270

Tab. 3.12.: SEC results of the different copolymer–compositions of *Series B*

Entry f_{nBMA}	time [min]	M_n [$g \cdot mol^{-1}$]	M_w [$g \cdot mol^{-1}$]	M_z [$g \cdot mol^{-1}$]	M_w/M_n	M_z/M_n
V28	60	18140 ±109	18420 ±92	18620 ±186	1.015 ±0.0081	1.026 ±0.0103
0.0	90	24460 ±171	24920 ±150	25560 ±256	1.019 ±0.0092	1.045 ±0.0209
	120	27940 ±279	28500 ±285	29360 ±881	1.020 ±0.0204	1.051 ±0.0420
	150	31750 ±95	32090 ±96	32560 ±228	1.011 ±0.0040	1.025 ±0.0082
	180	33900 ±136	34330 ±137	34810 ±278	1.013 ±0.0061	1.027 ±0.0092
V26	60	18710 ±75	18790 ±75	18860 ±170	1.004 ±0.0060	1.008 ±0.0101
0.2	90	22840 ±69	23000 ±46	23140 ±139	1.007 ±0.0040	1.013 ±0.0061
	120	26840 ±161	27150 ±162	27590 ±276	1.011 ±0.0091	1.028 ±0.0103
	150	28610 ±114	29090 ±116	29520 ±266	1.017 ±0.0061	1.032 ±0.0103
	180	30160 ±90	30660 ±92	31060 ±186	1.017 ±0.0041	1.030 ±0.0072
V24	60	18720 ±93	18910 ±95	19080 ±190	1.010 ±0.0071	1.019 ±0.0102
0.25	90	24060 ±192	24190 ±145	24310 ±243	1.005 ±0.0101	1.010 ±0.0202
	120	24250 ±97	24410 ±98	24570 ±221	1.007 ±0.0050	1.013 ±0.0091
	150	28200 ±84	28680 ±86	29180 ±204	1.017 ±0.0041	1.035 ±0.0072
	180	33720 ±101	33960 ±102	34180 ±239	1.007 ±0.0040	1.014 ±0.0071
V22	60	13220 ±79	13430 ±67	13620 ±136	1.016 ±0.0081	1.031 ±0.0103
0.33	90	16870 ±118	17110 ±171	17320 ±173	1.014 ±0.0101	1.026 ±0.0205
	120	16460 ±823	19940 ±80	20800 ±187	1.212 ±0.0061	1.264 ±0.0632
	150	19950 ±79	20070 ±80	20190 ±182	1.006 ±0.0060	1.012 ±0.0091
	180	23000 ±69	23190 ±70	26650 ±163	1.008 ±0.0040	1.015 ±0.0081
V21	60	13770 ±96	13220 ±132	13960 ±698	1.016 ±0.0102	1.065 ±0.0533
0.5	90	17420 ±87	17730 ±89	18000 ±180	1.018 ±0.0071	1.033 ±0.0103
	120	20630 ±83	21090 ±63	21570 ±151	1.023 ±0.0051	1.046 ±0.0084
	150	22830 ±69	23380 ±70	23960 ±144	1.024 ±0.0041	1.050 ±0.0074
	180	24050 ±120	25060 ±100	25980 ±260	1.042 ±0.0063	1.080 ±0.0108
V23	60	17920 ±86	18340 ±73	18680 ±187	1.023 ±0.0072	1.042 ±0.0104
0.66	90	22960 ±69	23360 ±70	23810 ±167	1.017 ±0.0051	1.037 ±0.0083
	120	25480 ±102	26130 ±78	26710 ±187	1.026 ±0.0051	1.048 ±0.0073
	150	28430 ±85	28960 ±87	29470 ±177	1.018 ±0.0041	1.036 ±0.0073
	180	31080 ±155	31750 ±159	32490 ±325	1.021 ±0.0072	1.045 ±0.0105
V25	60	18780 ±113	18910 ±113	19080 ±191	1.007 ±0.0081	1.016 ±0.0102
0.75	90	23560 ±94	23700 ±95	23850 ±191	1.006 ±0.0060	1.012 ±0.0091

Continuation on next page ...

Entry f_{nBMA}	time [min]	M_n [g · mol^{-1}]	M_w [g · mol^{-1}]	M_z [g · mol^{-1}]	M_w/M_n	M_z/M_n
	120	28390 ±57	28610 ±57	28810 ±115	1.008 ±0.0060	1.015 ±0.0051
	150	30020 ±120	30490 ±91	30920 ±216	1.016 ±0.0051	1.030 ±0.0082
	180	31920 ±128	33510 ±168	35800 ±358	1.050 ±0.0063	1.121 ±0.0112
V27	60	18640 ±112	19170 ±115	16640 ±166	1.028 ±0.0082	1.054 ±0.0105
0.8	90	25790 ±129	26330 ±132	26840 ±268	1.021 ±0.0072	1.040 ±0.0104
	120	28770 ±230	29530 ±207	30620 ±612	1.026 ±0.0103	1.064 ±0.0213
	150	30900 ±124	31800 ±159	33170 ±332	1.029 ±0.0072	1.073 ±0.0107
	180	33230 ±199	33960 ±204	34890 ±349	1.022 ±0.0082	1.050 ±0.0105
V29	60	14180 ±284	14380 ±288	14610 ±438	1.014 ±0.0203	1.030 ±0.0412
1.0	90	17660 ±88	18490 ±92	19420 ±194	1.047 ±0.0084	1.100 ±0.0220
	120	20630 ±413	21180 ±635	22110 ±1769	1.027 ±0.0411	1.072 ±0.0858
	150	21670 ±217	22260 ±200	22990 ±459	1.027 ±0.0103	1.061 ±0.0212
	180	24380 ±477	24670 ±247	25080 ±758	1.012 ±0.0202	1.029 ±0.0309

For experiment V23 the results of the absolute molar mass determinations are depicted in *Figure 3.19a*. The molar mass grew linear at the beginning up to 45 min and reached 17920 g · mol^{-1} after 60 min, but with times the growth curve attended and at the end the molar mass was 31080 g · mol^{-1}. Hence, the growth of the molar mass followed a bounded growth $M \approx M_\infty(1 - e^{-kt})$. *Figure 3.19b* shows the linear dependence of the molar mass M_n of the samples to the conversion p. In *Section 3.3.1* it was shown that $t \to 0 : -\ln(1-p) = k_1 \cdot t$ applied to the reaction kinetic and in this section it was displayed that $t \to \infty : M = k_2 \cdot p$ applied to the molar mass progress. These rules were valid for controlled reactions without termination reactions.

The measured molar masses were all lower than the relative peak masses. For experiment V23 the values are compared in *Table 3.13*.

Tab. 3.13.: Comparison of relative* and absolute molar masses of experiment V23 (f_{nBMA} = 0.66)

time [min]	V_E [ml]	relative M * [g · mol^{-1}]	absolute M [g · mol^{-1}]	ΔM [g · mol^{-1}]	[%]
60	27.42	20860	17920	2940	16.41
90	27.05	25190	22960	2230	9.71
120	26.83	28200	25480	2720	10.68
150	26.67	30640	28430	2210	7.77
180	26.49	33450	31080	2370	7.63

* calibrated against PS–Standard

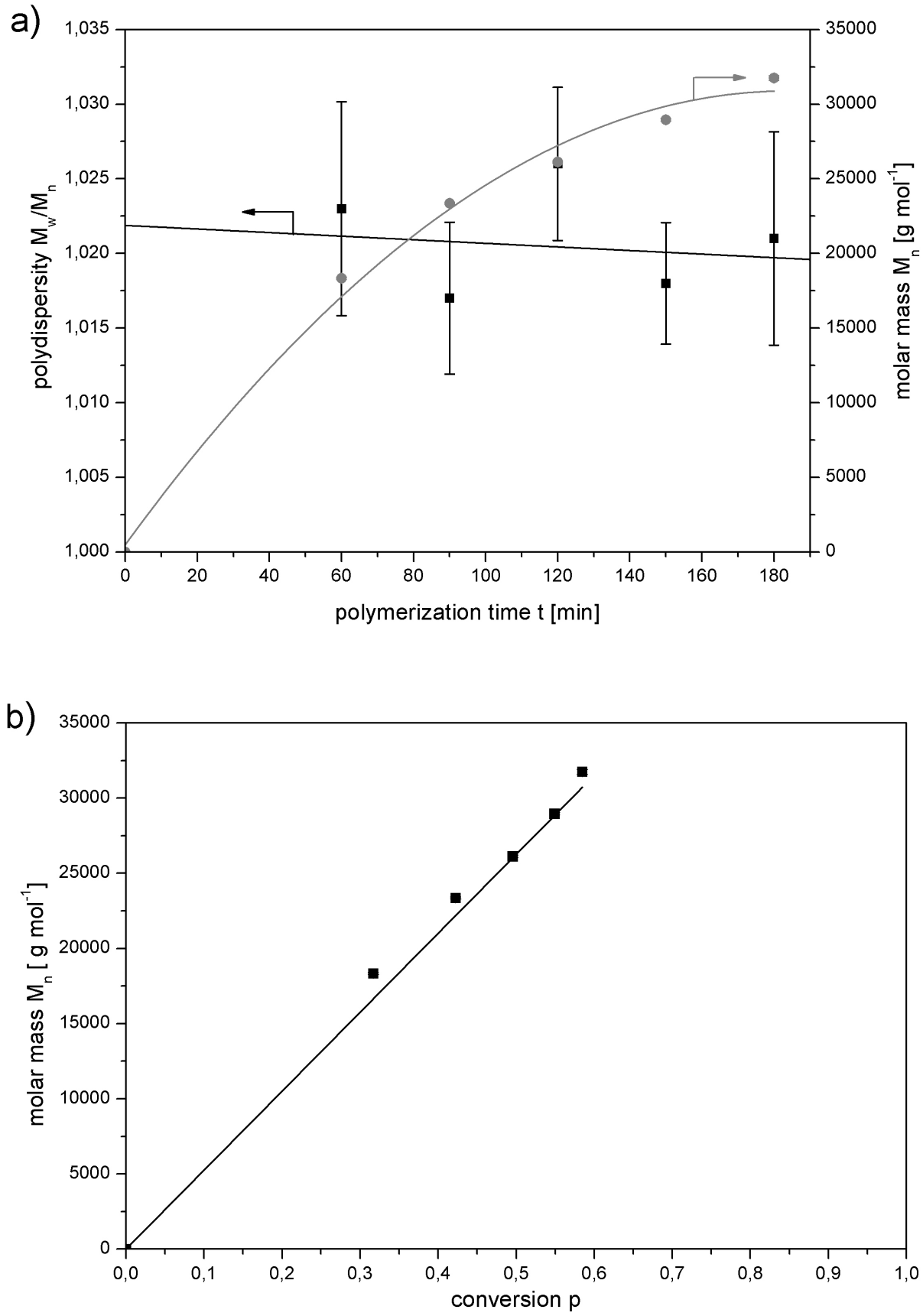

Fig. 3.19.: a) Polydispersities M_w/M_n and molar masses M_n of batch copolymer V23 (f_{nBMA} = 0.66) against time t; ■ polydispersity M_w/M_n, ● molar mass M_n; b) molar masses M_n of batch copolymer V23 (f_{nBMA} = 0.66) against conversion p

The difference between the relative and the absolute molar masses originated from the form of the RI–peak. Only at with a perfect distribution the molar masses of the peak maximum and the number average molecular weight would be the same. Any kind of termination reactions would lead to front– or back–tailing at the RI–peak and so to differences between the relative and the total molar mass. Fronting appears when a polymerization is terminated by a combination reaction and tailing by disproportionation. [79, 88] That the values of relative and absolute molar masses of the samples from batch copolymer V23 approached over the reaction time showed that there was a good control over the ATRP.

Figure 3.20 shows the dependence of M_n and PDI on the copolymer composition. The molecular weight (M_n) was fairly independent of the used copolymer composition ($M_n \approx 28500\,g \cdot mol^{-1}$), although the masses scattered considerably. The polydispersity of the samples was low (PDI = 1.02 . . . 1.08) and also independent of the copolymer composition. As with the results of the elementary analysis it was shown that the monomer composition of the reaction had no influence on the resulting copolymer.

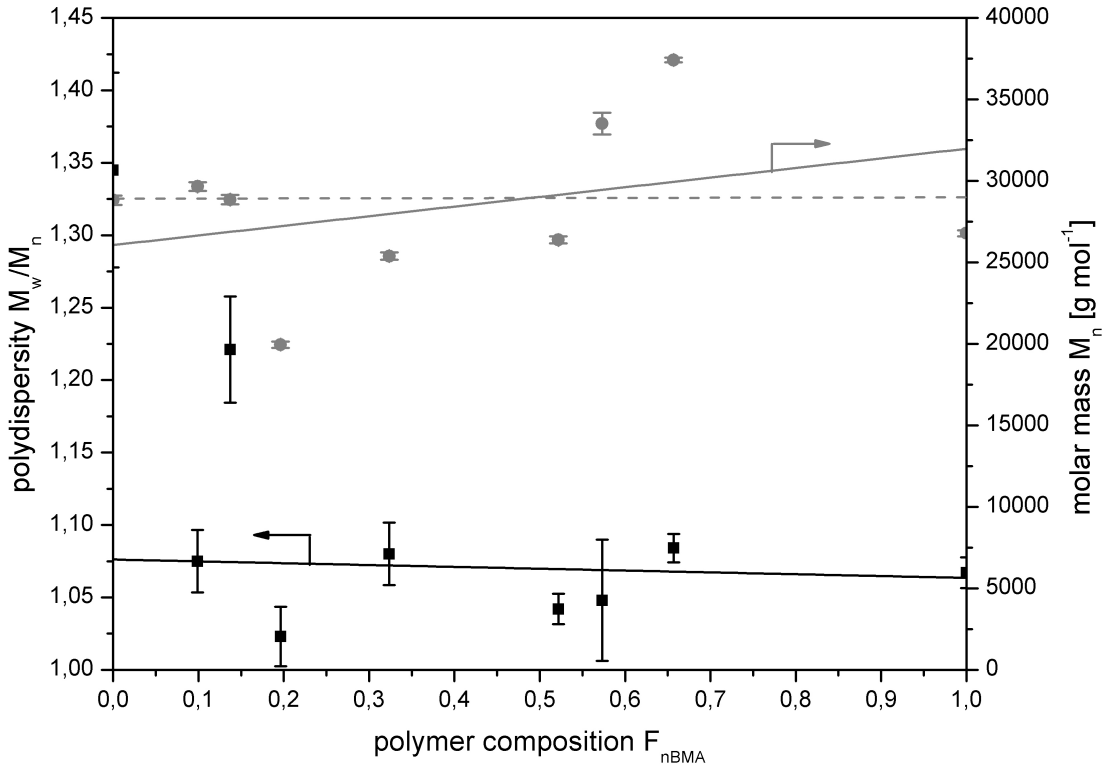

Fig. 3.20.: Polydispersities M_w/M_n and molar masses M_n of *Series A*; P[nBMA–co–tBMA]–copolymers ■ polydispersity M_w/M_n, ● molar mass M_n, dashed line – average molar mass

3.3.4. Thermal Behavior

The next kind of analysis was the differential scanning calorimetry. Here the thermal behavior of the copolymers was anlaysed mainly to determine the dependence of the glass transition

temperature T_g on the copolymer composition. All samples of *Series A* were measured with the following temperature program:

- precooling: RT to −50 °C
- standby for 20 min
- 1. heating: -50 to 200 °C
- 1. cooling: 200 to −50 °C
- 2. heating: -50 to 200 °C
- postcooling: 200 °C to RT

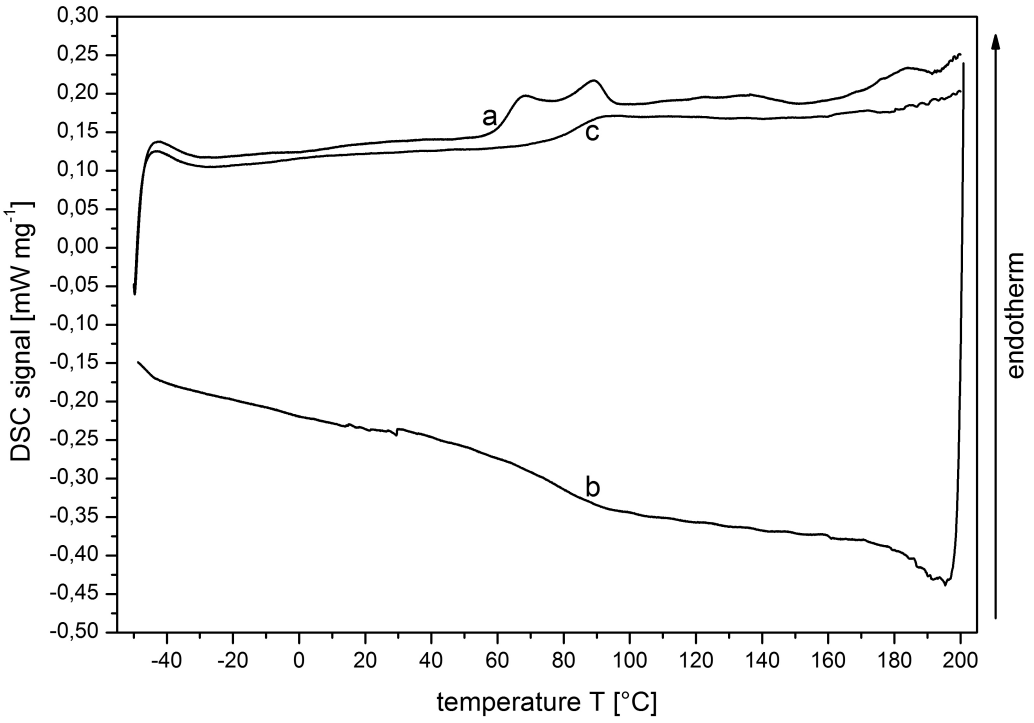

Fig. 3.21.: DSC thermogram of experiment V14 (F_{nBMA} = 0.14); a – first heating run, b – first cooling run, c – second heating run; heating rate $10\,K \cdot min^{-1}$

The samples of *Series B* were measured between -80 to 150 °C but with the same procedure because the analysis of *Series A* showed that it was not required to heat up to 200 °C. In *Figure 3.21* the thermogram of experiment V14 with both heating runs and the cooling run is depicted as an example.

Because the copolymers were completely amorphous, no melting or crystallization was observed. In the vicinity of T_g the measured heat flow exhibited a characteristic step, caused by the change of the materials heat capacity (Δc_p) upon softening from the solid glass into the liquid melt. [89] A schematic depiction of a theoretical DSC thermogram in the vicinity of

a glass transition is given in *Figure 3.22*. For the analysis of such a glass transition step the linear part of the DSC–signal before and after the step are extrapolated, see *Figure 3.22* lines a and b, and a tangent is applied trough the glass transition step, see *Figure 3.22* line c. The intersection between lines a and c is the starting point of the glass transition, T_{onset}, and the intersection between lines b and c the end point, T_{offset}. The point of inflection in this area was set as glass transition temperature T_g. The temperature range of the glass transition, the range between T_{offset} and T_{onset}, was defined as glass transition temperature range ΔT. (Note that the temperature at the point of inflection and the midpoint temperature (T_{midpt}) can, but do not necessarily, coincide.)

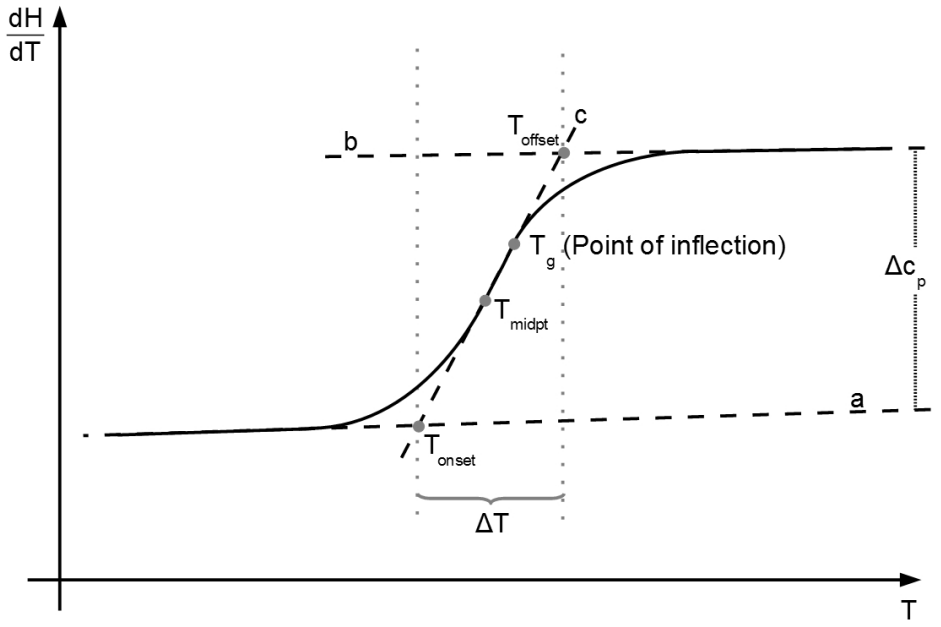

Fig. 3.22.: Scheme of a theoretical DSC thermogram in the vicinity of a glass transition

The first heating run showed a single glass transition overlaid by a relaxation peak in the range from 60 to 100 °C. To avoid effects of the sample thermal history only the second heating run was analyzed. With the analysis software of the DSC T_{onset} and T_{offset} of the glass transition region were determined and then the other values T_g, $\Delta T = T_{offset} - T_{onset}$ and Δc_p were calculated. [89] Also the midpoint of the glass transition region T_{midpt} were computed but these values was not used further. All second heating runs from the copolymers of *Series A* and all the samples of *Series B* which were taken during the batch copolymerization were analyzed that way. The second heating runs of the samples of V26 as an example for *Series B* are depicted in *Figure 3.23*. T_g, T_{onset} and T_{offset} as bounds of the glass area are marked there. The second heating runs of the batch copolymers of *Series A* are collated in *Figure 3.25* also with marked T_g, T_{onset} and T_{offset}. All the DSC results of the batch copolymerizations of *Series A* are summarized in *Table 3.14* and the one of *Series B* in *Table 3.15*.

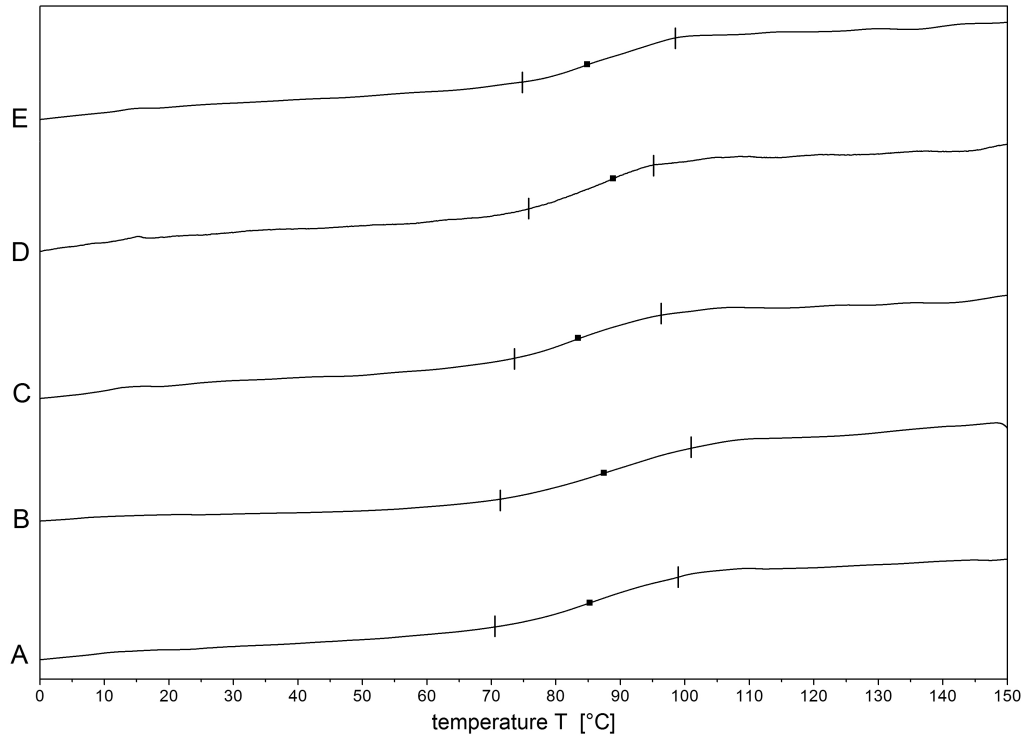

Fig. 3.23.: DSC thermograms of samples taken during the batch copolymerization V26 (f_{nBMA} = 0.20) with marked glass transition temperature range ΔT and temperature T_g (second heating runs, heating rate $10\,K \cdot min^{-1}$; A – 60 min, B – 90 min, C – 120 min, D – 150 min, E – 180 min of polymerization time)

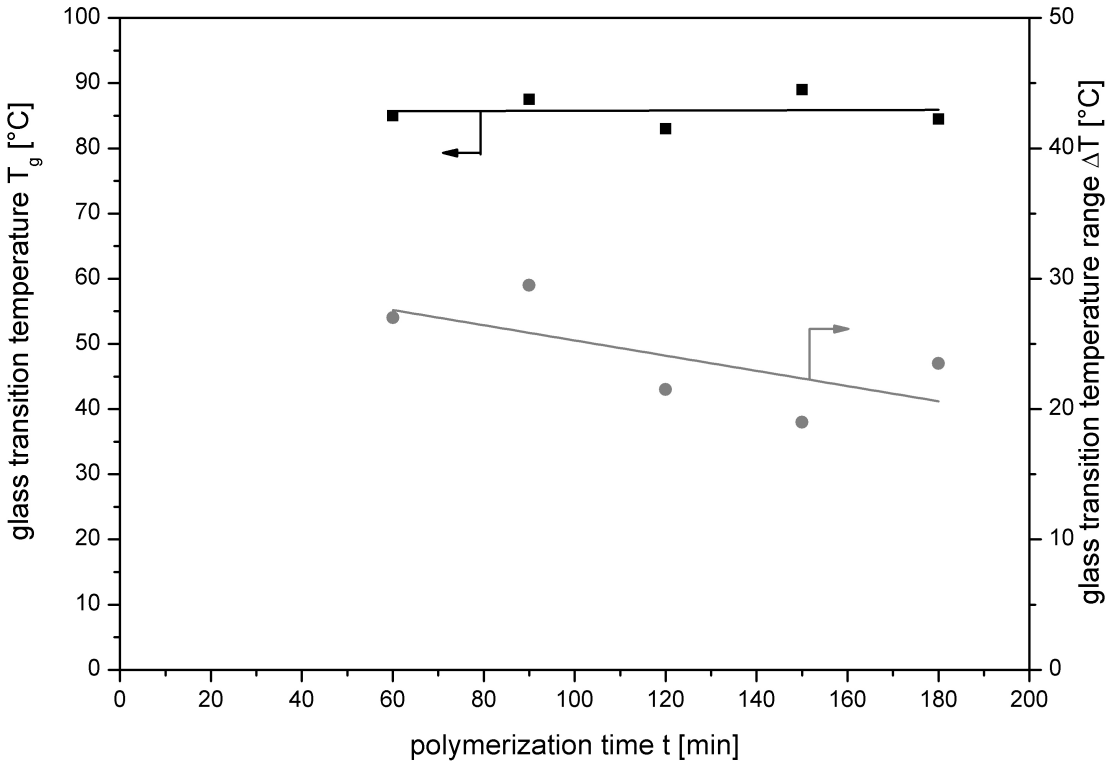

Fig. 3.24.: Glass transition temperature T_g and temperature range ΔT of the samples taken during the batch copolymerization V26 (f_{nBMA} = 0.20); ■ glass transition temperature T_g, ● glass transition temperature range ΔT

Tab. 3.14.: DSC results of the different copolymer compositions of *Series A*

Entry	F_{nBMA}	T_g^F [a] [°C]	T_{onset} [°C]	T_{midpt} [°C]	T_g [°C]	T_{offset} [°C]	ΔT [°C]	Δc_p [$J \cdot g^{-1} \cdot K^{-1}$]
V18	0.00	107.0[b]	96.0	103.0	107.5	111.0	15.0	0.223
V16	0.10	96.0	83.5	91.0	90.0	97.5	14.0	0.260
V14	0.14	92.0	75.0	82.5	83.0	89.5	14.5	0.234
V12	0.20	85.5	67.0	76.5	77.5	85.5	18.5	0.226
V11	0.32	74.0	55.5	64.5	63.0	72.0	16.5	0.249
V13	0.52	56.0	38.0	50.5	48.0	59.5	21.5	0.199
V15	0.57	52.0	38.0	48.0	48.0	55.5	17.5	0.223
V17	0.66	44.5	36.0	46.0	44.0	54.0	18.0	0.243
V19	1.00	20.0[c]	16.5	29.0	27.5	38.0	21.5	0.230

[a] calculated with *Fox–Equation 3.3.25*; from Literature [b] [90] and [c] [91]

Tab. 3.15.: DSC results of the different copolymer compositions of *Series B*

Entry F_{nBMA}	time [min]	T_{onset} [°C]	T_{midpt} [°C]	T_g [°C]	T_{offset} [°C]	ΔT [°C]	Δc_p [$J \cdot g^{-1} \cdot K^{-1}$]
V28	60	54.0	71.0	71.5	97.0	43.0	0.200
0.0	90	64.5	74.0	76.5	85.0	20.5	0.177
	120	66.0	75.0	73.5	83.5	17.0	0.167
	150	70.5	78.0	77.0	84.0	13.5	0.181
	180	73.5	82.5	81.5	91.0	18.0	0.202
V26	60	71.5	85.0	85.0	98.5	27.0	0.321
0.2	90	71.5	85.5	87.5	101.0	29.5	0.437
	120	74.0	86.0	83.0	96.0	21.5	0.238
	150	76.0	86.2	88.9	95.2	19.2	0.226
	180	74.8	87.0	84.5	98.3	23.5	0.267
V24	60	40.0	51.5	51.0	61.0	21.0	0.204
0.25	90	70.5	80.5	80.5	89.5	19.5	0.245
	120	65.0	77.5	77.0	89.5	25.0	0.308
	150	65.0	74.5	75.5	83.0	18.0	0.240
	180	70.0	77.0	76.0	82.5	12.5	0.185
V22	60	41.5	52.5	54.0	61.5	20.0	0.239
0.33	90	39.0	51.0	47.0	59.5	20.5	0.218
	120	52.5	61.0	60.5	69.5	17.0	0.238
	150	53.0	62.0	65.0	70.0	17.0	0.224
	180	52.4	64.0	64.5	76.5	24.0	0.182

Continuation on next page ...

Entry F_{nBMA}	time [min]	T_{onset} [°C]	T_{midpt} [°C]	T_g [°C]	T_{offset} [°C]	ΔT [°C]	Δc_p $[J \cdot g^{-1} \cdot K^{-1}]$
V21	60	46.0	57.0	58.5	70.0	24.0	0.209
0.5	90	34.0	44.5	41.5	52.5	18.5	0.187
	120	49.5	55.5	57.5	61.0	11.5	0.186
	150	43.0	53.5	48.5	61.5	18.5	0.204
	180	44.5	55.2	54.0	72.0	27.5	0.181
V23	60	45.5	53.0	55.5	59.5	14.0	0.250
0.66	90	41.0	51.5	53.5	63.0	22.0	0.240
	120	44.0	51.5	51.0	59.0	15.0	0.245
	150	42.5	49.5	49.5	55.5	13.0	0.218
	180	43.0	50.5	54.5	58.0	15.0	0.218
V25	60	33.5	45.0	45.5	54.5	21.0	0.248
0.75	90	33.0	42.5	44.5	50.5	17.5	0.224
	120	36.5	43.5	44.5	50.0	13.5	0.197
	150	34.5	44.5	41.5	52.5	18.0	0.234
	180	26.5	39.5	39.5	50.5	24.0	0.229
V27	60	20.5	37.0	37.0	52.0	31.5	0.232
0.8	90	32.5	40.5	42.5	47.5	15.0	0.227
	120	18.0	37.5	32.5	56.0	37.5	0.186
	150	20.0	35.0	33.0	49.0	28.5	0.191
	180	27.5	36.5	39.0	43.0	15.5	0.193
V29	60	54.0	71.0	71.5	97.0	43.0	0.200
1.0	90	64.5	74.0	76.5	85.0	20.6	0.177
	120	66.0	75.0	73.5	83.5	17.0	0.167
	150	70.5	78.0	77.0	84.0	13.5	0.181
	180	73.5	82.5	81.5	91.0	18.0	0.202

The second heating runs of the samples that were taken during the batch copolymerization of experiment V26, see *Figure 3.23*, did no vary significantly. So the glass transition temperature and the glass transition range did not change with the growing of the molar mass. *Figure 3.24* depicts T_g and ΔT against the polymerization time. The T_g staid constant over the whole polymerization and ΔT decreased slightly. Therefore the growth of the molar mass had no influence on the glass transition temperature and range. That was the same for all compositions of *Series B*.

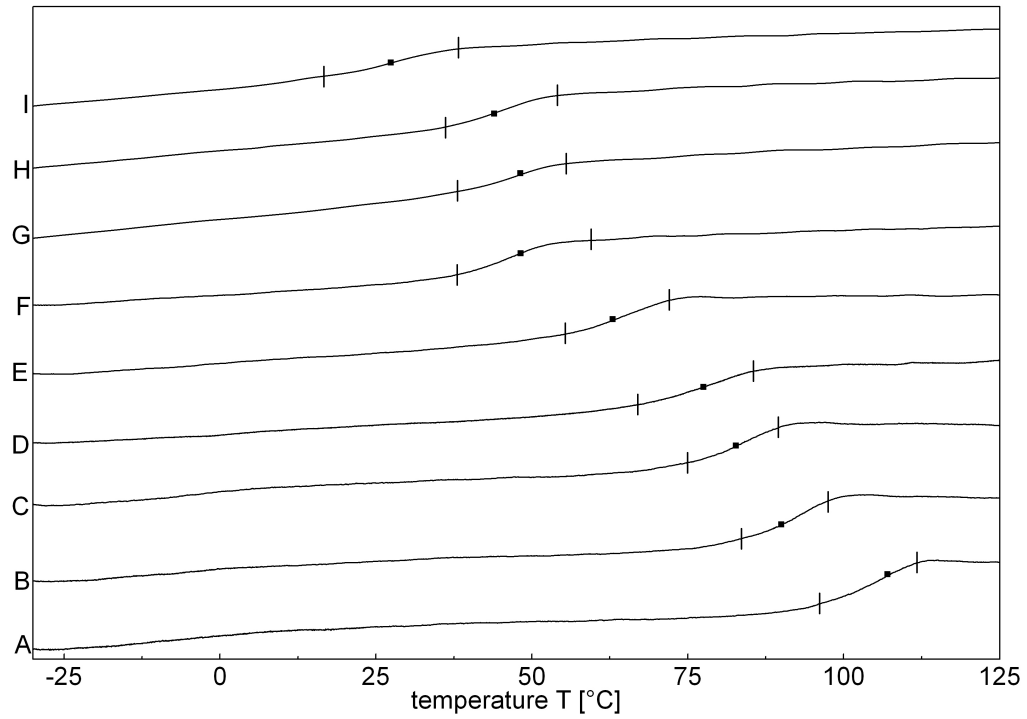

Fig. 3.25.: DSC thermograms of copolymers P[nBMA–co–tBMA] *Series A* with marked glass transition temperature range ΔT and temperature T_g; second heating runs, heating rate $10\,K \cdot min^{-1}$; A – $F_{nBMA} = 0.00$, B – $F_{nBMA} = 0.10$, C – $F_{nBMA} = 0.14$, D – $F_{nBMA} = 0.20$, E – $F_{nBMA} = 0.32$, F – $F_{nBMA} = 0.52$, G – $F_{nBMA} = 0.57$, H – $F_{nBMA} = 0.66$, I – $F_{nBMA} = 1.00$

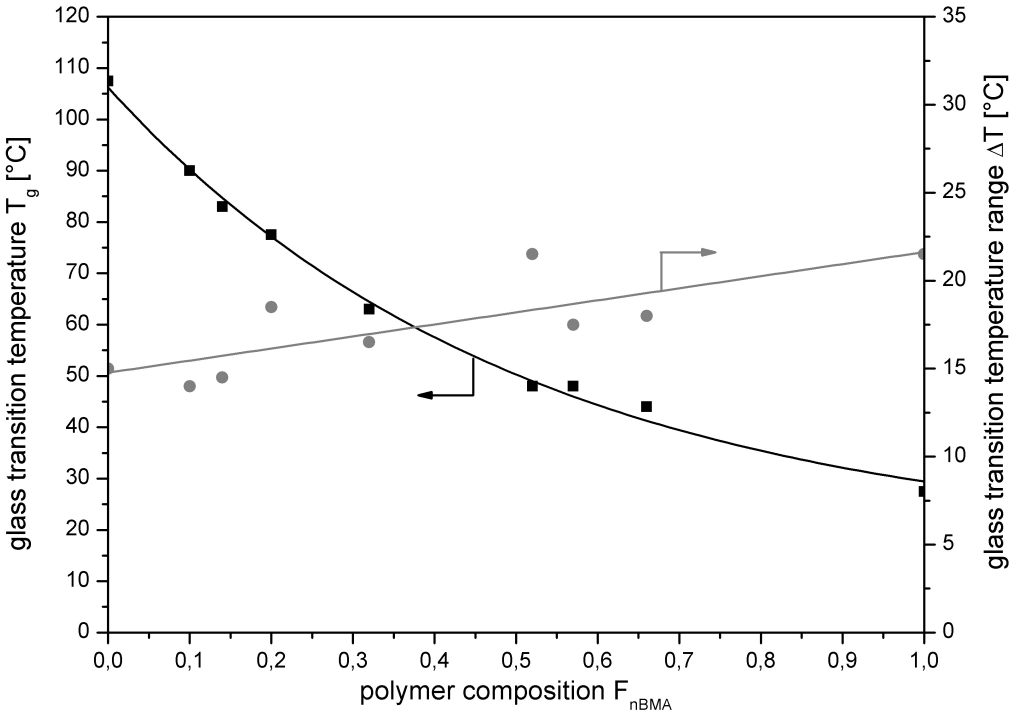

Fig. 3.26.: Glass transition temperature T_g and temperature range ΔT of copolymers P[nBMA–co–tBMA] *Series A*; ■ glass transition temperature T_g, ● glass transition temperature range ΔT

Figure 3.25 shows that there is a strong dependence of the glass transition temperature on the composition of the copolymer. T_g decreased systematically from 107.5 ℃ for PtBMA to 27.5 ℃ for PnBMA. The change of ΔT was not so obviously. The two values are also depicted in *Figure 3.26* against the copolymer composition to point out the trends more explicitly. The dependence of T_g on the copolymer composition was not linear over all compositions. Between F_{nBMA}=0.00 and 0.32 T_g fell linear with the rise of nBMA in the polymer chain. Then the curves became flatter. The equation of the fit is given in *Equation 3.3.23*. ΔT increased unsteady from 15 to 30 ℃. Even here the fit is given in *Equation 3.3.24*.

$$T_g = (17.018 \pm 4.757)\,℃ + (89.206 \pm 4.245)\,℃ \cdot e^{(-1.972 \pm 0.224)\,℃ \cdot F_{nBMA}} \tag{3.3.23}$$

$$\Delta T = (14.772 \pm 0.973)\,℃ + (6.853 \pm 1.966)\,℃ \cdot F_{nBMA} \tag{3.3.24}$$

The T_g–values of the homopolymers fitted good with literature. For PtBMA the literature [90] cited 107 ℃ which was equal to the measurements here and for PnBMA [91] 20 ℃ was named which was slightly higher than the value here (27.5 ℃) but it lay in the determined glass transition region. The theoretical glass transition temperature of a copolymer can be calculated by the *Fox–Equation* (cf. *Equation 3.3.25*). [19]

$$\frac{1}{T_g} = \frac{F_{nBMA}}{T_{g,PnBMA}} + \frac{1 - F_{nBMA}}{T_{g,PtBMA}} \tag{3.3.25}$$

The theoretical values of T_g of the different batch copolymers are listed in *Table 3.14*. All measured T_g of the copolymers were just slightly lower than the calculated ones from the *Fox–Equation 3.3.25*. So this equation is a good possibility to evaluate the glass transition temperature of the gradient copolymers.

Figure 3.27 shows the plot of the reciprocal of the glass transition temperature T_g of the copolymer of *Series A* against the copolymer composition. There the $1/T_g$ values rose nearly linear with the amount of nBMA in the copolymer. The fit is given in *Equation 3.3.26*.

$$\frac{1}{T_g} = (0.0027 \pm 2.614 \cdot 10^{-5})\,K^{-1} + (6.839 \cdot 10^{-4} \pm 5.283 \cdot 10^{-5})\,K^{-1} \cdot F_{nBMA} \tag{3.3.26}$$

with T_{g1} = T_g of PtBMA and T_{g2} = T_g of PnBMA

The *Fox–Equation* (*Equation 3.3.25*) was converted into *Equation 3.3.27* and then the values of intersection and slope of *Equation 3.3.26* were introduced into the equation. Therewith the values of T_g(PtBMA) and T_g(PBzMA) were calculated.

$$\frac{1}{T_g} = \frac{1}{T_{g1}} + \frac{T_{g1} - T_{g2}}{T_{g1} \cdot T_{g2}} \cdot F_{nBMA} \tag{3.3.27}$$

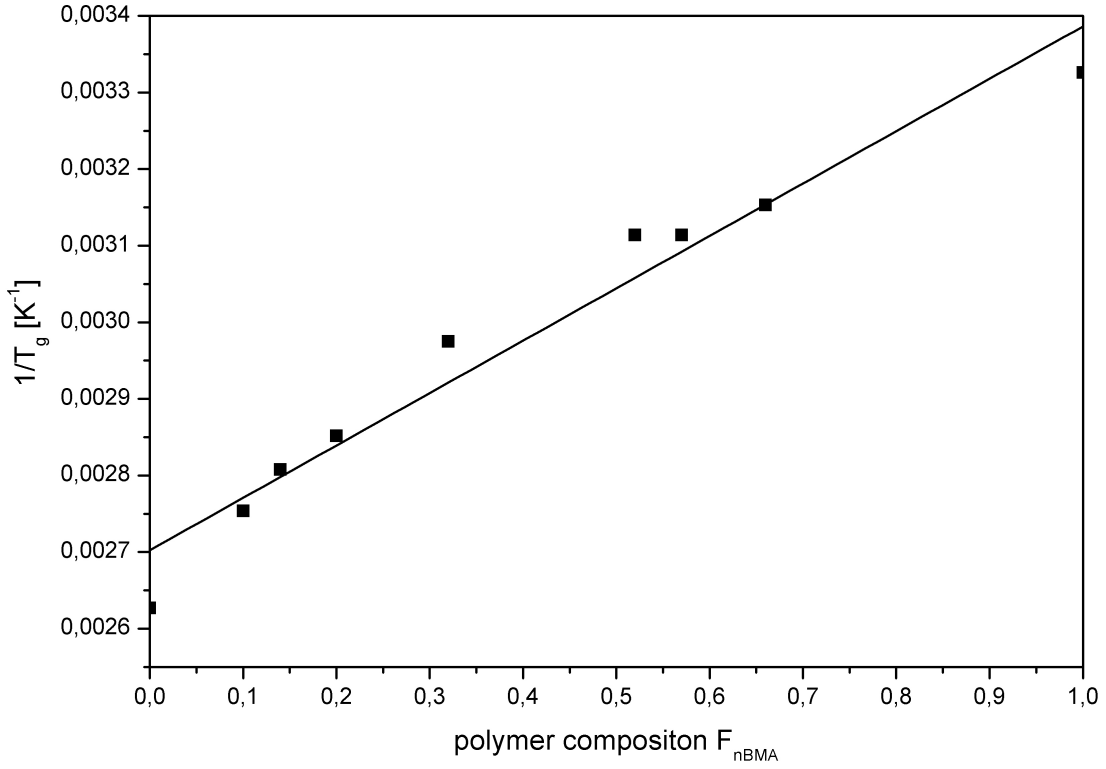

Fig. 3.27.: Reciprocal glass transition temperature T_g of *Series A* against copolymer composition

This linear relation between the glass transition temperature and the composition of the copolymer corresponded with the *Fox–Equation*. The solution of *Equation 3.3.27* with the values of *Equation 3.3.26* were the T_g of the homopolymers and gave 97.2℃ for T_{g1} which is a deviation of 9.6 % from the measured T_g and 9.1 % from the literature values of PtBMA and 22.4℃ for T_{g2} which is a deviation of 18.7 % from the measured T_g and 11.9 % from the literature values of PnBMA. Especially the value for T_{g2} of nBMA was obviously lower than the measured value. The difference to the literature values was not so high. For tBMA the calculated value was smaller than the measured one and the one from literature. With a difference of 10 % the calculated values from the fitting were tolerable. The determination of the glass transition temperatures of the homopolymers with the reciprocal glass transition temperature of the copolymers lead to sufficient results.

3.4. Summary

The copolymerization rates were measured with seven mixtures of nBMA and tBMA to determine the copolymerization rate constants as well as the instantaneous copolymer compositions of the P[nBMA–co–tBMA] copolymers during ATRP reactions as a function of the comonomer composition. The copolymerization parameters were measured ($r_{nBMA} = 0.475$, $r_{nBMA} = 0.886$). The kinetic studies revealed the occurrence of a well controlled polymerization reaction free of side reactions. The compositions of the resulting copolymers were anlaysed with elementary analysis and infra red spectroscopy. The elementary analysis showed that a

change in the monomer mixture had no influence on the polymerization. The different amount of *n*–butyl– and *tert*–butyl–groups inside the polymer chain could be represented in the IR–spectra qualitatively. The quantitative analysis of the IR–spectra resulted in a calibration curve for the copolymer composition out of the peak height of two specific bands. SEC studies supported the findings of the ^{1}H–NMR–spectroscopy–analysis by revealing narrow MWD without multimodalities or indications of termination reactions. The molecular weights were proportional to the monomer conversion, also indicating a high degree of control. The dn/dc values showed no direct relationship between the refractive index increment and the composition of the copolymer. DSC studies showed the glass transition temperatures depended on the copolymer composition and is well described by the *Fox–Equation*. During the batch polymerization the glass transition temperature did not change. The glass transition range is slightly independent on the conversion of the batch copolymerization and the copolymer composition.

4. Hydrolysis of Statistical Copolymers from n– and tert–Butyl Methacrylate

The aim of this thesis is to prepare a functional amphiphilic gradient copolymers. For that reason the *tert*–butyl group of P[tBMA–grad–nBMA] must be converted into a COOH–group via hydrolysis. In this chapter a statistical copolymer from nBMA and tBMA (P[nBMA–co–tBMA], cf. *Chapter 3*) was used as model compound to find an efficient hydrolysis procedure.

The *tert*–butyl group is a classical protections group of OH–groups in organic chemistry. [92] The standard method for the removal of a *tert*–butyl group is acid catalyzed hydrolysis. Especially the use of trifluoroacetic acid is well described in literature. [93] Also in polymer chemistry this cleavage reaction is often used to remove ester groups. Since (meth)acrylic acid can not be polymerized with ATRP [16], the indirect way using *tert*–butyl ester monomers is frequency applied. [94, 95, 96] Another acid that can be used as a cleavage catalyst is methanesulfonic acid. This acid is more often used in bio–organic chemistry for the hydrolysis of proteins [97, 98, 99] but is also known in polymer chemistry [100, 101]. A different way to convert the tert–butyl–ester–group to a carboxylic acid group is a hydrolysis under neutral conditions with trimethylsilyl iodide. This method was introduced because the reaction conditions are milder and it is also possible to work with acid sensitive educts. [102, 103, 104, 105]

4.1. Materials and Methods

4.1.1. Materials

In all hydrolysis experiments the same batch copolymer – P[nBMA–co–tBMA] with F_{nBMA} = 0.32 (experiment V11, *Chapter 3, Table 3.1*) – was used as substrate. The three hydrolysis reagents trifluoroacetic acid (TFA, 99 %, *Alfa Aesar*), methanesulfonic acid (MSA, ≤ 99.5 %, *Aldrich*) and trimethylsilyl iodide (TMSI, 97 %, *Alfa Aesar*, stabilized with copper) were used as received. The same applied to the used solvents chloroform (99.9 %, *Acros*, extra dry over molecular sieve, stabilized), THF (chromasolv, *Aldrich*) and *n*–pentane (*Aldrich*).

4.1.2. Hydrolysis with Trifluoroacetic Acid

P[nBMA–co–MAA]; V41: 0.2 g of the copolymer V11 were dissolved in 1.0 ml of $CHCl_3$ by stirring over night at room temperature. Then 0.37 ml trifluoroacetic acid (TFA) were

added. The mixture was stirred for 22 hours at room temperature. After that the flask was opened and the mixture was diluted with 5 ml THF. Subsequently the solution was dropped in 200 ml of icecold pentane. The precipitated polymer was filtered over a P4 glass filter and dried at room temperature in an oil pump vacuum over night.

^{1}***H–NMR:*** 0.65–1.25 ppm (broad peak, –CH_3, P[nBMA]); 1.3–1.45ppm (broad peak, –CH_2–, P[nBMA]); 1.5–1.61 ppm (broad peak, –CH_2–, P[nBMA]); 1.62–2.05 ppm (broad peak, –CH_3, P[nBMA], P[MAA]); 2.09 ppm (acetone); 3.33 ppm (H_2O); 3.8–4.0 ppm (broad peak, –OCH_2R, P[nBMA]); 12.1–12.5 ppm (broad peak, –COOH, P[MAA])

EA: 61.83 % C, 8.69 % H, (29.48 % O_{calc})

ATR–FTIR: 3600–2350 cm^{-1} (–COOH); 3050–2350 cm^{-1} (–CH_2–, –CH_3); 1725 cm^{-1} (–C=O); 1698 cm^{-1}; 1466 cm^{-1} (–CH_2–, –CH_3); 1388 cm^{-1}; 1256 cm^{-1} (nBu); 1156 cm^{-1} (–C–O–C–); 1065 cm^{-1} (nBu); 1019 cm^{-1}; 997 cm^{-1}; 963 cm^{-1} (nBu); 944 cm^{-1}; 844 cm^{-1}; 750 cm^{-1}; 520 cm^{-1}

4.1.3. Hydrolysis with Methanesulfonic Acid

P[nBMA–co–MAA]; V51: 0.2 g of the copolymer V11 were dissolved in 1.8 g (1.2 ml) $CHCl_3$ was stirred over night at room temperature. Subsequently 0.12 ml of methanesulfonic acid (MSA) were added and the mixture was stirred for 2 hours at room temperature. One spatula–spoon of sodium hydrogen carbonate was added, the mixture was stirred for 30 minutes. 5 ml THF were added, the mixture was filtered over a P4 glass filter and the solution was dropped into 200 ml of icecold pentane. The precipitated polymer was filtered over a P4 glass filter and dried at room temperature for two hours. The copolymer was re–dissolved in 1 ml THF and the solution was dropped into 200 ml of ice cooled water:methanol = 1:1 vol:vol mixture. The precipitated polymer was filtered over a P4 glass filter and dried at room temperature under oil pump vacuum over night.

^{1}***H–NMR:*** 0.65–1.25 ppm (broad peak, –CH_3, P[nBMA]); 1.3–1.45 ppm (broad peak, –CH_2–, P[nBMA]); 1.5–1.61 ppm (broad peak, –CH_2–, P[nBMA]); 1.62–2.05 ppm (broad peak, –CH_3, P[nBMA], P[MAA]); 3.33 ppm (H_2O); 3.8–4.0 ppm (broad peak, –OCH_2R, P[nBMA]); 12.1–12.5 ppm (broad peak, –COOH, P[MAA])

EA: 61.75 % C, 8.36 % H, (29.89 % O_{calc})

ATR–FTIR: 3600–2350 cm^{-1} (–COOH); 3050–2350 cm^{-1} (–CH_2–, –CH_3); 1723 cm^{-1} (–C=O); 1456 cm^{-1} (–CH_2–, –CH_3); 1367 cm^{-1}; 1247 cm^{-1} (nBu); 1142 cm^{-1} (–C–O–C–); 1064 cm^{-1} (nBu); 965 cm^{-1} (nBu); 943 cm^{-1}; 847 cm^{-1}; 802 cm^{-1}; 749 cm^{-1}; 697 cm^{-1}; 516 cm^{-1}; 468 cm^{-1}

4.1.4. Hydrolysis with Trimethylsilyl Iodide

P[nBMA–co–MAA]; V61: A 25 ml Schlenk flask was heated out with a hot gun, set to a temperature of 400 °C, under vacuum for five minutes and then flushed with nitrogen. 0.2 g of the copolymer were dissolved in 2 ml $CHCl_3$ in the flask under nitrogen counter–stream. After three freeze–melt– cycles the flask was filled with nitrogen and the solution was stirred over night at room temperature. 0.26 ml of trimethylsilyl iodide (TMSI) were added and the mixture was stirred for one hour at room temperature. Subsequently the flask was opened, the mixture was diluted with 5 ml THF and the solution was dropped into 50 ml icecold water. The polymer–water mixture was stirred over night at room temperature. The precipitated polymer was filtered over a P4 glass filter and was dried under vacuum over night at RT. The crude polymer was mixed with 1 ml THF and the solution was dropped slowly into 200 ml of ice cooled water:methanol = 1:1 vol:vol mixture and stirred for 2 hours. The precipitated polymer was filtered over a P4 glass filter and dried under vacuum for one hour at room temperature. This step was repeated for three times. The final product was dried in an oil pump vacuum at room temperature over night.

^{1}***H–NMR:*** 0.65–1.25 ppm (broad peak, –CH_3, P[nBMA]); 1.3–1.45 ppm (broad peak, –CH_2–, P[nBMA]); 1.5–1.61 ppm (broad peak, –CH_2–, P[nBMA]); 1.62–2.05 ppm (broad peak, –CH_3, P[nBMA], P[MAA]); 3.33 ppm (H_2O); 3.8–4.0 ppm (broad peak, –OCH_2R, P[nBMA]); 12.1–12.5 ppm (broad peak, –COOH, P[MAA])

EA: 61.83 % C, 8.66 % H, (29.77 % O_{calc})

ATR–FTIR: 3600–2350 cm^{-1} (–COOH); 3050–2350 cm^{-1} (–CH_2–, –CH_3); 1723 cm^{-1} (–C=O); 1698 cm^{-1}; 1466 cm^{-1} (–CH_2–, –CH_3); 1388 cm^{-1}; 1246 cm^{-1} (nBu); 1154 cm^{-1} (–C–O–C–); 1064 cm^{-1} (nBu); 1049 cm^{-1}; 963 cm^{-1} (nBu); 943 cm^{-1}; 843 cm^{-1}; 749 cm^{-1}; 632 cm^{-1}; 519 cm^{-1}

4.1.5. Characterization

All characterization–methods were the same as with the batch copolymers of *Chapter 3*. The used methods were:

- ^{1}H–NMR spectroscopy
- elementary analysis
- ATR–FTIR–spectroscopy
- size exclusion chromatography
- differential scanning calorimetry

The same instruments under the same conditions were used for the investigation of the resulting copolymers.

X–ray Fluorescence Spectroscopy

The XRF–measurement was performed with a PANalytival Axios spectrometer. The interpretation of the data was done with the device software SuperQ 5.0. The sample–pan was lined with a polypropylene film. The measurement was done under helium as protection gas.

Microscopy

The optical micrographes were taken with a with a Zeiss "Axio Imager.A1m" microscop and a Zeiss 10x/0.25 Pol objective in bright–field transmission mode. The sample was heated up on a Mettler Toledo FP82 HT Hot Stage controlled with a FP90 Central Processor. The sample was heated up from RT to 60 °C within 5 min and then the temperature was kept for 2 min. Subsequently the samples were heated up to 300 °C with 5 °C per minute. After 300 °C were reached the heating table was deactivated the sample was allowed to cool down to RT.

4.2. Results and Discussion

The classical acid catalyzed ester hydrolysis reaction is well known. The reaction scheme of it is depicted in *Figure 4.1.*

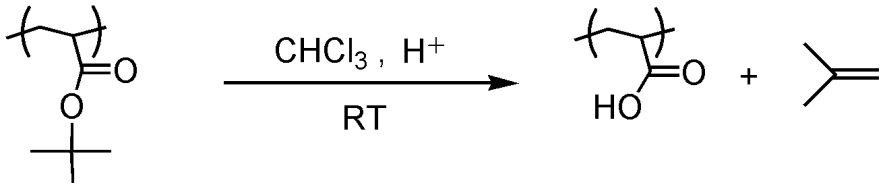

Fig. 4.1.: Reaction scheme of the acid catalyzed ester hydrolysis

The hydrolysis under neutral conditions with TMSI is a two step reaction. In a first step the *tert*–butyl group is replaced by a trimethylsilyl–group (TMS) that can be hydrolyzed in the presence of H_2O. The scheme of this is depicted in *Figure 4.2.*

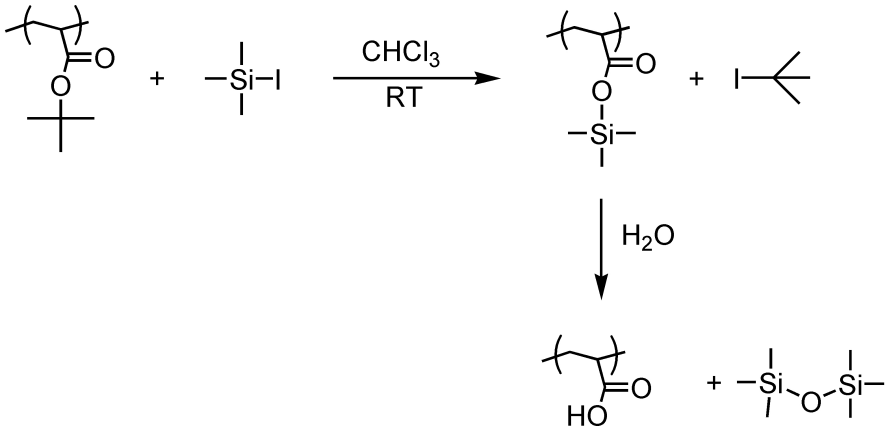

Fig. 4.2.: Reaction scheme of *tert*–butyl ester cleavage in the presence of $(CH_3)_3$Si–I

In this section the observations made with the hydrolysis reactions are described. The three experiments were outlined as *Series D.* The reaction procedure with the observations is given and also the analysis of the hydrolysis products and their discussion. Two of the reactions were acidic hydrolysis, one with TFA (V41) and another with MSA (V51) as reagent. The third cleavage reaction used TMSI (V61) as reagent, so under neutral conditions. In *Table 4.1* an overview on the three different hydrolysis reactions with conditions and yields is listed.

Tab. 4.1.: Hydrolysis experiments on P[nBMA$_{0.32}$–co–tBMA$_{0.68}$]

Educt	Product	Reagent	Conditions	yield [g]	yield [%]
V11	V41	TFA	RT; 1.0 ml CH_2Cl_2; 22 h	0.14	93.3
V11	V51	MSA	RT; 1.2 ml CH_2Cl_2; 2 h	0.12	80.0
V11	V61	TMSI	RT; 2.0 ml CH_2Cl_2; 1 h	0.12	80.0

Prior to the synthesis the required amount of hydrolysis reagent was calculated by means of *Equation 4.2.1*. The designations of the different variables and their values are given in *Table 4.2* together with the resulting volumes of the different entries.

$$V_{HR} = \frac{m \cdot F_{tBMA} \cdot x \cdot M_{HR}}{M_{tBMA} \cdot \delta_{HR}} \tag{4.2.1}$$

Tab. 4.2.: Variables and values of *Equation 4.2.1*

Variable	Unity	Designation	V11	TFA	MSA	TMSI
m		mass polymer	0.2			
F_{tBMA}		molar fraction of tBMA	0.68			
M_{tBMA}	$g \cdot mol^{-1}$	molar mass tBMA	142.2			
x		multiplicity factor HR		5	2	2
M_{HR}	$g \cdot mol^{-1}$	molar mass HR		114.02	96.11	200.09
δ_{HR}	$g \cdot ml^{-1}$	density HR		1.48	1.48	1.47
V_{HR}	ml	Volume HR		0.37	0.12	0.26

HR = hydrolysis reagent: TFA, MSA, TMSI

The polymer samples were stirred over night in CH_2Cl_2 to ensure the complete dissolution of the polymer. The first tested hydrolysis reagent was trifluoroacetic acid (cf. experiment V41, *Table 4.1*). After the addition of the TFA the mixture had to be stirred for 22 hours to obtain total conversion. The mixture appearance changed from colorless to light brown, simultaneously the batch became viscous over night. It was not necessary to remove the byproduct (2–methyl–1–propene) separately because it evaporated while stirring at room temperature due to its low bowling point of -6.9 °C. [106] After cleaning and drying the product V41 was a white powder.

The next reagent was methanesulfonic acid (cf. experiment V51, *Table 4.1*). The reaction was much faster than the hydrolysis with TFA. For total conversion only 2 hours were needed. Some minutes after the addition of MSA the mixture became a light brown gel. During the second hour the gel liquefied again. The synthesis instruction included the neutralization of the excess of acid after the reaction time. [101] The obtained solution was more easier to handle for purification. However, due to the presence of the neutralization, a second precipitation–step in a water : methanol mixture was necessary to obtain a salt–free polymer. Also the product V51 was a white powder after purification.

The last tested reagent was trimethylsilyl iodide (cf. experiment V61, *Table 4.1*). The reaction was much faster than the previous one. After the addition of the TMSI the mixture got dark brown because the reagent released iodine. The removal of the byproducts 2–iodo–2–methylpropane and 1,1,1,3,3,3– hexamethyldisiloxane was much more time consuming. Both have a boiling point around 100 °C [106] and so had to be washed out. After the first precipi-

tation of the polymer in water the polymer was dark brown. The precipitation was repeated for three times in water and methanol. With every precipitation the color of the product became more bright until it was also a white powder, finally.

The expected yield for total conversion was calculated according to *Equation 4.2.2.*

$$y_{theo} = \frac{m \cdot F_{tBMA} \cdot M_{MAA}}{M_{tBMA}} + m \cdot (1 - F_{tBMA}) \tag{4.2.2}$$

with y_{theo} – theoretical yield, m – mass of the polymer, F_{tBMA} – ratio of tBMA in the polymer = 0.68, M_{MAA} – molar mass of MAA = 86.09 $g \cdot mol^{-1}$, M_{tBMA} – molar mass of tBMA = 142.2 $g \cdot mol^{-1}$

At complete conversion a total yield of 0.15 g of the methacrylic acid copolymer should be obtained. The results for the three synthesis are given in *Table 4.1.* The highest yield gave experiment V41 with 93.3 % while the two other methods resulted in about 80 %. All yields were in an acceptable range.

The neutralization of the excess MSA with sodium hydrogen carbonate can lead to an exchange of the OH–groups to the respective sodium–salt. A sample of the hydrolysis–product of V51 was analyzed with XRF–spectroscopy to determine the amount of sodium inside the sample. Based on the fact that no sodium was found in the sample, any loss of OH–groups due to neutralization can be excluded.

Because of the change from *tert*–butyl–groups to OH–groups along the copolymer chain the solubility of the polymers should have changed. This was tested before the structural analysis of the products was done. The educt was well soluble in aprotic solvents like chloroform, acetone and THF but not in protic solvents like water and methanol. The products could be solved in DMSO and methanol, however, not in chloroform, acetone and THF. After some hours of stirring the respective polymer/ solvent mixture were still opaque. In water the hydrolysis products were also not soluble. The solubilities of the educt and the products are listed in *Table 4.3.* The change of the solubility from educt to product was characteristic for the change of the functional groups along the polymer chain.

Tab. 4.3.: Table of solubility of educt V11 and hydrolysis products *Series D*

Entry	H_2O	MeOH	DMSO	Acetone	CH_2Cl_2	THF
V11	–	–	n. m.*	+	+	+
V41	–	±	+	–	–	–
V51	–	±	+	–	–	–
V61	–	±	+	–	–	–

* n. m. ≡ not measured, 10 mg in 0.5 ml, RT, 6 h
\+ = soluble, – = insoluble, ± = difficultly soluble

With the results from the solubility–tests first the hydrolysis–products were analyzed by ^{1}H–NMR–spectroscopy, dissolved in DMSO–d_6 while educt V11 was measured in $CDCl_3$. The chemical shift in the ^{1}H–NMR–spectra of educt and products were not the same due to the different solvents but the comparison was still possible. The molecular structures of the educt and the product, together with the numbering of the carbons of the experiment V41 to 61 are shown in *Figure 4.3*. In *Figure 4.4* the ^{1}H–NMR–spectrum of the substrate material V11 and the spectra of the three hydrolysis products are depicted in comparison.

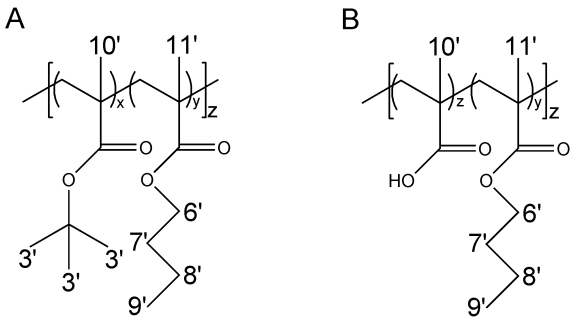

Fig. 4.3.: Molecular structures of educt V11 and products of polymers of *Series D* with carbon–atom labels; A – educt P[tBMA$_{0.32}$–co–nBMA$_{0.68}$] and B – product P[MAA$_x$–co–nBMA$_y$] (z = x + y = 1)

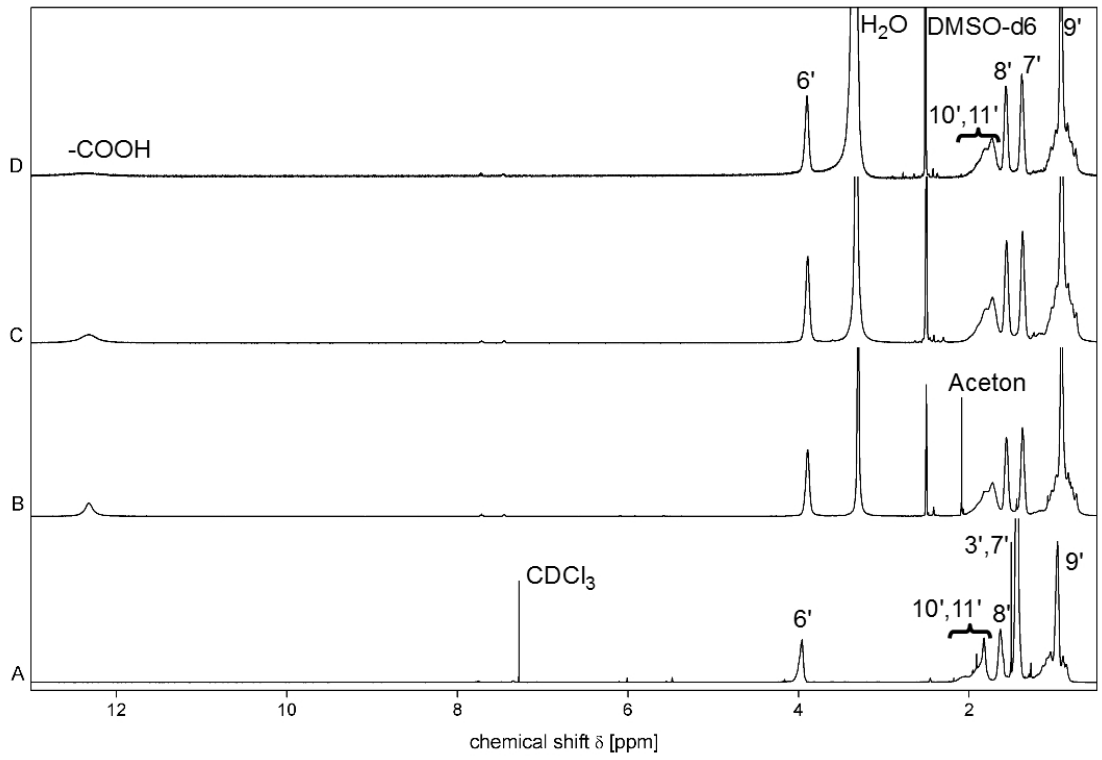

Fig. 4.4.: Comparison of ^{1}H–NMR–Spectra of educt V11 and the polymers of *Series D*; A – educt P[tBMA$_{0.32}$–co–nBMA$_{0.68}$] V11, B – V41 hydrolysis with TFA, C – V51 hydrolysis with MSA, D – V61 hydrolysis with TMSI

The intensity of the mixed broad peak ranging from 1.3 to 1.45 ppm caused by the signals of the protons 3' and 7' shrank relative to the signals 8' or 9' which remained constant on comparing educt and product. The reason was the absence of the signal 3' from the protons of the *tert*–butyl group in the product. The –COOH–signal could be monitored between 12.0 to 12.75 ppm. Furthermore it was clearly to see that water was used during the hydrolysis with TMSI. In all ^{1}H–NMR–spectra of *Series D* a H_2O signal was present, also because the DMSO–d_6 was not dry, but in the spectra of compound V61 the peak was much bigger than in the two other spectra. In the spectra of V41 an additional peak from acetone appeared from the NMR–tube which was not completely dry. The ^{1}H–NMR–spectra of V61 did not show signals in the range below 0 ppm. That means that no TMS–groups remained in the polymer chain and that the hydrolysis reaction under neural conditions proceeded completely. From the ^{1}H–NMR–spectra it can be concluded that all three reagents quantitatively removed the *tert*–butyl ester groups from the copolymer.

After the NMR–analysis the copolymers were assayed by elementary analysis. The results of these measurements are listed in *Table 4.4*. The theoretical values were calculated for a 100 % conversion of the hydrolysis of the polymer P[nBMA$_{0.32}$–co–MMA$_{0.68}$]. The measured values differed not much from the set values, hence virtually a total conversion of the *tert*–butyl to –COOH–groups had occurred. Furthermore, the well agreement between theoretical and experimental element composition showed that the resulting copolymers were clean and dry. Since all three entries showed the same values, all three synthesis methods gave fairly similar products.

Tab. 4.4.: Elementary analysis of educt V11 and the polymers of *Series D* with divergence from the set value

Entry		C [%]	ΔC	H [%]	ΔH	O [%]	ΔO
V11	theory	67.57		9.92		22.50	
	is	67.15	-0.42	9.76	-0.16	23.09	0.59
	theory	60.95		8.29		30.75	
V41	is	61.83	0.88	8.69	0.40	29.48	-1.27
V51	is	61.75	0.80	8.36	0.07	29.89	-0.86
V61	is	61.83	0.62	8.66	0.37	29.77	-0.98

The hydrolysis–products were also investigated by ATR–FTIR–spectroscopy and their spectra were compared with the IR–spectra of the educt. The IR–spectra of the four polymers are depicted in *Figure 4.5*. In *Section 3.3.2* two bands at 970 cm^{-1} and 850 cm^{-1} were introduced that are characteristic for the polymer–incorporated tBMA and nBMA units. When the two bands were observed the change of the spectra were pronounced. *Band 1* at 970 cm^{-1} caused by nBMA units did not change much, but *band 2* at 850 cm^{-1} representing tBMA differed strongly. The change was so strong that a comparison of peak height and peak area of educt

and products was not possible. The loss of band intensity at 850 cm^{-1} clearly indicates that the hydrolysis products no longer contained tBMA–ester side groups. Also the range between 3400 to 2400 cm^{-1} changed from educt to product. A broad band from 3100 to 3380 cm^{-1} appeared which could be assigned to the vibrational band of the carboxylic acid OH–group. A third change exhibited the band at 1710 cm^{-1} which is the vibrational band of the ester C=O group. In the IR–spectrum of the educt the band was a small singlet, while in the spectra of all products a broader doublet band was found. The double band maxima at 1720 cm^{-1} and 1700 cm^{-1}. The literature refers 1720 cm^{-1} to ester C=O vibration, while 1700 cm^{-1} belong to the vibration of carboxylic acid C=O groups. [85] In the spectrum of experiment V61 (hydrolysis with TMSI) the vibrational CH_3– and –CH_2– bands between 3050 to 2800 cm^{-1} increased obviously in comparison to the other spectra of experiment V41 (hydrolysis with TFA) and experiment V51 (hydrolysis with MSA). The second different of the spectrum from experiment V61 to the spectra from V41 and V51 was that the acid carbonyl vibration at 1700 cm^{-1} was less pronounced.

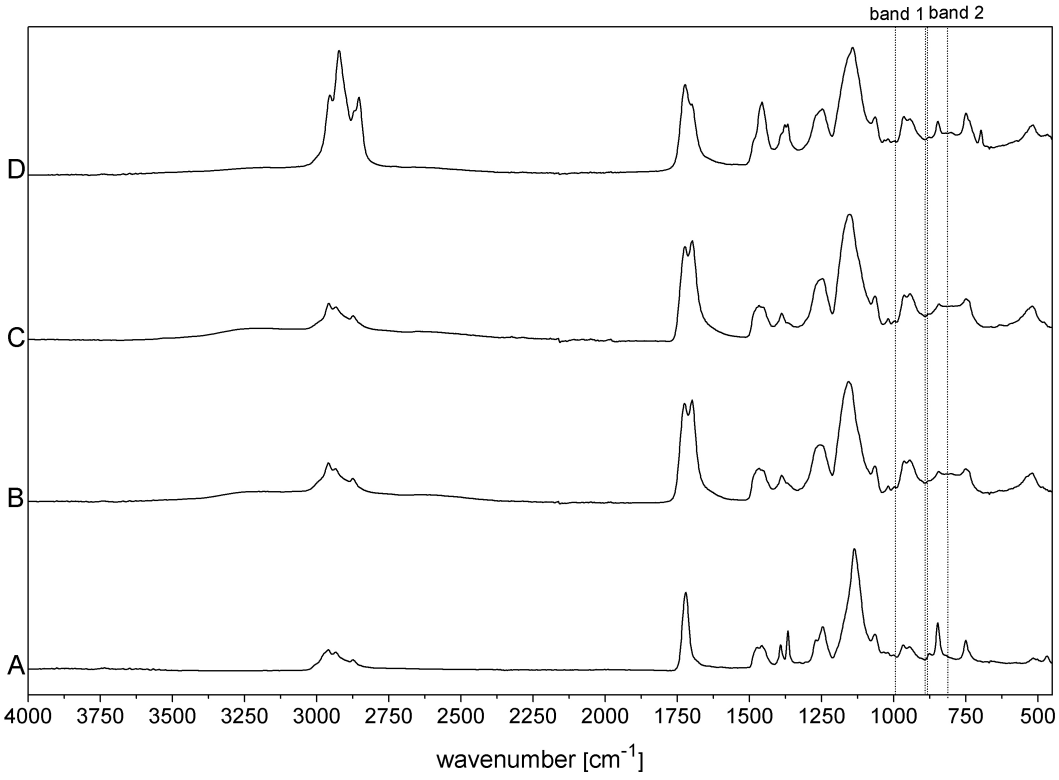

Fig. 4.5.: Comparison of the ATR–FTIR–spectra of educt V11 and the polymers of *Series D*; A – educt P[$tBMA_{0.32}$–co–$nBMA_{0.68}$] V11, B – V41 hydrolysis with TFA, C – V51 hydrolysis with MSA, D – V61 hydrolysis with TMSI (Spectra normalized to $A_{1136} = 1$)

After the structural analysis the molar masses of the polymers were determined. The hydrolyzed copolymers were not soluble in THF anymore, cf. *Table 4.3*. For the analysis with the SEC about 0.4 mg of the copolymer was mixed with 1 ml THF and two drops of TMSI. The mixture was stirred over night at RT and the copolymer was found to be dissolved the next day. The dn/dc of the solution could not be determined, because of the presence of

free TMSI: The brown liquid disturbed the measurement. For this reason only the relative molar mass based on a polystyrene–calibration ("PS–Standard–values") was determined from the elution volume V_E of the samples and *Equation 3.3.22*. The RI–detector signals of the samples from *Series D* are given in *Figure 4.6* together with the signal from the educt.

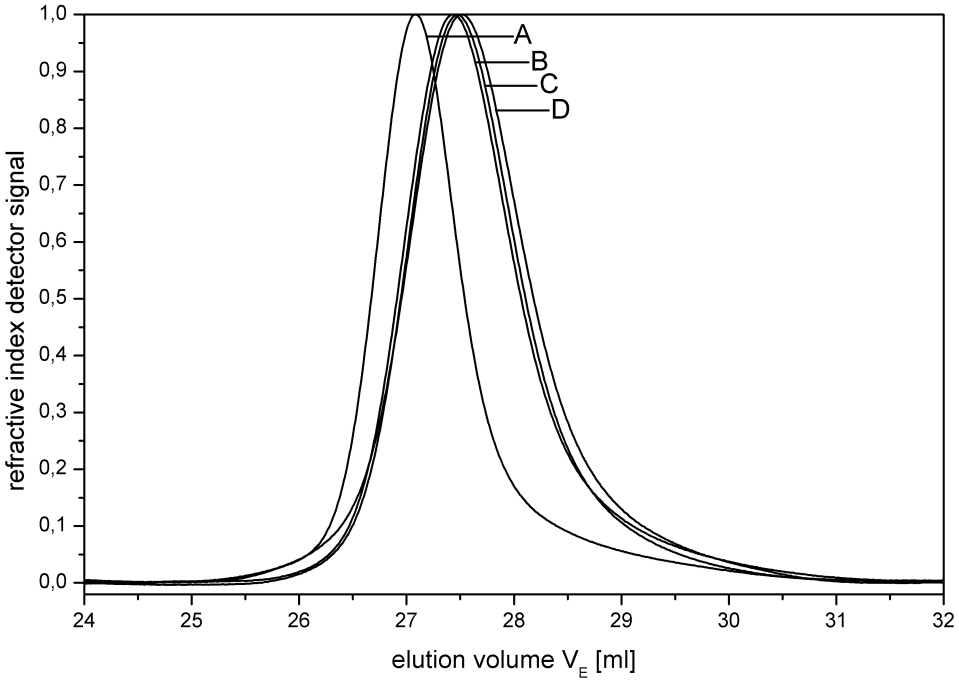

Fig. 4.6.: Comparison of SEC elution diagrams of educt V11 and the polymers of *Series D*; A – educt P[tBMA$_{0.32}$–co–nBMA$_{0.68}$] V11, B – V41 hydrolysis with TFA, C – V51 hydrolysis with MSA, D – V61 hydrolysis with TMSI

Tab. 4.5.: SEC results of the educt V11 and the polymers of *Series D*

Entry	V_E[a] [ml]	M[b] [g · mol^{-1}]	ΔM [g · mol^{-1}]	[%]
V11	27.26	22680		
V41	27.34	21760	920	4.06
V51	27.40	21080	1600	7.06
V61	27.42	20890	1790	7.89

[a] Peak elution volume
[b] relative values, based on PS–Standard calibration *Eq. 3.3.22*

The RI–curves of the three hydrolysis–products, very similar in shape and elution volume, were shifted towards higher elution volumes, i. e. lower molecular weights in comparison to the source material. The results are listed in *Table 4.5*. The molar masses of all three products were lower than the educt. They decreased between 4 to 8 %. However, the measured molar masses of the products were higher than expected, since the molar mass should be around 18600 g · mol^{-1}. This was an expectable result, due to the relative determination

of the molar weights. The differences between the relative and the absolute determination were shown in *Section 3.3.3*, *Table 3.13* for the batch copolymers of experiment V11 to V19. Furthermore relative weights were higher than the absolute ones. For a relative molecular weight determination only the maximum elution volume is used and this is always higher than the average molar mass of a sample.

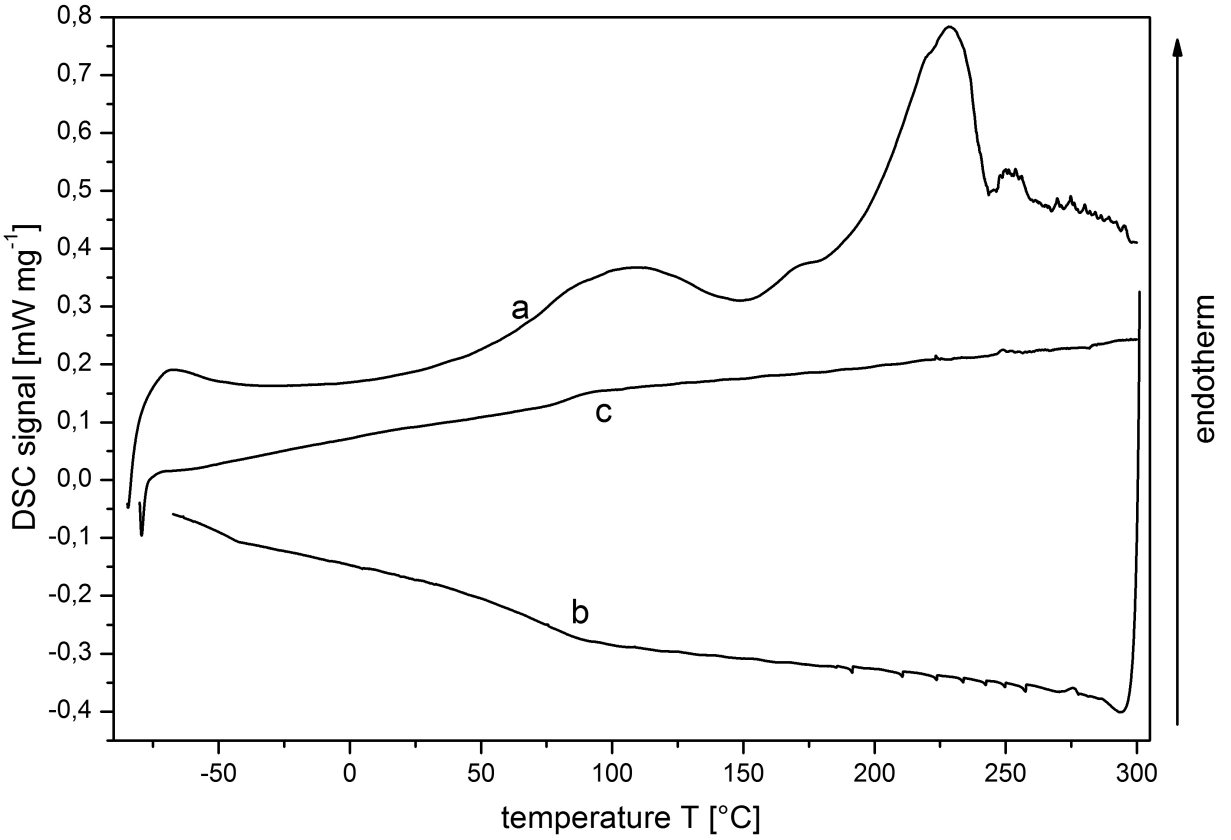

Fig. 4.7.: DSC thermogram of experiment V51 – hydrolysis with MSA; a – first heating run, b – first cooling run, c – second heating run; heating rate $10\,\mathrm{K}\cdot\mathrm{min}^{-1}$

In the final series of experiments the thermal behavior of the hydrolyzed copolymers was investigated. The samples were analyzed by means of differential thermal analysis (DSC) and thermo–optical–analysis (TOA). With DSC–measurements two heating runs from -80 to 300 °C and one cooling in between run have been performed. Note that the samples were measured in DSC–pans with a hole punched in the covering lid allowing for the evaporation of volatiles. The full DSC-thermogram of experiment V51 is given in *Figure 4.7*. The first heating run showed a broad endothermic peak between 50 °C and 150 °C and a second one between 160 °C and 240 °C. Above 240 °C the curve was noisy. The second heating run showed a small glass transition step around 90 °C. To find out if the samples lost weight, the DSC–pans were weighted before and after the DSC-measurement. The results are listed in *Table 4.6*, showing a weight loss of 12 to 15 % during the complete measuring cycle. That meaned the samples were decomposed by the heat and partly lost weight due to the evaporation of decomposition products.

Tab. 4.6.: Weight loss of substance weight during DSC measurement of the polymers of *Series D*

Entry	weighted portion	loss	
	[mg]	[mg]	[%]
V41	4.310	0.574	13.3
V51	11.384	1.730	15.2
V61	5.578	0.666	11.9

For an overview all three DSC thermograms of the hydrolyzed polymers in comparison to the thermogram of the educt V11 are depicted in *Figure 4.8*. During the first heating run the two broad peaks of the three products were the obvious differences to the educt. In the thermogram of the educt one peak between 50 °C and 85 °C during the first heating run. In the first heating run of the thermograms of the products the first peak was between was found 5 °C and 125 °C. There was a second peak in the first heating run between 150 °C and 275 °C. Since the educt was not heated up to 300 °C a comparison was not possible in this temperature range. The products were heated to a higher temperature, because at 150 °C an endotherm peak started to rise that was not present in the educt where instead a plateau followed a tiny endothermal signal. A further difference between the thermograms of educt and products was found during the second heating run. In the thermogram of the educt the second heating run showed a glass transition step at 63 °C. Such as step was not to find in the thermograms of any product even when the products were heated up to 200 °C or to 300 °C.

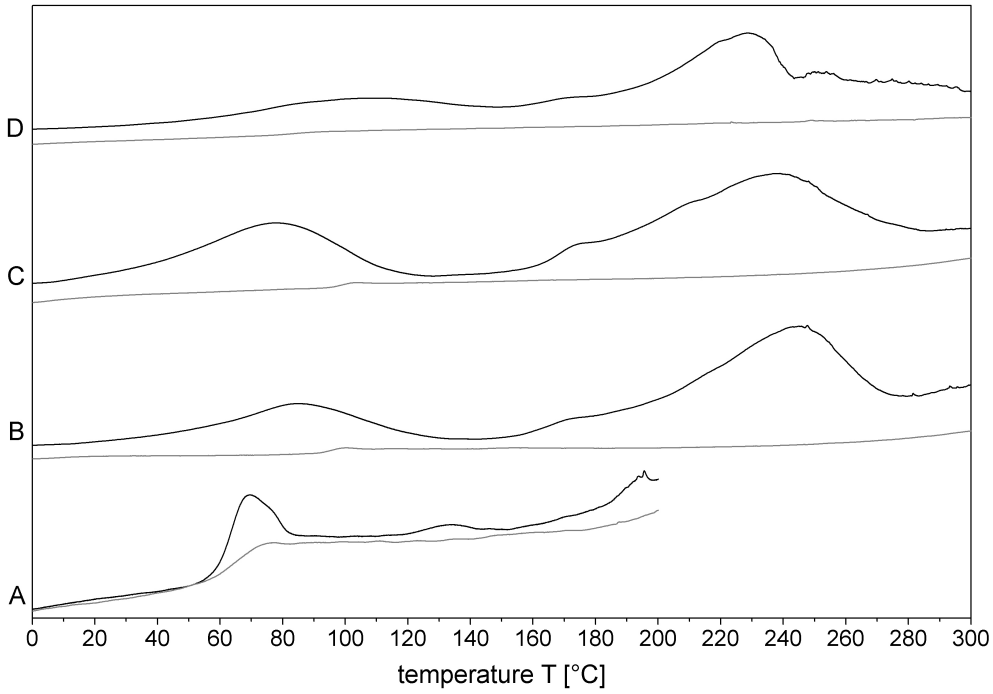

Fig. 4.8.: DSC thermograms of the first and second heating runs of educt V11 and hydrolysis–products *Series D* (A – educt P[tBMA$_{0.32}$–co–nBMA$_{0.68}$] V11, B – V41 hydrolysis with TFA, C – V51 hydrolysis with MSA, D – V61 hydrolysis with TMSI; black line – first heating run, grey line – second heating runs, heating rate $10\,\mathrm{K}\cdot\mathrm{min}^{-1}$

To optical out what happened during the DSC–measurements sample V51 was observed under the microscope while it was heated up from RT to 300 °C. Pictures, as shown in *Figure 4.9*, were taken during the heating-up at intervals of (i) $10\,°C \cdot min^{-1}$ between 80 °C and 190 °C, (ii) $5\,°C \cdot min^{-1}$ between 190 °C and 250 °C and (iii) $10\,°C \cdot min^{-1}$ between 250 °C and 300 °C.

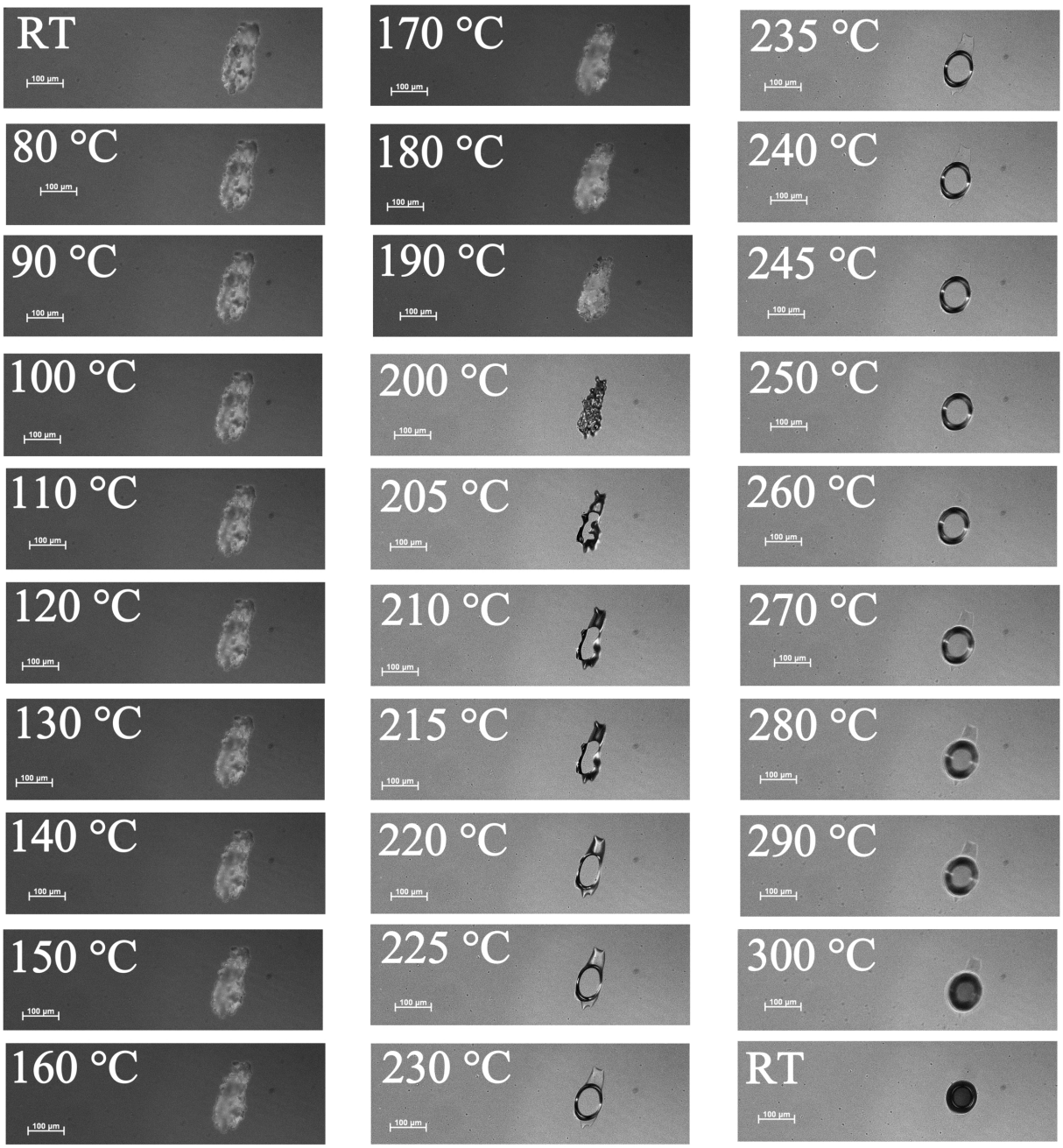

Fig. 4.9.: Thermo optical analysis of experiment V51 from RT to 300 °C

As was clearly seen the sample did not change up to 190 °C. Thus, the first peak in the DSC thermogram between 50 °C and 150 °C could be caused by evaporation of residual water or solvent. Above 190 °C the sample changed obviously. The samples became liquid and a gas bubble was formed. When a temperature of 300 °C was reached just a brown spot remained. Hence the second peak in the DSC thermogram resulted from the decomposition of the sample.

The observed small glass transition step at 95 ℃ must be attributed to the remaining, but thermally altered, i. e. cured residue of the sample and cannot be taken as a characteristic property of the original polymer.

4.3. Summary

The *tert*–butyl–ester groups of the educt polymer V11 P[nBMA$_{0.32}$–co–tBMA$_{0.68}$] have been cleaved to obtain P[nBMA$_{0.32}$–co–MAA$_{0.68}$] by means of TFA, MSA and TMSI. All three ways of hydrolysis worked well. The characterization with ^{1}H–NMR–spectroscopy and elementary analysis showed the absence of any *tert*–butyl–groups in the polymer chains and hence a complete conversion with all hydrolysis. The observed changes in the ATR–IR–spectra supported these findings. The vibrational band of OH-groups evolved and the fingerprint–region exhibited changes of the vibrational bands assigned to the *tert*–butyl–group that suggested its disappearance. The SEC proved a decrease in lower molar masses of *Series D*. The DSC analysis and the observation of a sample under the microscope during heating–up from RT to 300 ℃ demonstrated the decomposition of the sample above 190 ℃.

The three hydrolysis reactions gave similar results with respect to yield and degree of hydrolysis. The hydrolysis with TMSI was the fastest but the work–up was tedious. The hydrolysis with TFA gave slightly higher yields but needed much longer (22 h) than using MSA (2 h). For these reasons it was decided to exclusively use the methanesulfonic acid (MSA) hydrolysis procedure for all further hydrolysis reactions in the next steps of the thesis.

5. Synthesis of Gradient Copolymers from n– and tert–Butyl Methacrylate by means of Semibatch Polymerization

This part of the work describes the synthesis and the characterization of functional amphiphilic gradient copolymers. With the results from the kinetic studies on the statistical tBMA/nBMA copolymers (cf. *Section 3.3.1*) the monomer addition programs required for the semibatch polymerization of the gradient copolymers can be calculated. The resulting gradient copolymers P[tBMA–grad–nBMA] are analyzed in the same way as the statistical copolymers before and the results are compared. The four syntheses were subsumed under the term *Series C*.

5.1. Materials and Methods

5.1.1. Materials

Chemicals and pre–treated of chemicals were the same as detailed in *Section 3.1.1*.

- monomers
  - *n*–butyl methacrylate (nBMA, 99 %, *Sigma–Aldrich*)
  - *tert*–butyl methacrylate (tBMA, 98 %, *Alfa Aesar*)
- initiator: *para*–toluenesulfonyl chloride (pTSC, 98 %, *Sigma–Aldrich*)
- catalyst: copper(I) chloride (97 %, *Sigma–Aldrich*)
- ligand: N,N,N',N',N"–pentamethyldiethylenetriamine (PMDETA, 99 %, *Sigma–Aldrich*)
- solvent: 2–butanone (MEK, *BDH Prolabo*, chromasol.)

5.1.2. Semibatch Copolymerization of Gradient Copolymers

The experimental setup of the semibatch copolymerization is depicted in *Figure 5.1*. For the synthesis the two monomers were prepared separately. Here is described the preparation of polymer V31 as example: Two Schlenk flasks, one of 100 ml volume to hold the stock solution

and one of 50 ml to store the feed solution were heated out with a hot gun (air temperature $\approx$ 400 °C) under vacuum for five minutes and then flushed with nitrogen. Subsequently the stock solution consisting of 0.1411 g ($7.403 \cdot 10^{-4}$ mol) pTSC, 9.4364 g (0.0664 mol) tBMA, 0.1283 g ($7.403 \cdot 10^{-4}$ mol) PMDETA and 0.0733 g ($7.403 \cdot 10^{-4}$ mol) CuCl was weighted in a screw–cap glass. The mixture was rinsed into the 100 ml Schlenk flask with 9.4364 g MEK under nitrogen counter flow. In a second screw–cap glass was weighted in the feed solution monomer, 11.2338 g (0.0790 mol) nBMA. It was flushed into the 50 ml Schlenk flask with 11.2338 g MEK likewise under nitrogen counter stream. All investigated compositions are listed in *Table 5.1.*

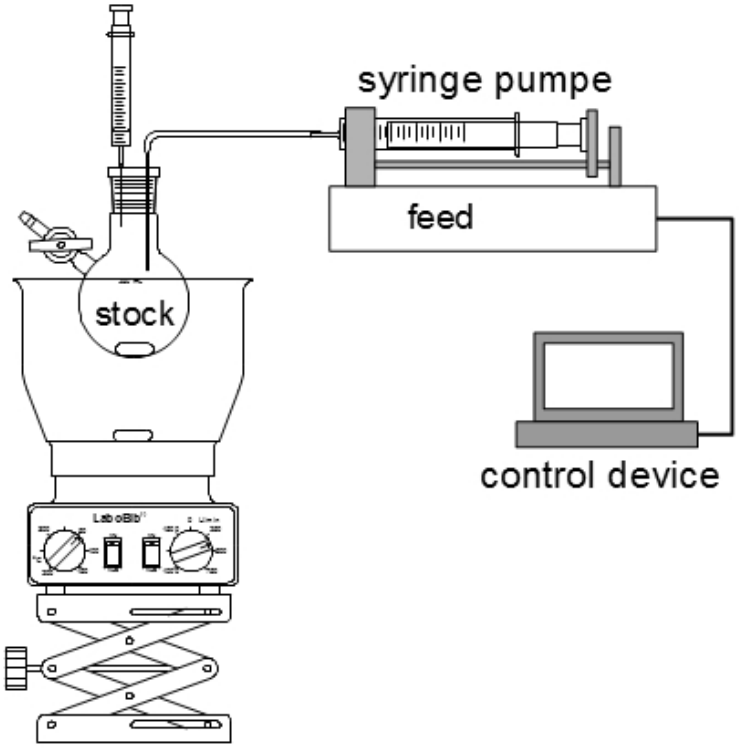

Fig. 5.1.: Experimental setup for semibatch copolymerization

The two solutions were degassed by means of five freeze–melting–cycles. Than the feed solution was transferred into a gas–tight syringe under nitrogen flow and mounted in the syringe pump. The stock solution was placed in an oil bath at 80 °C with stirring. At this time the sampling began. After 30 min for the pre–polymerization the monomer addition program was started.

During the polymerization aliquot samples with volumes of about 0.05 ml were taken at 0, 15, 30, 40, 50, 60, 70, 80, 90, 120, 150, 180, 210, 270, 330, 390, 450 and 1440 min. The samples were immediately given into 0.5 ml ice cooled $CDCl_3$ without further purification. Furthermore 1 ml samples were taken from the solution and precipitated in 20 ml of ice cooled water : methanol = 1 : 1 vol : vol mixture at 0, 90, 150, 210, 330 and 450 min.

Tab. 5.1.: Compositions of the semibatch copolymerization solutions of tBMA/nBMA – *Series C*

Entry	f^0_{tBMA}	Solution	Component	n [mol]	m [g]
V31	0.5	Stock	tBMA	0.0664	9.4364
			pTSC	$7.403 \cdot 10^{-4}$	0.1411
			PMDETA	$7.403 \cdot 10^{-4}$	0.1283
			CuCl	$7.403 \cdot 10^{-4}$	0.0733
			MEK	0.1309	9.4364
		Feed	nBMA	0.0790	11.2338
			MEK	0.1558	11.2338
V32	0.65	Stock	tBMA	0.0863	12.2673
			pTSC	$7.458 \cdot 10^{-4}$	0.1422
			PMDETA	$7.458 \cdot 10^{-4}$	0.1293
			CuCl	$7.458 \cdot 10^{-4}$	0.0738
			MEK	0.1701	12.2673
		Feed	nBMA	0.0553	7.8637
			MEK	0.1091	7.8637
V33	0.75	Stock	tBMA	0.0995	14.1546
			pTSC	$7.494 \cdot 10^{-4}$	0.1429
			PMDETA	$7.494 \cdot 10^{-4}$	0.1299
			CuCl	$7.494 \cdot 10^{-4}$	0.0742
			MEK	0.1963	14.1546
		Feed	nBMA	0.0395	5.6169
			MEK	0.0779	5.6169
V34	0.85	Stock	tBMA	0.1128	16.0419
			pTSC	$7.530 \cdot 10^{-4}$	0.1436
			PMDETA	$7.530 \cdot 10^{-4}$	0.1305
			CuCl	$7.530 \cdot 10^{-4}$	0.0745
			MEK	0.2225	16.0419
		Feed	nBMA	0.0237	3.3701
			MEK	0.0467	3.3701

The precipitated polymers were worked up by means of procedure *"work–up B"* as described in *Section 3.1.2* with the samples of *Series B* and also characterized by means of elementary analysis, ATR–FTIR–spectroscopy, SEC and DSC. After 24 h the reaction solution was cooled down and the polymer was precipitated in 600 ml water–methanol–solution, filtered and dried, also in accordance to *"work–up B"*. The precipitate was extracted first with 150 ml CH_2Cl_2 and 150 ml H_2O and then the water phase was extracted two times more with 50 ml CH_2Cl_2 each. The color of the organic phase shifted from green to colorless and of the aqueous phase from colorless to blue. The organic phases were combined and dried by vacuum evaporation. The resulting polymer was characterized as detailed in *Chapter 3, Section 3.1.2*. The polymer yields of the samples and of the completely worked–up semi–batch are listed in *Table 5.2*.

Tab. 5.2.: Polymer yields obtained from the 1–ml–samples and the final yield of the semi–batch copolymerizations of *Series C*

time	V31		V32		V33		V34	
[min]	[g]	[%]	[g]	[%]	[g]	[%]	[g]	[%]
60	0.10	22.88	0.12	27.75	0.09	22.25	0.10	22.79
90	0.17	39.43	0.16	37.64	0.15	35.64	0.17	40.81
150	0.23	54.42	0.23	53.20	0.24	55.99	0.23	54.23
210	0.27	63.84	0.26	60.90	0.26	62.08	0.30	70.84
330	0.28	66.66	0.33	78.20	0.37	87.56	0.38	88.62
450	0.32	75.99	0.41	97.59	0.42	99.02	0.42	98.08
1440	14.51	78.16	15.71	83.99	15.93	84.78	15.85	83.96

Experiment V31 (P[PtBMA–grad–nBMA], $f_{tBMA} = 0.5$, $F_{tBMA} = 0.53$):

^{1}***H–NMR:*** 0.6–0.8 ppm (broad peak, –CH_3, nBMA and P[nBMA]); 1.25–1.45 ppm (broad peak, –$C(CH_3)_3$, P[tBMA], –CH_2–, nBMA and P[nBMA]); 1.42 ppm (s, –$C(CH_3)_3$, tBMA); 1.5–1.6 ppm (broad peak, –CH_2–, nBMA and P[nBMA]); 1.7–1.9 ppm (broad peak, –CH_3, P[tBMA] and P[nBMA]); 1.9 ppm (s, –CH_3, tBMA); 1.8 ppm (s, –CH_3, nBMA); 3.8–3.95 ppm (broad peak, –OCH_2R, P[nBMA]); 4.0 ppm (t, OCH_2R, nBMA); 5.3 ppm (t, CH_2=C–, cis, tBMA); 5.4 ppm (t, CH_2=C–, cis, nBMA); 5.9 ppm (s, CH_2=C–, trans, tBMA); 6.0 ppm (s, CH_2=C–, trans, nBMA)

EA: 66.79 % C, 9.23 % H, (23.98 % O_{calc})

ATR–FTIR: 3050–2800 cm^{-1} (=CH_2, –CH_2–, –CH_3); 1720 cm^{-1} (–C=O); 1473 cm^{-1} (–CH_2–, –CH_3); 1456 cm^{-1} (–CH_2–, –CH_3); 1392 cm^{-1}; 1366 cm^{-1} (tBu); 1327 cm^{-1}; 1270 cm^{-1} (tBu); 1247 cm^{-1} (nBu); 1136 cm^{-1} (–C–O–C–); 1065 cm^{-1} (nBu); 1035 cm^{-1}; 1020 cm^{-1}; 1000 cm^{-1}; 967 cm^{-1} (nBu); 945 cm^{-1}; 876 cm^{-1} (tBu)

SEC: $dn/dc = 0.0853\,ml \cdot g^{-1}$; $M_n = 55050\,g \cdot mol^{-1}$; $M_w = 58890\,g \cdot mol^{-1}$; $M_z = 61900\,g \cdot mol^{-1}$

DSC: $T_{onset} = 52.0\,°C$; $T_{midpt} = 60.0\,°C$; $T_g = 60.5\,°C$; $T_{offset} = 67.0\,°C$; $\Delta C_p = 0.197\,J \cdot g^{-1} \cdot K^{-1}$

Experiment V32 to V34 (P[PtBMA–grad–nBMA]:

The signal patterns of V32 to V34 were identical to that of V31. Signal intensities are found in *Table 5.4*. The elementary analysis results are shown in *Table 5.7*. The band intensities of the ATR–FTIR–spectra are summarized in *Table 5.8*, SEC– and DSC–data in *Table 5.12* and *Table 5.13*, respectively.

5.1.3. Characterization

All characterization–methods were the same as with the batch copolymers of *Chapter 3*. The used methods were:

- ^{1}H–NMR spectroscopy
- elementary analysis
- ATR–FTIR–spectroscopy
- size exclusion chromatography
- differential scanning calorimetry

The same instruments under the same conditions were used for the investigation of the resulting copolymers.

5.2. Results and Discussion

The subsequent paragraph describes the preparation of the monomer–feed programs, the set–up and performance of the semi–batch experiments as well as the results of the analysis from the different semibatch polymerizations of the different compositions of P[tBMA–grad–nBMA] and also their discussion. The gradient copolymers were analyzed with the same methods as the statistical copolymers P[nBMA–co–tBMA] before and under the same conditions (cf. *Section 3.2*).

The theoretical initial value of the monomer amount for the all semibatch copolymerizations were 0.1264 mol, i. e. 0.0632 mol tBMA and nBMA for experiment V31, 0.08216 mol tBMA and 0.04424 mol nBMA for experiment V32, 0.0948 mol tBMA and 0.316 mol nBMA for experiment V33 and 0.10477 mol tBMA and 0.01896 mol nBMA for experiment V34. Actually it were used 5 % more tBMA and 25 % more nBMA. The amount of tBMA was enlarged because a pre–polymerization time of 30 min was used to ensure a smooth start of the ATRP–reaction. The nBMA–feed solution was larger to compensate for the dead volume of the syringe and the syringe pump. The amount of the other components were adapted respectively. The ratio of monomer to solvent was wt : wt 1 : 1 for the stock and also for the feed solution because the concentrations had to remain constant. The amount of the components of the initiator system was adjusted to the additional amount of tBMA for the pre– polymerization, because only the 5 % of tBMA were polymerized, prior to the start of the monomer feed.

5.2.1. Monomer Addition Program

The preparation of gradient copolymers was done by semibatch copolymerization. That meant one monomer in the stock solution, here *tert*–butyl methacrylate, together with the initiator compounds was submitted in a Schlenk flask. The second monomer in the feed solution, here *n*–butyl methacrylate, was continuously injected into the stock solution during the reaction. The required feeding rate which was expressed by means of the dimensionless parameter q, depending on the target gradient $\phi = dF_{tBMA}/dX_e$ and the copolymerization properties of the comonomer system. This is described by the *Equations 5.2.1* to *5.2.4*, taken from Literature [107].

$$\frac{dq}{dp} = -f_{tBMA}\frac{X_e\phi}{F'_{tBMA}}(q-p) + 1 - \frac{F_{tBMA}}{f_{tBMA}} \tag{5.2.1}$$

$$\frac{df_{tBMA}}{dp} = \frac{1}{q-p}\left\{f_{tBMA} - F_{tBMA} - \frac{dq}{dp}\cdot f_{tBMA}\right\} \tag{5.2.2}$$

$$\frac{dt}{dp} = \frac{1}{k(f_{efftBMA})}\frac{1}{q-p} \tag{5.2.3}$$

$$q = \frac{1+p}{2} \tag{5.2.4}$$

with ϕ = targeted copolymer compositional gradient, X_e = targeted length of the gradient block, $F'_{tBMA} = dF_{tBMA}/df_{tBMA}$, q = total monomer addition function, p = monomer conversion, F_{tBMA} = instantaneous molar fraction of tBMA in the copolymer, f_{tBMA} = instantaneous molar fraction of tBMA in the monomer mixture

In the differential equation system (DES) *5.2.1* to *5.2.4* the "polymer chain" related gradient $\phi = dF/dX$ is used. Since ϕ is a small number ($\Delta F \leq 1; X_n > 10$) in the subsequent text the "monomer conversion" related gradient $\phi_p = dF/dp$ will be used. Note, that ϕ, and ϕ_p are interrelated by the simple expression $\phi = X_{n,e}^{-1} \cdot \phi_p$. Four different target gradient copolymers ϕ were synthesized and investigated here. They are listed in *Table 5.3*. $\phi_p = dF_{tBMA}/dp$ was calculated according to *Equation 5.2.5*.

$$\lim_{p \to \infty} \phi_p \Rightarrow F_{tBMA,e} - 1 \tag{5.2.5}$$

Tab. 5.3.: Theoretical values for monomer addition program of *Series C*

Entry	target Gradient ϕ_p	f_{tBMA}^{final}	$F_{tBMA,e}$	$F_{cum,tBMA}$	q_0
V31	-1.0	0.50	0.0	0.50	0.50
V32	-0.7	0.65	0.3	0.65	0.65
V33	-0.5	0.75	0.5	0.75	0.75
V34	-0.3	0.85	0.7	0.85	0.85

$\phi_p = dF_{tBMA}/dp$, $q_0 = n_{tBMA,0}/(n_{tBMA,0} + n_{tBMA,e})$

The solution of the DES cannot be performed analytically, hence a numerical approximation was calculated by means of the program "GradMake". [107] Since the integration requires the knowledge of the dependence of the effective copolymerization rate constant k_{eff} from the actual monomer composition ($k_{eff,tBMA}$), the kinetic data of the tBMA/nBMA batch copolymerization experiments (cf. *Section 3.3.1*) were required. The total effective rate constant k_{eff} (cf. *Figure 3.8*) was plotted against the monomer composition of the tBMA as stock–monomer. The equation of the line of fit from this plot was converted to get the rate constant k_0 and the first–order term of the reactions rate polynomial k_{f1}, see *Equation 5.2.6* to *5.2.8*.

$$k_{eff}(f_{tBMA}) = k_0 + a \cdot f_{tBMA} \tag{5.2.6}$$

$$k_{f1} = \frac{a}{k_0} \tag{5.2.7}$$

$$k_{eff}(f_{tBMA}) = k_0 \cdot (1 + k_{f1} \cdot f_{tBMA}) \tag{5.2.8}$$

For the copolymerization tBMA and nBMA the equation of the line of fit (cf. *Equation 5.2.9*) and the equivalent of *Equation 5.2.8* was *Equation 5.2.10*.

$$k_{eff}(f_{tBMA}) = 1.8978 \cdot 10^{-4}\,s^{-1} - 5.19 \cdot 10^{-5}\,s^{-1} \cdot f_{tBMA} \tag{5.2.9}$$

$$k_{eff}(f_{tBMA}) = 1.8978 \cdot 10^{-4}\,s^{-1} \cdot (1 - 2.7347 \cdot 10^{-1} \cdot f_{tBMA}) \tag{5.2.10}$$

The two values $k_1 = 1.898 \cdot 10^{-4}\,s^{-1}$ and $k_{f1} = 2.735 \cdot 10^{-1}$ were integrated into the program "GradMake". In the program the monomer of the in the stock solution tBMA was labeled as "Monomer1" and the one in the feed solution nBMA as "Monomer2". "GradMake" solved the DES, calculated the time– dependent dosing rate (cf. *Figure 5.2*) and created a data–file containing the required volume–feed rates ("addition program") to control the syringe pump, see *Supplements A* to *D*.

The feeding program contained the respective feed time interval Δt with the related feed rate dV/dt as shown in the *Figure 5.2*.

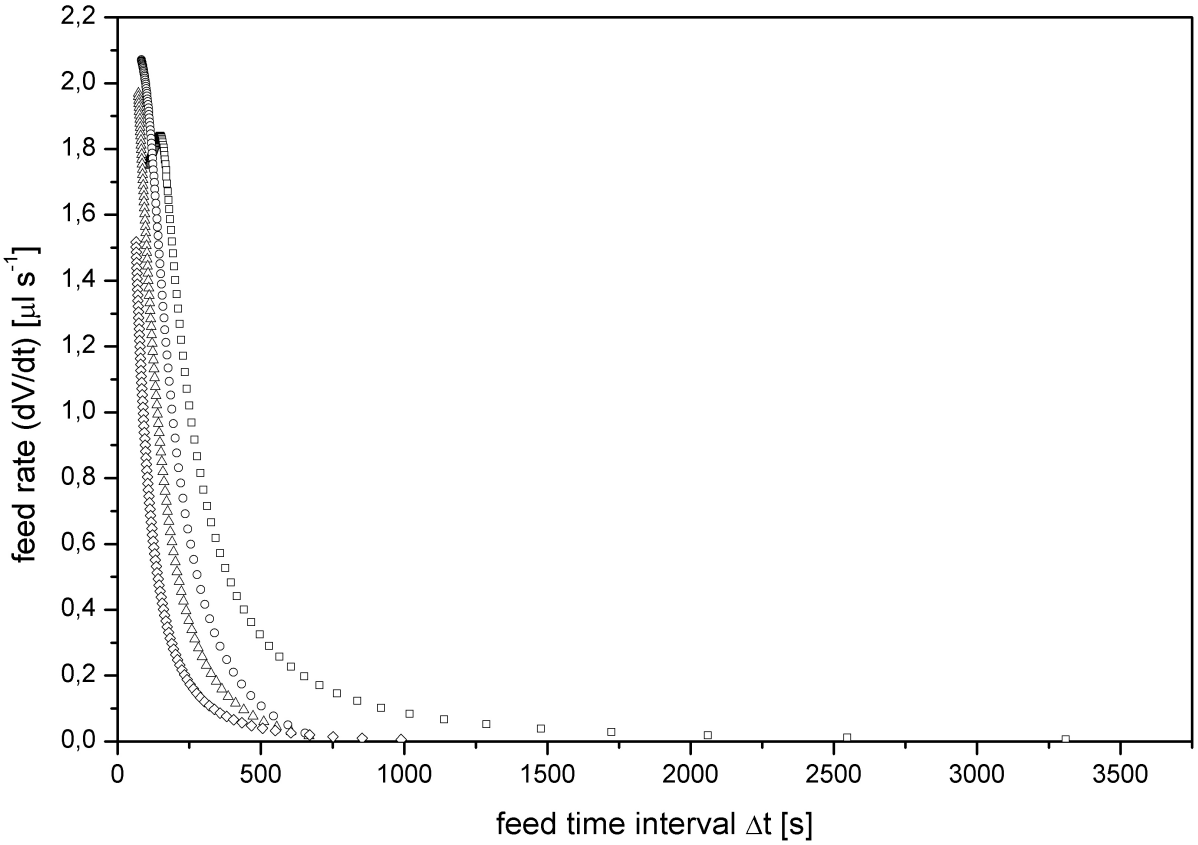

Fig. 5.2.: Feed rate per feed time intervals of the different monomer addition programs; V31 (□, $\phi_p = -1$, $f_{tBMA} = 0.5$), V32 (○, $\phi_p = -0.7$, $f_{tBMA} = 0.65$), V33 (△, $\phi_p = -0.5$, $f_{tBMA} = 0.75$), V34 (◇, $\phi_p = -0.3$, $f_{tBMA} = 0.85$)

The resulting differential volume per feed time $\Delta V(t)$ and the total volume V_{total} are shown in *Figures 5.3* and *5.4*. The total volume was the sum over all injected differential volumes up to the corresponding feed time (see *Equation 5.2.11*).

$$V_{total} = \int \frac{dV}{dt} dt = \sum_{i=1}^{n} \Delta V_i \tag{5.2.11}$$

$$t_{feed} = \int dt_{feed} = \sum_{i=1}^{n} \Delta t_{feed,i} \tag{5.2.12}$$

The resulting feed rates and volumes showed all nearly the same shapes, see *Figure 5.2* to *5.4*. At the start the feed rates were high and then they decreased. First the decrease was abrupt and then it flattened. During the first 100 min 60 % of the feed solution was injected, then the amount fell to very low values. The differential volume per feed time increased first up to a maximum, then the curves decreased strongly and ceased off. The slope of the decreasing curve tails decreased with lower values of ϕ_p ($\phi_p = -1$, $\phi_p = -0.7$, $\phi_p = -0.5$, $\phi_p = -0.3$). The total volume also showed that most of the feed solution was injected at the beginning of the copolymerizations. The total time of the monomer addition varied between the entries. Experiment V31 ($\phi_p = -1$) had a much longer feed time than the three others. Experiment V34 ($\phi_p = -0.3$) was a bit longer than the entries V32 ($\phi_p = -0.7$) and V33 ($\phi_p = -0.5$). Experiment V32 and V33 had nearly the same time of feeding.

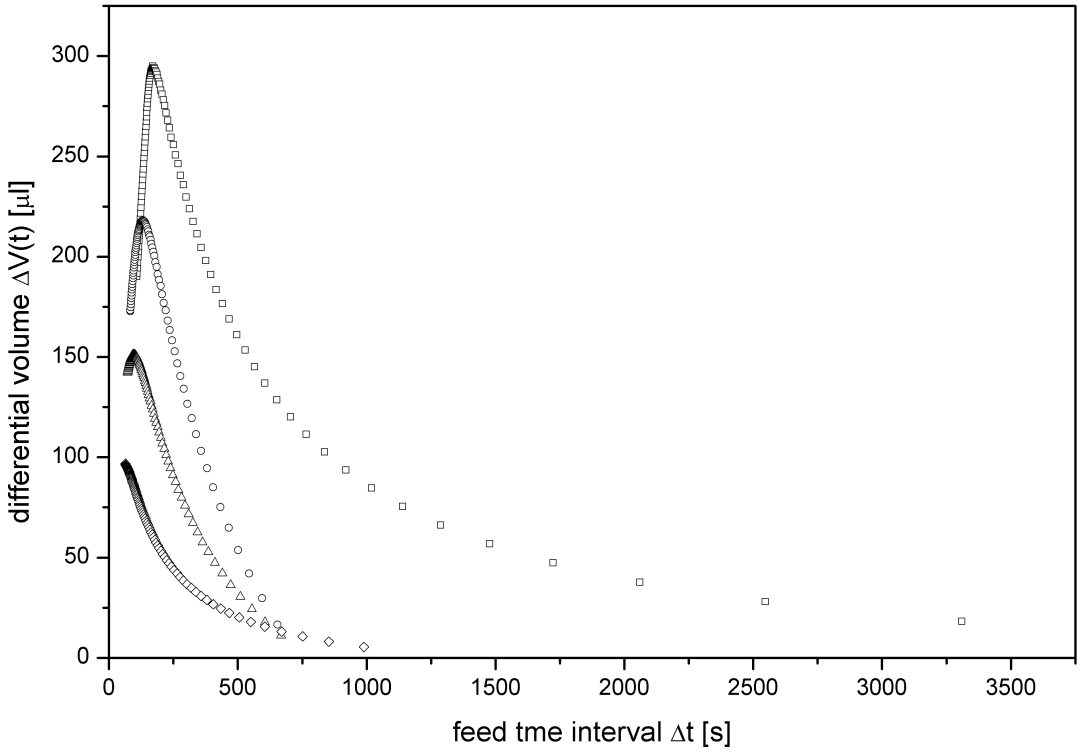

Fig. 5.3.: Differential volume per feed time intervals of the different monomer addition programs; V31 (□, $\phi_p = -1$, $f_{tBMA} = 0.5$), V32 (○, $\phi_p = -0.7$, $f_{tBMA} = 0.65$), V33 (△, $\phi_p = -0.5$, $f_{tBMA} = 0.75$), V34 (◇, $\phi_p = -0.3$, $f_{tBMA} = 0.85$)

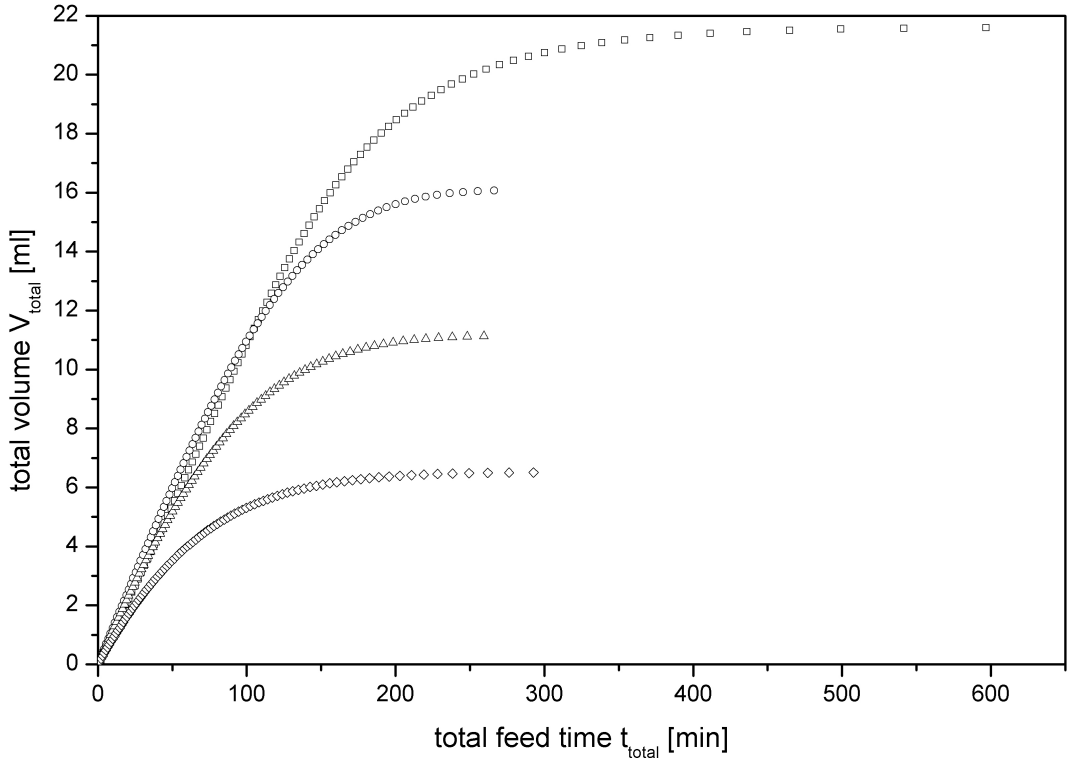

Fig. 5.4.: Total volume per total feed time of the different monomer addition programs; V31 (□, $\phi_p = -1$, $f_{tBMA} = 0.5$), V32 (○, $\phi_p = -0.7$, $f_{tBMA} = 0.65$), V33 (△, $\phi_p = -0.5$, $f_{tBMA} = 0.75$), V34 (◇, $\phi_p = -0.3$, $f_{tBMA} = 0.85$)

5.2.2. Kinetic Studies

NMR samples were taken during the semibatch gradient copolymerizations and analyzed to determine the monomer conversion p from the integrals of the ^{1}H–NMR–spectra signals and to determine the cumulative and instantaneous composition of the gradient copolymers, F_{cum} and F_{inst}, respectively. The change of the spectra during the course of reaction and the analyzed peaks are depicted in *Figure 5.6* exemplary for the four polymerizations, together with the corresponding proton signals of experiment V32 (ϕ_p = −0.7, f_{tBMA} = 0.65). The molecular structures of the monomers tBMA and nBMA and the resulting copolymer as well as the numbering of these carbons are shown in *Figure 5.5*.

In the first spectrum A, shown in *Figure 5.6*, taken at the start of the semibatch copolymerization, only the signals of the monomer tBMA, a singlet at 5.9 ppm (=CH_2^{cis}, 1), a triplet at 5.3 ppm (=CH_2^{trans}, 2) and a singlet at 1.8 ppm (–CH_3, 10) of the methacrylate part of the monomer and a singlet at 1.4 ppm of the *tert*–butyl group (3) together with the solvent signals of MEK at 0.96 ppm (t), 2.06 ppm (s) and 2.38 ppm (q) were present, certainly. The last ^{1}H–NMR–spectrum H, taken after 24 h, showed the sharp signals of both monomers and five broad signals of the polymer chain at 3.8 to 3.95 ppm (α–proton, 6'), 1.5 to 1.6 ppm (γ–proton, 8'), 1.3 to 1.45 ppm (β–proton, 7') and 0.6 to 0.8 ppm (δ–proton, 9') of the *n*–butyl group and at 1.3 to 1.45 ppm a signal caused by the *tert*–butyl group (3'). The solvent signals remained constant during the polymerization and in the relation to these signals the intensity changes of the monomer and polymer signals became observable. The same behavior was also noticed during the batch synthesis before, reported in *Section 3.3.1*. In all ^{1}H–NMR–spectra of the four semibatch gradient copolymerizations the peak areas A of the signals were determined for calculation of the monomer conversion.

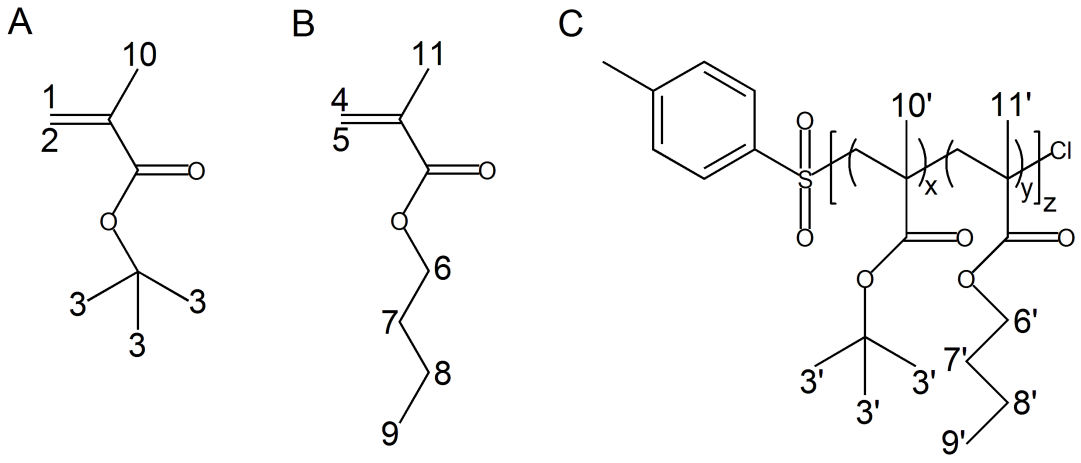

Fig. 5.5.: Molecular structures of the monomers (A) tBMA and (B) nBMA and (C) the copolymer P[tBMA–grad–nBMA] *Series C* with carbon–atom labels (z = x + y = 1)

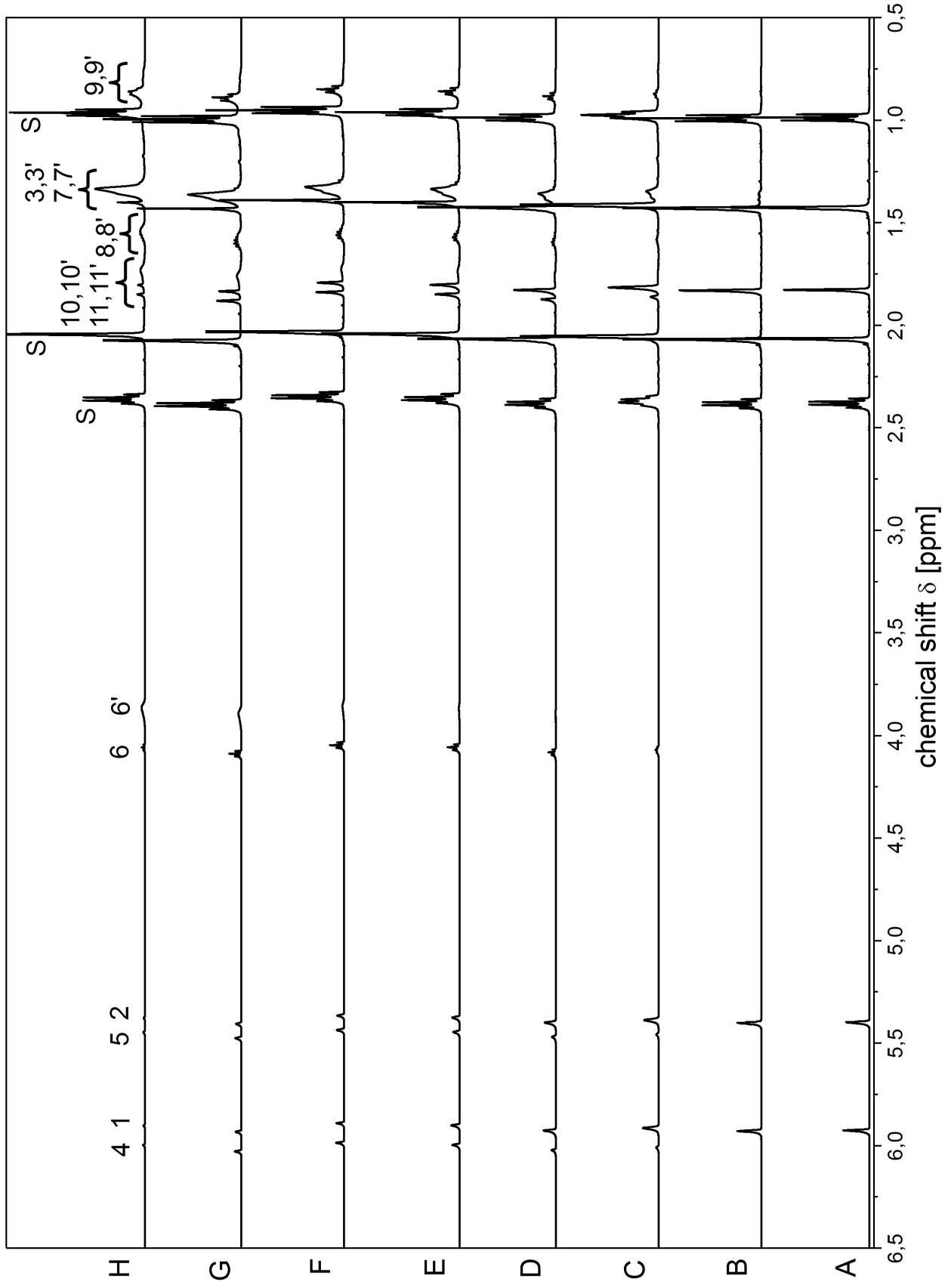

Fig. 5.6.: ^{1}H–NMR–spectra of experiment V32 (ϕ_p = −0.7, f_{tBMA} = 0.65) after reaction time of A – 0 min, B – 30 min, C – 60 min, D – 90 min, E – 180 min, F – 330 min, G – 450 min, H – 1440 min

The determination of the conversion of tBMA (p_{tBMA}) was done in the same way as described with the batch experiments in *Section 3.3*. The integrals A_1 (5.9 ppm) from a signal of the monomer tBMA, A_x (1.3–1.45 ppm), the mixed signal from the monomers and both functional groups in the polymer chain, and $A_{8,8'}$ (1.5–1.6 ppm) the γ–proton signal from the *n*–butyl group of the monomer and of the polymer were measured and with the *Equations 5.2.13* to *5.2.15* p_{tBMA} was calculated.

$$A_{tBMA} = \frac{A_x - A_8}{z} - A_1 \tag{5.2.13}$$

$$z = \frac{A_{x,0}}{A_{1,0}} \tag{5.2.14}$$

$$p_{tBMA} = \frac{A_{tBMA}}{A_1 + A_{tBMA}} \tag{5.2.15}$$

with A_x = integral intensity from 1.3 to 1.45 ppm of the same signal arising from parts of the monomers and the polymers; $A_{x,0}$ = integral intensity from 1.3 to 1.45 ppm at $t = 0$ min; A_1 = integral intensity from 5.9 ppm; $A_{1,0}$ = integral intensity from 5.9 ppm at $t = 0$ min; A_8 = integral intensity from 1.5 to 1.6 ppm; A_{tBMA} = integral intensity from 1.3 to 1.45 ppm only from the *tert*–butyl group of the polymer; z = signal intensity ratio of the *tert*–butyl group to the monomers vinylic CH_2=–protons = A_1

From the conversion of tBMA the amount of tBMA–units inside the polymer chain ($n_{tBMA,P}$) was determined, using *Equation 5.2.16*.

$$n_{tBMA,P} = p_{tBMA} \cdot n_{tBMA,0} \tag{5.2.16}$$

with $n_{tBMA,0}$ = the amount of tBMA in the stock solution at the beginning of the polymerization $t = 0$ min

The calculation of the amount of nBMA in the solution and inside the polymer chain differed from the determination used in the batch copolymerization, because the total amount of nBMA in the system depends on the injected mass of the feed solution up to a certain time. First the amount of nBMA in solution $n_{nBMA,S}$ was determined by means of the *Equations 5.2.17* to *5.2.19*.

$$n_{nBMA,total} = n_{nBMA,P} + n_{nBMA,S} \tag{5.2.17}$$

$$n_{nBMA,total} = n_{nBMA,S} \cdot \left(1 + \frac{n_{nBMA,P}}{n_{nBMA,S}}\right) \tag{5.2.18}$$

$$n_{nBMA,S} = \frac{n_{nBMA,total}}{\left(1 + \frac{n_{nBMA,P}}{n_{nBMA,S}}\right)} \tag{5.2.19}$$

with $n_{nBMA,total}$ = amount of nBMA in the whole system at the end of the polymerization,

$n_{nBMA,S}$ = the amount of nBMA in the stock solution and $n_{nBMA,P}$ = the amount of nBMA inside the polymer chain

Since $n_{nBMA,S}$ corresponds to A_6, the signal of the α–proton of the *n*–butyl group in the monomer nBMA, and $n_{nBMA,P}$ is proportional to $A_{6'}$, the peak of the α–proton of the *n*–butyl group in the polymer chain, $n_{nBMA,S}$ can be calculated. *Equation 5.2.19* becomes:

$$n_{nBMA,S} = \frac{n_{nBMA,total}}{\left(1 + \frac{A_{6'}}{A_6}\right)} \tag{5.2.20}$$

From the amount of nBMA in the solution, the amount of nBMA in the polymer chain $n_{nBMA,P}$ was obtained and with this result the conversion of nBMA (p_{nBMA}) was calculated. The results of the analysis of the NMR–spectra in view to the conversion of nBMA were listed in *Table 5.4*.

$$n_{nBMA,P} = n_{nBMA,total} - n_{nBMA,S} \tag{5.2.21}$$

$$p_{nBMA} = \frac{n_{nBMA,P}}{n_{nBMA,total}} \tag{5.2.22}$$

The conversions of the two monomers gave the total monomer conversion p of the whole system.

$$p = \frac{n_{tBMA,P} + n_{nBMA,P}}{n_{tBMA,0} + n_{nBMA,total}} \tag{5.2.23}$$

with $n_{tBMA,P}$ = amount of tBMA inside the polymer chain, $n_{nBMA,P}$ = amount of nBMA inside the polymer chain, $n_{tBMA,0}$ = the amount of tBMA in the stock solution at the beginning of the polymerization t = 0 min, $n_{nBMA,total}$ = amount of nBMA in the whole system at the end of the polymerization

The total conversions of the each sample taken during the copolymerizations of *Series C* are summarized in *Table 5.4*. A plot of the total conversions p of the semibatch copolymerizations V31 to V34 versus the reaction time is depicted in *Figure 5.7*. The graphs were relatively similar. In all four semibatch copolymerizations the conversion was linear up to 120 min. Then the curves leveled off. Only experiment V31 was slightly different, because the conversion p was lower than the three other experiments. However, all four reactions reached a final conversion of 91 ± 2 % after 24 h.

Tab. 5.4.: ^{1}H–NMR–signal areas and conversions during the different semibatch–copolymerizations of *Series C*

Entry f_{tBMA}	time t [min]	A_1	A_6	$A_{6'}$	$A_{8,8'}$	A_x	A_{tBMA}	p_{tBMA}	$n_{tBMA,P}$ [mol]	$n_{nBMA,S}$ [mol]	$n_{nBMA,P}$ [mol]	p_{nBMA}	p
V31	0	1.0000	0.0000	0.0000	0.0000	9.5347	0.0000	0.0000	0.0000	–	–	–	–
0.5	15	1.0000	0.0000	0.0000	0.0000	9.6240	0.0100	0.0099	0.0007	–	–	–	–
	30	1.0000	0.0000	0.0000	0.0000	9.9935	0.0488	0.0465	0.0031	–	–	–	0.0232
	40	41.3046	1.4338	0.0673	3.4732	425.8478	3.0206	0.0682	0.0045	0.0604	0.0028	0.0448	0.0565
	50	15.9792	1.6965	0.1265	3.4704	176.4562	2.1744	0.1198	0.0080	0.0588	0.0044	0.0694	0.0946
	60	9.5601	1.8185	0.1325	2.5234	111.4995	1.8762	0.1641	0.0109	0.0589	0.0043	0.0679	0.1160
	70	6.7606	1.9187	0.1130	2.9835	84.2260	1.7652	0.2070	0.0138	0.0597	0.0035	0.0556	0.1313
	80	4.7734	1.9138	0.1867	2.9393	62.7839	1.5069	0.2399	0.0159	0.0576	0.0056	0.0889	0.1644
	90	3.7915	1.9540	0.2343	2.9357	52.7310	1.4342	0.2745	0.0182	0.0564	0.0068	0.1071	0.1908
	120	2.1006	1.9914	0.3332	2.8245	34.6077	1.2348	0.3702	0.0246	0.0541	0.0091	0.1433	0.2568
	150	1.4080	1.9882	0.4288	2.7842	26.5093	1.0818	0.4345	0.0289	0.0520	0.0112	0.1774	0.3060
	180	1.0371	2.0210	0.5347	2.8027	22.1535	0.9936	0.4893	0.0325	0.0500	0.0132	0.2092	0.3493
	210	0.8044	2.0156	0.5887	2.9018	19.4068	0.9277	0.5356	0.0356	0.0489	0.0143	0.2261	0.3808
	270	1.0000	3.4936	1.2653	5.1487	28.5597	1.4568	0.5930	0.0394	0.0464	0.0168	0.2659	0.4294
	330	1.0000	4.3071	1.9419	6.6137	33.4436	1.8156	0.6448	0.0428	0.0436	0.0196	0.3108	0.4778
	390	1.0000	4.9673	2.6464	8.1955	38.2810	2.1573	0.6833	0.0454	0.0412	0.0220	0.3476	0.5154
	450	1.0000	5.3119	3.2131	9.0091	41.9321	2.4550	0.7106	0.0472	0.0394	0.0238	0.3769	0.5437
	1440	1.0000	8.1838	51.5710	62.9131	271.9619	20.9382	0.9544	0.0634	0.0087	0.0545	0.8630	0.9087
V32	0	1.0000	0.0000	0.0000	0.0000	9.4830	0.0000	0.0000	0.0000	–	–	–	–
0.65	15	1.0000	0.0000	0.0000	0.0000	9.5423	0.0063	0.0062	0.0005	–	–	–	–

Continuation on next page ...

Entry f_{tBMA}	time t [min]	A_1	A_6	$A_{6'}$	$A_{8,8'}$	A_x	A_{tBMA}	p_{tBMA}	$n_{tBMA,P}$ [mol]	$n_{nBMA,S}$ [mol]	$n_{nBMA,P}$ [mol]	p_{nBMA}	p
	30	1.0000	0.0000	0.0000	0.0000	10.1849	0.0740	0.0689	0.0060	0.0000	0.0000	0.0000	0.0448
	40	23.0386	1.9356	0.0000	4.3675	241.6561	1.9839	0.0793	0.0068	0.0442	0.0000	0.0000	0.0515
	50	10.5051	1.9911	0.0547	3.1921	120.5209	1.8674	0.1509	0.0130	0.0430	0.0012	0.0267	0.1075
	60	6.8555	2.0627	0.1102	2.8683	82.5312	1.5451	0.1839	0.0159	0.0420	0.0022	0.0507	0.1373
	70	4.8206	1.9841	0.1741	2.7609	61.5789	1.3819	0.2228	0.0192	0.0406	0.0036	0.0807	0.1731
	80	3.6998	2.0043	0.2327	2.6896	50.0746	1.2970	0.2596	0.0224	0.0396	0.0046	0.1040	0.2051
	90	2.9922	2.0170	0.2899	2.7119	43.2621	1.2839	0.3003	0.0259	0.0387	0.0056	0.1257	0.2392
	120	1.9528	2.0205	0.4068	2.7752	32.8878	1.2226	0.3850	0.0332	0.0368	0.0074	0.1676	0.3089
	150	1.4332	2.0161	0.5416	2.8691	27.9477	1.2114	0.4581	0.0395	0.0348	0.0094	0.2118	0.3719
	180	1.1708	2.0170	0.6973	2.9823	25.3108	1.1838	0.5028	0.0434	0.0329	0.0114	0.2569	0.4167
	210	1.0360	2.0147	0.8633	3.1588	25.4604	1.3158	0.5595	0.0483	0.0309	0.0133	0.3000	0.4687
	270	0.9071	2.0377	1.7889	4.2989	32.0094	2.0150	0.6896	0.0595	0.0235	0.0207	0.4675	0.6119
	330	0.9227	2.0248	1.3236	3.7102	28.1651	1.6561	0.6422	0.0554	0.0267	0.0175	0.3953	0.5558
	390	0.8988	2.0400	2.2827	4.8550	35.5591	2.3390	0.7224	0.0623	0.0209	0.0233	0.5281	0.6544
	450	0.8880	2.0503	2.7457	5.3167	40.0914	2.7791	0.7578	0.0654	0.0189	0.0253	0.5725	0.6930
	1440	0.7916	2.0746	10.7855	14.6120	107.1279	8.9644	0.9189	0.0793	0.0071	0.0371	0.8387	0.8908
V33	0	1.0000	0.0000	0.0000	0.0000	9.3237	0.0000	0.0000	0.0000	–	–	–	–
0.75	15	1.0000	0.0000	0.0000	0.0000	9.4687	0.0156	0.0153	0.0015	–	–	–	–
	30	1.0000	0.0000	0.0000	0.0000	9.7220	0.0427	0.0410	0.0041	–	–	–	0.0307
	40	24.8754	1.9536	0.0000	2.1409	253.6090	2.0955	0.0777	0.0077	0.0316	0.0000	0.0000	0.0583
	50	12.5537	1.9042	0.0578	2.4070	133.5571	1.5126	0.1075	0.0107	0.0307	0.0009	0.0295	0.0880
	60	8.6607	2.0026	0.1293	2.6412	98.8323	1.6561	0.1605	0.0160	0.0297	0.0019	0.0607	0.1356

Continuation on next page ...

Entry f_{tBMA}	time t [min]	A_1	A_6	$A_{6'}$	$A_{8,8'}$	A_x	A_{tBMA}	p_{tBMA}	$n_{tBMA,P}$ [mol]	$n_{nBMA,S}$ [mol]	$n_{nBMA,P}$ [mol]	p_{nBMA}	p
	70	6.4350	1.9912	0.2152	2.8863	78.9731	1.7256	0.2115	0.0210	0.0285	0.0031	0.0975	0.1830
	80	5.0724	1.9465	0.2395	2.7805	64.4906	1.5462	0.2336	0.0232	0.0281	0.0035	0.1096	0.2026
	90	4.2778	1.9678	0.3000	2.8950	58.9470	1.7340	0.2884	0.0287	0.0274	0.0042	0.1323	0.2494
	120	2.8943	1.9724	0.5085	2.9500	46.6700	1.7948	0.3828	0.0381	0.0251	0.0065	0.2050	0.3383
	150	2.4141	2.0661	0.7811	3.3636	45.4892	2.1040	0.4657	0.0463	0.0229	0.0087	0.2743	0.4179
	180	2.0114	2.0007	0.8761	3.3707	43.0139	2.2405	0.5269	0.0524	0.0220	0.0096	0.3045	0.4713
	210	1.8328	1.9979	1.0594	3.5278	43.1412	2.4159	0.5686	0.0566	0.0207	0.0110	0.3465	0.5131
	270	1.7103	1.9992	1.4427	3.9671	47.2073	2.9274	0.6312	0.0628	0.0184	0.0133	0.4192	0.5782
	330	1.6707	1.9891	1.8322	4.3050	53.0047	3.5525	0.6801	0.0677	0.0165	0.0152	0.4795	0.6300
	390	1.6738	1.9760	2.1191	4.6558	59.4273	4.2006	0.7151	0.0712	0.0153	0.0164	0.5175	0.6657
	450	1.6348	2.0009	2.6310	5.3361	62.9919	4.5490	0.7356	0.0732	0.0137	0.0180	0.5680	0.6937
	1440	1.4851	2.0479	10.7088	14.7867	177.4886	15.9653	0.9149	0.0910	0.0051	0.0265	0.8395	0.8960
V34	0	1.0000	0.0000	0.0000	0.0000	9.5093	0.0000	0.0000	0.0000	–	–	–	–
0.85	15	1.0000	0.0000	0.0000	0.0000	9.5413	0.0034	0.0034	0.0004	–	–	–	–
	30	1.0000	0.0000	0.0000	0.0000	9.6057	0.0101	0.0100	0.0011	–	–	–	0.0085
	40	40.0420	1.8527	0.0000	2.7814	398.8170	1.6052	0.0385	0.0044	0.0190	0.0000	0.0000	0.0328
	50	22.2797	2.1607	0.1319	5.0996	239.5269	2.3727	0.0963	0.0109	0.0179	0.0011	0.0575	0.0904
	60	14.1913	2.0333	0.2303	3.6810	161.4756	2.4024	0.1448	0.0163	0.0171	0.0019	0.1017	0.1383
	70	10.7938	2.0260	0.2355	3.8995	131.5417	2.6291	0.1959	0.0221	0.0170	0.0020	0.1041	0.1821
	80	8.2803	1.8678	0.2671	2.6008	104.9418	2.4819	0.2306	0.0260	0.0166	0.0024	0.1251	0.2148
	90	7.7248	2.0383	0.3685	3.1962	104.7342	2.9530	0.2766	0.0312	0.0161	0.0029	0.1531	0.2580
	120	5.5005	1.9991	0.5049	3.2467	86.0975	3.2121	0.3687	0.0416	0.0152	0.0038	0.2016	0.3436

Continuation on next page ...

Entry f_{tBMA}	time t [min]	A_1	A_6	$A_{6'}$	$A_{8,8'}$	A_x	A_{tBMA}	p_{tBMA}	$n_{tBMA,P}$ [mol]	$n_{nBMA,S}$ [mol]	$n_{nBMA,P}$ [mol]	p_{nBMA}	p
	150	4.5421	1.9717	0.6849	3.4290	79.9915	3.5092	0.4359	0.0492	0.0141	0.0049	0.2578	0.4092
	180	4.0056	1.9321	0.8461	3.6672	77.6919	3.7789	0.4854	0.0548	0.0132	0.0058	0.3046	0.4583
	210	3.8288	1.9861	1.1406	4.3276	84.2373	4.5745	0.5444	0.0614	0.0121	0.0069	0.3648	0.5174
	270	3.4602	1.9355	1.4764	4.3330	91.1475	5.6692	0.6210	0.0701	0.0108	0.0082	0.4327	0.5927
	330	3.1316	1.8125	1.8931	4.4611	94.1833	6.3036	0.6681	0.0754	0.0093	0.0097	0.5109	0.6445
	390	3.6391	1.9849	2.3357	5.8824	134.0922	9.8435	0.7301	0.0824	0.0087	0.0103	0.5406	0.7017
	450	3.4238	2.0242	3.3055	6.9271	144.0824	10.9995	0.7626	0.0860	0.0072	0.0118	0.6202	0.7413
	1440	2.9394	2.0075	15.6207	25.8145	473.0050	44.0873	0.9375	0.1058	0.0022	0.0168	0.8861	0.9298

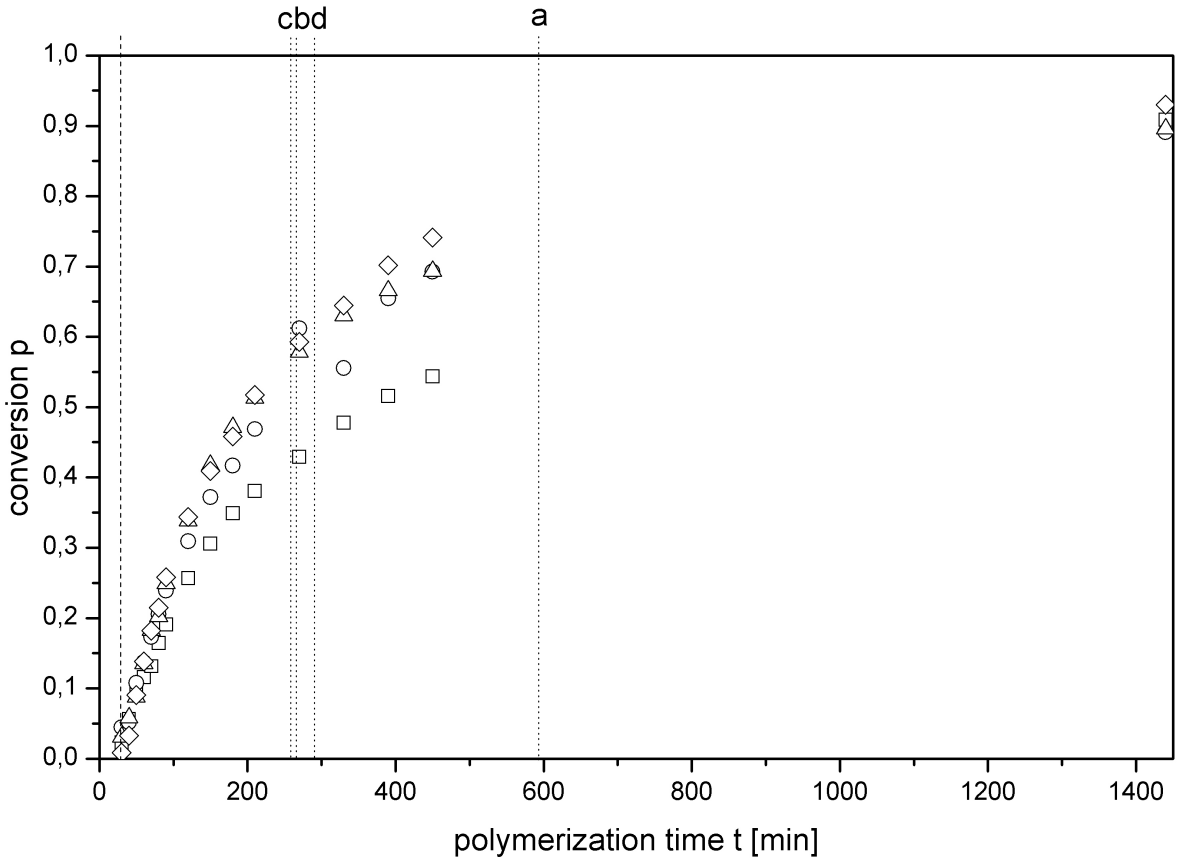

Fig. 5.7.: Conversion p of *Series C*; V31 (□, $\phi_p = -1$, $f_{tBMA} = 0.5$), V32 (○, $\phi_p = -0.7$, $f_{tBMA} = 0.65$), V33 (△, $\phi_p = -0.5$, $f_{tBMA} = 0.75$), V34 (◇, $\phi_p = -0.3$, $f_{tBMA} = 0.85$); dashed line – start of feed–solution injection, dotted lines – end of feed–solution–injection – a V31, b V32, c V33, d V34

With these results the cumulative and the instantaneous compositions of the gradient copolymers (F_{cum} and F_{inst}) were determined as well as their change during the polymerization, with help of *Equations 5.2.24* and *5.2.25*.

$$F_{cum}^{tBMA}(p) = \frac{1}{1 + \frac{n_{nBMA,P}}{n_{tBMA,P}}} \tag{5.2.24}$$

$$F_{inst}^{tBMA}(p) = F_{cum}^{tBMA}(p) + p \cdot \frac{\Delta F_{cum}^{tBMA}(p)}{\Delta p} \tag{5.2.25}$$

The results of these calculations applied to the four semibatch synthesis are listed in *Table 5.5* and depicted in the *Figures 5.8* and *5.9* (composition/time plot) and *Figures 5.10* and *5.11* (composition/conversion plot).

Some of the calculated values of the instantaneous compositions were higher than 1 and one value was lower than 0. These results must be chemical erroneous because the molar fraction of a monomer in a copolymer must be between 0 and 1. The incorrect data points are indicated by arrows in the *Figures 5.9* and *5.11*.

Tab. 5.5.: Kinetic results and compositions of the different copolymer compositions of experiments of *Series C*

Entry f_{tBMA}	time t [min]	p	F_{cum}	F_{inst} [a]	F_{inst} [b]	F_{inst} [c]	Entry f_{tBMA}	time t [min]	p	F_{cum}	F_{inst} [a]	F_{inst} [b]	F_{inst} [c]
V31	0	0.0000	–	–	–	–	V33	0	0.0000	–	–	–	–
0.5	15	0.0000	1.0000	1.0000	1.0000	1.0000	0.75	15	0.0000	1.0000	1.0000	1.0000	1.0000
	30	0.0232	1.0000	1.0000	0.9569	0.9910		30	0.0307	1.0000	1.0000	0.9597	0.9941
	40	0.0565	0.6149	-0.0393	0.5101	0.5931		40	0.0583	1.0000	3.1158	0.9236	0.9888
	50	0.0946	0.6446	0.7182	0.4690	0.6080		50	0.0880	0.9200	0.6832	0.8046	0.9031
	60	0.1160	0.7174	1.1118	0.5021	0.6726		60	0.1356	0.8929	0.8156	0.7153	0.8669
	70	0.1313	0.7964	1.4725	0.5527	0.7457						0.8736	
	80	0.1644	0.7393	0.4557	0.4342	0.6758		70	0.1830	0.8722	0.7926	0.8463	0.8372
					0.6960			80	0.2026	0.8704	0.8512	0.8416	0.8316
	90	0.1908	0.7292	0.6561	0.6789	0.6555		90	0.2494	0.8729	0.8861	0.8375	0.8251
	120	0.2568	0.7307	0.7366	0.6630	0.6315		120	0.3383	0.8547	0.7854	0.8066	0.7899
	150	0.3060	0.7201	0.6542	0.6395	0.6020		150	0.4179	0.8424	0.7780	0.7831	0.7624
	180	0.3493	0.7107	0.6350	0.6187	0.5758		180	0.4713	0.8449	0.8672	0.7780	0.7547
	210	0.3808	0.7134	0.7456	0.6130	0.5663		210	0.5131	0.8379	0.7510	0.7650	0.7396
	270	0.4294	0.7009	0.5902	0.5877	0.5350		270	0.5782	0.8258	0.7192	0.7438	0.7151
	330	0.4778	0.6856	0.5342	0.5596	0.5010		330	0.6300	0.8171	0.7104	0.7277	0.6964
	390	0.5154	0.6738	0.5124	0.5379	0.4747		390	0.6657	0.8131	0.7395	0.7187	0.6857
	450	0.5437	0.6645	0.4867	0.5212	0.4545		450	0.6937	0.8031	0.5546	0.7046	0.6702
	1440	0.9087	0.5374	0.2211	0.2979	0.1865		1440	0.8960	0.7744	0.6472	0.6472	0.6028

Continuation on next page ...

Entry f_{tBMA}	time t [min]	p	F_{cum}	F_{inst} [a]	F_{inst} [b]	F_{inst} [c]	Entry f_{tBMA}	time t [min]	p	F_{cum}	F_{inst} [a]	F_{inst} [b]	F_{inst} [c]
V32	0	0.0000	–	–	–	–	V34	0	0.0000	–	–	–	–
0.65	15	0.0000	1.0000	1.0000	1.0000	1.0000	0.85	15	0.0000	1.0000	1.0000	1.0000	1.0000
	30	0.0448	1.0000	1.0000	0.9423	0.9834		30	0.0085	1.0000	1.0000	0.9953	0.9991
	40	0.0515	1.0000	1.0000	0.9336	0.9843		40	0.0328	1.0000	2.3521	0.9820	0.9964
	50	0.1075	0.9168	0.7570	0.7784	0.8841		50	0.0904	0.9085	0.7651	0.8588	0.8986
	60	0.1373	0.8763	0.6895	0.6994	0.8344		60	0.1383	0.8942	0.8527	0.8180	0.8790
	70	0.1731	0.8436	0.6853	0.6207 0.8040	0.7908		70	0.1821	0.9178	1.0162	0.8176 0.9045	0.8979
	80	0.2051	0.8297	0.7411	0.7828	0.7672		80	0.2148	0.9163	0.9062	0.9006	0.8927
	90	0.2392	0.8235	0.7798	0.7688	0.7506		90	0.2580	0.9147	0.9053	0.8958	0.8864
	120	0.3089	0.8177	0.7922	0.7471	0.7236		120	0.3436	0.9157	0.9195	0.8905	0.8780
	150	0.3719	0.8086	0.7545	0.7235	0.6953		150	0.4092	0.9094	0.8703	0.8795	0.8646
	180	0.4167	0.7926	0.6441	0.6973	0.6656		180	0.4583	0.9044	0.8582	0.8709	0.8512
	210	0.4687	0.7846	0.7122	0.6774	0.6418		210	0.5174	0.8986	0.8473	0.8607	0.8419
	270	0.6119	0.7423	0.5616	0.6023	0.5559		270	0.5927	0.8950	0.8665	0.8516	0.8300
	330	0.5558	0.7603	0.5815	0.6332	0.5910		330	0.6445	0.8859	0.7731	0.8388	0.8153
	390	0.6544	0.7276	0.5105	0.5779	0.5282		390	0.7017	0.8891	0.9285	0.8378	0.8122
	450	0.6930	0.7210	0.6030	0.5625	0.5099		450	0.7413	0.8795	0.7000	0.8253	0.7983
	1440	0.8908	0.6814	0.5032	0.4777	0.4100		1440	0.9298	0.8627	0.7795	0.7946	0.7608

[a] calculated by *Eq. 5.2.25*; [b] calculated by *Eq. 5.2.35*; [c] calculated by *Eq. 5.2.35* with average slope

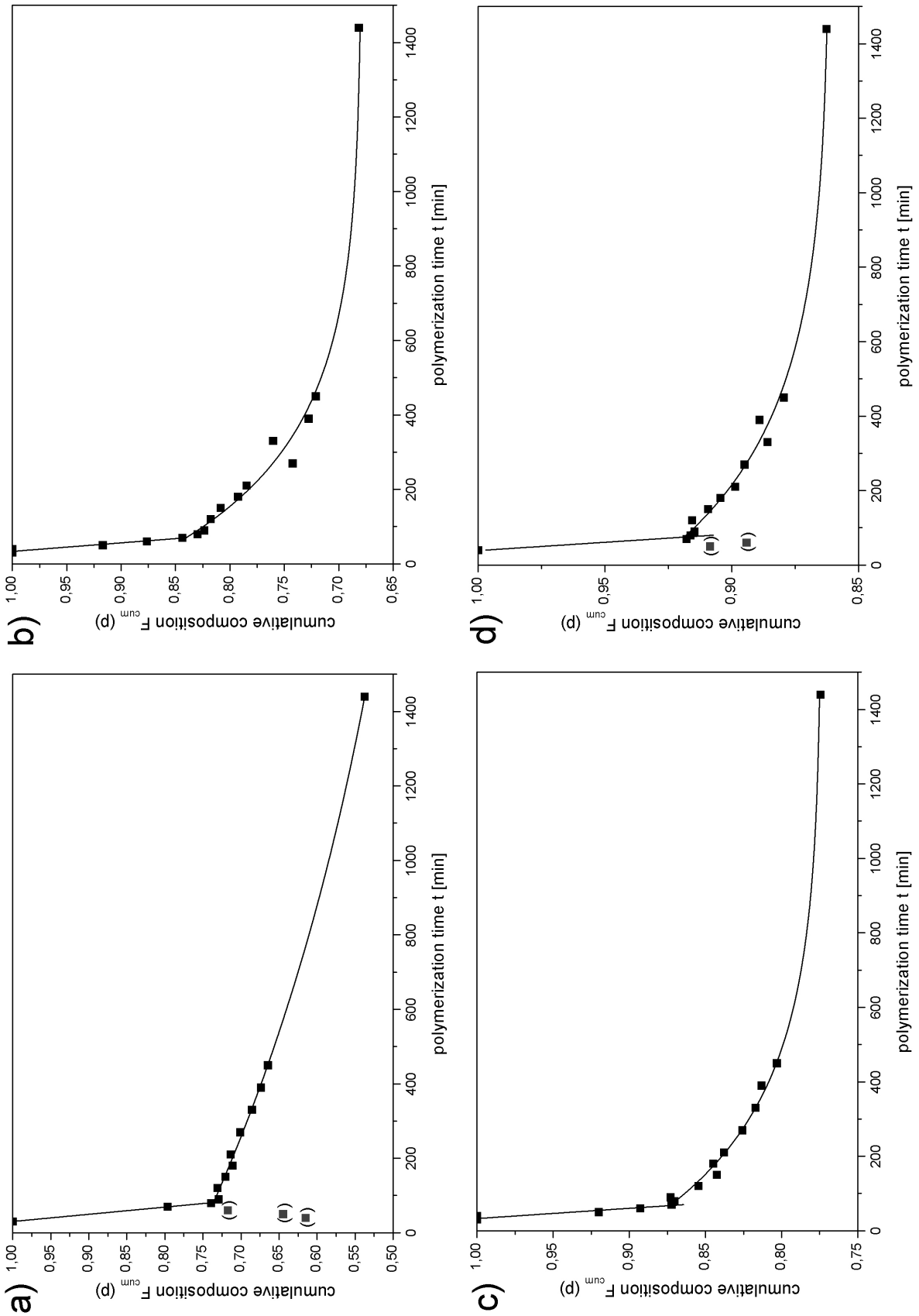

Fig. 5.8.: Plots of the cumulative compositions F_{cum} of gradient copolymers of *Series C* versus reaction time t (unconsidered values in brackets); a) V31 ($\phi_p = -1$, $f_{tBMA} = 0.5$), b) V32 ($\phi_p = -0.7$, $f_{tBMA} = 0.65$), c) V33 ($\phi_p = -0.5$, $f_{tBMA} = 0.75$), d) V34 ($\phi_p = -0.3$, $f_{tBMA} = 0.85$)

The cumulative composition $F_{cum,tBMA}$ of the early samples of V31 ($f_{tBMA} = 0.5$) and V34 ($f_{tBMA} = 0.85$) gave scattering values, see *Figure 5.8*. Some values differed so strong that they were not used in the analysis of the cumulative compositions. The points are shown with brackets in *Figures 5.8* and *5.10*. Beside this the compositional curves of the four polymerizations were consistent, although the slopes of the respective compositional curves were not consistent. All cumulative compositions first reduced strongly and then leveled off exponentially. F_{cum} is proportional to the conversion ($F_{cum} = \alpha \cdot p$), hence F(t) cannot become time–linear. The equations of the decreasing curve fractions are given with the *Equations 5.2.26* to *5.2.33*.

$$\text{V31}: \quad F_{cum}^{tBMA}(p_{<80min}) = (1.1559 \pm 0.0065) - (0.0052 \pm 0.0001) \cdot t \tag{5.2.26}$$

$$F_{cum}^{tBMA}(p_{\geq 80min}) = (0.3859 \pm 0.0390) + (0.3681 \pm 0.0368) \cdot e^{(-0.0007 \pm 0.0001) \cdot t} \tag{5.2.27}$$

$$\text{V32}: \quad F_{cum}^{tBMA}(p_{<70min}) = (1.1456 \pm 0.0333) - (0.0044 \pm 0.0006) \cdot t \tag{5.2.28}$$

$$F_{cum}^{tBMA}(p_{\geq 70min}) = (0.6789 \pm 0.0093) + (0.2048 \pm 0.0113) \cdot e^{(-0.0034 \pm 0.0005) \cdot t} \tag{5.2.29}$$

$$\text{V33}: \quad F_{cum}^{tBMA}(p_{<70min}) = (1.1184 \pm 0.0331) - (0.0036 \pm 0.0006) \cdot t \tag{5.2.30}$$

$$F_{cum}^{tBMA}(p_{\geq 70min}) = (0.7738 \pm 0.0042) + (0.1233 \pm 0.0047) \cdot e^{(-0.0032 \pm 0.0004) \cdot t} \tag{5.2.31}$$

$$\text{V34}: \quad F_{cum}^{tBMA}(p_{<80min}) = (1.0867 \pm 0.0339) - (0.0022 \pm 0.0005) \cdot t \tag{5.2.32}$$

$$F_{cum}^{tBMA}(p_{\geq 80min}) = (0.8613 \pm 0.0032) + (0.0709 \pm 0.0036) \cdot e^{(-0.0028 \pm 0.0004) \cdot t} \tag{5.2.33}$$

Both slopes decreased with the increase of tBMA in the copolymerization systems. All resulting polymers had a cumulative composition which was slightly higher than the theoretical expected values. The calculation of the instantaneous composition $F_{inst,tBMA}$ of the gradient copolymers gave scattering values with all four polymerizations, see *Figure 5.9*. These results were not very surprising. In *Equation 5.2.25* the differential quotient $(dF_{cum}/dp)_p$ was approximated by the differential quotient:

$$\frac{\Delta F_{cum}}{\Delta p} = \frac{F_{cum}^{i+1} - F_{cum}^{i}}{p^{i+1} - p^{i}} \tag{5.2.34}$$

This is a very crude approximation, which is known to be very sensitive to even small experimental errors in F_{cum} and p. Since the experimental error of the ^{1}H–NMR based on the determination of F_{cum} and p is between 5–10 %, the difference quotient calculation strongly amplified the deviations, and results in heavy scattering of the obtained instantaneous compositions, F_{inst}. To overcome the described problem, a second strategy of data evaluation was tried: It was attempted to fit a sufficient analytical function to the cumulative composition $F_{cum}(p)$. This function can smoothly be derived and the respective derivative $dF_{cum}^{(fit)}/dp$ can be used to calculate the instantaneous composition $F_{inst}(p)$ (cf. *Equation 5.2.35*).

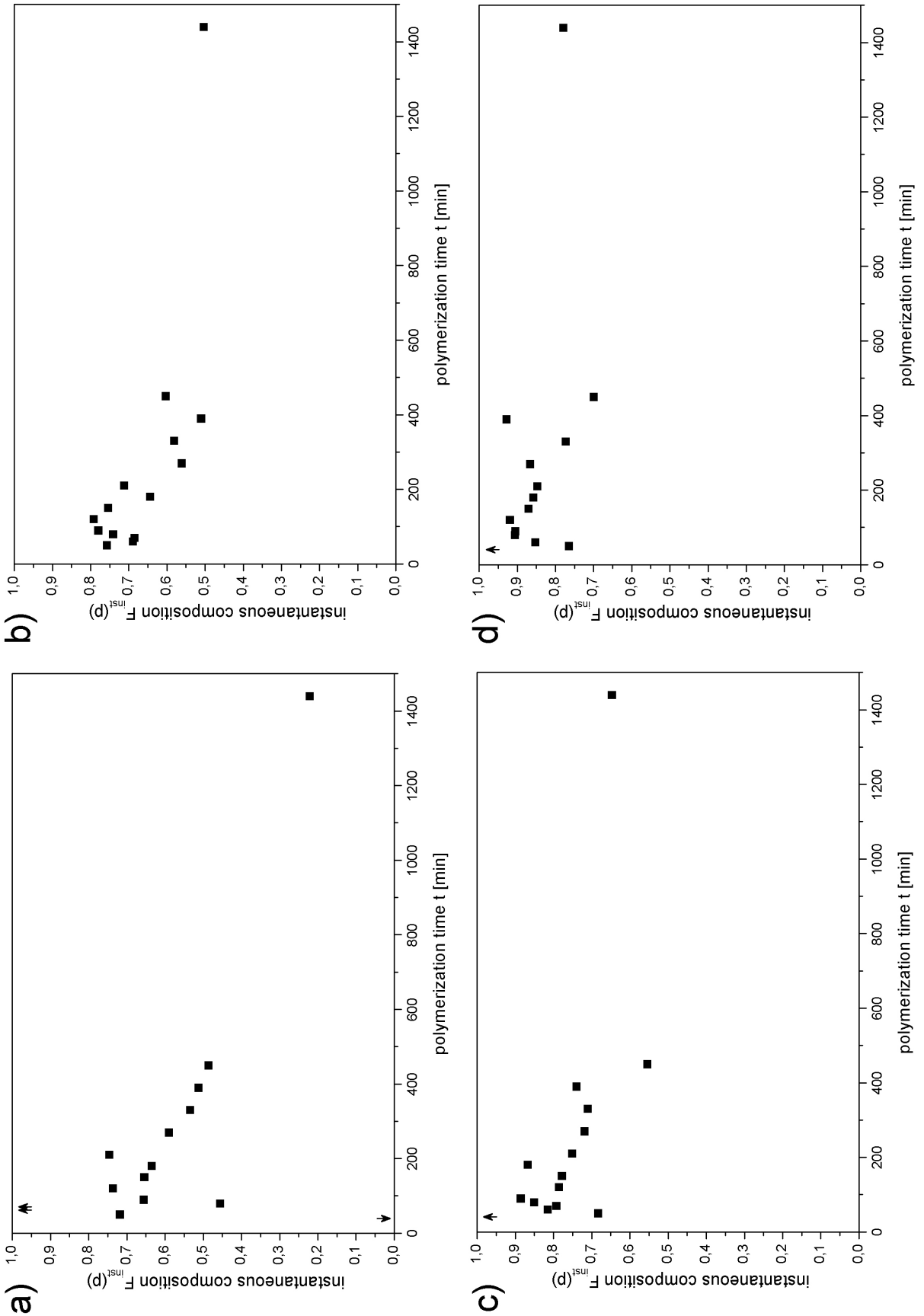

Fig. 5.9.: Plots of the instantaneous compositions F_{inst} of gradient copolymers of *Series C* versus reaction time t (chemical incorrect values indicated with arrows); a) V31 (ϕ_p = –1, f_{tBMA} = 0.5), b) V32 (ϕ_p = –0.7, f_{tBMA} = 0.65), c) V33 (ϕ_p = –0.5, f_{tBMA} = 0.75), d) V34 (ϕ_p = –0.3, f_{tBMA} = 0.85)

The plots of the cumulative compositions as a function of the conversions p, see *Figure 5.10*, showed that the $F_{cum}(p)$ of the four polymerizations changed in a similar fashion as the plot against polymerization time. First there was strong linear decrease up to an average conversion of about 16 %. Then the slope became flatter but remained linear for all four polymerizations up to 91 %. The value of conversion at which the slope changed will be called "changing point" (P_c) in the subsequent text. Hence, the curves $F_{cum}(p)$ can be well approximated by two linear functions of slope $s_i = (dF_{cum}/dp)^{(fit)}$ ($i = 1 : p < 0.16$, $i = 2 : 0.16 < p < 0.91$). In *Table 5.6* the two slopes and also the average slope are listed.

The instantaneous tBMA molar fraction of the copolymer was calculated by means of *Equation 5.2.35*, using slope s_1 in the conversion interval $p \in [0, 0.16]$ and slope s_2 with $p \geq [0.16]$. Hence, for each P_c two instantaneous compositions were calculated. Furthermore the instantaneous composition was calculated with the average slope of the cumulative composition and *Equation 5.2.35*.

$$F_{inst}^{tBMA}(p) = F_{cum}^{tBMA}(p) + p \cdot \left(\frac{dF_{cum}^{tBMA}(p)}{dp} \right)_i^{(fit)} \tag{5.2.35}$$

The results of the calculations of $F_{inst}(p)$ with the *Equations 5.2.25* and *5.2.35* are summarized in *Table 5.5* and the values are plotted in the *Figure 5.11*. Slope s_2 decreased with the increase of the tBMA–units in the polymer chain.

Like in *Figure 5.9* the data points, resulting from *Equation 5.2.25* scattered strongly. The reason was the described amplification of the compositional errors by numeric derivation like the one of the first calculation of the instantaneous composition. The instantaneous compositions which were calculated from *Equation 5.2.35* scattered less than the ones obtained with *Equation 5.2.25*, both, the values calculates by the slopes s_1 and s_2 and the values calculated by the average slope. The equation of the fits are given in *Equation 5.2.36*. The slopes of the fits are given in *Table 8.6*.

$$F_{inst}^{tBMA} = 1 - \phi_{p,i} \cdot p \tag{5.2.36}$$

with F_{inst}^{tBMA}= instantaneous molar fraction of tBMA in the gradient copolymer, p = total monomer conversion

The final F_{inst}^{tBMA} values of all four resulting copolymers were lower than the target compositions (see *Figure 5.11*, dotted line). However, the polymers can be described by an average gradient of $\phi_{p,av}$ (V31 = 0.77, V32 = 0.64, V33 = 0.41, V34 = 0.21) that is calculated by means of *Equation 5.2.35*, using the average slopes of the whole $F_{cum}(p)$–curves (s_{av}), see *Table 5.6*.

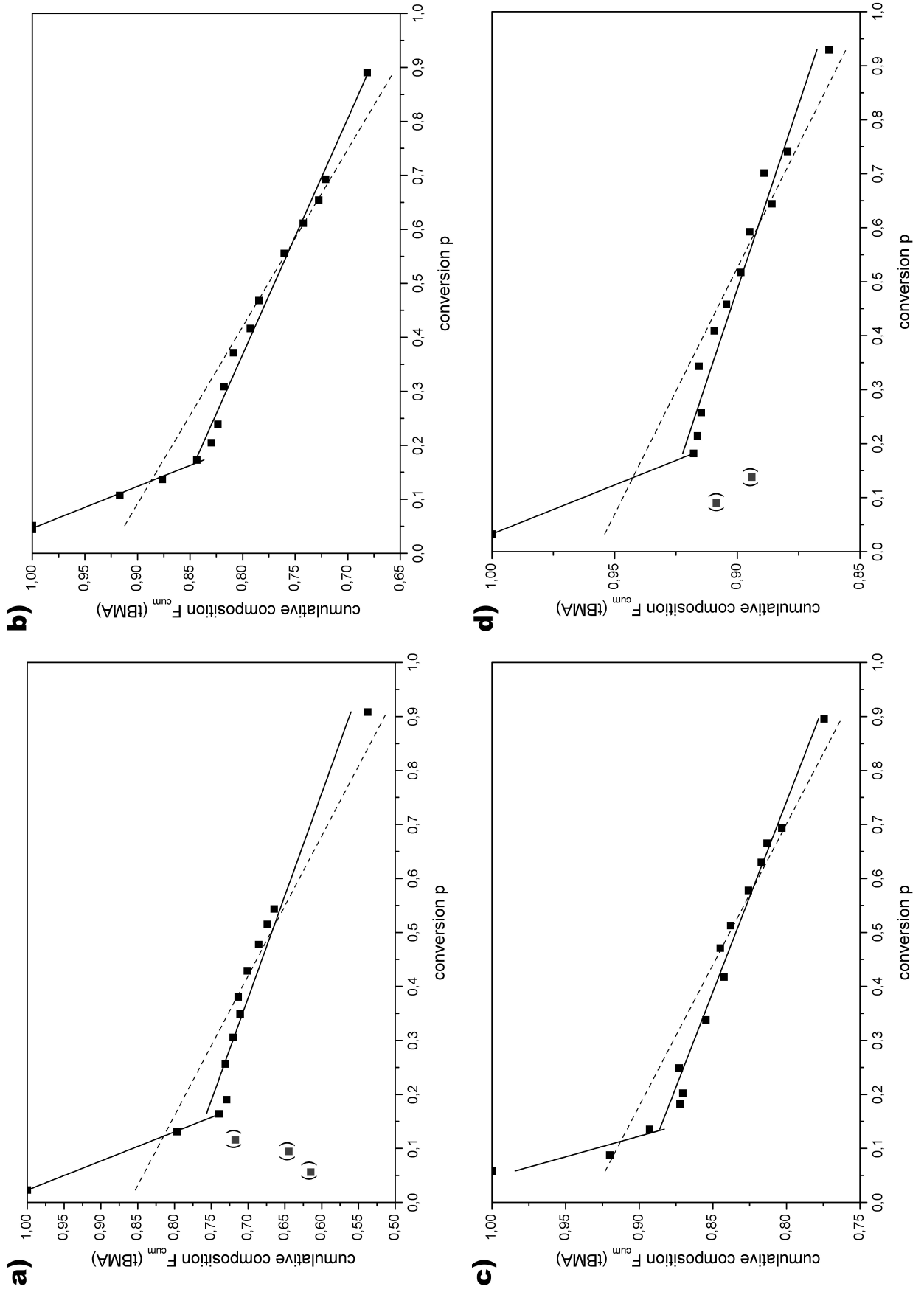

Fig. 5.10.: Plots of the cumulative compositions F_{cum} of gradient copolymers of *Series C* versus conversion p; a) V31 (ϕ_p = –1, f_{tBMA} = 0.5), b) V32 (ϕ_p = –0.7, f_{tBMA} = 0.65), c) V33 (ϕ_p = –0.5, f_{tBMA} = 0.75), d) V34 (ϕ_p = –0.3, f_{tBMA} = 0.85); dashed line – average slope; unconsidered value in brackets

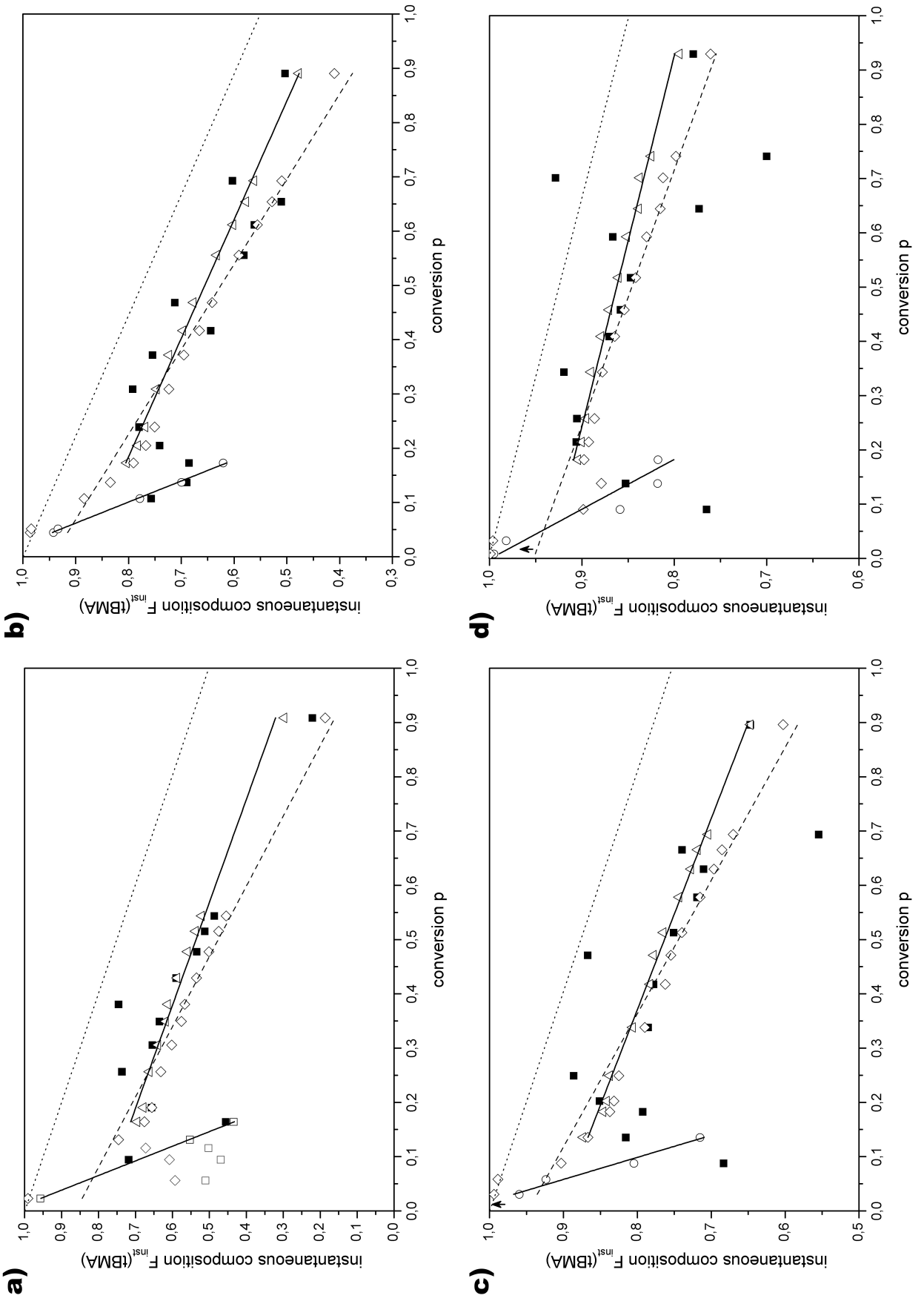

Fig. 5.11.: Plots of the instantaneous compositions F_{inst} of gradient copolymers of *Series C* versus conversion p; a) V31 ($\phi_p = -1$, $f_{tBMA} = 0.5$), b) V32 ($\phi_p = -0.7$, $f_{tBMA} = 0.65$), c) V33 ($\phi_p = -0.5$, $f_{tBMA} = 0.75$), d) V34 ($\phi_p = -0.3$, $f_{tBMA} = 0.85$); ■ F_{inst} calculated by *Equation 5.2.25*, □ F_{inst} calculated by *Equation 5.2.35*, △ F_{inst} calculated by *Equation 5.2.35* with average slope of F_{cum}; dashed line – average slope; dotted line – ideal run of the curve; chemical incorrect value indicated with arrow

Since however, these averages may cause misleading interpretations, the gradient copolymers will be named as V31 = $GP_{0.53}$, V32 = $GP_{0.46}$, V33 = $GP_{0.28}$ and V34 = $GP_{0.15}$ referring to the $\phi_{p,2}$ that dominates the polymer chain. The target compositions were $\phi_{p,target}$ are listed in *Table 5.3*. The differences were -48 % for V31, -34 % for V32, -44 % for V33 and -50 % for V34. Due to the binary slopes the resulting compositions differed strongly from the target values and due to the binary slopes the copolymers can be described as "double gradients".

Tab. 5.6.: Slopes of decreases of cumulative and instantaneous compositions against composition of experiments V31 to V34

Entry	f_{tBMA}	$\phi_{p,target}$	p	$s_i = \frac{dF_{cum}}{d_p}$	$\phi_p = \frac{dF_{inst}}{dp}$	$\Delta\phi_p$
V31	0.50	-1.0	0.00 ... 0.16	-1.8558 ± 0.0301	-3.7116 ± 0.0301	
			0.16 ... 0.91	-0.2636 ± 0.0224	-0.5273 ± 0.0224	-47 %
			0.00 ... 0.91	-0.3862 ± 0.0680	-0.7725 ± 0.0680	-23 %
V32	0.65	-0.7	0.00 ... 0.17	-1.2880 ± 0.0658	-2.5761 ± 0.0658	
			0.17 ... 0.89	-0.2287 ± 0.0081	-0.4574 ± 0.0081	-34 %
			0.00 ... 0.89	-0.3047 ± 0.0334	-0.6379 ± 0.0369	-10 %
V33	0.75	-0.5	0.00 ... 0.14	-1.3104 ± 0.5697	-2.4602 ± 0.3079	
			0.14 ... 0.90	-0.1419 ± 0.0063	-0.2838 ± 0.0063	-44 %
			0.00 ... 0.90	-0.1915 ± 0.0266	-0.4075 ± 0.0293	-18 %
V34	0.85	-0.3	0.00 ... 0.18	-0.5504 ± 0.0005	-1.0886 ± 0.2696	
			0.18 ... 0.93	-0.0732 ± 0.0050	-0.1463 ± 0.0050	-50 %
			0.00 ... 0.93	-0.1096 ± 0.0193	-0.2127 ± 0.0233	-30 %

The observed dependence of the compositional data from the monomer conversion suggested that the injection of the second monomer nBMA into the ATRP system of the initiator pTSC, the ligand PMDETA, the catalyst $Cu^{I}Cl/Cu^{II}Cl$ and the first monomer tBMA disturbed the equilibrium of the system. This kinetic effect could not be seen before in the batch experiments because there the monomer mixture ($n_{i,S}$, $n_{i,P}$, i = nBMA, tBMA) started in equilibrium. It can be seen from the composition–time data that the ATRP system required around 75 min until a new transient equilibrium was build up again. After this time the mixing ratio deviated from the assumptions which were used for the calculations of the injection program, hence the feed program did not fit to the existing monomer mixture. The fact that the feed solution had not the same temperature than the stock solution could also contribute to the disorder of the equilibrium. In further experiment the use of a heating bath would be useful. Other problems like contamination of the monomer with 4–methoxyphenol (the inhibitor which used for the storage of the monomers) or oxygen can be excluded, because these contaminants were eliminated by the filtration of the monomer over an excess of aluminium oxide and the performed freeze–melt–cycles. To solve this problem two way are possible: The complex–equilibrium can be introduced into the model of the injection program. The second way is to employ empirical relation of monomer feed. That means to test and change the feed program until it fits to the equilibrium changes of the monomer mixture.

5.2.3. Structural Analysis

As described with the batch polymerizations in *Section 3.3.2* the purity and the composition of the resulting copolymers was analyzed by means of elementary analysis. The results of the measurements and the differences between the theoretical and the analysis results are listed in *Table 5.7*.

The element compositions of the statistical copolymers (cf. *Tables 3.7* and *3.8*) and the gradient copolymers were nearly similar. Hence, both copolymerization method, batch and semibatch, gave consistent results. Moreover, the differences between the theoretical compositions and the measured values were small, indicating that the samples were free of pollution.

Tab. 5.7.: Results of the elementary analysis of the different gradient copolymer compositions of *Series C* with divergence from the set point

Entry f_{tBMA}	time [min]	C [%]	ΔC	H [%]	ΔH	O [%]	ΔO
set value		67.57		9.92		22.50	
V31	60	67.06	-0.51	9.28	-0.64	23.66	1.16
$GP_{0.53}$	90	67.22	-0.35	9.58	-0.34	23.20	0.70
0.5	150	66.56	-1.01	9.11	-0.81	24.33	1.83
	210	66.98	-0.59	8.96	-0.96	24.06	1.56
	330	67.24	-0.33	9.29	-0.63	23.47	0.97
	450	67.05	-0.52	9.10	-0.82	23.85	1.35
	1440	66.79	-0.78	9.23	-0.69	23.98	1.48
V32	60	67.06	-0.51	9.28	-0.64	23.66	1.16
$GP_{0.46}$	90	67.22	-0.35	9.58	-0.34	23.20	0.70
0.65	150	67.43	-0.14	9.34	-0.58	23.23	0.73
	210	67.55	-0.02	9.50	-0.42	22.95	0.45
	330	67.54	-0.03	9.38	-0.54	23.08	0.58
	450	67.18	-0.39	9.33	-0.59	23.49	0.99
	1440	67.10	-0.47	9.55	-0.37	23.35	0.85
V33	60	67.56	-0.01	9.38	-0.54	23.06	0.56
$GP_{0.28}$	90	67.75	0.18	9.35	-0.57	22.90	0.40
0.75	150	67.82	0.25	9.34	-0.58	22.84	0.34
	210	67.85	0.28	9.25	-0.67	22.90	0.40
	330	67.87	0.30	9.37	-0.55	22.76	0.26
	450	68.05	0.48	9.42	-0.50	22.53	0.03
	1440	67.93	0.36	9.60	-0.32	22.47	-0.03

Continuation on next page ...

Entry f_{tBMA}	time [min]	C [%]	ΔC	H [%]	ΔH	O [%]	ΔO
V34	60	67.42	-0.15	9.13	-0.79	23.45	0.95
$GP_{0.15}$	90	67.14	-0.43	9.38	-0.54	23.48	0.98
0.85	150	67.39	-0.18	9.17	-0.75	23.44	0.94
	210	67.48	-0.09	9.38	-0.54	23.14	0.64
	330	67.47	-0.10	9.11	-0.81	23.42	0.92
	450	67.51	-0.06	9.35	-0.57	23.14	0.64
	1440	66.63	-0.94	9.07	-0.85	24.30	1.80

Subsequently the gradient copolymers were investigated with ATR–FTIR–spectroscopy. From all samples which were taken during the semibatch copolymerizations IR–spectra were measured and anlaysed in view to the peak height and peak area of the two vibrational bands, at 970 cm^{-1} (*band 1*), specific for the *n*–butyl–chain, and at 850 cm^{-1} (*band 2*), caused by the *tert*–butyl–group. The values are summarized in *Table 5.8*. For the comparison purpose the spectra were normalized by setting the adsorption intensity of the vibrational band at 1136 cm^{-1} to one by dividing all intensities A_x by A_1.

Tab. 5.8.: Peak area and peak height of the analyzed ATR–FTIR–bands of gradient copolymers P[tBMA–grad–nBMA] of *Series C*

		band 1		*band 2*	
Entry f_{tBMA}	time [min]	peak area [cm^{-1}]	peak height	peak area [cm^{-1}]	peak height
V31	60	3.52	0.074	8.79	0.414
$GP_{0.53}$	90	3.88	0.083	9.16	0.412
0.5	150	4.02	0.082	8.62	0.404
	210	4.40	0.089	8.49	0.391
	330	4.93	0.102	8.14	0.367
	450	5.22	0.108	7.95	0.358
	1440	5.71	0.123	6.95	0.307
V32	60	3.11	0.065	8.37	0.399
$GP_{0.46}$	90	3.45	0.071	8.54	0.402
0.65	150	4.07	0.082	8.74	0.402
	210	4.16	0.085	8.26	0.381
	330	4.49	0.090	8.05	0.367
	450	4.75	0.096	8.15	0.368
	1440	5.09	0.105	8.06	0.367

Continuation on next page ...

		band 1		*band 2*	
Entry	time	peak area	peak height	peak area	peak height
f_{tBMA}	[min]	[cm^{-1}]		[cm^{-1}]	
V33	60	3.26	0.067	8.77	0.414
$GP_{0.28}$	90	3.77	0.075	9.35	0.430
0.75	150	3.99	0.079	8.91	0.413
	210	3.91	0.077	8.30	0.389
	330	4.14	0.082	8.44	0.392
	450	4.37	0.087	8.70	0.401
	1440	4.52	0.093	8.66	0.400
V34	60	3.09	0.066	8.77	0.417
$GP_{0.15}$	90	3.47	0.072	8.82	0.415
0.85	150	3.63	0.071	8.92	0.419
	210	3.68	0.073	8.77	0.412
	330	3.54	0.069	8.34	0.396
	450	4.07	0.078	9.24	0.422
	1440	4.22	0.091	9.59	0.451

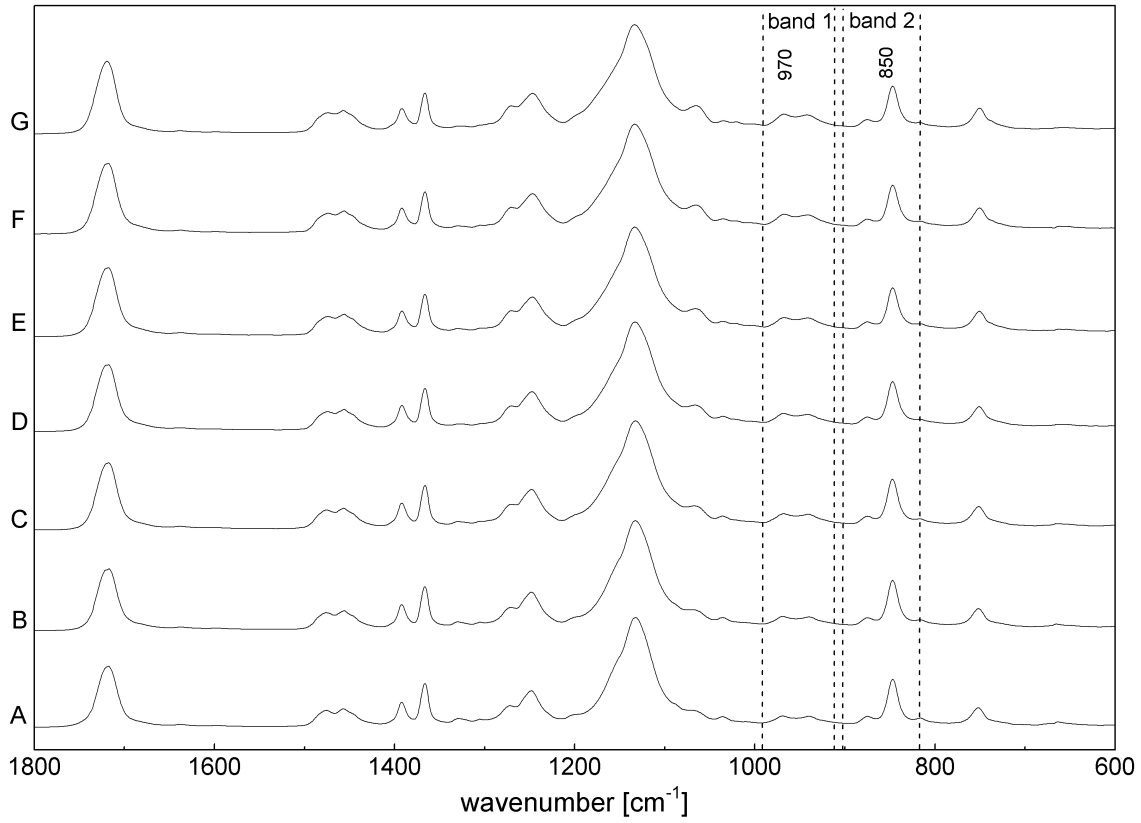

Fig. 5.12.: Finger print region of ATR–FTIR–spectra of samples of experiment V32 ($GP_{0.46}$, f_{tBMA} = 0.65); A – 60 min, B – 90 min, C – 150 min, D – 210 min, E – 330 min, F – 450 min and G – 1440 min of reaction time (Spectra normalized to A_{1136} = 1)

In *Figure 5.12* the fingerprint region of the samples of experiment V32 $GP_{0.46}$ (f_{tBMA} = 0.65) and in *Figure 5.13* an extended section of the spectra from 800 to 1000 cm^{-1} are shown to demonstrate the changes of the vibrational bands during the polymerization time more in detail. For *band 1* at 970 cm^{-1} the increase of the band was clearly recognizable. The decease of *band 2* at 850 cm^{-1} during the polymerization was, however, minimal. The incorporation of the nBMA, which was injected during the polymerization, inside the polymer chain lead to a constantly change of the composition of the copolymer and caused the rise of *band 1*. The changes of *band 2* were smaller during the polymerization time which must be attributed to a different extinction coefficient of the tBMA–units. Because the total amount of tBMA was present at the start of the synthesis the change was caused by the tBMA depletion of the solution. The IR–signal qualitatively support the NMR results.

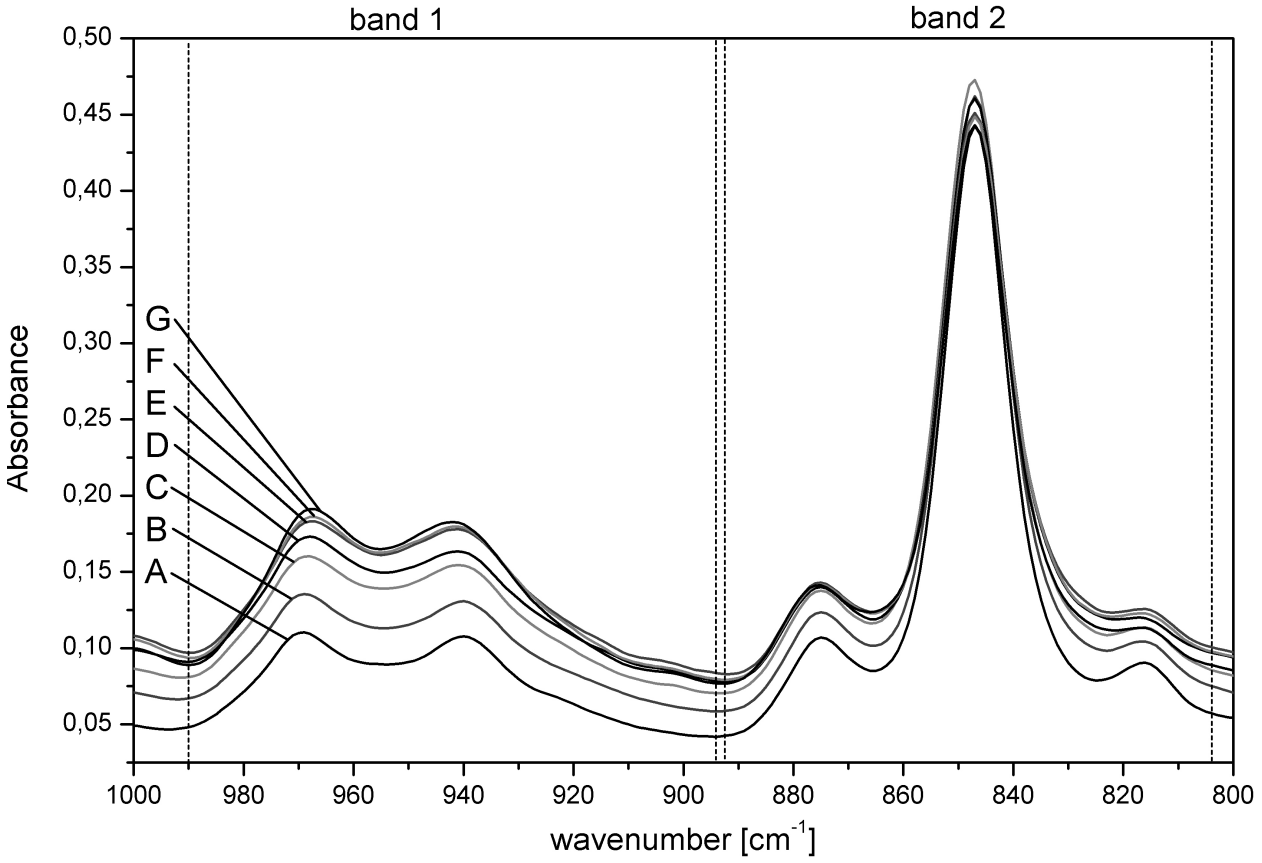

Fig. 5.13.: Section of ATR–FTIR–spectra of samples taken during experiment V32 ($GP_{0.46}$, f_{tBMA} = 0.65) with analyzed specific vibrational bands; A – 60 min, B – 90 min, C – 150 min, D – 210 min, E – 330 min, F – 450 min and G – 1440 min of reaction time (Spectra normalized to A_{1136} = 1)

In *Figure 5.14* the range of the absorption-spectra from 800 to 1000 cm^{-1} of the four resulting gradient copolymers are pictured to distinguish the differences between the compositions. The decrease of the amount of nBMA inside the polymer chain was represented in the IR–spectra with the decrease of the correlated vibrational *band 1*. *Band 2* did not show such a specific behavior between peak height/ area and copolymer composition.

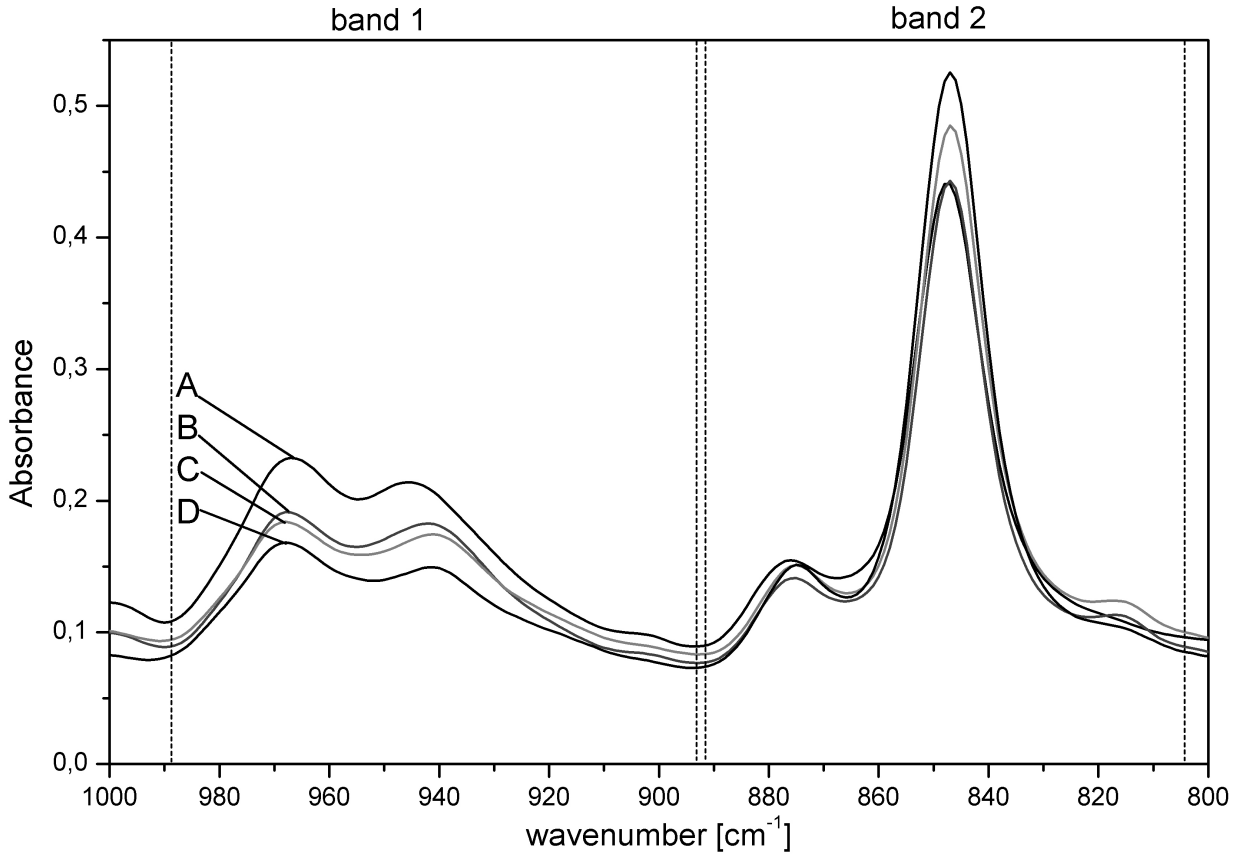

Fig. 5.14.: Section of ATR–FTIR–spectra of gradient copolymers P[tBMA–grad–nBMA] obtained after 1440 min of reaction time; A – $GP_{0.53}$ (V31, f_{tBMA} = 0.5), B – $GP_{0.46}$ (V32, f_{tBMA} = 0.65), C – $GP_{0.28}$ (V33, f_{tBMA} = 0.75), D – $GP_{0.15}$ (V33, f_{tBMA} = 0.85) (Spectra normalized to A_{1136} = 1)

The *Figures 5.15* and *5.16* depict the peak areas and peak heights of the two bands of the samples taken during the four semibatch copolymerizations. The *band 1* values of the peak area and the peak height increased during the polymerization and both values of *band 2* decreased. But the values of *band 2* scattered much more than that of *band 1*. In both graphs the values of *band 1* increased nearly linear at the beginning of the polymerization, then the rise leveled off. The values confirmed the observations from the *Figures 5.13* and *5.14*. Hence the peak height of *band 1* was used to determine the composition of the copolymer by a modified *Equation 3.3.20*, see *Equation 5.2.37*. The change was necessary because *Equation 3.3.20* was used to calculate F_{nBMA}.

$$F_{tBMA} = 1 - [(-0.524 \pm 0.081) + (9.862 \pm 1.278) \cdot PH_1 - (14.471 \pm 4.374) \cdot PH_1^2] \quad (5.2.37)$$

with F_{tBMA} = composition of the copolymer, PH_1 = peak height of *band 1*

The obtained compositions were compared with the cumulative compositions $F_{cum,tBMA}$ originating from the ^{1}H–NMR analysis. The results of these calculations are listed in *Table 5.9*. The compositions obtained from both methods did not differ much ($\lesssim 5\,\%$), expect from the first sample of experiment V31 taken at 60 min at 18 % conversion.

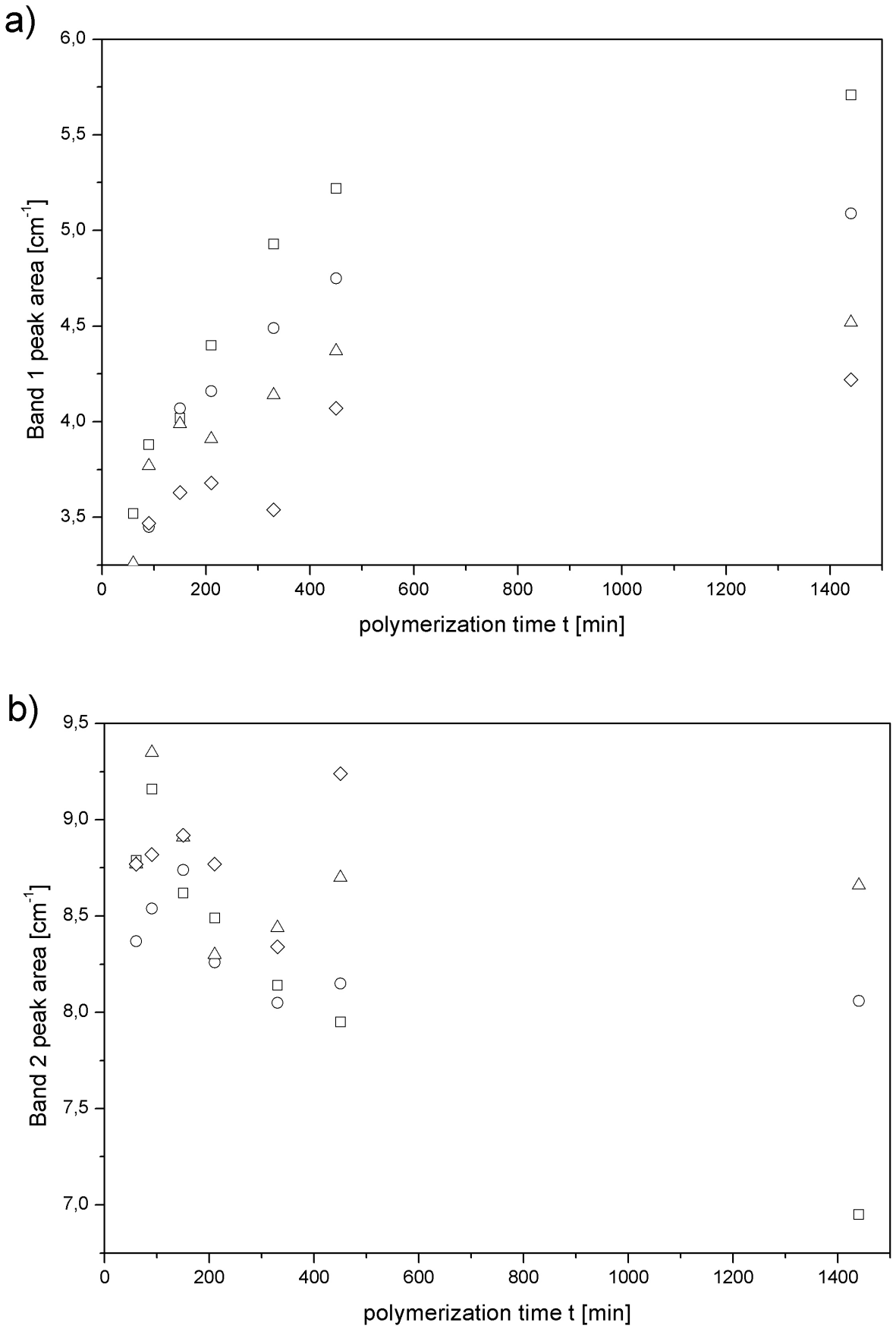

Fig. 5.15.: Plot of ATR–FTIR–spectra peak area a) *band 1* and b) *band 2* of gradient copolymers P[tBMA–grad–nBMA] *Series C* versus polymerization time t; $GP_{0.53}$ (□, V31, f_{tBMA} = 0.5), $GP_{0.46}$ (○, V32, f_{tBMA} = 0.65), $GP_{0.28}$ (△, V33, f_{tBMA} = 0.75), $GP_{0.15}$ (◇, V34, f_{tBMA} = 0.85)

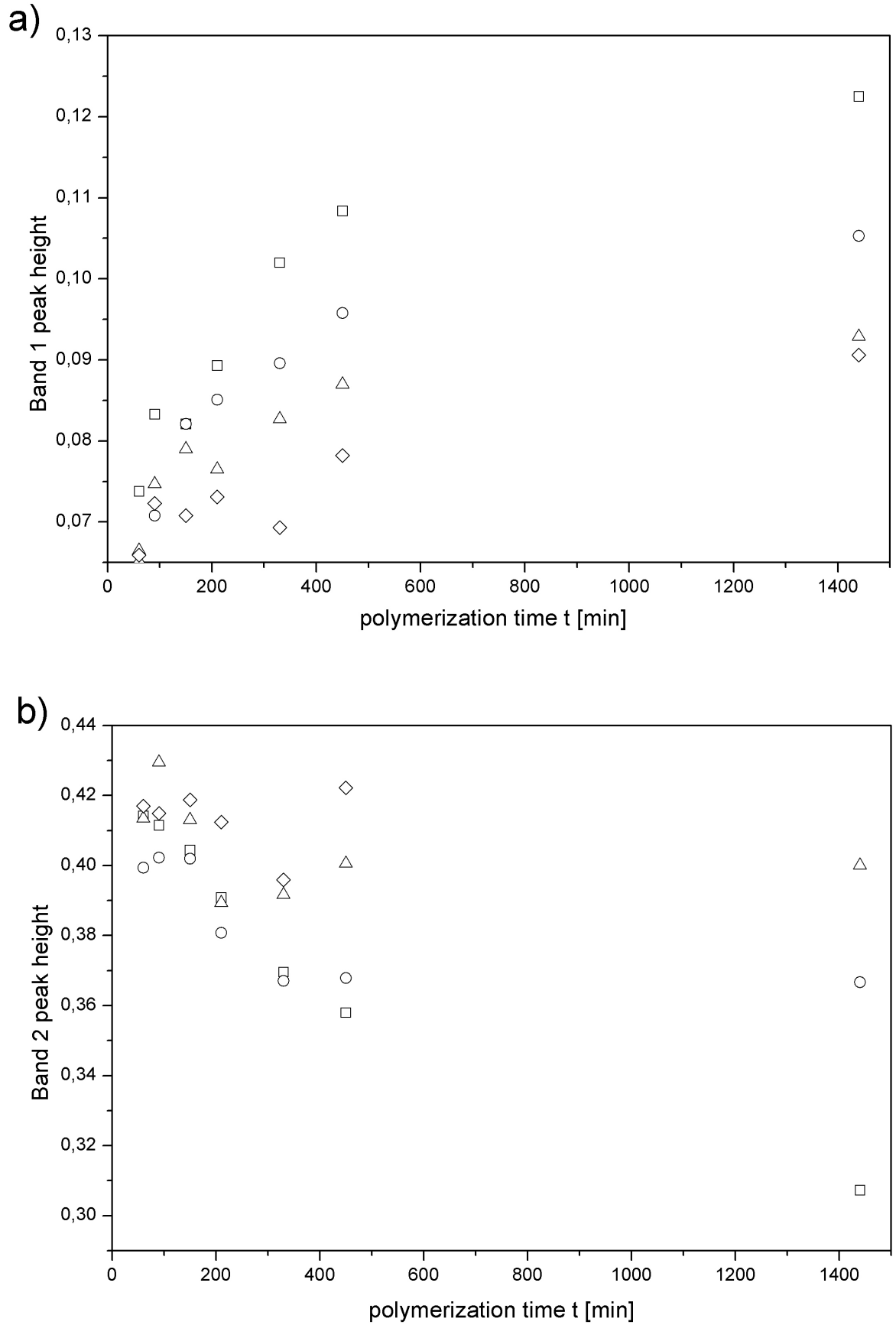

Fig. 5.16.: Plot of ATR–FTIR–spectra peak height a) *band 1* and b) *band 2* of gradient copolymers P[tBMA–grad–nBMA] *Series C* versus polymerization time t; $GP_{0.53}$ (□, V31, f_{tBMA} = 0.5), $GP_{0.46}$ (○, V32, f_{tBMA} = 0.65), $GP_{0.28}$ (△, V33, f_{tBMA} = 0.75), $GP_{0.15}$ (◇, V34, f_{tBMA} = 0.85)

Tab. 5.9.: Composition of gradient copolymers P[tBMA–grad–nBMA] of *Series C* calculated from peak height of *band 1*

Entry f_{tBMA}	time [min]	F_{nBMA} [a]	F_{cum}^{tBMA} [b] NMR	F_{cum}^{tBMA} [c] IR	ΔF [d]
V31	60	0.13	0.88	0.72	-0.16
$GP_{0.53}$	90	0.20	0.80	0.73	-0.07
0.5	150	0.19	0.81	0.72	-0.09
	210	0.24	0.76	0.71	-0.05
	330	0.33	0.67	0.69	0.02
	450	0.38	0.63	0.66	0.03
	1440	0.47	0.53	0.54	0.02
V32	60	0.05	0.95	0.88	-0.07
$GP_{0.46}$	90	0.10	0.90	0.82	-0.08
0.65	150	0.19	0.81	0.81	0.00
	210	0.21	0.79	0.78	-0.01
	330	0.24	0.76	0.76	0.00
	450	0.29	0.71	0.72	0.01
	1440	0.35	0.65	0.68	0.03
V33	60	0.07	0.93	0.89	-0.04
$GP_{0.28}$	90	0.13	0.87	0.87	0.00
0.75	150	0.17	0.84	0.84	0.00
	210	0.15	0.85	0.84	-0.01
	330	0.19	0.81	0.82	0.01
	450	0.22	0.78	0.80	0.02
	1440	0.27	0.73	0.77	0.04
V34	60	0.06	0.94	0.89	-0.05
$GP_{0.15}$	90	0.11	0.89	0.91	0.02
0.85	150	0.10	0.90	0.91	0.01
	210	0.12	0.88	0.90	0.02
	330	0.09	0.91	0.89	-0.02
	450	0.16	0.84	0.88	0.04
	1440	0.25	0.75	0.86	0.11

[a] calculated with *Eq. 3.3.20*

[b] calculated with *Eq. 5.2.37*

[c] calculated from ^{1}H–NMR–spectra

[d] $\Delta F = F_{cum}^{tBMA}(IR) - F_{cum}^{tBMA}(NMR)$

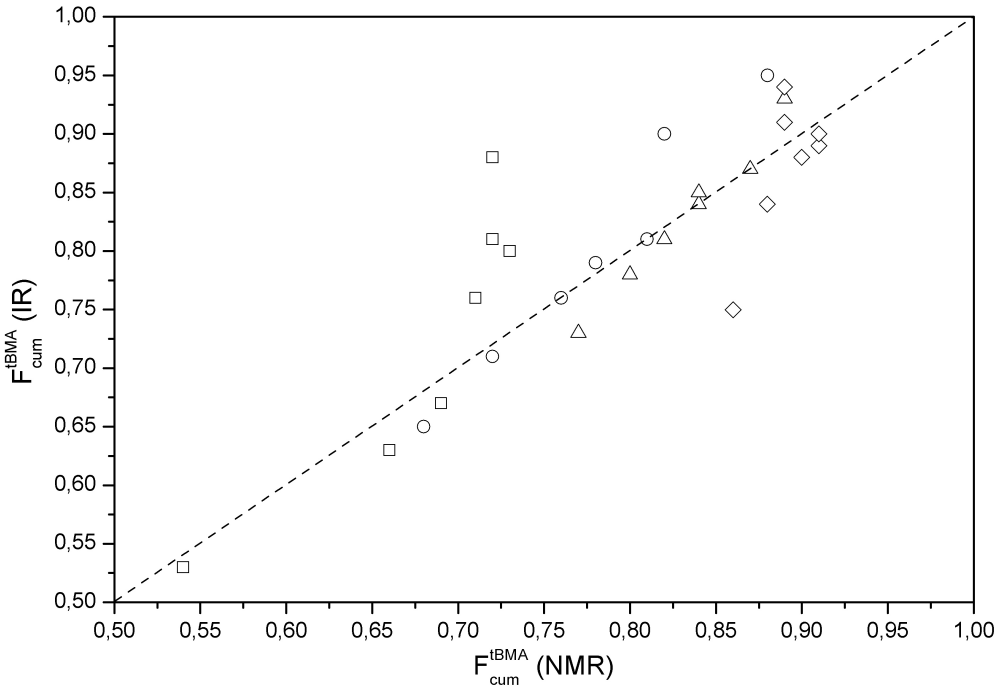

Fig. 5.17.: Interrelation of the cumulative compositions calculated from ^{1}H–NMR and from ATR–FTIR; $GP_{0.53}$ (□, f_{tBMA} = 0.5), $GP_{0.46}$ (○, f_{tBMA} = 0.65), $GP_{0.28}$ (△, f_{tBMA} = 0.75), $GP_{0.15}$ (◇, f_{tBMA} = 0.85), dashed line – ideal curve

With *Figure 5.17* the consensus between the compositions obtained from ^{1}H–NMR and from ATR–FTIR was determined. In case of perfect agreement the data points should be located on a straight line of slope s = 1. As a general tendency it can be noticed that tBMA contents of the gradient copolymers below 70 mol% gave good agreements, with the IR–values to be ≈2–4 mol% below the NMR–based compositions. At higher tBMA molar fraction strong data scattering was observed that, however, depended on the investigated polymer. While the points of $GP_{0.46}$ and $GP_{0.28}$ well fitted, $GP_{0.53}$ and $GP_{0.15}$ deviated from the ideal curve.

5.2.4. Molecular Weight Characterization

The finally obtained gradient copolymers of the semibatch copolymerizations and also the precipitated samples were analyzed with size exclusion chromatography. In *Figure 5.18* the elution diagrams based on the signal of the RI–detector of the samples which were taken during the polymerization at different times at experiment V32 ($GP_{0.46}$, f_{tBMA} = 0.65) are depicted as an example. All the RI–signals gave monomodal peaks, hence over the whole time of the semibatch copolymerization no termination reactions occurred. Furthermore the signals shifted to lower elution volumes with higher polymerization times of the sample, indicating an increasing molar mass of the samples. The RI–signals from all samples of the three other semibatch reactions looked alike. All four semibatch copolymerizations worked well with respect to the reaction control.

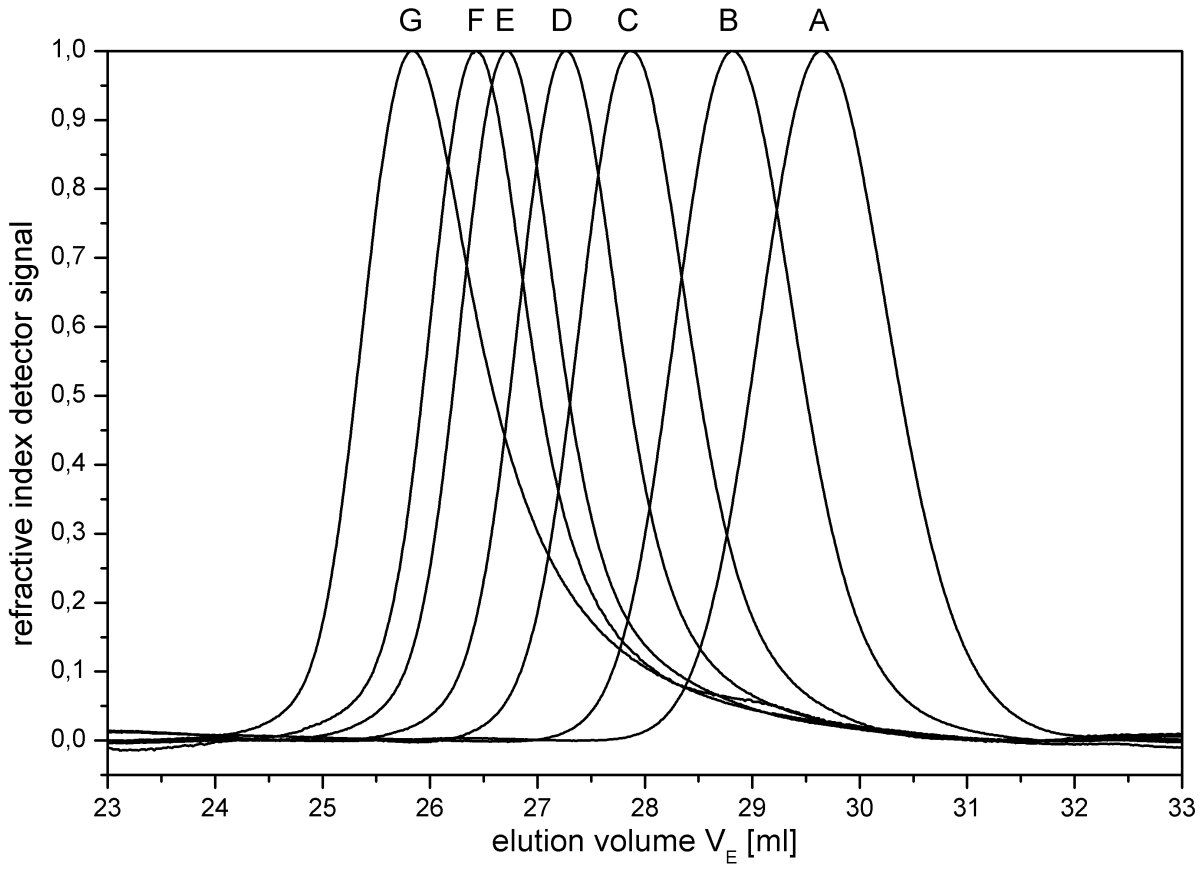

Fig. 5.18.: Elution diagrams of the samples of experiment V32 ($GP_{0.46}$, f_{tBMA} = 0.65); A – 60 min, B – 90 min, C – 150 min, D – 210 min, E – 330 min, F – 450 min and G – 1440 min of reaction time

With the calibration curve arising from polystyrene standards that was used in *Section 3.3.3, Figure 3.15*, the relative molar masses of the samples were calculated from the maximum elution volume V_E of the RI–signals. The elution volumes of the RI–signals of all samples of the four semibatch copolymerizations and the calculated relative molar masses are listed in *Table 5.11*. The values of the relative molar masses rose nearly linear at the beginning of all four copolymerizations than the slopes flattened. Because for the determination of the relative molar mass just one point of the RI–signal was used, not the whole sample was covered with this kind of molar mass determination. To account for this effect the absolute molar masses of the sample were determined. The next step was the determination of the differential refractive index increments dn/dc of the resulting gradient copolymers because these values are necessary for the calculation of the absolute molar mass of the polymers from light scattering data. This was done the same way as described with the statistical copolymers of experiment V11 to V19 in THF at 25 °C, cf. *Section 3.3.3*. The results of these measurements are listed in *Table 5.10* and are pictured in *Figure 5.19*.

A clear dependence of dn/dc from the copolymer composition could not be found just like it was for the statistical copolymer. However the dn/dc–values of the four gradient copolymers lay in a small range from $0.080\,ml \cdot g^{-1}$ to $0.087\,ml \cdot g^{-1}$, this is the same range that was found

with the statistical copolymers, cf. *Table 3.10*, which had dn/dc values between 0.0612 ml · g^{-1} and 0.0988 ml · g^{-1}.

Tab. 5.10.: Differential refractive index increment dn/dc of the different copolymer compositions of *Series C*

Entry	GradCoPo	F_{tBMA}	dn/dc [ml · g^{-1}]
V31	$GP_{0.53}$	0.54	0.0853 ± 0.0003
V32	$GP_{0.46}$	0.68	0.0843 ± 0.0004
V33	$GP_{0.28}$	0.77	0.0870 ± 0.0011
V34	$GP_{0.15}$	0.86	0.0799 ± 0.0017

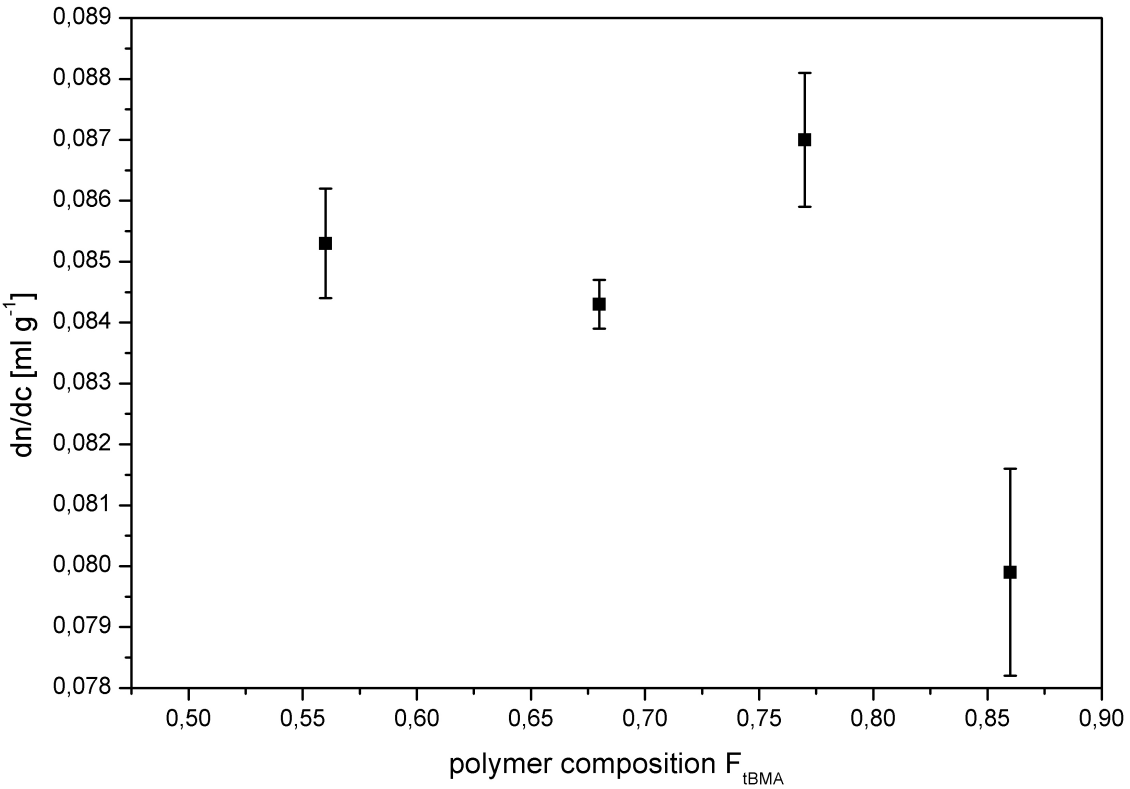

Fig. 5.19.: Differential refractive index increments dn/dc of the final different gradient copolymer compositions of P[tBMA–grad–nBMA]

With the results from the determination of dn/dc the molecular weight averages (M_n, M_w, M_z) and from these the polydispersity indices PDI (M_w/M_n, M_z/M_n) of the samples of the four semibatch copolymerizations were determined in the same way as for the statistical copolymers in *Section 3.3.3*. *Figure 5.20* depicts the RI– and the 90°–MALS– detector signals of the elution–diagram of the resulting gradient copolymer V34 ($GP_{0.15}$). From the angle dependence of the scattered light intensity and the known dn/dc–value of = 0.0799 ml · g^{-1} (cf. *Table 5.10*) the absolute molecular weight of a fraction at a given elution volume can be derived. The calculated molecular weights are also shown in *Figure 5.20* (right axis). Since the RI–signal is proportional to the weight fraction of the eluted polymer, the complete

molecular weight distribution (MWD) of the measured polymer can be obtained and with this the molecular weight averages and the polydispersity indices can be calculated.

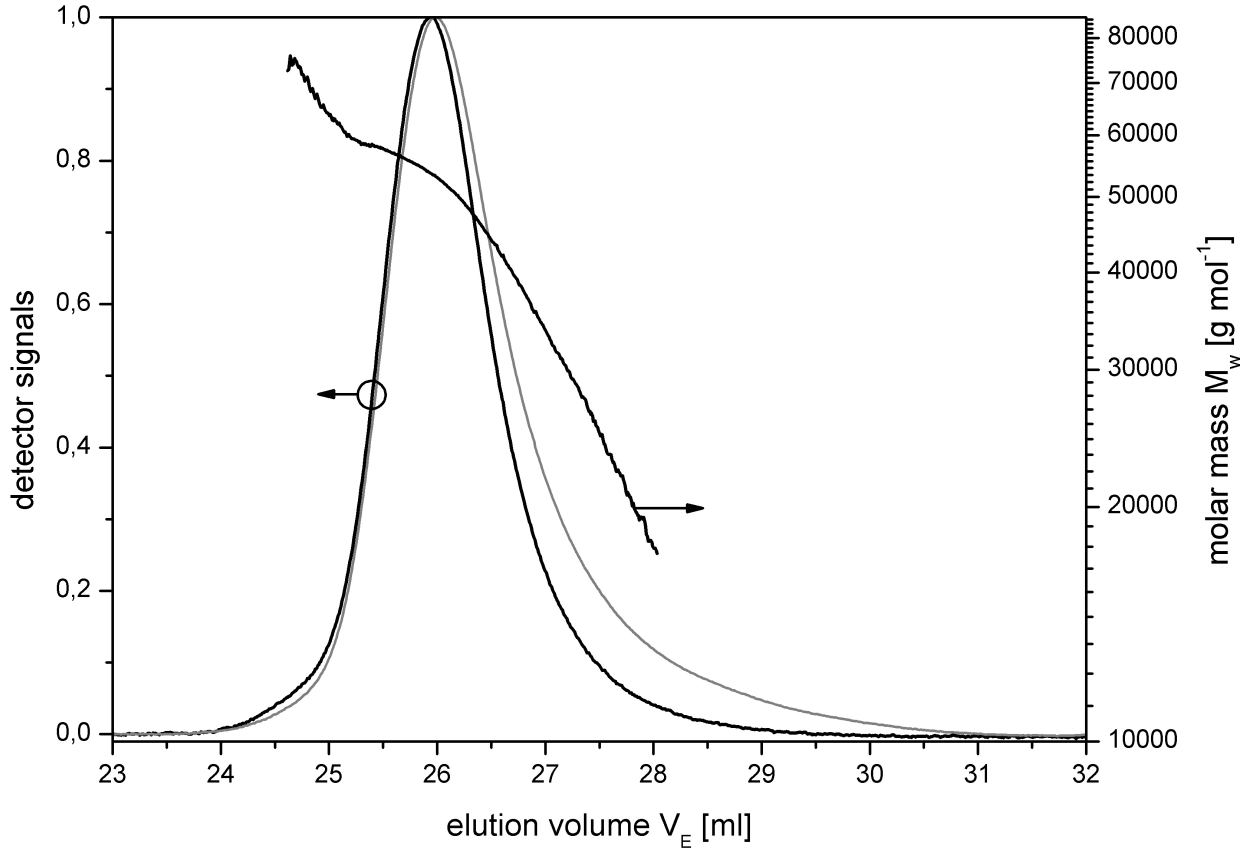

Fig. 5.20.: SEC elution diagrams and molar masses of gradient copolymer V34 ($GP_{0.15}$, f_{tBMA} = 0.85) obtained after 1440 min of reaction time; black curve – light scattering signal, grey curve – refractive index signal

The obtained values are detailed in *Table 5.12*. Both detector signals in *Figure 5.20* did not show fronting or tailing which indicated the lack of termination and chain extension reaction during the reaction time of 1440 min.

Tab. 5.11.: Comparison of relative* and absolute molar masses of the different gradient copolymer compositions of P[tBMA–grad–nBMA]

Entry	time	V_E	relative M*	absolute M	ΔM	
f_{tBMA}	[min]	[ml]	[g · mol^{-1}]	[g · mol^{-1}]	[g · mol^{-1}]	[%]
V31	60	29.98	5679	5208	471	-9.04
$GP_{0.53}$	90	29.17	8575	7824	751	-9.60
0.5	150	28.22	13952	13880	72	-0.52
	210	27.68	18281	17900	381	-2.13
	330	27.05	25175	25060	115	-0.46
	450	26.69	30259	31110	-851	2.74

Continuation on next page ...

Entry f_{tBMA}	time [min]	V_E [ml]	relative M* [g · mol^{-1}]	absolute M [g · mol^{-1}]	ΔM [g · mol^{-1}]	[%]
	1440	25.37	59132	58890	242	-0.41
V32	60	29.63	6792	6633	159	-2.40
$GP_{0.46}$	90	28.80	10339	10620	-281	2.65
0.65	150	27.87	16599	17040	-441	2.59
	210	27.27	22517	23270	-753	3.23
	330	26.71	30032	30660	-628	2.05
	450	26.42	34791	35890	-1099	3.06
	1440	25.83	46905	47210	-305	0.65
V33	60	29.22	8363	7297	1066	-14.61
$GP_{0.28}$	90	28.37	12886	12230	656	-5.36
0.75	150	27.30	22229	21710	519	-2.39
	210	26.84	28083	27840	243	-0.87
	330	26.45	34152	35640	-1488	4.18
	450	26.17	39508	38000	1508	-3.97
	1440	25.52	54819	49860	4959	-9.94
V34	60	29.41	7603	8174	-571	6.99
$GP_{0.15}$	90	28.44	12425	13680	-1255	9.18
0.85	150	27.54	19672	20850	-1178	5.65
	210	27.21	23296	26000	-2704	10.40
	330	26.64	31023	33380	-2357	7.06
	450	26.37	35701	37520	-1819	4.85
	1440	25.94	44411	47270	-2859	6.05

* calibrated against PS–Standard

Tab. 5.12.: SEC results of *Series C*

Entry f_{tBMA}	time [min]	M_n [g · mol^{-1}]	M_w [g · mol^{-1}]	M_z [g · mol^{-1}]	M_w/M_n	M_z/M_n
V31	60	4987 ±150	5208 ±208	5566 ±612	1.044 ±0.052	1.116 ±0.134
$GP_{0.53}$	90	7431 ±149	7824 ±235	8340 ±334	1.053 ±0.021	1.122 ±0.056
0.5	150	13640 ±136	13880 ±139	14220 ±427	1.018 ±0.020	1.043 ±0.031
	210	17550 ±176	17900 ±179	18230 ±365	1.020 ±0.020	1.039 ±0.021
	330	24360 ±146	25060 ±125	25560 ±256	1.029 ±0.008	1.049 ±0.010
	450	30570 ±122	31110 ±124	31550 ±252	1.017 ±0.005	1.032 ±0.009
	1440	55050 ±165	58890 ±118	61900 ±310	1.070 ±0.004	1.124 ±0.007

Continuation on next page ...

Entry f_{tBMA}	time [min]	M_n [g · mol^{-1}]	M_w [g · mol^{-1}]	M_z [g · mol^{-1}]	M_w/M_n	M_z/M_n
V32	60	6170 ±123	6633 ±265	7948 ±1431	1.075 ±0.054	1.288 ±0.232
$GP_{0.46}$	90	10180 ±204	10620 ±212	11190 ±560	1.043 ±0.031	1.099 ±0.066
0.65	150	16550 ±1655	17040 ±153	17520 ±350	1.029 ±0.010	1.058 ±0.021
	210	22470 ±225	23270 ±465	24120 ±965	1.036 ±0.021	1.073 ±0.043
	330	28650 ±2865	30660 ±153	31900 ±319	1.070 ±0.011	1.113 ±0.011
	450	34050 ±681	35890 ±718	37230 ±1862	1.054 ±0.032	1.093 ±0.055
	1440	43190 ±389	47210 ±236	50200 ±502	1.093 ±0.011	1.162 ±0.012
V33	60	6924 ±208	7297 ±219	8067 ±807	1.054 ±0.042	1.165 ±0.128
$GP_{0.28}$	90	11730 ±117	12230 ±122	12680 ±380	1.043 ±0.021	1.081 ±0.032
0.75	150	20840 ±146	21710 ±130	22450 ±225	1.041 ±0.009	1.077 ±0.022
	210	26890 ±269	27840 ±278	28950 ±869	1.035 ±0.021	1.077 ±0.032
	330	35260 ±705	35640 ±713	36020 ±1081	1.011 ±0.020	1.022 ±0.041
	450	35210 ±317	38000 ±190	39840 ±398	1.079 ±0.011	1.131 ±0.011
	1440	45380 ±227	49860 ±150	53050 ±371	1.099 ±0.007	1.169 ±0.011
V34	60	7527 ±301	8174 ±490	10440 ±2088	1.086 ±0.076	1.387 ±0.291
$GP_{0.15}$	90	13040 ±391	13680 ±684	15210 ±2890	1.049 ±0.063	1.166 ±0.222
0.85	150	20230 ±405	20850 ±417	22120 ±1327	1.031 ±0.031	1.094 ±0.066
	210	25110 ±251	26000 ±234	26760 ±535	1.035 ±0.021	1.066 ±0.021
	330	32160 ±289	33380 ±200	34580 ±346	1.038 ±0.010	1.075 ±0.022
	450	35210 ±211	37520 ±150	39190 ±353	1.066 ±0.009	1.113 ±0.011
	1440	43720 ±437	47270 ±378	49820 ±996	1.081 ±0.011	1.140 ±0.023

The results of the SEC analysis were compared for the different copolymer compositions and the change over the polymerization time (*Figure 5.21*) respectively the conversion (*Figure 5.22*) of the four reactions. In any case the MWD was very narrow with PDI = M_w/M_n ranging from 1.03 to 1.10. For most practical purposes the polymers can be regarded as fairly monodisperse ($\overline{M}_w \approx \overline{M}_n$).

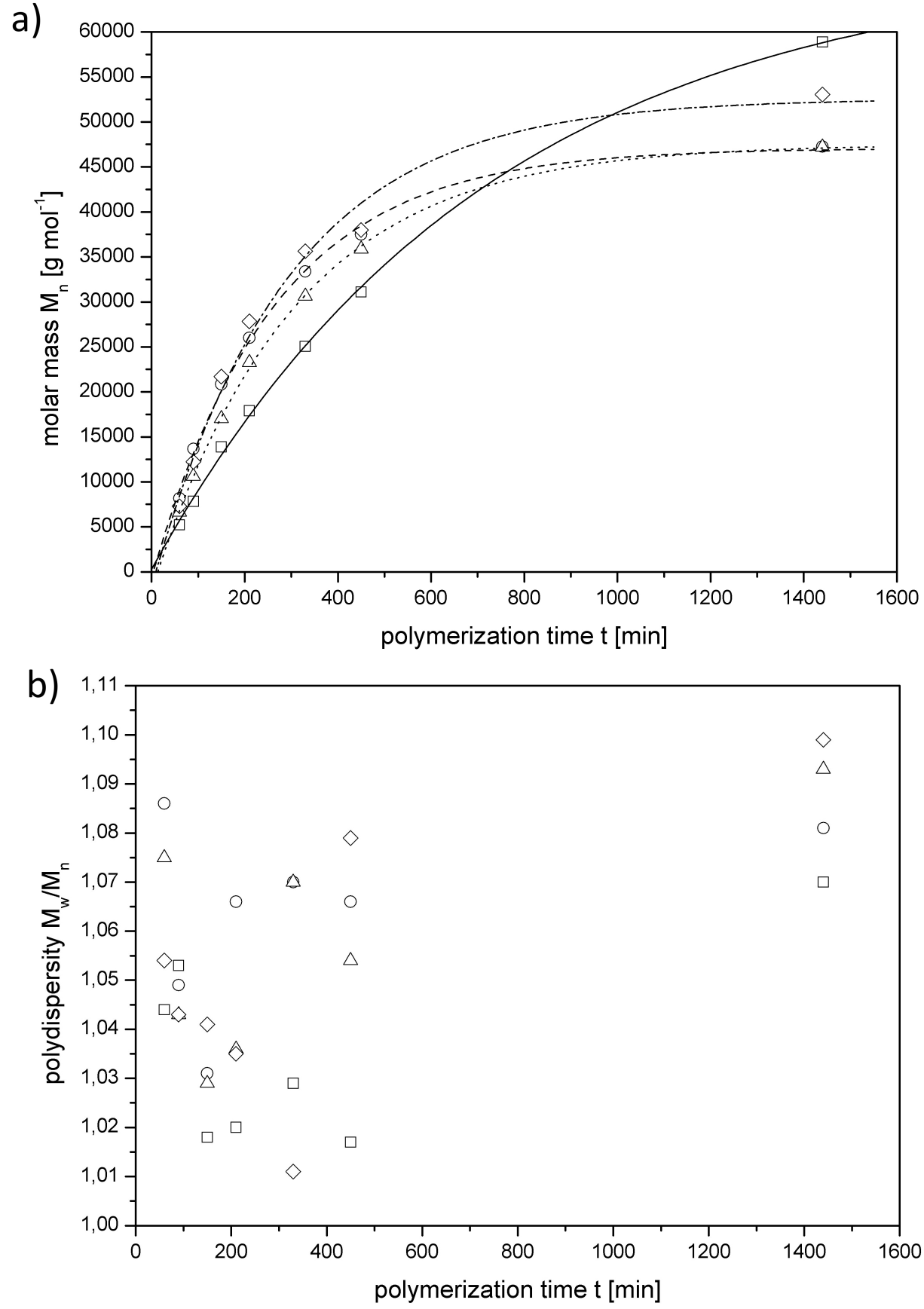

Fig. 5.21.: a) Molar masses M_n and b) polydispersities against reaction time t of *Series C*; $GP_{0.53}$ (□/ solid line, V31, f_{tBMA} = 0.5), $GP_{0.46}$ (○/ dashed line, V32, f_{tBMA} = 0.65), $GP_{0.28}$ (△/ dotted line, V33, f_{tBMA} = 0.75), $GP_{0.15}$ (◇/ dotted–dashed line, V34, f_{tBMA} = 0.85)

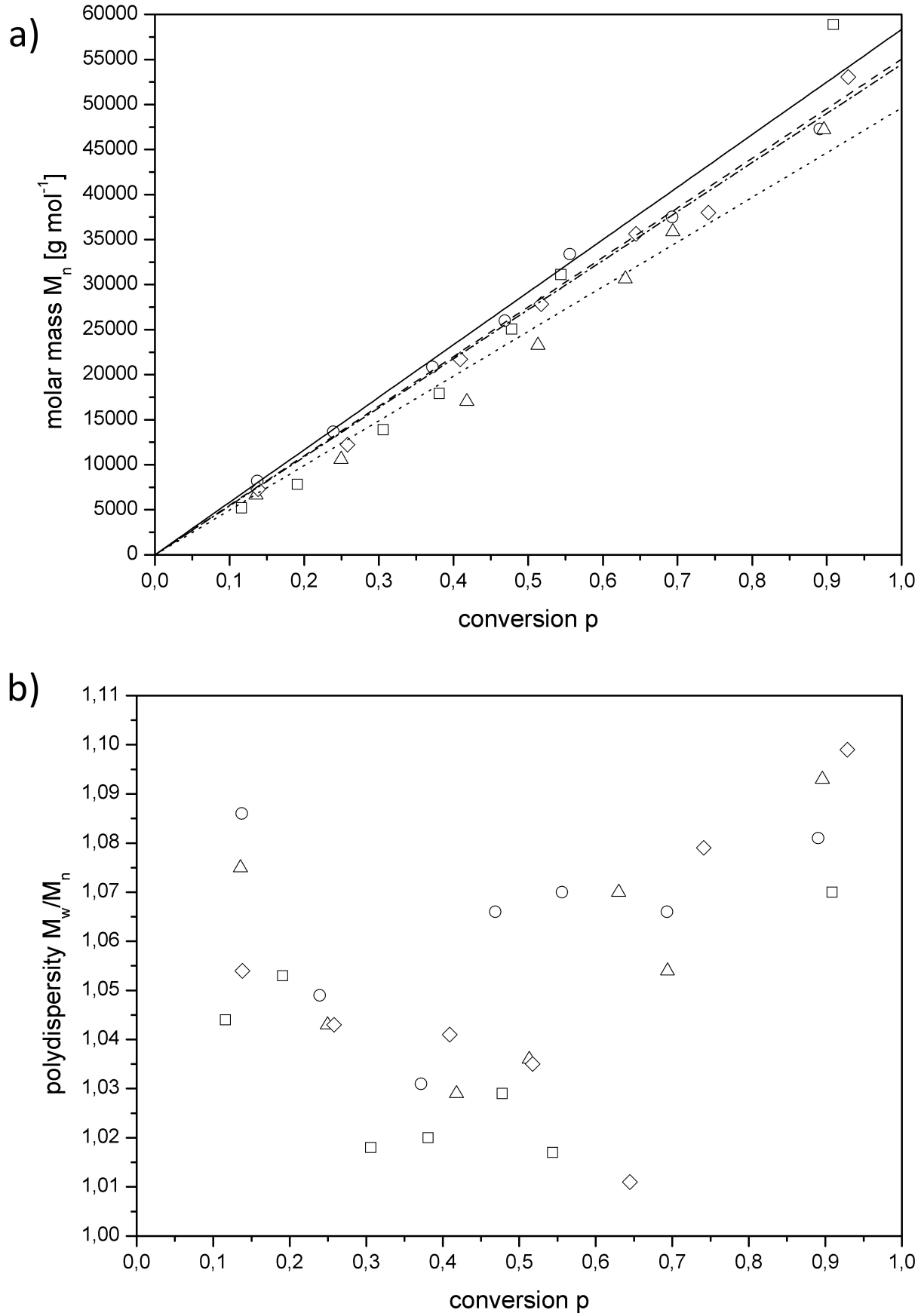

Fig. 5.22.: a) Molar masses M_n and b) polydispersities against conversion p of *Series C*; $GP_{0.53}$ (□/ solid line, V31, f_{tBMA} = 0.5), $GP_{0.46}$ (○/ dashed line, V32, f_{tBMA} = 0.65), $GP_{0.28}$ (△/ dotted line, V33, f_{tBMA} = 0.75), $GP_{0.15}$ (◇/ dotted–dashed line, V34, f_{tBMA} = 0.85)

As well as the relative molar masses the absolute molar masses increased linearly up to 210 min then the slopes flattened in all four entries. The development of the molar mass M_n during the four semibatch copolymerizations of the gradient copolymers was nearly the same as during the batch copolymerizations of the statistical copolymers (cf *Figure 3.19*). At the beginning of all four semibatch polymerizations the slope was linear over the first 210 min. However, the final masses M_w of the gradient copolymers were higher than then molar masses of the statistical copolymers because the polymerization time was much longer (1440 min instead of 180 min). The average final molar mass M_n of the statistical copolymers was $\approx 28500\,g \cdot mol^{-1}$. In the semibatch copolymerizations of the gradient copolymers an average final molar mass of $\approx 50100\,g \cdot mol^{-1}$ was reached. The polymerization time of the semibatch experiment was eight times longer than of the batch experiments. But the final average molar mass of the gradient copolymers of *Series C* has not even the double size. So the mass growth of the semibatch reactions were much slower than the batch reactions. A relation between the polydispersity PDI and the polymerization time t was not obvious. That was also a repetition of the results of the statistical copolymers from the batch copolymerizations of *Series A* and *Series B*. But all PDI values were very low with maximal 1.10. The range of the PDI of the gradient copolymers stayed constant during the semibatch polymerizations.

A linear relation between the development of the molar masses M_n and the total conversion of the monomers p during the semibatch experiments was found. The fitted curves originated all in (0,0). This behavior is typical for controlled radical polymerizations. [108] The data points had an average slope of $543\,g \cdot mol^{-1}$, see *Equations 5.2.38* to *5.2.41*.

$$V31, GP_{0.53}: \; M_n = (58335 \pm 3035)\,g \cdot mol^{-1} \cdot p(f_{tBMA,0.50}) \tag{5.2.38}$$

$$V32, GP_{0.46}: \; M_n = (55040 \pm 1000)\,g \cdot mol^{-1} \cdot p(f_{tBMA,0.65}) \tag{5.2.39}$$

$$V33, GP_{0.28}: \; M_n = (49614 \pm 1547)\,g \cdot mol^{-1} \cdot p(f_{tBMA,0.75}) \tag{5.2.40}$$

$$V34, GP_{0.15}: \; M_n = (54448 \pm 1059)\,g \cdot mol^{-1} \cdot p(f_{tBMA,0.85}) \tag{5.2.41}$$

The depiction of the polydispersities PDI of the samples of the four copolymers versus the conversion p gave no relation of the PDI and the conversion p. This was the same observation as with the PDI/reaction time plot. However, the values of the PDI were very low over the whole conversion range. In literature on gradient copolymers which had been synthesized by ATRP the PDI–values were up to 1.5. [109, 110, 111] Hence, it can be stated that the reaction control was good over the whole conversion.

5.2.5. Thermal Behavior

The thermal behavior of the gradient copolymers was examined to determine the temperature range of the glass transition region ΔT and the glass transition temperature T_g. The samples of the precipitated copolymers of *Series C* were analyzed in the same way and the same

temperature range as the statistical copolymers of *Series B* (cf. *Section 3.3.4*). The applied DSC program parameters were:

- precooling: RT to −80 °C
- standby for 20 min
- 1. heating: −80 to 150 °C
- 1. cooling: 150 to −80 °C
- 2. heating: −80 to 150 °C
- postcooling: 150 °C to RT

In *Figure 5.23* the thermogram of the sample of experiment V34 ($GP_{0.15}$, f_{tBMA} = 0.85) which was taken after 60 min polymerization time with both heating runs and the cooling run is depicted as an example. The first heating run showed a glass transition overlaid by a relaxation peak between 60 °C and 90 °C. The second heating run showed a glass transition step nearly in the same range as the peak in the first run. Only the second heating runs of all samples taken during the four semibatch polymerizations were anlaysed with respect to T_{onset}, T_{offset}, T_g, T_{midpt}, ΔT and Δc_p. [89] The analysis followed the description in *Section 3.3.4*. The complete results of the analysis of the second heating runs from all samples of *Series C* are listed in *Table 5.13*.

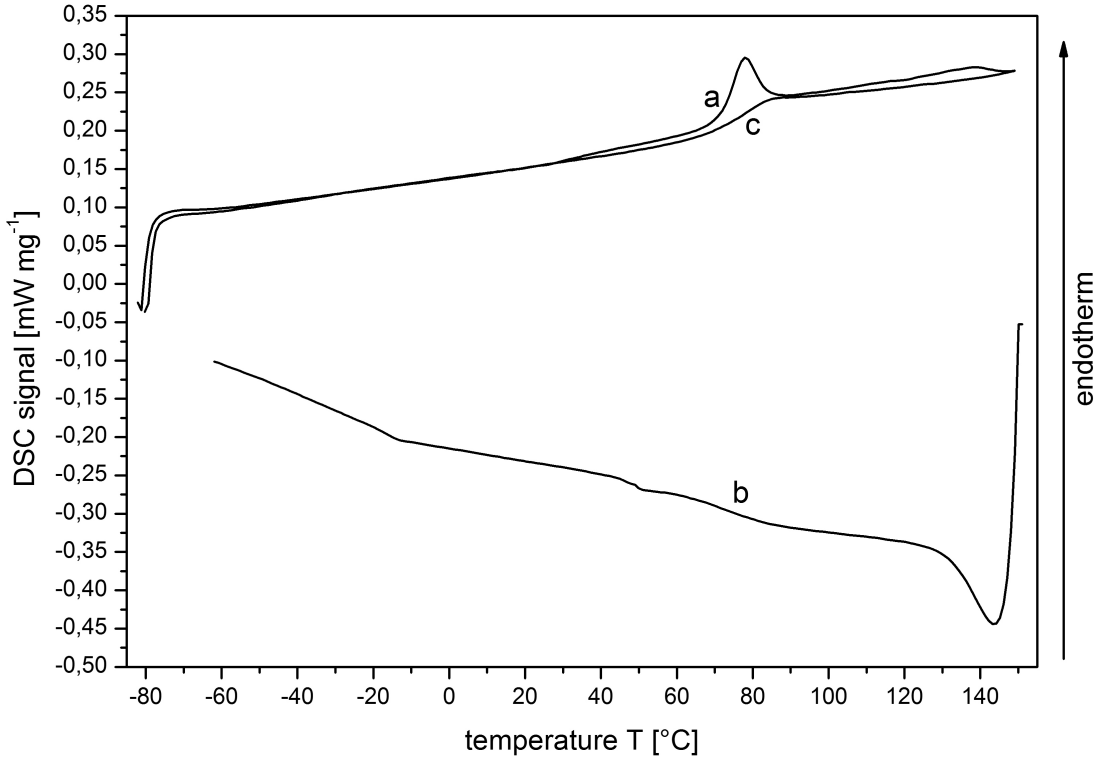

Fig. 5.23.: DSC thermogram of gradient copolymer V34 ($GP_{0.15}$, f_{tBMA} = 0.85, reaction time t = 60 min); a – first heating run, b – first cooling run, c – second heating run; heating rate $10\,K \cdot min^{-1}$

Tab. 5.13.: DSC results of the different gradient copolymers of *Series C*

Entry f_{tBMA}	time t [min]	T_{onset} [°C]	T_{midpt} [°C]	T_g [°C]	T_{offset} [°C]	ΔT [°C]	Δc_p [$J \cdot g^{-1} \cdot K^{-1}$]
V31	60	50.5	60.0	56.0	67.0	16.5	0.169
$GP_{0.53}$	90	61.0	72.0	72.0	87.0	26.0	0.191
0.5	150	60.0	71.5	70.0	82.0	22.0	0.252
	210	56.5	67.0	69.5	75.0	18.5	0.194
	330	55.5	65.5	69.5	73.5	18.0	0.180
	450	54.0	63.0	63.5	69.5	15.5	0.163
	1440	52.0	60.0	60.5	67.0	15.0	0.197
V32	60	54.5	65.0	65.0	73.0	18.5	0.204
$GP_{0.46}$	90	53.5	64.0	64.5	72.5	19.0	0.227
0.65	150	53.0	64.5	64.0	73.5	20.5	0.241
	210	50.5	54.0	63.0	74.0	23.5	0.200
	330	42.0	58.5	54.5	73.0	31.0	0.197
	450	40.0	59.5	52.5	75.5	35.5	0.231
	1440	46.0	57.0	60.0	66.0	20.0	0.190
V33	60	58.5	67.0	70.0	75.0	16.0	0.248
$GP_{0.28}$	90	62.5	69.5	71.0	76.0	13.0	0.218
0.75	150	51.5	64.5	64.0	75.5	23.5	0.263
	210	53.0	67.5	60.5	83.5	30.5	0.209
	330	56.5	66.0	62.0	72.5	16.0	0.157
	450	50.0	59.0	60.5	66.5	16.5	0.220
	1440	60.0	69.0	68.5	76.0	16.0	0.207
V34	60	67.5	73.5	79.0	81.0	13.5	0.256
$GP_{0.15}$	90	54.5	64.0	63.5	72.0	17.5	0.213
0.85	150	63.0	70.0	73.5	77.0	14.0	0.224
	210	61.0	70.5	73.0	78.0	17.0	0.230
	330	62.5	71.5	72.5	79.5	17.0	0.230
	450	65.5	73.5	73.5	80.5	15.0	0.223
	1440	75.5	86.0	84.0	95.5	20.0	0.254

The thermograms of the second heating runs from the samples of experiment V32 ($GP_{0.46}$, f_{tBMA} = 0.65) are depicted in *Figure 5.24* exemplarily for the four gradient copolymers. The limits of the glass transition range ΔT, T_{onset} and T_{offset}, are marked there, as well as the glass transition temperature T_g. The glass transition temperature T_g shifted from 65 °C (curve A, t = 60 min) to lower temperature of 52.5 °C up to a polymerization time of 450 min. However, the last samples taken at 1440 min had a higher glass transition temperature of 60 °C. The

glass transition temperature range ΔT expanded from 18.5 to 35.5 °C over the first 450 min. The sample which was taken after 1440 min had a smaller ΔT of 20 °C.

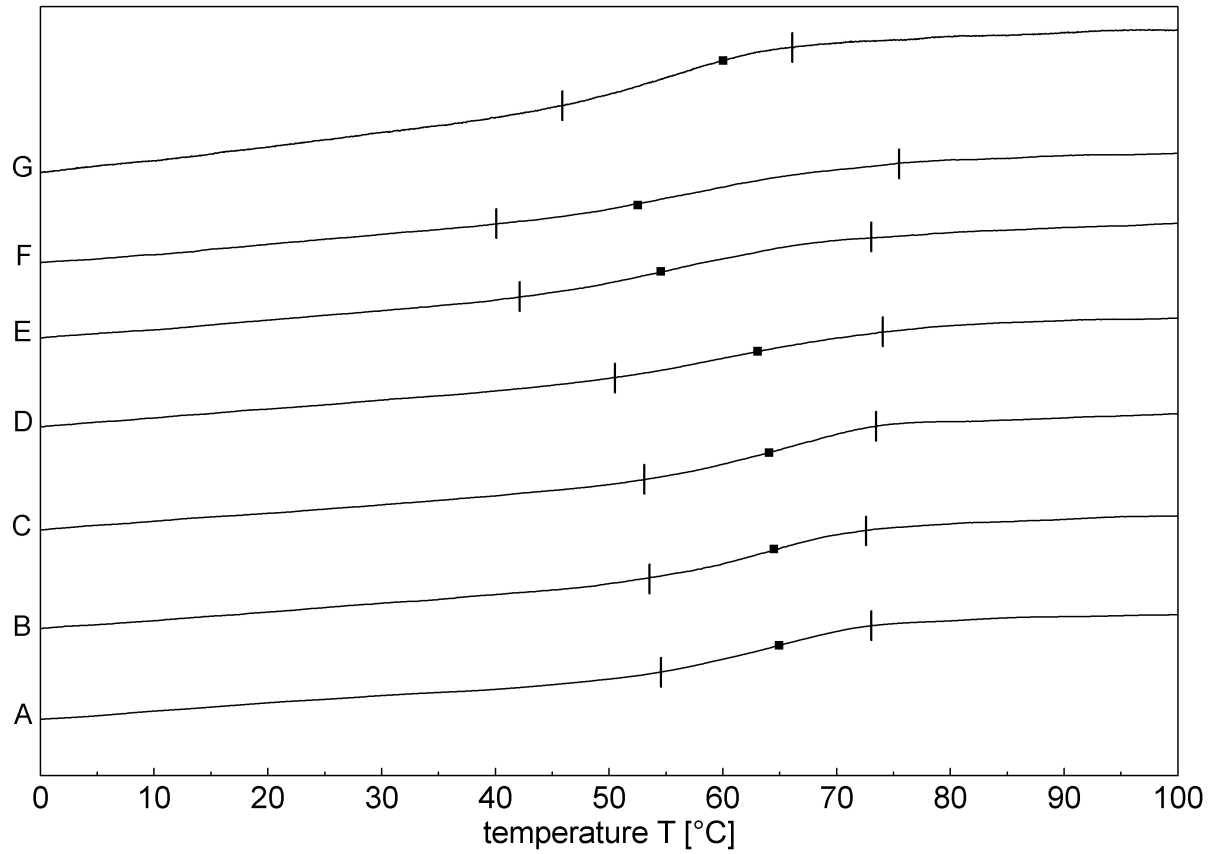

Fig. 5.24.: DSC thermograms of experiment V32 ($GP_{0.46}$, f_{tBMA} = 0.65) with marked glass transition temperature range T_{onset}, T_{offset} and glass transition temperature T_g; second heating runs, heating rate $10\,K \cdot min^{-1}$; A – 60 min, B – 90 min, C – 150 min, D – 210 min, E – 330 min, F – 450 min and G – 1440 min of reaction time

The plot of the glass transition temperatures T_g and temperature ranges ΔT of all semibatch copolymerization samples against the polymerization time t is depicted in *Figure 5.25*, while *Figure 5.26* shows analogues plots versus the monomer conversion p.

The results of the DSC–measurements varied obviously between the four semibatch copolymerizations. The glass transition temperature T_g of the samples from experiment V31 ($GP_{0.53}$, f_{tBMA} = 0.5) slightly decreased from 72 to 60.5 °C during the polymerization time, see *Figure 5.25a*. The decrease of the glass transition temperature range ΔT was strong up to a polymerization time of 450 min from 26 to 15 °C. Between 450 min and 1440 min was no obviously change. The values of the glass transition temperature T_g samples of experiment V32 ($GP_{0.46}$, f_{tBMA} = 0.65) decreased up to 450 min polymerization time from 65 to 52.5 °C and then up to 1440 min T_g increased to 60 °C, see *Figure 5.25b*. The values of the glass transition temperature range ΔT proceeded contrary. First they rose from 18.5 to 35.5 °C and then they fell to 20 °C.

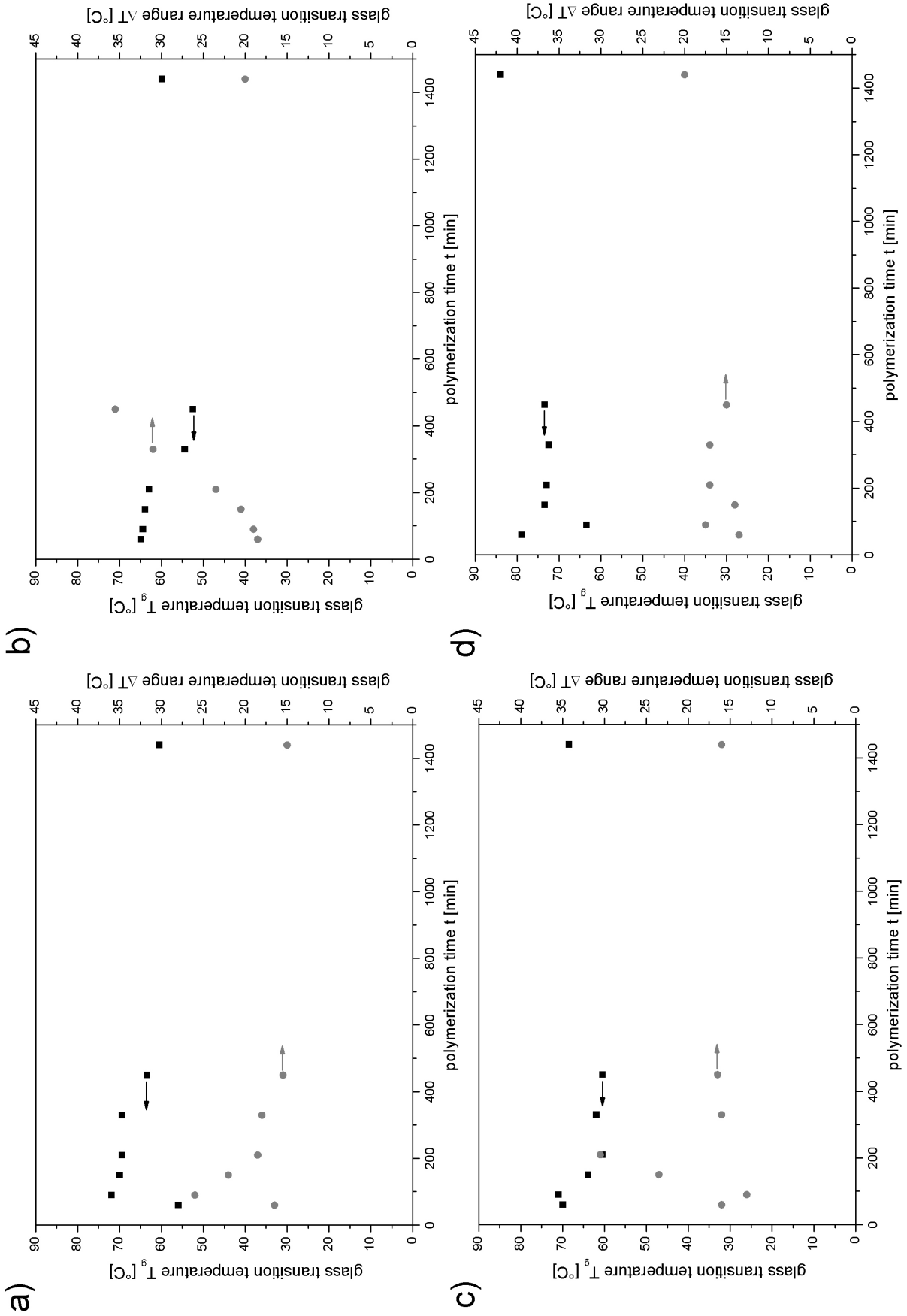

Fig. 5.25.: Plot of the glass transition temperature T_g (■) and the glass transition region ΔT (●) versus the polymerization time t of *Series C*; a) V31 ($GP_{0.53}$, f_{tBMA} = 0.5), b) V32 ($GP_{0.46}$, f_{tBMA} = 0.65), c) V33 ($GP_{0.28}$, f_{tBMA} = 0.75), d) V34 ($GP_{0.15}$, f_{tBMA} = 0.85)

Figure 5.25c shows the polymerization time depending values of the samples taken during experiment V33 ($GP_{0.28}$, f_{tBMA} = 0.75). Here the data points of T_g first declined up to 450 min of polymerization time from 70 to 60.5 ℃ and then they raised to 68.5 ℃ at 1440 min. The analysis of the glass transition temperature range showed scattering values around 16 ℃. The T_g values from the samples of experiment V34 ($GP_{0.15}$, f_{tBMA} = 0.85) (see *Figure 5.25d*) slightly decreased from 79 ℃ T_g to 73.5 ℃ T_g up to 450 min of polymerization time and then increase again to 84 ℃ at 1440 min. For ΔT the values scattered and increased from 13.5 to 20 ℃.

In *Figure 5.26a* the plots of the glass transition temperature T_g and the glass transition region ΔT of the samples from experiment V31 ($GP_{0.53}$, f_{tBMA} = 0.5) against the conversion p are given. The first values at 11 % p did not fit to the other values. There was an increase from 56 to 72 ℃ at T_g and from 16.5 to 26 ℃ at ΔT from 11 to 20 % conversion. The residual T_g values slightly decrease from 72 to 60.5 ℃ and the ΔT values also decrease with a stronger slope from 26 to 15 ℃. The T_g and ΔT values of the samples of experiment V32 ($GP_{0.46}$, f_{tBMA} = 0.65) are plotted in *Figure 5.26b*. The data points of the glass transition temperature declined from 65 ℃ to 52.5 ℃ up to a conversion of 70 % and then declined to 60 ℃ again. The glass transition temperature range first rose from 18.5 to 35.5 ℃ up to 70 % and then fell to 20 ℃. In *Figure 5.26c* are the T_g– and ΔT–values of the samples of experiment V33 ($GP_{0.28}$, f_{tBMA} = 0.75) displayed. The glass transition temperature scattered between 60 ℃ and 70 ℃ and the glass transition temperature range scattered around 16 ℃. The glass transition temperature of the samples of experiment V34 ($GP_{0.15}$, f_{tBMA} = 0.85), see *Figure 5.26d*, was nearly linear around 75 ℃ up to a conversion of 80 %. Then T_g increased up to 84 ℃. The values of ΔT increased from 13.5 to 20 ℃.

The dependence of the glass transition temperature constantly changed with the composition of the four entries, according to the *Fox–Flory–Theory*. [71, 112] Theoretically the T_g should decrease with increase of the amount of nBMA inside the polymer chain because PnBMA has a lower glass transition temperature than PtBMA. [90, 91] Only for V32 ($GP_{0.46}$, f_{tBMA} = 0.65) this was obviously noticeable. The values of the samples of the three other entries only fall slightly. But in all four entries the T_g–value of the last sample, taken after 1440 min, was higher than the one taken at 450 min.

The glass transition temperature range ΔT of the statistical copolymers of *Series A* rose slightly with the increase of nBMA inside the polymer chain (see *Figure 3.26*). According to the literature [14, 15] the temperature range of the correlated gradient copolymers with an equal composition should have a broader glass transition temperature range that lay between the glass transition temperature of the homopolymers.

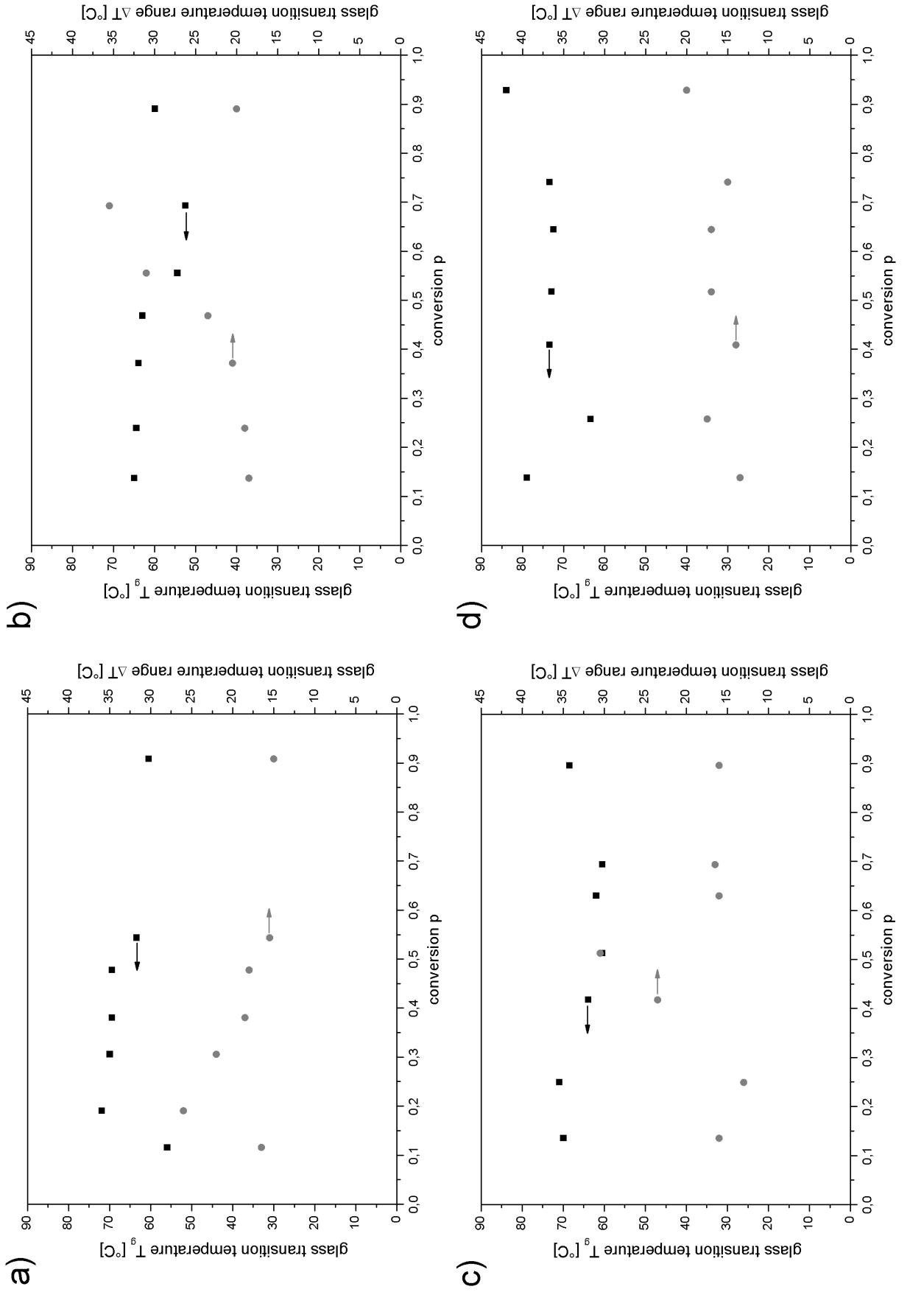

Fig. 5.26.: Plot of the glass transition temperature T_g (■) and the glass transition region ΔT (●) versus the conversion p of *Series C*; a) V31 ($GP_{0.53}$, f_{tBMA} = 0.5), b) V32 ($GP_{0.46}$, f_{tBMA} = 0.65), c) V33 ($GP_{0.28}$, f_{tBMA} = 0.75), d) V34 ($GP_{0.15}$, f_{tBMA} = 0.85)

The broadening of the glass transition temperature range with the increase of nBMA inside the polymer chain could be observed for V32 ($GP_{0.46}$, f_{tBMA} = 0.65). Hence, the glass transition temperature range of the samples of this developed as expected. The three other semibatch copolymerization did not show this behavior. When the values of ΔT of the statistical copolymers and the gradient copolymers were compared, cf. *Tables 3.14*, *3.15* and *5.13*, no obvious difference was observed.

For statistical copolymers the glass transition temperature can be described with *Fox's* equation (cf. *Section 3.3.4*). This analysis was also applied to the gradient copolymers, using *Equation 5.2.42*.

$$\frac{1}{T_g} = \frac{F_{tBMA}}{T_{g,tBMA}} + \frac{F_{nBMA}}{T_{g,nBMA}} \tag{5.2.42}$$

with $T_{g,tBMA}$ = 107 °C [90] and $T_{g,nBMA}$ = 20 °C [91]

The results of the calculations are listed in *Table 5.14*. For the copolymers $GP_{0.46}$, $GP_{0.28}$ and $GP_{0.15}$ the *Fox–Equation* gave temperature that were close to the measured T_g within 2 to 8 °C. But the calculated glass transition temperatures of the samples of $GP_{0.53}$ did not agree to the measured temperatures. The measured T_g values were all distinctly higher than the calculated *Fox*–T_g–values. The differences lay between 17 °C and 28 °C. The gradients of the copolymers $GP_{0.46}$, $GP_{0.28}$ and $GP_{0.15}$ obviously be to small, hence, there was no substantial difference between the monomer distribution in the gradient–copolymers and the statistical copolymers.

Tab. 5.14.: Theoretical and measured glass transition temperature of *Series C*

Entry f_{tBMA}	time [min]	F_{tBMA}	F_{nBMA} [a]	T_g(*Fox*) [b] [°C]	T_g(DSC) [c] [°C]	ΔT_g [d] [°C]
V31	60	0.59	0.41	38.6	56.0	17.4
$GP_{0.53}$	90	0.72	0.28	48.3	72.0	23.7
0.5	150	0.67	0.33	43.6	70.0	26.4
	210	0.67	0.33	44.0	69.5	25.5
	330	0.64	0.36	41.4	69.5	28.1
	450	0.62	0.38	40.3	63.5	23.2
	1440	0.56	0.44	36.8	60.5	23.7
V32	60	0.88	0.12	69.6	65.0	-4.6
$GP_{0.46}$	90	0.82	0.18	60.5	64.5	4.0
0.65	150	0.81	0.19	58.4	64.0	5.6
	210	0.78	0.22	55.2	63.0	7.8

Continuation on next page ...

Entry f_{tBMA}	time [min]	F_{tBMA}	F_{nBMA} [a]	T_g(*Fox*) [b] [°C]	T_g(DSC) [c] [°C]	ΔT_g [d] [°C]
	330	0.76	0.24	52.4	54.5	2.1
	450	0.72	0.28	48.3	52.5	4.2
	1440	0.68	0.32	44.8	60.0	15.2
V33	60	0.89	0.11	73.0	70.0	-3.0
$GP_{0.28}$	90	0.87	0.13	68.9	71.0	2.1
0.75	150	0.84	0.16	63.5	64.0	0.5
	210	0.84	0.16	62.8	60.5	-2.3
	330	0.82	0.18	59.6	62.0	2.4
	450	0.80	0.20	57.6	60.5	2.9
	1440	0.77	0.23	54.0	69.0	15.0
V34	60	0.89	0.11	73.3	79.0	5.7
$GP_{0.15}$	90	0.91	0.09	78.0	63.5	-14.5
0.85	150	0.91	0.09	76.8	73.5	-3.3
	210	0.90	0.10	74.2	73.0	-1.2
	330	0.89	0.11	71.5	72.5	1.0
	450	0.88	0.12	70.2	73.5	3.3
	1440	0.86	0.14	67.0	84.0	17.0

[a] $F_{nBMA} = 1 - F_{tBMA}$; [b] calculated with *Eq. 5.2.42*

[c] measured with DSC; [d] $\Delta T_g = T_g$(DSC) - T_g(*Fox*)

5.3. Summary

Based on the kinetic investigations on batch–copolymerizations of the different monomer compositions of *n*–butyl and *tert*–butyl methacrylate the monomer addition programs of semibatch copolymerizations to generate gradient copolymers with different compositional gradients have been calculated. Four different monomer compositions were polymerized with tBMA as the stock and nBMA as the feed. The analysis of the ^{1}H–NMR–spectra of the samples taken over the reaction time showed that the conversion of all entries increased linear at the beginning of the polymerization and then leveled off. After 1440 min the conversion reached around 91 % in all cases. From the monomer conversions the cumulative and the instantaneous copolymer compositions of all samples was calculated. The cumulative compositions showed a decrease in tBMA–contend up to the intended composition with all four semibatch reactions. The instantaneous compositions also decreased. The slope of the decrease was too strong up to 16 % of monomer conversion and from 16 to 91 % monomer conversion the slope was too small. But the gradient was constant within these regions. Therewith the semibatch copolymerization yielded in linear gradient copolymers with a con-

stant gradient between a conversion of 16 to 91 %. Over the whole reaction the copolymers can be described as "double–gradients". Elementary analysis showed the samples to be free of pollution. The analysis of the samples with ATR–FTIR–spectroscopy gave spectra with the same characteristic vibrational bands that were found for the statistic copolymers. The calibration curve that was developed with the statistic copolymers could also be applied to the gradient copolymers and gave similar compositions as obtained by ^{1}H–NMR–analysis. The SEC–measurements gave elution–diagrams without fronting or tailing, demonstrating a good reaction control even over 1440 min. The molar masses grew regularly for the experiments V32 ($GP_{0.46}$), V33 ($GP_{0.28}$) and V34 ($GP_{0.15}$), while experiment V31 ($GP_{0.53}$) of higher molar weight. The low polydispersities of all samples were well below 1.1, which also indicated the good reaction control. DSC thermal analysis revealed a remarkable decrease of the T_g, as well as a strong increase of the glass transition temperature range with growing of the isolated samples of experiment V32 ($GP_{0.46}$). The measured T_g of the gradient copolymers do not obey the *Fox–Flory*–Rule of the copolymers glass temperature. Semi–batch copolymers of the experiments V33 ($GP_{0.28}$) and V34 ($GP_{0.15}$) exhibited a similar behavior of T_g and ΔT on conversion p, however, they all could be described by means of *Fox*–Equation and hence behave like random copolymers. It must be concluded that P[tBMA–grad–nBMA] copolymers only behave thermally different from their random analogs if the compositional gradient dF/dp exceeds a value of about 0.8. At all four reactions the last sample, taken at 1440 min, the values of T_g were higher than the one taken at 450 min, although they should be lower. The reason could be that the last sample was not a small one of 1 ml but rather was taken from the final precipitated copolymer.

6. Hydrolysis of Gradient Copolymers from n– and tert-Butyl Methacrylate

Since the declared aim of this thesis was to prepare a functional amphiphilic gradient copolymer P[MAA–grad–nBMA], the next step is the cleavage of the tert–butyl–ester side groups of the gradient copolymers P[tBMA–grad–nBMA] which were synthesized in *Chapter 5*. In *Chapter 4* a model compound – the statistical copolymer P[nBMA–co–tBMA] – was used to find an efficient hydrolysis procedure, demonstrating the hydrolysis with methanesulfonic acid to give the best results. This chapter shows the hydrolysis of the final gradient copolymers V31 to V34 (*Series C*) to result compounds V71 to V74 (*Series E*).

6.1. Materials and Methods

The chemicals and the synthesis method were the same as described in *Section 4.1.*

6.1.1. Materials

The hydrolysis reagent was methanesulfonic acid (MSA, ≤ 99.5 %, *Aldrich*). It was used as received. The same applied to the used solvents chloroform (99.9 %, *Acros*, extra dry over molecular sieve, stabilized), THF (chromasolv, *Aldrich*) and *n*–pentane (*Aldrich*).

6.1.2. General Procedure

0.25 g of the copolymer were dissolved in 2.25 g (1.5 ml) $CHCl_3$ and was stirred over night at room temperature. Then the respective amount of methanesulfonic acid (MSA) was added, see *Table 6.1.* The mixture was stirred for 2 hours at room temperature. A spatula–spoon of sodium hydrogen carbonate was added and this mixture was stirred for 30 min. Subsequently 5 ml THF were added and the mixture was filtered over a P4 glass filter. Afterward the solution was dropped into 200 ml of ice–cold pentane. The precipitated polymer was filtered over P4 glass filter and dried at room temperature for two hours. Then the copolymer was re–dissolved in 1 ml THF and the solution was dropped into 200 ml of an ice cooled water : methanol = 1 : 1 vol:vol mixture. The precipitated polymer was filtered over P4 glass filter and dried at room temperature under an oil–pump vacuum over night. The yields are listed in *Table 6.1.*

Experiment V71 (P[MAA–grad–nBMA], $F_{MAA} = 0.53$):

^{1}H–NMR: 0.65–1.22 ppm (broad peak, –CH_3, P[nBMA]); 1.3–1.46 ppm (broad peak, –CH_2–, P[nBMA]); 1.49–1.63 ppm (broad peak, –CH_2–, P[nBMA]); 1.64–2.15 ppm (broad peak, –CH_3, P[nBMA], P[MAA]); 3.33 ppm (H_2O); 3.8–4.0 ppm (broad peak, –OCH_2R, P[nBMA]); 12.1–12.5 ppm (broad peak, –COOH, P[MAA])

EA: 62.45 % C, 8.66 % H, (28.88 % O_{calc})

ATR–FTIR: 3600–2300 cm^{-1} (–COOH); 3050–2750 cm^{-1} (–CH_2–, –CH_3); 1724 cm^{-1} (–C=O); 1699 cm^{-1}; 1468 cm^{-1} (–CH_2–, –CH_3); 1389 cm^{-1}; 1244 cm^{-1} (nBu); 1154 cm^{-1} (–C–O–C–); 1065 cm^{-1} (nBu); 1020 cm^{-1}; 998 cm^{-1}; 964 cm^{-1} (nBu); 945 cm^{-1}; 844 cm^{-1}; 800 cm^{-1}; 749 cm^{-1}; 518 cm^{-1}

Experiment V72 to V74 (P[MAA–grad–nBMA]:

The ^{1}H– and IR–spectra of the compounds V72 to V74 exhibited the same signals, i. e. band positions as observed in the analogous copolymer V71. The ^{1}H–NMR–spectra are shown in *Figure 6.2*, the FTIR–spectra are depicted in *Figure 6.3*. The elemental analysis results the four experiments are listed in *Table 6.2*, SEC– and DSC–data in *Table 6.3* and *Table 6.4*, respectively.

6.1.3. Characterization

All characterization–methods were the same as with the batch copolymers of *Chapter 3*. The used methods were:

- ^{1}H–NMR spectroscopy
- elementary analysis
- ATR–FTIR–spectroscopy
- size exclusion chromatography
- differential scanning calorimetry

The same instruments under the same conditions were used for the investigation of the resulting copolymers.

6.2. Results and Discussion

This section describes the observations on the hydrolysis reaction performed with the gradient copolymers of V31 to V34. Also the results of the analysis of the hydrolysis products are given. The products were compared with the educts and the differences between the four products were investigated.

The amount of added MSA depended on the amount of tBMA inside the polymer chain. It was calculated in an analogous way as for the statistical copolymers. *Equation 6.2.1* was used for the gradient copolymers.

$$V_{MSA} = \frac{m \cdot F_{tBMA} \cdot x \cdot M_{MSA}}{M_{tBMA} \cdot \delta_{MSA}} \tag{6.2.1}$$

with V_{MSA} – Volume of the methanesulfonic acid, m – mass of the polymer, F_{tBMA} – ratio of tBMA in the polymer chain, x – multiplicity factor for the hydrolysis reagent = 2, M_{tBMA} – molar mass of tBMA = $142.2\,g \cdot mol^{-1}$, M_{MSA} – molar mass of the methanesulfonic acid = $96.11\,g \cdot mol^{-1}$ and δ_{MSA} – density of the methanesulfonic acid = $1.48\,g \cdot ml^{-1}$

The reactions proceeded in the same way as observed with the model hydrolysis in *Section 4.2*. However, a second precipitation was not only necessary to remove the formed salt: After the first precipitation from pentane the hydrolysis products were brown oils, hence a second purification step was needed. After the purification steps the resulting copolymers were obtained in form of light yellow powders.

The theoretical yields depend on the copolymer composition F_{tBMA}, they were calculated in the same way as in *Section 4.2*, but using *Equation 6.2.2*.

$$y_{theo} = \frac{m \cdot F_{tBMA} \cdot M_{MAA}}{M_{tBMA}} + m \cdot (1 - F_{tBMA}) \tag{6.2.2}$$

with y_{theo} – theoretical yield, m – mass of the polymer, F_{tBMA} – ratio of tBMA in the polymer, M_{MAA} – molar mass of MAA = $86.09\,g \cdot mol^{-1}$, M_{tBMA} – molar mass of tBMA = $142.2\,g \cdot mol^{-1}$

The results of the two calculations, the needed volumes of methanesulfonic acid and the theoretical yields, as well as the resulting and percentage yields of the four hydrolysis reactions are listed in *Table 6.1*.

The rise of *tert*–butyl–group contents inside the polymer chain of the educts and therewith of the COOH–group molar fraction in the products lead to a decrease of the reaction yield. That was due to the change in the solubility of the hydrolysis products. The higher the amount of COOH–groups, the better was the solubility of the copolymer in water. The hydrolysis products were precipitated in a mixture of water and methanol (vol:vol 1:1) to purify the

copolymers. To keep the comparability of the reactions, the precipitation mixture was not changed. A fraction of the copolymers was not precipitated and this amount became larger with increasing COOH–group content of the polymer chains.

Tab. 6.1.: Amount of added MSA and yields of hydrolysis products of *Series E*

Educt	F_{tBMA}	V_{MSA}	yield		
			theoretical	actual	
		[ml]	[g]	[g]	[%]
V71	0.56	0.13	0.19	0.15	78.95
V72	0.68	0.16	0.18	0.12	66.67
V73	0.77	0.18	0.17	0.11	64.71
V74	0.86	0.20	0.16	0.09	56.25

In analogy to the statistical copolymers the hydrolyzed gradient copolymers were dissolved in DMSO-d6 for ^{1}H–NMR–spectroscopy. The resulting ^{1}H–NMR–spectra are represented in *Figure 6.2* (black lines) together with the corresponding ^{1}H–NMR–spectra of the educts (grey lines). The molecular structures of the educts and the products with the numbering of the carbons are shown in *Figure 6.1.* The changes between the spectra of the educts and the products were distinct. The intensity of the mixed broad peak ranging from 1.3 to 1.45 ppm caused by the signals 3' and 7' shrank relative to the signals 8' or 9' which remained constant. The reason was the absence of the signal 3' from the protons of the *tert*–butyl group in the product. The –COOH–signal could be monitored between 12.0 to 12.75 ppm. In all ^{1}H–NMR–spectra of the products a H_2O signal was present because the DMSO–d_6 was not dry. In the spectra of V34 an additional peak from CH_2Cl_2 appeared because the NMR–tube was not completely dry. From the ^{1}H–NMR–spectra it can be concluded that all *tert*–butyl–ester groups were removed.

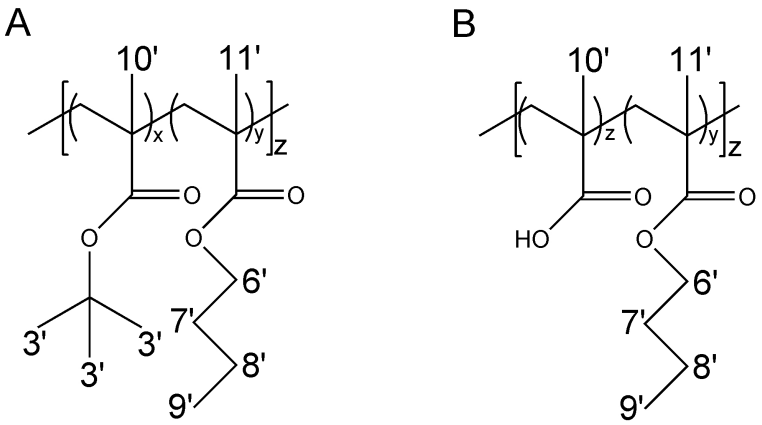

Fig. 6.1.: Molecular structures of educts *Series C* and products *Series E* with carbon–atom labels; A – educt P[tBMA–grad–nBMA] and B – product P[MAA–grad–nBMA] (z = x + y = 1)

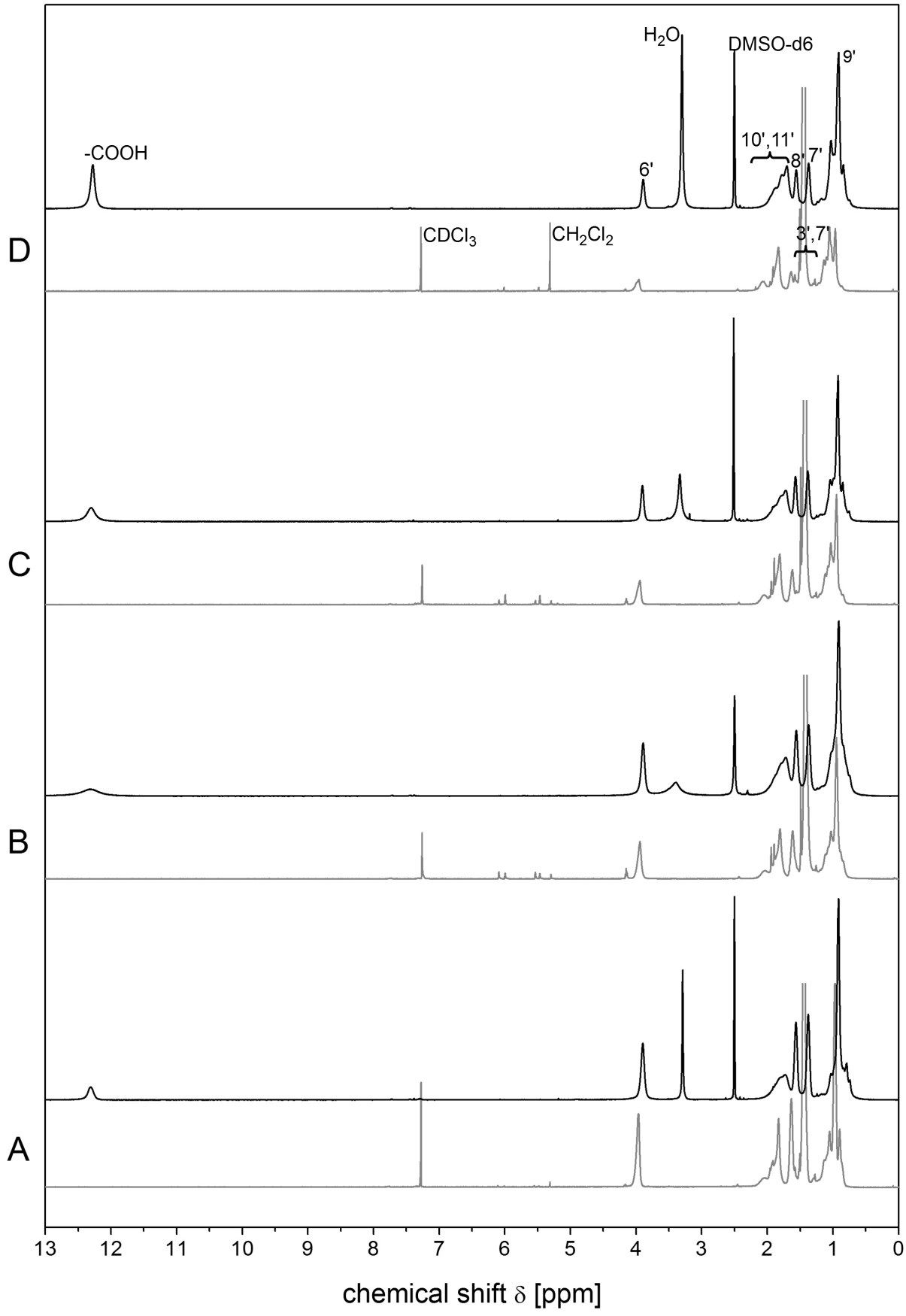

Fig. 6.2.: Comparison of ^{1}H–NMR–spectra of educts of *Series C* and hydrolysis–products of *Series E*; grey line – educt, black line – product; A: V31/V71 $F_{nBMA} = 0.44$, B: V32/V72 $F_{nBMA} = 0.32$, C: V33/V73 $F_{nBMA} = 0.23$, D: V34/V74 $F_{nBMA} = 0.14$

The NMR–analysis is followed by the investigation of the hydrolyzed gradient copolymers by elementary analysis and ATR–FTIR–spectroscopy.

The results of the elementary analysis are listed in *Table 6.2*. The theoretical values were calculated for 100 % conversion of the hydrolysis of the educts. The results showed different tendencies of the three elements. The amount of carbon had to fall from *Series E* because the amount of removed *tert*–butyl inside the polymer chain rose. In fact the amount of carbon decreased stronger than calculated and the difference between set value and actual values became higher with the increase of F_{MAA}. The amount of hydrogen also had to fall with the rise of MMA. Here the measured values fitted good to the set values for all four hydrolysis. The amount of oxygen had to increase with the decrease tBMA/ rise of MMA inside the polymer chain. The measured values of oxygen were also higher than they should, expect experiment V71. Moreover, the difference between the set values and the measured one became higher with the rise of MMA. An explanation of the enlargement of the differences is the deterioration of the precipitation behavior in the water : methanol mixture at the end of the synthesis for the purification of the polymer. The hydrolyzed copolymer could be contaminated with solvents or other chemicals which was used during the synthesis even if the ^{1}H–NMR–spectra did not point to something like that. In any case, the good fits of the values of experiment V71 to the targeted values and the fact that the differences of the other entries showed tendencies into the right direction meant that all four reactions worked well.

Tab. 6.2.: Results of the elementary analysis of educts and hydrolysis–products of *Series E* with divergence from the set values

Entry	F_{nBMA}		C [%]	ΔC	H [%]	ΔH	O [%]	ΔO
V31	0.44	theory	67.57		9.92		22.50	
		is	66.79	-0.78	9.23	-0.69	23.98	1.48
V71		theory	62.45		8.66		28.88	
		is	62.59	0.14	8.64	-0.02	28.77	0.11
V32	0.32	theory	67.57		9.92		22.50	
		is	67.10	-0.47	9.55	-0.37	23.35	0.85
V72		theory	60.95		8.29		30.75	
		is	59.30	-1.65	8.15	-0.14	32.55	1.79
V33	0.23	theory	67.57		9.92		22.50	
		is	67.93	0.36	9.60	-0.32	22.47	-0.03
V73		theory	59.69		7.98		32.32	
		is	57.14	-2.55	7.84	-0.14	35.02	2.70
V34	0.14	theory	67.57		9.92		22.50	
		is	66.63	-0.94	9.07	-0.85	24.30	1.80
V74		theory	58.30		7.64		34.06	
		is	54.37	-3.93	7.60	-0.04	38.04	3.97

The second part of the structure analysis was the ATR–FTIR–spectroscopy. The resulting spectra of the four hydrolyzed gradient copolymers (black lines) are depicted in *Figure 6.3* together with the educts (grey lines). In the four spectra the vibrational bands that were analyzed in the same way as the educts before are marked to show the differences between the educts and the products.

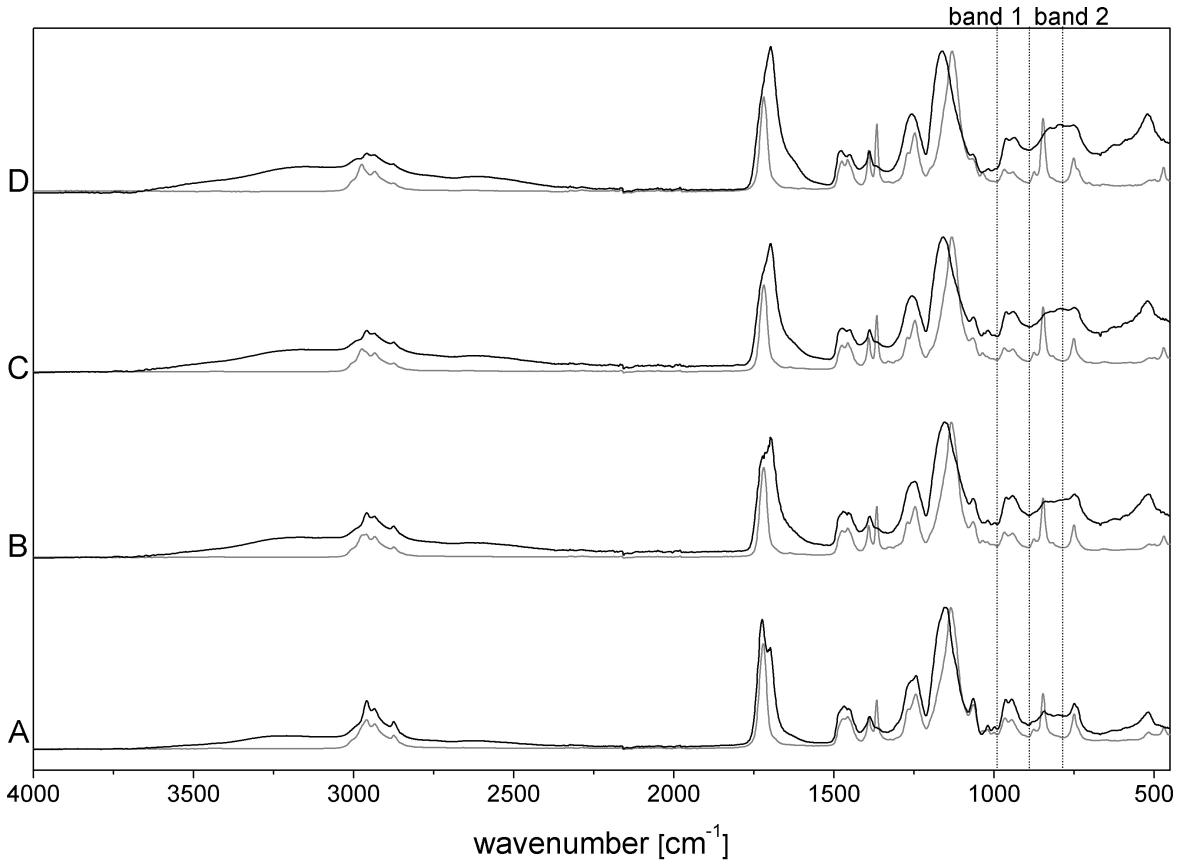

Fig. 6.3.: Comparison of ATR–FTIR–spectra of educts *Series C* and hydrolysis–products of *Series E*; grey line – educt, black line – product; A: V31/V71 $F_{nBMA} = 0.44$, B: V32/V72 $F_{nBMA} = 0.32$, C: V33/V73 $F_{nBMA} = 0.23$, D: V34/V74 $F_{nBMA} = 0.14$ (Spectra normalized to $A_{1136} = 1$)

In *Section 3.3.2* two bands at 970 cm^{-1} and 850 cm^{-1} were introduced that are characteristic for polymer-incorporated tBMA and nBMA units, respectively. *Band 1* at 970 cm^{-1} for nBMA did not change so much but *band 2* at 850 cm^{-1} for tBMA differed obviously from the educt–spectrum to spectra of the products. The changes of *band 2* were so strong and influenced also *band 1*. Therewith the analysis of peak height and peak area of both bands was not possible anymore. The change of band intensity at 850 cm^{-1} clearly indicates that the hydrolysis products no longer contained tBMA–ester side groups. The band merged with the band at 750 cm^{-1}. The higher the amount of MAA inside the copolymer chain the stronger the fusion of the two bands. Also the band at 1370 cm^{-1} shrank with the hydrolysis. A third change exhibited the band at 1710 cm^{-1} which is the vibrational bands of ester–C=O group. In the IR–spectrum of the educt the band was a small singlet. The product–spectra instead had broad doublets at that region and with the increase of the MMA–amount that band

became even wider. The double band exhibited maxima at 1720 cm^{-1} and 1700 cm^{-1}. The literature refers 1720 cm^{-1} to ester–C=O vibration, while 1700 cm^{-1} belong to the vibrations of carboxylic acid–C=O groups. [87] Further the range $\tilde{\nu} > 3000\,cm^{-1}$ changed from educt to product in all four cases. A broad band ranging from 2500 to 3500 cm^{-1} appeared which could be assigned to the vibrational band of the carboxylic acid OH–group. That broad region got stronger with the rise of the MMA-amount. All in all the changes in the ATR–FTIR–spectra from the educts to the products and the differences of the products among themselves showed that the hydrolysis reactions worked well.

The next analysis was the size exclusion chromatography (SEC). As with the hydrolyzed statistical copolymers also the products of *Series E* were not soluble in THF. As described in *Section 4.2* about 0.4 mg of the copolymer was mixed with 1 ml THF and two drops of TMSI and the mixture was stirred over night at RT. The copolymer became THF–soluble, because the carboxyl groups were converted into non–polar trimethylsilyl–esters. Since the presence of non–covalent fixed TMSI disturbed the dn/dc determination, only the relative molar mass of the copolymers were calculated from the maximum elution volume of the samples and *Equation 3.3.22* which based on a polystyrene–calibration–curve ("PSS–values"). The resulting elution diagrams of the RI–detector signals are depicted in *Figure 6.4* and the results are listed in *Table 6.3*.

Tab. 6.3.: SEC results of educts *Series C* and hydrolysis–products of *Series E*

Entry	F_{nBMA}	V_E [a] [ml]	M [b] [$g \cdot mol^{-1}$]	ΔM [$g \cdot mol^{-1}$]	[%]
V31	0.44	25.37	59132		
V71		25.59	53031	6101	10.32
V32	0.32	25.83	46905		
V72		26.17	39403	7502	15.36
V33	0.23	25.52	54819		
V73		26.17	39519	15300	27.91
V34	0.14	25.94	44411		
V74		26.81	28544	15867	35.73

[a] Peak elution volume
[b] relative values, based on PS–Standard calibration *Eq. 3.3.22*

As well as the product elution–curves of the RI–detector signals also the four educt elution–curves were monomodal with the same shape, indeed they were shifted towards higher elution volumes, i. e. lower molecular weights. The molar masses of all four products were lower than the educt and the differences became higher with a higher amount of tBMA respectively MAA inside the polymer chain. The difference between the molar mass of the educts and the products decreased from 10.32 to 35.73 %.

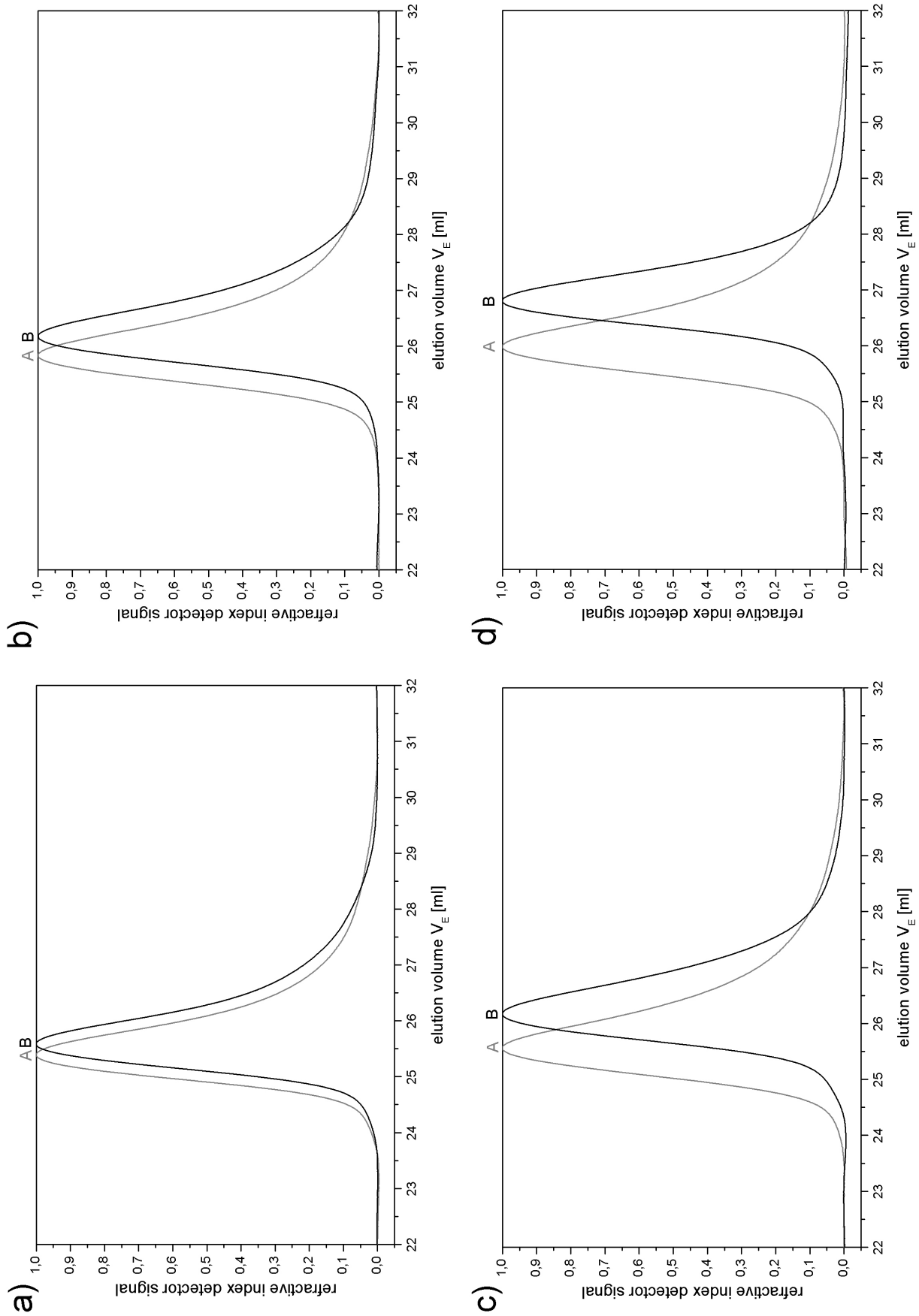

Fig. 6.4.: Comparison of SEC elution diagrams of educts *Series C* and hydrolysis–products of *Series E*; A grey line – educt, B black line – product; a: V31/V71 $F_{nBMA} = 0.44$, b: V32/V72 $F_{nBMA} = 0.32$, c: V33/V73 $F_{nBMA} = 0.23$, d: V34/V74 $F_{nBMA} = 0.14$

The calculated relative molar masses were slightly higher than the expected one, around 10 %, which was caused by the fact that for a relative molecular weight determination only the maximum elution volume is used and this is always higher than the average molar mass of a sample. Only for experiment V74 the calculated and the expected relative molar masses fitted good together. In terms of SEC the results of the hydrolysis reactions were as expected.

The investigation of the thermal behavior was the next part of analysis. The samples of *Series E* were heated up two times from −80 to 200 °C with a cooling run in between (dT/dt = 10 K/min). The samples were not measured up to 300 °C because from *Section 4.2* it was known that the hydrolyzed polymer–samples will decompose. In *Figure 6.5* the two heating runs and the cooling run of experiment V71 is represented as an example for the four measurements.

The thermograms of the first heating run showed an endothermic peak between 15 to 115 °C likewise the thermograms of the statistical copolymers, cf. *Figure 4.7*. This signal was attributed to the evaporation of remanding solvents , i. e. H_2O ("emission peak"). At 190 °C the beginning of the second peak showed. The DSC–trace of the cooling run and the second heating run did not show any peak or other changes, hence, no regeneration of the sample was detected as it was found with the statistical copolymers of *Section 4.2*. In *Figure 6.6* the first heating runs of the compounds of *Series E* are pictured.

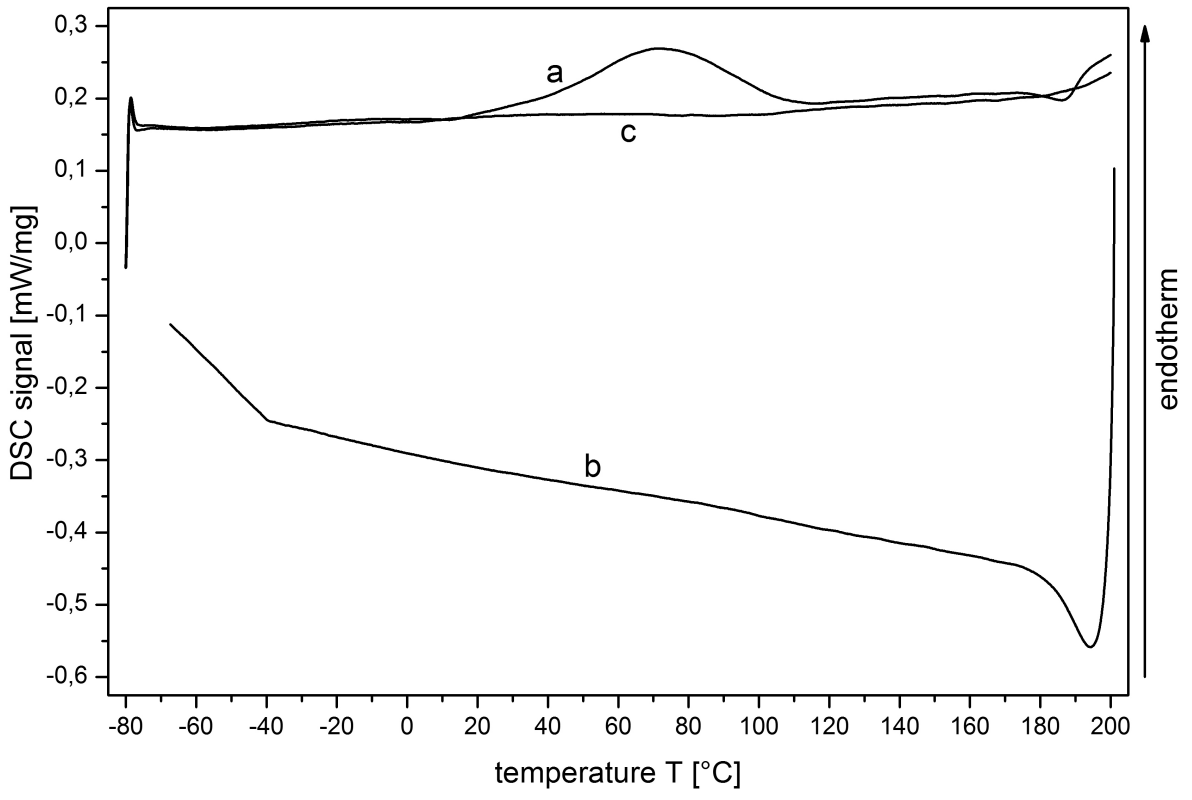

Fig. 6.5.: DSC thermogram of experiment V71 (P[$MAA_{0.56}$-grad-$nBMA_{0.44}$]); a – first heating run, b – first cooling run, c – second heating run; heating rate 10 K · min^{-1}

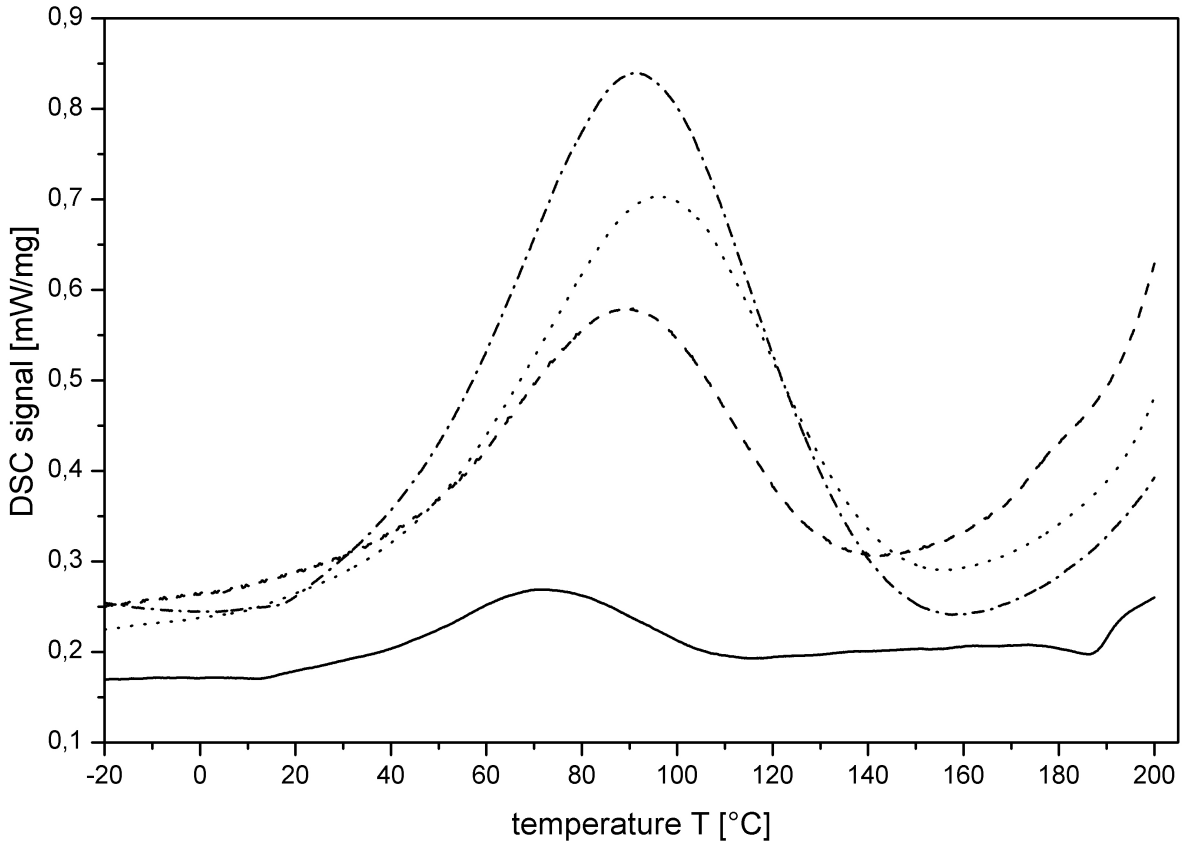

Fig. 6.6.: DSC thermograms of the hydrolysis products of *Series E*; first heating runs, heating rate 10 $K \cdot min^{-1}$; solid line – V71 ($F_{MAA} = 0.56$), dashed line – V72 ($F_{MAA} = 0.68$), dotted line – V73 ($F_{MAA} = 0.77$), dashed–dotted line – V74 ($F_{MAA} = 0.86$)

All thermograms exhibited an endothermic peak in the same temperature range as substance V71. The peaks got broader and higher with the increase of MMA inside the polymer chain. Regarding to this evident coherence between the shape of the endothermic peak and the composition of the copolymer, the peak area and peak height were determined. The results are listed in *Table 6.4* and plotted in *Figure 6.7*.

Tab. 6.4.: DSC results of hydrolysis–products of *Series E*

Entry	F_{MAA}	Area $[J \cdot g^{-1}]$	T_{Peak} [°C]	T_{onset} [°C]	T_{offset} [°C]	Width [°C]	Height $[mW \cdot mg^{-1}]$
V71	0.56	23.7	70.5	34.5	106.8	53.7	0.0845
V72	0.68	98.1	89.9	47.3	129.6	63.2	0.2863
V73	0.77	166.8	95.6	41.1	137.6	70.9	0.4366
V74	0.86	221.3	90.7	37.5	133.2	70.9	0.5949

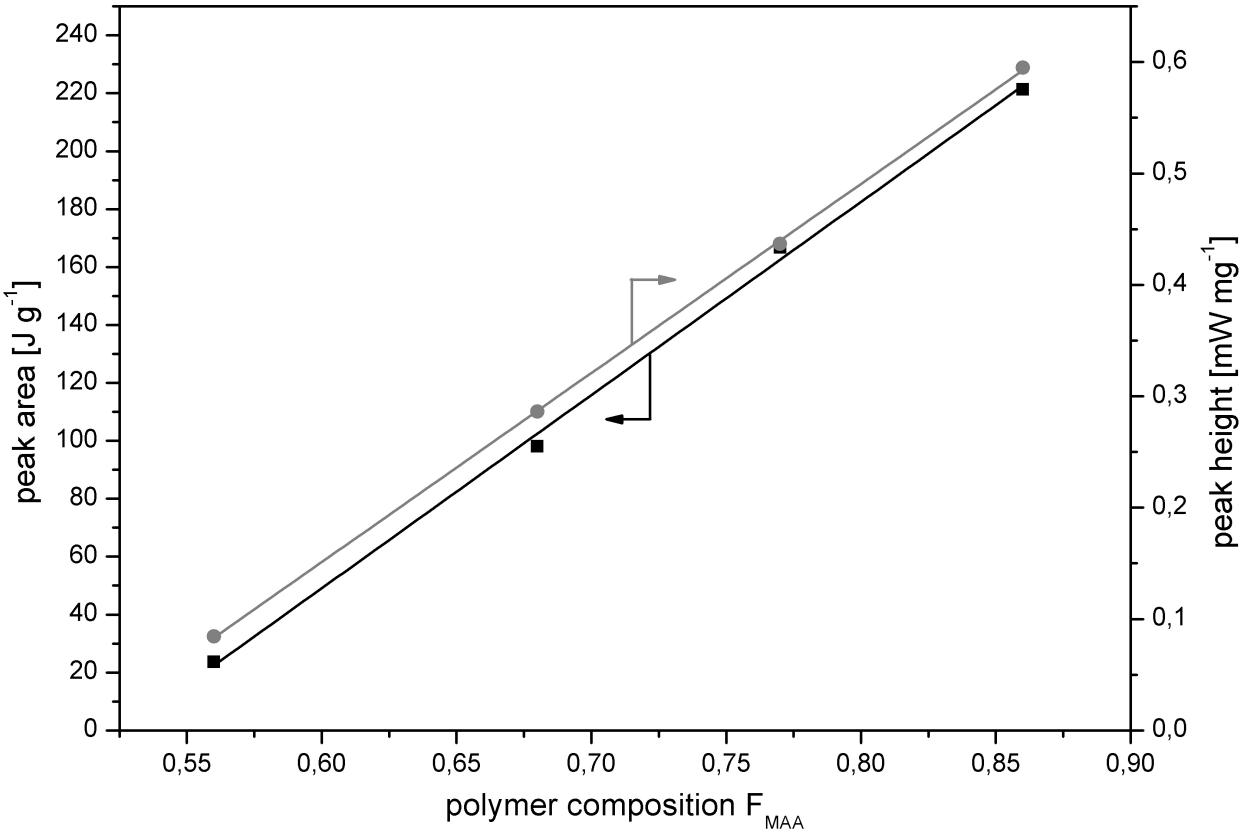

Fig. 6.7.: Plot of peak area ■ and peak height ● of the endothermic peak between 15 °C and 150 °C between against composition of *Series E*

Both values, the peak area and the peak height, showed a linear dependence on the MAA contents of the copolymers. With the increase of the COOH–group–fraction of in the polymer chain also the peak area and peak height rose. The equations of the two fits are given in *Equation 6.2.3* and *6.2.4*.

$$\text{peak area} = (-351.30 \pm 14.74)\,\text{J} \cdot \text{g}^{-1} + (667.28 \pm 20.30)\,\text{J} \cdot \text{g}^{-1} \cdot \text{F}_{\text{MAA}} \tag{6.2.3}$$

$$\text{peak height} = (-0.87 \pm 0.01)\,\text{mW} \cdot \text{mg}^{-1} + (1.70 \pm 0.01)\,\text{mW} \cdot \text{mg}^{-1} \cdot \text{F}_{\text{MAA}} \tag{6.2.4}$$

The energy which is needed for the decomposition of the hydrolyzed copolymers rises linear with an increase of methacrylic acid units inside the polymer chain. The independence of the peak area and the peak height from the composition of the copolymers implies that the the peak did not results from the emission of solvents but from the decomposition of COOH-groups of the polymers.

6.3. Summary

The *tert*–butyl groups of the P[tBMA–grad–nBMA] gradient copolymers were hydrolytically cleaved by means of methanesulfonic acid (MSA). The characterization of the hydrolyzed copolymers of *Series E* with ^{1}H–NMR–spectroscopy and elementary analysis showed the absence of *tert*–butyl–groups in the polymer chains and a total conversion for all hydrolysis. The elementary analysis fitted well for experiment V71, with the values from the three other substances tended into the right directions. The changes in the IR–spectra supported the good results of the ^{1}H–NMR–spectroscopy. The vibrational band of the OH–groups occurred and the fingerprint– region change in case of the vibrational bands from the *tert*–butyl–group. The changes were so vigorous that an analysis of the vibrational band of nBMA was not possible anymore. The molar mass decreased obviously. With the increase of the MAA–amount inside the polymer chain the shift to lower molar masses became higher. The DSC analysis showed broad endothermic peaks for all copolymers in the same region and the samples did not regenerate after the first heating run. This was the same behavior as observed with samples of the statistical copolymers. The peak area and the peak height of the endothermic peaks rose linear with increase of the MAA–amount inside the polymer chains, hence the needed energy of decomposition increase linear. All four hydrolysis of the resulting gradient copolymers worked well and four amphiphilic gradient copolymers with different composition have successfully be obtained.

7. Synthesis of Statistic Copolymers from Benzyl Methacrylate and tert–Butyl Methacrylate by means of Batch Polymerization

The second monomer system that was investigated in the context of this PhD thesis was composed of benzyl methacrylate and *tert*–butyl methacrylate. In close analogy to the system with *n*– and *tert*–butyl methacrylate statistical copolymers have been prepared first for comparative purpose by means of Atom Transfer Radical Polymerization (ATRP) [16]. These batch experiments were carried out to measure (i) the rate of polymerization of the two monomers, (ii) the composition of the copolymers, as well as (iii) the molecular weights of the products in dependence of the monomer–educt mixture and the reaction time and (iv) the thermal behavior of the resulting polymers and their change during the polymerization. The evaluated data were used to calculate the respective rate constants and to construct the copolymerization diagram of the system BzMA/tBMA.

7.1. Materials and Methods

The batch synthesis with benzyl methacrylate and *tert*–butyl methacrylate as monomers was done under the same conditions as the ATRP with the monomers *n*– and *tert*–butyl methacrylate. (CuCl : pTSC : PMDETA = 1 : 1 : 1 as initiator system, initiator : monomer 1 : 175, solvent MEK, monomer : solvent wt : wt 1:1, T = 80 °C).

7.1.1. Materials

Benzyl methacrylate (BzMA, 98 %, *Alfa Aesar*) and *tert*–butyl methacrylate (tBMA, 98 %, *Alfa Aesar*) were purified via filtration over 1.5 g basic Al_2O_3 (*Sigma–Aldrich*) per 1 g monomer to remove the inhibitor 4–methoxyphenol. 2–Butanone (MEK, *BDH Prolabo*, chromasol.) was dried with boron oxide B_2O_3 (99.9 %, *Sigma–Aldrich*) as described in literature [83]. Copper(I) chloride (97 %, *Sigma–Aldrich*) was given into a tenfold amount of glacial acetic acid and heated under reflux for five hours. Subsequently the grey powder was washed with 100 ml ethanol and 100 ml acetone and then dried in vacuo at 60 °C over night. (following

[84]) N,N,N',N',N"– Pentamethyldiethylenetriamine (PMDETA, 99 %, *Sigma–Aldrich*) and *para*–toluenesulfonyl chloride (pTSC, 98 %, *Sigma–Aldrich*) were used as received.

7.1.2. Batch Copolymerization of Statistical Copolymers

Two series of batch experiments were performed. *Series F* (experiments V81 to V89, *Table 7.1*) consisted of preparative syntheses without sampling and *Series G* (experiments V91 to V94, *Table 7.2*) consisted of analytical copolymerizations with samples taken for EA–, ATR–FTIR–, SEC– and DSC–analysis. The setup of the batch synthesis of BzMA and tBMA was the same as for the batch synthesis, see *Figure 7.1.*

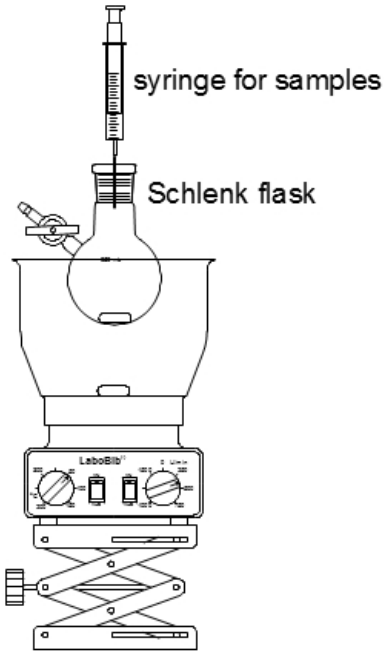

Fig. 7.1.: Experimental setup for batch copolymerization

Series F was performed in analogy to *Series A*, cf. *Section 3.1.2.* A 25 ml Schlenk flask was heated out with a hot gun (air temperature ≈ 400 °C) under vacuum for five minutes and then flushed with nitrogen. The chemicals were weighted in a screw–cap glass in a specific order: First 0.0313 g ($1.81 \cdot 10^{-4}$ mol) pTSC was weighted, followed by the respective amounts of the two monomers, e. g. 2.7843 g (0.0158 mol) BzMA and 2.2468 g (0.0158 mol) tBMA (cf. *Table 7.1*). When the pTSC was dissolved, 0.0344 g ($1.81 \cdot 10^{-4}$ mol) PMDETA, and 0.0179 g ($1.81 \cdot 10^{-4}$ mol) CuCl were added. The mixture was rinsed into the Schlenk flask with 5.0310 g of the solvent MEK under nitrogen flow. Then the flask was sealed with a rubber septum. Subsequently the solution was degassed by means of 5 freeze–melt–cycles, flooded with nitrogen and then heated up to 80 °C for 3 hours. During the reaction time 0.05 ml samples were taken periodically by means of a syringe through the sealed septum at 0, 15, 30, 45, 60, 90, 120, 150 and 180 min for ^{1}H–NMR analysis. The 0.05 ml aliquot samples were given into 0.5 ml cold $CDCl_3$ without further purification.

After 3 hours the Schlenk flask was removed from the oil bath. The reactions mixture was cooled to 20 ℃ with a mixture of ice and water. Afterward the solution was diluted with 20 ml of MEK, filtered over 30 g Al_2O_3 and two–thirds of the solvent was removed by vacuum distillation. The residual mixture of polymer, monomers, initiator components and remaining solvent was slowly dropped into 500 ml of an cooled water : methanol (1 : 1 vol : vol) mixture with −50 ℃. The temperature of the precipitation–solution was observed with a cooling–mixture of isopropyl alcohol and liquid nitrogen. The precipitated polymer was filtered over a P4 glass filter and dried at 25 ℃ under vacuum over night. This technique is donated as *work–up C* in the text throughout. The yields of the polymerizations are listed in *Table 7.1*.

For *Series G*, the analog to *Series B* (cf. *Section 3.1.2*) 0.0689 g ($3.61 \cdot 10^{-4}$ mol) pTSC, 0.0626 g ($3.61 \cdot 10^{-4}$ mol) PMDETA, 0.0357 g ($3.61 \cdot 10^{-4}$ mol) CuCl were mixed with the corresponding amount of the monomers and MEK (cf. *Table 7.2*). The preparation of the Schlenk flask, the mixture and the transfer of the chemicals were performed as described with *Series G* but using a 50 ml Schlenk flask. The same holds true with the synthesis temperature, the reaction time as well as the working up procedure. Reaction conditions and yields are summarized in *Table 7.2*. In *Series G* 1 ml aliquot samples were taken, at 0, 60, 90, 120, 150, 180 min for SEC analysis and another 0.05 ml sample were treated as described with *Series F* and used for ^{1}H–NMR analysis.

SEC–samples were worked up differently from the final polymer. The SEC–sample–work–up procedure is denoted as *work–up D*. 1 ml of the solution was dropped into 20 ml of a cooled water : methanol = 1 : 1 vol:vol mixture which was cooled with isopropyl alcohol and liquid nitrogen to −50 ℃. The precipitated polymer was separated by centrifugation and dried at 25 ℃ under vacuum over night. The precipitate was dissolved in 5 ml CH_2Cl_2 and transferred into a separatory funnel. 5 ml H_2O were added and thoroughly shaken. The organic phase was separated and given into a round-bottom flask. The water phase was extracted two times more each with 2 ml CH_2Cl_2. All organic phased were combined and the solvent was removed by vacuum evaporation. The polymer yields of the copolymers isolated from the samples are listed in *Table7.2*.

All the precipitated, cleaned and dried copolymers were examined with elemental analysis, ATR–FTIR, SEC and DSC. The respective composition data of all performed test polymerizations are summarized in *Tables 7.1 and 7.2*.

Tab. 7.1.: Monomer compositions and final yields of BzMA–tBMA batch copolymerization experiments – *Series F*

Entry	BzMA [mol]	tBMA [mol]	BzMA:tBMA	f_{BzMA}	m_{BzMA} [g]	m_{tBMA} [g]	m_{MEK} [g]	yield [g]	yield [%]
V81	0.0158	0.0158	1:1	0.50	2.7843	2.2468	5.0310	3.62	71.49
V82	0.0105	0.0211	1:2	0.33	1.8503	3.0004	4.8519	3.61	73.95
V83	0.0211	0.0105	2:1	0.66	3.7182	1.4931	5.2102	4.15	79.20
V84	0.0079	0.0237	1:3	0.25	1.3921	3.3701	4.7623	3.13	65.23
V85	0.0237	0.0079	3:1	0.75	4.1764	1.1234	5.2998	3.59	67.35
V86	0.0063	0.0253	1:4	0.20	1.1102	3.5977	4.7085	3.04	64.16
V87	0.0253	0.0063	4:1	0.80	4.4584	0.8959	5.3535	4.70	87.26
V88	–	0.0316	0:1	0.00	–	4.4935	4.4935	2.88	63.68
V89	0.0316	–	1:0	1.00	5.5686	–	5.5686	4.12	73.54

Tab. 7.2.: Monomer compositions and final yields of BzMA–tBMA batch copolymerization experiments – *Series G*

Entry	BzMA [mol]	tBMA [mol]	BzMA:tBMA	f_{BzMA}	m_{BzMA} [g]	m_{tBMA} [g]	m_{MEK} [g]	yield [g]	yield [%]
V91	0.0316	0.0316	1:1	0.50	5.5686	4.4935	10.0621	7.0909	69.99
V92	0.0211	0.0421	1:2	0.33	3.7182	5.9866	9.7048	6.3808	65.29
V93	0.0421	0.0211	2:1	0.66	7.4189	3.0004	10.4193	7.2422	69.04
V94	0.0632	–	1:0	1.00	11.1371	–	11.1371	5.6621	65.48

Tab. 7.3.: Time–conversion data obtained from samples taken during the batch copolymerization reactions of BzMA and tBMA *(Series G)*

time [min]	Entry	yield [g]	yield [%]	Entry	yield [g]	yield [%]
60	V91	0.26	58.40	V92	0.21	47.52
90		0.32	72.16		0.28	65.13
120		0.36	82.78		0.32	72.50
150		0.38	86.76		0.38	87.25
180		0.39	87.78		0.40	90.88
60	V93	0.25	56.02	V94	0.27	59.48
90		0.35	79.51		0.32	71.28
120		0.39	88.09		0.34	75.14
150		0.39	86.68		0.36	79.10
180		0.41	91.26		0.38	84.06

T = 80 °C, [M] = xx mol $\cdot$ l^{-1}, I:M = 1:175

Experiment V88 (PtBMA):

^{1}***H–NMR:*** 1.25–1.45 ppm (broad peak, –C(CH_3)$_3$, P[tBMA]); 1.42 ppm (s, –C(CH_3)$_3$, tBMA); 1.7–1.9 ppm (broad peak, –CH_3, P[tBMA]); 1.9 ppm (s, –CH_3, tBMA); 5.3 ppm (t, CH_2=C–, cis, tBMA); 5.9 ppm (s, CH_2=C–, trans, tBMA)

EA: 65.30 % C, 9.54 % H, (25.16 % O_{calc})

ATR–FTIR: 3100–2800 cm^{-1} (=CH_2, –CH_2–, –CH_3); 1717 cm^{-1} (–C=O); 1476 cm^{-1} (–CH_2–, –CH_3); 1457 cm^{-1} (–CH_2–, –CH_3); 1392 cm^{-1}; 1366 cm^{-1} (tBu); 1331 cm^{-1}; 1248 cm^{-1} (tBu); 1132 cm^{-1} (–C–O–C–); 1036 cm^{-1}; 969 cm^{-1}; 940 cm^{-1}; 875 cm^{-1} (tBu); 847 cm^{-1}; 752 cm^{-1}; 522 cm^{-1}; 500 cm^{-1}; 471 cm^{-1}

SEC: dn/dc = 0.0612 $ml \cdot g^{-1}$; M_n = 30820 $g \cdot mol^{-1}$; M_w = 31620 $g \cdot mol^{-1}$; M_z = 33570 $g \cdot mol^{-1}$

DSC: T_{onset} = 96.0 °C; T_{midpt} = 103.0 °C; T_g = 107.5 °C; T_{offset} = 111.0 °C; ΔC_p = 0.223 $J \cdot g^{-1} \cdot K^{-1}$

Experiment V89 (PBzMA):

^{1}***H–NMR:*** 1.7–1.9 ppm (broad peak, –CH_3, P[BzMA]); 1.8 ppm (s, –CH_3, BzMA); 4.8–5.1 ppm (broad peak, –OCH_2R, P[BzMA]); 5.2 ppm (s, OCH_2R, BzMA); 5.5 ppm (t, CH_2=C–, cis, BzMA); 6.1 ppm (s, CH_2=C–, trans, BzMA); 7.3–7.43 ppm (broad peak, aromatic ring, BzMA and P[BzMA])

EA: 73.82 % C, 6.66 % H, (19.52 % O_{calc})

ATR–FTIR: 3050–2800 cm^{-1} (=CH_2, –CH_2–, –CH_3, aromatic ring); 1722 cm^{-1} (–C=O); 1497 cm^{-1}; 1484 cm^{-1} (–CH_2–, –CH_3); 1455 cm^{-1} (–CH_2–, –CH_3); 1388 cm^{-1}; 1367 cm^{-1}; 1318 cm^{-1}; 1294 cm^{-1}; 1260 cm^{-1}; 1236 cm^{-1}; 1138 cm^{-1} (–C–O–C–); 1081 cm^{-1}; 1060 cm^{-1}; 1029 cm^{-1}; 964 cm^{-1} (Bz); 912 cm^{-1}; 846 cm^{-1}; 826 cm^{-1}; 747 cm^{-1} (Bz); 733 cm^{-1}; 695 cm^{-1} (Bz); 583 cm^{-1}; 527 cm^{-1}; 458 cm^{-1}

SEC: dn/dc = 0.1351 $ml \cdot g^{-1}$; M_n = 5284 $g \cdot mol^{-1}$; M_w = 55960 $g \cdot mol^{-1}$; M_z = 59460 $g \cdot mol^{-1}$

DSC: T_{onset} = 96.0 °C; T_{midpt} = 103.0 °C; T_g = 107.5 °C; T_{offset} = 111.0 °C; ΔC_p = 0.223 $J \cdot g^{-1} \cdot K^{-1}$

Experiment V81 (P[BzMA–co–tBMA], $f_{BzMA} = 0.5$, $F_{BzMA} = 0.33$):

^{1}H–NMR: 1.25–1.45 ppm (broad peak, –C(CH_3)$_3$, P[tBMA]); 1.42 ppm (s, –C(CH_3)$_3$, tBMA); 1.7–1.9 ppm (broad peak, –CH_3, P[tBMA] and P[BzMA]); 1.9 ppm (s, –CH_3, tBMA); 1.8 ppm (s, –CH_3, BzMA); 4.8–5.1 ppm (broad peak, –OCH_2R, P[BzMA]); 5.2 ppm (s, OCH_2R, BzMA); 5.3 ppm (t, CH_2=C–, cis, tBMA); 5.5 ppm (t, CH_2=C–, cis, BzMA); 5.9 ppm (s, CH_2=C–, trans, tBMA); 6.1 ppm (s, CH_2=C–, trans, BzMA); 7.3–7.43 ppm (broad peak, aromatic ring, BzMA and P[BzMA])

EA: 71.20 % C, 8.18 % H, (20.62 % O_{calc})

ATR–FTIR: 3125–2800 cm^{-1} (=CH_2, –CH_2–, –CH_3, aromatic ring); 1717 cm^{-1} (–C=O); 1476 cm^{-1} (–CH_2–, –CH_3); 1455 cm^{-1} (–CH_2–, –CH_3); 1392 cm^{-1}; 1367 cm^{-1} (tBu); 1319 cm^{-1}; 1248 cm^{-1} (tBu); 1134 cm^{-1} (–C–O–C–); 1030 cm^{-1}; 967 cm^{-1} (Bz); 912 cm^{-1}; 876 cm^{-1}; 846 cm^{-1} (tBu); 749 cm^{-1} (Bz); 696 cm^{-1} (Bz); 584 cm^{-1}; 528 cm^{-1}; 461 cm^{-1}

SEC: dn/dc = 0.1135 $ml \cdot g^{-1}$; M_n = 30880 $g \cdot mol^{-1}$; M_w = 31570 $g \cdot mol^{-1}$; M_z = 32300 $g \cdot mol^{-1}$

DSC: T_{onset} = 45.0 °C; T_{midpt} = 56.5 °C; T_g = 52.5 °C; T_{offset} = 70.5 °C; ΔC_p = 0.140 $J \cdot g^{-1} \cdot K^{-1}$

7.1.3. Characterization

All characterization–methods were the same as with the batch copolymers of *Chapter 3*. The used methods were:

- ^{1}H–NMR spectroscopy
- elementary analysis
- ATR–FTIR–spectroscopy
- size exclusion chromatography
- differential scanning calorimetry

The same instruments under the same conditions were used for the investigation of the resulting copolymers.

7.2. Results and Discussion

In following paragraph the results of the analyzes from the different statistical copolymers from benzyl and *tert*–butyl methacrylate P[BzMA–co–tBMA] as well as their discussion is given.

The ATRP–polymerizations were carried out in analogy to the copolymerization of *n*– and *tert*–butyl methacrylate (cf. *Chapter 3*) using toluolsulfonyl chloride (pTSC) as the initiator, $Cu^{I}Cl$ as the catalyst and N,N,N',N',N"–pentamethyldiethylenetriamine (PMDETA) as the ligand. The initial ratio of the substances was $pTSC : CuCl : PMDETA : Mon = 1 : 1 : 1 : 175$. The reactions were carried out in 2–butanone (MEK) as solvent 80 °C. The ratio of monomer to solvent was wt : wt 1 : 1 (cf. experimental part *Section 7.1.2*). Two series of copolymerization were performed. *Series F*, see *Table 7.1*, were preparative syntheses just with sampling for ^{1}H–NMR–analysis, and *Series G*, see *Table 7.2*, were preparative syntheses with sampling for ^{1}H–NMR–, IR–, SEC– and DSC–analysis. The resulting copolymers were filtered over Al_2O_3 to remove the CuCl, subsequently precipitated in an mixture of water:methanol vol : vol 1 : 1 that was cooled down to −50 °C by a mixture of liquid nitrogen and isopropyl alcohol, filtered over a P4 glass filter and dried at 25 °C under vacuum over night. This technique was called *"work–up C"*. The samples for ^{1}H–NMR were used without further purification. The other samples were precipitated also in an mixture of water and methanol with vol:vol 1:1 that was cooled down to −50 °C by liquid nitrogen and isopropyl alcohol. The precipitated polymers were separated from the liquid phase by centrifugation and dried over night at 25 °C under vacuum. The polymers were re–dissolved in dichloromethane and transferred in a separation funnel. Water was added and the CuCl was extracted. The polymer– dichloromethane solution was clear and green. After the extraction the organic phase was clear and colorless and the water phase was clear and blue. The organic phase was separated and the solvent was removed by vacuum evaporation. This technique was called *"work–up D"*. The resulting polymers were white and amorphous powders. The work–ups of the *Series F* and *G* were different to the work–ups of *Series A* and *B* relating to the temperature of the precipitation–solution of methanol and water. The precipitation of the copolymers with BzMA–units only worked well when the methanol–water–mixture had a temperature obviously under −40 °C especially for copolymers with low conversion.

7.2.1. Kinetic Studies

In a first series of copolymerization experiments (*Series F*) preparative batch synthesis were performed to measure the rate of copolymerization as well as the resulting copolymer compositions. Aliquot samples were taken after 0, 15, 30, 45, 60, 90, 120, 150 and 180 min and analyzed by means of ^{1}H–NMR–spectroscopy. The ^{1}H–NMR–spectra were analyzed regarding the conversion p of the monomers which was the basis for the calculation of the reaction rates. The signals in the resulting spectra were assigned to the structure elements of the

monomers and the copolymer as shown in Table 7.4. The position of the peaks were taken from literature [85].

Within the subsequent text the numbers of the appropriate carbons from the chemical structure, that is shown in *Figure 7.3*, are given in the brackets. The BzMA as monomer showed a singlet signal at 6.1 ppm and a triplet at 5.5 ppm originating from the vinyl–group (4 and 5) and a singlet at 1.8 ppm caused by the methyl–group (11) of the methacrylate group. The benzyl–unit exhibited a singlet of the benzylic methylene–group (6) at 5.2 ppm and a broad multiplet was caused the aromatic ring protons (7, 8, 9) between 7.5 to 7.2 ppm. The BzMA–part of the polymer is represented in the spectra by broad peaks around 5.0 to 4.8 ppm for the methylene–group (6') and from 7.5 to 7.2 ppm for the aromatic ring protons.

Tab. 7.4.: Position and assignments of the signals in the ^{1}H–NMR–spectra of the prepared P[BzMA–co–tBMA] polymers

δ [ppm]	Multiplicity	No. of carbons	Carbon No.*	Structure element
1.25–1.4	broad peak	9H	3'	–C(CH_3)$_3$, P[tBMA]
1.42	s	2H	3	–C(CH_3)$_3$, tBMA
1.7–1.9	broad peak	4H	10',11'	–CH_2–backbone, P[BzMA] and P[tBMA]
1.9	s	3H	10	–CH_3, tBMA
1.8	s	3H	11	–CH_3, BzMA
4.75–5.05	broad peak	2H	6'	–OCH_2R, P[BzMA]
5.2	s	2H	6	–OCH_2R, BzMA
5.3	t	1H	2	CH_2=C–, cis, tBMA
5.5	t	1H	5	CH_2=C–, cis, BzMA
5.9	s	1H	1	CH_2=C–, trans, tBMA
6.1	s	1H	4	CH_2=C–, trans, BzMA
7.2–7.5	broad peak	5H	7-9,7'-9'	aromatic ring, BzMA and P[BzMA]

* cf. *Figure 7.2*

Hence the signals, resulting from the aromatic rings of the monomer and polymer, appear in the same chemical shift region, and become mutually overlapped. The methacrylate–part of the tBMA monomer shows a singlet at 5.9 ppm, a triplet at 5.3 ppm and a singlet at 1.9 ppm (1, 2, 10) and the *tert*–butyl group gave rise to a singlet at 1.9 ppm (3). The broad signal between circa 1.25 to 1.4 ppm is caused by the *tert*–butyl group of PtBMA (3'). The CH_2–signals of the polymer–backbone (10', 11') are present in form of a broad peak ranging from 1.7 to 1.9 ppm. The peaks around 2.4 (quartet), 2.1 (singlet) and 1.0 (triplet) ppm belong to solvent MEK.

The changes of the ^{1}H–NMR–spectra during the polymerization are shown in *Figure 7.4* and in more detail *Figure 7.5*. The intensities of the different monomer–signals decrease in relation to the solvent peaks which remain constant during the polymerization. The signal 6' of the methylene–group of the benzyl–part of PBzMA appears and increases over time to become a

very broad peak from 4.8 to 5.1 ppm. Especially for the broad peak around 1.25 to 1.4 ppm this is very obvious, because there is also the *tert*–butyl group signal of the PtBMA which rises in intensity. In the region between 1.7 to 1.9 ppm the CH_2–signal of the polymer–backbone (10', 11') grow in comparison to the solvent–signals next neighbored to the corresponding monomer peaks (10, 11). The broad peak of the polymer (10', 11') overlapped with the two monomer signals (10, 11). In *Figure 7.5* only the spectra of three samples, taken at 0, 90 and 180 min, were depicted to point out the differences more in detail.

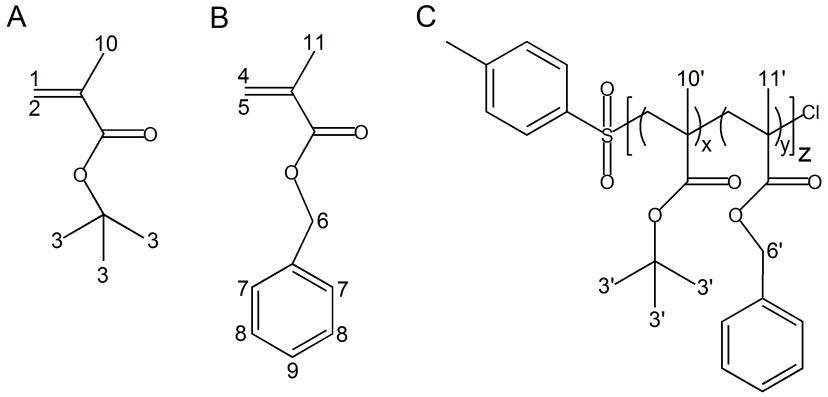

Fig. 7.2.: Molecular structures of the monomers (A) tBMA and (B) nBMA and (C) the resulting copolymer of *Series F* and *G* with carbon–atom labels (z = x + y = 1)

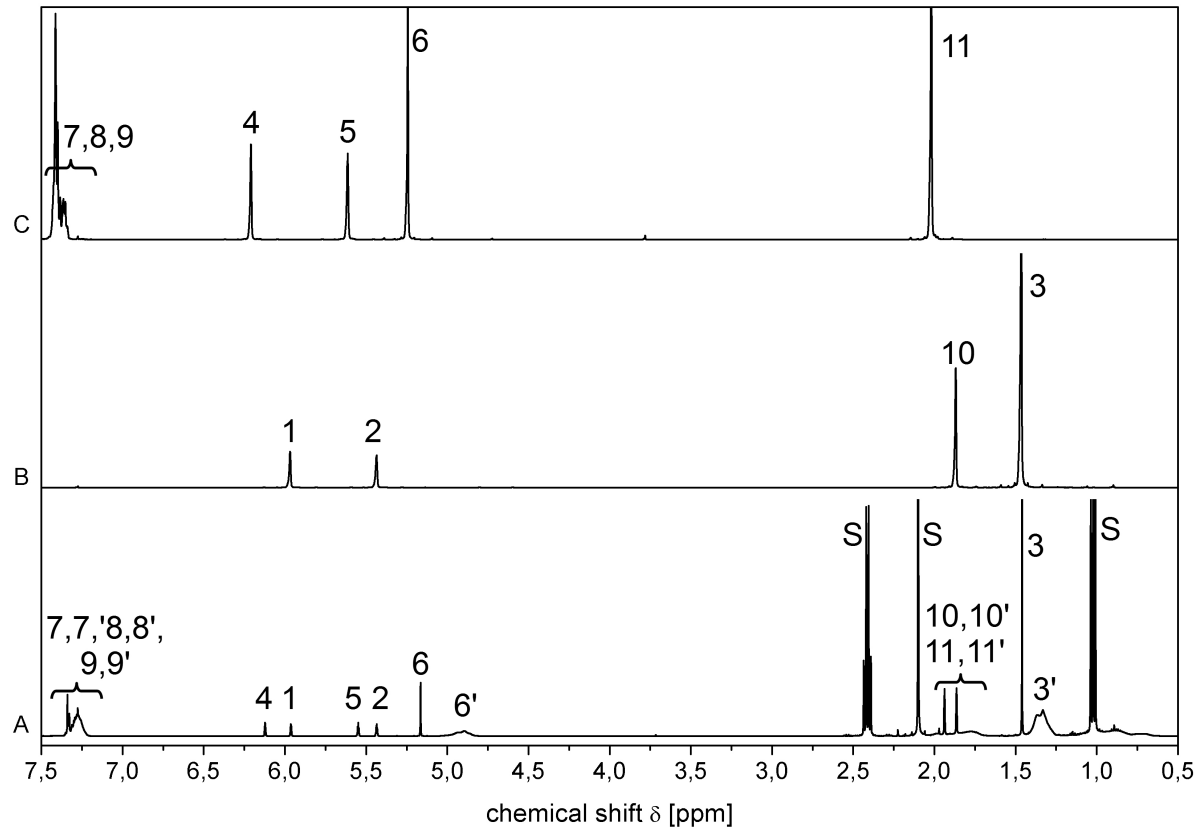

Fig. 7.3.: ^{1}H–NMR–spectrum of (A) reaction mixture V81 (f_{BzMA} = 0.5; BzMA:tBMA = 1:1, I:M = 1:175, T = 80 °C) after 180 min reaction time, (B) tBMA and (C) BzMA (S = solvent signals: MEK)

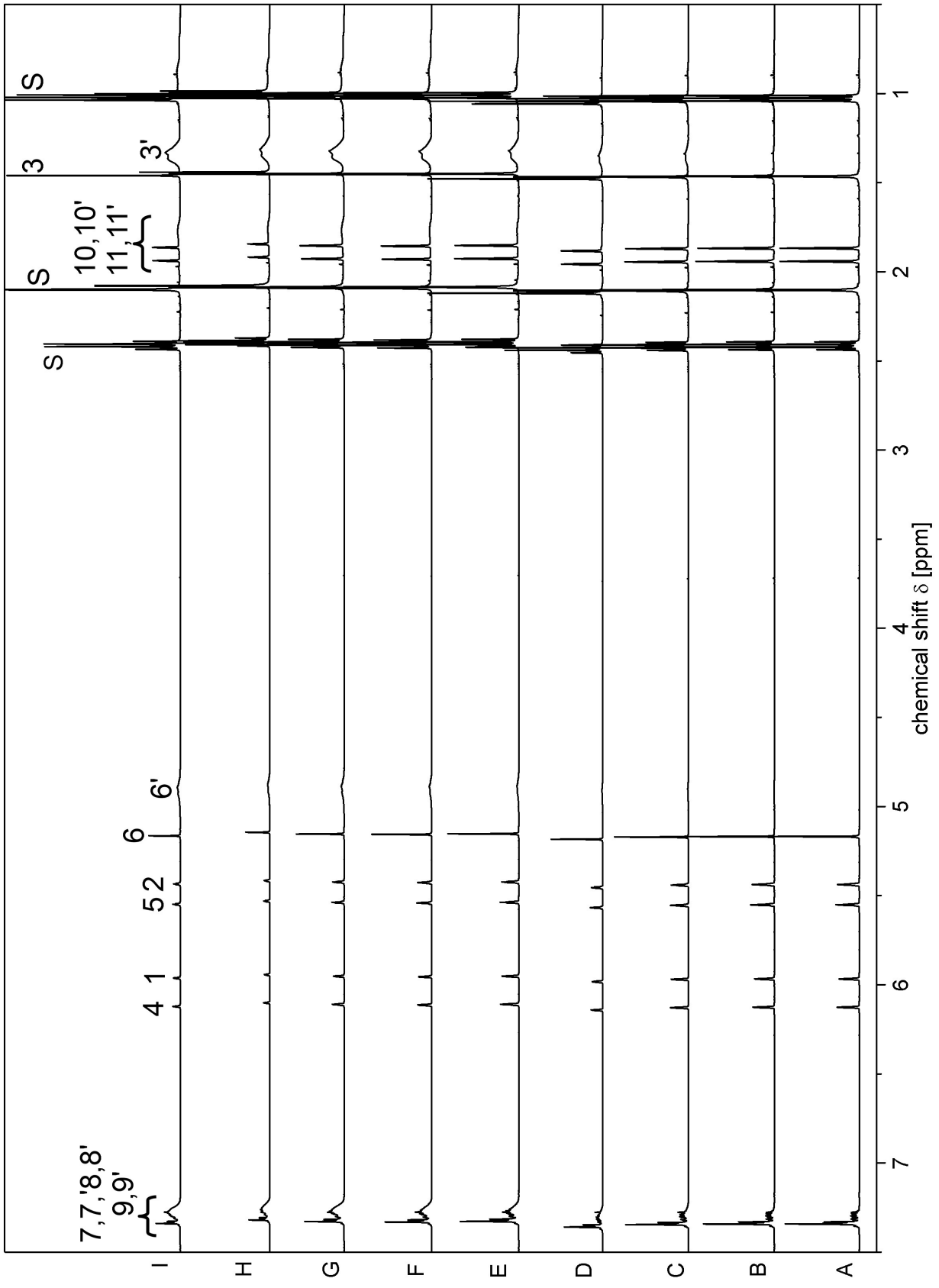

Fig. 7.4.: ^{1}H–NMR–spectra of samples, taken from the copolymerization mixture V81 (f_{BzMA} = 0.5) at different polymerization times; A – 0 min, B – 15 min, C – 30 min, D – 45 min, E – 60 min, F – 90 min, G – 120 min, H – 150 min and I – 180 min

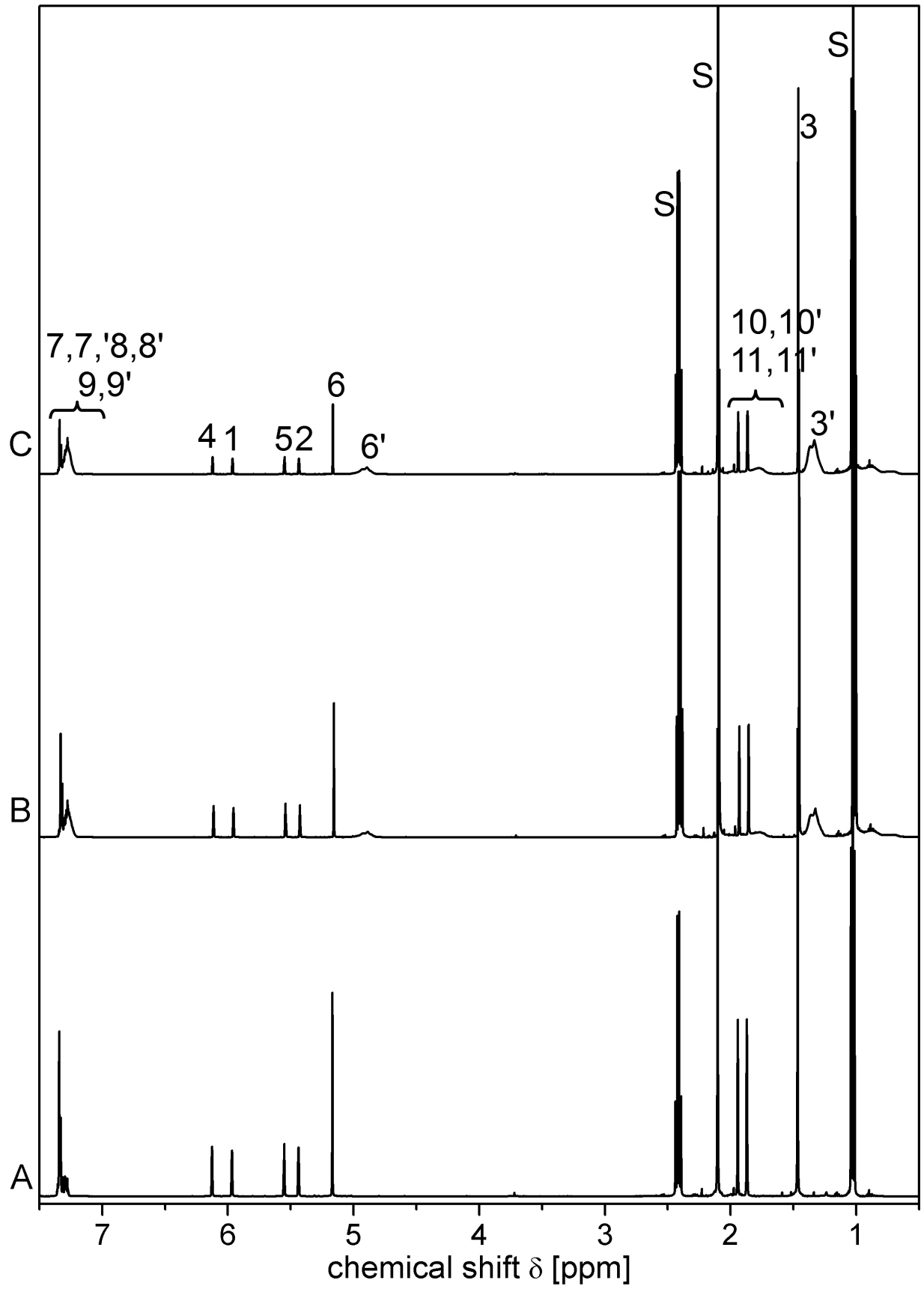

Fig. 7.5.: ^{1}H–NMR–spectra of samples, taken from the copolymerization mixture V81 (f_{BzMA} = 0.5) at different polymerization times; A – 0 min, B – 90 min and C – 180 min

The determination of the kinetic data were done in the same way as with the first monomer–system consisting of *n*– and *tert*–butyl methacrylate, cf. *Section 3.3.1*. However, since the signals of the monomers and the different parts of the polymer were more separated here, the calculations of conversion and composition differed slightly. The peak areas of the signals 3, 3', 6, 6' were measured and the molar ratios of monomers to polymer were calculated by means of *Equations 7.2.1 to 7.2.2*.

To determine of the conversion of BzMA (p_{BzMA}) the integrals of the methylene–group (6, 6'), cf. *Figure 7.2*, of the monomer (A_6) and that of the polymer ($A_{6'}$) were used, respectively (cf. *Equation 7.2.1*).

$$p_{BzMA} = \frac{A_{6'}}{A_6 + A_{6'}} \tag{7.2.1}$$

with A_6 = integral intensity at 5.15 to 5.2 ppm; $A_{6'}$ = integral intensity at 4.75 to 5.05 ppm

To determine the conversion of the *tert*–butyl methacrylate (p_{tBMA}) the signals (3) (cf. *Figure 7.2*) of the CH_3–groups of the monomers *tert*–butyl group (A_3) and the respective signal 3' of the polymer ($A_{3'}$) were taken (cf. *Equation 7.2.2*).

$$p_{tBMA} = \frac{A_{3'}}{A_3 + A_{3'}} \tag{7.2.2}$$

with A_3 = integral intensity at 1.41 to 1.43 ppm; $A_{3'}$ = integral intensity at 1.25 to 1.4 ppm

The values of the integrals A3, A3', A6 and A6' as well as the results of the *Equations 7.2.1* and *7.2.2* and the total conversions of the ^{1}H–NMR–samples taken from the experiments of *Series F* are listed in *Table 7.5*.

Tab. 7.5.: Values of integrated ^{1}H–NMR signals and calculated conversions of *Series F*

Entry	time	Integral				conversion p		
f_{BzMA}	[min]	A_6	$A_{6'}$	A_3	$A_{3'}$	BzMA	tBMA	total
V81	0	2.0224	0.0000	9.2353	0.0000	0.0000	0.0000	0.0000
0.5	15	2.0016	0.1407	9.2660	0.8582	0.0657	0.0848	0.0424
	30	2.0090	0.3867	9.3239	2.3050	0.1614	0.1982	0.1319
	45	1.9970	0.8374	9.2860	4.6241	0.2954	0.3324	0.2469
	60	1.9943	1.2573	9.3304	6.2966	0.3867	0.4029	0.3492
	90	2.0281	1.9860	9.6231	10.7179	0.4948	0.5269	0.4568
	120	2.0028	2.9955	9.3524	14.5993	0.5993	0.6095	0.5521
	150	1.9966	3.9167	9.4110	19.3527	0.6624	0.6728	0.6361

Continuation on next page ...

Entry	time	Integral				conversion p		
f_{BzMA}	[min]	A_6	$A_{6'}$	A_3	$A_{3'}$	BzMA	tBMA	total
	180	1.9989	4.9077	9.4311	23.5377	0.7106	0.7139	0.6881
V82	0	1.0082	0.0000	9.2194	0.0000	0.0000	0.0000	0.0000
0.33	15	1.0180	0.0571	9.3560	0.8666	0.0531	0.0848	0.0735
	30	1.0010	0.2461	9.1438	2.6446	0.1973	0.2243	0.2132
	45	1.0111	0.4160	9.0590	4.3804	0.2915	0.3259	0.3113
	60	1.0174	0.6365	9.2788	6.5334	0.3849	0.4132	0.3997
	90	1.0229	1.1314	9.3340	10.8969	0.5252	0.5386	0.5288
	120	1.0244	1.7262	9.4333	16.5355	0.6276	0.6367	0.6273
	150	1.0207	2.2494	9.5183	21.4296	0.6879	0.6924	0.6840
	180	1.0275	2.6931	9.3805	26.1495	0.7238	0.7360	0.7246
V83	0	4.0301	0.0000	9.1938	0.0000	0.0000	0.0000	0.0000
0.66	15	4.0160	0.4483	9.0465	1.2264	0.1004	0.1194	0.1057
	30	3.9676	1.3199	9.0896	3.5185	0.2496	0.2791	0.2568
	45	3.9663	2.3039	9.1446	5.9529	0.3674	0.3943	0.3726
	60	4.0232	3.3837	9.2261	8.5694	0.4568	0.4816	0.4604
	90	4.0680	5.5007	9.4635	13.7825	0.5749	0.5929	0.5751
	120	4.0482	7.7074	9.3692	19.3662	0.6556	0.6740	0.6551
	150	4.0656	10.2164	9.4021	24.5129	0.7153	0.7228	0.7106
	180	4.0214	12.2106	9.3955	29.5497	0.7523	0.7588	0.7469
V84	0	1.9861	0.0000	27.2459	0.0000	0.0000	0.0000	0.0000
0.25	15	1.9821	0.0479	27.3688	3.3937	0.0236	0.1103	0.0886
	30	2.0192	0.3598	27.9387	8.4613	0.1512	0.2325	0.2121
	45	2.0065	0.7611	27.6912	13.4766	0.2750	0.3274	0.3143
	60	2.0094	1.1077	27.7138	19.6707	0.3554	0.4151	0.4002
	90	2.0112	1.8800	27.9923	29.8045	0.4831	0.5157	0.5075
	120	2.0090	2.6068	27.5274	42.3970	0.5648	0.6063	0.5959
	150	1.9693	3.3238	26.4227	49.4054	0.6280	0.6515	0.6456
	180	2.0332	4.2821	28.9001	67.1780	0.6781	0.6992	0.6939
V85	0	6.4157	0.0000	9.2641	0.0000	0.0000	0.0000	0.0000
0.75	15	6.1985	0.1034	9.2683	0.7522	0.0164	0.0751	0.0311
	30	6.1308	0.7052	9.2083	1.4728	0.1032	0.1379	0.1118
	45	6.2208	1.5010	9.2964	2.9317	0.1944	0.2398	0.2057
	60	6.2071	2.2437	9.4738	3.9783	0.2655	0.2957	0.2731
	90	6.2349	3.5492	9.5060	6.1634	0.3628	0.3933	0.3704

Continuation on next page ...

Entry	time	Integral				conversion p		
f_{BzMA}	[min]	A_6	$A_{6'}$	A_3	$A_{3'}$	BzMA	tBMA	total
	120	6.1867	4.9558	9.4331	8.7090	0.4448	0.4800	0.4536
	150	6.2826	6.4227	9.5111	11.0087	0.5055	0.5365	0.5133
	180	6.3463	8.0051	9.6801	13.5456	0.5578	0.5832	0.5641
V86	0	0.4940	0.0000	9.1973	0.0000	0.0000	0.0000	0.0000
0.2	15	0.4963	0.0110	9.2914	0.4592	0.0217	0.0471	0.0420
	30	0.4963	0.0515	9.2705	1.5923	0.0940	0.1466	0.1361
	45	0.4996	0.1226	9.3487	2.4551	0.1970	0.2080	0.2058
	60	0.5007	0.1640	9.3795	3.6282	0.2467	0.2789	0.2725
	90	0.5172	0.3085	9.2966	6.1193	0.3736	0.3970	0.3923
	120	0.5016	0.4271	9.1413	8.3745	0.4599	0.4781	0.4745
	150	0.5043	0.5729	9.3300	10.9769	0.5318	0.5406	0.5388
	180	0.5097	0.6790	9.5909	13.5739	0.5712	0.5860	0.5830
V87	0	8.5802	0.0000	8.8779	0.0000	0.0000	0.0000	0.0000
0.8	15	7.8303	0.5422	9.0172	1.2350	0.0648	0.1205	0.0759
	30	8.0086	1.9111	9.1275	3.0004	0.1927	0.2474	0.2036
	45	7.9935	3.7154	9.1748	5.5965	0.3173	0.3789	0.3296
	60	7.9470	5.5590	9.2542	7.3912	0.4116	0.4440	0.4181
	90	7.8407	9.4919	9.1722	12.5558	0.5476	0.5779	0.5537
	120	7.8682	13.6865	9.2351	17.8601	0.6350	0.6592	0.6398
	150	7.8497	18.2042	9.2486	23.6625	0.6987	0.7190	0.7028
	180	7.9037	24.0751	9.4728	31.3315	0.7529	0.7679	0.7559
V88	0	–	–	9.3873	0.0000	–	0.0000	0.0000
0.0	15	–	–	9.2505	0.4831	–	0.0496	0.0496
	30	–	–	9.4404	1.4668	–	0.1345	0.1345
	45	–	–	9.4383	2.5480	–	0.2126	0.2126
	60	–	–	9.3901	3.6854	–	0.2819	0.2819
	90	–	–	9.5863	5.9845	–	0.3843	0.3843
	120	–	–	9.4846	8.1597	–	0.4625	0.4625
	150	–	–	9.8736	10.2475	–	0.5093	0.5093
	180	–	–	9.6371	11.8756	–	0.5520	0.5520
V89	0	2.0096	0.0000	–	–	0.0000	–	0.0000
1.0	15	2.0079	0.2506	–	–	0.1110	–	0.1110
	30	2.0142	0.7716	–	–	0.2770	–	0.2770
	45	2.0071	1.4185	–	–	0.4141	–	0.4141

Continuation on next page ...

Entry	time	Integral				conversion p		
f_{BzMA}	[min]	A_6	$A_{6'}$	A_3	$A_{3'}$	BzMA	tBMA	total
	60	2.0442	2.4578	–	–	0.5459	–	0.5459
	90	2.0319	3.7708	–	–	0.6498	–	0.6498
	120	2.0271	5.4785	–	–	0.7299	–	0.7299
	150	2.0428	7.8666	–	–	0.7939	–	0.7939
	180	2.0569	10.4657	–	–	0.8357	–	0.8357

Figure 7.6a depicts a representative time conversion curve as obtained with reaction V81 (*Table 7.1,* $f_{BzMA} = 0.5$). The conversion of both the monomers increased steadily, however, the initial slope of the curves was larger than that of the later stages of the reaction. Note that both monomers were consumed with similar rate in the present example. In the absence of side reactions the reaction kinetic of an ATRP homopolymerization is of pseudo–first–order. [16] As long as the monomer composition of the reaction mixture is not altered during the course of a copolymerization this kinetic law should be valid, too. With copolymerizations the effective rate constant k_{eff} may depend on the monomer composition.

$$\frac{d[M]}{dt} = -k_{eff} \cdot [M] \qquad \text{with } [M] = [M]_1 + [M]_2 \tag{7.2.3}$$

with [M] = total monomer concentration, $[M]_i$ = concentration of monomer i, k_{eff} = effective rate constant of copolymerization

At least the low conversion, initial stages of a copolymerization reaction can be described by *Equation 7.2.3*. Hence, a first order kinetic plot of $(-\ln(1-p))$ was set up. The calculated conversions of the samples were inserted into *Equation 7.2.3* and the results were also plotted in *Figure 7.6b*. The rate constants of the monomers (k_{BzMA} and k_{tBMA}) were determined from the initial slope of a regression line in the range of small conversions ($\ln(1-p) < 0.5$) of the kinetic plots. The first four data points (up to a reaction time of 45 min) of all members of *Series F* were used and became located on straight lines (cf. *Figure 7.6*) up to conversion of about 30 %. This result was similar to the one of *Series A*. The continuity during all the polymerizations and over all the monomer compositions was a signal for the very well control over the reaction by ATRP. Note that the time–unit was changed from minutes to seconds, because in the literature rate constants are given in s^{-1} by default. The resulting kinetic plot with the two regression lines for experiment V81 is given in *Figure 7.6b* exemplarily.

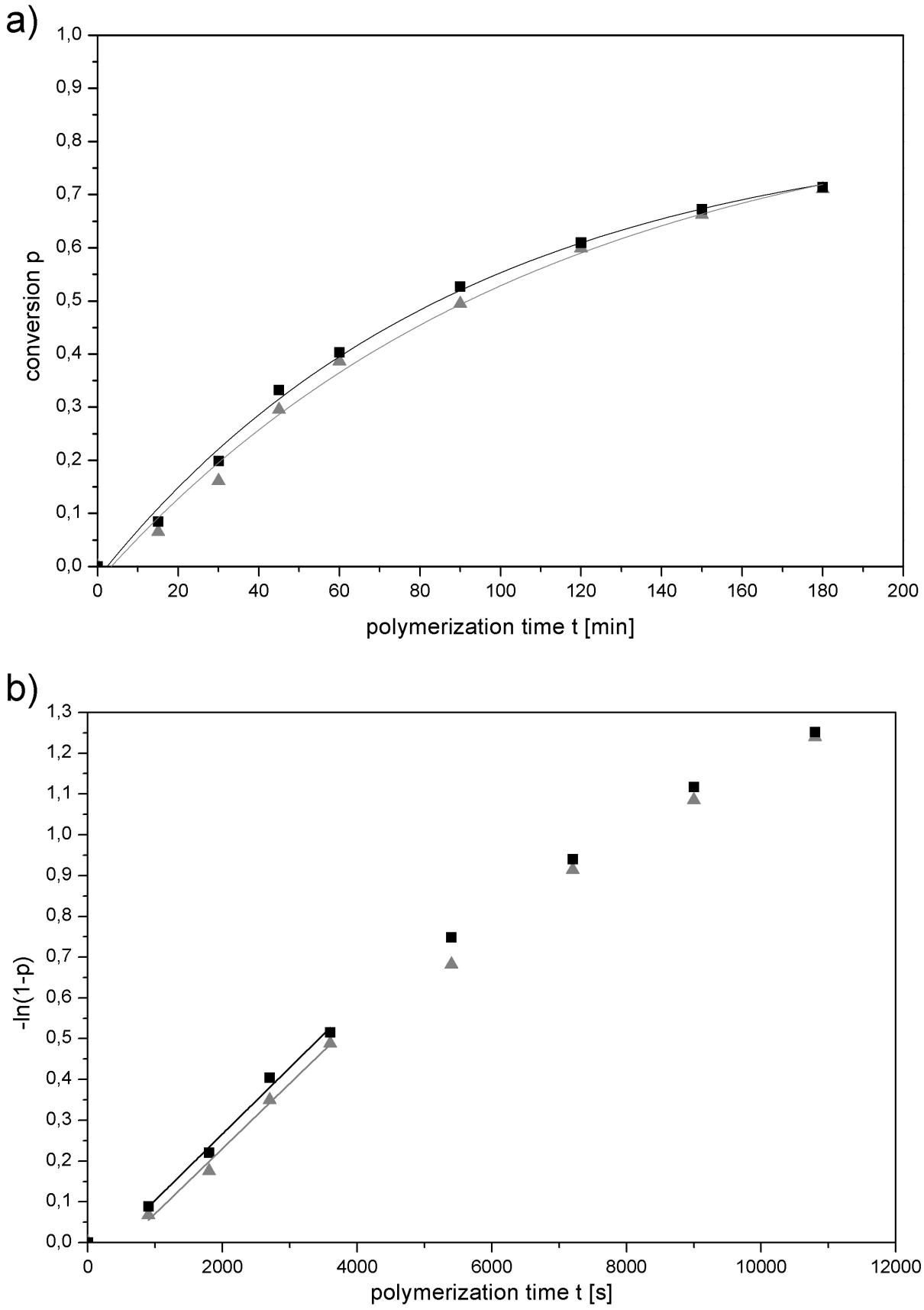

Fig. 7.6.: Monomer conversion and first order kinetic plot based on the NMR–evaluation of experiment V81 (f_{BzMA} = 0.5); a) conversion p versus time [min]; b) First order kinetic parameters versus time [s]; ■ tBMA, ▲ BzMA

The rate constants $k_{BzMA}(f_{BzMA})$ and $k_{tBMA}(f_{BzMA})$ as obtained from the experiments using the monomer ratios f_{BzMA} = 0, 0.2, 0.25, 0.33, 0.5, 0.66, 0.75, 0.8 and 1 (cf. *Table 7.6*) were plotted against the monomer molar fraction of BzMA and a regression line was calculated for the data points. In a binary ATRP–copolymerization the consumption of each monomer obeys a pseudo first order–reaction kinetics, as long as the monomer–mixture composition does not change. Hence, one can describe the initial stages of the copolymerization by means of *Equation 7.2.4 and 7.2.5*.

$$-\ln(1 - p_{BzMA}) = k_{BzMA}(f_{BzMA}) \cdot t \tag{7.2.4}$$

$$-\ln(1 - p_{tBMA}) = k_{tBMA}(f_{BzMA}) \cdot t \tag{7.2.5}$$

In these equations $k_i(f_{BzMA})$ represent the composition–dependent rate constants of the respective monomer. *Figure 7.6b* depicts the respective kinetic plot obtained from the data of experiment V81. An analogous analysis was performed with all obtained time conversion data of reactions V82 to V89. The measured individual rate constants $k_i(f_i)$ are summarized in *Table 7.6*. *Figure 7.7* depicts a plot of the individual monomer rate constant $k_i(f_{BzMA})$ (i = BzMA, tBMA) versus the initial molar fraction of BzMA in the monomer mixture, f_{BzMA}. BzMA ($k_{BzMA} = 2.22 \cdot 10^{-4} s^{-1}$) polymerized about twice as fast as tBMA ($k_{BzMA} = 9.45 \cdot 10^{-5} s^{-1}$). The measured effective rate constants of the copolymerizations lay within this range. Between f_{BzMA} = 0.2 and 0.8, while it seems that $k_{eff}(f_{BzMA})$ exhibits a more strong change between f_{BzMA} = 0 – 0.2 ($dk/df \approx 2.46 \cdot 10^{-4} s^{-1}$) and f_{tBMA} = 0.8 – 1 ($dk/df \approx 2.63 \cdot 10^{-4} s^{-1}$) the values only slightly increased ($1.2 \ldots 1.8 \cdot 10^{-4}$). The rise fitted to values of the homopolymerizations.

Tab. 7.6.: Kinetic results and copolymer compositions of the different copolymer compositions of *Series F*

Entry	f_{BzMA}	k_{BzMA} [s^{-1}]	$k_{eff\,BzMA}$ [s^{-1}]	k_{tBMA} [s^{-1}]	$k_{eff\,tBMA}$ [s^{-1}]	k_{eff} [s^{-1}]	F_{BzMA}[a]
V88	0.00	–	$1.46 \cdot 10^{-4}$	$9.45 \cdot 10^{-5}$	$1.41 \cdot 10^{-4}$	$1.41 \cdot 10^{-4}$	0.00
V86	0.20	$1.01 \cdot 10^{-4}$	$1.53 \cdot 10^{-4}$	$1.01 \cdot 10^{-4}$	$1.51 \cdot 10^{-4}$	$1.51 \cdot 10^{-4}$	0.11
V84	0.33	$1.58 \cdot 10^{-4}$	$1.58 \cdot 10^{-4}$	$1.64 \cdot 10^{-4}$	$1.57 \cdot 10^{-4}$	$1.57 \cdot 10^{-4}$	0.14
V82	0.25	$1.56 \cdot 10^{-4}$	$1.55 \cdot 10^{-4}$	$1.50 \cdot 10^{-4}$	$1.53 \cdot 10^{-4}$	$1.53 \cdot 10^{-4}$	0.20
V81	0.50	$1.60 \cdot 10^{-4}$	$1.64 \cdot 10^{-4}$	$1.63 \cdot 10^{-4}$	$1.65 \cdot 10^{-4}$	$1.64 \cdot 10^{-4}$	0.33
V83	0.66	$1.75 \cdot 10^{-4}$	$1.70 \cdot 10^{-4}$	$1.88 \cdot 10^{-4}$	$1.73 \cdot 10^{-4}$	$1.71 \cdot 10^{-4}$	0.48
V85	0.75	$1.09 \cdot 10^{-4}$	$1.73 \cdot 10^{-4}$	$9.97 \cdot 10^{-5}$	$1.77 \cdot 10^{-4}$	$1.74 \cdot 10^{-4}$	0.61
V87	0.80	$1.73 \cdot 10^{-4}$	$1.75 \cdot 10^{-4}$	$1.69 \cdot 10^{-4}$	$1.79 \cdot 10^{-4}$	$1.76 \cdot 10^{-4}$	0.67
V89	1.00	$2.22 \cdot 10^{-4}$	$1.82 \cdot 10^{-4}$	–	$1.89 \cdot 10^{-4}$	$1.82 \cdot 10^{-4}$	1.00

[a] calculated from *Equation 7.2.14*

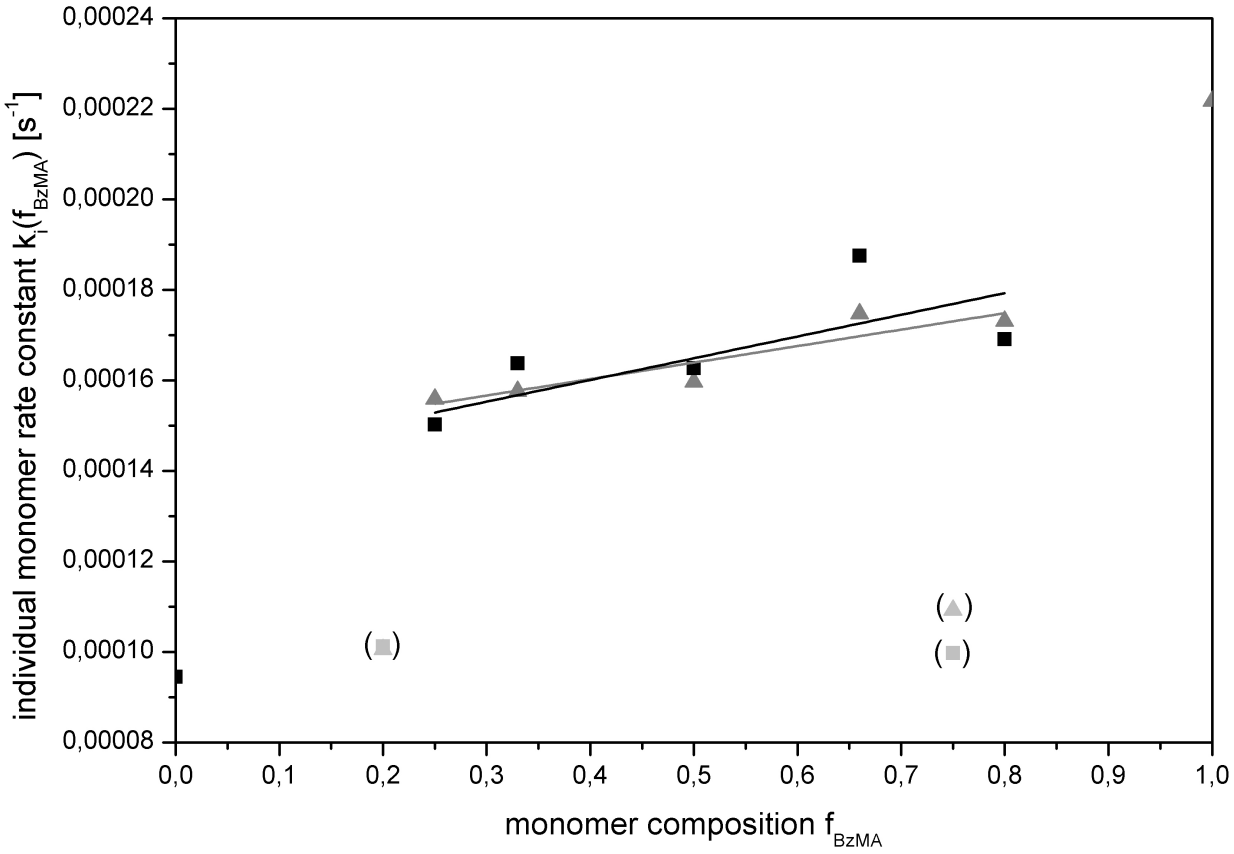

Fig. 7.7.: Plot of the individual monomer rate constants k_{BzMA} and k_{tBMA} versus the BzMA–content of the monomer feed ratio; ■ tBMA, ▲ BzMA; not included values in brackets

In the interval $f_{BzMA} \in [0.2, 0.8]$ the rate constants were approximated by straight lines, their low slopes ($m_{Bz} = \frac{dk_{BzMA}}{df_{BzMA}} = 3.64 \cdot 10^{-5} \pm 1.19 \cdot 10^{-5}$, $m_{tB} = \frac{dk_{tBMA}}{df_{BzMA}} = 4.80 \cdot 10^{-5} \pm 3.19 \cdot 10^{-5}$) indicating a very weak dependence of the copolymerization rate on the monomer mixture composition. These results were much the same as for *Series A*. Both fitted lines are shown in *Figure 7.8*. The disregarded values are set into brackets.

If both monomers are consumed according to a first–order kinetics, the sum of both monomer concentrations $[M] = [M_{BzMA}] + [M_{tBMA}]$ must follow the same law. Hence, the total rate of copolymerization will follow *Equation 7.2.3*, with k_{eff} representing the monomer mixture dependence effective rate constant. It can be shown that k_{eff} is related to the monomer composition f_{BzMA} and the individual rate constant according to *Equation 7.2.10*. With the equations of the regression lines from the rate constants and the monomer composition of the different feed ratios the effective rate constants of the monomers ($k_{eff,BzMA}$ and $k_{eff,tBMA}$) were calculated (see *Equations 7.2.6 and 7.2.7*).

$$k_{eff,BzMA} = a_{k_{BzMA}} + b_{k_{BzMA}} \cdot f_{BzMA} \tag{7.2.6}$$

$$k_{eff,tBMA} = a_{k_{tBMA}} + b_{k_{tBMA}} \cdot f_{tBMA} \tag{7.2.7}$$

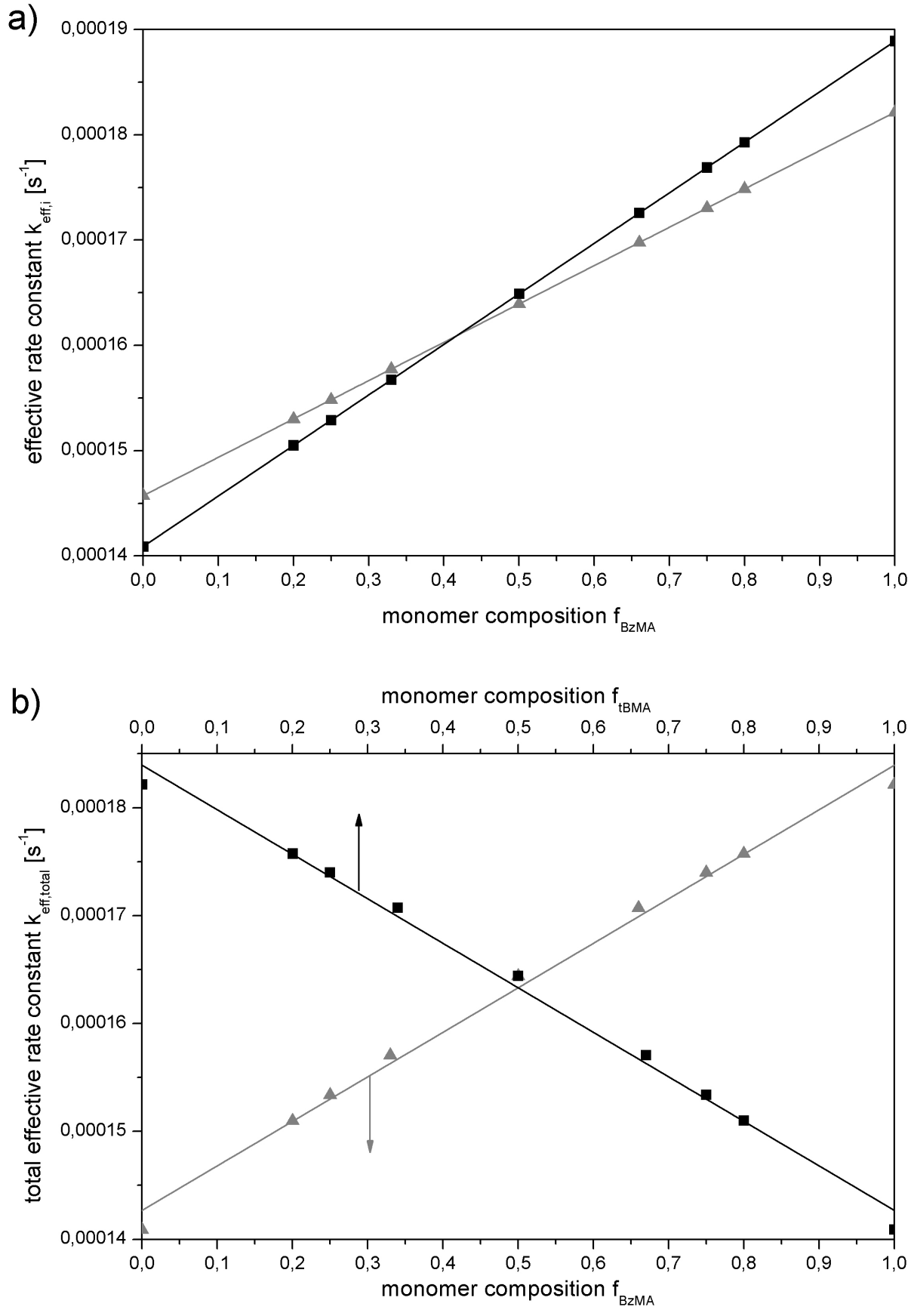

Fig. 7.8.: Effective rate constants of the individual monomer consumptions $k_{eff,i}$ and total effective rate constants $k_{eff.total,total}$ of the total reaction for the different monomer feed ratios of *Series F* – assuming that the fit equations to be valid in $f_{BzMA} \in [0,1]$; a) effective monomer rate constants $k_{eff,BzMA}$ (▲) (*Eq. 7.2.8*) and $k_{eff,tBMA}$ (■) (*Eq. 7.2.9*); b) total effective rate constant $k_{eff}(f_{BzMA})$ (▲) (*Eq. 7.2.11*) and $k_{eff}(f_{tBMA})$ (■) (*Eq. 7.2.12*)

The fit of *Equations 7.2.6* and *7.2.7* to the experimental data of *Table 7.6* gave the resulted in *Equations 7.2.8* and *7.2.9*.

$$k_{eff,BzMA} = \left(1.46 \cdot 10^{-4} \pm 7.03 \cdot 10^{-6}\right) s^{-1} + \left(3.64 \cdot 10^{-5} \pm 1.19 \cdot 10^{-5}\right) s^{-1} \cdot f_{BzMA} \quad (7.2.8)$$

$$k_{eff,tBMA} = \left(1.41 \cdot 10^{-4} \pm 1.88 \cdot 10^{-5}\right) s^{-1} + \left(4.80 \cdot 10^{-5} \pm 3.19 \cdot 10^{-5}\right) s^{-1} \cdot f_{BzMA} \quad (7.2.9)$$

The data points here lied on straight lines for both monomers, cf. *Figure 7.8a*. The values of the effective rate constants were used to determine the copolymerizations total effective rate constant (k_{eff}) with *Equation 7.2.10*.

$$k_{eff} = f_1 \cdot k_1 + f_2 \cdot k_2 \quad (7.2.10)$$

The total rate constant was expressed either in terms of the molar fraction of BzMA in the reaction mixture (f_{BzMA}, cf. *Equation 7.2.11*) or in dependence of f_{tBMA} (cf. *Equation 7.2.12*).

$$k_{eff}(f_{BzMA}) = \left(1.43 \cdot 10^{-4}\right) s^{-1} + \left(4.12 \cdot 10^{-5}\right) s^{-1} \cdot f_{BzMA} \quad (7.2.11)$$

$$k_{eff}(f_{tBMA}) = \left(1.84 \cdot 10^{-4}\right) s^{-1} - \left(4.12 \cdot 10^{-5}\right) s^{-1} \cdot f_{tBMA} \quad (7.2.12)$$

The results are pictured in *Figure 7.8b*, to demonstrate the linear relation. All the results of the previous calculations are summarized in *Table 7.6*.

The measured rate constances were also used to determine the instantaneous polymer composition $\frac{d[BzMA]}{d[tBMA]}$ of the resulting copolymers by means of *Equation 7.2.13*.

$$F_{BzMA} = \frac{R_{BzMA}}{R_{BzMA} + R_{tBMA}} = \frac{f_{BzMA} \cdot k_{BzMA}}{k_{BzMA} + f_{tBMA} \cdot k_{tBMA}} \quad (7.2.13)$$

with R_i = rate of copolymerization of monomer i, k_i = effective, composition dependent individual rate constant of monomer i, f_i = molar fraction of monomer i in the reaction mixture

The copolymerization diagram of benzyl and *tert*–butyl methacrylate as obtained from *Equation 7.2.13* is shown in *Figure 7.9*. The compositions of the resulting copolymers from *Series F* were summarized in *Table 7.6*. At any monomer composition f_{BzMA} the monomer tBMA copolymerized faster than BzMA, resulting in copolymers that contained less BzMA than was initially present in the monomer mixture.

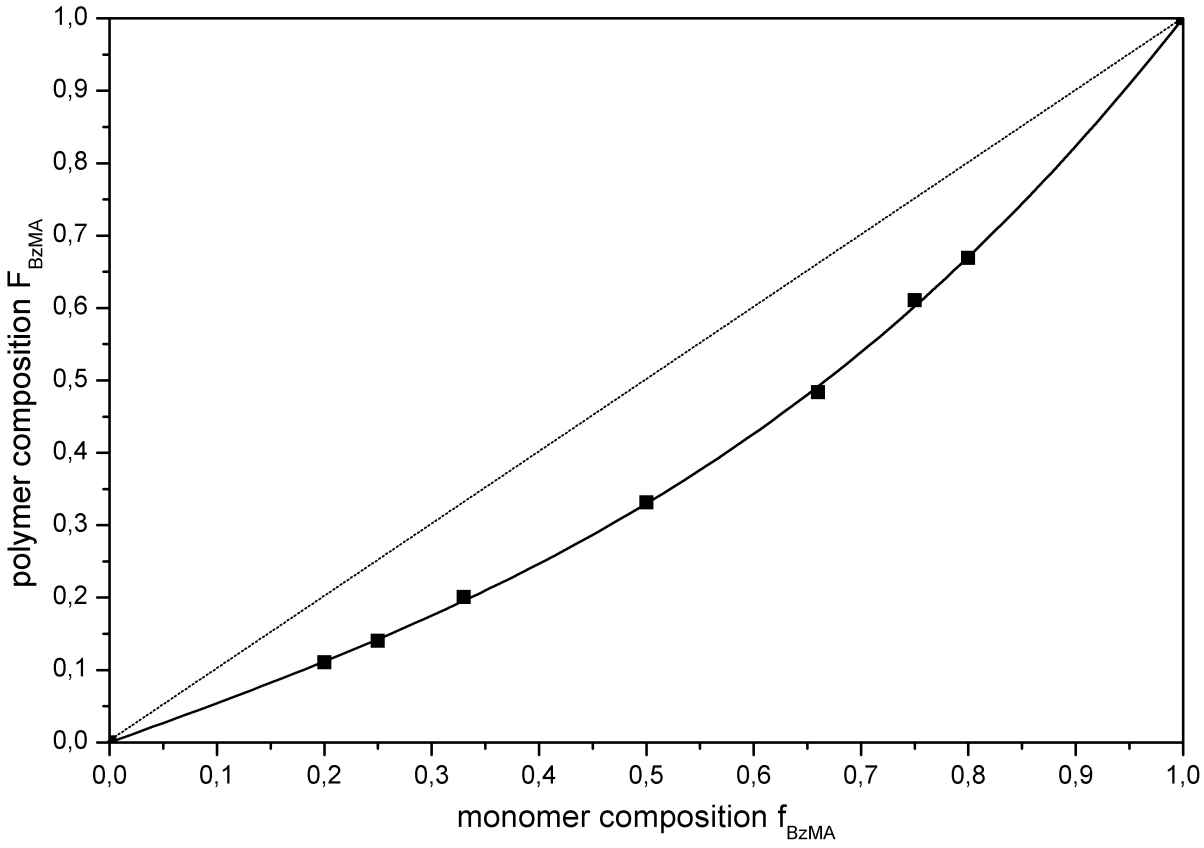

Fig. 7.9.: Copolymerization diagram for benzyl– and tert–butyl–methacrylate; dashed line for ideal random copolymerization, solid line for line of fit: $r_{BzMA} = 0.517$, $r_{tBMA} = 2.055$; compositions determinded by *Eq. 7.2.13*

Such a copolymerization diagram is described in the terminal–model by means of the *Lewis–Mayo–Equation* with one reactivity ratio larger and one reactivity ratio smaller than one. [20, 86]

$$F_1 = \frac{d[M_1]}{d[M_1] + d[M_2]} = \frac{r_1 f_1^2 + f_1 f_2}{r_1 f_1^2 + 2 f_1 f_2 + r_2 f_2^2} \tag{7.2.14}$$

with r_i = reactivity ratio, i. e. copolymerization parameter of monomer i, f_i = molar fraction of monomer i in the reaction mixture, F_i = instantaneous molar fraction of monomer i incorporated on the copolymer, $d[M_i]$ = different change of the concentration of monomer i due to a differential conversion, (1) = BzMA and (2) = tBMA

The monomer reactivity ratios were determined by a least–square fit of *Equation 7.2.14* to the data points of *Figure 7.9* to yield $r_{BzMA} = 0.517 \pm 0.02$ and $r_{tBMA} = 2.055 \pm 0.06$. A comparison of the values with literature data was not possible, since copolymerization reactivity ratios of this system have not yet been published.

Comparison of kinetic results from batch copolymerizations of nBMA/tBMA and BzMA/tBMA

In the following paragraph the results of the kinetic analysis of *Series A*, the batch copolymerizations of *n*–butyl methacrylate and *tert*–butyl methacrylate, and *Series F*, the batch copolymerizations of benzyl methacrylate and *tert*–butyl methacrylate, are compared. The values of the effective rate constants $k_{eff,i}$ of the two series are given in *Figure 7.10.*

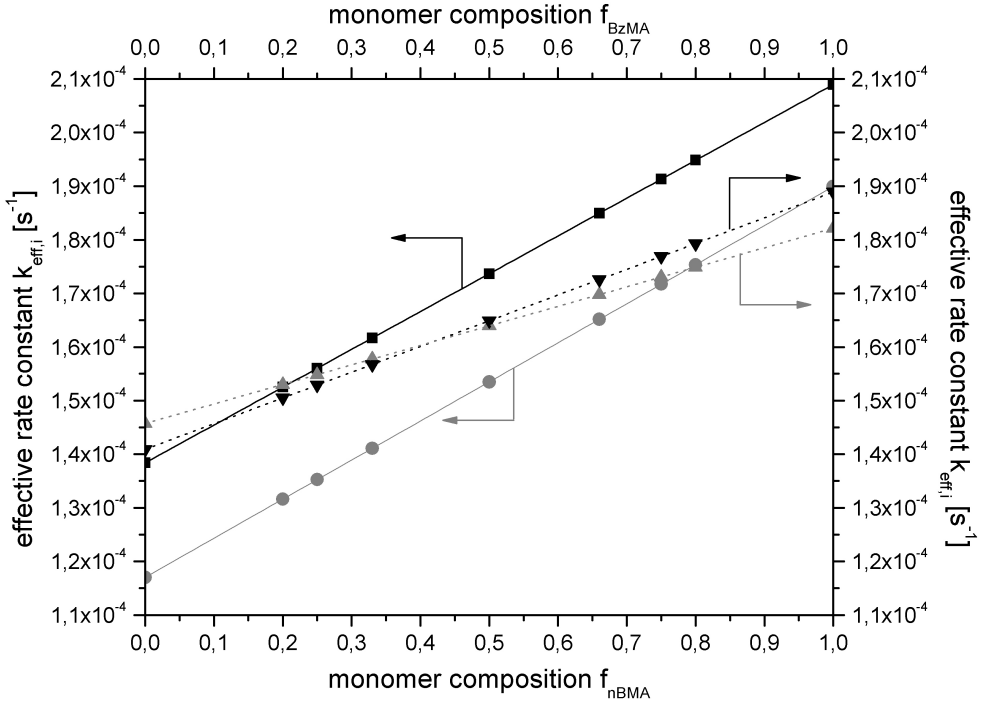

Fig. 7.10.: Comparison of the effective rate constants $k_{eff,i}$ of the batch copolymerization *Series A* (left axis, solid lines, ● nBMA, ■ tBMA) and *Series F* (right axis, dashed lines, ▲ BzMA, ▼ tBMA)

The effective rate constants $k_{eff,i}$ of the two monomers of both series laid on straight lines. For *Series A* (● nBMA, ■ tBMA), the values differed just slightly. The difference shrunk from $2.14 \cdot 10^{-5}\,s^{-1}$ at $f_{nBMA} = 0$ to $1.90 \cdot 10^{-5}\,s^{-1}$ at $f_{nBMA} = 1$. The effective rate constant values of the two monomers of *Series F* (▲ BzMA, ▼ tBMA) differed less. The average difference of the effective rate constants of *Series F* was $3.23 \cdot 10^{-6}\,s^{-1}$. The effective rate constants of $f_{tBMA} = 0$ of *Series A* was $1.38 \cdot 10^{-4}\,s^{-1}$ and also both values of *Series F* were in that region, for $f_{tBMA} = 0$ at $1.41 \cdot 10^{-4}\,s^{-1}$ and $f_{BzMA} = 0$ at $1.46 \cdot 10^{-4}\,s^{-1}$. The effective rate constant of $f_{nBMA} = 0$ was obviously lower than the three others with $1.17 \cdot 10^{-4}\,s^{-1}$. The values of $f_i = 1$ were distributed in a different way. For tBMA of *Series A* it was $2.10 \cdot 10^{-4}\,s^{-1}$ and the three other monomers gave obviously lower values, for nBMA $1.90 \cdot 10^{-4}\,s^{-1}$, for BzMA $1.82 \cdot 10^{-4}\,s^{-1}$ and for tBMA of *Series F* $1.89 \cdot 10^{-4}\,s^{-1}$. So the slops of the two monomers of *Series A* were higher than the slops of the monomers of *Series F*. Within a series the slops were relatively equal, for *Series A* at $7.18 \cdot 10^{-5}\,s^{-1}$ and for *Series F* at $4.22 \cdot 10^{-5}\,s^{-1}$.

The total effective rate constants $k_{eff}(f_i)$ of the two series are given in *Figure 7.11.*

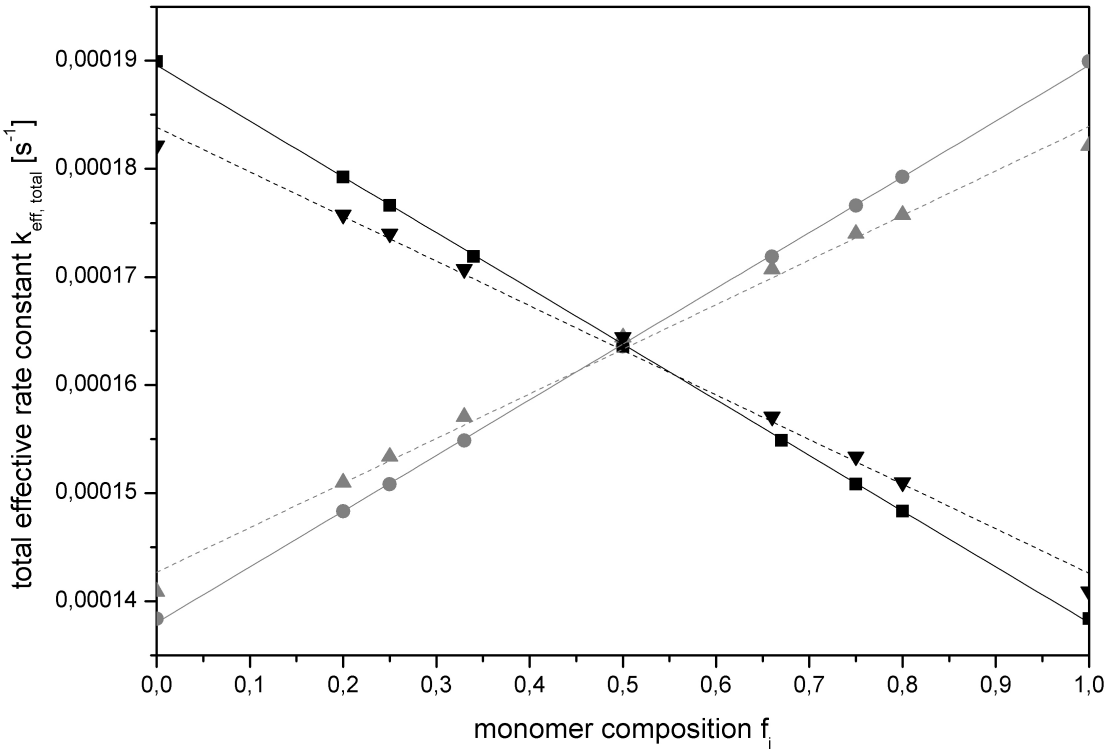

Fig. 7.11.: Comparison of total effective rate constant $k_{eff,total}$ of the batch copolymerization *Series A* (i = nBMA, solid lines, ● nBMA, ■ tBMA) and *Series F* (i = BzMA, dashed lines, ▲ BzMA, ▼ tBMA), assuming the individual monomer rate constants to vary linear over $f_i \in [0,1]$

The total effective rate constants $k_{eff}(f_i)$ of the monomers of both series laid on straight lines. The midpoint of both series for $f_i = 0.5$ was at $1.64 \cdot 10^{-4}\,s^{-1}$. For $f_i = 0$ the total effective rate constants of *Series A* were $1.38 \cdot 10^{-4}\,s^{-1}$ for nBMA (●) and $1.90 \cdot 10^{-4}\,s^{-1}$ for tBMA (■) and for *Series F* $1.41 \cdot 10^{-4}\,s^{-1}$ for BzMA (▲) and $1.82 \cdot 10^{-4}\,s^{-1}$ for tBMA (▼). The slope of *Series A* was $5.15 \cdot 10^{-5}\,s^{-1}$ for nBMA, respectively $-5.15 \cdot 10^{-5}\,s^{-1}$ for tBMA and of *Series F* the slope was $4.12 \cdot 10^{-5}\,s^{-1}$ for BzMA, respectively $-4.12 \cdot 10^{-5}\,s^{-1}$ for tBMA, so the slope of *Series A* was obviously higher than the one of *Series F.*

In *Figure 7.12* the two copolymerization diagrams are shown. The values of the compositions of the copolymers F_i of both monomer systems (*Series A* ●, *Series F* ▲) showed no obviously differences. Both copolymerization can be described in the terminal–model by means of the *Lewis–Mayo–Equation* with one reactivity ratio larger and one reactivity ratio smaller than one. The monomer reactivity ratios of *Series A* were $r_{nBMA} = 0.475 \pm 0.05$ and $r_{tBMA} = 0.886 \pm 0.05$ and of *Series F* $r_{BzMA} = 0.517 \pm 0.02$ and $r_{tBMA} = 2.055 \pm 0.06$. For *Series A* the reactivity ratios differed not strong. A distinct difference was between the values of *Series F.* The reactivity ratios of nBMA and BzMA were slightly similar. But the values of tBMA of the two systems differed very strongly.

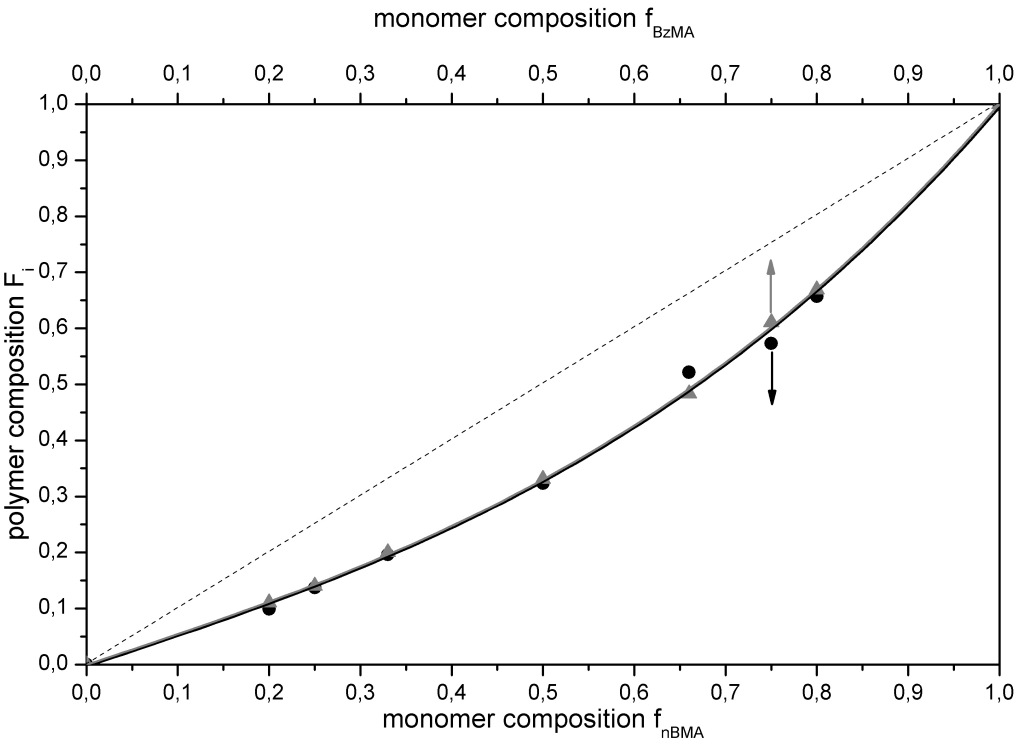

Fig. 7.12.: Comparison of copolymerization diagrams of the batch copolymerization *Series A* (i = nBMA, ●, black line) and *Series F* (i = BzMA, ▲, grey line), dashed line for ideal random copolymerization

The effective rate constants $k_{eff,i}$ and the total effective rate constants $k_{eff}(f_i)$ were in the same range for both series and the compositions of the resulting copolymers F_i of both series were nearly the same. There was a large difference between the reactivity ratios of tBMA in the two monomer system.

7.2.2. Structural Analysis

The next investigations referred to the compositional analysis of the copolymers. First the elementary analysis of all resulting copolymers of *Series F* and *Series G* is detailed. The purity and the composition of the resulting copolymers was controlled with it. The molecular formula of the *tert*–butyl methacrylate is $C_8H_{14}O_2$ (67.57 % C, 9.92 % H, 22.50 % O), the one of benzyl methacrylate $C_{11}H_{12}O_2$ (74.98 % C, 6.86 % H, 18.16 % O). The calculation of the theoretical values of the three element–contents had to be done for each member of *Series F* and *Series G* to accommodate for the different copolymer compositions. With the analysis method described in *Section 3.2.2* the content of only C and H can be measured, while the amount of O had to be calculated from the difference to 100 %. The results of the elementary analysis of *Series F* are listed in *Table 7.7* and the ones of *Series G* in *Table 7.8*. Furthermore the differences between the theoretical values and the analysis results are given. As part of the initiator–molecule pTSC in each polymer–chain one sulfur–atom occurs, however, its amount was below the detection limit of the elementary analysis device of around 2 %.

The theoretical values showed two tendencies which based on the different ratios of BzMA– and tBMA–units along the copolymer chains. The amount of carbon increased proportional to the molar fraction of BzMA inside the polymer chain and the amounts of hydrogen and oxygen decreased. The differences between theoretical values and measured values were relatively small (< 3.2 %).

Tab. 7.7.: Results of the elementary analysis of the different copolymer compositions of *Series F* with divergence from the theoretical value

Entry	F_{BzMA}		C [%]	ΔC	H [%]	ΔH	O [%]	ΔO
V88	0.00	theory	67.57		9.92		22.50	
		is	65.30	-2.27	9.54	-0.38	25.16	2.65
V86	0.11	theory	68.56		9.51		21.92	
		is	68.53	-0.03	8.93	-0.58	22.54	0.62
V84	0.15	theory	68.86		9.39		21.75	
		is	69.41	0.55	8.90	-0.49	21.69	-0.06
V82	0.19	theory	69.28		9.22		21.50	
		is	72.43	3.15	7.56	-1.66	20.02	-1.49
V81	0.33	theory	70.39		8.76		20.85	
		is	71.20	0.81	8.18	-0.58	20.62	-0.23
V83	0.48	theory	71.55		8.28		20.17	
		is	69.66	-1.89	8.65	0.36	21.70	1.53
V85	0.61	theory	72.46		7.90		19.63	
		is	73.12	0.66	7.26	-0.65	19.63	-0.01
V87	0.67	theory	72.87		7.74		19.40	
		is	72.65	-0.22	7.51	-0.23	19.84	0.44
V89	1.00	theory	74.98		6.86		18.16	
		is	73.82	-1.16	6.66	-0.21	19.52	1.36

Tab. 7.8.: Results of the elementary analysis of the different copolymer compositions of *Series G* with divergence from the theoretical value

Entry f_{BzMA}	time [min]		C [%]	ΔC	H [%]	ΔH	O [%]	ΔO
V92		theory	69.28		9.22		21.50	
0.33	60	is	70.42	1.14	8.40	-0.82	21.18	-0.32
	90		71.04	1.76	8.14	-1.08	20.82	-0.68
	120		70.63	1.35	8.42	-0.81	20.96	-0.54
	150		70.74	1.46	8.11	-1.11	21.15	-0.35
	180		70.76	1.48	8.50	-0.72	20.74	-0.76
V91		theory	70.39		8.76		20.85	
0.5	60	is	71.25	0.86	7.40	-1.37	21.36	0.50

Continuation on next page ...

Entry f_{BzMA}	time [min]		C [%]	ΔC	H [%]	ΔH	O [%]	ΔO
	90		71.65	1.26	7.68	-1.08	20.67	-0.18
	120		71.02	0.63	7.37	-1.40	21.62	0.77
	150		71.64	1.25	7.57	-1.19	20.79	-0.06
	180		71.83	1.44	7.56	-1.20	20.61	-0.24
V93		theory	71.55		8.28		20.17	
0.66	60	is	72.89	1.34	7.46	-0.82	19.65	-0.52
	90		72.66	1.11	7.45	-0.83	19.89	-0.28
	120		72.99	1.44	7.50	-0.78	19.51	-0.66
	150		73.05	1.50	7.46	-0.82	19.49	-0.68
	180		73.01	1.46	7.51	-0.77	19.48	-0.69
V94		theory	74.98		6.86		18.16	
1.00	60	is	74.88	-0.10	6.65	-0.21	18.47	0.31
	90		75.02	0.04	6.74	-0.12	18.24	0.08
	120		74.78	-0.20	6.70	-0.16	18.52	0.36
	150		74.82	-0.16	6.70	-0.16	18.48	0.32
	180		74.95	-0.03	6.74	-0.12	18.31	0.15

That implied that all samples, expect the ones of V88 and V82, were free of pollution, such as solvents etc, and that the reactions worked in the same way independent from the monomer composition. That the samples of experiment V88 and V82 exhibited higher deviations may be caused by the greater difficulty to isolate purity samples and dry the copolymers from benzyl methacrylate and *tert*–butyl methacrylate. So remainders of solvents, in particular H_2O, caused these differences. A further drying step did not improve the results. Over all the results of the elementary analysis showed that the polymers are nearly free of pollution. The differences were consistence mostly over all compositions. That means that all the reactions worked in the same way independent from the monomer composition. That was a good requirement for the semibatch polymerization where the monomer composition will change continuously during the reaction.

In a next step the copolymer compositions were calculated from the amount of carbon and hydrogen that were measured by the elementary analysis. Two calibration curves, one for each element, were constructed from the theoretical amount of the elements of the two homopolymers, see *Figure 7.13*. The linear equations of the two elements contents, depending on F_{BzMA} are given in *Equations 7.2.15* and *7.2.16*.

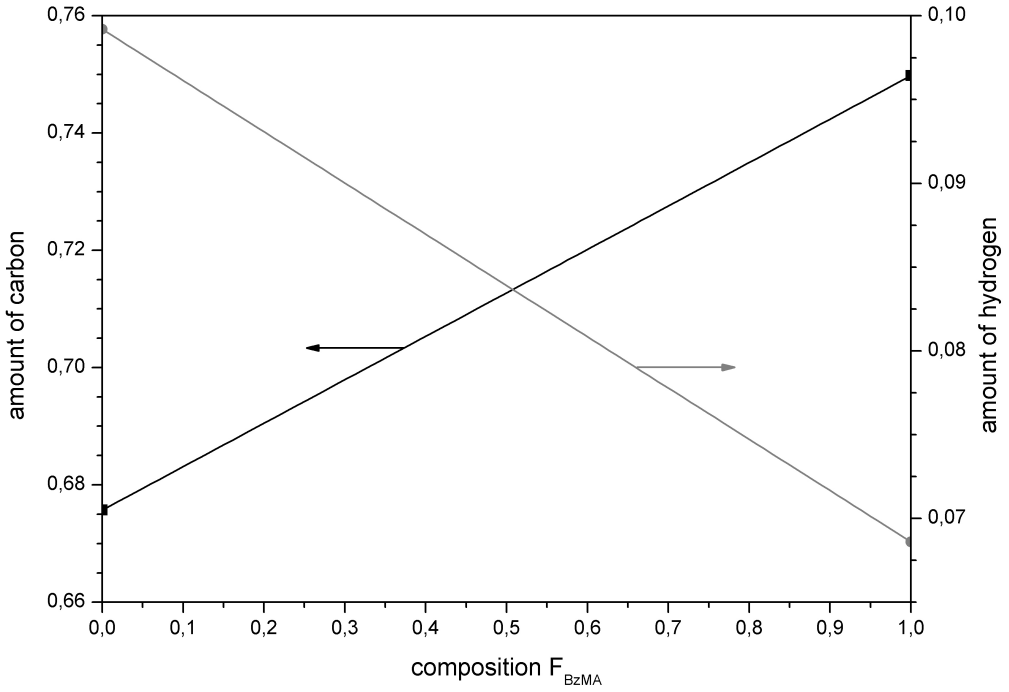

Fig. 7.13.: Calibration curves to determine F_{BzMA} from the element content of carbon (black line) and hydrogen (grey line) for P[BzMA–co–tBMA]

$$C = 0.6757 + 0.0741 \cdot F_{BzMA} \tag{7.2.15}$$

$$H = 0.0992 - 0.0306 \cdot F_{BzMA} \tag{7.2.16}$$

The equations is resolved for the composition and with the amounts of carbon, respectively hydrogen, taken from elementary analysis the compositions were calculated. The results are listed in *Tables 7.9* and *7.10*.

Tab. 7.9.: Compositions of copolymers of *Series F* resulting from ^{1}H–NMR–analysis F^{NMR}_{BzMA} and elementary analysis F^{EA}_{BzMA}

Entry	f_{BzMA}	F^{NMR}_{BzMA} [a]	$F^{EA,C}_{BzMA}$ [b]	ΔF^{C}_{BzMA} [c]	$F^{EA,H}_{BzMA}$ [d]	ΔF^{H}_{BzMA} [c]
V88	0.00	0.00	-0.31	-0.31	0.12	0.12
V86	0.20	0.11	0.13	0.02	0.32	0.21
V84	0.25	0.15	0.25	0.10	0.33	0.18
V82	0.33	0.19	0.66	0.47	0.77	0.58
V81	0.50	0.33	0.49	0.16	0.57	0.24
V83	0.66	0.48	0.28	-0.20	0.42	-0.06
V85	0.75	0.61	0.75	0.14	0.87	0.26
V87	0.85	0.67	0.69	0.02	0.79	0.12
V89	1.00	1.00	0.84	-0.16	1.07	0.07

[a] calculated from ^{1}H–NMR–spectra

[b] calculated from *Eq. 7.2.15*

[c] $\Delta F^{x}_{BzMA} = F^{EA,x}_{BzMA} - F^{NMR}_{BzMA}$; [d] calculated from *Eq. 7.2.16*

Tab. 7.10.: Compositions of copolymers of *Series G* resulting from ^{1}H–NMR–analysis F^{NMR}_{BzMA} and elementary analysis F^{EA}_{BzMA}

Entry f_{BzMA}	time [min]	F^{NMR}_{BzMA} [a]	$F^{EA,C}_{BzMA}$ [b]	ΔF^{C}_{BzMA} [c]	$F^{EA,H}_{BzMA}$ [d]	ΔF^{H}_{BzMA} [c]
V91	60	0.47	0.50	0.03	0.82	0.35
0.50	90	0.46	0.55	0.09	0.73	0.27
	120	0.48	0.47	-0.01	0.83	0.35
	150	0.48	0.55	0.07	0.77	0.29
	180	0.48	0.57	0.09	0.77	0.29
V92	60	0.27	0.38	0.11	0.50	0.23
0.33	90	0.29	0.47	0.18	0.58	0.29
	120	0.30	0.41	0.11	0.49	0.19
	150	0.38	0.43	0.05	0.59	0.21
	180	0.30	0.43	0.13	0.46	0.16
V93	60	0.63	0.72	0.09	0.80	0.17
0.66	90	0.64	0.69	0.05	0.81	0.17
	120	0.64	0.73	0.09	0.79	0.15
	150	0.64	0.74	0.10	0.80	0.16
	180	0.64	0.73	0.09	0.79	0.15
V94	60	1.00	0.99	-0.01	1.07	0.07
1.00	90	1.00	1.01	0.01	1.04	0.04
	120	1.00	0.97	-0.03	1.05	0.05
	150	1.00	0.98	-0.02	1.05	0.05
	180	1.00	1.00	0.00	1.04	0.04

[a] calculated from ^{1}H–NMR–spectra; [b] calculated from *Eq. 7.2.15*

[c] $\Delta F^{x}_{BzMA} = F^{EA,x}_{BzMA} - F^{NMR}_{BzMA}$; [d] calculated from *Eq. 7.2.16*

The compositions $F^{EA,H}_{tBMA}$ calculated from the hydrogen content differed obviously from the compositions which were determined from the ^{1}H–NMR–spectra of the precipitated copolymers for both elements carbon and hydrogen. The differences could be caused by various problems. One possibility is that there is still solvent in the sample. But the ^{1}H–NMR–spectra did not show the presence of residual solvents or considerable amounts of monomers, hence, that was not the reason for the deviations. An other possible problem could be that the samples were inhomogeneous. For a NMR–measurement 10 mg of the copolymer was used, for an EA–measurement only 2.5 mg. So the problem of an inhomogeneous substance will be increase at the elementary analysis. But the resulting copolymers were apparently consistent. A third possibility is that the pollution happened during the measurement itself. The measurement of standards in periodical intervals should avoid that.

The next kind of structural analysis was the ATR–FTIR–spectroscopy. Before the IR–spectra of the polymers were measured, the spectra of the monomers were gathered to find the characteristic vibration bands that can be used to distinguish monomers and polymer units. These spectra of benzyl methacrylate and *tert*–butyl methacrylate are shown in *Figure 7.14*. Note that the ATR–FTIR is a reflection measurement technique. The intensity of an IR–band depends on the penetration depth of the IR radiation ($\approx 0.1 \ldots 1.0 \cdot \lambda$), but not on the sample thickness as long as the measurement film in much thicker than the longest measured wavelength. [87] For the comparison purposes the spectra were normalized by setting the adsorption intensity of the vibrational band at 1134 cm^{-1} to one by dividing all intensities A_x by A_1.

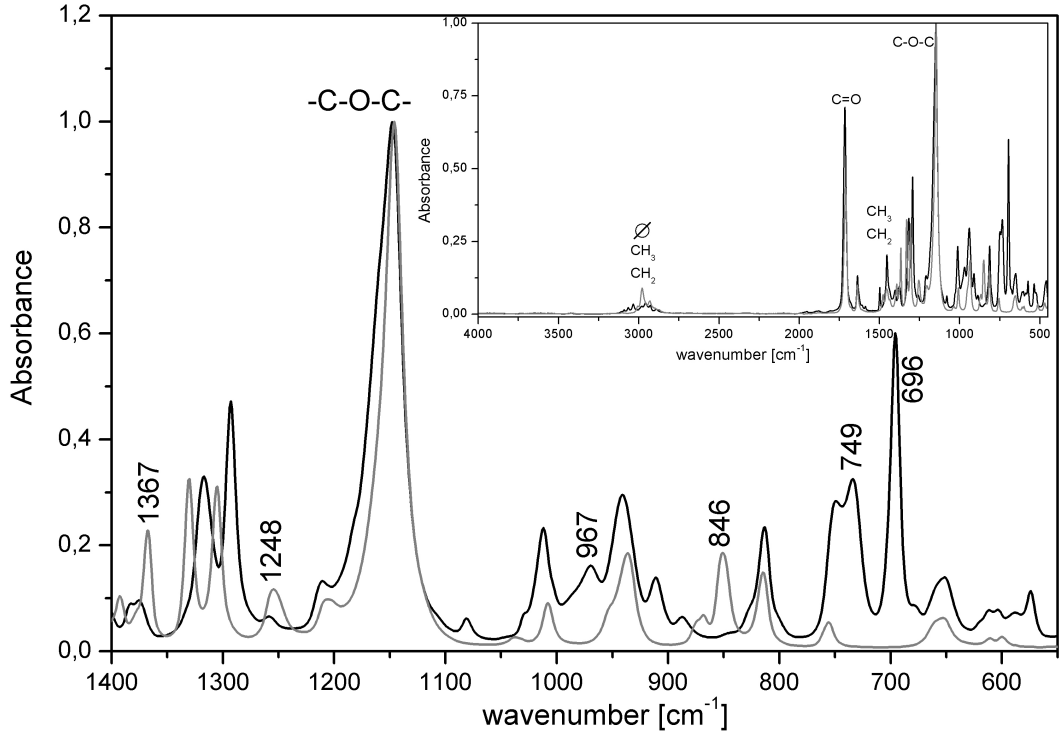

Fig. 7.14.: Finger print region of the ATR–FTIR–spectra of BzMA and tBMA (black line – BzMA, grey line – tBMA). Insert: full MIR–spectra (Spectra normalized to $A_{1134} = 1$)

In the spectra the peaks were equal for both the monomers that belonged to the methacrylate–part of the molecules. The vibrational bands of $=CH_2$, $-CH_2-$ and $-CH_3$ was found between 3125 to 2800 cm^{-1}, but the one for $=CH_2$ which was located higher than 3000 cm^{-1} was merely weak and imperceptible. The vibrational band of C=O was located at 1717 cm^{-1}, for $-CH_2-$ and $-CH_3$ at 1476 cm^{-1} and 1455 cm^{-1} and for C–O–C at 1134 cm^{-1}. These were the same vibrational bands than for the first monomer mixture of *Section 3.3.2*. The differences between the two spectra resulted from the two different ester–groups of the monomers. The broad mixed band between 3125 to 2800 cm^{-1} also contained the vibrational band of the aromatic ring of the BzMA. The benzyl–group and the *tert*–butyl–group became particularly visible between 600 cm^{-1} and 1400 cm^{-1}. tBMA showed distinct bands at 1367 cm^{-1}, 1248 cm^{-1} and 846 cm^{-1}. That were the same characteristic vibrational band than before in *Series A*.

The characteristic bands for BzMA laid at 967 cm^{-1}, 749 cm^{-1} and 796 cm^{-1}. Because these bands are within the finger print region it was not possible to assign the vibrational bands to specific vibrations of the functional groups of the molecules.

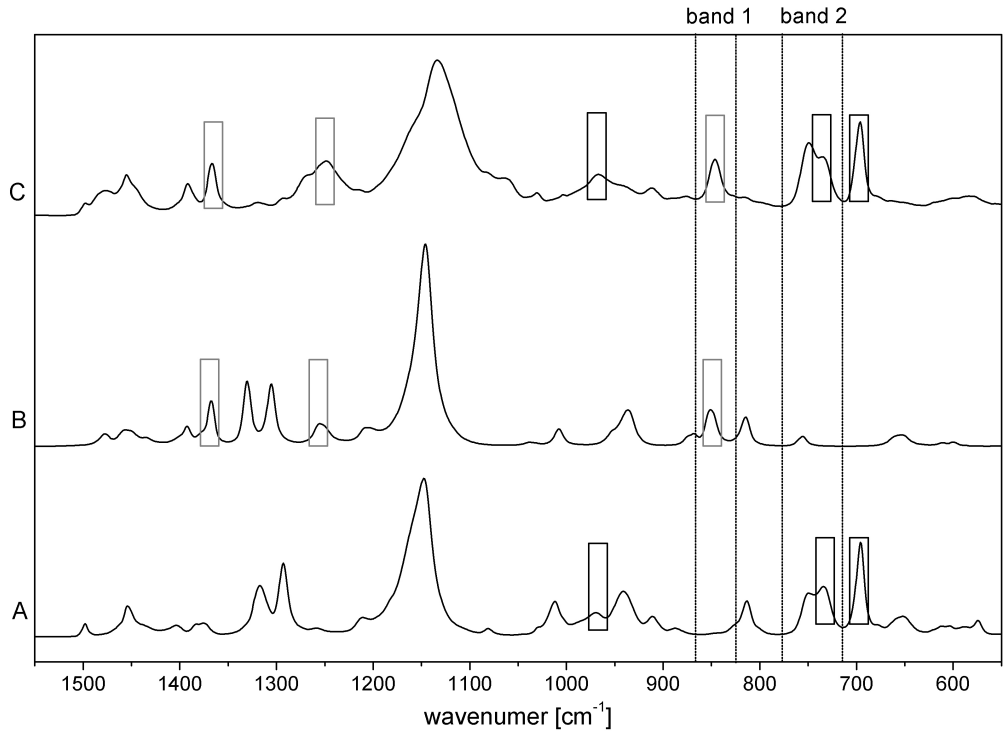

Fig. 7.15.: Comparison of the finger print region of the ATR–FTIR–spectra of A – BzMA, B – tBMA and C – experiment V81 (F_{BzMA} = 0.33); □ – BzMA specific bands, □ – tBMA specific bands; analyzed bands were marked with dashed lines (Spectra normalized to A_{1134} = 1)

The IR–spectrum of the statistic copolymer of experiment V81 (F_{BzMA} = 0.33) from *Series F*, containing both the benzyl– and the *tert*–butyl–ester groups is given in *Figure 7.15* together with the spectra of the two monomers to work out the differences between the copolymers and the two monomers. The three vibrational bands that were characteristic for BzMA and also the three bands for tBMA were marked there in the spectra of the polymer and the corresponding monomer–spectra. However, several bands in each monomer spectra did not have corresponding bands in the polymer spectrum. They were at 815 cm^{-1} and 1010 cm^{-1} in both monomer spectra, at 1290 cm^{-1} and 1320 cm^{-1} in the BzMA spectrum and at 1305 cm^{-1} and 1330 cm^{-1} in the tBMA spectrum. In the polymer spectrum were no bands in the region between 1290 cm^{-1} and 1350 cm^{-1}. Hence that bands resulted from the vibration of $=CH_2$. [87]

The band at 850 cm^{-1} (*band 1*) characteristic for tBMA and the one at 730 cm^{-1} (*band 2*) caused by BzMA were most suited for the investigation of the copolymer compositions. They were clearly separated and could be investigated well in view to peak area (PA) and peak height (PH). In *Figure 7.16* these two vibrational bands of the IR–spectra of the different copolymers from *Series F* are compared. It was recognizable that with the change in copolymer composition the peak area and the peak height changed. *Band 1* is a characteristic band

from tBMA and with the rise of the amount of *tert*–butyl–group in the copolymer chain also the band intensity increased. Conversely, the intensity of *band 2* which is characteristic for the benzyl–group decreased. To show that behaviors more precisely the peak area and the peak height of the two bands were determined and then the composition of the samples, taken from analysis of ^{1}H–NMR–spectra, was plotted against the peak area and the peak height. This is depicted in *Figure 7.17* and further the values are listed in *Table 7.11.*

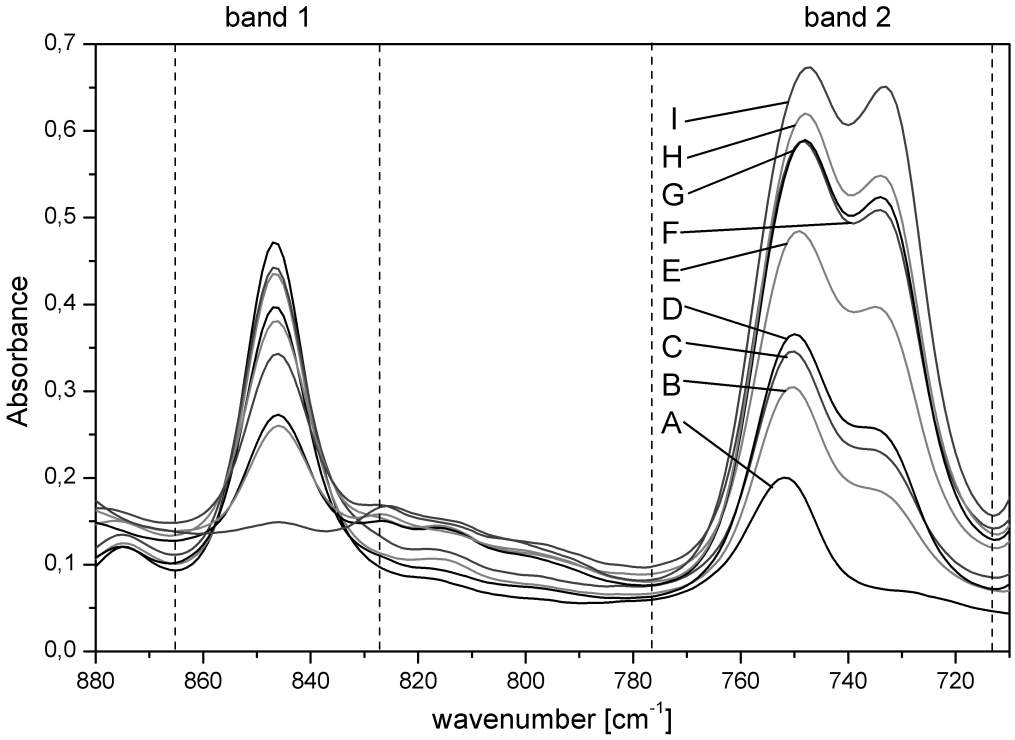

Fig. 7.16.: Analyzed section of the ATR–FTIR–spectra of the different copolymer compositions of P[tBMA–co–BzMA]; A – F_{BzMA} = 0.00, B – F_{BzMA} = 0.11, C – F_{BzMA} = 0.15, D – F_{BzMA} = 0.19, E – F_{BzMA} = 0.33, F – F_{BzMA} = 0.48, G – F_{BzMA} = 0.61, H – F_{BzMA} = 0.67, I – F_{BzMA} = 1.00 (Spectra normalized to A_{1134} = 1)

Tab. 7.11.: Peak area and peak height of the analyzed ATR–FTIR–bands of *Series F*

		band 1		*band 2*	
Entry	F_{BzMA}[a]	peak area [cm^{-1}]	peak height	peak area [cm^{-1}]	peak height
V88	0.00	5.72	0.386	2.91	0.147
V86	0.11	5.61	0.343	5.76	0.237
V84	0.15	5.80	0.339	6.72	0.267
V82	0.19	5.00	0.305	7.91	0.300
V81	0.33	4.98	0.258	10.89	0.383
V83	0.48	4.24	0.207	13.89	0.471
V85	0.61	3.77	0.157	14.62	0.490
V87	0.67	3.31	0.136	15.27	0.515
V89	1.00	2.09	0.055	17.82	0.557

[a] calculated from ^{1}H–NMR–spectra

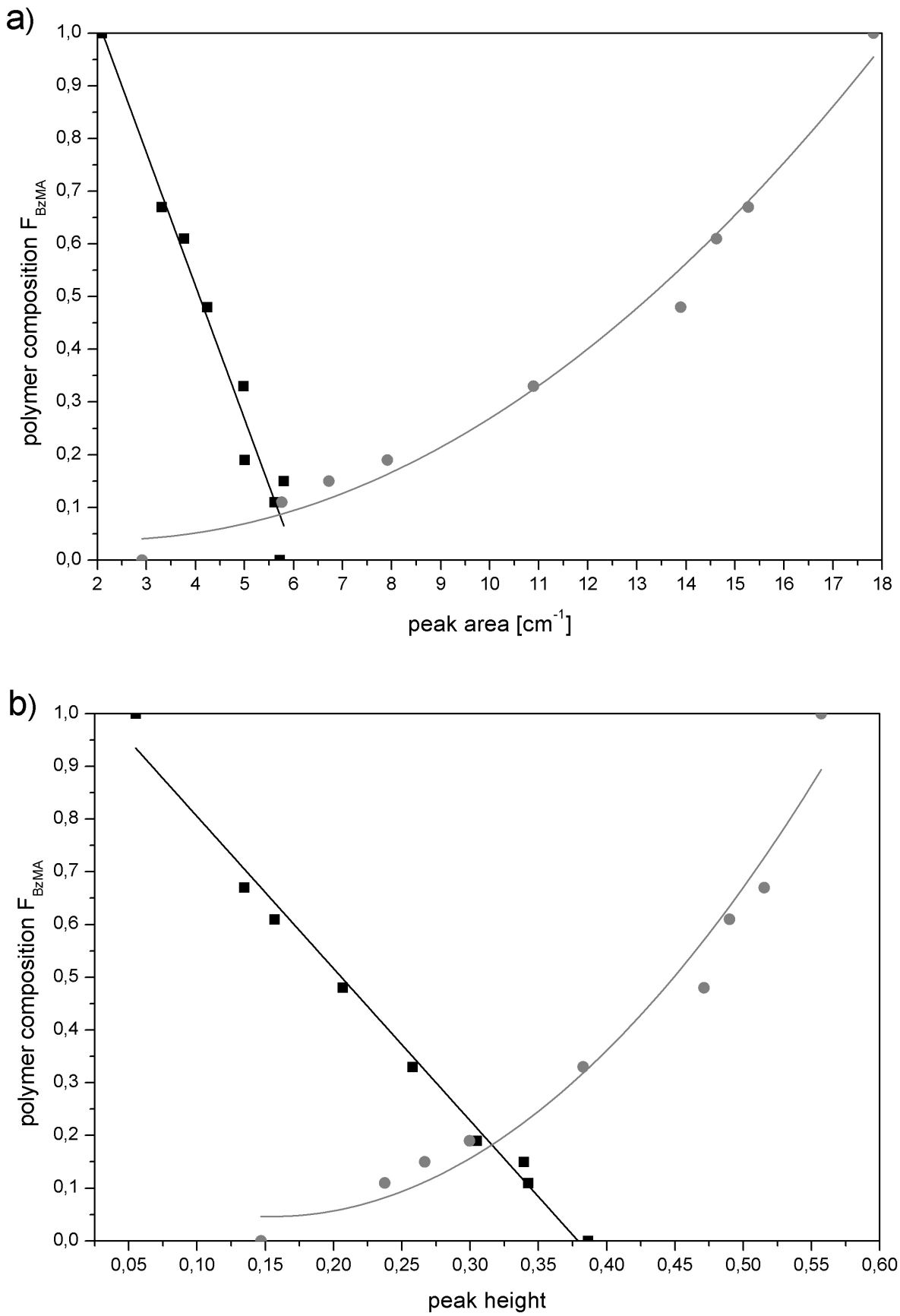

Fig. 7.17.: ATR–FTIR calibration curves, relating the composition of the copolymers P[BzMA–co–tBMA] of *Series F* to a) peak area and b) peak height of *band 1* (850 cm^{-1}, ■) and *band 2* (730 cm^{-1}, ●)

All values, peak area and peak height of both vibrational bands, changed with the change of copolymer composition F_{BzMA}. The mentioned decrease of *band 1* and the increase of *band 2* is reflected by the *Equations 7.2.17 to 7.2.20*.

$$\begin{aligned} F_{BzMA}(PA_1) &= (1.532 \pm 0.079)\,cm^{-1} \\ &\quad - (0.253 \pm 0.017)\,cm^{-1} \cdot PA_1 \end{aligned} \tag{7.2.17}$$

$$\begin{aligned} F_{BzMA}(PA_2) &= (0.055 \pm 0.076)\,cm^{-1} \\ &\quad - (0.0158 \pm 0.017)\,cm^{-1} \cdot PA_2 + (0.004 \pm 0.001)\,cm^{-1} \cdot PA_2^2 \end{aligned} \tag{7.2.18}$$

$$\begin{aligned} F_{BzMA}(PH_1) &= (1.093 \pm 0.031) \\ &\quad - (2.885 \pm 0.116) \cdot PH_1 \end{aligned} \tag{7.2.19}$$

$$\begin{aligned} F_{BzMA}(PH_2) &= (0.171 \pm 0.192) \\ &\quad - (1.618 \pm 1.173) \cdot PH_2 + (5.233 \pm 1.610) \cdot PH_2^2 \end{aligned} \tag{7.2.20}$$

With the copolymer system nBMA/tBMA the fitting of the peak height of vibrational bands worked better than the peak area fits (see *Figure 3.13*). Here, with *Series F* (tBMA/BzMA), no greater difference between the error–estimations of the peak area– and the peak height–fits was found. Hence, both values were qualified for the use as calibration curve to determine the composition of the copolymers. This monomer system can be analyzed quantitatively by means of ATR–FTIR spectroscopy. Because peak height measurement is the classical way of IR–analysis, and because of the comparability with *Series A*, the peak height method will be used to build the calibration curve.

7.2.3. Molecular Weight Characterization

The investigation procedure of the resulting copolymers from benzyl methacrylate and *tert*–butyl methacrylate was the same as for the first monomer mixture with *n*– and *tert*–butyl methacrylate, cf. *Section 3.3.3*. So after the investigation of the kinetic and the structure, the resulting polymers were also investigated with size exclusion chromatography.

In common with *Series A* and *Series B* the experiments of *Series F* were repeated in larger batches, *Series G* (cf. *Section 7.1.2*), to allow for sampling of sufficient larger quantities to obtain enough polymer per sample for a SEC analysis. On one hand that was done for the verification of the polymerization control and on the other hand to find out how the molar mass growth during the polymerization via the samples from *Series G*. The control of the polymerization can be judged by the polydispersity of the polymer, because the lower the PDI the better the control. With a perfect control over the reaction the PDI would be $1 + \frac{1}{x_1}$. [41] During the polymerization the first sample was taken after one hour because at earlier times the conversion was not sufficiently high to support the analysis. Other samples were taken every 30 min up to 3 hours. The procedure of sampling and work–up was also the same

as described with *Series B*, *Section 3.1.2*, to maintain the comparability of the two systems.

Figure 7.18 shows the elution diagrams (RI–signals) of the samples from batch copolymerization V93. With growing reaction time the peaks of the elution diagrams became shifted to lower elution volumes, from 27.9 to 26.7 ml. Hence, the molar mass of the copolymers became larger during the course of the reaction. All the GPC–analysis of the samples of *Series G* showed this behavior. In view to the growth of the molar mass all the entries of *Series G* worked well and just like *Series B*, cf. *Section 3.3.3*. The RI–signals also demonstrated the absence of side reactions over the course of reaction, due to the lack of multimodality and front- or back–tailing effects.

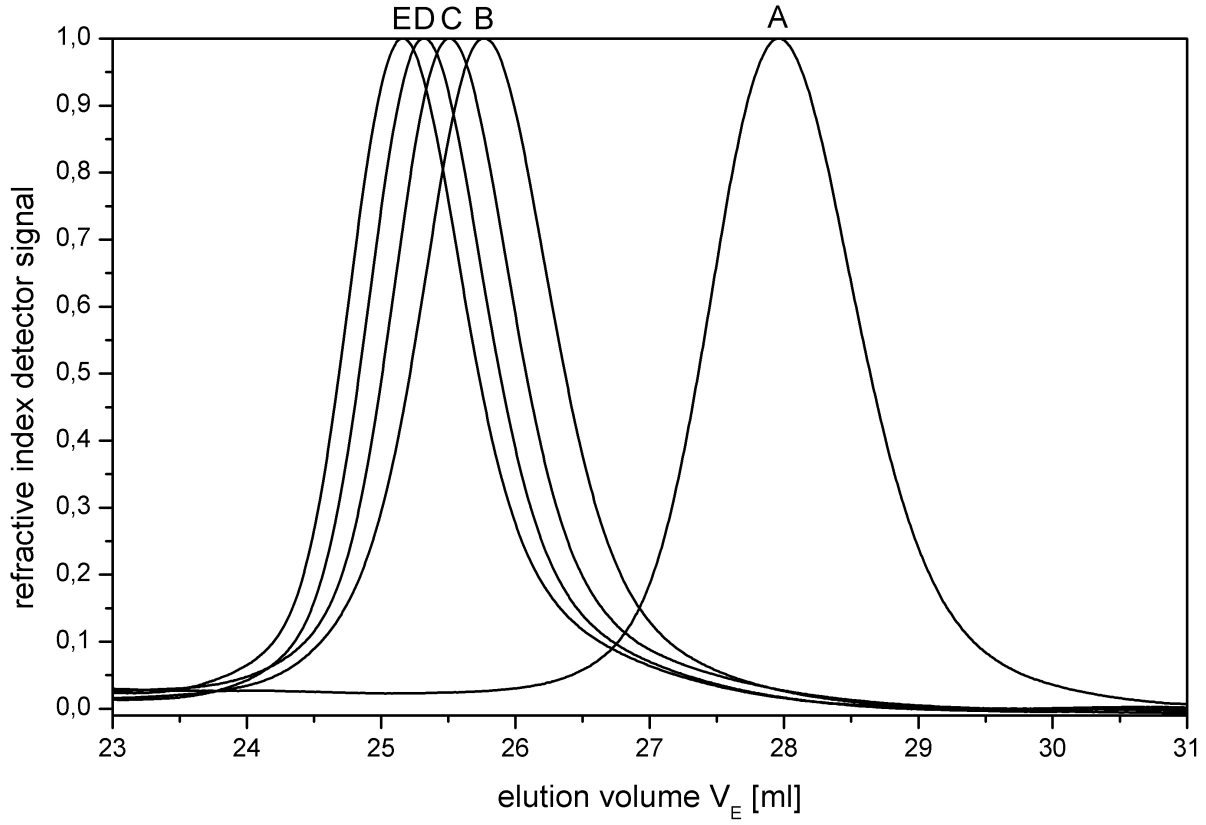

Fig. 7.18.: SEC elution diagrams of the samples of batch copolymerization V93 ($f_{BzMA} = 0.66$) at reaction times of A – 60 min, B – 90 min, C – 120 min, D – 150 min, E – 180 min

The calibration curve arising from narrow distributed linear polystyrene standards (see *Equation 3.3.22*) was used together with the the maximum elution–volume of the RI–elution curve for the determination of the relative molar masses of the copolymers. The molar masses rose linear from 16420 to 30130 $g \cdot mol^{-1}$ during the polymerization. The results of the calculations are listed in *Table 7.15*. Because of the fact that only one point of the RI–peak the maximum elution–volume was used for the determination of the relative molar mass the results only reflected just one part of the sample. Therefore the absolute molar masses of the samples were also determined.

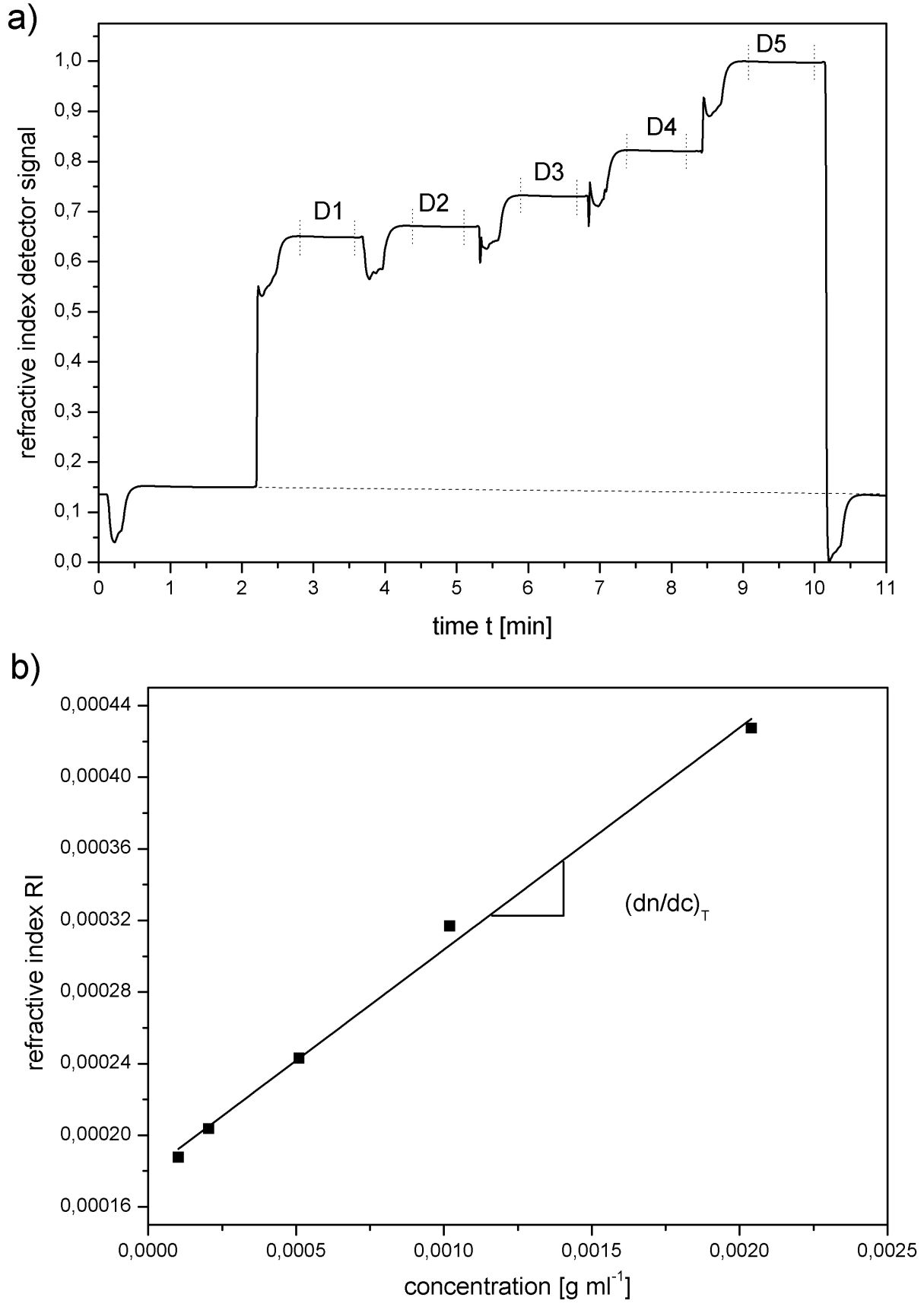

Fig. 7.19.: Refractive index increment of polymer V82 (F_{BzMA} = 0.2); a) elution diagram of solutions D1 – 0.1 mg · ml^{-1}, D2 – 0.2 mg · ml^{-1}, D3 – 0.5 mg · ml^{-1}, D4 – 1.0 mg · ml^{-1}, D5 – 2.0 mg · ml^{-1} (dashed vertical lines) and THF – baseline (dashed horizontal line); b) determination of dn/dc – concentrations against refractive index (dn/dc = 0.1246 ± 0.0025 g · mol^{-1}); in THF at 25 °C

As described in *Section 3.3.3* for the determination of the absolute molar masses of the samples by means of static light scattering first the differential refractive index increment (dn/dc) of the resulting polymers from *Series G* must be measured, see *Section 2.4*. Moreover a correlation between polymer composition and dn/dc in THF as solvent at 25 °C was investigated.

Five different concentrations of each copolymer (V81 to V89) were injected one after another; before and after the polymer solution pure THF was injected. Then the gathered diagram was analyzed. First a baseline between the solvent levels was drawn and the regions of the different concentrations were marked. An example of such a time/n–diagram obtained from the copolymer V82 is depicted in *Figure 7.19a*. The five obtained refractive indices $n(c_i)$ of the concentration series were plotted against the concentrations c_i (see *Figure 7.19b*).

The measured refractive indices of the polymer solutions fairly laid on a straight line of positive slope. The slope of the fitted linear function is the differential refractive index increment dn/dc of copolymer V82 in THF at 25 °C. The other copolymers of *Series F* were investigated in an analogous way. The measured differential refractive index increments of the copolymers are summarized in *Table 7.12* while *Figure 7.20* depicts a plot of the dn/dc versus the molar fraction of BzMA (F_{BzMA}) in the respective substance. There was a rough tendency between the copolymer composition and the dn/dc of the polymer. With rise of the amount of BzMA inside the polymer chain the values of dn/dc also increased. The values changed from 0.0695 to 0.1351 $ml \cdot g^{-1}$. Up to a composition of $F_{BzMA} = 0.5$ the gain was higher ($\sim 0.59 = \Delta[dn/dc]$) than from F_{BzMA} 0.5 to 1.0 ($\sim 0.03 = \Delta[dn/dc]$). Literature values of the dn/dc for PBzMA or PtBMA in THF at 25 °C were not available.

Tab. 7.12.: Differential refractive index increment dn/dc of the different copolymer compositions of *Series F*

Entry	F_{BzMA}	dn/dc [$ml \cdot g^{-1}$]
V88	0.00	0.0612 ± 0.0019
V86	0.11	0.0814 ± 0.0050
V84	0.15	0.0873 ± 0.0016
V82	0.19	0.1246 ± 0.0025
V81	0.33	0.1135 ± 0.0025
V83	0.48	0.1059 ± 0.0050
V85	0.61	0.1207 ± 0.0022
V87	0.66	0.1198 ± 0.0019
V89	1.00	0.1351 ± 0.0028

The measured dn/dc values of P[BzMA–co–tBMA] copolymers in THF were used to analyze the molecular weight distributions and to determine the absolute molar masses of the BzMA/tBMA copolymers of *Series F* and *G* (batch copolymerization, cf. *Section 7.1.2*) by means of online MALS during SEC characterization.

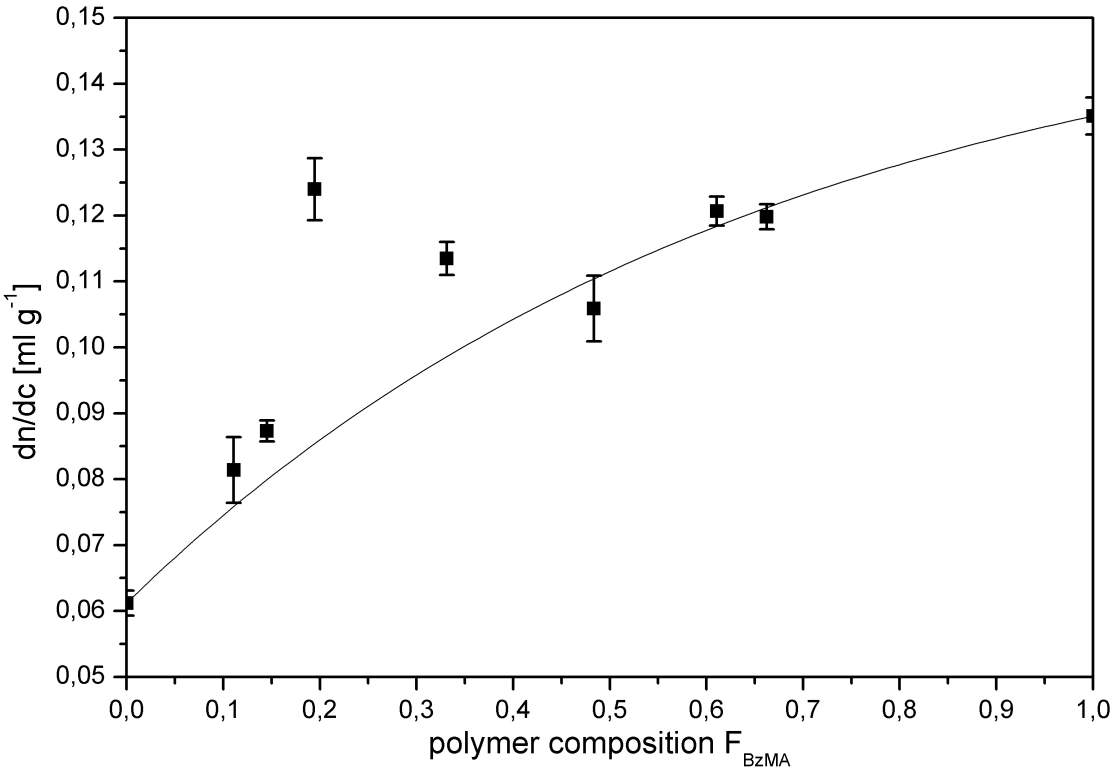

Fig. 7.20.: Plot of the measured differential refractive index increments dn/dc of the solutions of P[BzMA–co–tBMA] copolymers (Polymers of *Series F*, cf. *Table 7.1*, THF, 25 °C)

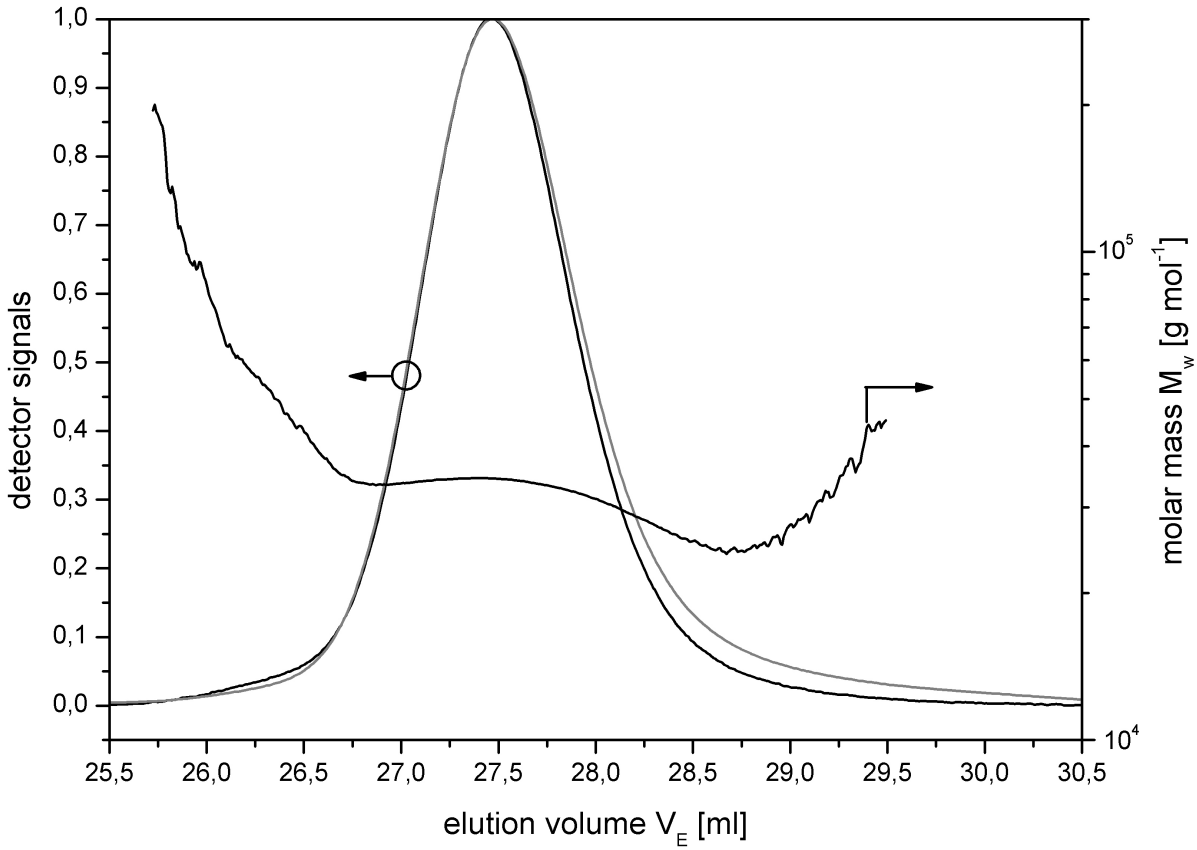

Fig. 7.21.: SEC elution diagrams and molar masses of experiment V85 (F_{BzMA} = 0.61); black curve – light scattering signal, grey curve – refractive index signal

Figure 7.21 depicts the RI– and the 90°–MALS–detector signals of the elution–diagram of P[BzMA–co–tBMA] copolymer V85 (F_{BzMA} = 0.61). The signals were analyzed in the same way as before the data from the SEC analysis of *Series A* and *Series B*, cf. *Section 3.3.3*. From the angle dependence of the scattered light intensity and the known dn/dc–value of dn/dc = 0.1207 ml · g^{-1} (cf. *Table 7.12*) the absolute molecular weight of a fraction at a given elution volume can be derived (cf. *Section 2.4*). The calculated molecular weights are shown in *Figure 7.21* (right axis). Since the RI–signal is proportional to the weight fraction of the eluted polymer, the complete molecular weight distribution (MWD) of the measured polymer can be obtained. Both detector signals were also monomodal without fronting and tailing. This result was also a repetition of the results from the first monomer mixture. From the MWD the molecular weight averages (M_n, M_w, M_z) and the polydispersity indices M_w/M_n respectively M_z/M_n was calculated. The obtained values are detailed in *Table 7.13* for *Series F* and in *Table 7.14* for *Series G*.

Tab. 7.13.: SEC results of the different copolymer-compositions of *Series F*

Entry	F_{BzMA}	M_n [g · mol^{-1}]	M_w [g · mol^{-1}]	M_z [g · mol^{-1}]	M_w/M_n	M_z/M_n
V88	0.00	30820 ± 616	31620 ± 949	33570 ± 4364	1.026 ± 0.0308	1.089 ± 0.1416
V86	0.11	33510 ± 235	34590 ± 138	35730 ± 357	1.032 ± 0.0083	1.066 ± 0.0107
V84	0.15	33050 ± 331	35990 ± 180	37900 ± 758	1.089 ± 0.0109	1.147 ± 0.0229
V82	0.19	36600 ± 256	38980 ± 156	40570 ± 406	1.065 ± 0.0085	1.109 ± 0.0111
V81	0.33	30880 ± 278	31570 ± 221	32300 ± 323	1.022 ± 0.0102	1.046 ± 0.0209
V83	0.48	34250 ± 343	36520 ± 292	38170 ± 763	1.066 ± 0.0213	1.115 ± 0.0223
V85	0.61	33020 ± 198	33580 ± 201	34590 ± 692	1.017 ± 0.0092	1.048 ± 0.0210
V87	0.66	49870 ± 150	54050 ± 108	57090 ± 171	1.084 ± 0.0033	1.145 ± 0.0046
V89	1.00	52840 ± 159	55960 ± 112	59460 ± 297	1.059 ± 0.0042	1.125 ± 0.0068

Tab. 7.14.: SEC results of the different copolymer-compositions of *Series G*

Entry f_{BzMA}	time [min]	M_n [g · mol^{-1}]	M_w [g · mol^{-1}]	M_z [g · mol^{-1}]	M_w/M_n	M_z/M_n
V92	60	14370 ±144	14890 ±134	15380 ±308	1.036 ±0.0104	1.070 ±0.0214
0.33	90	21570 ±194	22920 ±138	27150 ±543	1.063 ±0.0106	1.259 ±0.0252
	120	23870 ±239	24930 ±199	27800 ±556	1.045 ±0.0105	1.165 ±0.0350
	150	26530 ±265	28010 ±224	35210 ±1056	1.056 ±0.0106	1.327 ±0.0398
	180	26940 ±269	29200 ±146	31720 ±317	1.084 ±0.0108	1.177 ±0.0235
V91	60	23050 ±184	27080 ±162	34890 ±349	1.175 ±0.0118	1.513 ±0.0303
0.5	90	28140 ±141	31990 ±64	37060 ±148	1.137 ±0.0068	1.317 ±0.0092
	120	30060 ±301	35430 ±354	69970 ±3499	1.179 ±0.0236	2.328 ±0.1164
	150	33070 ±331	35190 ±704	39140 ±2740	1.064 ±0.0213	1.183 ±0.0828

Continuation on next page ...

Entry f_{BzMA}	time [min]	M_n [$g \cdot mol^{-1}$]	M_w [$g \cdot mol^{-1}$]	M_z [$g \cdot mol^{-1}$]	M_w/M_n	M_z/M_n
	180	32580 ±652	35380 ±354	38030 ±1521	1.086 ±0.0326	1.167 ±0.0467
V93	60	23960 ±144	25330 ±152	26750 ±268	1.057 ±0.0095	1.116 ±0.0223
0.66	90	33740 ±270	36320 ±218	39690 ±794	1.076 ±0.0108	1.176 ±0.0235
	120	37530 ±375	40710 ±204	44340 ±443	1.085 ±0.0109	1.181 ±0.0236
	150	41910 ±293	45130 ±181	49570 ±496	1.077 ±0.0086	1.183 ±0.0118
	180	44070 ±353	47850 ±191	51880 ±415	1.085 ±0.0098	1.177 ±0.0118
V99	60	32090 ±225	34970 ±105	37600 ±301	1.090 ±0.0087	1.172 ±0.0117
1.0	90	40710 ±122	42740 ±128	45270 ±272	1.500 ±0.0060	1.112 ±0.0078
	120	44560 ±134	48690 ±97	53120 ±319	1.093 ±0.0044	1.192 ±0.0083
	150	47230 ±142	51550 ±103	55710 ±223	1.091 ±0.0044	1.180 ±0.0059
	180	47400 ±190	53330 ±160	58280 ±408	1.125 ±0.0056	1.230 ±0.0098

For experiment V93 (f_{nBMA} = 0.66) the results of the absolute molar mass determination are depicted against the reaction time in *Figure 7.22a*. The molar mass grew linear at the beginning and reached 25330 $g \cdot mol^{-1}$ after 60 min, but with times the growth curve attended and at the end the molar mass was 47850 $g \cdot mol^{-1}$. Hence, the growth of the molar mass followed a bounded growth $M \approx M_\infty(1 - e^{-kt})$. *Figure 3.19b* shows the linear dependence of the molar mass M_w of the samples to the conversion p. In *Section 7.2.1* it was shown that $t \to 0 : -\ln(1 - p) = k_1 \cdot t$ applied to the reaction kinetic and in this section it was displayed that $t \to \infty : M = k_2 \cdot p$ applied to the molar mass progress. These rules were valid for controlled reactions without termination reactions.

Tab. 7.15.: Comparison of relative* and absolute molar masses of experiment V93 (f_{nBMA} = 0.66)

time [min]	V_E [ml]	relative M* [$g \cdot mol^{-1}$]	absolute M [$g \cdot mol^{-1}$]	ΔM [$g \cdot mol^{-1}$]	[%]
60	27.90	16420	25330	8915	35.19
90	27.32	22040	36320	14278	39.31
120	27.07	24990	40710	15716	38.61
150	26.86	37780	45130	17354	38.45
180	26.70	30130	47850	17718	37.03

* calibrated against PS–Standard

The measured absolute molar masses were all larger than the relative peak masses. For experiment V93 the values are compared in *Table 7.15*. With the increase of the reaction time also the difference between the relative and the absolute molar mass increased, from ΔM of 8915 to 17718 $g \cdot mol^{-1}$. The variance depended on the different approach of the determination methods.

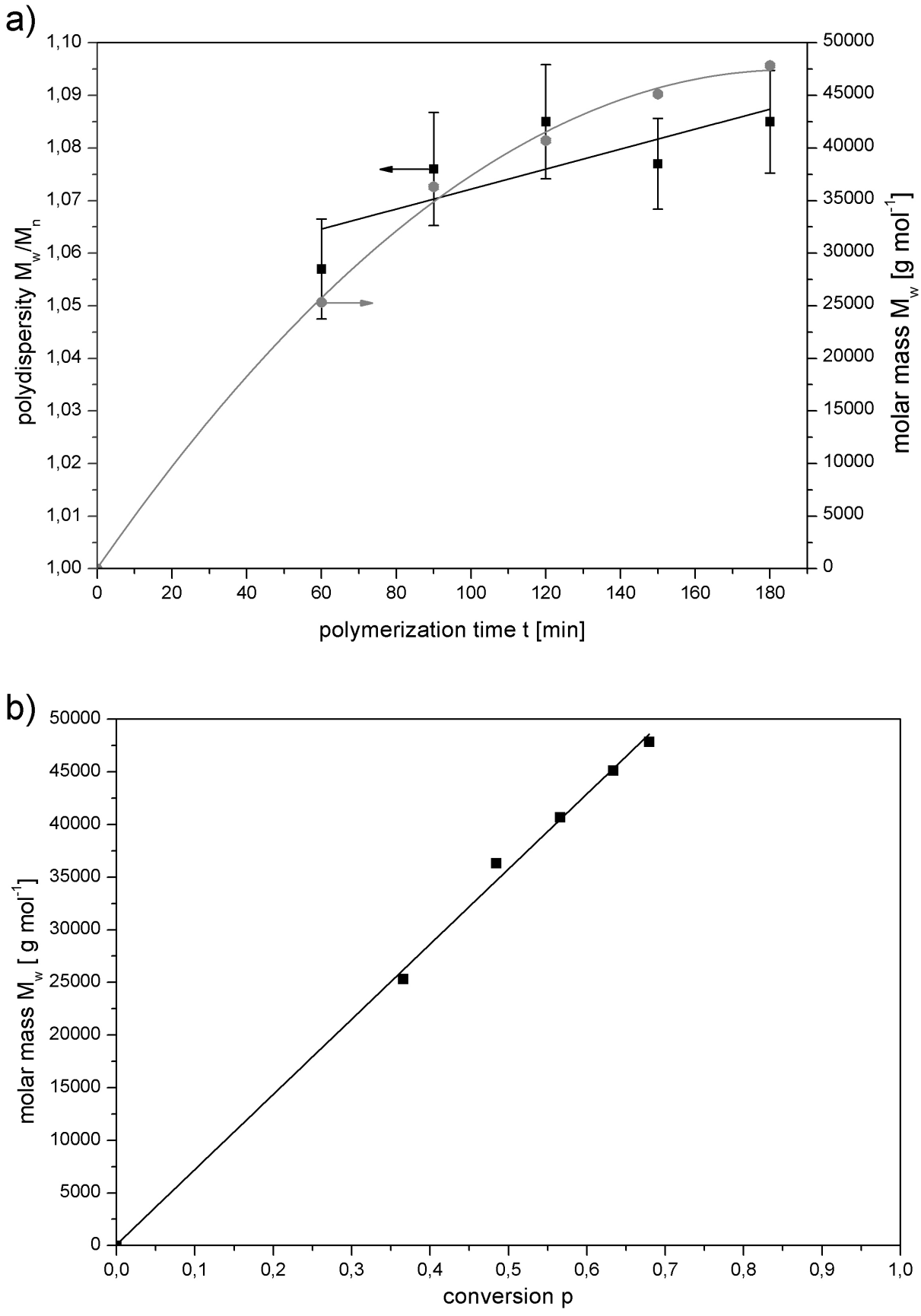

Fig. 7.22.: a) Polydispersities M_w/M_n and molar masses M_n of batch copolymer V93 (f_{BzMA} = 0.66) against polymerization time t; ■ polydispersity M_w/M_n, ● molar mass M_w; b) molar masses M_n of batch copolymer V93 (f_{BzMA} = 0.66) against conversion p

For the determination of the relative molar mass only the maximum elution volume of the RI–curve is used, that means only one point of the whole measurement. The absolute molar mass is determined from the complete database of the measurement and displays the molecular weight distribution of the whole sample.

Figure 7.23 shows the dependence of M_n and PDI on the copolymer composition. The molecular weight (M_n) was fairly independent of the used copolymer composition ($M_n \approx 38800\,g \cdot mol^{-1}$), although the masses scattered considerably. The polydispersity of the samples was low (PDI = 1.02 . . . 1.09) and also independent of the copolymer composition. As with the results of the elementary analysis it was shown that the monomer composition of the reaction had no influence on the resulting copolymer.

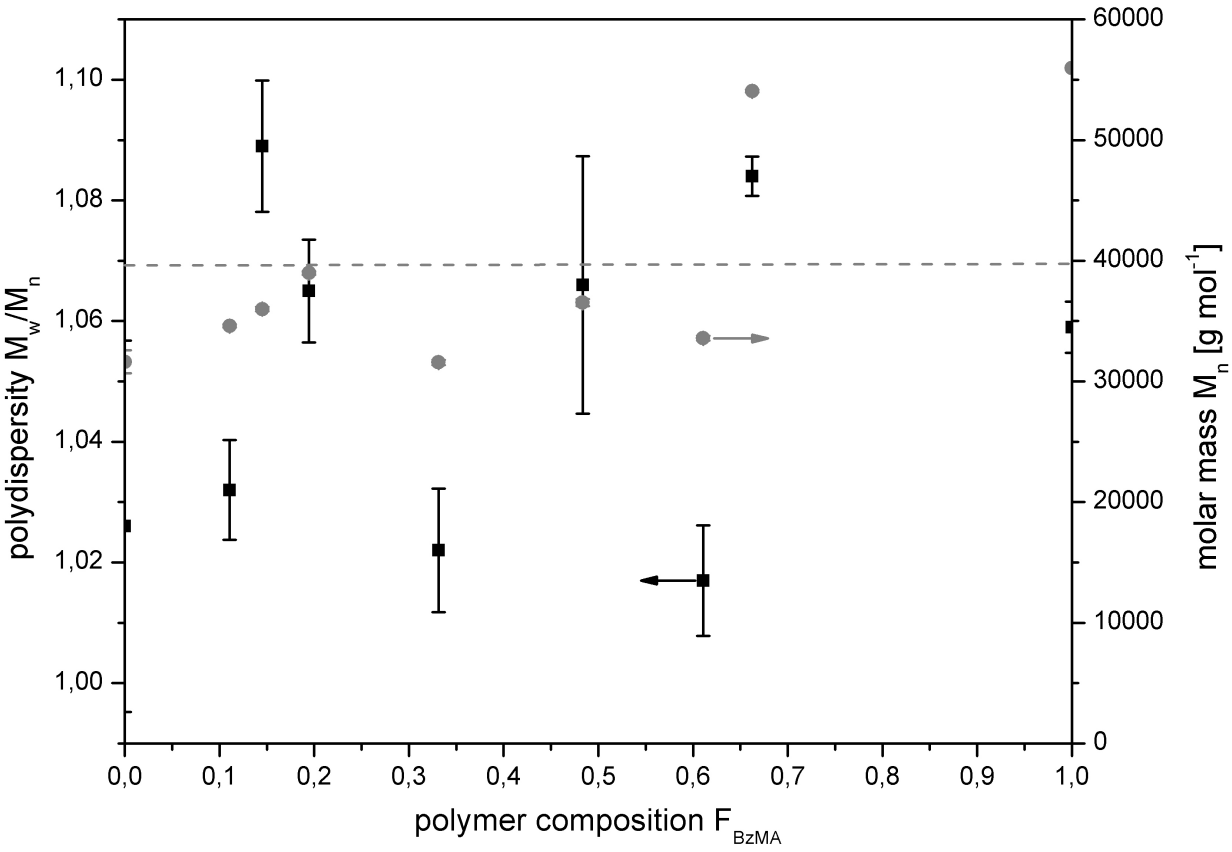

Fig. 7.23.: Polydispersities M_w/M_n and molar masses M_n of *Series F* P[BzMA–co–tBMA]–copolymers; ■ polydispersity M_w/M_n and ● molar mass M_n, dashed line – average molar mass

Comparison of molecular weight characterizations from batch copolymerizations of nBMA/tBMA and BzMA/tBMA

In the next paragraph the results of the SEC analysis of *Series A* and *Series F* are compared to work out the similarities and the differences of the two monomer mixtures. The resulting molar masses M_n of the final copolymers of *Series A* and *Series F* are given in *Figure 7.25* and the polydispersities PDI in *Figure 7.27*.

The dn/dc values of *Series A* and *Series F* are compared in *Figure 7.24*. The values of *Series A* were all lower than the one of *Series F*. The progression of the values from *Series F* were slightly more consistent than the one of *Series A*.

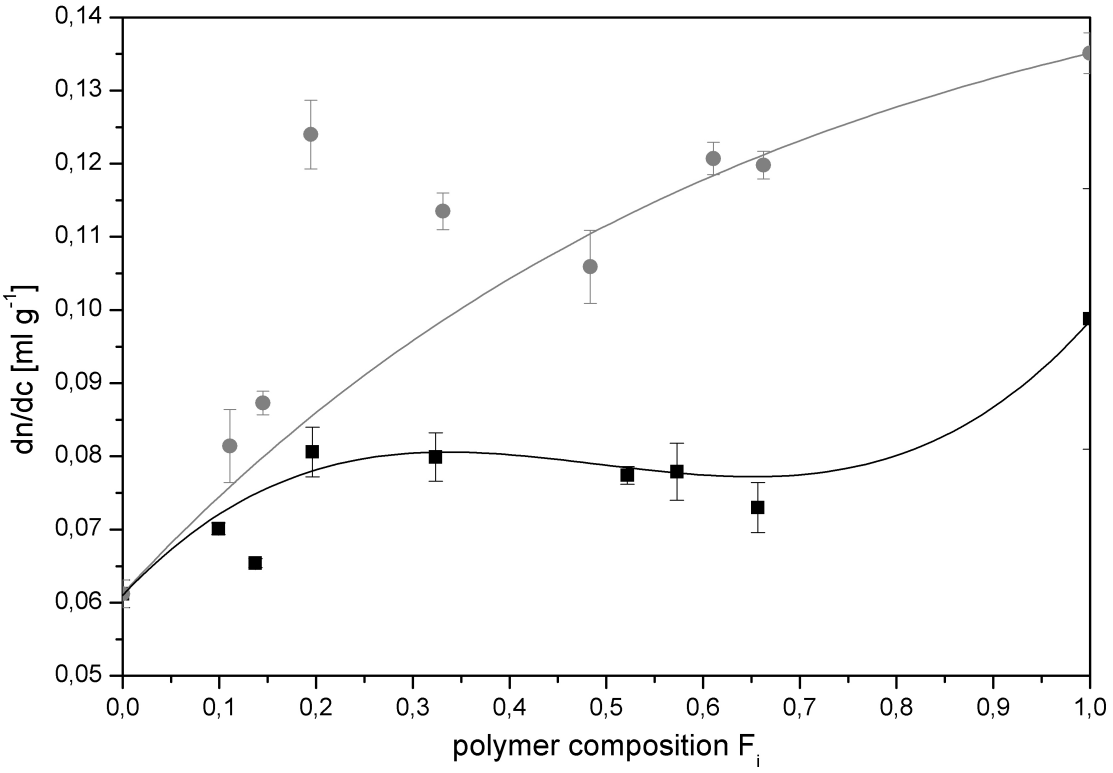

Fig. 7.24.: Comparison of the differential refractive index increments dn/dc of the solutions of the two copolymer series (Polymers of ■ *Series A*, i = nBMA, cf. *Table 3.10*, and ● *Series F*, i = BzMA cf. *Table 7.12*, THF, 25 °C)

The molar masses of *Series F* were higher than the ones of *Series A*. The average molar mass of *Series A* was $28500\,g \cdot mol^{-1}$ and the one of *Series F* was $39200\,g \cdot mol^{-1}$. Especially the homopolymers of BzMA had a obviously higher M_n than the homopolymer of nBMA.

Beside the absolute molar masses of the copolymers, the two copolymerization system were also compared by the degree of polymerization X_n, to compensate the different molar masses of the monomers nBMA and BzMA. The degree of polymerization considers the number of incorporated monomer units in the polymer-chain and not their molar mass, see *Equation 7.2.21*.

$$X_n = \frac{M_n}{F_1 \cdot M_1 + F_2 \cdot M_2} \tag{7.2.21}$$

with M_n = molar mass of the copolymer, F_i = molar fraction of monomer i, M_i = molar mass of monomer i ($M_{tBMA/nBMA} = 142.2\,g \cdot mol^{-1}$ and $M_{BzMA} = 176.21\,g \cdot mol^{-1}$)

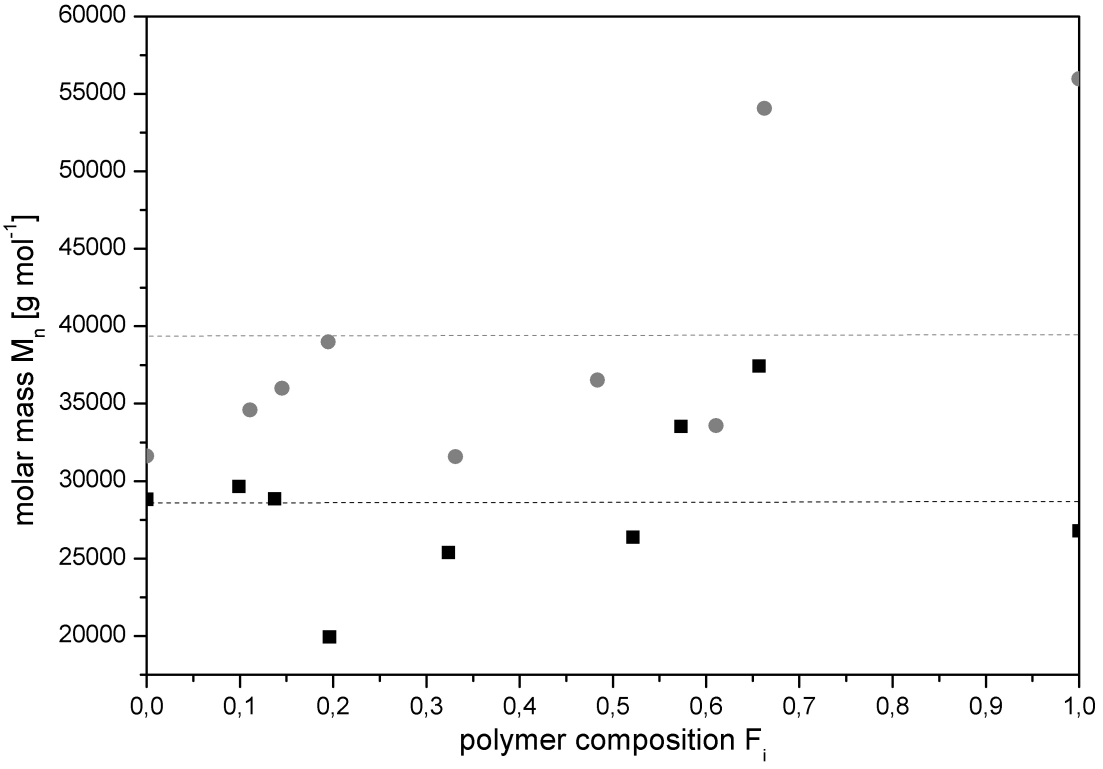

Fig. 7.25.: Comparison of a) molar masses M_n of *Series A* (■, i = nBMA, cf. *Table 3.11*) and *Series F* (●, i = BzMA, cf. *Table 7.13*) against copolymer composition, dashed lines – average molar mass

The degree of polymerization of the copolymers of *Series A* and *Series F* are listed in *Table 7.16* and shown in *Figure 7.26*. In *Series A* the X_n–values laid between 140 and 260. While in *Series F* the degree of polymerization ranged from X_n = 205 to 260 between F_{BzMA} = 0 and F_{BzMA} = 0.61. Hence, X_n(BzMA/tBMA) is in the same region as X_n of the copolymers from tBMA and nBMA. The copolymers with F_{BzMA} = 0.66 and F_{BzMA} = 1 had a degree of polymerization of 330, respectively 320. Larger amounts of BzMA inside the polymer is coupled to higher X_n–values.

Tab. 7.16.: Degree of polymerization X_n of the copolymers of *Series A* P[nBMA–co–tBMA] and *Series F* P[BzMA–co–tBMA]

F_{nBMA}	X_n	F_{BzMA}	X_n
0.00	202.67	0.00	222.36
0.10	208.58	0.11	236.97
0.14	202.88	0.15	244.60
0.20	140.30	0.19	261.93
0.32	178.55	0.33	205.72
0.52	185.51	0.48	230.20
0.57	235.72	0.61	206.05
0.66	263.15	0.66	328.12
1.00	188.40	1.00	317.58

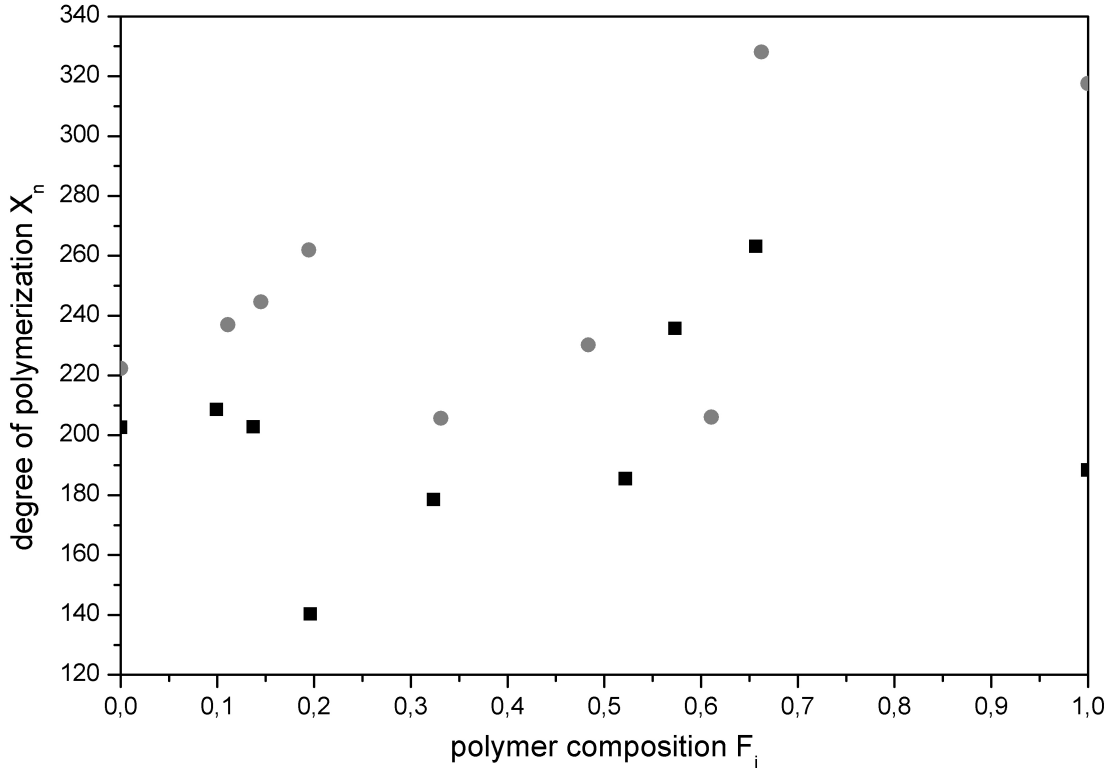

Fig. 7.26.: Comparison of degree of polymerization X_n of *Series A* (■, i = nBMA) and *Series F* (●, i = BzMA) against copolymer composition

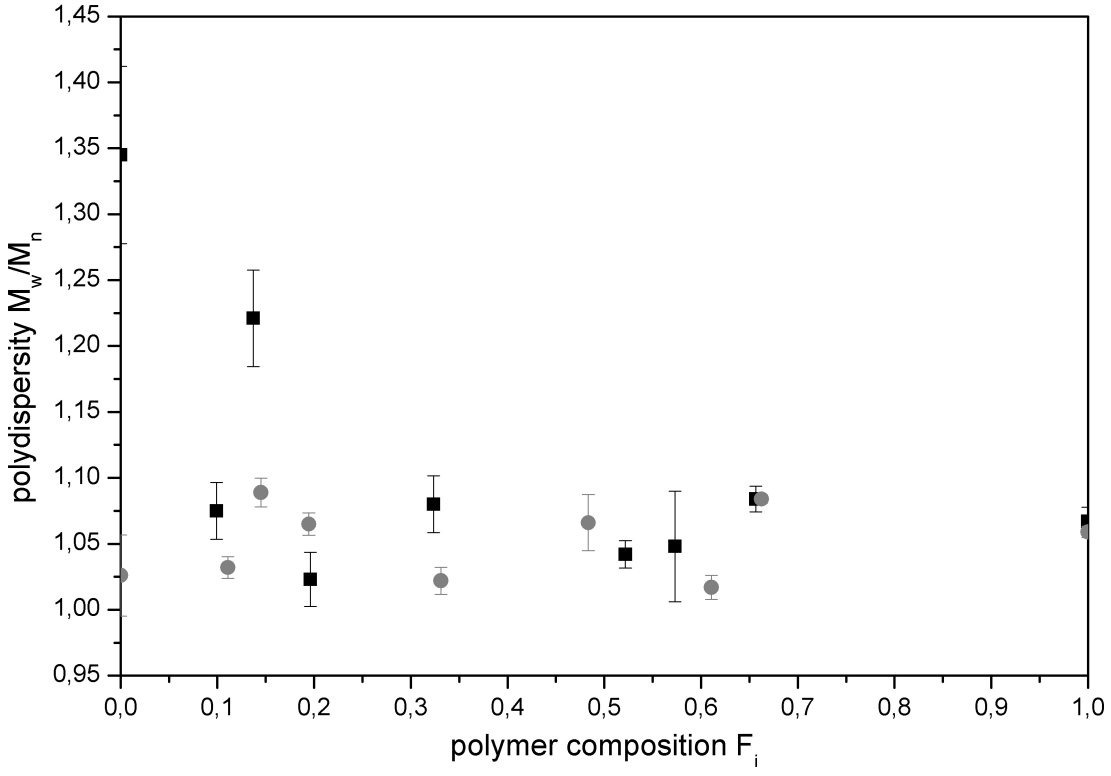

Fig. 7.27.: Comparison of polydispersities M_w/M_n of *Series A* (■, i = nBMA) and *Series F* (●, i = BzMA) against copolymer composition

The polydispersities PDI were nearly the same with both monomer mixtures. They were low (PDI < 1.1) with two exceptions. F_{nBMA} = 0 had a PDI of 1.345 and F_{BzMA} = 0 a PDI of 1.221. The low PDI–values and their narrow distribution on changing t comonomer–content showed that the two controlled radical copolymerizations worked well, independent of the monomer mixture.

7.2.4. Thermal Behavior

The next kind of analysis was the differential scanning calorimetry. Here the thermal behavior of the copolymers was analyzed mainly to determine the dependence of the glass transition temperature T_g on the copolymer composition. All samples of *Series F* were measured with the following temperature program:

- precooling: RT to −50 °C
- standby for 20 min
- 1. heating: −50 to 200 °C
- 1. cooling: 200 to −50 °C
- 2. heating: −50 to 200 °C
- postcooling: 200 °C to RT

Note that the same temperature program was used to analyze *Series A* to maintain the compatibility of investigations, cf. *Section 3.3.4*.

The samples of *Series F* were measured between −80 to 150 °C as with *Series B* but with otherwise equal DSC program because the analysis of *Series A* showed that it was not required to heat up to 200 °C. In *Figure 7.28* the thermogram of experiment V81 with both heating and the cooling runs is depicted as an example.

The first heating run showed a single glass transition step overlaid by a relaxation peak in the range from 30 to 80 °C. To avoid effects of the sample thermal history only the second heating run was analyzed. With the analysis software of the DSC, T_{onset} and T_{offset} of the glass transition region were determined and then the other values T_g, $\Delta T = T_{offset} - T_{onset}$ and Δc_p were calculated. [89] Also the midpoint of the glass transition region T_{midpt} was computed but these values were not used further. The procedure was the same as described before for the first monomer mixture in *Section 3.3.4*. All second heating runs from the copolymers of *Series F* and all the samples of *Series G* which were taken during the batch copolymerization were analyzed that way. The second heating runs of the samples of V92 as an example for *Series G* are depicted in *Figure 7.29*. T_g, T_{onset} and T_{offset} as bounds of the glass area are marked there. The second heating runs of the batch copolymers of *Series F* are collected

in *Figure 7.31*, also with marked T_g, T_{onset} and T_{offset}. All the DSC results of the batch copolymerizations of *Series F* are summarized in *Table 7.17* and the one of *Series G* in *Table 7.18*.

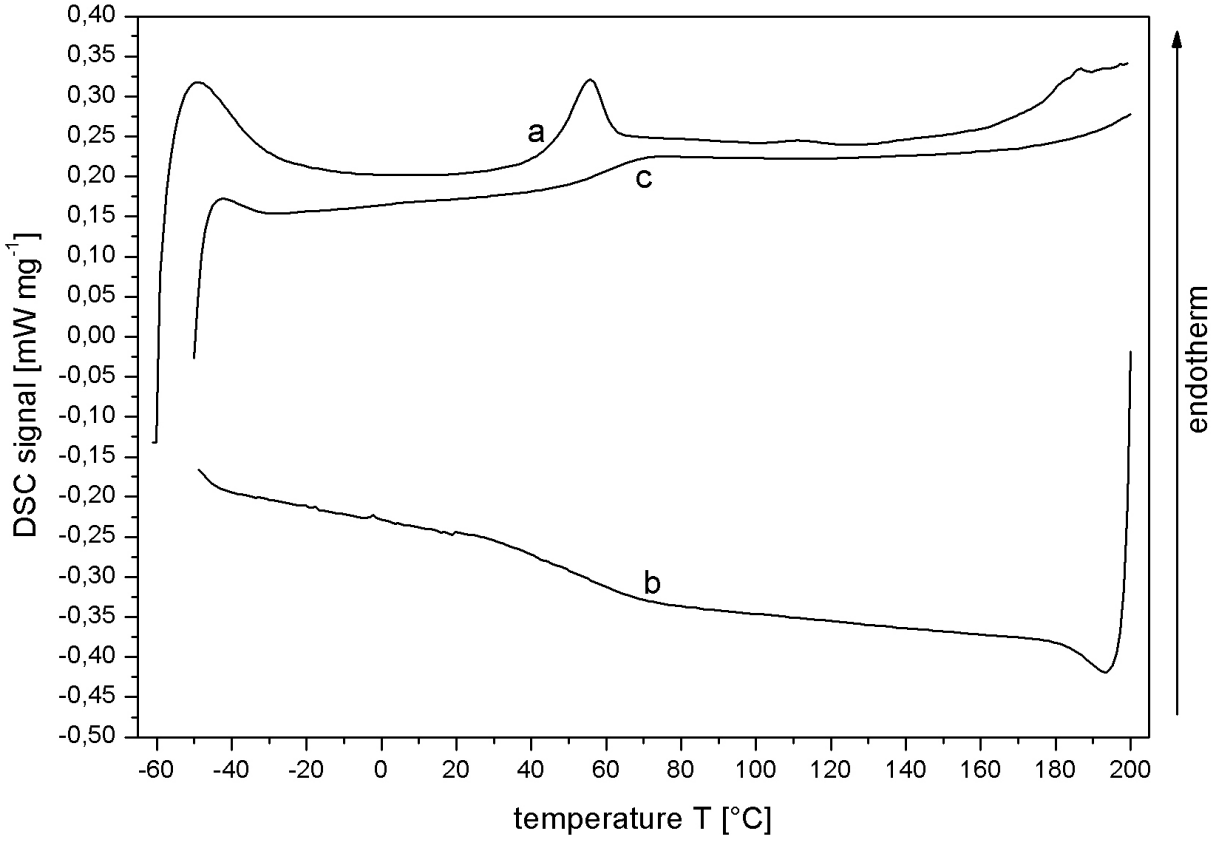

Fig. 7.28.: DSC thermogram of experiment V81 (F_{BzMA} = 0.33); a – first heating run, b – first cooling run, c – second heating run; heating rate $10\,K \cdot min^{-1}$

Tab. 7.17.: DSC results of the different copolymer compositions of *Series F*

Entry	F_{BzMA}	$T_g^{F\ a}$ [°C]	T_{onset} [°C]	T_{midpt} [°C]	T_g [°C]	T_{offset} [°C]	ΔT [°C]	Δc_p $[J \cdot g^{-1} \cdot K^{-1}]$
V88	0.00	107.0[b]	96.0	103.0	107.5	111.0	15.0	0.223
V86	0.11	94.0	67.0	82.5	81.5	99.0	32.0	0.220
V84	0.15	90.0	73.5	81.5	83.0	89.0	15.5	0.175
V82	0.19	86.0	43.5	50.0	55.5	57.5	14.0	0.222
V81	0.33	75.5	45.0	56.5	52.5	70.5	25.5	0.140
V83	0.48	66.5	47.0	63.0	66.0	77.0	30.0	0.254
V85	0.61	60.2	39.0	49.5	54.0	58.5	19.5	0.206
V87	0.66	58.0	17.5	32.5	29.5	43.0	25.5	0.215
V89	1.00	47.0[c]	24.0	34.0	36.5	42.5	18.5	0.239

[a] calculated with *Fox–Equation 7.2.23*; from Literature [b] [90] and [c] [113]

Tab. 7.18.: DSC results of the different copolymer compositions of *Series G*

Entry F_{BzMA}	time [min]	T_{onset} [°C]	T_{midpt} [°C]	T_g [°C]	T_{offset} [°C]	ΔT [°C]	Δc_p $[J \cdot g^{-1} \cdot K^{-1}]$
V92	60	61.5	69.5	70.0	77.0	15.5	0.263
0.33	90	59.5	69.0	71.5	77.5	18.0	0.253
	120	58.0	64.5	66.0	71.0	13.0	0.215
	150	51.0	60.0	63.0	66.5	15.5	0.198
	180	62.5	69.0	71.0	75.0	12.5	0.238
V91	60	30.0	37.5	39.0	43.5	13.5	0.249
0.5	90	47.5	59.0	58.5	69.0	21.5	0.244
	120	58.0	65.5	61.0	71.5	13.5	0.184
	150	42.0	50.5	51.5	58.0	16.0	0.247
	180	42.0	50.5	51.5	58.0	16.0	0.214
V93	60	48.5	57.0	56.0	64.5	16.0	0.281
0.66	90	53.5	62.0	65.5	68.5	15.0	0.311
	120	44.0	51.5	53.5	58.0	14.0	0.241
	150	39.0	48.5	47.5	55.5	16.5	0.255
	180	44.0	51.0	52.0	56.5	12.5	0.244
V94	60	42.5	48.0	51.5	53.5	11.0	0.264
1.0	90	49.0	55.5	56.0	60.5	11.5	0.278
	120	36.5	43.5	46.5	50.0	13.5	0.277
	150	38.0	43.5	48.0	50.0	12.0	0.274
	180	35.0	42.0	43.0	48.0	13.0	0.278

The second heating runs of the samples that were taken during the batch copolymerization of experiment V92, see *Figure 7.29*, did not vary significantly between the first four samples. Only the last sample, taken after 180 min, showed a slight shift to higher temperature. So the glass transition temperature and the glass transition range did not change obviously with the growing of the molar mass. *Figure 7.30* depicts T_g and ΔT against the polymerization time. The T_g staid constant over the whole polymerization and also ΔT decreased only marginally. Therefore the growth of the molar mass had no influence on the glass transition temperature and range. That was the same with all compositions of *Series G*. An analogous behavior was also found with the P[nBMA–co–tBMA]–copolymers of *Series B*.

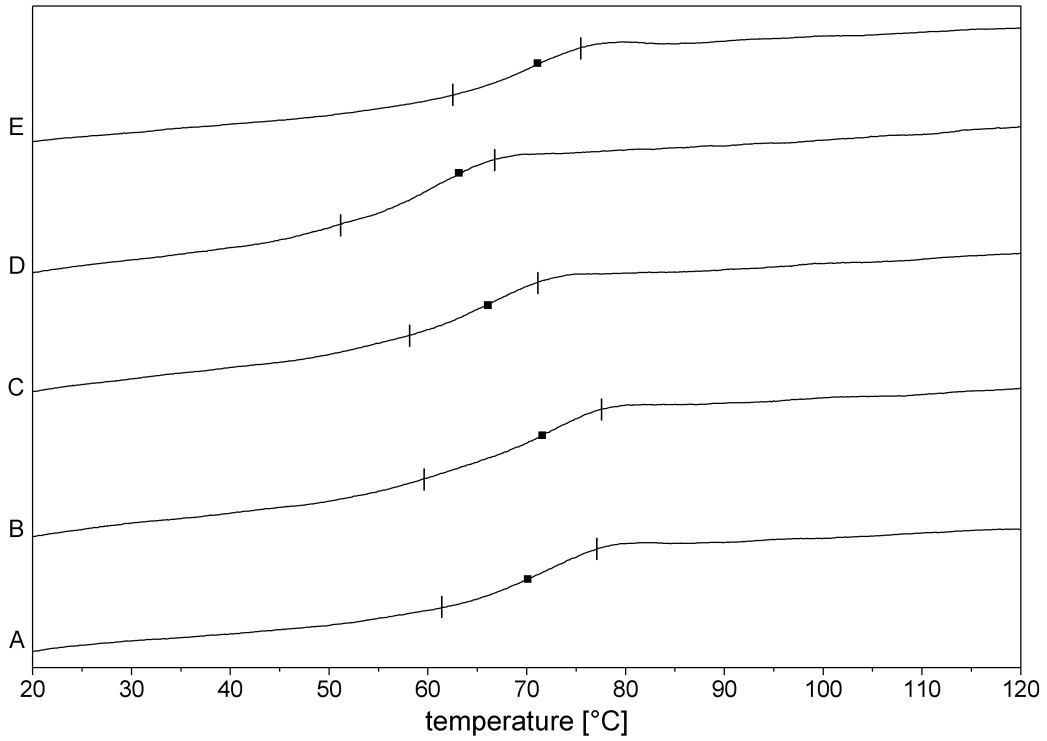

Fig. 7.29.: DSC thermograms of samples taken during the batch copolymerization V92 (f_{BzMA} = 0.33) with marked glass transition temperature range ΔT and temperature T_g (second heating runs, heating rate $10\,K \cdot min^{-1}$; A – 60 min, B – 90 min, C – 120 min, D – 150 min, E – 180 min of polymerization time

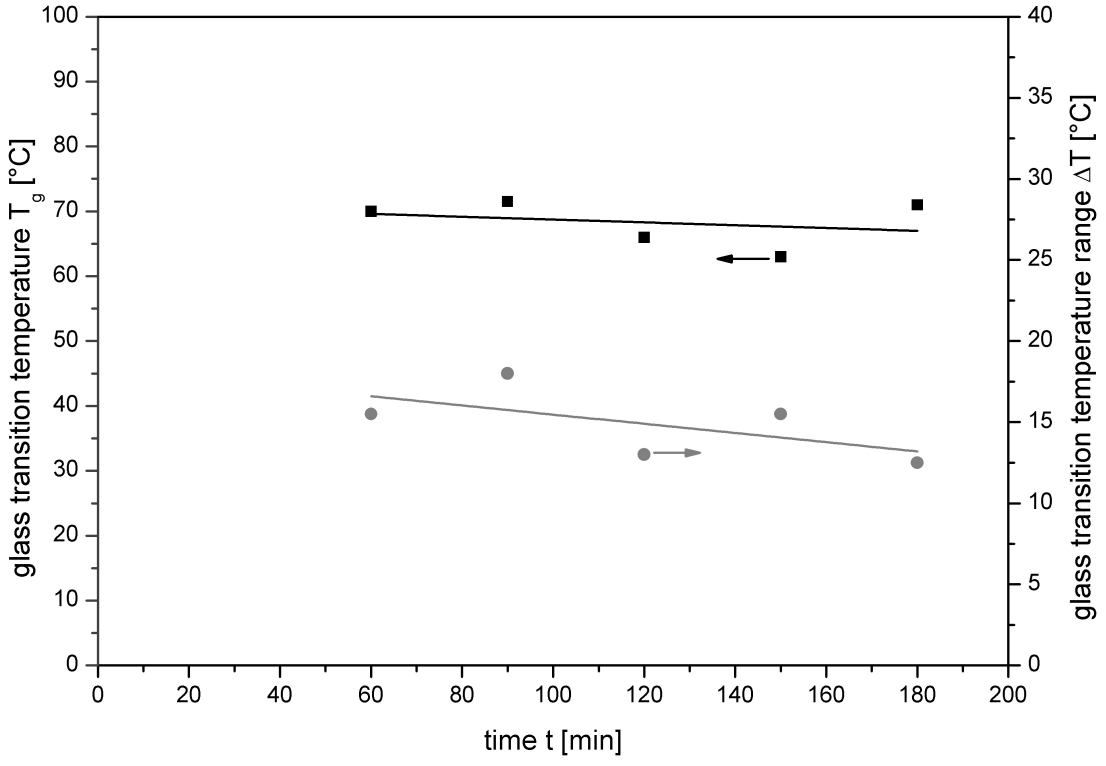

Fig. 7.30.: Glass transition temperature T_g and temperature range ΔT of the samples taken during the batch copolymerization V92 (f_{BzMA} = 0.33); ■ glass transition temperature T_g and ● glass transition region ΔT

Figure 7.31 shows that there is some kind of dependence of the glass transition temperature on the composition of the copolymer. T_g decreased from 107.5 ℃ for PtBMA to 36.5 ℃ for PBzMA. The change of ΔT was not consistent. The two values are also plotted in *Figure 7.32* against the copolymer composition to point out the trends more explicitly. The dependence of T_g on the copolymer composition was not linear over all compositions. Between $F_{BzMA} = 0.00$ and 0.33 T_g fell linear with the rise of BzMA in the polymer chain. Then the curves became flatter. The equation of the fit is given in *Equation 7.2.22*. ΔT did not show a dependence to the copolymer composition.

$$T_g = (39.006 \pm 10.488)\,°C + (67.127 \pm 13.192)\,°C \cdot e^{(-4.0960 \pm 2.093)\,°C \cdot F_{BzMA}} \tag{7.2.22}$$

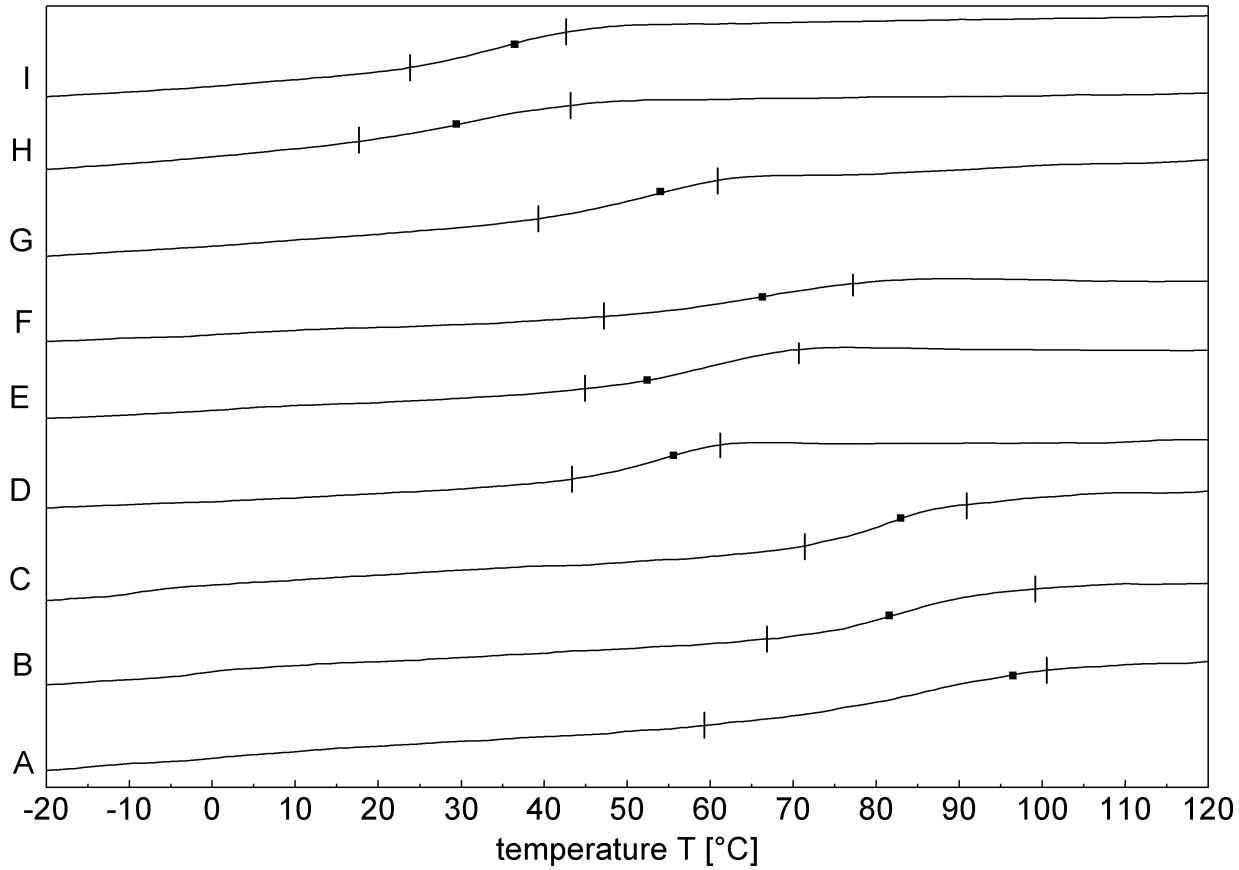

Fig. 7.31.: DSC thermograms of copolymers P[BzMA–co–tBMA] *Series F* with marked glass transition temperature range ΔT and temperature T_g; second heating runs, heating rate $10\,K \cdot min^{-1}$; A – $F_{BzMA} = 0.00$, B – $F_{BzMA} = 0.11$, C – $F_{BzMA} = 0.15$, D – $F_{BzMA} = 0.19$, E – $F_{BzMA} = 0.33$, F – $F_{BzMA} = 0.48$, G – $F_{BzMA} = 0.61$, H – $F_{BzMA} = 0.66$, I – $F_{BzMA} = 1.00$

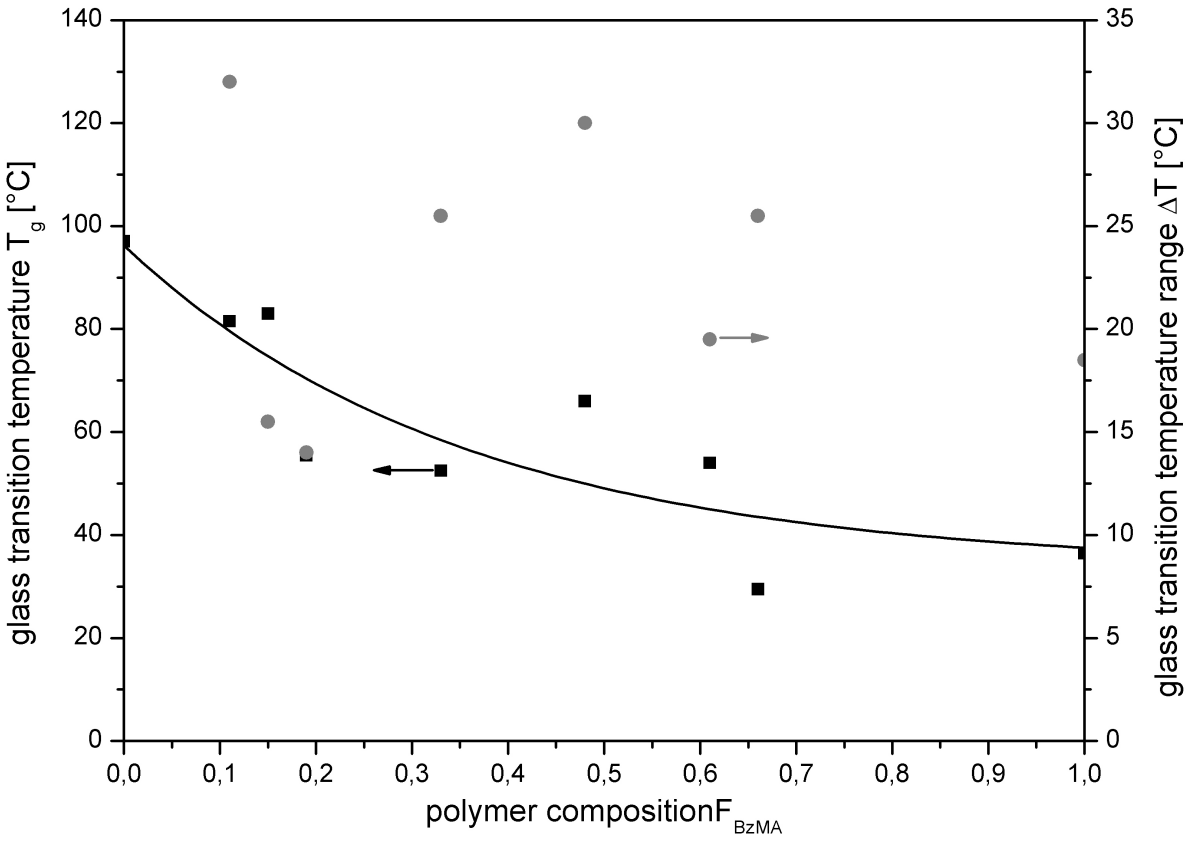

Fig. 7.32.: Glass transition temperature T_g and temperature range ΔT of copolymers P[BzMA–co–tBMA] *Series F*; ■ glass transition temperature T_g and ● glass transition region ΔT

The measured T_g–values of PtBMA agreed well to the known literature values. Reference [90] stated 107 °C which was nearly the same as the present measurements (107.5 °C). For PBzMA [113] T_g = 47 °C is given which is about 10 °C higher than the measured value (36.5 °C). Despite the discrepancy of the values of PBzMA, the literature values were used to fit the *Fox–Equation* (*7.2.23*) to the glass transition temperature of the prepared copolymers. [19]

$$\frac{1}{T_g} = \frac{F_{BzMA}}{T_{g,PBzMA}} + \frac{1 - F_{BzMA}}{T_{g,PtBMA}} \tag{7.2.23}$$

The *Fox*–T_g–values of the different batch copolymers are listed in *Table 7.17*. All measured T_g of the copolymers were lower than the ones calculated from the *Fox–Equation 7.2.23*. The difference was around 10 °C what was the same difference than between the measured T_g of BzMA of the homopolymers and its literature value. So this equation is a good possibility to estimate the glass transition temperature of the gradient copolymers, because the differences were the same. In both cases, calculation and measurement, the T_g–values decreased with the increasing of BzMA inside the polymer chain.

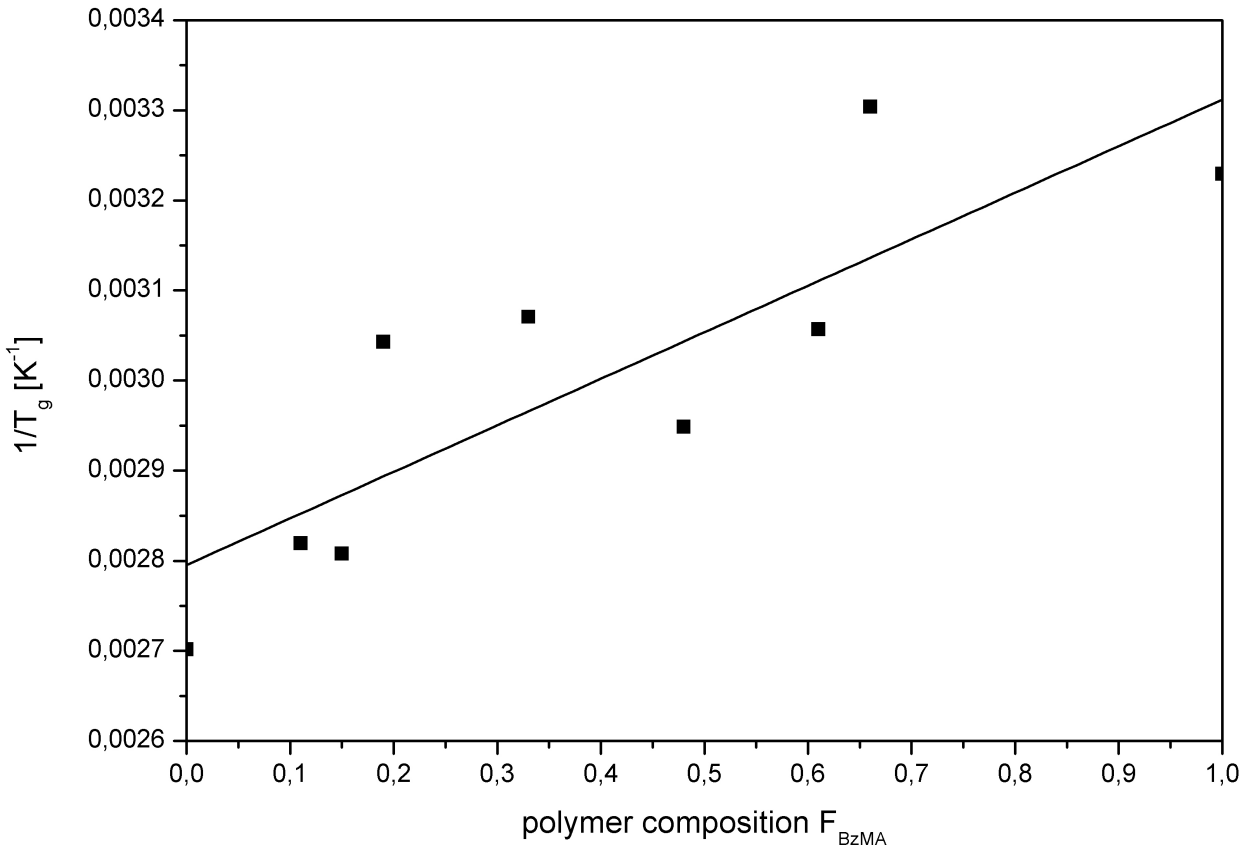

Fig. 7.33.: Reciprocal glass transition temperature T_g of *Series F* against copolymer composition

Figure 7.33 shows the plot of the reciprocal of the glass transition temperature T_g of the copolymer of *Series F* against the copolymers composition. There the $1/T_g$ values rose roughly linear with the amount of BzMA in the copolymer but in all cases the T_g–values of the copolymers exceeded their corresponding *Fox*–values strongly. The fit is given in *Equation 7.2.24*.

$$\frac{1}{T_g} = (0.0028 \pm 6.882 \cdot 10^{-5})\,K^{-1} + (5.514 \cdot 10^{-4} \pm 1.386 \cdot 10^{-4})K^{-1} \cdot F_{BzMA} \qquad (7.2.24)$$

with $T_{g1} = T_g$ of PtBMA and $T_{g2} = T_g$ of PBzMA

The *Fox–Equation* (*Equation 7.2.23*) was converted into *Equation 7.2.25* and then the values of intersection and slope of *Equation 7.2.24* were introduced into the equation. Therewith the values of T_g(PtBMA) and T_g(PBzMA) were calculated.

$$\frac{1}{T_g} = \frac{1}{T_{g1}} + \frac{T_{g1} - T_{g2}}{T_{g1} \cdot T_{g2}} \cdot F_{BzMA} \qquad (7.2.25)$$

The solution of *Equation 7.2.25* with the values of *Equation 7.2.24* for T_g of tBMA was 84.0 °C which is a deviation of 21.9 % from the measured T_g and 21.5 % from the literature value. The resulting T_g of PBzMA was 24.2 °C which is a deviation of 33.7 % from the measured T_g and 48.5 % from the literature value. The determination of the glass transition temperatures

of the homopolymers with the reciprocal glass transition temperature of the copolymers did not lead to sufficient results.

Comparison of the thermal behavior of the batch copolymers of nBMA/tBMA and BzMA/tBMA

In *Figure 7.34* the measured glass transition temperature T_g of the different copolymer compositions of *Series A* P[nBMA–co–tBMA] and *Series F* P[BzMA–co–tBMA] are depicted. The values of *Series F* scattered more than the values of *Series A*. Up to a composition of F_{BzMA}/ F_{nBMA} of 0.55 the glass transition temperature T_g of the copolymers containing benzyl methacrylate were lower than the T_g of the copolymers with *n*–butyl methacrylate. Then the curves intersected and the T_g of the copolymers from *Series F* were higher. Because the homopolymer PBzMA exhibits a higher glass transition temperature than PnBMA it was expected that all T_g values of *Series F* were higher than the ones of *Series A*. However, the scattering of the values of *Series F* made the fitting only an approximation.

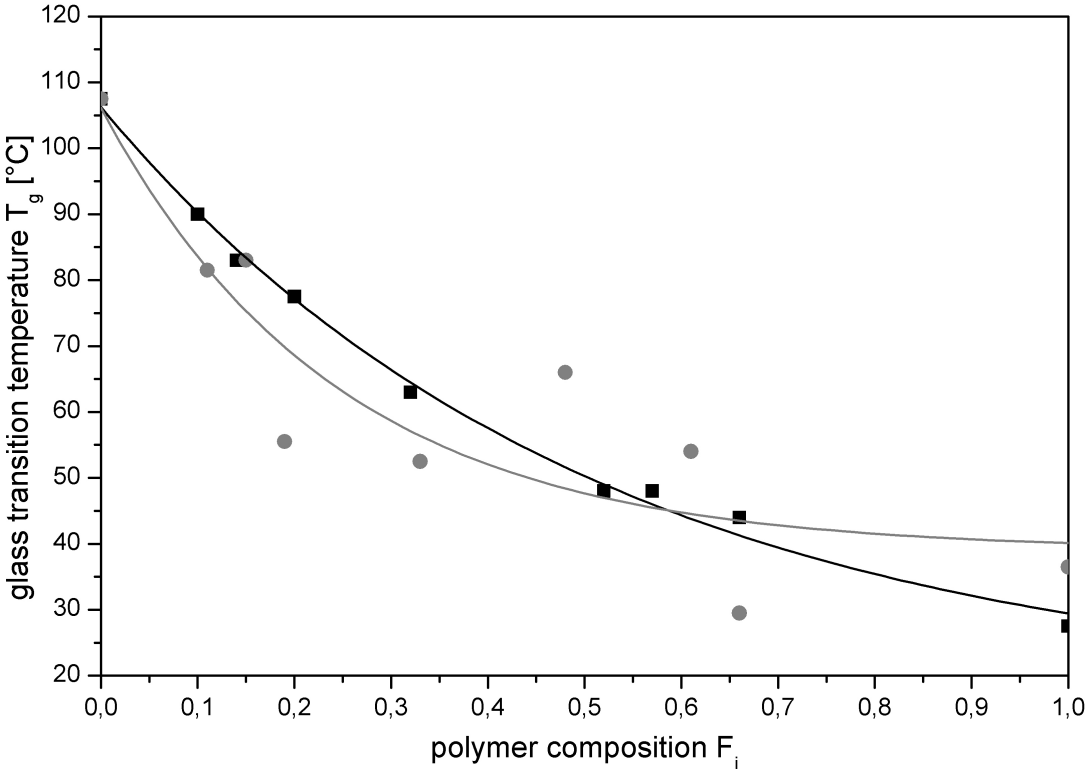

Fig. 7.34.: Comparison of glass transition temperature T_g of ■ *Series A* P[nBMA–co–tBMA] and ● *Series F* P[BzMA–co–tBMA] against copolymer composition

The reciprocal glass transition temperatures of *Series A* and *Series F* is compared in *Figure 7.35*. Again it was clearly to see that the values of *Series F* scattered obviously more than the one of *Series A*. The scattering was the reason why the analysis of the DSC–values of *Series F* did not gave as good results as the one of *Series A*.

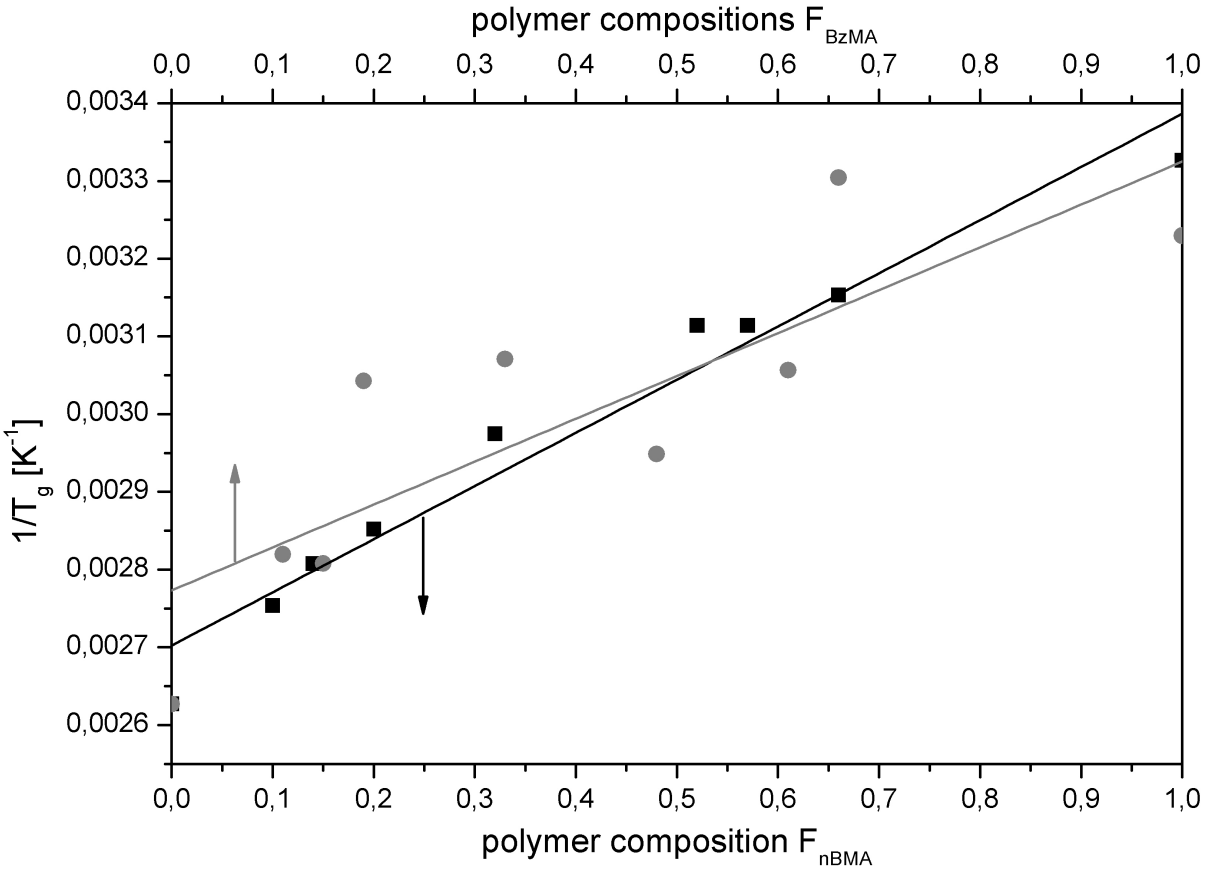

Fig. 7.35.: Comparison of reciprocal glass transition temperature T_g of ■ *Series A* and ● *Series F* against copolymer composition

7.3. Summary

The copolymerization rates of seven mixtures of BzMA and tBMA were measured to determine the copolymerization rate constants as well as the instantaneous copolymer compositions of the P[BzMA–co–tBMA] copolymers during the ATRP reactions as a function of the comonomer composition. The kinetic studies revealed the occurrence of a well controlled polymerization reaction free of side reactions. The copolymerization parameters were measured ($r_{BzMA} = 0.517$, $r_{tBMA} = 2.055$). The compositions of the resulting copolymers were analyzed with elementary analysis and infra red spectroscopy. The results of the elementary analysis showed that the polymers are nearly free of pollution. That means that all the reactions worked in the same way independent from the monomer composition. A calculation of the composition from the measured amounts of carbon or hydrogen leads to values which a obviously different from the compositions resulting from the analysis of the ^{1}H–NMR–analysis. The different amount of benzyl– and *tert*–butyl–groups inside the polymer chain were quantitatively represented in the IR–spectra. The quantitative analysis of the IR–spectra resulted in a calibration curve allowing for the copolymer composition determination from measurements of the peak height of two specific bands at 850 cm^{-1} for tBMA and 730 cm^{-1} for BzMA. SEC studies supported the findings of the ^{1}H–NMR–spectroscopy–analysis by revealing nar-

row MWD, without multimodalities or indications of termination reactions. The molecular weights were proportional to the monomer conversion, also indicating a high degree of control. The dn/dc values showed no direct relationship between the refractive index increment and the composition of the copolymer. DSC studies showed the glass transition temperatures slightly depended on the copolymer composition and can not well be described by *Fox's* equation. During the batch polymerization the glass transition temperature of the isolated samples did not change. The glass transition range is independent on the conversion of the batch copolymerization and the copolymer composition.

8. Synthesis of Gradient Copolymer from Benzyl and tert–Butyl Methacrylate by means of Semibatch Polymerization

This part of the work describes the synthesis and the characterization of functional amphiphilic gradient copolymers from benzyl methacrylate and *tert*–butyl methacrylate . With the results from the kinetic studies on the statistical tBMA/BzMA copolymer (cf. *Section 7.2.1*) the monomer addition program required for the semibatch polymerization of the gradient copolymer can be calculated. The resulting gradient copolymer P[tBMA–grad–BzMA] is analyzed in the same way as the statistical copolymers before and the results were compared.

8.1. Materials and Methods

8.1.1. Materials

Chemicals and pre–treated of chemicals were the same as detailed in *Chapter 7*.

- monomers
  - benzyl methacrylate (BzMA, 98 %, *Alfa Aesar*)
  - *tert*–butyl methacrylate (tBMA, 98 %, *Alfa Aesar*)
- initiator: *para*–toluenesulfonyl chloride (pTSC, 98 %, *Sigma–Aldrich*)
- catalyst: copper(I) chloride (97 %, *Sigma–Aldrich*)
- ligand: N,N,N',N',N"–pentamethyldiethylenetriamine (PMDETA, 99 %, *Sigma–Aldrich*)
- solvent: 2–butanone (MEK, *BDH Prolabo*, chromasol.)

8.1.2. Semibatch Copolymerization of Gradient Copolymers

The experimental setup of the semibatch copolymerization is depicted in *Figure 8.1.*

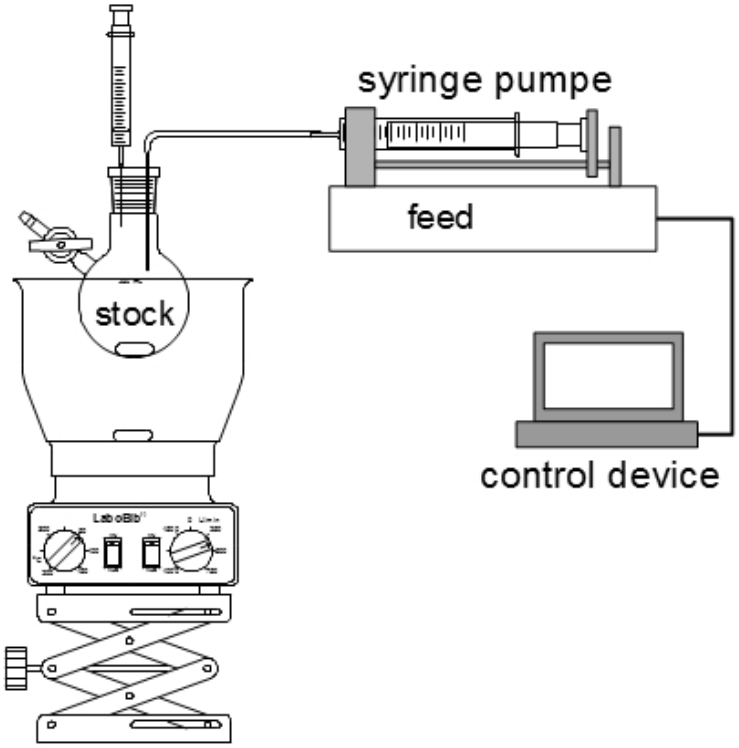

Fig. 8.1.: Experimental setup for semibatch copolymerization

For the synthesis the two monomers were prepared separately. Two Schlenk flasks, one of 100 ml volume to hold the the stock solution and one of 50 ml for the feed solution were heated out with a hot gun (air temperature ≈ 400 °C) under vacuum for five minutes and then flushed with nitrogen. Subsequently the stock solution consisting of 0.1411 g ($7.403 \cdot 10^{-4}$ mol) pTSC, 9.4364 g (0.0664 mol) tBMA, 0.1283 g ($7.403 \cdot 10^{-4}$ mol) PMDETA and 0.0733 g ($7.403 \cdot 10^{-4}$ mol) CuCl was weighted in a screw–cap glass. The mixture was rinsed into the 100 ml Schlenk flask with 9.4364 g MEK under nitrogen counter flow. In a second screw–cap glass was weighted in the feed solution monomer, 13.9214 g (0.0790 mol) BzMA. It was flushed into the 50 ml Schlenk flask with 13.9214 g MEK likewise under nitrogen counter stream. The composition is also listed in *Table 8.1.*

Tab. 8.1.: Composition of the semibatch copolymerization of tBMA and BzMA

Entry	f^0_{tBMA}			n [mol]	m [g]
V101	0.5	Stock	tBMA	0.0664	9.4364
			pTSC	$7.403 \cdot 10^{-4}$	0.1411
			PMDETA	$7.403 \cdot 10^{-4}$	0.1283
			CuCl	$7.403 \cdot 10^{-4}$	0.0733
			MEK	0.1309	9.4364
		Feed	BzMA	0.0790	13.9214
			MEK	0.1931	13.9214

The two solutions were degassed by means of five freeze–melting–cycles. Than the feed solution was transferred into a gas–tight syringe under nitrogen flow and mounted in the syringe pump. The stock solution was placed in an oil bath at 80 ℃ with stirring. At this time the sampling began. After 30 min for the pre–polymerization the monomer addition program was started.

During the polymerization aliquot samples with volumes of about 0.05 ml were taken at 0, 15, 30, 40, 50, 60, 70, 80, 90, 120, 150, 180, 210, 270, 330, 390, 450 and 1440 min. The samples were immediately given into 0.5 ml ice cooled $CDCl_3$ without further purification. Furthermore 1 ml samples were taken from the solution and precipitated in 20 ml of water : methanol = 1 : 1 vol : vol (temperature −50 ℃) mixture at 60, 90, 150, 210, 330 and 450 min.

The precipitated polymers were worked up by means of procedure *"work–up D"* as described in *Section 7.1.2* with the samples of *Series G* and also characterized by means of elementary analysis, ATR–FTIR–spectroscopy, SEC and DSC. After 24 h the reaction solution was cooled down and the polymer was precipitated in 600 ml water–methanol–solution, filtered and dried, also in accordance to *"work–up D"*. The precipitate was extracted first with 150 ml CH_2Cl_2 and 150 ml H_2O and then the water phase was extracted two times more with 50 ml CH_2Cl_2 each. The color of the organic phase shifted from green to colorless in the organic phase and from colorless to blue in the aqueous phase. The organic phases were combined and dried by vacuum evaporation. The resulting polymer was characterized as detailed in *Chapter 7, Section 7.1.2*. The polymer yields of the samples and of the completely worked–up semi–batch are listed in *Table 8.2*.

Tab. 8.2.: Polymer yields obtained from the 1–ml–samples and the final yield of the semi–batch copolymerization of experiment V101

time	[g]	[%]
60	0.07	14.91
90	0.15	33.93
150	0.22	51.72
210	0.32	72.08
330	0.42	95.23
450	0.43	97.80
1440	16.44	79.36

[1] ***H–NMR:*** 1.25–1.45 ppm (broad peak, $–C(CH_3)_3$, P[tBMA]); 1.42 ppm (s, $–C(CH_3)_3$, tBMA); 1.7–1.9 ppm (broad peak, $–CH_3$, P[tBMA] and P[BzMA]); 1.9 ppm (s, $–CH_3$, tBMA); 1.8 ppm (s, $–CH_3$, BzMA); 4.8–5.1 ppm (broad peak, $–OCH_2R$, P[BzMA]); 5.2 ppm (s, OCH_2R, BzMA); 5.3 ppm (t, CH_2=C–, cis, tBMA); 5.5 ppm (t, CH_2=C–, cis, BzMA); 5.9 ppm (s, CH_2=C–, trans, tBMA); 6.1 ppm (s, CH_2=C–, trans, BzMA); 7.3–7.43 ppm (broad peak, aromatic ring, BzMA and P[BzMA])

EA: 71.20 % C, 8.18 % H, (20.62 % O_{calc})

ATR–FTIR: 3125–2800 cm^{-1} (=CH_2, –CH_2–, –CH_3, aromatic ring); 1717 cm^{-1} (–C=O); 1476 cm^{-1} (–CH_2–, –CH_3); 1455 cm^{-1} (–CH_2–, –CH_3); 1392 cm^{-1}; 1367 cm^{-1} (tBu); 1319 cm^{-1}; 1248 cm^{-1} (tBu); 1134 cm^{-1} (–C–O–C–); 1030 cm^{-1}; 967 cm^{-1} (Bz); 912 cm^{-1}; 876 cm^{-1}; 846 cm^{-1} (tBu); 749 cm^{-1} (Bz); 696 cm^{-1} (Bz); 584 cm^{-1}; 528 cm^{-1}; 461 cm^{-1}

SEC: dn/dc = 0.1135 $ml \cdot g^{-1}$; M_n = 30880 $g \cdot mol^{-1}$; M_w = 31570 $g \cdot mol^{-1}$; M_z = 32300 $g \cdot mol^{-1}$

DSC: T_{onset} = 45.0 °C; T_{midpt} = 56.5 °C; T_g = 52.5 °C; T_{offset} = 70.5 °C; ΔC_p = 0.140 $J \cdot g^{-1} \cdot K^{-1}$

8.1.3. Characterization

All characterization–methods were the same as with the batch copolymers of *Chapter 3*. The used methods were:

- ^{1}H–NMR spectroscopy
- elementary analysis
- ATR–FTIR–spectroscopy
- size exclusion chromatography
- differential scanning calorimetry

The same instruments under the same conditions were used for the investigation of the resulting copolymers.

8.2. Results and Discussion

The subsequent paragraph describes the preparation of the monomer–feed programs, the set–up and performance of the semi–batch experiments as well as the results of the analysis from the semibatch polymerization of P[tBMA–grad–BzMA] and also its discussion. The gradient copolymer was analyzed with the same methods as the statistical copolymers P[BzMA–co–tBMA] before and under the same conditions (cf. *Section 3.2*).

The theoretical initial value of the monomer amount was 0.1264 mol, i. e. 0.0632 mol tBMA and BzMA. Actually it were used 5 % more tBMA and 25 % more BzMA. The amount of tBMA was enlarged because a pre–polymerization time of 30 min was used to ensure a smooth start of the ATRP–reaction. The BzMA–feed solution was larger to compensate for the dead volume of the syringe and the syringe pump. The amount of the other components were adapted respectively. The ratio of monomer to solvent was wt : wt 1 : 1 for the stock and also for the feed solution because the concentrations had to remain constant. The amount of the components of the initiator system was adjusted to the additional amount of tBMA for the pre–polymerization, because only the 5 % of tBMA were polymerized, prior to the start of the monomer feed.

8.2.1. Monomer Addition Program

The preparation of the gradient copolymer was done by semibatch copolymerization. That meaned the monomer in the stock solution together with the initiator compounds, here *tert*–butyl methacrylate, was submitted in a Schlenk flask. The second monomer in the feed solution, here benzyl methacrylate, was continuously injected into the stock solution during the polymerization. The required feeding rate which was expressed by means of the dimensionless parameter q, depending on the target gradient $\phi = dF_{nBMA}/dX_e$ and the copolymerization properties of the comonomer system. This is described by the *Equations 8.2.1* to *8.2.4*, taken from Literature [107].

$$\frac{dq}{dp} = -f_{tBMA}\frac{X_e\phi}{F'_{tBMA}}(q-p) + 1 - \frac{F_{tBMA}}{f_{tBMA}} \tag{8.2.1}$$

$$\frac{df_{tBMA}}{dp} = \frac{1}{q-p}\left\{f_{tBMA} - F_{tBMA} - \frac{dq}{dp}\cdot f_{tBMA}\right\} \tag{8.2.2}$$

$$\frac{dt}{dp} = \frac{1}{k(f_{efftBMA})}\frac{1}{q-p} \tag{8.2.3}$$

$$q = \frac{1+p}{2} \tag{8.2.4}$$

with ϕ = targeted copolymer compositional gradient, X_e = targeted length of the gradient block, $F'_{tBMA} = dF_{tBMA}/df_{tBMA}$, q = total monomer addition function, p = monomer conversion, F_{tBMA} = instantaneous molar fraction of tBMA in the copolymer, f_{tBMA} = instantaneous

molar fraction of tBMA in the monomer mixture

In the differential equation system (DES) *8.2.1* to *8.2.4* the "polymer chain" related gradient $\phi = dF/dX$ is used. Since ϕ is a small number ($\Delta F \leq 1; X_n > 10$) in the subsequent text the "monomer conversion" related gradient $\phi_p = dF/dp$ will be used. Note, that ϕ, and ϕ_p are interrelated by the simple expression $\phi = X_{n,e}^{-1} \cdot \phi_p$. One target gradient copolymer $\phi = -1.0$ was synthesized and investigated here, as shown in *Table 8.3.* $\phi_p = dF_{tBMA}/dp$ was calculated according to *Equation 8.2.5.*

$$\lim_{p \to \infty} \phi_p \Rightarrow F_{tBMA,e} - 1 \tag{8.2.5}$$

Tab. 8.3.: Theoretical values for monomer addition program of experiment V101

target gradient ϕ_p	f_{tBMA}^{final}	$F_{tBMA,e}$	$F_{cum,tBMA}$	q_0
-1.0	0.50	0.0	0.50	0.50
$\phi_p = dF_{tBMA}/dp$, $q_0 = n_{tBMA,0}/(n_{tBMA,0} + n_{tBMA,e})$				

The solution of the DES cannot be performed analytically, hence a numerical approximation was calculated by means of the program "GradMake". [107] Since the integration requires the knowledge of the dependence of the effective copolymerization rate constant k_{eff} from the actual monomer composition ($k_{eff,tBMA}$), the kinetic data of the tBMA/BzMA batch copolymerization experiments (cf. *Section 7.2.1*) were required. The total effective rate constant k_{eff} (cf. *Figure 7.8*) was plotted against the monomer composition of the tBMA as stock–monomer. The equation of the line of fit from this plot was converted to get the rate constant k_0 and the first–order term of the reactions rate polynomial k_{f1}, see *Equation 8.2.6* to *8.2.8.*

$$k_{eff}(f_{tBMA}) = k_0 + a \cdot f_{tBMA} \tag{8.2.6}$$

$$k_{f1} = \frac{a}{k_0} \tag{8.2.7}$$

$$k_{eff}(f_{tBMA}) = k_0 \cdot (1 + k_{f1} \cdot f_{tBMA}) \tag{8.2.8}$$

For the copolymerization tBMA and BzMA the equation of the line of fit (cf. *Equation 8.2.9*) and the equivalent of *Equation 8.2.8* was *Equation 8.2.10.*

$$k_{eff}(f_{tBMA}) = 1.8394 \cdot 10^{-4} s^{-1} - 4.1246 \cdot 10^{-5} s^{-1} \cdot f_{tBMA} \tag{8.2.9}$$

$$k_{eff}(f_{tBMA}) = 1.8394 \cdot 10^{-4} s^{-1} \cdot (1 - 2.2424 \cdot 10^{-1} \cdot f_{tBMA}) \tag{8.2.10}$$

The two values $k_1 = 1.898 \cdot 10^{-4}\,s^{-1}$ and $k_{f1} = 2.242 \cdot 10^{-1}$ were integrated into the program "GradMake". In the program the monomer of the in the stock solution tBMA was labeled

as "Monomer1" and the one in the feed solution BzMA as "Monomer2". "GradMake" solved the DES, calculated the time–dependent dosing rate (cf. *Figure 8.2*) and created a data–file containing the required volume–feed rates ("addition program") to control the syringe pump, see *Supplement E.*

The addition program contained the respective feed time interval Δt with the related feed rate dV/dt as shown in the *Figure 8.2.* The resulting differential volume per feed time $\Delta V(t)$ and the total volume V_{total} are shown in *Figures 8.3* and *8.4.* The total volume was the sum over all injected differential volumes up to the corresponding feed time (see *Equation 8.2.11*).

$$V_{total} = \int \frac{dV}{dt} dt = \sum_{i=1}^{n} \Delta V_i \tag{8.2.11}$$

$$t_{feed} = \int dt_{feed} = \sum_{i=1}^{n} \Delta t_{feed,i} \tag{8.2.12}$$

The feed rate per feed time, see *Figure 8.2*, started with the highest rate and then the values fall strongly and leveled off. The feed volume per feed time, see *Figure 8.3*, showed nearly the same shape. The representation of the total volume against the total addition time in *Figure 8.4* shows that during the first 85 min the half of the feed solution was added and the curve level off. Up to 200 min most of the solution was injected.

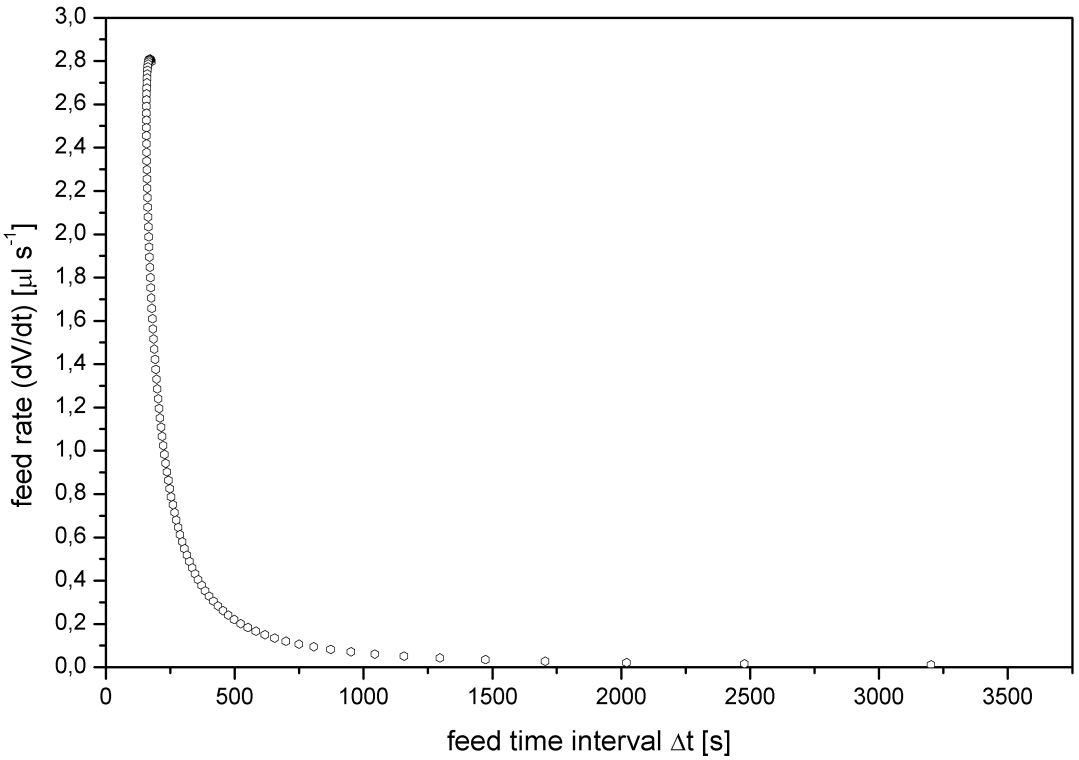

Fig. 8.2.: Feed rate per feed time intervals of experiment V101 ($\phi_p = -1$, $f_{tBMA} = 0.5$)

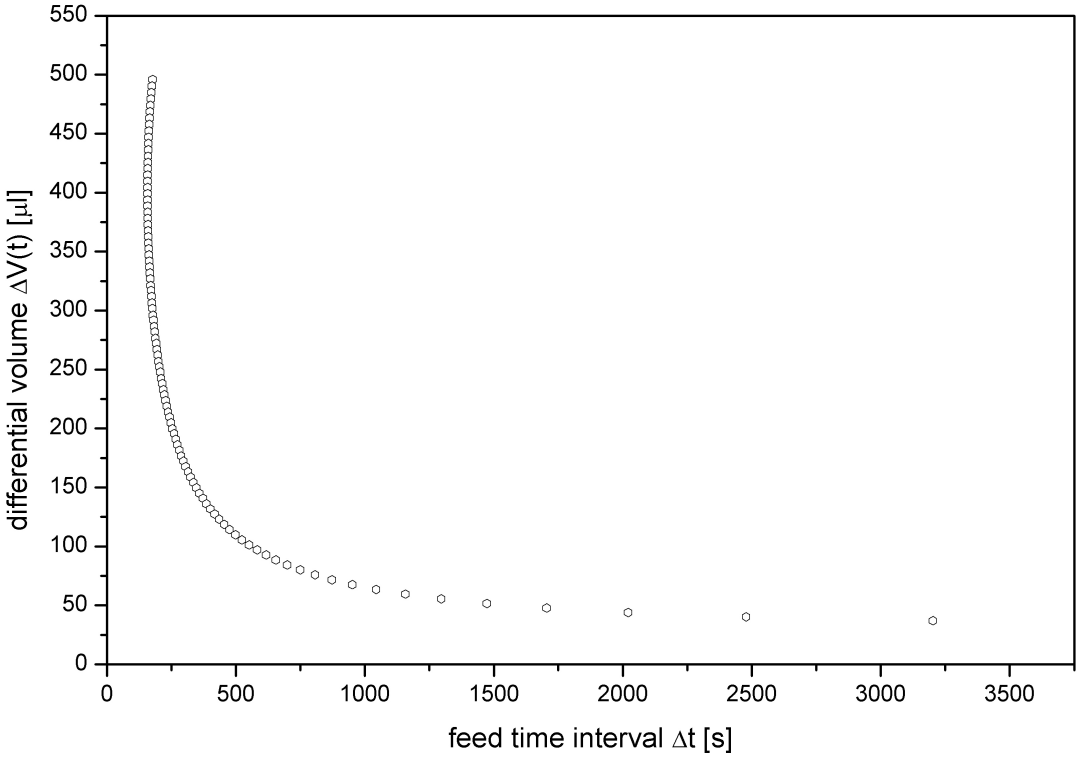

Fig. 8.3.: Differential volume per feed time intervals of experiment V101 ($\phi_p = -1$, $f_{tBMA} = 0.5$)

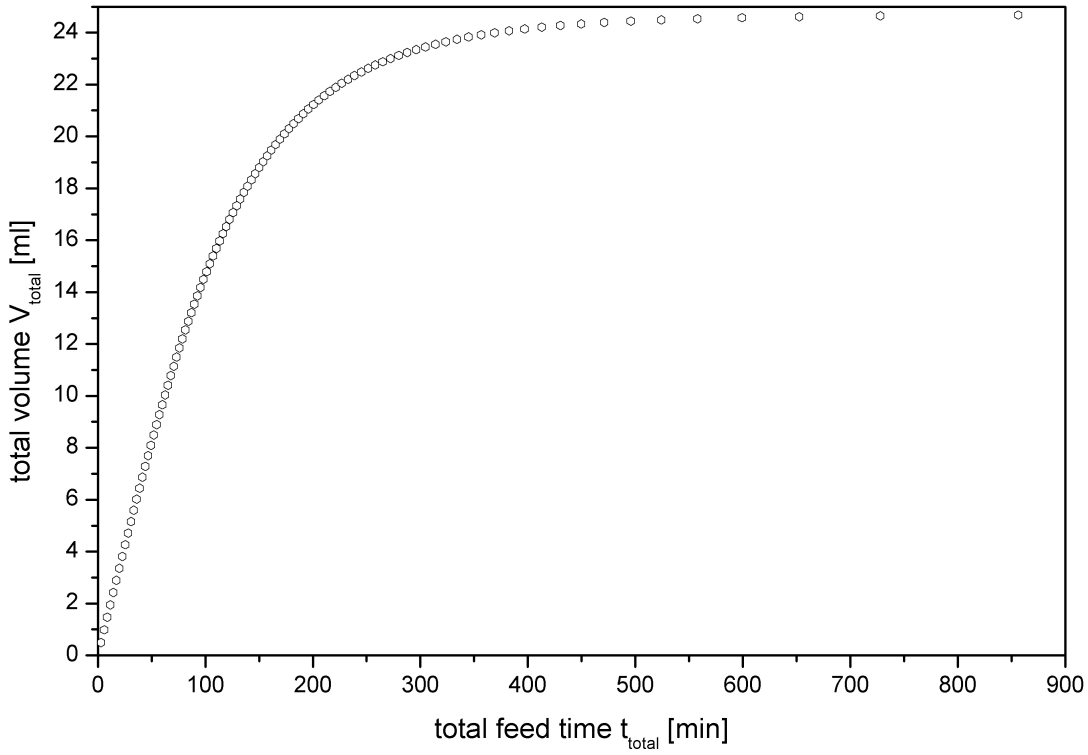

Fig. 8.4.: Total volume per total feed time of experiment V101 ($\phi_p = -1$, $f_{tBMA} = 0.5$)

8.2.2. Kinetic Studies

NMR samples were taken during the semibatch gradient copolymerization and analyzed to determine the monomer conversion p from the integrals of the ^{1}H–NMR–spectra and to determine the cumulative and instantaneous composition of the gradient copolymer, F_{cum} and F_{inst}, respectively. The change of the spectra during the course of reaction and the analyzed peaks are depicted in *Figure 8.6*. The molecular structures of the monomers tBMA and BzMA and the resulting copolymer as well as the numbering of their carbon atom are shown in *Figure 8.5*.

In the first spectrum A, shown in *Figure 8.6*, taken at the start of the semibatch copolymerization, only the signals of the monomer tBMA a singlet at 5.9 ppm (=CH_2^{cis}, 1), a triplet at 5.3 ppm (=CH_2^{trans}, 2) and a singlet at 1.8 ppm (–CH_3, 10) of the methacrylate part of the monomer and a singlet at 1.4 ppm of the *tert*–butyl group (3) together with the solvent signals of MEK at 0.96 ppm (t), 2.06 ppm (s) and 2.38 ppm (q) were present, certainly. The last ^{1}H–NMR–spectrum H, taken after 24 h, showed the sharp signals of both monomers and the two broad signals of the polymer chain at 4.75 to 5.05 ppm (–OCH_2R, 6') and at 1.25 to 1.4 ppm a signal caused by the *tert*–butyl group (3'). The solvent signals remained constant during the polymerization and in the relation to these signals the intensity changes of the monomer signals became observable. The same behavior was also noticed during the batch synthesis before, reported in *Section 7.2.1*. In all ^{1}H–NMR–spectra of the semibatch gradient copolymerization the peak areas A of the signals were determined for calculation of the monomer conversion.

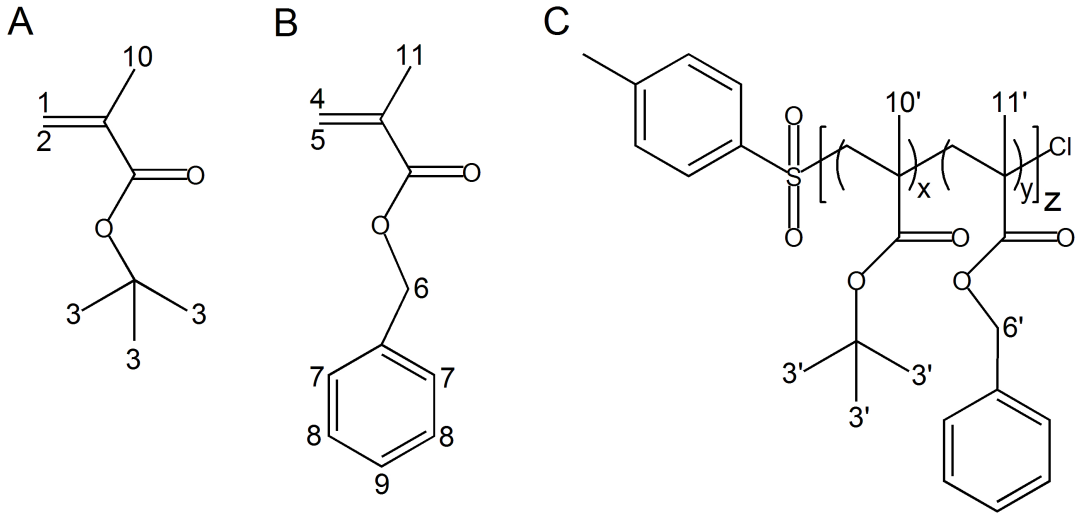

Fig. 8.5.: Molecular structures of the monomers (A) tBMA and (B) BzMA and (C) the copolymer P[tBMA–grad–BzMA] with carbon–atom labels (z = x + y = 1)

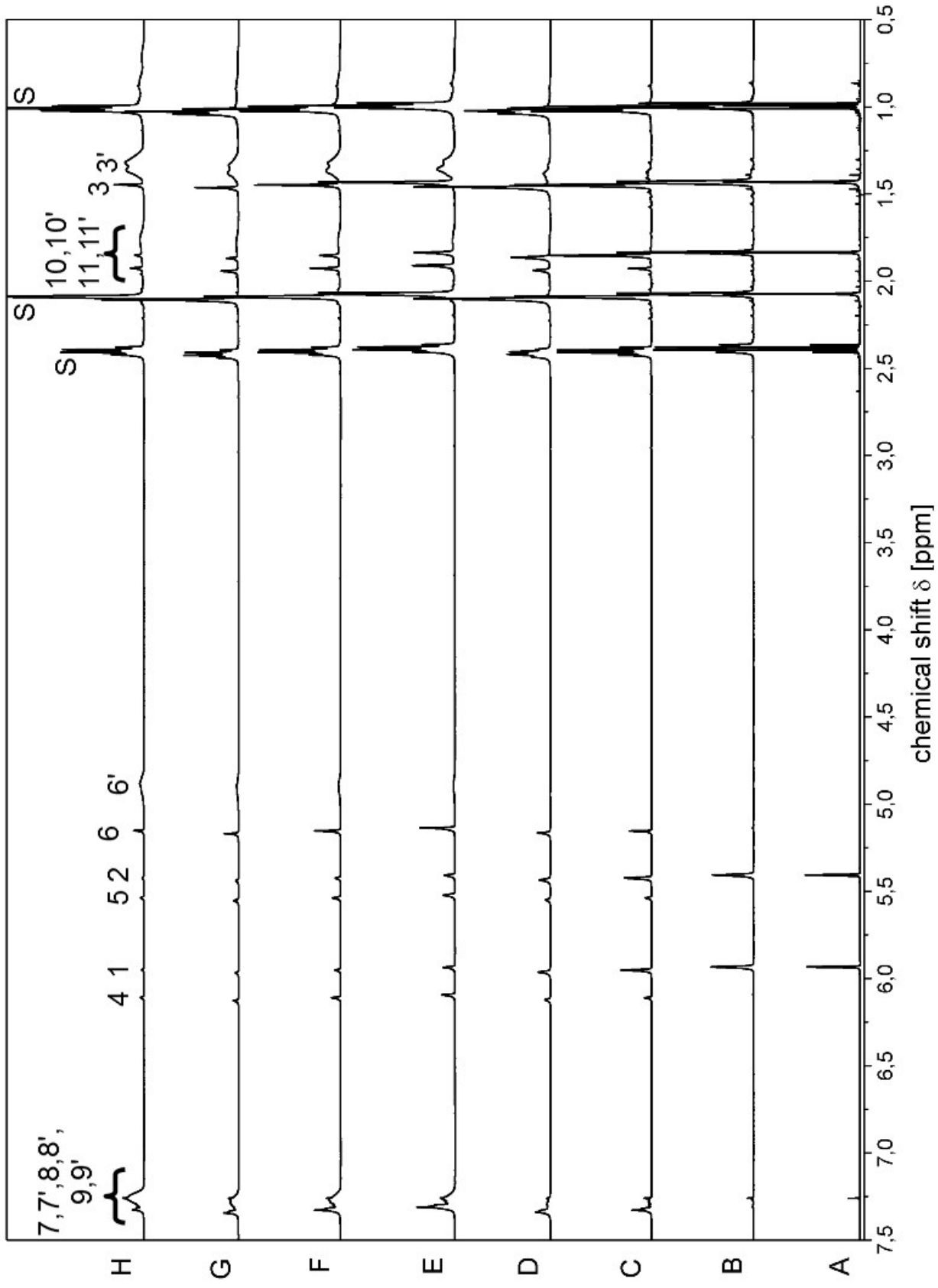

Fig. 8.6.: ^{1}H–NMR–spectra of experiment V101 ($\phi_p = -1$, $f_{tBMA} = 0.5$) after reaction time of A – 0 min, B – 30 min, C – 60 min, D – 90 min, E – 180 min, F – 330 min, G – 450 min, H – 1440 min

The determination of the conversions of the monomers (p_{tBMA} and p_{BzMA}) was done in the same way as for the statistical copolymers in *Section 7.2.1*. To determine of the conversion of BzMA (p_{BzMA}) the integrals of the methylene–group–protons (6, 6') of the monomer (A_6) and that of the polymer ($A_{6'}$) were used, respectively (cf. *Equation 8.2.13*).

$$p_{BzMA} = \frac{A_{6'}}{A_6 + A_{6'}} \tag{8.2.13}$$

with A_6 = integral intensity at 5.15 to 5.2 ppm; $A_{6'}$ = integral intensity at 4.75 to 5.05 ppm

To determine the conversion of the *tert*–butyl methacrylate (p_{tBMA}) the signals (3) of the CH_3–groups of the monomers *tert*–butyl group (A_3) and the signal 3' of the polymer ($A_{3'}$) were taken (cf. *Equation 8.2.14*).

$$p_{tBMA} = \frac{A_{3'}}{A_3 + A_{3'}} \tag{8.2.14}$$

with A_3 = integral intensity at 1.41 to 1.43 ppm; $A_{3'}$ = integral intensity at 1.25 to 1.4 ppm

From the conversion of each monomer the respectively amount of tBMA– and BzMA–units in the polymer chain, $n_{tBMA,P}$ and $n_{BzMA,P}$, are calculated with *Equation 8.2.15*.

$$n_{i,P} = p_i \cdot n_{i,0} \tag{8.2.15}$$

with $n_{i,0}$ representing the amount of monomer i in a solution at the beginning of the polymerization $t = 0$ min

The conversions of the two monomers gave the total monomer conversion p of the whole system.

$$p = \frac{n_{tBMA,P} + n_{BzMA,P}}{n_{tBMA,0} + n_{BzMA,total}} \tag{8.2.16}$$

with $n_{tBMA,P}$ = amount of tBMA inside the polymer chain, $n_{BzMA,P}$ = amount of BzMA inside the polymer chain, $n_{tBMA,0}$ = the amount of tBMA in the stock solution at the beginning of the polymerization $t = 0$ min, $n_{BzMA,total}$ = amount of BzMA in the whole system at the end of the polymerization

The total conversions of the each sample taken during the copolymerization are summarized in *Table 8.4*. A plot of the total conversion p of the semibatch copolymerizations V101 versus the reaction time is depicted in *Figure 8.7*. After a short induction period of about 60 min, the conversion rose linear up to 150 min, then the curve leveled off. After 24 h the conversion reached 86 %.

Tab. 8.4.: ^{1}H–NMR–signal areas and conversions during semibatch–copolymerization V101

time t [min]	A_6	$A_{6'}$	A_3	$A_{3'}$	p_{tBMA}	$n_{tBMA,P}$ [mol]	p_{BzMA}	$n_{BzMA,P}$ [mol]	p
0	0.0000	0.0000	9.4062	0.0000	0.0000	0.0000	–	–	–
15	0.0000	0.0000	9.2463	0.2446	0.0258	0.0017	–	–	–
30	0.0000	0.0000	9.1500	0.3576	0.0376	0.0025	–	–	–
40	1.8546	0.0075	109.7198	5.4143	0.0470	0.0031	0.0040	0.0003	0.0255
50	1.9601	0.0218	58.7244	4.5891	0.0725	0.0048	0.0110	0.0007	0.0417
60	1.9397	0.0493	40.3055	3.5410	0.0808	0.0054	0.0248	0.0016	0.0528
70	1.9810	0.0539	30.8116	4.2860	0.1221	0.0081	0.0265	0.0017	0.0743
80	2.0080	0.1468	24.4559	4.5528	0.1570	0.0104	0.0681	0.0043	0.1125
90	1.9990	0.3222	20.6631	5.7063	0.2164	0.0144	0.1388	0.0088	0.1776
120	1.9598	0.4600	13.2861	7.0341	0.3462	0.0230	0.1901	0.0120	0.2681
150	1.9781	0.7591	10.1434	8.2177	0.4476	0.0297	0.2773	0.0175	0.3624
180	2.2052	1.0019	9.4759	9.6520	0.5046	0.0335	0.3124	0.0197	0.4085
210	2.5078	1.3808	9.5124	11.8201	0.5541	0.0368	0.3551	0.0224	0.4546
270	2.9209	2.3737	9.5988	16.7431	0.6356	0.0422	0.4483	0.0283	0.5420
330	3.1632	3.2613	9.7836	21.3357	0.6856	0.0455	0.5076	0.0321	0.5966
390	3.3022	4.1189	9.8353	24.5922	0.7143	0.0474	0.5550	0.0351	0.6347
450	3.2809	4.8772	9.9388	28.8275	0.7436	0.0494	0.5978	0.0378	0.6707
1440	3.6480	17.2825	10.8227	85.0253	0.8871	0.0589	0.8257	0.0522	0.8564

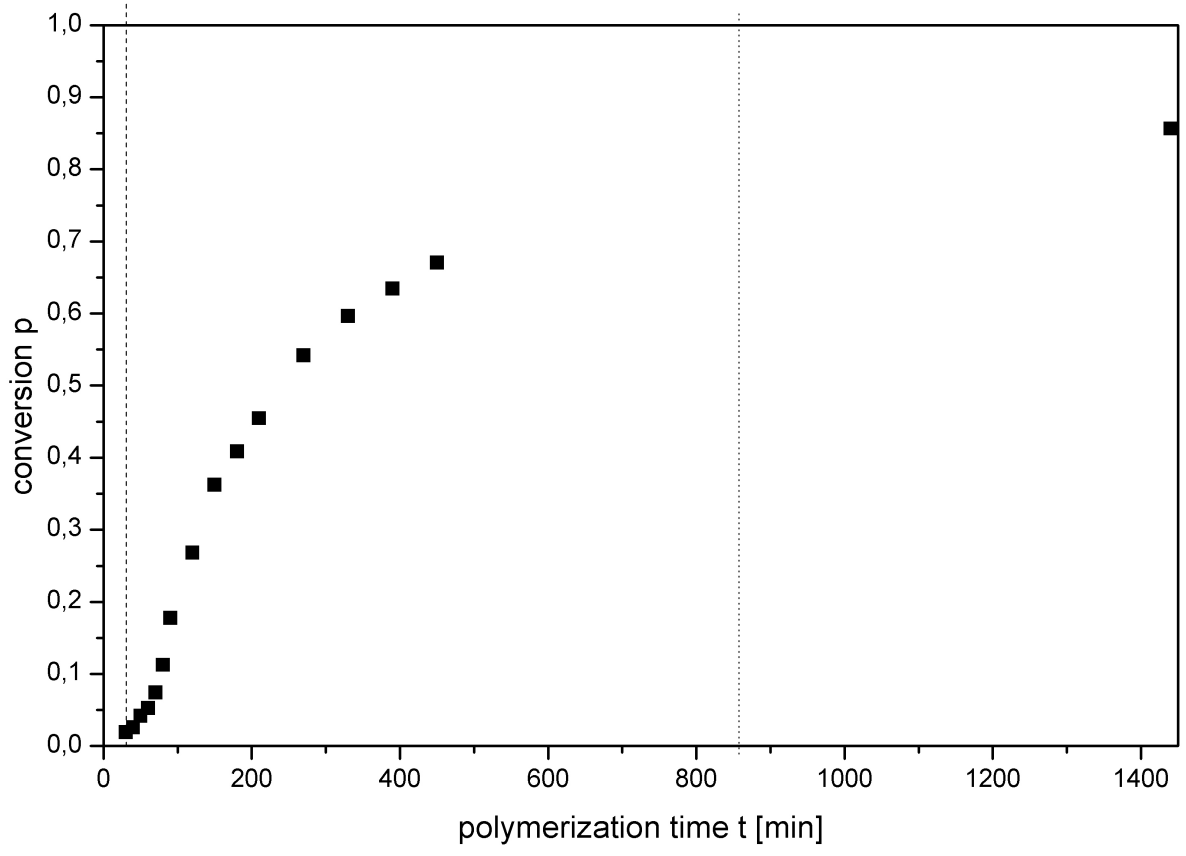

Fig. 8.7.: Conversion p of experiment V101 (ϕ_p = −1, f_{tBMA} = 0.5); dashed line – start of feed–solution–injection, dotted line – end of feed–solution–injection

With these results the cumulative and the instantaneous compositions of the gradient copolymer (F_{cum} and F_{inst}) were determined as well as their change during the polymerization, with help of *Equations 8.2.17* and *8.2.18*.

$$F_{cum}^{tBMA}(p) = \frac{1}{1 + \frac{n_{BzMA,P}}{n_{tBMA,P}}} \tag{8.2.17}$$

$$F_{inst}^{tBMA}(p) = F_{cum}^{tBMA}(p) + p \cdot \frac{\Delta F_{cum}^{tBMA}(p)}{\Delta p} \tag{8.2.18}$$

The results of these calculations applied to the semibatch synthesis are listed in *Table 8.5* and depicted in the *Figures 8.8* and *8.9* (composition/time plot) and *Figures 8.10* and *8.11* (composition/conversion plot).

One of the calculated values of the instantaneous composition ($t = 40\,min$, F_{inst} [a]) was higher than 1. This result must be chemical erroneous because the molar fraction of a monomer in a copolymer must be between 0 and 1. The incorrect data point is indicated by an arrow in the *Figures 8.9* and *8.11*. The value at $t = 120\,min$ differed so strong that it was not used in the analysis of the cumulative compositions. The point is shown with brackets in *Figures 8.8* and *8.10*. Beside this the compositional curves of the polymerization was consistent. However, the slope of the compositional curve was not consistent.

Tab. 8.5.: Kinetic results and compositions of the different copolymer compositions of experiment V101

time t [min]	p	F_{cum}	F_{inst} [a]	F_{inst} [b]	F_{inst} [c]
30	–	1.0000	1.0000	0.9489	0.9912
40	0.0255	0.9246	3.4302	0.8554	0.9127
50	0.0417	0.8738	0.7904	0.7607	0.8544
60	0.0528	0.7739	0.1374	0.6308	0.7494
70	0.0743	0.8289	0.9276	0.6275	0.7943
80	0.1125	0.7076	0.3159	0.4026 0.6815	0.6553
90	0.1776	0.6209	0.3618	0.5797	0.5383
120	0.2681	0.6567	0.7308	0.5946	0.5320
150	0.3624	0.6290	0.5300	0.5450	0.4603
180	0.4085	0.6292	0.6307	0.5345	0.4391
210	0.4546	0.6211	0.5468	0.5157	0.4096
270	0.5420	0.5983	0.4467	0.4726	0.3461
330	0.5966	0.5866	0.4468	0.4483	0.3089
390	0.6347	0.5749	0.3153	0.4277	0.2795
450	0.6707	0.5665	0.3754	0.4110	0.2544
1440	0.8564	0.5302	0.3137	0.3316	0.1317

[a] calculated by *Eq. 8.2.18*
[b] calculated by *Eq. 8.2.22*
[c] calculated by *Eq. 8.2.22* with average slope

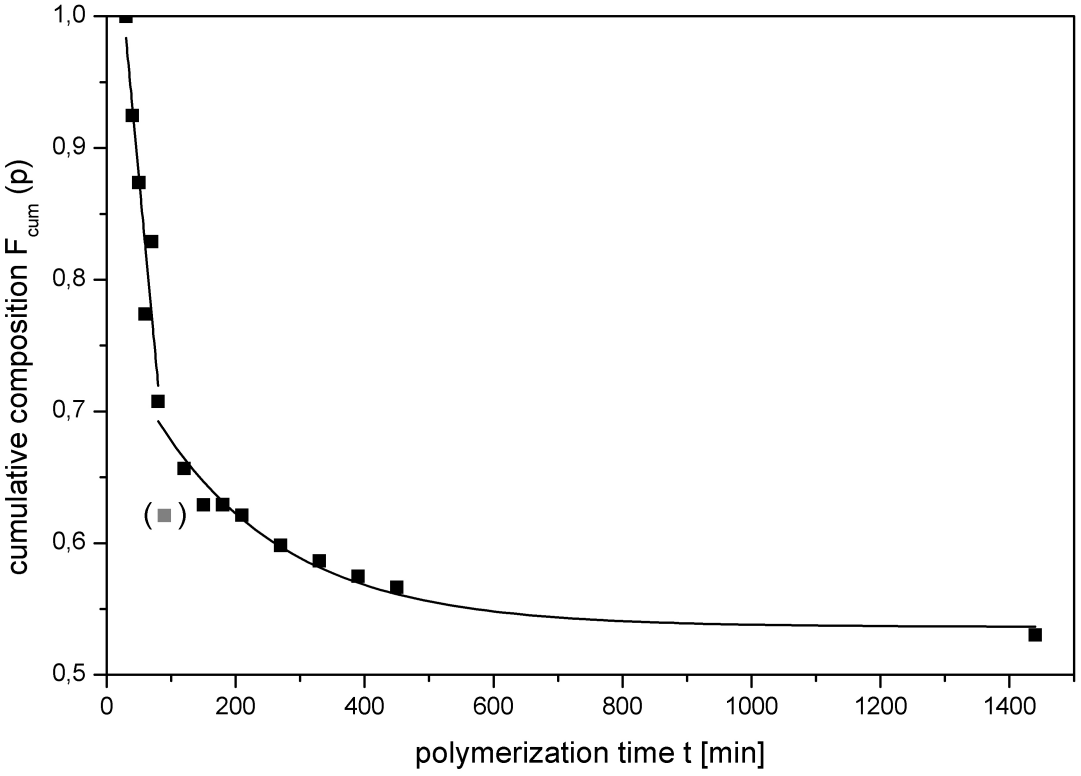

Fig. 8.8.: Plot of the cumulative compositions F_{cum} of gradient copolymer V101 ($\phi_p = -1$, $f_{tBMA} = 0.5$) versus the reaction time t (unconsidered value in brackets)

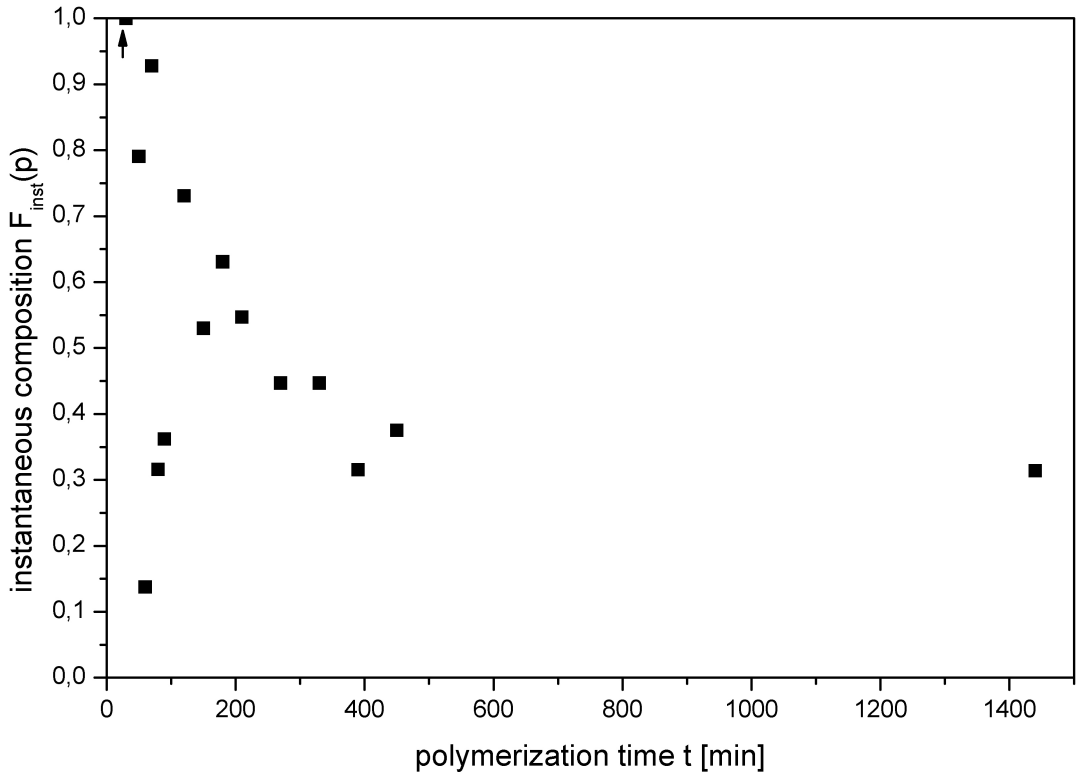

Fig. 8.9.: Plot of the instantaneous compositions F_{inst} of gradient copolymer V101 ($\phi_p = -1$, $f_{tBMA} = 0.5$) versus the reaction time t (obtained with *Eq. 8.2.18*; chemical incorrect value indicated with arrow)

The cumulative composition as a function of the polymerization time first reduced strongly but fairly linear in time up to 80 min and then leveled off exponentially. F_{cum} is proportional to the conversion ($F_{cum} = \alpha \cdot p$), hence F(t) cannot become time–linear. The two decreases are described with the *Equations 8.2.19* and *8.2.20*.

$$F_{cum}^{tBMA}(p_{<80min}) = (1.1420 \pm 0.0546) - (0.0053 \pm 0.0009) \cdot t \tag{8.2.19}$$

$$F_{cum}^{tBMA}(p_{\geq 80min}) = (0.5365 \pm 0.0096) + (0.2325 \pm 0.0194) \cdot e^{(-0.0050 \pm 0.0008) \cdot t} \tag{8.2.20}$$

The resulting polymer had a cumulative composition which was slightly higher than the theoretically expected value of 0.5. The calculation of the instantaneous composition $F_{inst,tBMA}$ of the gradient copolymers by means of *Equation 8.2.18* gave scattering values, see *Figure 8.9*. This result was not very surprising. In *Equation 8.2.18* the differential quotient $(dF_{cum}/dp)_p$ was approximated by the differential quotient:

$$\frac{\Delta F_{cum}}{\Delta p} = \frac{F_{cum}^{i+1} - F_{cum}^{i}}{p^{i+1} - p^{i}} \tag{8.2.21}$$

This is a very crude approximation, which is known to be very sensitive to even small experimental errors in F_{cum} and p. Since the experimental error of the ^{1}H–NMR based on the determination of F_{cum} and p is between 5–10 %, the difference quotient calculation strongly amplified the deviations, an results in heavy scattering of the obtained instantaneous compositions, F_{inst}. To overcome the described problem, a second strategy of data evaluation was tried: It was attempted to fit a sufficient analytical function to the cumulative composition $F_{cum}(p)$. This function can smoothly be derived and the respective derivative $dF_{cum}^{(fit)}/dp$ can be used to calculate the instantaneous composition $F_{inst}(p)$ (cf. *Equation 8.2.22*).

The plot of the cumulative compositions as a function of the conversions p, is shown in *Figure 8.10*. The curve consists of two linear segments of considerable different slope. Up to a monomer conversion of 11 % the cumulative composition decreased with a slope of $s_1 = dF_{cum}/dp = -2.7105 \pm 0.6685$, while the second segment of the plot exhibited a slope $s_2 = -0.2319 \pm 0.0091$ ($p = 0.11 \ldots 0.85$). The value of conversion at which the slope changed will be called "changing point" (P_c) in the subsequent text. Hence, the curve $F_{cum}(p)$ can be well approximated by two linear functions of slope $s_i = (dF_{cum}/dp)^{(fit)}$ ($i = 1 : p < 0.11$, $i = 2 : 0.11 < p < 0.85$). In *Table 8.6* the two slopes and also the average slope are listed.

The instantaneous tBMA molar fraction of the copolymer was calculated by means of *Equation 8.2.22*, using slope s_1 in the conversion interval $p \in [0, 0.11]$ and slope s_2 with $p \geq [0.11]$.

$$F_{inst}^{tBMA}(p) = F_{cum}^{tBMA}(p) + p \cdot \left(\frac{dF_{cum}^{tBMA}(p)}{dp} \right)_i^{(fit)} \tag{8.2.22}$$

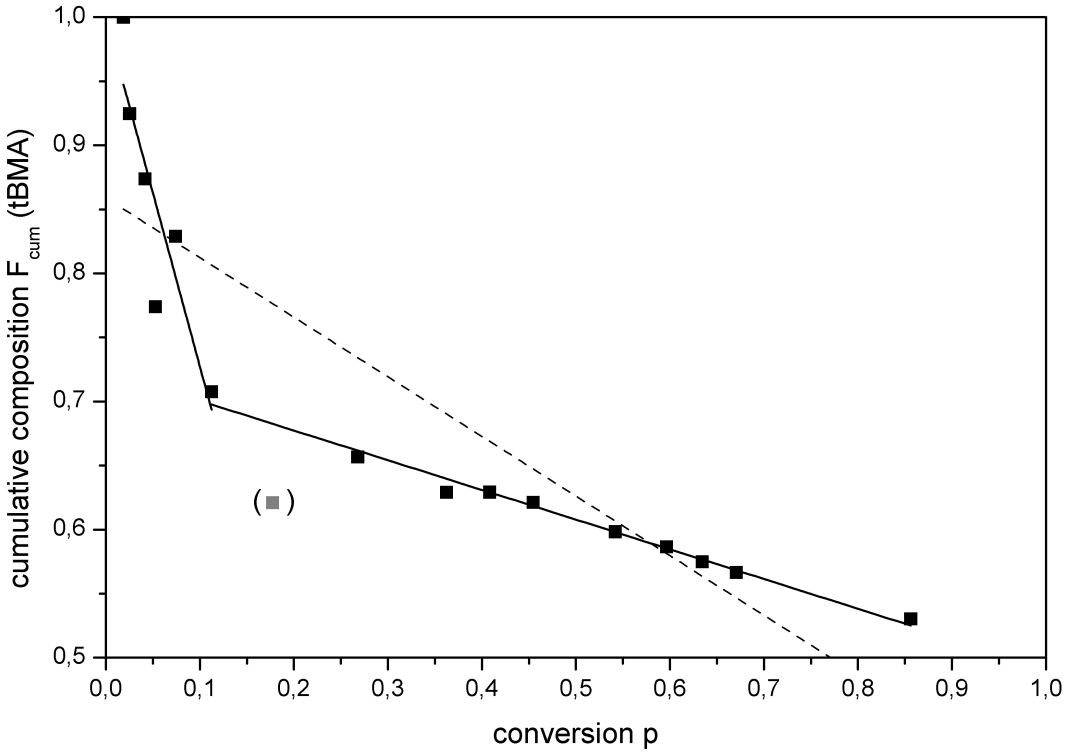

Fig. 8.10.: Plot of the cumulative compositions F_{cum} of gradient copolymer V101 ($\phi_p = -1$, f_{tBMA} = 0.5) versus the conversion p; dashed line – average slope; unconsidered value in brackets

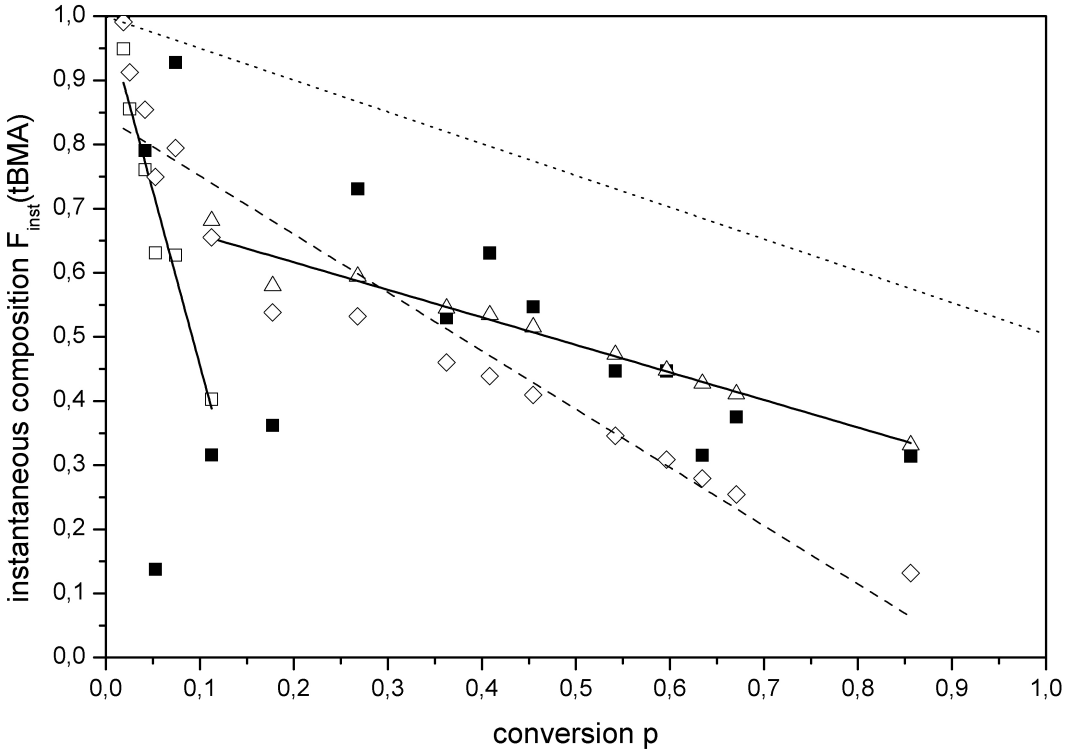

Fig. 8.11.: Plot of the instantaneous compositions F_{inst} of gradient copolymer V101 ($\phi_p = -1$, f_{tBMA} = 0.5) versus the conversion p; ■ F_{inst} calculated by *Equation 8.2.18*, □ F_{inst} calculated by *Equation 8.2.22*, △ F_{inst} calculated by *Equation 8.2.22* with average slope of F_{cum}; dashed line – average slope; dotted line – ideal run of the curve

Hence, for P_c two instantaneous compositions were calculated. Furthermore the instantaneous composition was calculated with the average slope of the cumulative composition and *Equation 8.2.22*. The results of the calculations of $F_{inst}(p)$ with the *Equations 8.2.18* and *8.2.22* are summarized in *Table 8.5* and the values are plotted in the *Figure 8.11*.

Like in *Figure 8.9* the data points, resulting from *Equation 8.2.18* scattered strongly. The reason was the described amplification of the compositional errors by numeric derivation like the one of the instantaneous composition. The instantaneous compositions which were calculated from *Equation 8.2.22* scattered less than the ones obtained with *Equation 8.2.18*, both the values calculates by the slopes s_1 and s_2 and the values calculated by the average slope. The resulting $F_{inst}(p)$ values from *Equation 8.2.22* show also two slopes with a "changing point" at $P_c \approx 0.11$. The equation of the fits are given in the *Equation 8.2.23*. The slopes of the fits are given in *Table 8.6*.

$$F_{inst}^{tBMA} = 1 - \phi_{p,i} \cdot p \tag{8.2.23}$$

with F_{inst}^{tBMA}= instantaneous molar fraction of tBMA in the gradient copolymer, p = total monomer conversion

The final F_{inst}^{tBMA} value was lower than the target composition of 0.5 (see *Figure 8.11*, dotted line). However, the polymer can be described by an average gradient of $\phi_{p,av} \approx -0.91$ that is calculated by means of *Equation 8.2.22*, using the average slope of the whole $F_{cum}(p)$–curve ($s_{av} = -0.47$). Since however, these averages may cause misleading interpretations, the gradient copolymer V101 will be denamed as $GP_{0.43}$, referring to the $\phi_{p,2} \approx -0.43$ that dominates the polymer chain. Due to the binary slope the resulting compositions differed strongly from the target value of -1.0 and due to the binary slopes the copolymer can be described as "double gradient". As a result the physical properties of the gradient copolymer are determined by the main gradient $\phi_{p,2}$.

Tab. 8.6.: Slopes of decreases of cumulative and instantaneous compositions against composition of experiment V101

$\phi_{p,target}$	p	$s_i = \frac{dF_{cum}}{d_p}$	$\phi_p = \frac{dF_{inst}}{dp}$	$\Delta\phi_p$
-1.0	0.00 ... 0.11	-2.7105 ± 0.6685	-5.4210 ± 0.6685	
	0.11 ... 0.85	-0.2319 ± 0.0091	-0.4292 ± 0.0262	-57 %
	0.00 ... 0.85	-0.4654 ± 0.0654	-0.9094 ± 0.0728	-9 %

The observed dependence of the compositional data from the monomer conversion suggested that the injection of the second monomer BzMA into the ATRP system of the initiator pTSC, the ligand PMDETA, the catalyst $Cu^{I}Cl/Cu^{II}Cl$ and the first monomer tBMA disturbed the equilibrium of the system. This kinetic effect could not be seen before in the batch experiments because there the monomer mixture ($n_{i,S}$, $n_{i,P}$, i = BzMA, tBMA) started in equilibrium. It

can be seen from the composition–time data that the ATRP system required around 75 min until a new transient equilibrium was build up again. After this time the mixing ratio deviated from the assumptions which were used for the calculations of the injection program, hence the feed program did not fit to the existing monomer mixture. The fact that the feed solution had not the same temperature than the stock solution could also contribute to the disorder of the equilibrium. In further experiment the use of a heating bath would be useful. Other problems like contamination of the monomer with 4–methoxyphenol (the inhibitor which used for the storage of the monomers) or oxygen can be excluded, because these contaminants were eliminated by the filtration of the monomer over an excess of aluminium oxide and the performed freeze–melt–cycles. To solve this problem two way are possible: The complex–equilibrium can be introduced into the model of the injection program. The second way is to employ empirical relation of monomer feed. That means to test and change the feed program until it fits to the equilibrium changes of the monomer mixture.

Comparison of Kinetic Results from Semibatch Copolymerizations of nBMA/tBMA and BzMA/tBMA

In the following paragraph the results of the kinetic analysis of the experiments V31 (P[tBMA–grad–nBMA] $GP_{0.53}$) and V101 (P[tBMA–grad–BzMA] $GP_{0.43}$), both with f_{tBMA} = 0.5, respectively $\phi_p = -1.0$, of the semibatch copolymerizations are compared. In *Figure 8.12* the conversions of the two experiments are depicted.

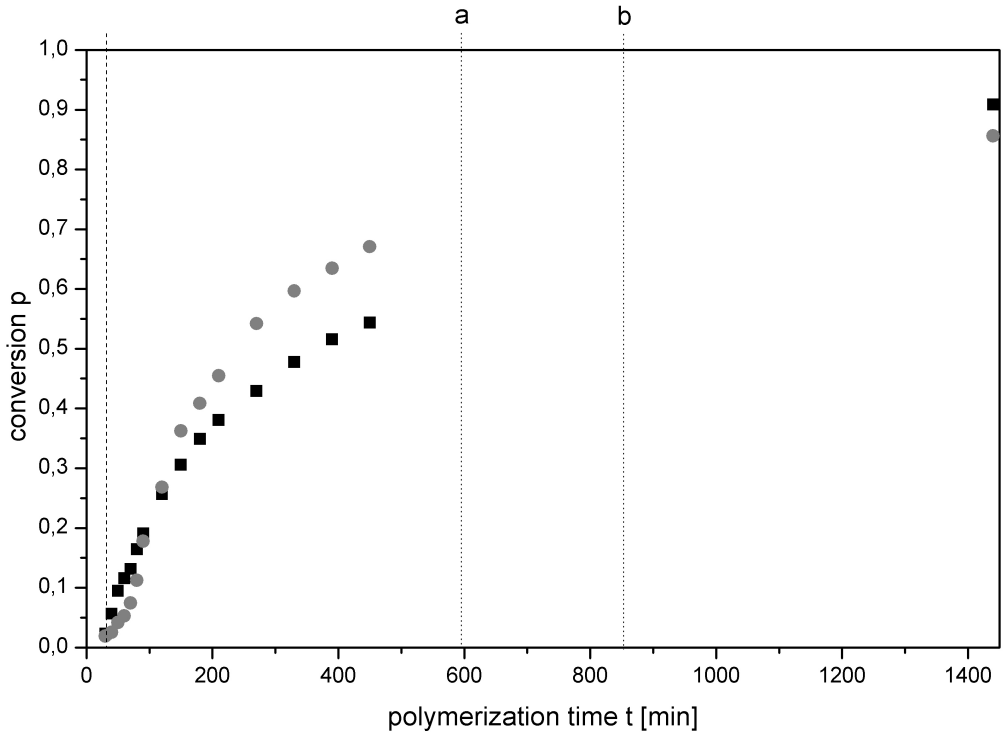

Fig. 8.12.: Conversion p of experiment P[tBMA–grad–nBMA] $GP_{0.53}$ (■, V31) and P[tBMA–grad–BzMA] $GP_{0.43}$ (●, V101); dashed line – start of feed–solution injection, dotted lines – end of feed–solution–injection – a V31, b V101

In the semibatch copolymerization V31 the conversion was linear up to 120 min. Then the curve leveled off. The reaction reached a final conversion of 91 % after 24 h. The conversion of the semibatch copolymerization V101 showed a short induction period of about 60 min, then the conversion rose linear up to 150 min, and finally the curve also leveled off. After 24 h the conversion reached 86 %.

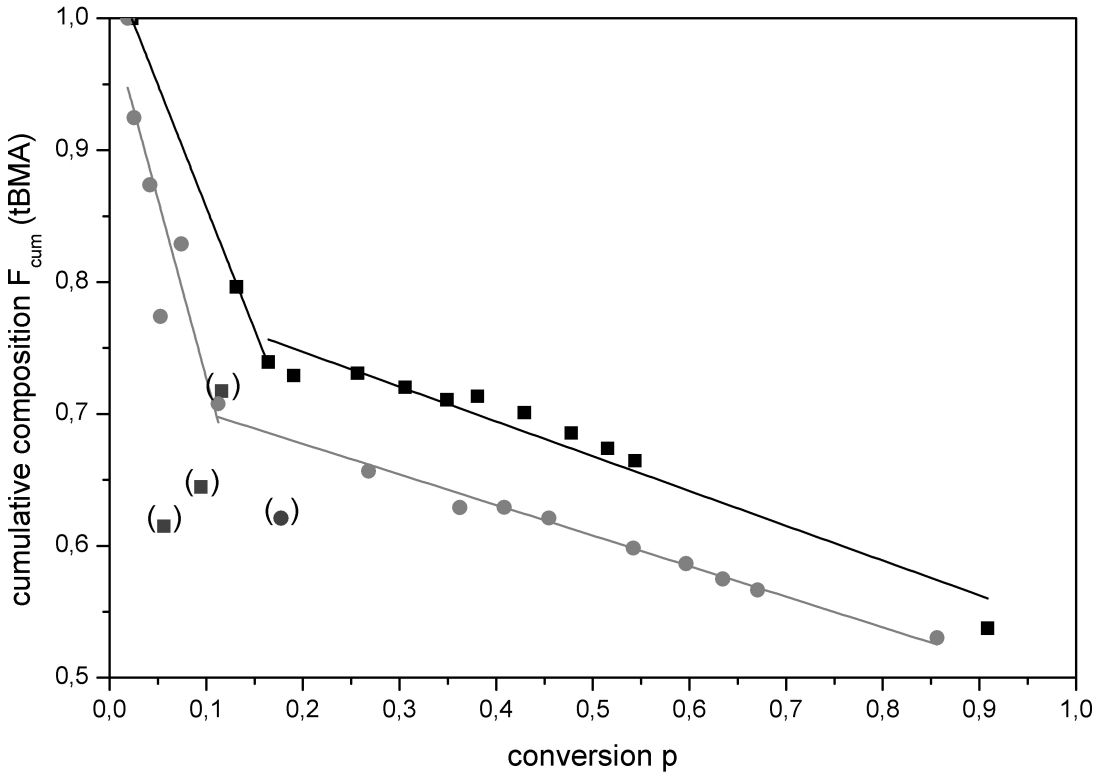

Fig. 8.13.: Plots of cumulative compositions F_{cum} of P[tBMA–grad–nBMA] $GP_{0.53}$ (■, V31) and P[tBMA–grad–BzMA] $GP_{0.43}$ (●, V101) against conversion p (unconsidered values in brackets)

In *Figure 8.13* the cumulative compositions are plotted against the conversion for the two monomer systems. The slope s_1 of the F_{cum}–values of copolymer $GP_{0.43}$ ($s_1 = -2.71 \pm 0.04$) was higher than s_1 of the values of $GP_{0.53}$ ($s_1 = -1.86 \pm 0.03$). The "chaning point" in the curves laid at $P_c = 0.16$ for $GP_{0.53}$ and at $P_c = 0.11$ for $GP_{0.43}$. In contrast the slope s_2 of the values of $GP_{0.43}$ ($s_2 = -0.23 \pm 0.01$) was lower than s_2 of the values of $GP_{0.53}$ ($s_2 = -0.26 \pm 0.02$). Since the concentrations and the conditions of the reactions were the same the differences of the cumulative compositions depend the different monomer compositions with tBMA– and nBMA–units in $GP_{0.53}$ and tBMA– and BzMA–units in $GP_{0.43}$.

The plot of the values of the instantaneous compositions F_{inst} against the conversion p of the two experiments are shown in *Figure 8.14*. Due to the fact that the values of the instantaneous compositions were calculated from the values and the slopes of the cumulative compositions, the differences of the values of F_{cum} were amplified at the values and the slopes of the instantaneous compositions of the two gradient copolymers.

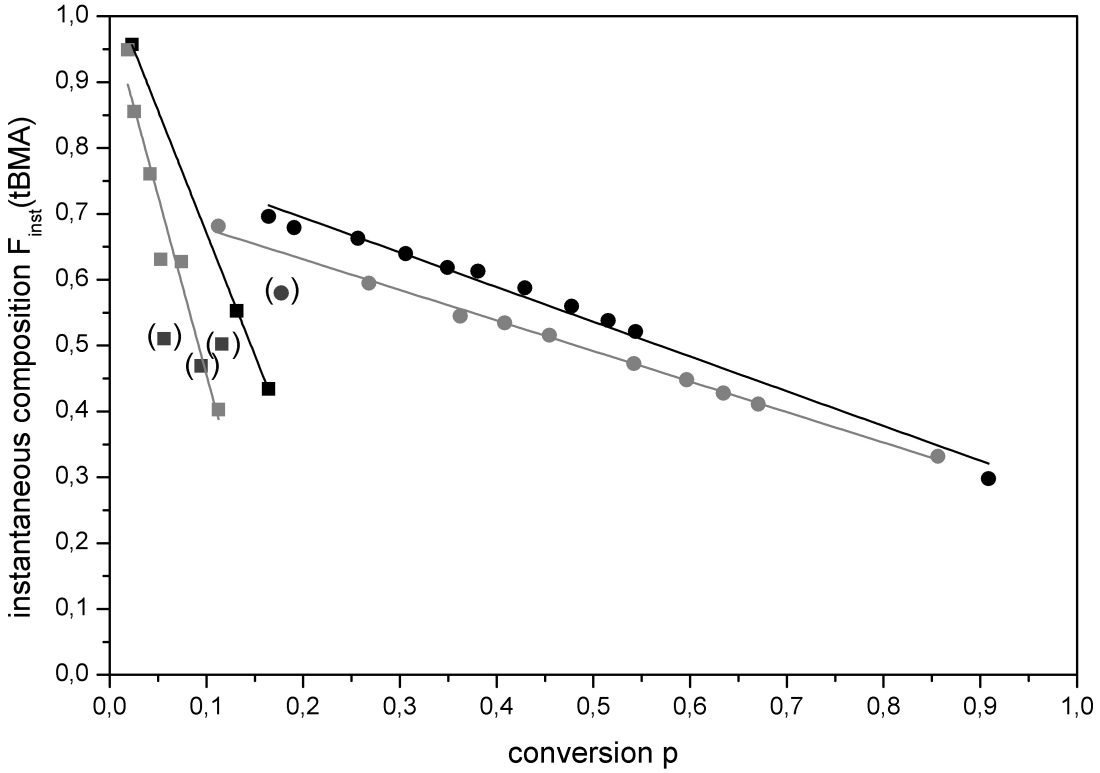

Fig. 8.14.: Plots of instantaneous compositions F_{inst} of (■) P[tBMA–grad–nBMA] $GP_{0.53}$, f_{tBMA} = 0.5, and (●) P[tBMA–grad–BzMA] $GP_{0.43}$, f_{tBMA} = 0.5 against conversion p (unconsidered values in brackets)

The overall process of the cumulative and the instantaneous compositions of the two semibatch copolymerizations were nearly the same. The different values result from the different kinetic behavior of nBMA and BzMA. Despite the differences both semibatch copolymerizations gave "double gradients". The main part of the gradient structure of both copolymers is represented by $\phi_{p,2}$. Thereby the physical behavior of the gradient copolymer is determined by $\phi_{p,2}$.

8.2.3. Structural Analysis

As described with the batch polymerizations in *Section 7.2.2* the purity and the composition of the resulting copolymers were analyzed by means of elementary analysis. The results of the measurements and the differences between the theoretical and the analysis results are listed in *Table 8.7*.

The element compositions of the statistical copolymers (cf. *Tables 7.7* and *7.8*) and the gradient copolymers were nearly similar. Hence, both copolymerization method, batch and semibatch, gave consistent results. Moreover, the differences between the theoretical compositions and the measured values were small, expect the sample t = 60 min, indicating that the samples were free of pollution.

Tab. 8.7.: Results of the elementary analysis of the samples taken during experiment V101 ($GP_{0.43}$, $f_{tBMA} = 0.5$) with divergence from the set point

time [min]	F_{cum}		C [%]	ΔC	H [%]	ΔH	O [%]	ΔO
60	0.77	theory	69.54		9.11		21.35	
		is	67.72	-1.82	8.38	-0.74	23.91	2.56
90	0.62	theory	70.76		8.61		20.63	
		is	68.86	-0.68	8.46	-0.65	22.68	1.34
150	0.63	theory	70.70		8.63		20.67	
		is	70.51	0.97	8.05	-1.06	21.44	0.10
210	0.62	theory	70.76		8.61		20.63	
		is	70.51	0.97	7.81	-1.30	21.68	0.33
330	0.59	theory	71.02		8.50		20.48	
		is	71.04	1.50	7.75	-1.36	21.21	-0.14
450	0.57	theory	71.18		8.43		20.39	
		is	70.87	1.33	7.73	-1.38	21.40	0.05
1440	0.53	theory	71.45		8.32		20.23	
		is	71.08	1.54	7.81	-1.30	21.11	-0.23

As well as for the statistical copolymers also for the gradient copolymers the data from elementary analysis were used to calculated the composition of the polymers. The fitted calibration curves from the amount of carbon and hydrogen, see *Section 7.2.2, Figure 7.13*, were adapted for the calculations. That was necessary because the equations were established for the amount of BzMA inside the polymer–chain F_{BzMA} and the composition of the gradient copolymers was described by the amount of tBMA inside the polymer–chain F_{tBMA}. So for the determination of the compositions from the amount of carbon *Equation 8.2.24* was used and for the determination from the amount of hydrogen *Equation 8.2.25*.

$$F_{tBMA} = 1 - \frac{C - 0.6757}{0.0741} \tag{8.2.24}$$

$$F_{tBMA} = 1 - \frac{H - 0.0992}{-0.0306} \tag{8.2.25}$$

The results of the calculations are given in *Table 8.8*.

The compositions $F_{tBMA}^{EA,H}$ calculated by the amount of hydrogen which was measured by elementary analysis differed obviously from the compositions which were determined from the ^{1}H–NMR–spectra of the precipitated copolymers. The composition which were calculated from the amount of carbon differed strongly only for the first two samples taken after 60 min and 90 min of reaction time. The calculations with the measured carbon amount from other five samples gave compositions that fitted good with the compositions calculated from ^{1}H–NMR–spectra. So for higher conversions the amount of carbon measured by elementary analysis is also a possibility to calculate the composition of the copolymers.

Tab. 8.8.: Compositions of copolymers of experiment V101 ($GP_{0.43}$, $f_{tBMA} = 0.5$) resulting from ^{1}H–NMR–analysis and elementary analysis

time [min]	$F^{NMR\ a}_{tBMA}$	$F^{EA,C\ b}_{tBMA}$	$\Delta F^{C}_{tBMA}{}^{c}$	$F^{EA,H\ d}_{tBMA}$	$\Delta F^{H}_{tBMA}{}^{c}$
60	0.77	0.98	0.21	0.50	-0.28
90	0.62	0.83	0.21	0.52	-0.10
150	0.63	0.60	-0.03	0.39	-0.24
210	0.62	0.60	-0.02	0.31	-0.31
330	0.59	0.53	-0.05	0.29	-0.30
450	0.57	0.55	-0.01	0.28	-0.28
1440	0.53	0.53	0.00	0.31	-0.22

[a] calculated from ^{1}H–NMR–spectra; [b] calculated from *Eq. 8.2.24*
[c] $\Delta F^{x}_{tBMA} = F^{EA,x}_{tBMA} - F^{NMR}_{tBMA}$; [d] calculated from *Eq. 8.2.25*

The differences between the values from the hydrogen amount and the NMR–measurements could not be caused by a solvent like water because the compositions calculated from the hydrogen amount were to low and the ^{1}H–NMR–spectra did not show the presence of residual solvents. Also the presence of monomers in the sample could falsify the measures amount but even they were not monitored in the NMR–spectra. An other possible problem could be that the samples were inhomogeneous. For a NMR–measurement 10 mg of the copolymer was used, for an EA–measurement only 2.5 mg. So the problem of an inhomogeneous substance will be increase at the elementary analysis. But the resulting copolymers were apparently consistent. A third possibility is that the pollution happened during the measurement itself. The measurement of standards in periodical intervals should avoid that.

Subsequently the copolymers P[tBMA–grad–BzMA] were investigated with ATR–FTIR–spectroscopy. From all samples which were taken during the semibatch copolymerization IR–spectra were measured and analyzed in view to the peak height and peak area of the two vibrational bands, at 850 cm^{-1} (*band 1*), specific for the *tert*–butyl–group, and at 730 cm^{-1} (*band 2*), caused by the benzyl–group. The values are summarized in *Table 8.9.*

Tab. 8.9.: Peak area and peak height of the analyzed ATR–FTIR–bands the samples taken during experiment V101 ($GP_{0.43}$, $f_{tBMA} = 0.5$)

	band 1		*band 2*	
time [min]	peak area [cm^{-1}]	peak height	peak area [cm^{-1}]	peak height
60	4.10	0.301	5.18	0.207
90	4.37	0.317	6.97	0.270
150	4.22	0.297	8.84	0.322
210	3.32	0.248	9.02	0.331
330	3.75	0.269	10.37	0.383
450	3.75	0.267	10.98	0.392
1440	3.78	0.266	10.83	0.378

For the comparison purposes the spectra were normalized by setting the adsorption intensity of the vibrational band at 1134 cm^{-1} to one by dividing all intensities A_x by A_1. In *Figure 8.15* the fingerprint region of the samples of experiment V101 $GP_{0.43}$ (f_{tBMA} = 0.5) and in *Figure 8.16* an extended section of the spectra from 700 to 900 cm^{-1} are shown to demonstrate the changes of the vibrational bands during the polymerization time more in detail. For *band 1* at 850 cm^{-1} the increase of the band was clearly recognizable. The decease of *band 2* at 730 cm^{-1} during the polymerization was, however, minimal. The incorporation of the BzMA, which was injected during the polymerization, inside the polymer chain lead to a constantly change of the composition of the copolymer and caused the rise of *band 2*.

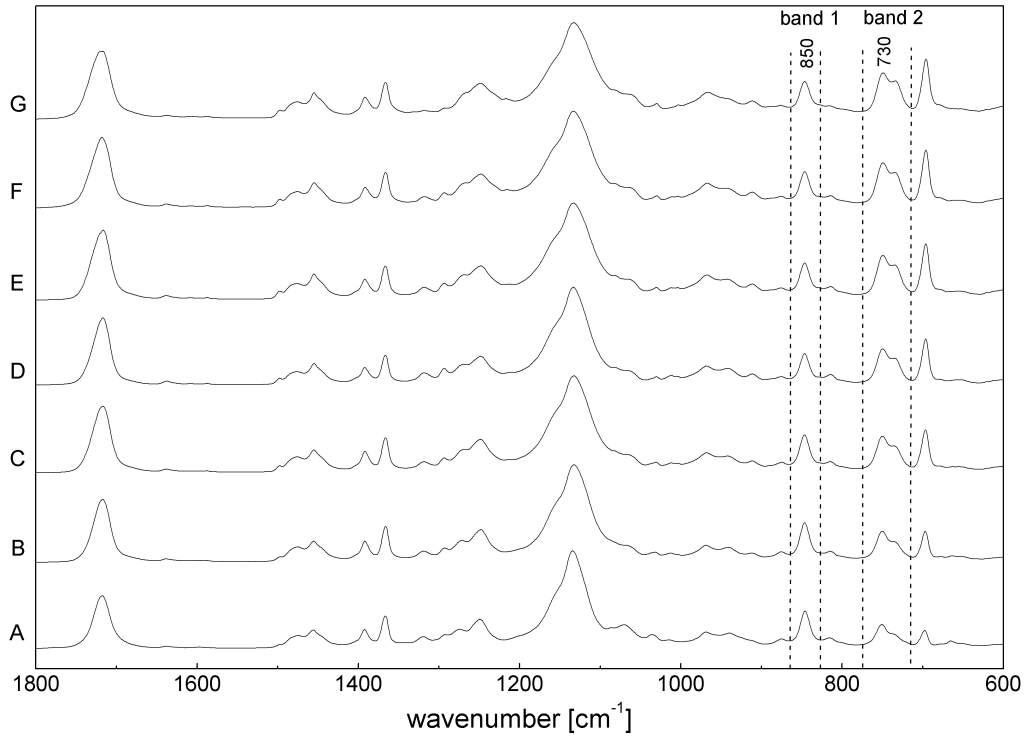

Fig. 8.15.: Finger print region of ATR–FTIR – spectra of samples of experiment V101 ($GP_{0.43}$, f_{tBMA} = 0.5); A – 60 min, B – 90 min, C – 150 min, D – 210 min, E – 330 min, F – 450 min and G – 1440 min of reaction time (Spectra normalized to A_{1134} = 1)

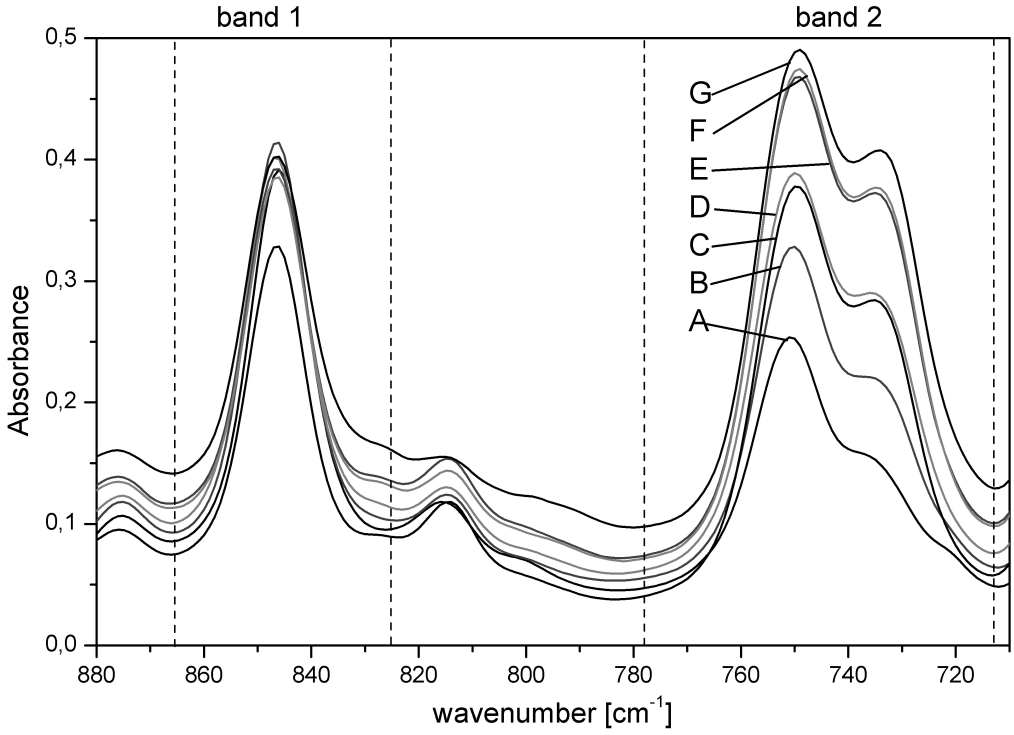

Fig. 8.16.: Section of ATR–FTIR–spectra of samples taken during experiment V101 ($GP_{0.43}$, f_{tBMA} = 0.65) with analyzed specific vibrational bands; A – 60 min, B – 90 min, C – 150 min, D – 210 min, E – 330 min, F – 450 min and G – 1440 min of reaction time (Spectra normalized to A_{1134} = 1)

The changes of *band 1* were smaller during the polymerization time which must be attributed to a different extinction coefficient of the tBMA–units. Because the total amount of tBMA was present at the start of the synthesis the change was caused by the tBMA depletion of the solution. The IR–signal qualitatively support the NMR results.

The *Figures 8.17* and *8.18* depict the peak areas and peak heights of the two bands of the samples taken during the semibatch copolymerization. The *band 1* values of the peak area slightly decreased. Up to 200 min of reaction time the values scattered. The values of the peak area of *band 2* increased exponentially. The run of the values of the peak height gave similar results. For *band 1* the values decreased exponentially and for *band 2* there was an exponential increase. The values confirmed the observations from the *Figure 8.16*. Hence the peak height of *band 2* was used to determine the composition of the copolymer by a modified *Equation 7.2.20*, see *Equation 8.2.26*. The change was necessary because with *Equation 7.2.20* F_{nBMA} was calculated. The obtained compositions were compared with the cumulative compositions $F_{cum,tBMA}$ originating from the ^{1}H–NMR analysis.

$$F_{tBMA} = 1 - [(0.171 \pm 0.192) - (1.618 \pm 1.173) \cdot PH_2 + (5.233 \pm 1.610) \cdot PH_2^2] \qquad (8.2.26)$$

with F_{tBMA} = composition of the copolymer, PH_2 = peak height of *band 2*

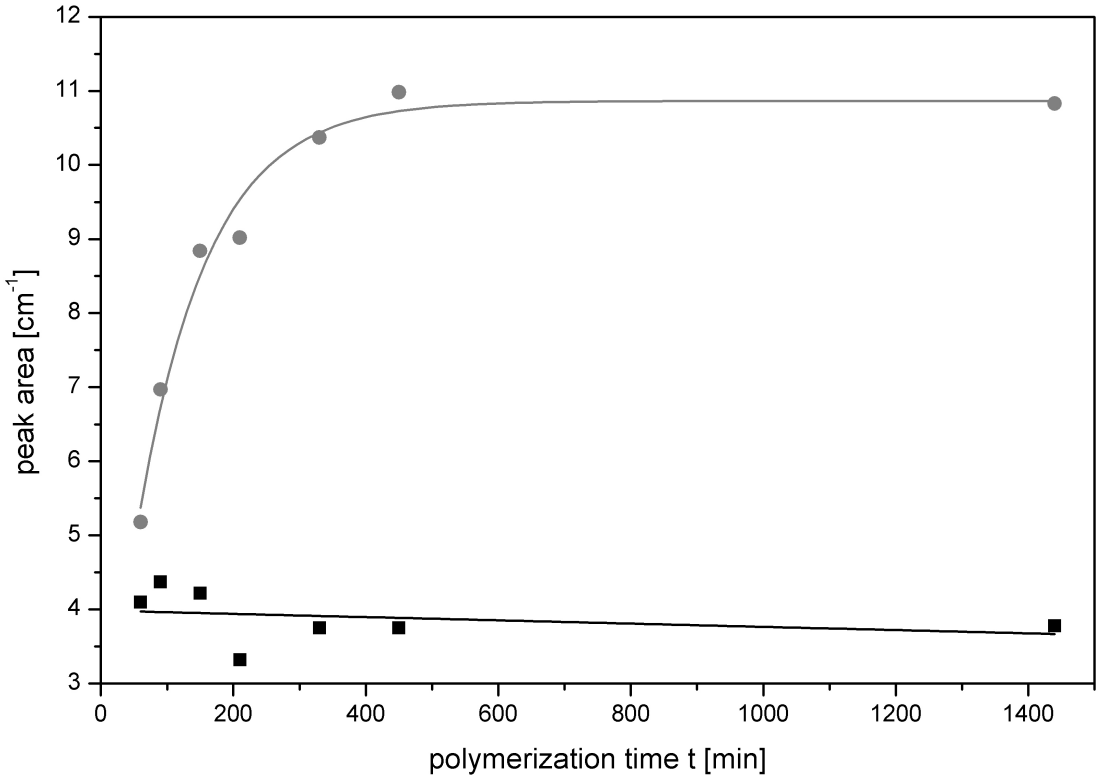

Fig. 8.17.: Plot of peak areas of ATR–FTIR–spectra *band 1* (■) and *band 2* (●) of P[tBMA–grad–BzMA] $GP_{0.43}$ (f_{tBMA} = 0.65) versus polymerization time t

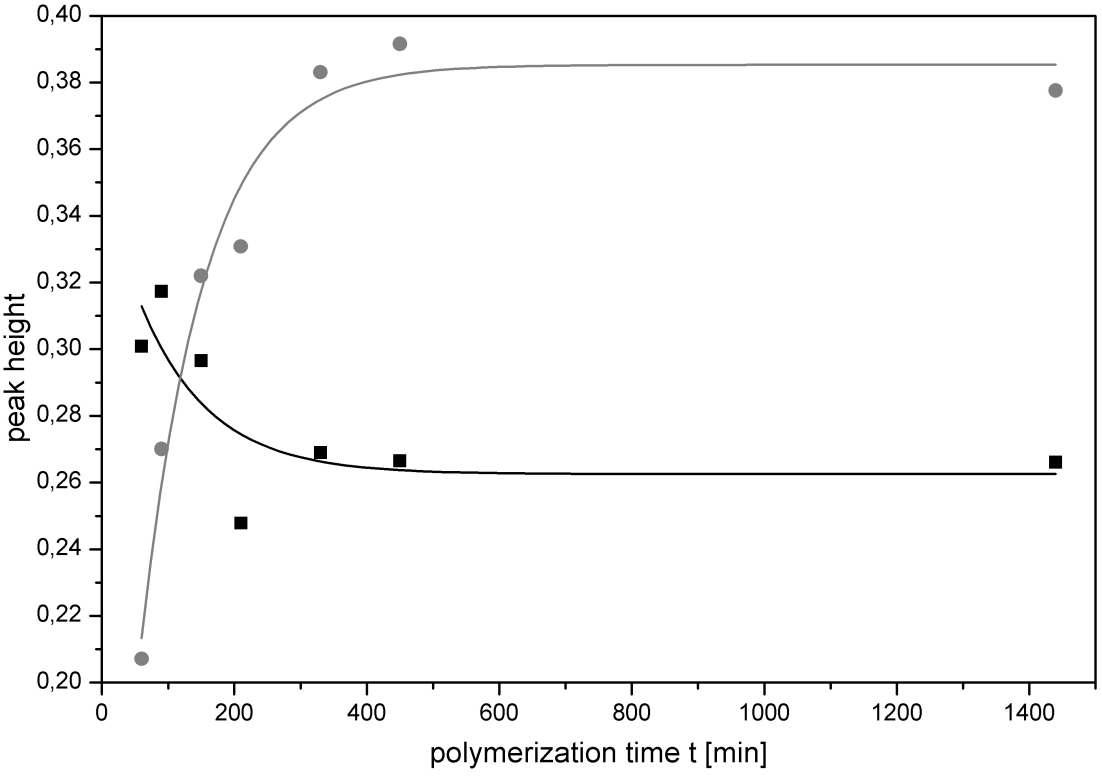

Fig. 8.18.: Plot of peak heights of ATR–FTIR–spectra *band1* (■) and *band 2* (●) of P[tBMA–grad–BzMA] $GP_{0.43}$ (f_{tBMA} = 0.65) versus polymerization time t

The results of these calculations are listed in *Table 8.10*. The compositions obtained from the two methods differed strongly. The compositions calculated from the peak height of *band 2* were all smaller than the ones calculated from NMR–spectra. The differences were between 15 % and 40 %.

Tab. 8.10.: Composition of gradient copolymer $GP_{0.43}$ calculated from peak height of *band 2*

time [min]	F_{BzMA} [a]	F^{tBMA}_{cum} [b] NMR	F^{tBMA}_{cum} [c] IR	ΔF [d]
60	0.06	0.94	0.77	-0.17
90	0.12	0.88	0.62	-0.26
150	0.19	0.81	0.63	-0.19
210	0.21	0.72	0.62	-0.17
330	0.32	0.68	0.59	-0.09
450	0.34	0.66	0.57	-0.09
1440	0.34	0.69	0.53	-0.16

[a] calculated with *Eq. 7.2.20*
[b] calculated with *Eq. 8.2.26*
[c] calculated from ^{1}H–NMR–spectra
[d] $\Delta F = F^{tBMA}_{cum}(IR) - F^{tBMA}_{cum}(NMR)$

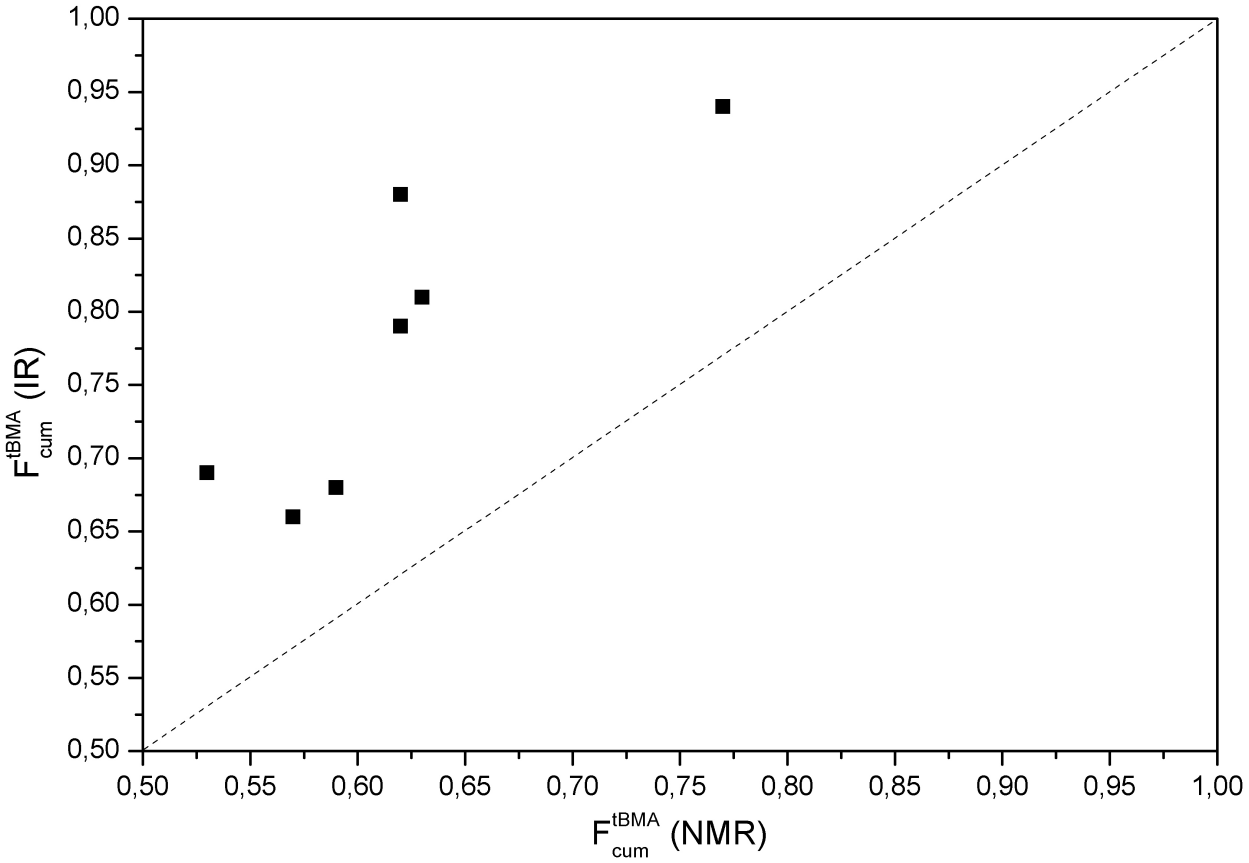

Fig. 8.19.: Interrelation of the cumulative compositions calculated from ^{1}H–NMR and from ATR–FTIR of $GP_{0.43}$ (f_{tBMA} = 0.65); dashed line – ideal curve

With *Figure 8.19* the missing consensus between the compositions from ^{1}H–NMR and ATR–IR is demonstrated. In case of perfect agreement the data points should be located on a straight line of slope s = 1. The compositions calculated from the values obtained by IR–spectra increased like the values from ^{1}H–NMR–spectra but they were all obviously higher and also did not develop linear. It is concluded better not to use FTIR–based methods to determine the composition of gradient tBMA/BzMA copolymers.

8.2.4. Molecular Weight Characterization

The finally obtained gradient copolymer of the semibatch copolymerization V101 and also the precipitated samples were analyzed with size exclusion chromatography. The elution diagrams based on the signal of the RI–detector of the samples which were taken during the polymerization at different times are shown in *Figure 8.20* together with experiment V101 ($GP_{0.43}$, f_{tBMA} = 0.5). All the RI–signals gave monomodal peaks, hence over the whole time of the semibatch copolymerization no termination reactions occurred. Furthermore the signals shifted to lower elution volumes with higher polymerization times of the sample, indicating an increasing molar mass of the samples.

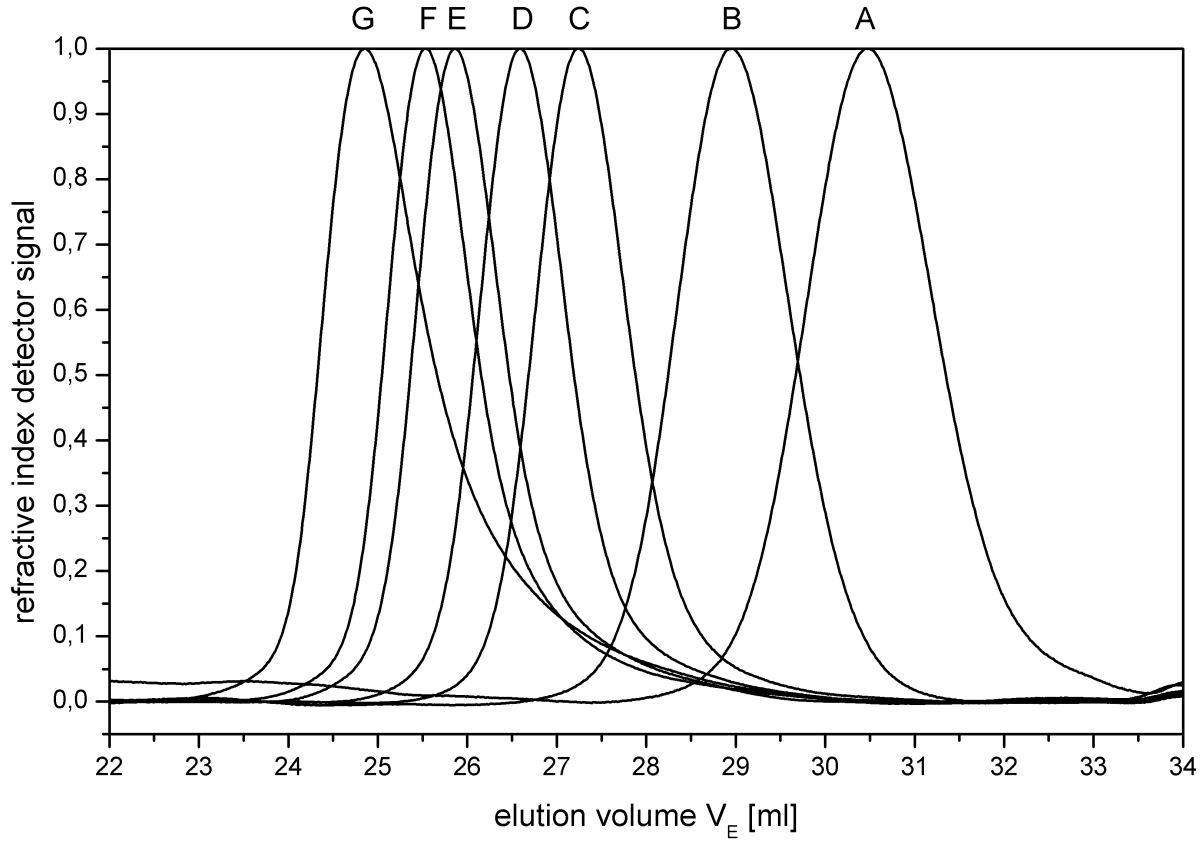

Fig. 8.20.: Elution diagrams of the samples of experiment V101 ($GP_{0.43}$, f_{tBMA} = 0.5); A – 60 min, B – 90 min, C – 150 min, D – 210 min, E – 330 min, F – 450 min and G – 1440 min of reaction time

With the same calibration curve arising from polystyrene standards that was used in *Section 3.3.3, Figure 3.15*, the relative molar masses of the samples were calculated from the maximum elution volume V_E of the RI–signals. The elution volumes of the RI–signals from the samples of the semibatch copolymerization and the calculated relative molar masses are listed in *Table 8.11*. The values of the relative molar masses rose nearly linear at the beginning than the slopes flattened. Because for the determination of the relative molar mass just one point of the RI–signal was used not the whole sample was covered. To account for this effect the absolute molar masses of the sample were determined.

The next step was the determination of the differential refractive index increments dn/dc of the resulting gradient copolymer because this value are necessary for the calculation of the absolute molar mass of the polymers from light scattering data, see *Section 2.4*. This was done the same way as described with the statistical copolymers of experiment V81 to V89 in THF at 25 °C, cf. *Section 7.2.3*. $GP_{0.43}$ (F_{tBMA} = 0.53) had a differential refractive index increment of $0.1234 \pm 0.0099\,ml \cdot g^{-1}$. That was in the same range than the statistical copolymers of BzMA and tBMA, see *Table 7.12*.

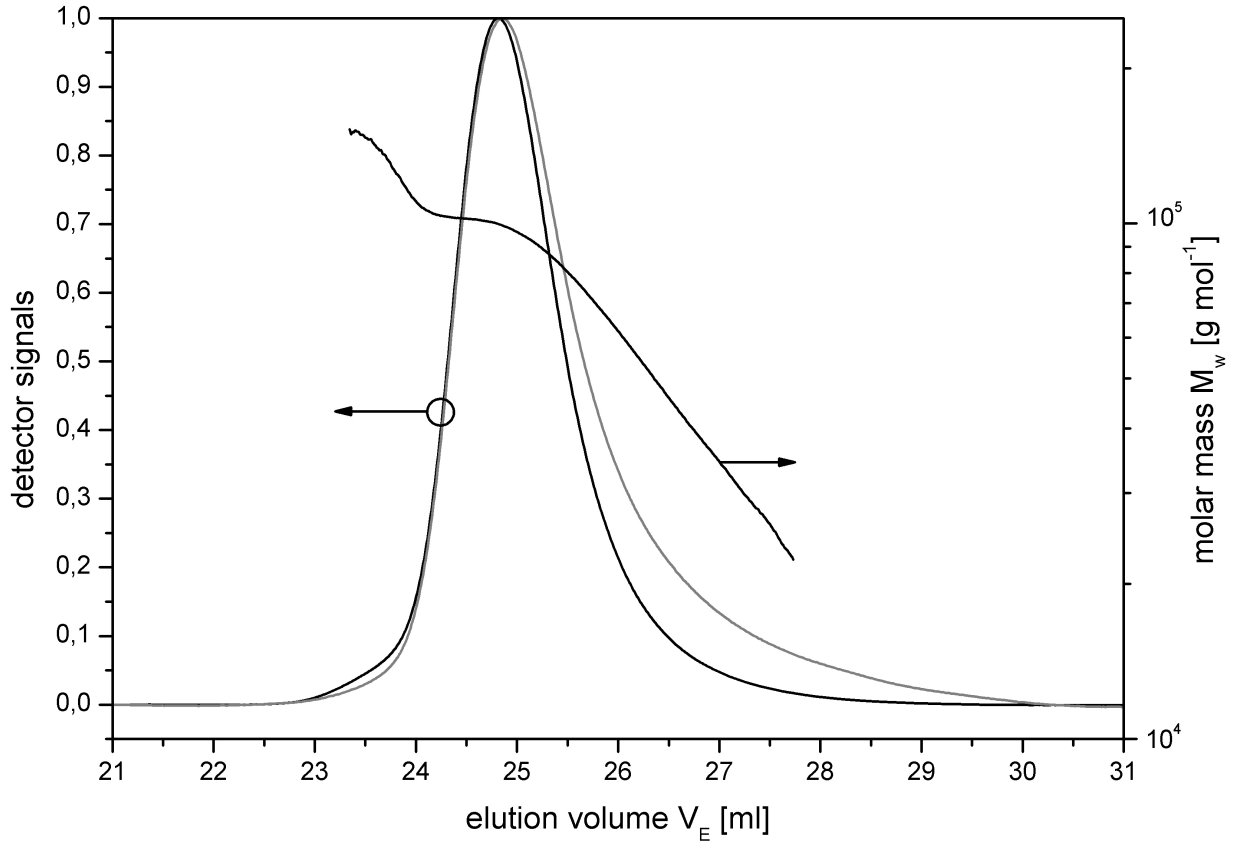

Fig. 8.21.: SEC elution diagrams and molar masses of gradient copolymer $GP_{0.43}$ (f_{tBMA} = 0.5) obtained after 1440 min of reaction time; black curve – light scattering signal, grey curve – refractive index signal

With the results from the determination of dn/dc the molecular weight averages (M_n, M_w, M_z) and from these the polydispersity indices PDI (M_w/M_n, M_z/M_n) of the samples of the semibatch copolymerization were determined in the same way as for the statistical copolymers in *Section 7.2.3*. *Figure 8.21* depicts the RI– and the 90°–MALS–detector signals of the elution–diagram of resulting gradient copolymer $GP_{0.43}$.

From the angle dependence of the scattered light intensity and the known dn/dc–value of dn/dc = $0.1234\,ml \cdot g^{-1}$ the absolute molecular weight of a fraction at a given elution volume can be derived. The calculated molecular weights are also shown in *Figure 8.21* (right axis). Since the RI–signal is proportional to the weight fraction of the eluted polymer, the complete molecular weight distribution (MWD) of the measured polymer can be obtained and with this the molecular weight averages and the polydispersity indices can be calculated. The obtained values are detailed in *Table 8.12*. Both detector signals in *Figure 8.21* did not show fronting or tailing which indicated the lack of termination and chain extension reaction during the reaction time of 1440 min.

Tab. 8.11.: Comparison of relative* and absolute molar masses of of the different gradient copolymer compositions of P[tBMA–grad–BzMA] $GP_{0.43}$

time [min]	V_E [ml]	relative M* $[g \cdot mol^{-1}]$	absolute M $[g \cdot mol^{-1}]$	ΔM $[g \cdot mol^{-1}]$	[%]
60	30.48	4407	3247	1160	-35.72
90	28.96	9567	9293	274	-2.95
150	27.24	22939	23290	-351	1.51
210	26.58	32044	34570	-2526	7.31
330	25.87	46057	53180	-7123	13.39
450	25.53	54727	62740	-8013	12.77
1440	24.85	77143	84520	-7377	8.73

* calibrated against PS–Standard

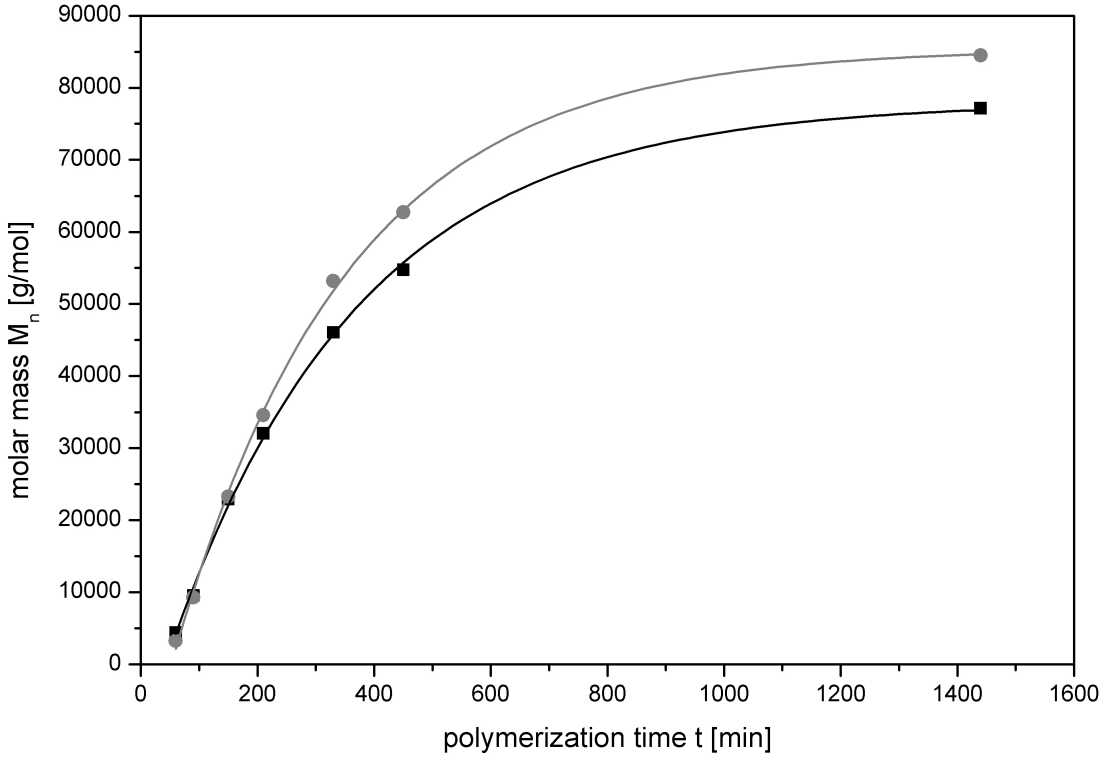

Fig. 8.22.: Comparison of relative (■) and absolute (●) molar masses M_n of $GP_{0.43}$ (f_{tBMA} = 0.5)

In *Figure 8.22* the relative molar masses, calculated from the calibrations curve of PS standards, and the absolute molar masses, calculated from the LS–signal and dn/dc value, are compared. Up to a reaction time of 150 min the masses were similar. After that with rising of the polymerization time the difference between the relative and the absolute molar masses became greater. But the shape of the curves of the values were similar and different by less than 14 % (t = 330 min).

Tab. 8.12.: SEC results of experiment V101

time [min]	M_n [g · mol^{-1}]	M_w [g · mol^{-1}]	M_z [g · mol^{-1}]	M_w/M_n	M_z/M_n
60	2978 ±119	3247 ±162	3689 ±553	1.087 ±0.065	1.235 ±0.185
90	8514 ±255	9293 ±372	12510 ±2252	1.091 ±0.055	1.469 ±0.264
150	22300 ±89	23290 ±70	24160 ±169	1.044 ±0.005	1.083 ±0.009
210	33180 ±133	34570 ±104	35630 ±249	1.042 ±0.005	1.074 ±0.009
330	50710 ±101	53180 ±53	55040 ±165	1.049 ±0.003	1.085 ±0.004
450	59690 ±119	62740 ±125	64920 ±260	1.051 ±0.003	1.088 ±0.005
1440	74730 ±224	84520 ±169	90640 ±181	1.131 ±0.003	1.213 ±0.005

The results of the SEC analysis against the polymerization time are plotted in *Figure 8.23* and against the conversion in *Figure 8.24*. The MWD was very narrow with PDI = M_w/M_n ranging from 1.04 to 1.13. For most practical purposes the copolymer can be regarded as fairly monodisperse ($\overline{M}_w \approx \overline{M}_n$).

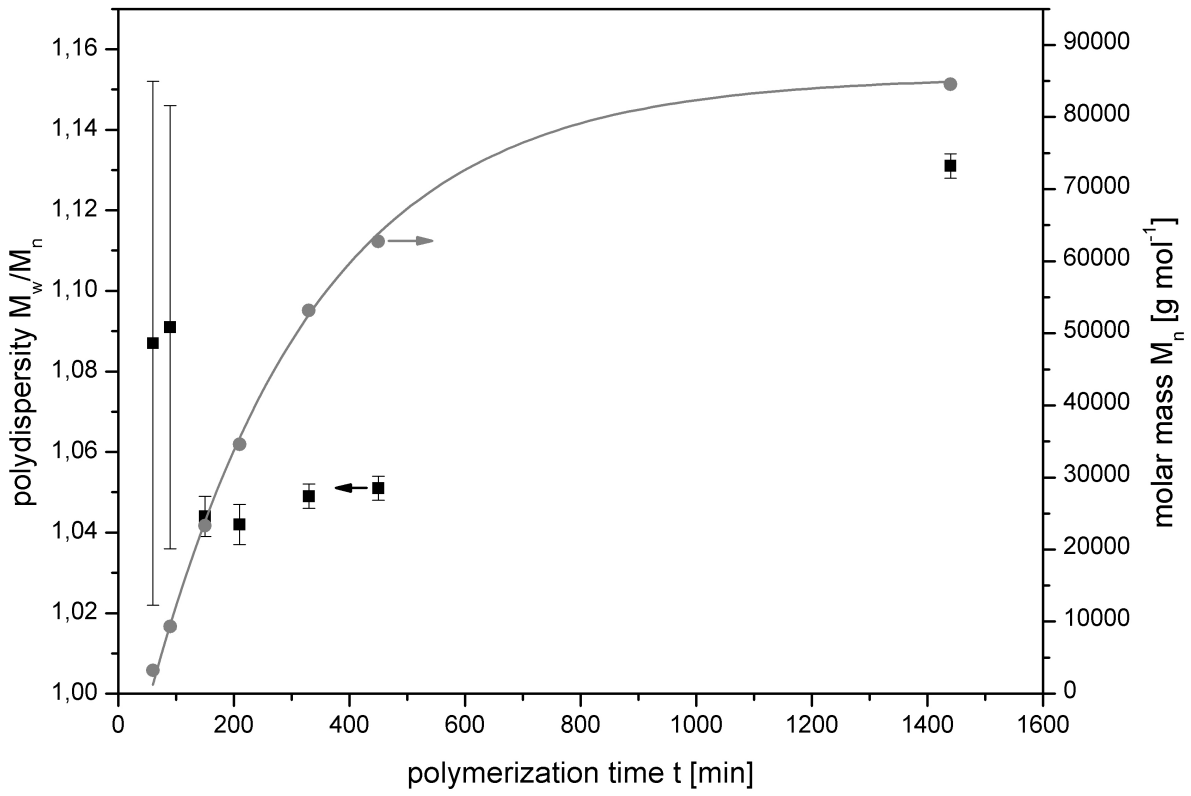

Fig. 8.23.: Molar masses M_n and polydispersities against reaction time t of $GP_{0.43}$ (f_{tBMA} = 0.5)

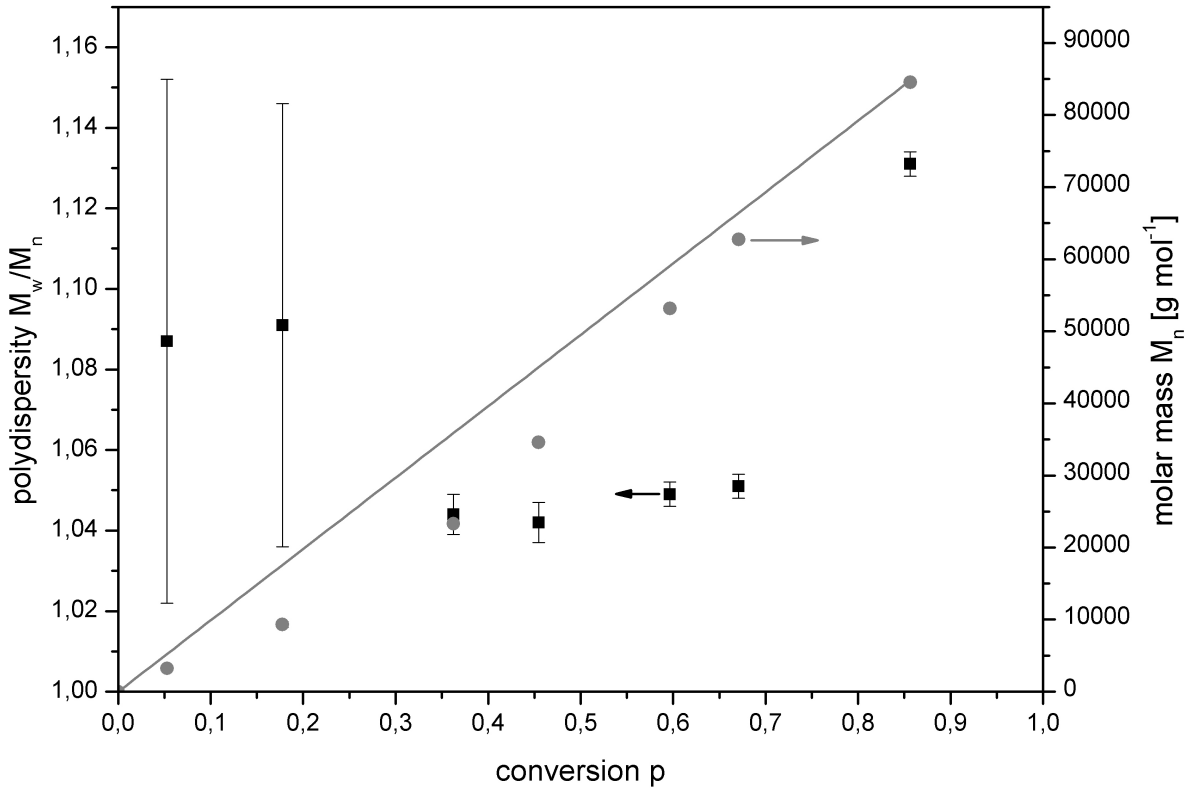

Fig. 8.24.: Molar masses M_n and polydispersities against conversion p of $GP_{0.43}$ (f_{tBMA} = 0.5)

As well as the relative molar masses the absolute molar masses increased linearly up to 160 min then the slopes flattened. The development of the molar mass M_n during the semibatch gradient copolymerization was nearly the same as during the batch copolymerizations of the statistical copolymers (cf. *Figure 7.22*). At the beginning of the polymerizations the slope was linear in the first 160 min. However, the final mass M_w of the gradient copolymer from the semibatch copolymerization was higher than the molar masses of the statistical copolymers resulting from the batch copolymerizations because the polymerization time was much longer (1440 min instead of 180 min). The average final molar mass M_n which was reached in the batch copolymerizations was $\approx 38800\,g \cdot mol^{-1}$. In the semibatch copolymerizations an average final molar mass of $\approx 74700\,g \cdot mol^{-1}$ was reached. The polymerization time of the semibatch experiment was eight times longer than that of the batch experiments, but the final molar mass of $GP_{0.43}$ is only twice as large. Hence, the mass growth of the gradient copolymer was much slower than that of the batch reactions. A relation between the polydispersity PDI and the polymerization time t was not obvious. That was also a repetition of the results from the statistical copolymers of *Series F* and *Series G*. PDI values were very low (PDI < 1.13), the range of the PDI stayed constant during the semibatch polymerization.

A linear relation between the development of the molar masses M_n and the total conversion of the monomers p during the semibatch experiments was found. The fitted curve originated in (0,0), a behavior that is typical for controlled radical polymerizations. [108]

$$V101, GP_{0.43}: \; M_n = (99014 \pm 42)\,g \cdot mol^{-1} \cdot p(f_{tBMA,0.50}) \tag{8.2.27}$$

The depiction of the polydispersities PDI of the samples versus the conversion p gave no relation of the PDI and the conversion p. This was the same observation than at the PDI/reaction time plot. However, the values of the PDI were very low over the whole conversion range. In literature gradient copolymers which had been synthesized by ATRP the PDI–values were up to 1.5. [109, 110, 111] Hence, it can be stated that the reaction was good over the whole conversion.

Comparison of Molecular Weight Characterizations from Semibatch Copolymerizations of nBMA/tBMA and BzMA/tBMA

In the following paragraph the results of the SEC analysis of the experiments V31 (P[tBMA–grad–nBMA] $GP_{0.53}$) and V101 (P[tBMA–grad–BzMA] $GP_{0.43}$), both with $f_{tBMA} = 0.5$, respectively $\phi_p = -1.0$, of the semibatch copolymerizations are compared. The degree of polymerization was calculated with *Equation 7.2.21* from the molar masses to eliminate the differences of the molar masses of the monomers *n*–butyl methacrylate and benzyl methacrylate. The X_n–values are listed with the corresponding conversions and compositions in *Table 8.13*.

Tab. 8.13.: Degree of polymerization X_n of the gradient copolymers of P[tBMA–grad–tBMA] V31 and P[BzMA–co–tBMA] V101

V31			V101		
p	X_n	PDI	p	X_n	PDI
0.1160	36.6245	1.044	0.0528	21.6627	1.087
0.1908	55.0211	1.053	0.1776	59.9190	1.091
0.3060	97.6090	1.018	0.3624	150.4356	1.044
0.3808	125.8790	1.020	0.4545	222.9095	1.042
0.4778	176.2307	1.029	0.5966	340.3310	1.049
0.5437	218.7764	1.017	0.6707	399.7627	1.051
0.9087	414.1350	1.070	0.8564	534.3392	1.131

In *Figure 8.25* the degree of polymerization of the samples of the two experiments are depicted against the conversion p. The X_n–values of the samples decreased nearly linear during both experiments, however, the graphs have different slopes. The slope during the semibatch copolymerization V101 was larger than during the polymerization V31. In *Figure 8.26* the polydispersities of the samples taken during the two semibatch copolymerizations are depicted. The PDI–values of the samples of copolymerization V31 were all lower than the PDI–values of the samples of experiment V101. Expect the last sample of experiment V101 all values lay under 1.14.

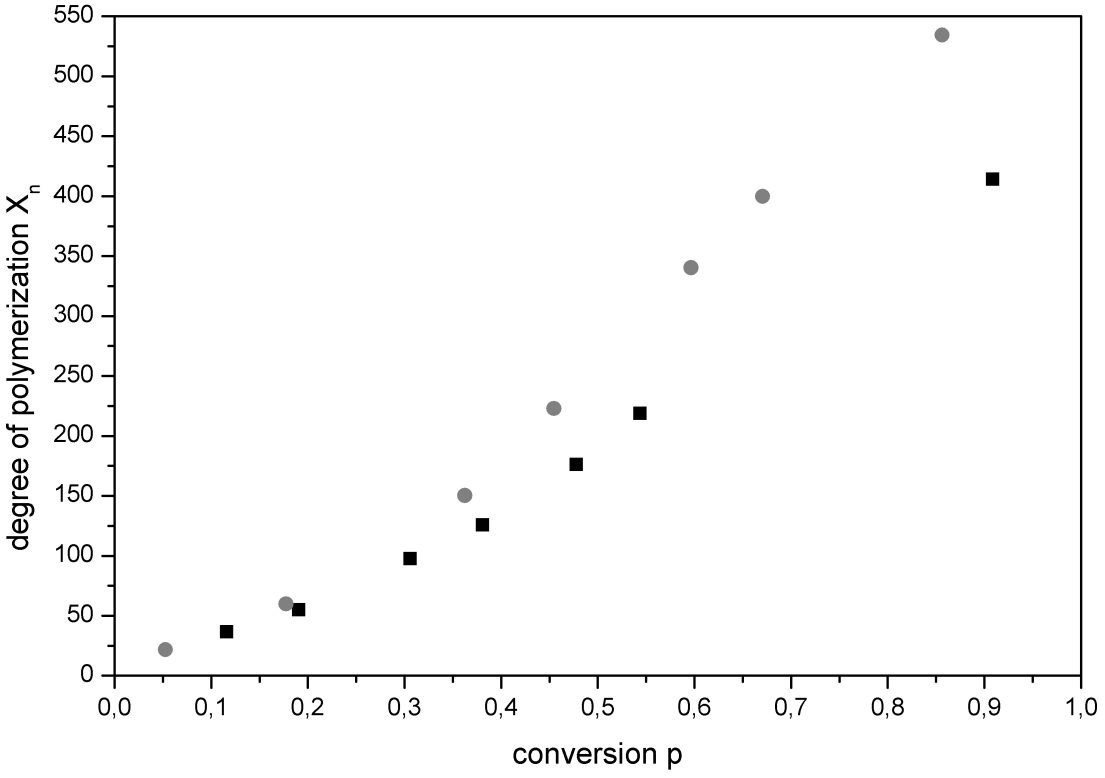

Fig. 8.25.: Comparison of degree of polymerization X_n of gradient copolymers of ■ P[tBMA–grad–tBMA] V31 and ● P[BzMA–co–tBMA] V101 against copolymer composition

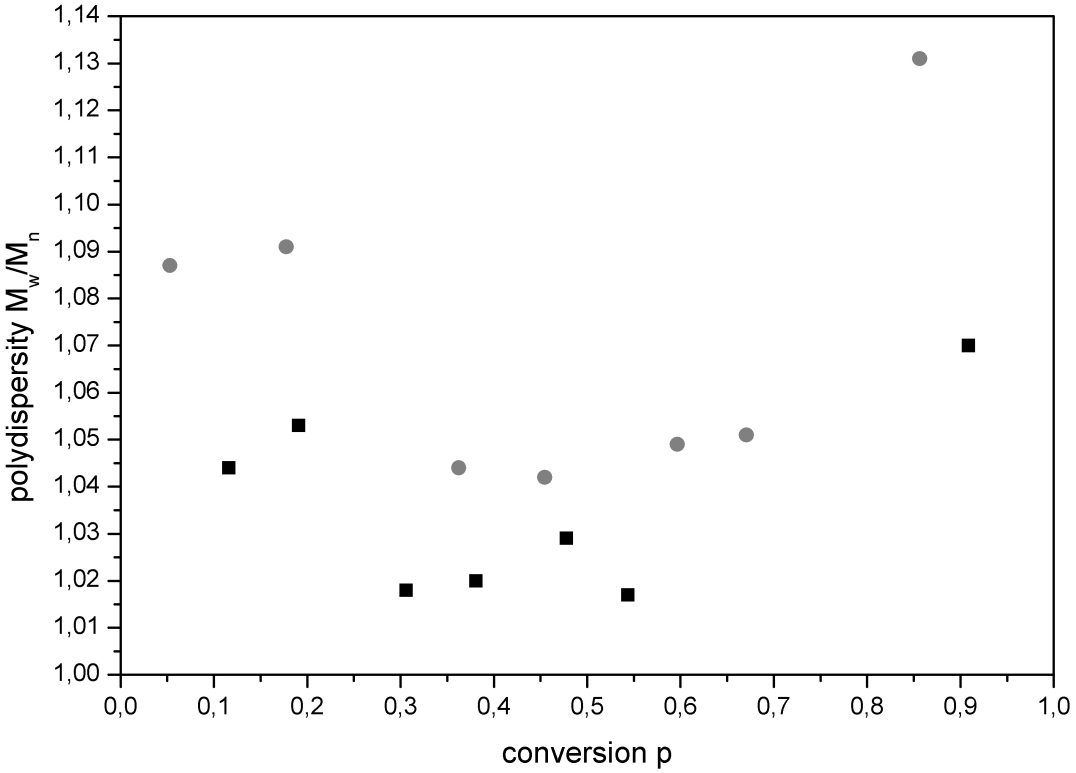

Fig. 8.26.: Comparison of polydispersities M_w/M_n of gradient copolymers of ■ P[tBMA–grad–tBMA] V31 and ● P[BzMA–co–tBMA] V101 against copolymer composition

The low values of polydispersity during both semibatch copolymerizations reflects the good control of the ATRP–system during the both semibatch copolymerizations.

8.2.5. Thermal Behavior

The thermal behavior of the gradient copolymer was examined to determine the temperature range of the glass transition region ΔT and the glass transition temperature T_g. The samples of the precipitated copolymers of experiment V101 were analyzed in the same way and the same temperature range as the statistical copolymers of *Series G* (cf. *Section 7.2.4*). The applied DSC program parameters were:

- precooling: RT to −80 °C
- standby for 20 min
- 1. heating: −80 to 150 °C
- 1. cooling: 150 to −80 °C
- 2. heating: −80 to 150 °C
- postcooling: 150 °C to RT

In *Figure 8.27* the thermogram of the sample which was taken after 60 min of polymerization time is depicted with both heating runs and the cooling run is depicted as an example. The first heating run showed a glass transition overlaid by a relaxation peak between 45 °C and 75 °C. The second heating run showed a glass transition step nearly in the same range as the peak of the first run. Only the second heating runs of all samples taken during the four semibatch polymerizations were analyzed with respect to T_{onset}, T_{offset}, T_g, T_{midpt}, ΔT and Δc_p. [89] The analysis followed the description in *Section 3.3.4*. The complete results of the analysis of the second heating runs from all samples of experiment V101 are listed in *Table 8.14*.

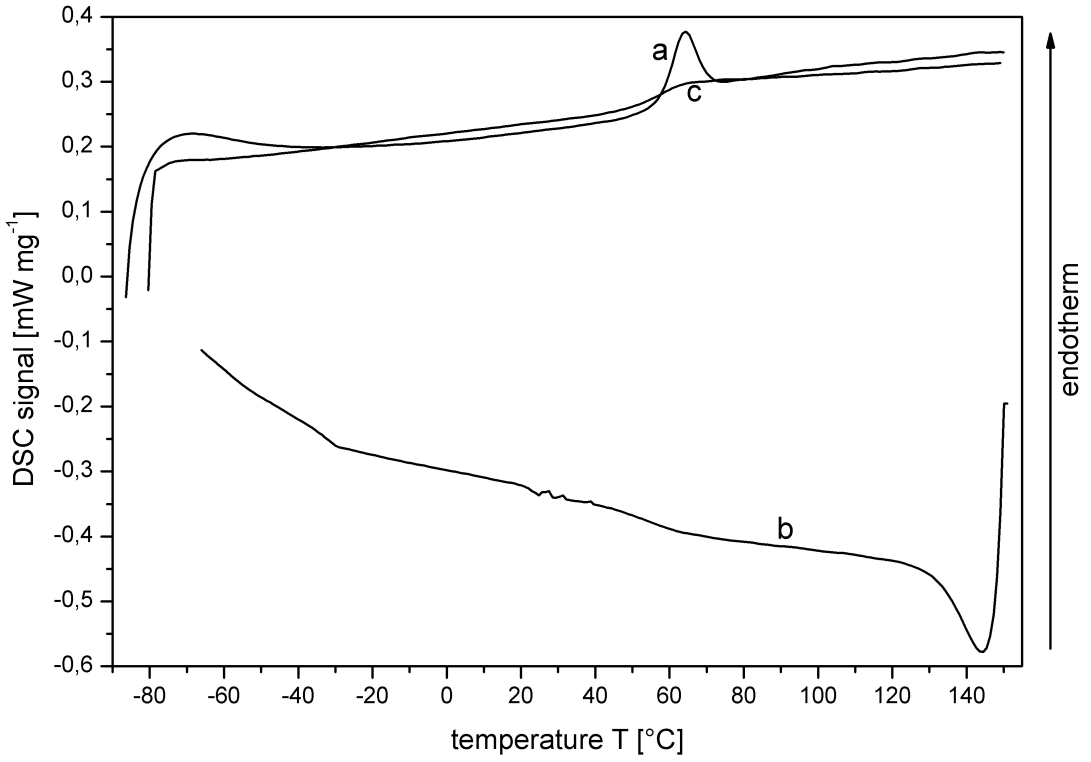

Fig. 8.27.: DSC thermogram of gradient copolymer V101 ($GP_{0.43}$, f_{tBMA} = 0.5, reaction time t = 60 min); a – first heating run, b – first cooling run, c – second heating run; heating rate $10\,K \cdot min^{-1}$

Tab. 8.14.: DSC results of experiment V101

time t [min]	T_{onset} [°C]	T_{midpt} [°C]	T_g [°C]	T_{offset} [°C]	ΔT [°C]	Δc_p $[J \cdot g^{-1} \cdot K^{-1}]$
60	37.0	49.5	45.5	57.0	7.5	0.137
90	55.0	70.5	74.5	83.0	12.5	0.269
150	30.0	43.5	45.0	53.0	9.5	0.219
210	16.0	28.5	29.5	37.5	9.0	0.196
330	24.5	35.0	37.0	42.0	7.0	0.201
450	27.5	40.5	42.5	49.0	8.5	0.210
1440	47.5	57.0	56.5	64.5	7.5	0.212

The thermograms of the second heating runs of the samples of experiment 101 ($GP_{0.43}$, f_{tBMA} = 0.5) are depicted in *Figure 8.28*. The limits of the glass transition range ΔT, T_{onset} and T_{offset}, are marked there, as well as the glass transition temperature T_g. The glass transition temperature T_g scattered between 29.5 °C and 74.5 °C. A dependence between polymerization time and T_g was not noticeable. The glass transition temperature range ΔT ranged from 7.5 to 12.5 °C. Also for this value no dependence on the polymerization time was found.

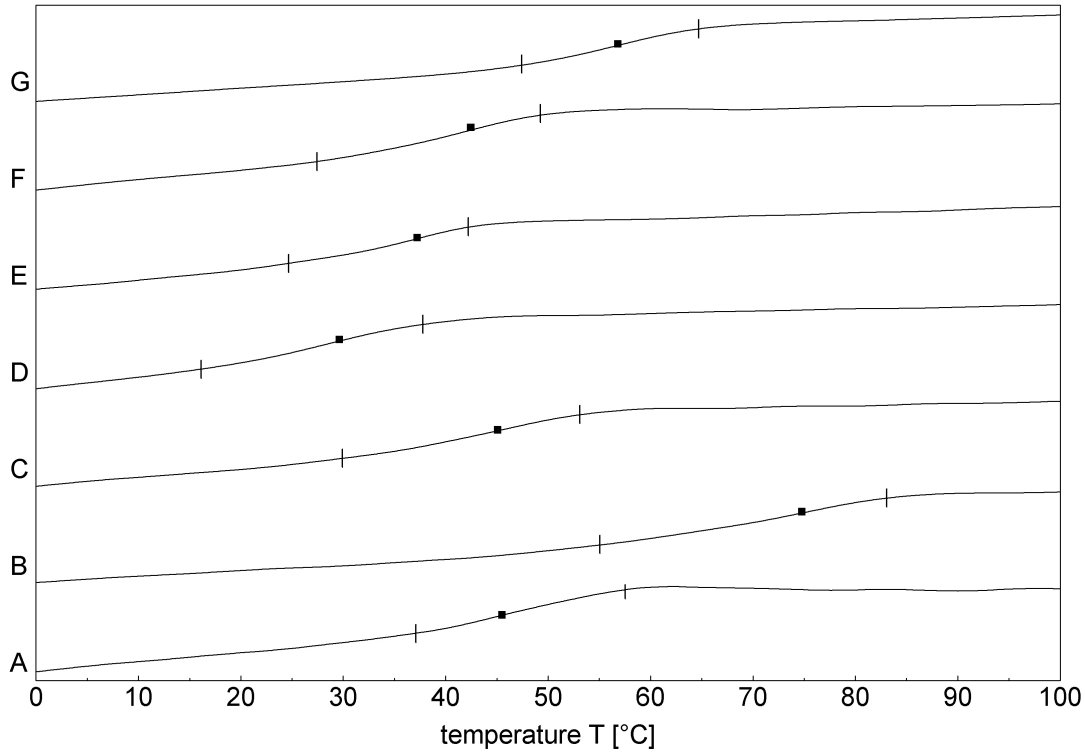

Fig. 8.28.: DSC thermograms of $GP_{0.43}$ (f_{tBMA} = 0.5) with marked glass transition temperature range T_{onset}, T_{offset} and glass transition temperature T_g; second heating runs, heating rate $10\,K \cdot min^{-1}$; A – 60 min, B – 90 min, C – 150 min, D – 210 min, E – 330 min, F – 450 min and G – 1440 min of reaction time

The plot of the glass transition temperatures T_g and temperature ranges ΔT of the samples of experiment V101 against the polymerization time t are depicted in *Figure 8.29*, while *Figure 8.30* shows an analogues plot versus the monomer conversion p.

The glass transition temperature T_g did not show a clear dependence on the polymerization time. But from 210 to 1440 min the values increased exponentially. The values of the glass transition temperature range ΔT laid in a narrow range between 7 °C and 13 °C and they were nearly linear.

Likewise the glass transition temperature did not show a dependence to the conversion p. The T_g–values increased, decreased and increased again with the rise of the conversion. The glass transition temperature range showed relatively straight values over the conversion p.

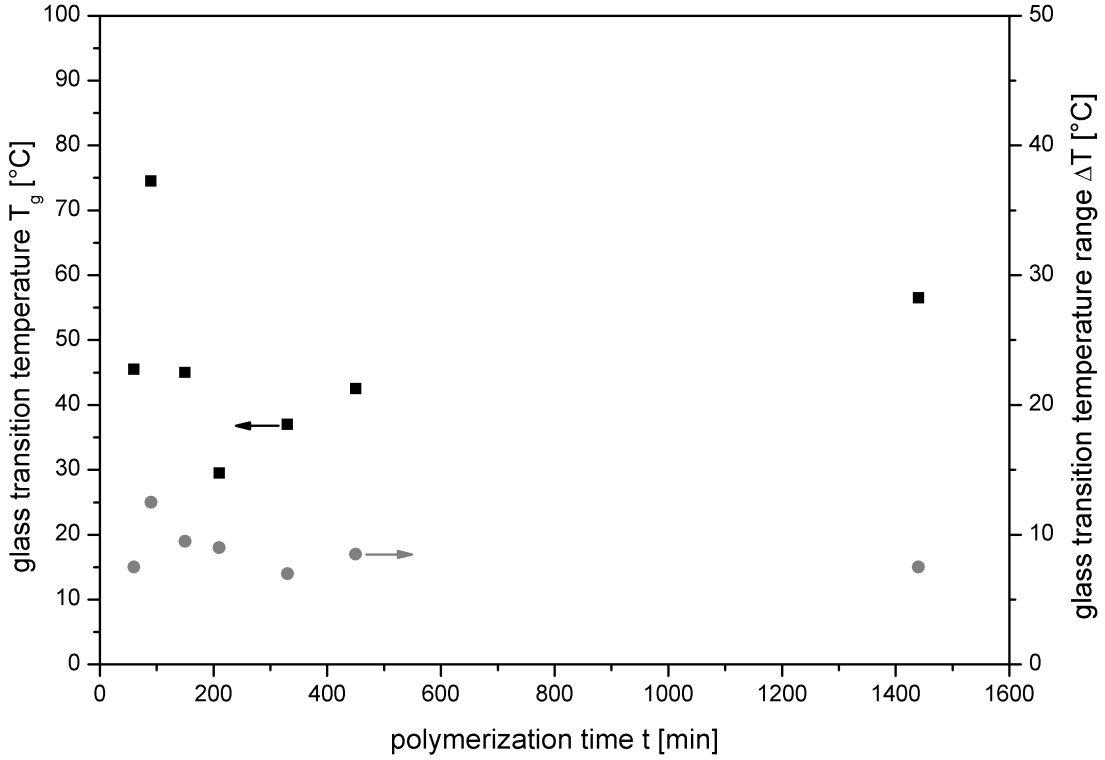

Fig. 8.29.: Plot of the glass transition temperature T_g (■) and the glass transition region ΔT (●) of $GP_{0.43}$ (f_{tBMA} = 0.5) against polymerization time t

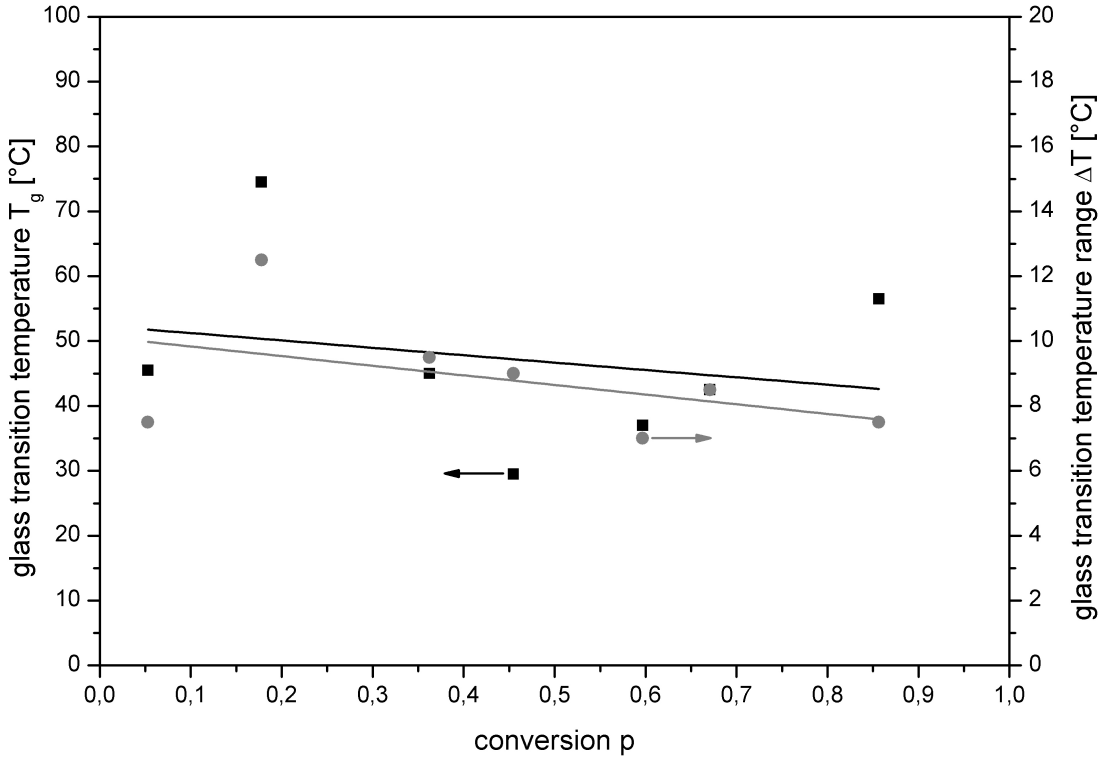

Fig. 8.30.: Plot of the glass transition temperature T_g (■) and the glass transition region ΔT (●) of $GP_{0.43}$ (f_{tBMA} = 0.5) against conversion p

The glass transition temperature of P[tBMA–co–BzMA] copolymers (*Series F*) can not be described well with *Fox*–Equation (cf. *Section 7.2.4*), because a difference of 10 ℃ between the calculated and measured values was found. However, this analysis was also applied to the gradient copolymers, using *Equation 8.2.28*. The results of the calculations are listed in *Table 8.15*.

$$\frac{1}{T_g} = \frac{F_{tBMA}}{T_{g,tBMA}} + \frac{F_{BzMA}}{T_{g,BzMA}} \tag{8.2.28}$$

with $T_{g,tBMA}$ = 107℃ [90] and $T_{g,nBMA}$ = 47℃ [113]

Tab. 8.15.: Theoretical and measured glass transition temperature of experiment V101

time [min]	F_{tBMA}	F_{BzMA} [a]	T_g(*Fox*) [b] [℃]	T_g(DSC) [c] [℃]	ΔT_g [d] [℃]
60	0.77	0.23	83.0	45.5	-37.5
90	0.62	0.38	72.1	74.5	2.4
150	0.63	0.37	72.6	45.0	-27.6
210	0.62	0.38	72.1	29.5	-42.6
330	0.59	0.41	70.0	37.0	-33.0
450	0.57	0.43	68.9	42.5	-26.4
1440	0.53	0.47	66.9	56.5	-10.4

[a] $F_{BzMA} = 1 - F_{tBMA}$; [b] calculated with *Eq. 8.2.28*
[c] measured with DSC; [d] $\Delta T_g = T_g$(DSC) - T_g(*Fox*)

The differences between the calculated and measured glass transition temperatures were high (> 25℃) for the most of the samples. Only with the sample taken at 90 min of polymerization time the calculated and the measured value were similar while the sample taken at 1440 min showed a the difference of 10℃. Since similar discrepancies have been found with the statistical copolymers, the system tBMA/BzMA is not suitable to a *Fox–Equation* based description. The glass transition temperatures T_g of the samples of the gradient copolymer $GP_{0.43}$ were in the same range as the glass transition temperatures of the samples of *Series G*, see *Table 7.18*. The glass transition temperature range ΔT of the samples of the gradient copolymer $GP_{0.43}$ were lower than the ΔT–values of the statistical copolymers of *Series G*.

Comparison of the Thermal Behavior of the Semibatch Copolymers of nBMA/tBMA and BzMA/tBMA

In the following paragraph the results of the DSC analysis of the experiments V31 (P[tBMA–grad–nBMA] $GP_{0.53}$) and V101 (P[tBMA–grad–BzMA] $GP_{0.43}$), both with f_{tBMA} = 0.5, respectively $\phi_p = -1.0$, of the semibatch copolymerizations are compared. In *Figure 8.31* the glass transition temperatures of the samples which were taken during the semibatch copolymerizations V31 and V101 are depicted.

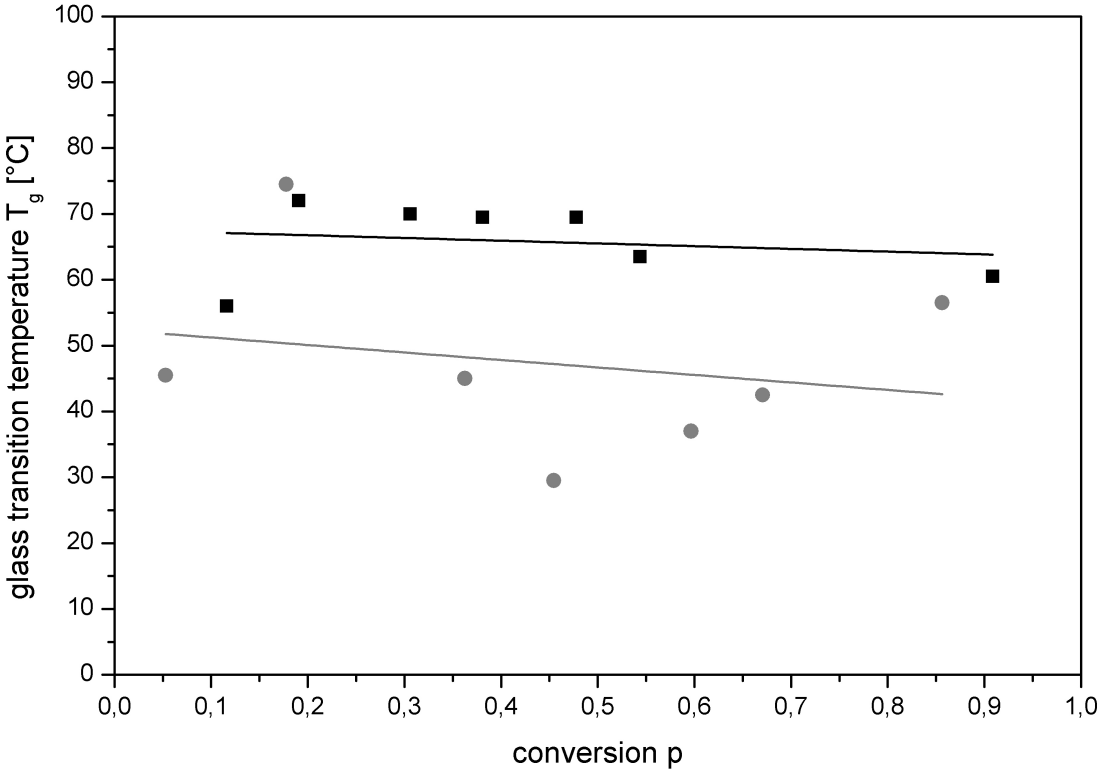

Fig. 8.31.: Comparison of glass transition temperature T_g of copolymers of ■ P[tBMA–grad–tBMA] V31 and ● P[BzMA–co–tBMA] V101 against copolymer composition

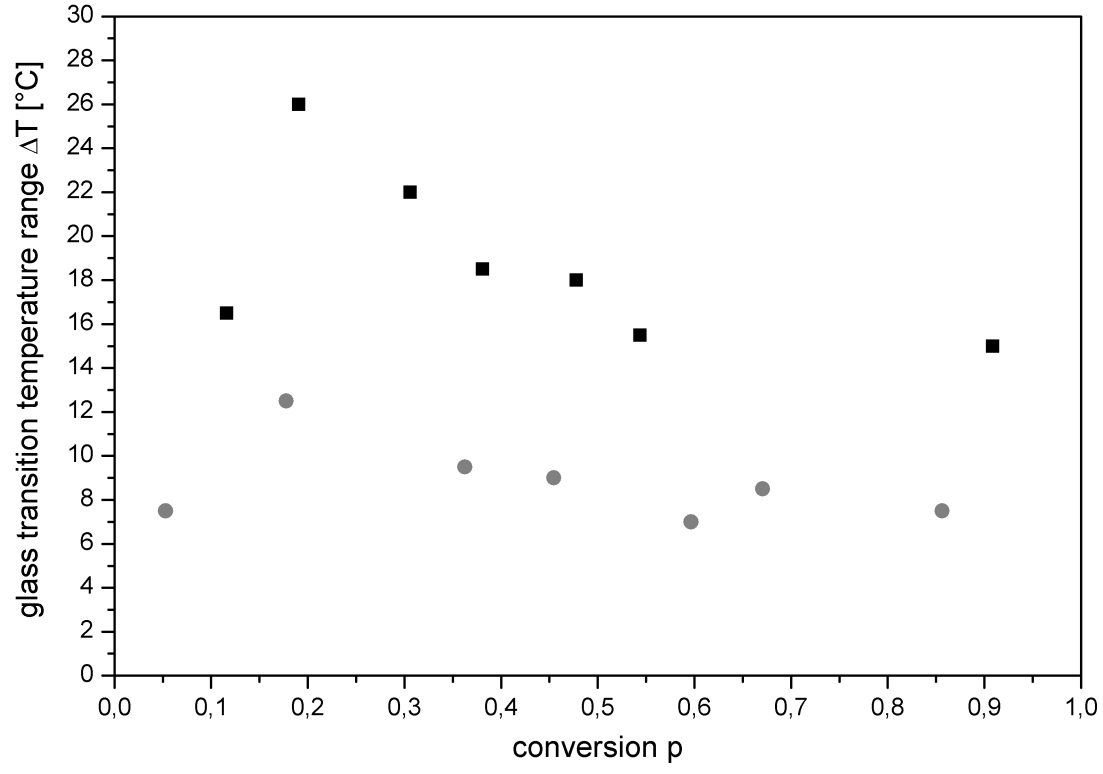

Fig. 8.32.: Comparison of glass transition temperature range ΔT of copolymers of ■ P[tBMA–grad–tBMA] V31 and ● P[BzMA–co–tBMA] V101 against copolymer composition

The glass transition temperature T_g of the samples of the copolymerization V31 were higher than the T_g–values of the samples of copolymerization V101 and the range of the values is smaller at the samples of V31 than the value–range of the samples of experiment V101. During both experiments the values scattered. The samples at experiments V31 the scattering was less strong. The differences between the T_g–values of copolymerization V101 was higher. That the values of the samples of semibatch copolymerization V31 were higher depends on the monomer–compositions of the two systems. Poly[benzyl methacrylate] has a lower glass transition temperature than poly[*tert*–butyl methacrylate].

In *Figure 8.32* the values of the glass transition temperature ranges ΔT of the samples from the semibatch synthesis V31 and V101 are depicted. The values of the samples of V31 are all higher than the values of the samples of V101. For both synthesis the sample–values increased from the first to the second value and the decreased from the second to the sixth value of V31 and to the fifth value of V101. Between the last two values of V31 and the last three values of V101 the values were nearly constant.

8.3. Summary

Based on the kinetic investigations on batch–copolymerizations of the different monomer compositions of *tert*–butyl–methacrylate (monomer 1) and benzyl methacrylate (monomer 2) the monomer addition program of semibatch copolymerization to generate a gradient copolymer has been calculated for a semibatch copolymerization with tBMA as the stock–monomer and BzMA as the feed–monomer. The analysis of the ^{1}H–NMR–spectra of the samples taken over the reaction time showed that the conversion increased linear at the beginning of the polymerization and then leveled off. After 1440 min the conversion reached around 85 %. From the monomer conversions the cumulative and the instantaneous copolymer compositions of all samples were calculated. The cumulative compositions showed a decrease in tBMA–content, the instantaneous compositions also decreased. The slope of the decrease was too strong up to 11 % of monomer conversion and from 11 to 85 % monomer conversion the slope was too small. Hence, the obtained gradient copolymer V101 is characterized by "double gradient" structure, with a large gradient ($\phi_p = -5.42$) over ~ 11 % of the chain length and a low gradient ($\phi_p = -0.43$) along the rest of the chain. Therewith the semibatch copolymerization yielded in a linear gradient copolymer with a constant gradient between a conversion of 11 to 85 %. Over the whole reaction the copolymer can be described as "double–gradient". Elementary analysis showed the samples to be free of pollution. A calculation of the composition from the measured amounts of carbon leads to values which did not a obviously different from the compositions resulting from the analysis of the ^{1}H–NMR–analysis. The analysis of the samples with ATR–FTIR–spectroscopy gave spectra with the same characteristic vibrational bands that were found for the statistic copolymers. The calibration curve that was developed with the statistic copolymers could also be applied to the gradient copolymer, but

gave compositions that fitted badly to the compositions obtained by ^{1}H–NMR–analysis. The SEC–measurements gave elution–diagrams without fronting or tailing, demonstrating a good reaction control even over 1440 min. The molar masses grew regularly. The polydispersities of all samples were well below 1.15, which also indicated the good reaction control. DSC thermal analysis revealed no dependence of the T_g to reaction time or composition of V101. The glass transition temperature range stayed constant during the reaction. The measured T_g of the copolymers do not obey the *Fox–Flory*–rule of the copolymers glass temperature. The glass transition temperature of the samples of experiment V101 were in the same range than the T_g–values of the statistical copolymers of *Series G* and the glass transition temperature range of the samples of the gradient semibatch copolymerization were lower than the ΔT–values of the samples of the statistical batch copolymerization of *Series G*.

9. Hydrolysis of Statistic and Gradient Copolymers from Benzyl Methacrylate and tert–Butyl Methacrylate

The aim of this thesis is to prepare a functional amphiphilic gradient copolymer. For that reason the *tert*–butyl group of P[tBMA–grad–BzMA] must be converted to a COOH–group via hydrolysis. In this chapter one statistical copolymer from BzMA and tBMA P[BzMA–co–tBMA] (V81), cf. *Chapter 7*, and the gradient copolymer P[tBMA–grad–BzMA] (V101) were hydrolyzed to obtain P[BzMA–co–MAA] (V111), respectively P[MAA–grad–BzMA] (V121).

The *tert*–butyl group is a classical protections group in organic chemistry for –COOH–groups. [92] The standard method for the removal of a *tert*–butyl group is acid catalyzed hydrolysis. Especially the use of trifluoroacetic acid is well described in literature [93]. Also in polymer chemistry this cleavage reaction is often used to remove ester groups. Since (meth)acrylic acid can not be polymerized with ATRP, the indirect way using *tert*–butyl ester monomers is frequency used. [94, 95, 96] Another acid that can be used as a cleavage catalyst is methanesulfonic acid. This acid is more often used in bio–organic chemistry for the hydrolysis of proteins [97, 98, 99] but is also known in polymer chemistry. [100, 101] A different way to convert the *tert*–butyl–ester–group to a carboxylic acid group is a hydrolysis under neutral conditions with trimethylsilyl iodide. This method was introduced because the reaction conditions are milder and it is also possible to work with acid sensitive educts. [102, 103, 104, 105] In *Chapter 4* the use of methanesulfonic acid was found to be the most effective way for the hydrolysis of the copolymers from *tert*– and *n*–butyl methacrylate. And because of the compatibility it was also used for the hydrolysis of the copolymers with *tert*–butyl and benzyl methacrylate.

9.1. Materials and Methods

The chemicals and the synthesis method were the same as described in *Section 4.1.*

9.1.1. Materials

The hydrolysis reagent was methanesulfonic acid (MSA, ≤ 99.5 %, *Aldrich*). It was used as received. The same applied to the used solvents chloroform (99.9 %, *Acros*, extra dry over molecular sieve, stabilized), THF (chromasolv, *Aldrich*) and *n*–pentane (*Aldrich*).

9.1.2. Hydrolysis of Statistical Copolymer

V111: 0.2 g of the copolymer V81 were dissolved in 1.8 g (1.2 ml) $CHCl_3$ and was stirred over night at room temperature. Then 0.27 g (0.18 ml) MSA were added. The mixture was stirred for 2 hours at room temperature. A spatula–spoon of sodium hydrogen carbonate was added and this mixture was stirred for 30 min. Subsequently 5 ml THF were added and the mixture was filtered over a P4 glass filter. Afterward the solution was dropped into 200 ml of ice–cold pentane. The precipitated polymer was filtered over P4 glass filter and dried at room temperature for two hours. Then the copolymer was re–dissolved in 1 ml THF and the solution was dropped into 200 ml of an ice cooled water : methanol = 1 : 1 vol : vol mixture. The precipitated polymer was filtered over P4 glass filter and dried at room temperature under an oil–pump vacuum over night.

^{1}***H–NMR:*** 0.55–0.73 ppm (broad peak); 0.74–1.17 ppm (broad peak); 1.55–2.08 ppm (broad peak, $–CH_3$, P[BzMA], P[MAA]); 3.40 ppm (H_2O); 3.71–3.90 ppm (broad peak); 4.8–5.04 ppm (broad peak, $–OCH_2R$, P[BzMA]); 7.04–7.49 ppm (broad peak, aromatic ring, P[BzMA]); 12.13–12.56 ppm (broad peak, –COOH, P[MAA])

EA: 67.33 % C, 7.00 % H, (25.67 % O_{calc})

ATR–FTIR: 3600–2360 cm^{-1} (–COOH); 3110– 2800 cm^{-1} (=CH_2, $–CH_2–$, $–CH_3$, aromatic ring); 1724 cm^{-1} (–C=O); 1703 cm^{-1} (–C=O); 1484 cm^{-1} ($–CH_2–$, $–CH_3$); 1455 cm^{-1} ($–CH_2–$, $–CH_3$); 1389 cm^{-1}; 1367 cm^{-1}; 1259 cm^{-1}; 1147 cm^{-1} (–C–O–C–); 1029 cm^{-1}; 964 cm^{-1} (Bz); 912 cm^{-1}; 826 cm^{-1}; 801 cm^{-1}; 750 cm^{-1} (Bz); 697 cm^{-1} (Bz); 587 cm^{-1}; 528 cm^{-1}; 460 cm^{-1}

9.1.3. Hydrolysis of Gradient Copolymer

V121: 0.25 g of the copolymer V101 were dissolved in 2.25 g (1.5 ml) $CHCl_3$ and was stirred over night at room temperature. Then 0.27 g (0.18 ml) MSA were added. The mixture was stirred for 2 hours at room temperature. A spatula–spoon of sodium hydrogen carbonate was added and this mixture was stirred for 30 min. Subsequently 5 ml THF were added and the

mixture was filtered over a P4 glass filter. Afterward the solution was dropped into 200 ml of ice–cold pentane. The precipitated polymer was filtered over P4 glass filter and dried at room temperature for two hours. Then the copolymer was re–dissolved in 1 ml THF and the solution was dropped into 200 ml of an ice cooled water : methanol = 1 : 1 vol : vol mixture. The precipitated polymer was filtered over P4 glass filter and dried at room temperature under an oil–pump vacuum over night.

^{1}***H–NMR:*** 0.57–0.74 ppm (broad peak); 0.75–1.22 ppm (broad peak); 1.59–2.09 ppm (broad peak, $-CH_3$, P[BzMA], P[MAA]); 3.56 ppm (H_2O); 4.8–5.08 ppm (broad peak, $-OCH_2R$, P[BzMA]); 7.23–7.45 ppm (broad peak, aromatic ring, P[BzMA]); 12.15–12.59 ppm (broad peak, –COOH, P[MAA])

EA: 65.36 % C, 6.81 % H, (27.83 % O_{calc})

ATR–FTIR: 3650–2390 cm^{-1} (–COOH); 3115–2790 cm^{-1} ($=CH_2$, $-CH_2-$, $-CH_3$, aromatic ring); 1726 cm^{-1} (–C=O); 1699 cm^{-1} (–C=O); 1483 cm^{-1} ($-CH_2-$, $-CH_3$); 1455 cm^{-1} ($-CH_2-$, $-CH_3$); 1389 cm^{-1}; 1368 cm^{-1}; 1257 cm^{-1}; 1149 cm^{-1} (–C–O–C–); 1030 cm^{-1}; 964 cm^{-1} (Bz); 912 cm^{-1}; 825 cm^{-1}; 801 cm^{-1}; 750 cm^{-1} (Bz); 697 cm^{-1} (Bz); 586 cm^{-1}; 526 cm^{-1}; 460 cm^{-1}

9.2. Results and Discussion

This section describes the observations on the hydrolysis reactions performed with the statistical copolymer V81 and the gradient copolymer V101. Also the results of the analysis of the hydrolysis products are given. The products were compared with the educts. Further the differences between the hydrolyzed statistical and gradient copolymer were investigated.

The amount of added MSA depends on the amount of tBMA inside the polymer chains. It was calculated with *Equation 9.2.1* for both copolymers consisting of *tert*–butyl methacrylate (monomer 1) and benzyl methacrylate (monomer 2).

$$V_{MSA} = \frac{m \cdot F_{tBMA} \cdot x \cdot M_{MSA}}{M_{tBMA} \cdot \delta_{MSA}} \tag{9.2.1}$$

with V_{MSA} – Volume of the methanesulfonic acid, m – mass of the polymer, F_{tBMA} – ratio of tBMA in the polymer chain, x – multiplicity factor for the hydrolysis reagent = 2, M_{tBMA} – molar mass of tBMA = 142.2 g · mol^{-1}, M_{MSA} – molar mass of the methanesulfonic acid = 96.11 g · mol^{-1} and δ_{MSA} – density of the methanesulfonic acid = 1.48 g · ml^{-1}

Also the theoretical yields depend on the copolymer composition F_{tBMA}. They were calculated in the same way as in *Section 4.2*, using *Equation 9.2.2*.

$$y_{theo} = \frac{m \cdot F_{tBMA} \cdot M_{MAA}}{M_{tBMA}} + m \cdot (1 - F_{tBMA}) \tag{9.2.2}$$

with y_{theo} – theoretical yield, m – mass of the polymer, F_{tBMA} – ratio of tBMA in the polymer, M_{MAA} – molar mass of MAA = 86.09 g · mol^{-1}, M_{tBMA} – molar mass of tBMA = 142.2 g · mol^{-1}

The results of the two calculations, the needed volumes of methanesulfonic acid and the theoretical yields, as well as the resulting and percentage yields of the two hydrolysis reactions are listed in *Table 9.1*.

Tab. 9.1.: Amount of added MSA and yields of the hydrolysis products V111 and V121

Product	Educt		F_{tBMA}	weighted mass [g]	V_{MSA} [ml]	yield theo [g]	yield actual [g]	yield actual [%]
V111	P[tBMA–co–BzMA]	V81	0.67	0.20	0.12	0.15	0.12	83.80
V121	P[tBMA–grad–BzMA]	V101	0.53	0.25	0.12	0.20	0.16	80.22

The reactions proceeded in the same way than the model synthesis in *Section 4.2*. Some minutes after the addition of MSA the mixture of both experiments became a light brown gel. During the second hour the gels liquefied again. The added sodium hydrogen carbonate neutralized the excess of acid after the reaction time. Because a byproduct of this step is a

salt, after the precipitation in *n*–pentane a second precipitation in water/ methanol was done. However, the second precipitations was not only necessary to remove the formed salt. After the first precipitations from *n*–pentane the hydrolysis products were light brown powders, hence a second purification step was needed. After the purification steps the resulting copolymers were obtained in form of white powders. The yields of both hydrolysis were around 80 %. The structure of the copolymers had no influence on the behavior of the educts during the reaction.

The solubility–properties of these hydrolysis products V111 and V121 were same as that of the P[nBMA–co–MAA], reported in *Chapter 4* (*Table 4.3*). Using a benzyl ester group instead of the *n*–butyl group had no influence on the solubility of the hydrolyzed copolymer: The hydrolyzed copolymers V111 and V121 were dissolved in DMSO-d6 for ^{1}H–NMR–spectroscopy. The resulting ^{1}H–NMR–spectra of the two hydrolysis products (B) are presented in *Figures 9.2* and *9.3* together with the corresponding ^{1}H–NMR–spectra of the educts (A). The molecular structures of the educts and the products with the numbering of the carbons are shown in *Figure 9.1.*

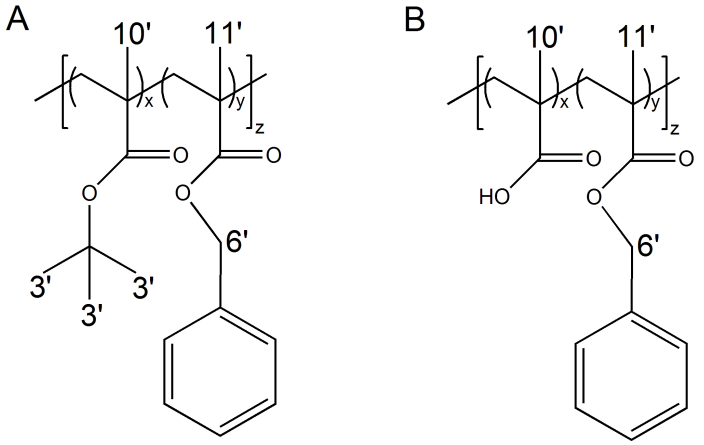

Fig. 9.1.: Molecular structures of educt V81, respectively V101, and product V111, respectively V121, with carbon–atom labels; A – educt P[$tBMA_x$–co–$BzMA_y$] and B – product P[MAA_x–co–$BzMA_y$] (z = x + y = 1)

The changes between the spectra of the educts and the products were distinct and for both hydrolysis the changes were the same. The intensity of the broad peak ranging from 1.25 to 1.55 ppm caused by the signals of the proton 3' shrank relative to the signals 6' from 4.8 ppm to 5.1 ppm, which remained constant. The reason was the absence of the signal 3' from the protons of the *tert*–butyl group in the products. In the spectra of the hydrolysis products the broad –COOH–signal could be monitored between 12.0 to 12.75 ppm. In the ^{1}H–NMR–spectra of the products additionally a H_2O signal was present because the DMSO–d6 was not dry. That the signal of the *tert*–butyl–group disappeared nearly completely indicated a total conversion of both educts.

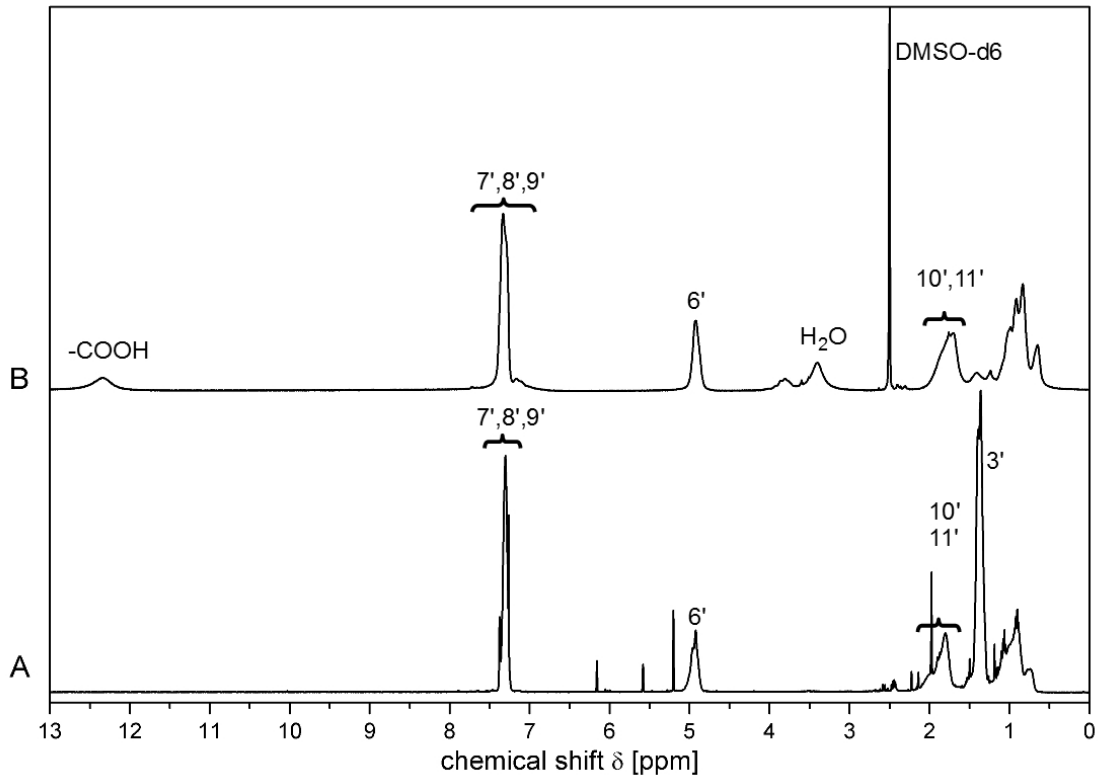

Fig. 9.2.: Comparison of ^{1}H–NMR–Spectra of educt V81 and product V111 (A: educt P[tBMA$_{0.67}$–co–BzMA$_{0.33}$]), V81; B: hydrolysis product P[MAA$_{0.67}$–co–BzMA$_{0.33}$], V111)

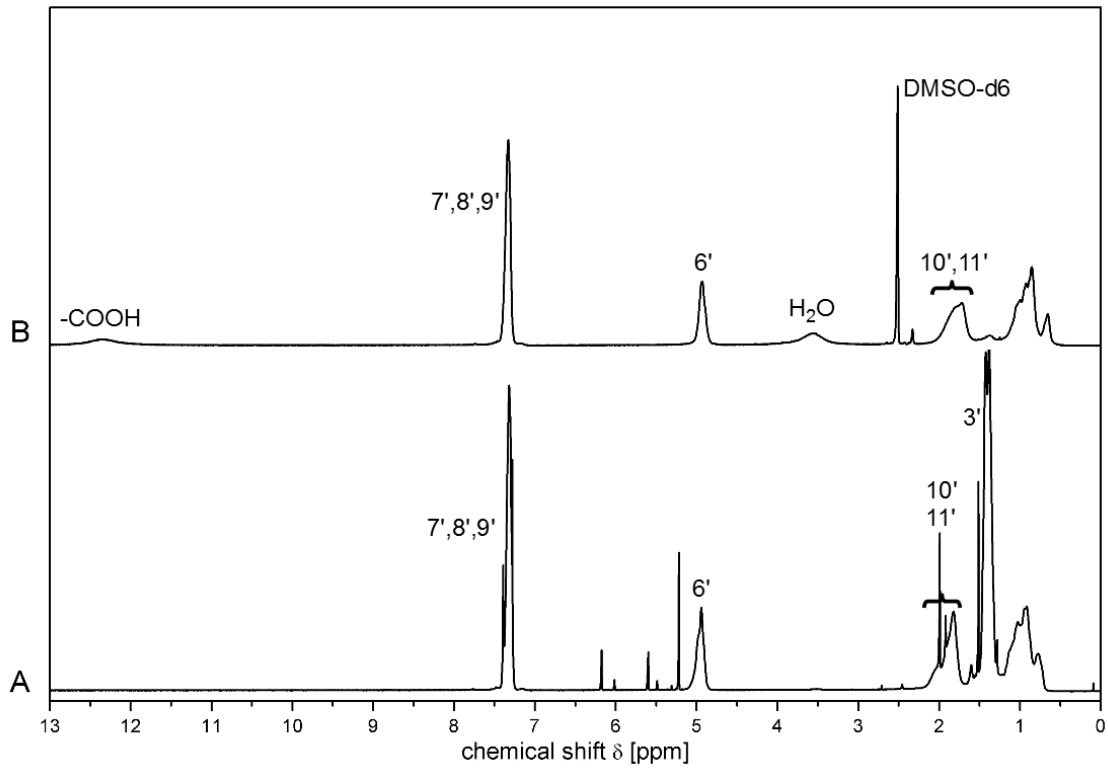

Fig. 9.3.: Comparison of ^{1}H–NMR–Spectra of educt V101 and product V121 (A: educt P[tBMA$_{0.53}$–grad–BzMA$_{0.47}$], V101; B: hydrolysis product P[MAA$_{0.53}$–grad–BzMA$_{0.47}$], V121)

The NMR–analysis is followed by the investigation of the hydrolyzed copolymers by elementary analysis and ATR–FTIR–spectroscopy. The results of the elementary analyzes are listed in *Table 9.2*. The theoretical values were calculated for 100 % conversion of the hydrolysis of the educts.

Tab. 9.2.: Results of the elemental analysis of educts V81 and V101 and hydrolysis–products V111 and V121 with divergence from the set values

Entry	F_{BzMA}		C [%]	ΔC	H [%]	ΔH	O [%]	ΔO
V81	0.33	theory	70.39		8.76		20.85	
		is	71.20	0.81	8.18	-0.58	20.62	-0.23
V111		theory	65.43		6.94		27.62	
		is	67.33	1.90	7.00	0.06	25.67	-1.96
V101	0.47	theory	71.45		8.32		20.23	
		is	71.08	1.54	7.81	-1.30	21.11	-0.23
V121		theory	68.17		6.92		24.91	
		is	65.36	-2.81	6.81	-0.12	27.83	2.92

The results of the two products were slightly different. The statistical copolymer V111 showed a small excess of carbon and a little less oxygen. At the gradient copolymer V121 the amount of carbon was slightly lower than calculated and for oxygen slightly higher. The differences were higher at the gradient copolymer than at the statistical copolymer. But in both cases the differences were justifiable. The results of the elementary analysis showed that the resulting copolymers were clean and dry.

In a next step the compositions of the copolymers was calculated from the content of carbon and hydrogen that were measured by means of elementary analysis like it was done with the educts. The different calibration curves were needed with the amounts of carbon and hydrogen of homopolymers PMAA and PBzMA as basis. These calibration curves are depicted in *Figure 9.4* and the corresponding linear equations are given as *Equations 9.2.3* and *9.2.4*.

$$C = 0.7498 - 0.1971 \cdot F_{MAA} \tag{9.2.3}$$

$$H = 0.0686 + 0.0017 \cdot F_{MAA} \tag{9.2.4}$$

The equations were recalculated for the composition and with the amounts of carbon, respectively hydrogen, taken from elementary analysis the compositions were calculated. The results are listed in *Table 9.3*.

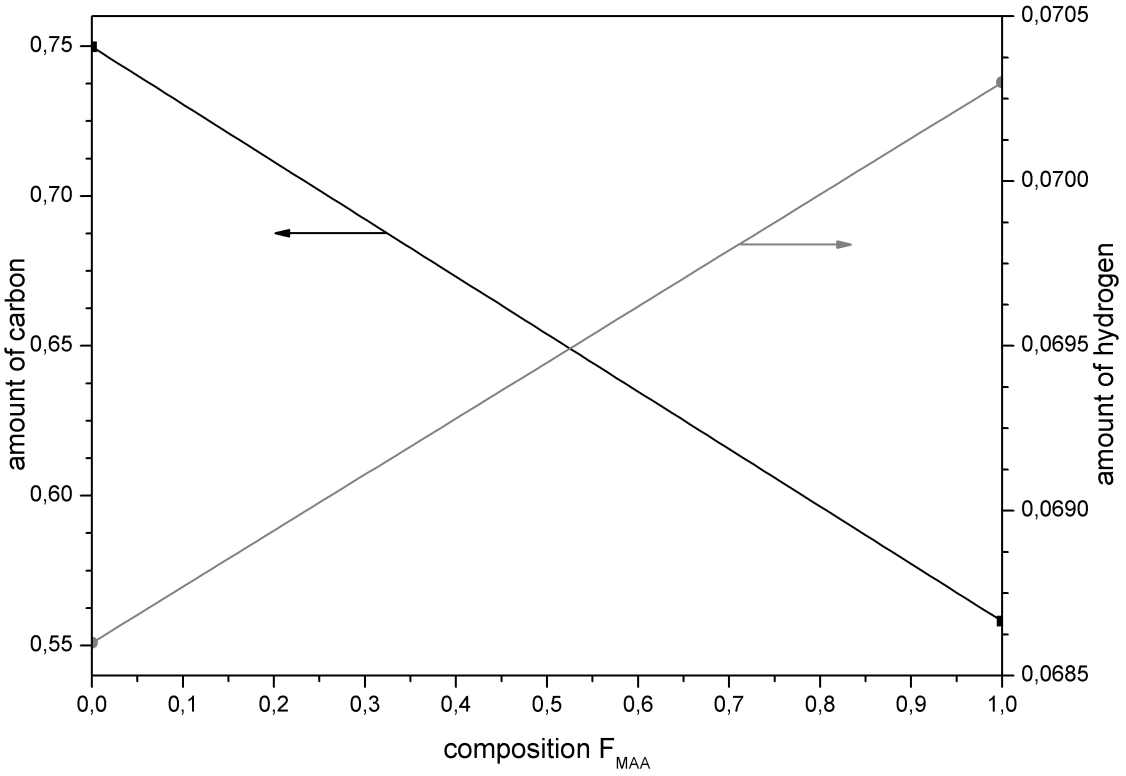

Fig. 9.4.: Calibration curves of amount of carbon (black line) and hydrogen (grey line) in P[MAA–co–BzMA]

Tab. 9.3.: Compositions of the copolymers of experiment V111 and V121 resulting from ^{1}H–NMR–analysis and elementary analysis

entry [min]	F^{NMR}_{MAA} [a]	$F^{EA,C}_{MAA}$ [b]	ΔF^{C}_{MAA} [c]	$F^{EA,H}_{MAA}$ [d]	ΔF^{H}_{MAA} [c]
V111	0.67	0.40	-0.27	0.83	0.16
V121	0.53	0.50	-0.03	–0.32	–0.85

[a] calculated from ^{1}H–NMR–spectra; [b] calculated from *Eq. 9.2.3*
[c] $\Delta F^{x}_{MAA} = F^{EA,x}_{MAA} - F^{NMR}_{MAA}$; [d] calculated from *Eq. 9.2.4*

The compositions $F^{EA,x}_{tBMA}$ calculated by elementary analysis differed obviously from the compositions which were determined from the ^{1}H–NMR–spectra of the precipitated copolymers for both elements carbon and hydrogen, expect the composition of V111 that was calculated from the amount of carbon. The differences could be caused by various problems: The presence of a residual solvent can be a reason for the large differences. However, the ^{1}H–NMR–spectra did not show the presence of solvents and therewith this can be excluded. The ^{1}H–NMR–spectra also did not contain signal which resulted from the presence of monomers. Inhomogeneity of the sample is also possible as a problem. The amount of polymer which was taken at a NMR–measurement is 10 mg and at an EA–measurement 2.5 mg. Hence, the smaller mass taken for the sample of the EA–measurement would be intensified a problem like inhomogeneity. The resulting copolymers were apparently consistent. Therewith, inhomogeneity can be

excluded. A third possibility is that the pollution happened during the measurement itself. The measurement of standards in periodical intervals should avoid that.

The ATR–FTIR–spectra of the educts (grey lines) and the corresponding product–spectra (black lines) are depicted in *Figures 9.5* and *9.6*. The vibrational bands in the IR–spectra were analyzed in view to changing which were caused by the hydrolysis.

In *section 7.2.2* two bands at 850 cm^{-1} and 730 cm^{-1} were introduced that are characteristic of polymer-incorporated tBMA and BzMA units, respectively. *Band 2* at 730 cm^{-1} of BzMA did not change so much but *band 1* at 850 cm^{-1} for tBMA differed obviously. The changes of *band 1* were strong and also influenced *band 2*. Therewith the analysis of peak height and peak area of both bands was not possible anymore. The loss of band intensity at 850 cm^{-1} clearly indicates that the hydrolysis products no longer contained tBMA–ester side groups. Also the intensity of the bands at 1370 cm^{-1} and 1390 cm^{-1} shrank with the hydrolysis. A third change exhibited the band at 1710 cm^{-1} which is the vibrational bands of ester–C=O–group. In the IR–spectrum of the educts the band was a small singlet. The product–spectra instead had a broader doublet at that region. The double band exhibited maxima at 1720 cm^{-1} and 1700 cm^{-1}. The literature refers 1720 cm^{-1} to ester–C=O vibration, while 1700 cm^{-1} belong to the vibrations of carboxylic acid–C=O groups. [87] Further the range $\tilde{\nu} > 3000\,cm^{-1}$ changed from educt to product in both cases. A broad band ranging from 2350 to 3700 cm^{-1} appeared which could be assigned to the vibrational band of the carboxylic acid OH–group. All in all the changes in the IR–spectra of the educts to the product–spectra and the differences of the product–spectra among themselves showed that both hydrolysis reactions worked well. Between the IR–spectra of the two products was no obvious difference. Hence, the structural sequence on the polymer chain has no influence on the IR–spectra.

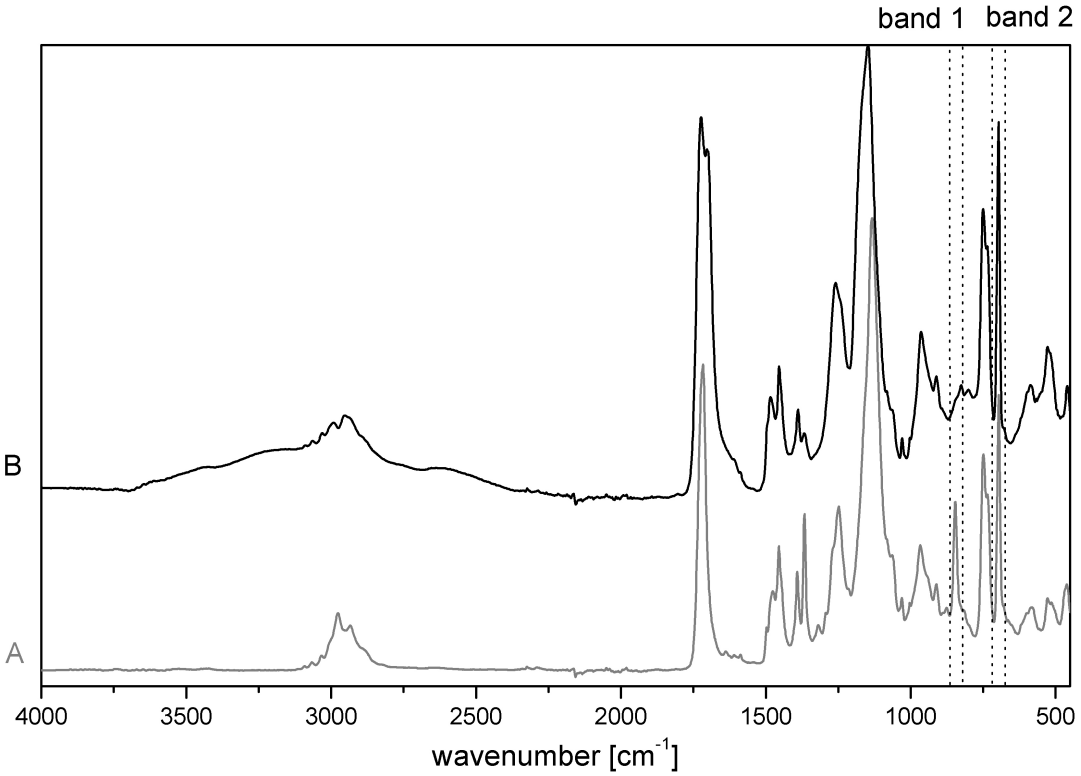

Fig. 9.5.: Comparison of ATR–FTIR–spectra of educt V81 and product V111 (A: educt P[tBMA$_{0.67}$–co–BzMA$_{0.33}$], V81; B: hydrolysis product P[MAA$_{0.67}$–co–BzMA$_{0.33}$], V111) (Spectra normalized to $A_{1134} = 1$)

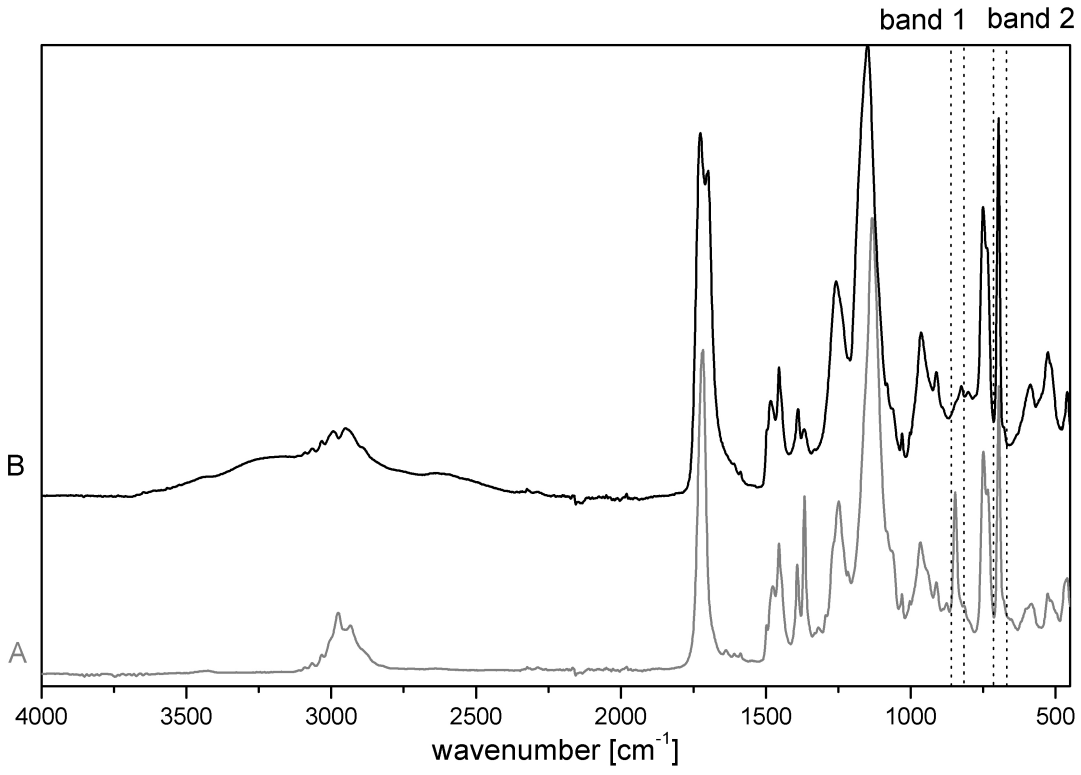

Fig. 9.6.: Comparison of ATR–FTIR–spectra of educt V101 and product V121 (A: educt P[tBMA$_{0.53}$–grad–BzMA$_{0.47}$], V101; B: hydrolysis product P[MAA$_{0.53}$–grad–BzMA$_{0.47}$], V121) (Spectra normalized to $A_{1134} = 1$)

The next type of analysis was the size exclusion chromatography (SEC). As with the hydrolyzed copolymers of *Chapter 4* also the products of V111 and V121 were not soluble in THF. As described in *Section 4.2* about 0.4 mg of the copolymer was mixed with 1 ml THF and two drops of TMSI and the mixture was stirred over night at RT. The copolymer became THF–soluble, because the carboxyl groups were converted into non–polar trimethylsilyl–esters. Since the presence of non–covalent fixed TMSI disturbed the dn/dc determination, only the relative molar mass of the copolymers were calculated from the maximum elution volume of the samples and *Equation 3.3.22* which based on a a polystyrene–calibration ("PS–Standard–values"). The resulting elution diagrams of the RI–detector signals are depicted in *Figure 9.7* and the calculated relative molar masses are listed in *Table 9.4*.

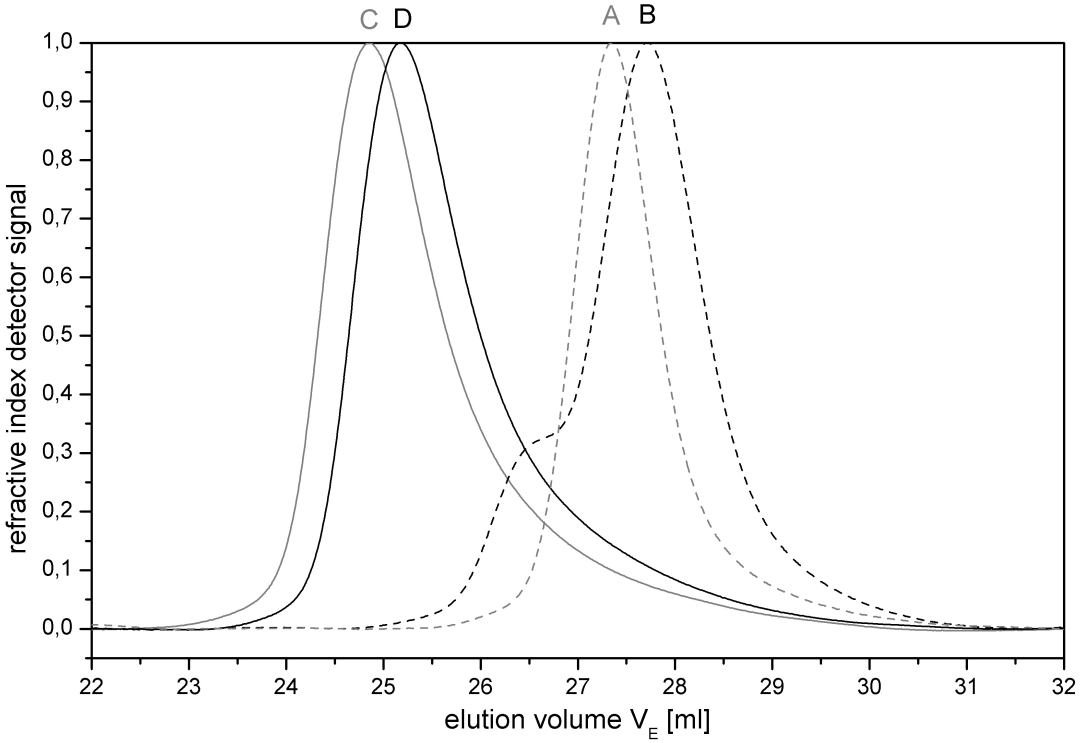

Fig. 9.7.: Comparison of SEC elution diagrams of the educts V81 and V101 as well as the products V111 and V121 (A: educt P[tBMA$_{0.67}$–co–BzMA$_{0.33}$], V81; B: hydrolysis product P[MAA$_{0.67}$–co–BzMA$_{0.33}$], V111; C: educt P[tBMA$_{0.53}$–grad–BzMA$_{0.47}$], V101; D: hydrolysis product P[MAA$_{0.53}$–grad–BzMA$_{0.47}$], V121)

Tab. 9.4.: SEC results of experiments V81, V111, V101 and V121

Entry	F_{BzMA}	V_E[a] [ml]	M_w[b] [g · mol^{-1}]	ΔM_w [g · mol^{-1}]	[%]
V81	0.33	27.34	21767		
V111		27.70	18111	3656	16.80
V101	0.47	24.85	77143		
V121		25.18	65317	11826	15.33

[a] Peak elution volume

[b] relative values, based on PSS calibration *Eq. 3.3.22*

The refractive index elution diagram of the sample of the copolymer V111 was bimodal. It shows a step on the left side. The reason for this could be the problem of solubility of the sample in THF. The elution diagram of the RI–detector of the sample of the copolymer V121 was monomodal as the elution diagram of the educt–sample. For both experiments the signals of the product–samples shifted towards higher elution volumes, i. e. lower molecular weights. The molar masses of the products were lower than the educts. In both cases the molar mass shrunk around 15 %. The calculated relative molar masses were slightly higher than the expected ones. The molar mass of the copolymer V111 should be 25 % lower than the molar mass of the educt and the molar mass of the copolymer V121 19 %. That was caused by the fact that for a relative molecular weight determination only the maximum elution volume is used and this is always higher than the average molar mass of a sample.

The investigation of the thermal behavior was the next part of analysis. The samples of the experiments V111 and V121 were heated up for two times from −80 to 200 °C with a cooling run in between (dT/dt = 10 K/min). The samples were not measured up to 300 °C as in *Section 4.2*, because it was known that the hydrolyzed polymer–samples will decompose. In *Figure 9.8* the two heating runs and the cooling run of both experiments V111 and V121 are represented.

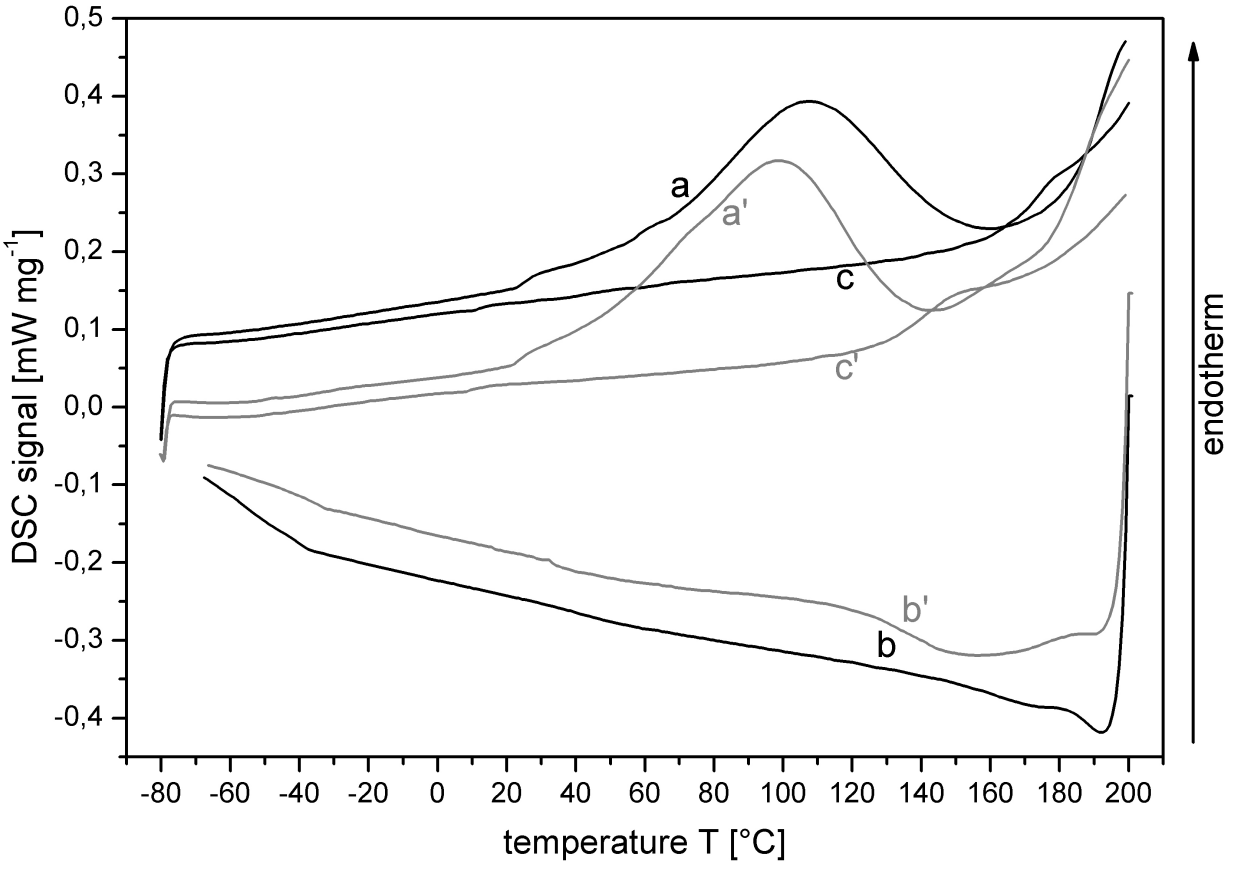

Fig. 9.8.: DSC thermograms of hydrolyzed copolymer V111 (black line) and V121 (grey line); a/a' – first heating run, b/b' – first cooling run, c/c' – second heating run; heating rate $10\,\mathrm{K}\cdot\mathrm{min}^{-1}$

Both thermograms of the first heating run exhibited an endothermic peak in the temperature range from 20 to 160 ℃. Then the DSC–signal increased. The second heating run and the cooling run did not show peaks or glass transition steps. The DSC–thermograms of P[nBMA–co–MAA], see *Section 4.2* also shows a similar endothermic peak during the first heating run. So also the hydrolyzed copolymers V111 and V121 decomposed during the first heating run. The peak area and peak height of the first heating runs of the thermograms of hydrolyzed copolymers V111 and V121 were determined and the results are listed in *Table 9.5*.

Tab. 9.5.: DSC results of hydrolysis–products of copolymers from experiment V111 and V121

Entry	F_{MAA}	Area $[J \cdot g^{-1}]$	T_{Peak} [℃]	T_{onset} [℃]	T_{offset} [℃]	Width [℃]	Height $[mW \cdot mg^{-1}]$
V111	0.67	23.7	70.5	34.5	106.8	53.7	0.0845
V121	0.53	98.1	89.9	47.3	129.6	63.2	0.2863

The peak area and the peak height of the endothermic peak of the sample V111, the statistical copolymer, was lower than the values of the gradient copolymer V121, although the amount of MAA inside the statistical copolymer was higher than in the gradient copolymer. The structure of the gradient copolymer lead to a stronger decomposition than the one of the statistical copolymer even if the amount of MAA in the gradient copolymer chain was lower than in the copolymer chain of the statistical copolymer.

9.3. Summary

The *tert*–butyl groups of the statistical and the gradient copolymer from *tert*–butyl methacrylate and benzyl methacrylate were hydrolytically cleaved by means of methanesulfonic acid (MSA). The characterization of the hydrolyzed copolymers with ^{1}H–NMR–spectroscopy and elementary analysis showed the absence of *tert*–butyl–groups in the polymer chains, and hence, a total conversion of the hydrolysis. The elementary analysis results agreed decently to the structure of both experiments. A calculation of the monomer molar fraction from the measured contents of carbon or hydrogen leads to values which obviously differed from the compositions resulting from the ^{1}H–NMR–analysis. The changes in the ATR-FTIR-spectra supported the good results of the ^{1}H–NMR–spectroscopy. The vibrational band of the OH-group occurred and the fingerprint–region change in case of the vibrational bands from the *tert*–butyl–group. The changes were so vigorous that an analysis of the vibrational band of BzMA was not possible. The RI–detector signals of copolymer V111 was bimodal what could be caused by the problem of the solubility of the hydrolyzed polymer in THF. The detector signals of the sample from copolymer V121 was monomodal. The SEC exhibited the decrease of the molar masses. The DSC analysis showed broad endothermic peaks for both copolymers in the same region and the samples did not regenerate after the first heating run. The peak area and the peak height of the endothermic peak of the statistical copolymer

V111 were lower than the ones of the gradient copolymer V121, despite the higher amount of MAA inside the statistical copolymer. Both hydrolysis of the copolymers worked well and an amphiphilic statistical and an amphiphilic gradient copolymer have successfully be obtained.

10. Synthesis of AB–Di–Block Copolymers from tert–Butyl Methacrylate and n–Butyl or Benzyl Methacrylate

This part describes the synthesis of AB–di–block copolymers from *tert*–butyl methacrylate as the block A and *n*–butyl methacrylate, respectively benzyl methacrylate, as the block B. The AB–di–block copolymers were synthesized to compare of the high structured copolymer with the unstructured statistical copolymers and the semi–structured gradient copolymers. The prepared block copolymers were aimed to be composed of the same length $P[A]_{0.5}$–b–$P[B]_{0.5}$. Moreover, the two resulting block copolymers were hydrolyzed with the same method than the statistical and the gradient copolymers before.

10.1. Materials and Methods

For compatibility reasons the AB–di–block copolymers were synthesized with the same materials and the former methods than the former statistical and gradient copolymers.

10.1.1. Materials

First are listed the chemicals which were used for the copolymerizations of the block copolymers. The treatments of chemicals were the same as detailed in *Sections 3.1.1* and *7.1.1.*

- monomers
  - *tert*–butyl methacrylate (tBMA, 98 %, *Alfa Aesar*)
  - *n*–butyl methacrylate (nBMA, 99 %, *Sigma–Aldrich*)
  - benzyl methacrylate (BzMA, 98 %, *Alfa Aesar*)
- initiator: *para*–toluenesulfonyl chloride (pTSC, 98 %, *Sigma–Aldrich*)
- catalyst: copper(I) chloride (97 %, *Sigma–Aldrich*)
- ligand: N,N,N',N',N"–pentamethyldiethylenetriamine (PMDETA, 99 %, *Sigma–Aldrich*)

- solvent: 2–butanone (MEK, *BDH Prolabo*, chromasol.)

The chemicals which were used for the hydrolysis are listed in the following. They were used as received.

- methanesulfonic acid (MSA, $\leq 99.5\,\%$, *Aldrich*)
- chloroform (99.9 %, *Acros*, extra dry over molecular sieve, stabilized)
- THF (chromasolv, *Aldrich*)
- *n*–pentane (*Aldrich*)

10.1.2. Synthesis of Block A – Macro Initiator

The block copolymers were also synthesized by Atom Transfer Radical Polymerization with the same system than the statistical and the gradient copolymers in *Chapters 3, 5, 7* and *8*. The experimental setup is depicted in *Figure 10.1*.

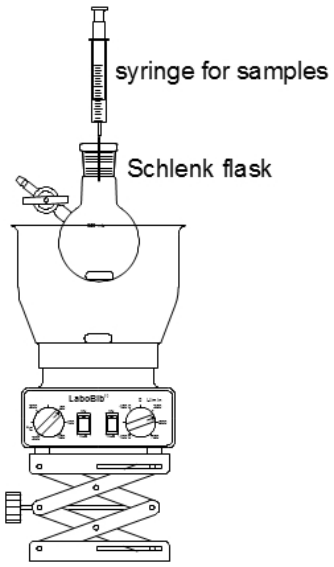

Fig. 10.1.: Experimental setup for batch block–copolymerization

A 50 ml Schlenk flask was heated out with a hot gun (air temperature ≈ 400 °C) under vacuum for five minutes and then flushed with nitrogen. The chemicals were weighted in a screw–cap glass in a specific order: First 0.0689 g ($3.61 \cdot 10^{-4}$ mol) pTSC was weighted, followed by the monomer tBMA, 8.9870 g (0.0632 mol). When the pTSC was dissolved, 0.0626 g ($3.61 \cdot 10^{-4}$ mol) PMDETA, and 0.0357 g ($3.61 \cdot 10^{-4}$ mol) CuCl were added. The mixture was rinsed into the Schlenk flask with 8.9870 g of the solvent MEK under nitrogen flow. Then the flask was sealed with a rubber septum. Subsequently the solution was degassed by means of 5 freeze–melt–cycles, flooded with nitrogen and then heated up to 80 °C for 45 minutes. At the start and the end of the reaction 0.05 ml samples were taken for ^{1}H–NMR analysis. Each 0.05 ml of aliquot–sample was given into 0.5 ml cold $CDCl_3$ without further purification.

After the reaction the Schlenk flask was removed from the oil bath. The flask was floated with air and the reactions mixture was cooled to 20 °C with a mixture of ice and water. Then the solution was dropped into 500 ml of a ice cooled water : methanol = 1 : 1 vol : vol mixture. The precipitated polymer was filtered over a P4 glass filter and dried at 45 °C under vacuum over night. The precipitated was dissolved in 20 ml CH_2Cl_2 and transferred into a separatory funnel. 20 ml H_2O were added and thoroughly shaken. The organic phase was separated and given into a round–bottom flask. The water phase was extracted two times more each with 10 ml CH_2Cl_2. All organic phased were combined. The solvent was removed by vacuum evaporation. The yield of the polymer is listed in *Table 10.1.*

Experiment V150 (PtBMA):
^{1}***H–NMR:*** 1.35–1.50 ppm (broad peak, –C$(CH_3)_3$, P[tBMA]); 1.45 ppm (s, –C$(CH_3)_3$, tBMA); 1.84–1.89 ppm (broad peak, –CH_3, P[tBMA]); 1.85 ppm (s, –CH_3, tBMA); 5.42 ppm (t, CH_2=C–, cis, tBMA); 5.95 ppm (s, CH_2=C–, trans, tBMA)

EA: 66.59 % C, 9.57 % H, (23.84 % O_{calc})

ATR–FTIR: 3100–2800 cm^{-1} (=CH_2, –CH_2–, –CH_3); 1718 cm^{-1} (–C=O); 1476 cm^{-1} (–CH_2–, –CH_3); 1457 cm^{-1} (–CH_2–, –CH_3); 1392 cm^{-1}; 1366 cm^{-1} (tBu); 1330 cm^{-1}; 1248 cm^{-1} (tBu); 1132 cm^{-1} (–C–O–C–); 1036 cm^{-1}; 969 cm^{-1}; 840 cm^{-1}; 875 cm^{-1} (tBu); 847 cm^{-1}; 816 cm^{-1}; 752 cm^{-1}; 666 cm^{-1}; 514 cm^{-1}; 497 cm^{-1}; 471 cm^{-1}

SEC: dn/dc = 0.0612 ml · g^{-1}; M_n = 11060 g · mol^{-1}; M_w = 11620 g · mol^{-1}; M_z = 12420 g · mol^{-1}

DSC: T_{onset} = 64.0 °C; T_{midpt} = 75.5 °C; T_g = 77.0 °C; T_{offset} = 85.0 °C; Δc_p = 0.247 J · g^{-1} · K^{-1}

10.1.3. Synthesis of Block B

The experimental setup was the same as for the macro initiator, see *Figure 10.1.* A 25 ml Schlenk flask was heated out with a hot gun (air temperature ≈ 400 °C) under vacuum for five minutes and then flushed with dry nitrogen. The chemicals were weighted in a screw–cap glass in a specific order: First 0.5246 g ($4.51 \cdot 10^{-5}$ mol) of the macroinitiator PtBMA was weighted in, followed by the monomer (Block B_1: 1.1234 g (0.0079 mol) nBMA, Block B_2: 1.3921 g (0.0079 mol) BzMA. Then 0.0078 g ($4.51 \cdot 10^{-5}$ mol) PMDETA, and 0.0045 g ($4.51 \cdot 10^{-5}$ mol) CuCl were added. The mixture was rinsed into the Schlenk flask with 1.6479 g of the solvent MEK for Block B_1 or 1.9167 g MEK for Block B_2 under nitrogen flow. Then the flask was sealed with a rubber septum. Subsequently the solution was degassed by means of 5 freeze–melt– cycles, flooded with nitrogen and then heated up to 80 °C for 1 hour. At the beginning and the end of the reaction 0.05 ml samples were taken for ^{1}H–NMR analysis. The 0.05 ml of aliquot–sample were given into 0.5 ml cold $CDCl_3$ without further purification.

After the reaction the Schlenk flask was removed from the oil bath. The flask was floated with air and the reactions mixture was cooled to 20 °C with a mixture of ice and water. Then the solution was dropped into 50 ml of a ice cooled water : methanol = 1 : 1 vol : vol mixture. The precipitated polymer was filtered over a P4 glass filter and dried at 45 °C under vacuum over night. The precipitated was dissolved in 5 ml CH_2Cl_2 and transferred into a separatory funnel. 5 ml H_2O were added and thoroughly shaken. The organic phase was separated and given into a round–bottom flask. The water phase was extracted two times more each with 2 ml CH_2Cl_2. All organic phased were combined. The solvent was removed by vacuum evaporation. The yield of the polymer is listed in *Table 10.1.*

Experiment V151 P[PtBMA–b–nBMA]:

^{1}***H–NMR:*** 0.86–0.94 ppm (broad peak, $–CH_3$, nBMA and P[nBMA]); 1.46–1.30 ppm (broad peak, $–C(CH_3)_3$, P[tBMA], $–CH_2–$, nBMA and P[nBMA]); 1.43 ppm (s, $–C(CH_3)_3$, tBMA); 1.52–1.65 ppm (broad peak, $–CH_2–$, nBMA and P[nBMA]); 1.72–1.82 ppm (broad peak, $–CH_3$, P[tBMA] and P[nBMA]); 1.84 ppm (s, $–CH_3$, tBMA); 1.88 ppm (s, $–CH_3$, nBMA); 3.82–3.99 ppm (broad peak, $–OCH_2R$, P[nBMA]); 4.09 ppm (t, OCH_2R, nBMA); 5.41 ppm (t, CH_2=C–, cis, tBMA); 5.48 ppm (t, CH_2=C–, cis, nBMA); 5.94 ppm (s, CH_2=C–, trans, tBMA); 6.03 ppm (s, CH_2=C–, trans, nBMA)

EA: 68.14 % C, 8.97 % H, (22.89 % O_{calc})

ATR–FTIR: 3080–2800 cm^{-1} (=CH_2, $–CH_2–$, $–CH_3$); 1721 cm^{-1} (–C=O); 1473 cm^{-1} ($–CH_2–$, $–CH_3$); 1512 cm^{-1}; 1456 cm^{-1} ($–CH_2–$, $–CH_3$); 1392 cm^{-1}; 1367 cm^{-1} (tBu); 1321 cm^{-1}; 1270 cm^{-1} (tBu); 1244 cm^{-1} (nBu); 1135 cm^{-1} (–C–O–C–); 1065 cm^{-1} (nBu); 1020 cm^{-1}; 1002 cm^{-1}; 967 cm^{-1} (nBu); 944 cm^{-1}; 876 cm^{-1} (tBu); 750 cm^{-1}; 657 cm^{-1}; 605 cm^{-1}; 581 cm^{-1}; 517 cm^{-1}; 472 cm^{-1};

SEC: dn/dc = 0.0772 $ml \cdot g^{-1}$; M_n = 23590 $g \cdot mol^{-1}$; M_w = 29310 $g \cdot mol^{-1}$; M_z = 34340 $g \cdot mol^{-1}$

DSC: glass transition 1: T_{onset} = 32.0 °C; T_{midpt} = 49.0 °C; T_g = 54.5 °C; T_{offset} = 62.0 °C; Δc_p = 0.187 $J \cdot g^{-1} \cdot K^{-1}$; glass transition 2: T_{onset} = 100.0 °C; T_{midpt} = 103.0 °C; T_g = 103.5 °C; T_{offset} = 105.5 °C; Δc_p = 0.074 $J \cdot g^{-1} \cdot K^{-1}$

Experiment V152 P[PtBMA–b–BzMA]:

^{1}***H–NMR:*** 1.22–1.54 ppm (broad peak, $–C(CH_3)_3$, P[tBMA]); 1.47 ppm (s, $–C(CH_3)_3$, tBMA); 1.69–1.91 ppm (broad peak, $–CH_3$, P[tBMA] and P[BzMA]); 1.86 ppm (s, $–CH_3$, tBMA); 1.95 ppm (s, $–CH_3$, BzMA); 4.79–4.97 ppm (broad peak, $–OCH_2R$, P[BzMA]); 5.18 ppm (s, OCH_2R, BzMA); 5.45 ppm (t, CH_2=C–, cis, tBMA); 5.56 ppm (t, CH_2=C–, cis, BzMA); 5.98 ppm (s, CH_2=C–, trans, tBMA); 6.14 ppm (s, CH_2=C–, trans, BzMA); 7.18–7.41 ppm (broad peak, aromatic ring, BzMA and P[BzMA])

EA: 72.17 % C, 7.49 % H, (20.34 % O_{calc})

ATR–FTIR: 3140–2800 cm^{-1} (=CH_2, –CH_2–, –CH_3, aromatic ring); 1719 cm^{-1} (–C=O); 1478 cm^{-1} (–CH_2–, –CH_3); 1455 cm^{-1} (–CH_2–, –CH_3); 1392 cm^{-1}; 1367 cm^{-1} (tBu); 1318 cm^{-1}; 1294 cm^{-1}; 1246 cm^{-1} (tBu); 1135 cm^{-1} (–C–O–C–); 1030 cm^{-1}; 967 cm^{-1} (Bz); 912 cm^{-1}; 877 cm^{-1}; 847 cm^{-1} (tBu); 827 cm^{-1}; 749 cm^{-1} (Bz); 696 cm^{-1} (Bz); 581 cm^{-1}; 527 cm^{-1}; 459 cm^{-1}

SEC: dn/dc = 0.1151 $ml \cdot g^{-1}$; M_n = 25040 $g \cdot mol^{-1}$; M_w = 31030 $g \cdot mol^{-1}$; M_z = 34700 $g \cdot mol^{-1}$

DSC: glass transition 1: T_{onset} = 24.5 °C; T_{midpt} = 34.5 °C; T_g = 31.0 °C; T_{offset} = 43.0 °C; Δc_p = 0.212 $J \cdot g^{-1} \cdot K^{-1}$; glass transition 2: T_{onset} = 58.5 °C; T_{midpt} = 63.0 °C; T_g = 59.0 °C; T_{offset} = 60.0 °C; Δc_p = 0.024 $J \cdot g^{-1} \cdot K^{-1}$

10.1.4. Hydrolysis

0.25 g of the block copolymer were dissolved in 2.25 g (1.5 ml) $CHCl_3$ and was stirred over night at room temperature. Then the respective amount of methanesulfonic acid (MSA) was added, see *Table 10.11.* The mixture was stirred for 2 hours at room temperature. A spatula–spoon of sodium hydrogen carbonate was added and this mixture was stirred for 30 min. Subsequently 5 ml THF were added and the mixture was filtered over a P4 glass filter. Afterward the solution was dropped into 200 ml of ice–cold *n*–pentane. The precipitated polymer was filtered over P4 glass filter and dried at room temperature for two hours. Then the copolymer was re–dissolved in 1 ml THF and the solution was dropped into 200 ml of an ice cooled water : methanol = 1 : 1 vol : vol mixture. The precipitated polymer was filtered over P4 glass filter and dried at room temperature under an oil–pump vacuum over night. The yields are also listed in *Table 10.11.*

Experiment V161 P[PMAA–b–nBMA]:

^{1}***H–NMR:*** 0.65–1.25 ppm (broad peak, –CH_3, P[nBMA]); 1.3–1.45 ppm (broad peak, –CH_2–, P[nBMA]); 1.5–1.61 ppm (broad peak, –CH_2–, P[nBMA]); 1.62–2.05 ppm (broad peak, –CH_3, P[nBMA], P[MAA]); 3.33 ppm (H_2O); 3.8–4.0 ppm (broad peak, –OCH_2R, P[nBMA]); 12.1–12.5 ppm (broad peak, –COOH, P[MAA])

EA: 61.75 % C, 8.36 % H, (29.89 % O_{calc})

ATR–FTIR: 3600–2350 cm^{-1} (–COOH); 3050–2350 cm^{-1} (–CH_2–, –CH_3); 1723 cm^{-1} (–C=O); 1456 cm^{-1} (–CH_2–, –CH_3); 1367 cm^{-1}; 1247 cm^{-1} (nBu); 1142 cm^{-1} (–C–O–C–); 1064 cm^{-1} (nBu); 965 cm^{-1} (nBu); 943 cm^{-1}; 847 cm^{-1}; 802 cm^{-1}; 749 cm^{-1}; 697 cm^{-1}; 516 cm^{-1}; 468 cm^{-1}

Experiment V162 P[PMAA–b–BzMA]:

^{1}***H–NMR:*** 0.55–0.73 ppm (broad peak); 0.74–1.17 ppm (broad peak); 1.55–2.08 ppm (broad peak, $-CH_3$, P[BzMA], P[MAA]); 3.40 ppm (H_2O); 3.71–3.90 ppm (broad peak); 4.8–5.04 ppm (broad peak, $-OCH_2R$, P[BzMA]); 7.04–7.49 ppm (broad peak, aromatic ring, P[BzMA]); 12.13–12.56 ppm (broad peak, –COOH, P[MAA])

EA: 67.33 % C, 7.00 % H, (25.67 % O_{calc})

ATR–FTIR: 3600–2360 cm^{-1} (–COOH); 3110–2800 cm^{-1} ($=CH_2$, $-CH_2-$, $-CH_3$, aromatic ring); 1724 cm^{-1} (–C=O); 1703 cm^{-1} (–C=O); 1484 cm^{-1} ($-CH_2-$, $-CH_3$); 1455 cm^{-1} ($-CH_2-$, $-CH_3$); 1389 cm^{-1}; 1367 cm^{-1}; 1259 cm^{-1}; 1147 cm^{-1} (–C–O–C–); 1029 cm^{-1}; 964 cm^{-1} (Bz); 912 cm^{-1}; 826 cm^{-1}; 801 cm^{-1}; 750 cm^{-1} (Bz); 697 cm^{-1} (Bz); 587 cm^{-1}; 528 cm^{-1}; 460 cm^{-1}

10.1.5. Characterization

All characterization–methods were the same as with the batch copolymers of *Chapter 3*. The used methods were:

- ^{1}H–NMR spectroscopy
- elementary analysis
- ATR–FTIR–spectroscopy
- size exclusion chromatography
- differential scanning calorimetry

The same instruments under the same conditions were used for the investigation of the resulting copolymers.

10.2. Results and Discussion of the Block Copolymerizations

To prepare P[tBMA]–b–P[nBMA] and P[tBMA]–b–P[BzMA] AB–di–block copolymers, a P[tBMA]–B_i macroinitiator was prepared in the first step. The block copolymers were obtained by subsequent growth of the second monomer on this starter block. The synthesis of the macro initiator P[tBMA] was performed by means of the same ATRP system that was used to prepare the statistical copolymers in *Section 3*, using *para*–toluolsulfonyl chloride (pTSC) as the initiator, Cu^ICl as the catalyst and N,N,N',N',N"–pentamethyldiethylenetriamine (PMDETA) as the ligand. The initial ratio of the substances was pTSC : CuCl : PMDETA : Mon = 1 : 1 : 1 : 175. The reactions were carried out in 2–butanone (MEK) as solvent at 80 °C. The ratio of monomer to solvent was wt : wt 1 : 1 (*Table 10.1*). The reaction was stopped after 45 min because it was known from the synthesis of the homopolymer P[tBMA] in *Section 3* that after that time range around 20 % monomer conversion are reached which is the target value for the macro initiator of Block A to exhibit a degree of polymerization of about X_n = 35. The resulting copolymers were precipitated in an ice–cooled mixture of water and methanol with vol : vol 1 : 1, then the precipitated polymers were separated from the liquid phase by filtration and dried over night at 45 °C under vacuum. The polymers were re–dissolved in dichloromethane and transferred in a separation funnel. Water was added and the CuCl was extracted. The polymer–dichloromethane solution was clear and green. After the extraction the organic phase was clear and colorless and the water phase was clear and blue. The organic phase was separated and the solvent was removed by vacuum evaporation. The resulting polymer was a white powder. The yield of the macroinitiator was 1.85 g (20 %), as shown in *Table 10.1, V150 A*.

Tab. 10.1.: Compositions and yields of the solutions for polymerizations of block–copolymers

Entry	Block	Component	n [mol]	m [g]	yield
V150	A	tBMA	0.0632	8.9870	1.85 g
		pTSC	$3.61 \cdot 10^{-4}$	0.0689	20.45 %
		PMDETA	$3.61 \cdot 10^{-4}$	0.0626	
		CuCl	$3.61 \cdot 10^{-4}$	0.0357	
		MEK		8.9870	
V151	AB_1	nBMA	0.0079	1.1234	1.22 g
		P[tBMA]	$4.51 \cdot 10^{-5}$	0.5246	74.12 %
		PMDETA	$4.51 \cdot 10^{-5}$	0.0078	
		CuCl	$4.51 \cdot 10^{-5}$	0.0045	
		MEK		1.6479	
V152	AB_2	BzMA	0.0079	1.3921	1.12 g
		P[tBMA]	$4.51 \cdot 10^{-5}$	0.5246	58.30 %
		PMDETA	$4.51 \cdot 10^{-5}$	0.0078	
		CuCl	$4.51 \cdot 10^{-5}$	0.0045	
		MEK		1.9167	

For the synthesis of the block copolymers with the P[tBMA] macroinitiator, resulting from experiment V150 as block A, the ATRP system was adapted respectively with the same ratios of monomer to initiator system and monomer to solvent. The compositions of the two reaction mixtures in experiments V151 and V152 are listed in *Table 10.1* together with the corresponding yields. After the reaction time of 1 hour in both cases the reactions were stopped by floating the Schlenk flask with air and cooling down the reaction mixtures. The work–up of the reaction mixtures and the resulting copolymers was done in the same way as for Block A. The reaction time was enlarged from 45 min to 1 hour form Block A to Block B because the conversion curves of the statistical copolymers flattened with higher conversions and because the used macro initiator already contained a certain amount of monomer units. The yields of the two experiments are also listed in *Table 10.1*. The yields of the two copolymerizations were unexpected high contrary to the assumption of the flat conversion curve. With the use of *Equation 10.2.1* the compositions of the AB–di–block copolymers were calculated. Hence, no symmetric AB–di–block–copolymers have been obtained in view of gravimetry, instead compound V151 is of the composition $P[tBMA]_{35}$–b–$P[nBMA]_{130}$, while polymer V152 exhibits $P[tBMA]_{35}$–b–$P[BzMA]_{101}$.

$$\bar{X}_n^{Block} = \frac{[M]_0}{[I]_0} \cdot p \tag{10.2.1}$$

with $\bar{X}_n^{Block}$ = degree of polymerization of a block copolymer, $[M]_0$ = monomer concentration at the start of the polymerization, $[I]_0$ = initiator concentration at the start of the polymerization, p = conversion

In following paragraphs the results of the analyzes from the two block copolymers P[tBMA]–b–P[nBMA] and P[tBMA]–b–P[BzMA], and also their discussion is described.

10.2.1. Kinetic Studies

At the start and at the end of the experiments V150, V151 and V152 samples were taken for the analysis with ^{1}H–NMR–spectroscopy. The ^{1}H–NMR–spectra were analyzed regarding the conversion p of the monomers. The signals in the resulting spectra were assigned to the structure elements of the monomers and the copolymer as shown in *Table 10.2*. The position of the peaks were taken from literature [63] and [85].

The structures of the monomers and the block copolymers are depicted in *Figure 10.2* together with the numbering of the carbon–atoms for the assignment of the peaks in the ^{1}H–NMR–spectra. *Figure 10.3* shows the ^{1}H–NMR–spectrum of the reactions mixtures of the experiments V150, V151 and V152 at the end of the polymerization times. In this figure the signals are assigned to the corresponding carbon–atoms of the monomers and the polymer chain.

Tab. 10.2.: Position and assignments of the signals in the obtained ^{1}H–NMR–spectra of AB–di–block copolymers

δ [ppm]	Multiplicity	No. of carbons	Carbon No.*	Structure element
0.6–0.8	broad peak	3H	9,9'	–CH_3, nBMA and P[nBMA] side chain
1.25–1.45	broad peak	9H	3'	–$C(CH_3)_3$, P[tBMA]
		2H	7,7'	–CH_2–, nBMA and P[nBMA] side chain
1.42	s	9H	3	–$C(CH_3)_3$, tBMA
1.5–1.6	broad peak	2H	8,8'	–CH_2–, nBMA and P[nBMA] side chain
1.7–1.95	broad peak	3H	10'	–CH_3 backbone, P[tBMA]
		3H	11'	–CH_3 backbone, P[nBMA]
		3H	18'	–CH_3 backbone, P[BzMA]
1.85	s	3H	10	–CH_3, tBMA
1.9	s	3H	11	–CH_3, nBMA
1.95	s	3H	18	–CH_3, BzMA
3.8–3.95	broad peak	2H	14'	–OCH_2R, P[nBMA]
4.0	t	2H	14	–OCH_2R, nBMA
4.75–5.05	broad peak	2H	6'	–OCH_2R, P[BzMA]
5.2	s	2H	6	–OCH_2R, BzMA
5.4	t	1H	2	CH_2=C–, cis, tBMA
5.5	t	1H	5	CH_2=C–, cis, nBMA
5.55	t	1H	13	CH_2=C–, cis, BzMA
5.9	s	1H	1	CH_2=C–, trans, tBMA
6.0	s	1H	4	CH_2=C–, trans, nBMA
6.1	s	1H	12	CH_2=C–, trans, BzMA
7.2–7.5	broad peak	5H	15–17	aromatic ring, BzMA
		5H	15'–17'	aromatic ring, P[BzMA]

* cf. *Figure 10.2*

In *Figure 10.3A* the resulting mixture of experiment V150 is given. The monomer tBMA is represented by a singlet at 5.9 ppm (1), a triplet at 5.4 ppm (2), a singlet at 1.85 ppm (10) and a singlet at 1.42 ppm (3). The broad signal between 1.25 ppm and 1.45 ppm (3') is caused by the *tert*–butyl groups of the polymer chain and the one between 1.7 ppm and 1.95 ppm (10') by the CH_2–group of the polymer–backbone. The resulting P[tBMA] is the basis of the two following block copolymers. The signals at circa 2.4 ppm (quartet), 2.1 ppm (singlet) and 1.0 ppm (triplet) ppm belong to MEK.

Figure 10.3B shows the resulting mixture of experiment V151 which is the synthesis of P[tBMA]–b–P[nBMA]. A little rest of the monomer tBMA gave barely visible signals at

5.9 ppm (1) and 5.4 ppm (2). The monomer for the second block B_1 nBMA give a singlet signal at 6.0 ppm (4), a triplet at 5.5 ppm (5) and a singlet at 1.85 ppm (11) for the methacrylate part. The *n*–butyl chain is represented by the signals at 4.0 ppm (6) for the α–protons, at 1.25–1.45 ppm (7) for the β–protons, at 1.5–1.6 ppm (8) for the γ–protons and at 0.6–0.8 ppm (9) for the δ–protons. The signals of the polymerized β–, γ– and δ–protons appear in the same chemical regions and become mutually overlapped. Additionally the signal of the β–protons interferes with the broad signal of the polymerized *tert*–butyl–group of P[tBMA]. The α–proton signal of the P[nBMA] appears between 4.75 ppm and 5.05 ppm (6'). The signal of the CH_2–group of the polymer–backbone (10') overlap with the signal of the CH_2–backbone–group of P[tBMA] between 1.7 ppm and 1.95 ppm.

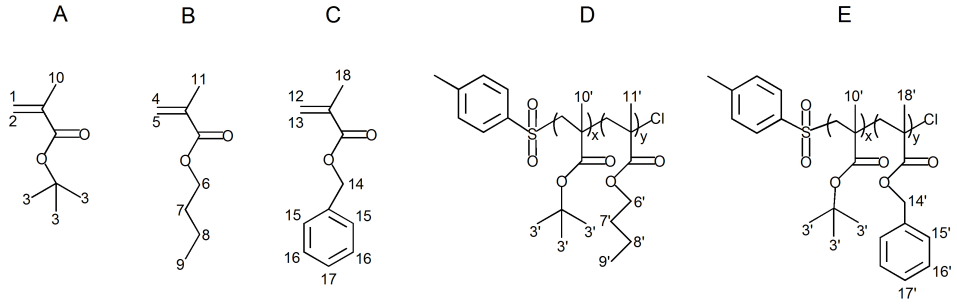

Fig. 10.2.: Molecular structures of the monomers (A) tBMA, (B) nBMA and (C) BzMA and the resulting block copolymers of (D) experiment V151 and (E) experiment V152 with carbon–atom labels (x + y = 1)

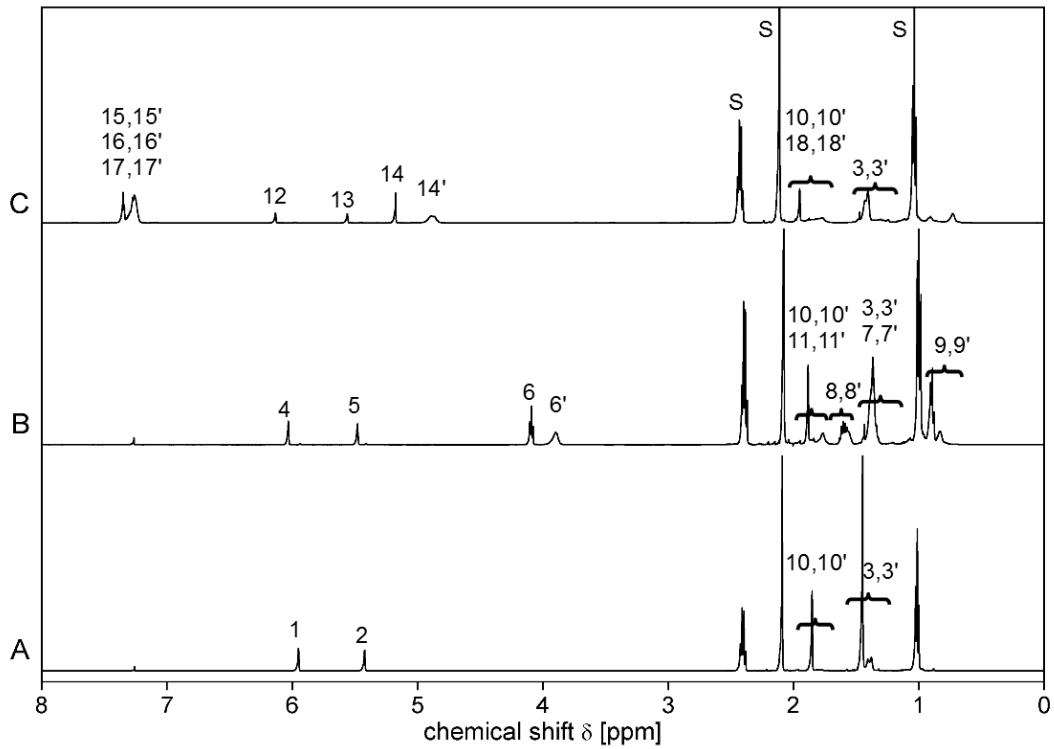

Fig. 10.3.: ^{1}H–NMR–spectra of (A) the macroinitiator P[tBMA]–B_i (V150) after 45 min reaction time, (B) block copolymer P[tBMA]–b–P[nBMA] (V151) and (C) block copolymer P[tBMA]–b–P[BzMA] (V152) after 60 min reaction time (I:M = 1:175, T = 80 °C, S = solvent signals: MEK)

Figure 10.3C depicts the ^{1}H–NMR–spectrum of experiment V152 at the end of the polymerization time with BzMA as monomer for Block B_2. As in *Figure 10.3B* there are barely visible signals of the monomeric tBMA at 5.9 ppm (1) and 5.4 ppm (2). The singlet signal at 6.1 ppm (12), the triplet at 5.55 ppm (13) and the singlet at 1.95 ppm (18) are caused by the methacrylate–part of the monomer BzMA. The singlet signal at 4.0 ppm (14) represented the methylene–group of BzMA and the broad signal between 7.2 and 7.5 ppm (15–17) the benzylic ring. A broad signal between 3.8 ppm and 3.95 ppm (18') is caused by the methylene–group inside the polymer chain. The methylene–groups of the polymerized BzMA–units (14') is located between 4.79 ppm and 4.97 ppm. The CH_2–group of the BzMA–part of the polymer backbone lay in the same region than the other CH_2–group in the polymer backbone of tBMA between 1.7 and 1.95 ppm. The benzylic ring inside the polymer chain show a broad signal with the same chemical shift than the benzyl–ring of the monomer between 7.2 ppm and 7.5 ppm (15'–17').

Tab. 10.3.: Integrals and conversion of experiments V150, V151 and V152

entry	A1	A6/A14	A6'/A14'	A8,8'	A3,3' A7,7'	A3'	conversion p
V150	1.00	–	–	–	11.56	0.28	0.22
V151	0.03	2.05	2.16	4.47	13.45	0.97	0.51
V152	0.02	2.05	3.81	–	14.88	1.63	0.65

The peak area of the signals 1 and 3/3' in *Figure 10.3A* were determined and with these values the conversion of the monomer tBMA of experiment V150 was calculated with *Equations 10.2.2* and *10.2.3*. The results are listed in *Table 10.3*.

$$A_{3'} = \frac{A_{3,3'}}{9} - A_1 \tag{10.2.2}$$

$$p_{tBMA} = \frac{A_{3'}}{A_{3'} + A_1} \tag{10.2.3}$$

with $A_{3,3'}$ = integral intensity at 1.25 to 1.45 ppm; A_1 = integral intensity at 5.9 ppm

The conversion of the monomer nBMA of experiment V151 was calculated from the peak areas of the signals 6 and 6' with the *Equation 10.2.4* and the conversion of BzMA of experiment V152 from the peak areas of the signals 14 and 14' with the *Equation 10.2.5*. The results of the two calculations are listed in *Table 10.3*.

$$p_{nBMA} = \frac{A_{6'}}{A_{6'} + A_6} \tag{10.2.4}$$

$$p_{BzMA} = \frac{A_{14'}}{A_{14'} + A_{14}} \tag{10.2.5}$$

with A_6 = integral intensity at 5.2 ppm; $A_{6'}$ = integral intensity at 4.75 to 5.05 ppm; A_{14} =

integral intensity at 4.0 ppm; $A_{14'}$ = integral intensity at 3.8 to 3.95 ppm

The calculated conversions fit to the measured gravimetric yields, c. f. *Table 10.1.* For the determination of the composition of the two AB–di–block copolymers from the ^{1}H–NMR–spectra, the precipitated copolymers were analyzed by ^{1}H–NMR–spectroscopy, even as the macro initiator. The spectra are depicted in *Figure 10.4.* All three spectra show that the precipitated polymers contained non–converted monomers. It was not possible to wash these out of the polymer coils.

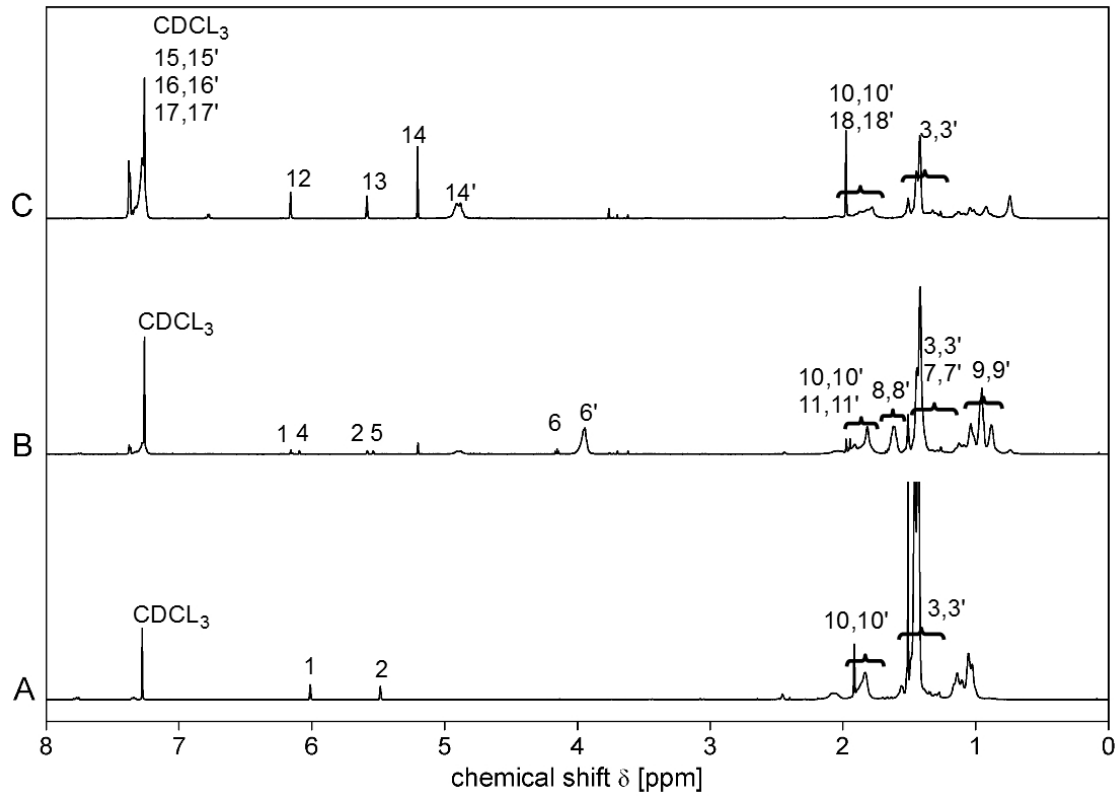

Fig. 10.4.: ^{1}H–NMR–spectra of precipitated (A) macroinitiator P[tBMA]–B_i (V150) after 45 min reaction time, (B) block copolymer P[tBMA]–b–P[nBMA] (V151) and (C) block copolymer P[tBMA]–b–P[BzMA] (V152) after 60 min reaction time (I:M = 1:175, T = 80 °C, S = solvent signals: MEK)

The composition of the block copolymers V151 and V152 was calculated from the ratio of the intensity of the integrals 3' and 6', respectively 3' and 14', of the ^{1}H–NMR–spectra of the precipitated AB–di–block copolymers. The peak areas of the different signals are given in *Table 10.4.*

Tab. 10.4.: Peak ares of precipitated AB–di–block copolymers V151 and V152

entry	A1	A6/A14	A6'/A14'	A8,8'	A3,3' A7,7'	A3'	F_{tBMA}	F_{nBMA}/ F_{BzMA}
V151	0.05	0.10	2.00	2.25	12.42	1.08	0.52	0.48
V152	0.01	0.87	2.00	–	8.18	0.90	0.47	0.53

For the determination of the peak area of the integral 3' in the ^{1}H–NMR–spectrum of experiment V151 the interfering peak areas of the integrals 3, 7 and 7' had to be subtracted from the mixed intensity of the integral (3,3', 7,7'), see *Equation 10.2.6*. The signal caused by the β–protons is equal to the signal caused by the γ–protons of the *n*–butyl chain, so the peak area of signal 8,8' was subtracted from the peak area of the mixed signal. The signal of the monomeric *tert*–butyl–group was eliminated by the subtraction of the value of the peak area of integral 1.

$$A_{3'} = \frac{A_{3'} - A_{8,8'}}{9} - A_1 \tag{10.2.6}$$

The integrals 3 and 3' interfere in the ^{1}H–NMR–spectrum of experiment V152 as in the spectrum of experiment V150. Hence the peak area of integral A3' was calculated with *Equation 10.2.2*. The values of the peak areas of the integrals 6' and 14' were divided by 2 and then the ratios of the two units in the polymer chain were determined. The results of the calculations are given in *Table 10.4*. The compositions of the two resulting block copolymers are

- V151: P[A]–b–P[B_1]: P[tBMA]$_{0.52}$–b–P[nBMA]$_{0.48}$
- V152: P[A]–b–P[B_2]: P[tBMA]$_{0.47}$–b–P[BzMA]$_{0.53}$

The compositions of both block copolymers were nearly the same and in both copolymers the blocks are of equal length. Hence, the target compositions were reached. When the compositions of the AB–di–block copolymers were calculated from the conversion with *Equation 10.2.1*, the copolymer with A – B_1 = nBMA is P[tBMA]$_{35}$–b–P[nBMA]$_{130}$ and the one with A – B_2 = BzMA is P[tBMA]$_{35}$–b–P[BzMA]$_{101}$. The NMR–spectra of the precipitated polymers, the macro initiator and both AB–di–block copolymers, showed rests of monomers. That means the weighted yields were too high. One reason for the differences are the remained monomers in the precipitated polymers which falsified the amounts of the yields. Another possibility is that there was a loss of control during the ATRP which means that *Equation 10.2.1* do not obtain. For the following analysis the compositions which were calculated from the ^{1}H–NMR–spectra of the precipitated AB–di–block copolymers are used because the results from the yields probably erroneous.

10.2.2. Structural Analysis

The next investigations referred to the compositional analysis of the block copolymers. First the elementary analysis of the resulting copolymers is detailed. Here the purity and the composition of the resulting copolymers were controlled. The results of the measurements and the differences between the theoretical and the analysis results are listed in *Table 10.5*.

Tab. 10.5.: Results of the elementary analysis of the experiments V150, V151 and V152

entry	F_{tBMA}		C [%]	ΔC	H [%]	ΔH	O [%]	ΔO
V150	1.00	theory	67.57		9.92		22.50	
		is	66.59	-0.98	9.57	-0.36	23.84	1.34
V151	0.52	theory	67.57		9.92		22.50	
		is	68.14	0.57	8.97	-0.96	22.89	0.39
V152	0.47	theory	71.89		8.14		19.97	
		is	72.17	0.28	7.49	-0.65	20.34	0.37

The elementary analysis yielded two results. In all measurements the differences to the theoretical values were small. That implied that all samples were free of pollution from solvents. The small amounts of the non–converted monomers did not influenced the elementary analysis essentially. When the samples were compared all the values were very similar. Hence, the three polymerizations proceeded in equal measure.

Subsequently the macro initiator and the two block copolymers were investigated with ATR–FTIR–spectroscopy. The finger print regions of the three IR–spectra are depicted in *Figure 10.5* with marked specific bands of the *n*–butyl–, *tert*–butyl– and benzyl–units.

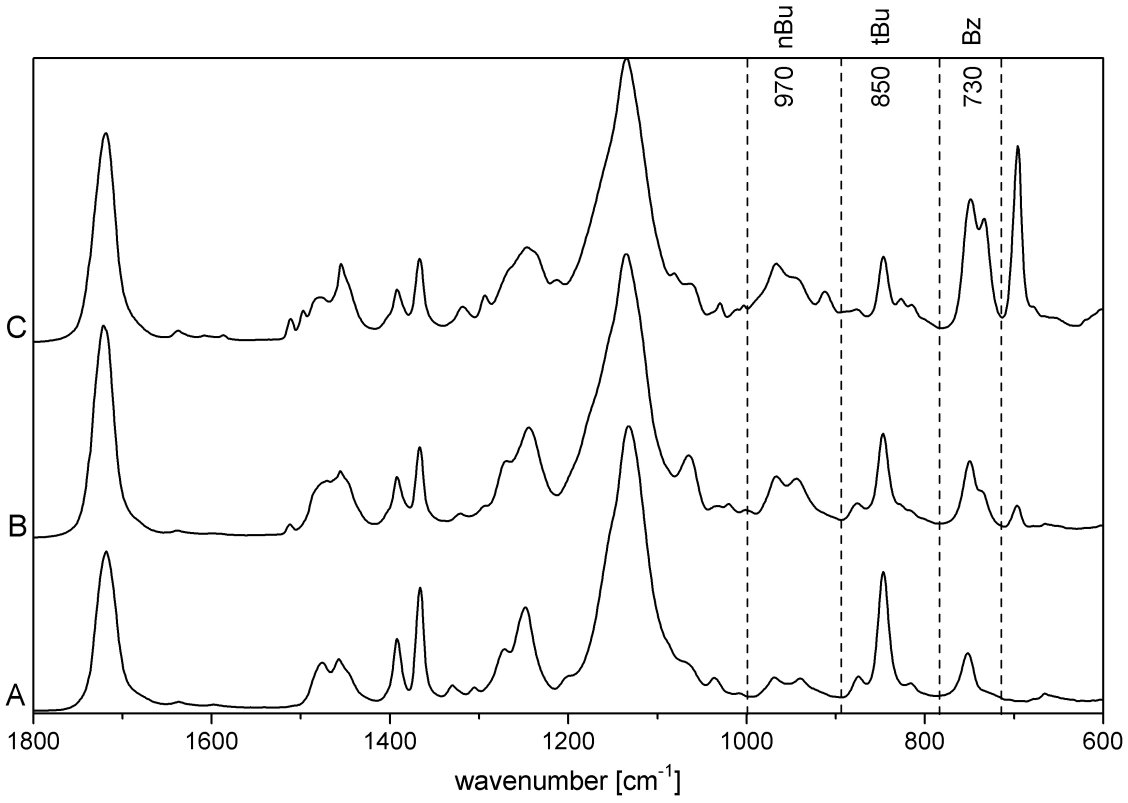

Fig. 10.5.: Finger print region of ATR–FTIR–spectra of (A) V150 macro initiator P[tBMA] and block copolymers (B) V151 $P[tBMA]_{0.52}$–b–$P[nBMA]_{0.48}$ and (C) V152 $P[tBMA]_{0.47}$–b–$P[BzMA]_{0.53}$

The three spectra show nearly the same peaks between 1800 cm^{-1} and 1000 cm^{-1}. Below 1000 cm^{-1} are the three vibrational bands which are specific for the three different functional groups. The band at 970 cm^{-1} represents the *n*–butyl–group, the one at 850 cm^{-1} the *tert*–butyl–group and the one at 730 cm^{-1} the benzyl–group. The peak area and the peak height of these three vibrational bands were determined. The results are listed in *Table 10.6.*

Tab. 10.6.: Peak area and peak height of the analyzed ATR–FTIR–bands of experiments V150, V151 and V152

		band nBu		*band tBu*		*band Bz*	
Entry	F_{tBMA}	peak area [cm^{-1}]	peak height	peak area [cm^{-1}]	peak height	peak area [cm^{-1}]	peak height
V150	1.00	3.24	0.068	9.22	0.435	3.35	0.156
V151	0.52	6.14	0.133	7.47	0.306	5.38	0.223
V152	0.47	6.81	0.150	5.26	0.217	11.78	0.422

The peak area and the peak height of the vibrational band caused by the *n*–butyl–ester group increased from the sample of the macro initiator P[tBMA] (V150) to the block copolymer $P[tBMA]_{0.52}$–b–$P[nBMA]_{0.48}$ (V151). That was caused by the addition of the block B_1 with nBMA groups. In contrast the peak area and the peak height of *band tBu* decreased. The results fitted good to the results of the investigations of peak area and peak height of the statistical copolymers with nBMA– and tBMA–units, see *Section 3.3.2*, and the respective gradient copolymers, see *Section 5.2.3*.

The vibrational band which is caused by the benzyl group also increased in view to the peak area and the peak height from the sample of the macro macro initiator (V150) to the block copolymer $P[tBMA]_{0.47}$–b–$P[BzMA]_{0.53}$ (V152). Even here the peak area and peak height of *band tBu* decreased. The changes caused by the addition of block B_2 confirm to the analyzes of the statistical copolymers with BzMA– and tBMA–units, see *Section 7.2.2*, and the respective gradient copolymer, see *Section 8.2.3*.

The changes of the vibrational bands from the ATR–FTIR–spectrum of the sample of the macro initiator to the spectra of the samples the two AB–di–block copolymers are obvious and in agreement with the results from the statistical and gradient copolymers before.

10.2.3. Molecular Weight Characterization

The macro initiator of experiment V150 and the obtained block copolymers of experiments V151 and V152 were analyzed with size exclusion chromatography. The elution diagrams based on the signal of the RI–detector of the samples are shown in *Figure 10.6.* The RI–signal of experiment V150 gives a monomodal peak, hence, during the polymerization no termination reactions occurred. The RI–signals of the samples of experiments V151 and

V152 showed tailing to the low molecular weight. That occurs either because of the presence of non–converted macro initiator or because of a slight loss of control, i. e. termination reactions. The macro initiator and the two block copolymers were investigated by diffusion ordered NMR spectroscopy (DOSY–NMR). The spectra of the three samples are depicted in *Figure 10.7*. The diffusion index (= -log D, D = diffusion coefficient) of the macro initiator is between - 8.8 ppm and - 8.9 ppm, see *Figure 10.7a*. A smaller molecule has a higher diffusion index than a larger molecule. Hence, with the addition of the second block to the macro initiator the diffusion index of the copolymer must decrease. *Figure 10.7b* shows the DOSY–NMR spectrum of P[tBMA]$_{0.52}$–b–P[nBMA]$_{0.48}$. The diffusion index is between - 8.95 ppm and - 9.1 ppm. *Figure 10.7c* shows the DOSY–NMR spectrum of P[tBMA]$_{0.47}$–b–P[BzMA]$_{0.53}$. The diffusion index is between - 9.2 ppm and - 9.3 ppm. The diffusion indices of both block copolymers were obviously lower than the one of the macro initiator. Additional, the DOSY–NMR spectra of both block copolymers do not show signals between - 8.8 ppm and - 8.9 ppm. Therewith, the total amount of the macro initiator was converted during the reactions and the DOSY–NMR measurement excludes the presence of non–converted or terminated macromolecules. That implies that the reaction control at the ATRP of the second block was not as good as during the synthesis of the macro initiator, causing a low–molecular weight tailing in the SEC–elution diagram (c. f. *Figure 10.6*).

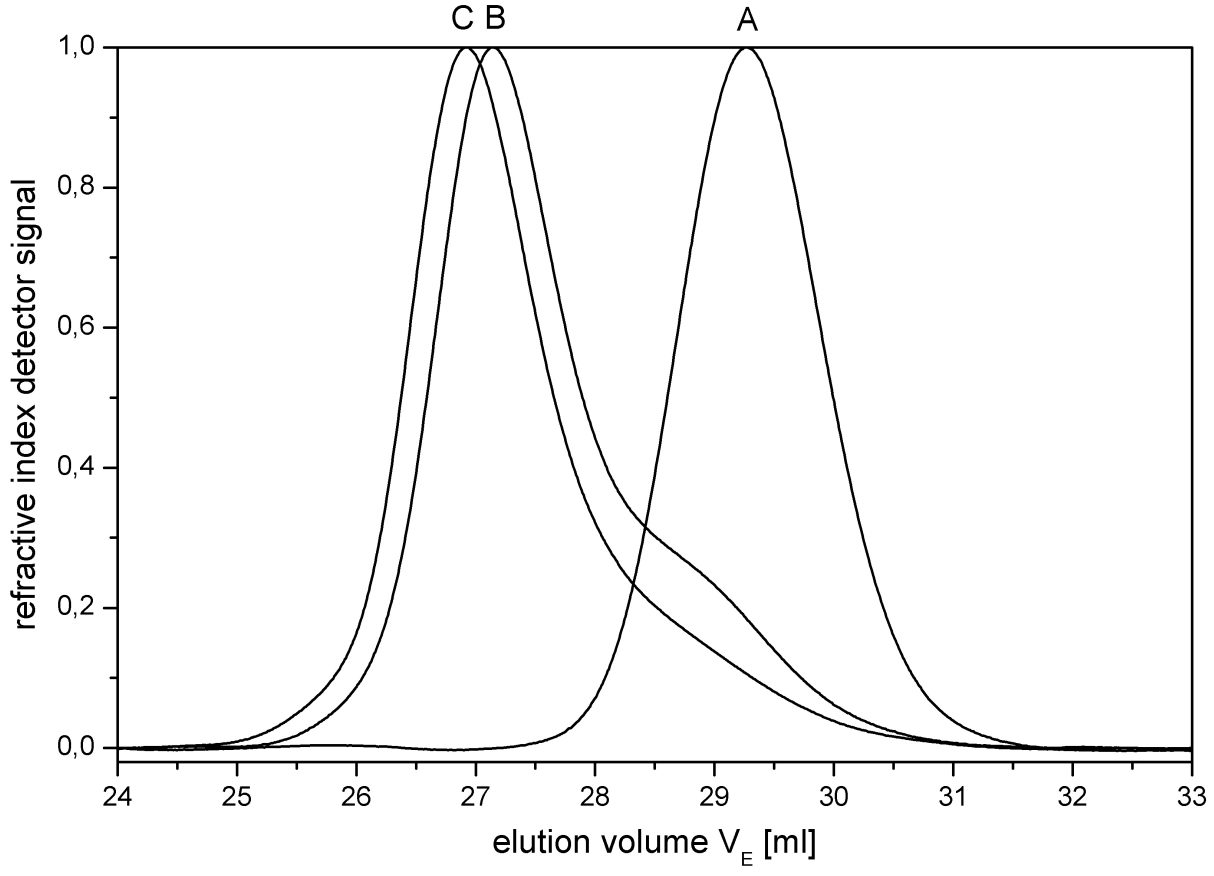

Fig. 10.6.: SEC elution diagrams of the samples of (A) V150 macro initiator P[tBMA] and block copolymers (B) V151 P[tBMA]$_{0.52}$–b–P[nBMA]$_{0.48}$ and (C) V152 P[tBMA]$_{0.47}$–b–P[BzMA]$_{0.53}$

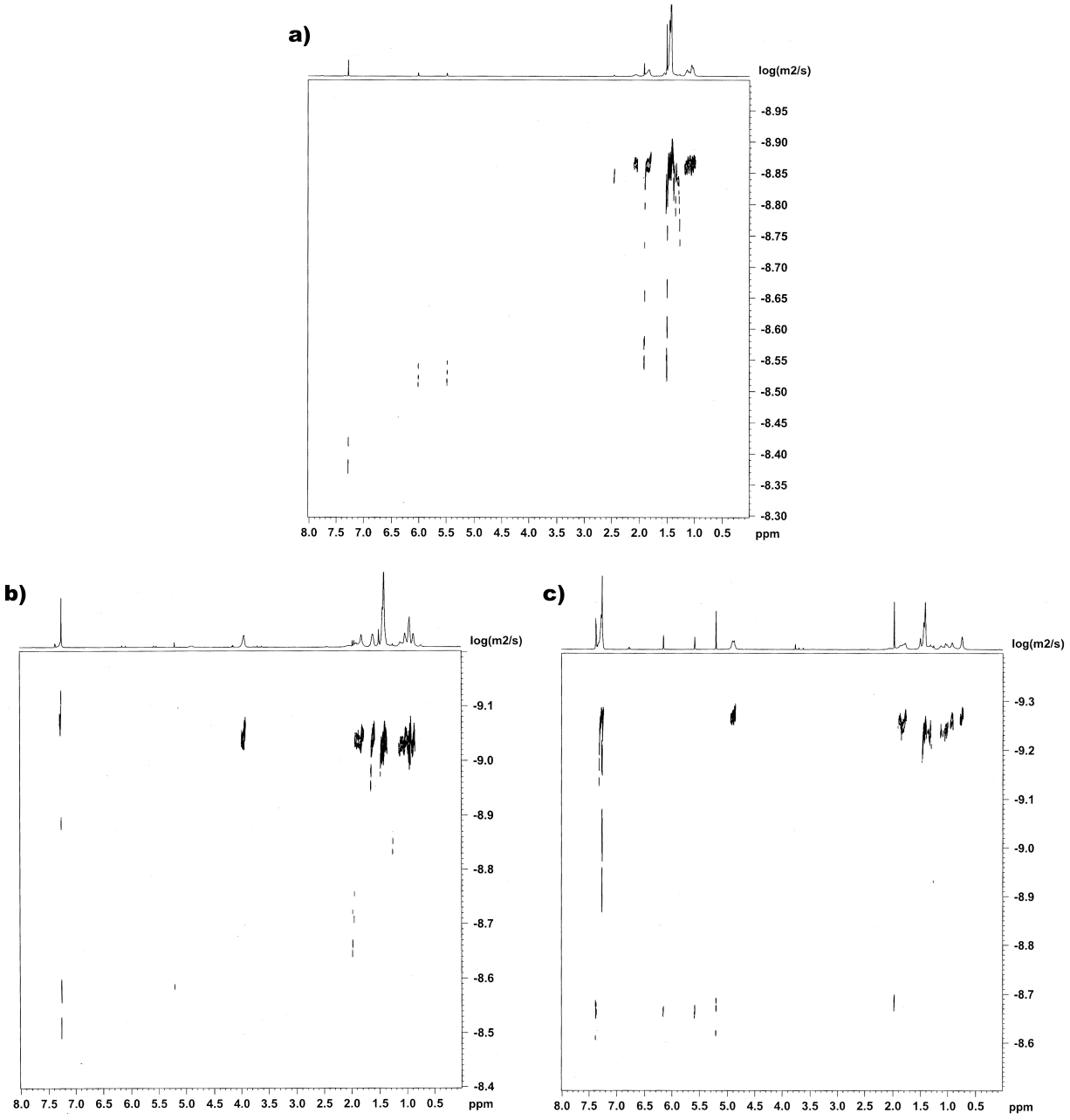

Fig. 10.7.: DOSY–NMR spectra of the samples of a) V150 macro initiator P[tBMA] and block copolymers b) V151 P[tBMA]$_{0.52}$–b–P[nBMA]$_{0.48}$ and c) V152 P[tBMA]$_{0.47}$–b–P[BzMA]$_{0.53}$

The maximum elution volume V_E of both block copolymers were nearly the same and both were obviously lower than the V_E of the macro initiator. Hence, the molar masses were higher. They are listed in *Table 10.9*. The increase of the molar mass resulted from the polymerizations of the second blocks to the first block, the macro initiator of P[tBMA]. Both copolymerizations worked similar. With the calibration curve arising from polystyrene standards that was used in *Section 3.3.3, Figure 3.15*, the relative molar masses of the samples were calculated from the maximum elution volume V_E of the RI–signals. The elution volumes of the RI–signals from the three samples and the calculated relative molar masses are listed in *Table 10.9* likewise. The relative molar masses of the final block copolymers were around

three times higher than the macro initiator. The difference was much higher than expected after the analyzes of the ^{1}H–NMR–spectra of the precipitated copolymers. The relative molar mass is a hunch, because for the determination just one point of the RI–signal was used not the whole sample was covered. To account for this effect the absolute molar masses of the sample were determined.

The next step was the determination of the differential refractive index increments dn/dc of the resulting AB–di–block copolymers because these values are necessary for the calculation of the absolute molar mass of the polymers from light scattering data, see *Section 2.4*. This was done the same way as described with the statistical copolymers of experiment V11 to V19 in THF at 25 °C, cf. *Section 3.3.3*. The results of these measurements are listed in *Table 10.7*.

Tab. 10.7.: Differential refractive index increment dn/dc of experiments V150, V151 and V152

Entry	F_{tBMA}	dn/dc [ml · g^{-1}]
V150	1.00	0.0612 ±0.0019
V151	0.52	0.0772 ±0.0024
V152	0.47	0.1151 ±0.0008

The differential refractive index increment of the three polymers changed obviously with the composition. The dn/dc value from the sample of V150 to the sample of V151 increased slightly. That this values increase with a added amount of nBMA inside the copolymer chain was observed previously at the statistical copolymers with nBMA– and tBMA–units, c. f. *Table 3.10*. The difference between the sample of V150 and V152 was much higher. Also this result agree with the measured dn/dc–values of the statistical copolymers with BzMA– and tBMA–units, c. f. *Table 7.12*.

With the results from the determination of dn/dc the molecular weight averages (M_n, M_w, M_z) and from these the polydispersity indices PDI (M_w/M_n, M_z/M_n) of the samples of the macro initiator and the two AB–di–block copolymers were determined in the same way as for the statistical copolymers in *Section 3.3.3*. *Figure 10.8* depicts the RI– and the 90°–MALS–detector signals of the elution–diagram of the sample of the macro initiator V150. From the angle dependence of the scattered light intensity and the known dn/dc–value of dn/dc = 0.0612 ml · g^{-1} (cf. *Table 10.7*) the absolute molecular weight of a fraction at a given elution volume can be derived, see *Section 2.4*. The calculated molecular weights are also shown in *Figure 10.8* (right axis). Since the RI–signal is proportional to the weight fraction of the eluted polymer, the complete molecular weight distribution (MWD) of the measured polymer can be obtained and with this the molecular weight averages and the polydispersity indices can be calculated. The obtained values are detailed in *Table 10.8*.

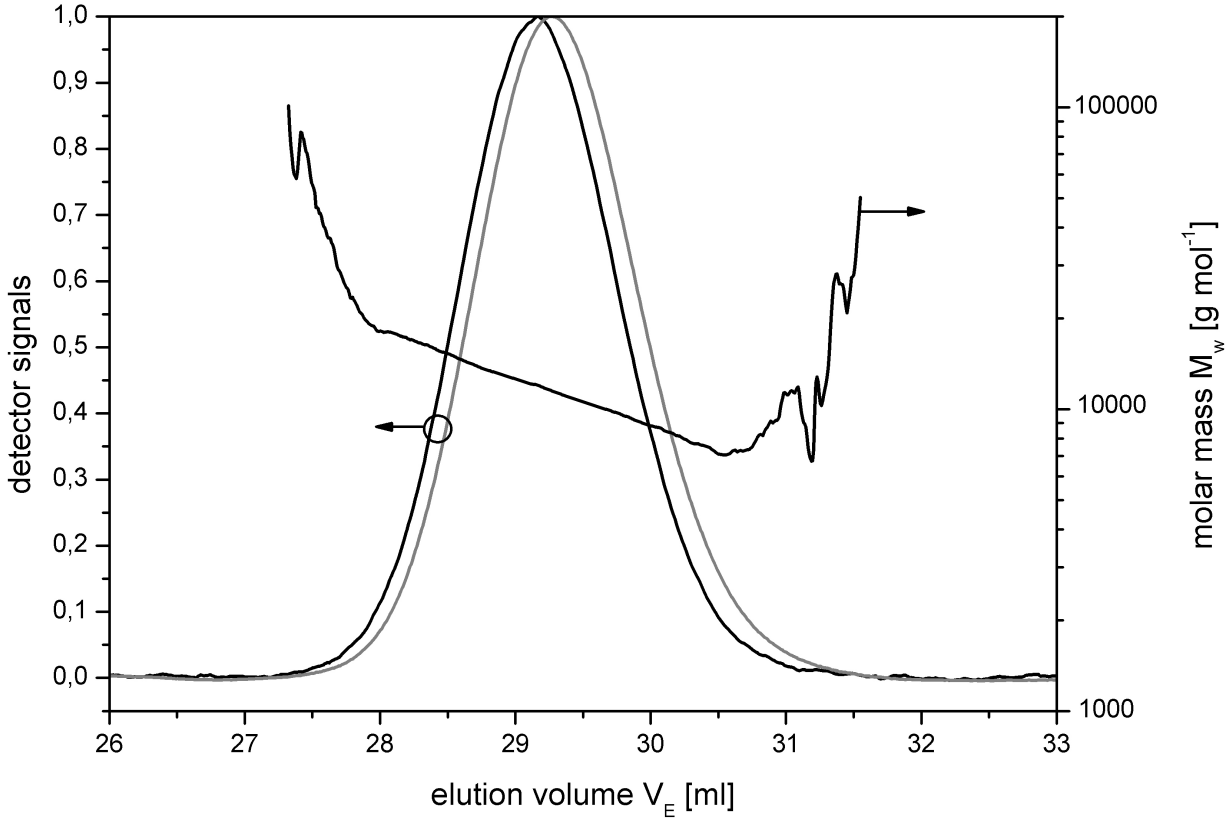

Fig. 10.8.: SEC elution diagrams and molar masses of macro initiator P[tBMA] (experiment V150); black curve – light scattering signal, grey curve – refractive index signal

Tab. 10.8.: SEC results of V150, V151 and V152

entry	F_{BzMA}	M_n [g · mol^{-1}]	M_w [g · mol^{-1}]	M_z [g · mol^{-1}]	M_w/M_n	M_z/M_n
V150	1.00	11060 ±221	11620 ±232	12420 ±621	1.051 ±0.021	1.124 ±0.067
V151	0.52	23590 ±236	29310 ±176	34340 ±343	1.242 ±0.025	1.456 ±0.029
V152	0.47	25300 ±228	31120 ±93	34720 ±208	1.230 ±0.011	1.373 ±0.014

The absolute molar mass of the macro initiator (10660 g · mol^{-1}) is half as high as the absolute molar mass of the P[tBMA] of experiment V18 (21420 g · mol^{-1}), see *Table 3.11.* The PDI–values of the sample of experiment V150 is narrow with 1.051. So the polymerization worked good and the resulting mass fitted good to the intended application of the polymer as macro initiator for the block copolymerizations when the molar mass of the resulting block copolymer should be around 25000 to 30000 g · mol^{-1}, which is the range of the molar masses of the statistical copolymers with nBMA– and tBMA–units, see *Table 3.11* and the statistical copolymers with BzMA– and tBMA–unit, see *Table 7.13.*

The molar masses of the samples of the two AB–di–block copolymers (V151 $P[tBMA]_{0.52}$–b–$P[nBMA]_{0.48}$ = 23590 g · mol^{-1} and V152 $P[tBMA]_{0.47}$–b–$P[BzMA]_{0.53}$ = 25300 g · mol^{-1}) are

two–times higher than M_n of the macro initiator P[tBMA]. That results confirm the calculations of the compositions of the ^{1}H–NMR–spectra of the precipitated polymers. The polydispersities of the samples of the two block copolymers are high, up to 1.23. Hence, the assumption from the shape of the RI–detector signals that there was a residue of non–converted macro initiator in the samples or a loss of control during the polymerizations of the second block was corroborated. The differences of the composition determinations from the yields and from the ^{1}H–NMR–spectra also refer to this loss of control.

The absolute molar masses which were determined from the LS–detector signals and the dn/dc–values are lower then the relative molar masses determined from the maximum elution volumes of the RI–detector signals. For the determination of the relative molar mass only the maximum elution volume of the RI–curve is used, that means only one point of the whole measurement. The absolute molar mass is determined from the complete database of the measurement and displays the molecular weight distribution of the whole sample.

Tab. 10.9.: Comparison of relative* and absolute molar masses of experiments V150, V151 and V152

entry	F_{tBMA}	V_E [ml]	relative M* [g · mol^{-1}]	absolute M [g · mol^{-1}]	ΔM [g · mol^{-1}]	[%]
V150	1.00	29.26	8223	11060	-2832	25.65
V151	0.52	27.15	23983	23590	393	-1.66
V152	0.47	26.92	26933	25300	1633	-6.45

* calibrated against PS–Standard

The resulting molar masses are in the same range then the statistical copolymers of the *Sections 3* and *7*. But the polydispersities were obviously higher. Hence, during the polymerization of the second block the control over the synthesis by the ATRP–system was lost.

10.2.4. Thermal Behavior

The thermal behavior of the two AB–di–block copolymers was examined to determine the temperature ranges of the glass transition regions ΔT and the glass transition temperatures T_g of the two glass transition steps which are expected. The theoretical thermograms of statistical, gradient and AB–di–block copolymers are described and compared in *Section 2.3*.

The samples of the macro initiator V150 and the two block copolymers V151 and V152 were measured in the same temperature range as the gradient copolymers of *Sections 5* and *8*. The applied DSC program parameters were:

- precooling: RT to -80 °C
- standby for 20 min

- 1. heating: -80 to 150 ℃
- 1. cooling: 150 to -80 ℃
- 2. heating: -80 to 150 ℃
- postcooling: 150 ℃ to RT

In *Figure 10.9* the thermogram of the macro initiator V150 with both heating runs and the cooling run are shown and *Figure 10.10* depicts the thermograms of the two AB–di–block copolymers V151 and V152 also with both heating runs and the cooling run.

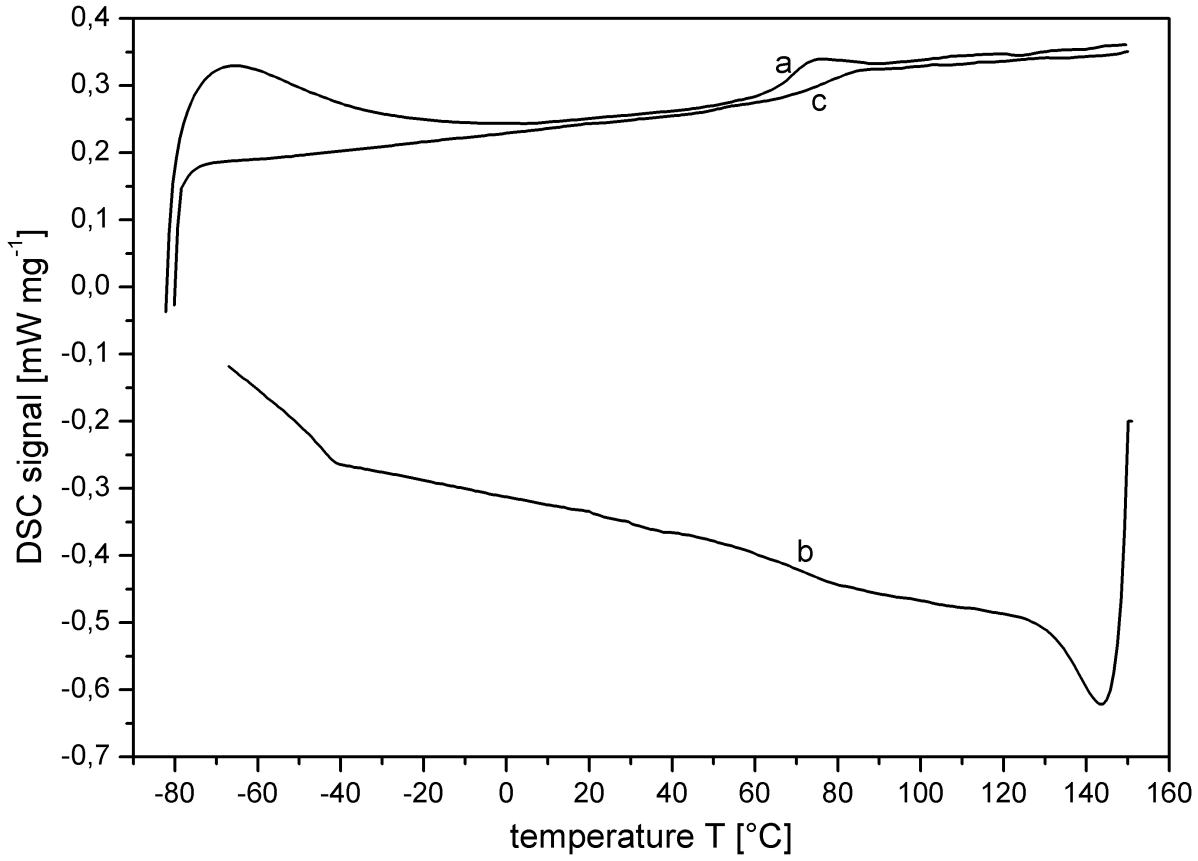

Fig. 10.9.: DSC thermogram of macro initiator P[tBMA] (experiment V150); a – first heating run, b – first cooling run, c – second heating run; heating rate $10\,\mathrm{K}\cdot\mathrm{min}^{-1}$

The first heating runs showed a single glass transition step overlaid by a relaxation peak in the range from 55 to 90 ℃ for the sample of the macro initiator V150, from 40 ℃ to 75 ℃ for the sample of V151 and 25 to 50 ℃ for the sample of V152. To avoid effects of the sample thermal history only the second heating runs were analyzed. With the analysis software of the DSC, T_{onset} and T_{offset} of the glass transition regions were determined and then the other values T_g, $\Delta T = T_{offset} - T_{onset}$ and Δc_p were calculated. [89] Also the midpoint of the glass transition region T_{midpt} was computed but these values were not used further. The procedure was the same as described before for the monomer mixtures in *Section 3.3.4*. The second heating runs of the three samples of the experiments V150, V151 and V152 are depicted in

Figure 10.11 with marked T_g, T_{onset} and T_{offset} as bounds of the glass area. All the DSC results of the samples of the three experiments are summarized in *Table 10.10*.

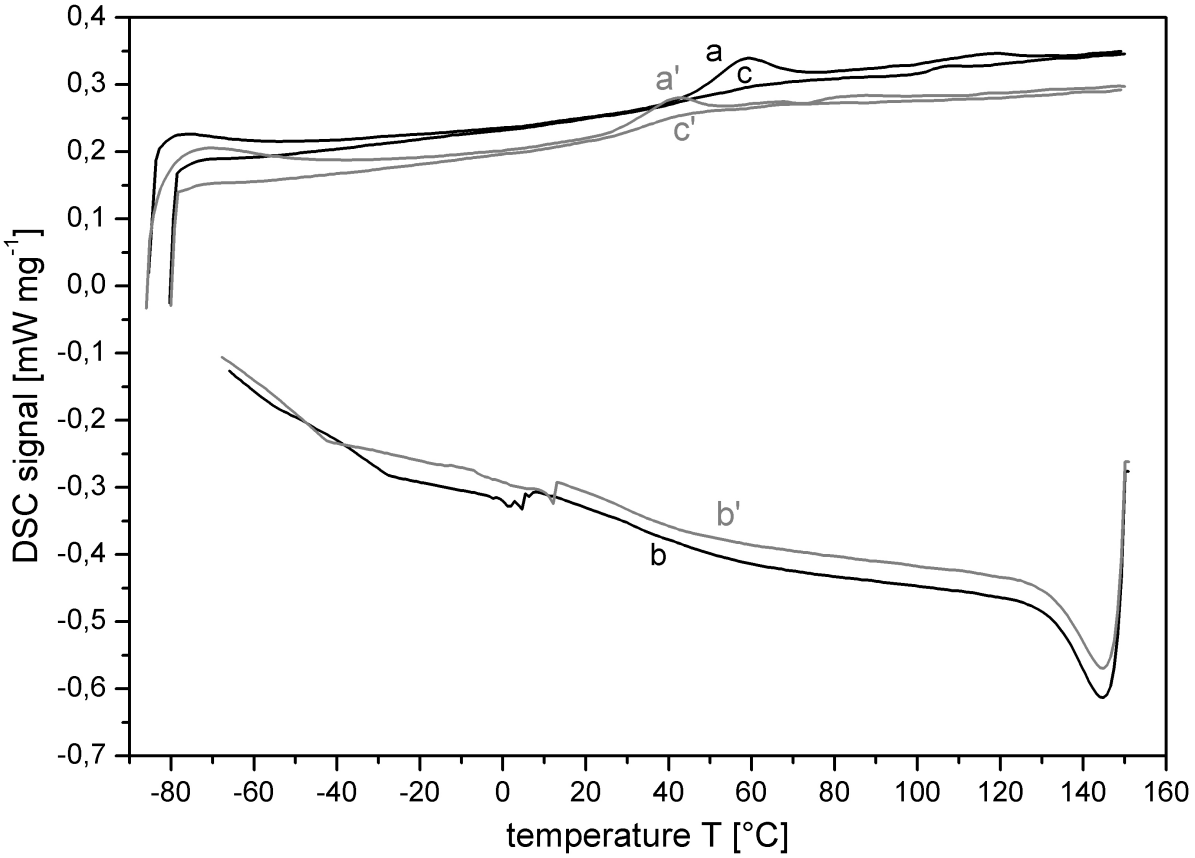

Fig. 10.10.: DSC thermogram of copolymer V151 ($P[tBMA]_{0.52}$–b–$P[nBMA]_{0.48}$, black line) and V152 ($P[tBMA]_{0.47}$–b–$P[BzMA]_{0.53}$, grey line); a/a' – first heating run, b/b' – first cooling run, c/c' – second heating run; heating rate 10 $K \cdot min^{-1}$

Tab. 10.10.: DSC results of experiments V150, V151 and V152

entry	F_{tBMA}	T_g–step	T_{onset} [°C]	T_{midpt} [°C]	T_g [°C]	T_{offset} [°C]	ΔT [°C]	Δc_p [$J \cdot g^{-1} \cdot K^{-1}$]
V150	1.00		63.0	74.0	77.0	84.5	21.5	0.264
V151	0.52	I	39.0	56.5	54.5	64.0	25.0	0.147
		II	100.5	103.0	103.5	105.5	5.0	0.068
V152	0.47	I	27.0	39.0	31.0	43.5	16.5	0.146
		II	58.0	62.5	59.0	63.5	5.5	0.023

The second heating run of the sample of the macro initiator showed a glass transition step between 63 °C and 84.5 °C, with the glass transition temperature at 77 °C. For high molecular weigh P[tBMA] the literature [90] cited a T_g of 107 °C. But this values was measured for P[tBMA] with a M_n of 25000 $g \cdot mol^{-1}$. In *Section 3.3.4* a T_g of 107.5 °C was measured for a P[tBMA] with 21420 $g \cdot mol^{-1}$. The macro initiator had a molar mass of 11060 $g \cdot mol^{-1}$, see *Table 10.8*. So the difference of the between the measured T_g and the T_g–value taken from

literature was caused by the different molar masses of the analyzed samples.

The second heating run of the sample of the block copolymer with tBMA– and nBMA–units $P[tBMA]_{0.52}$–b–$P[nBMA]_{0.48}$ showed two glass transition steps. The first step lay between 39 ℃ and 64 ℃ with a glass transition at 54.5 ℃, the second step between 100.5 ℃ and 105.5 ℃ and a T_g at 103.5 ℃. Even the second heating run of the sample of the block copolymer with tBMA– and BzMA–units $P[tBMA]_{0.47}$–b–$P[BzMA]_{0.53}$ showed two glass transition steps. The first step lay between 27 ℃ and 43.5 ℃ with a glass transition at 31 ℃, the second step between 58 ℃ and 63.5 ℃ and a T_g at 59 ℃. For both block copolymers the second glass transition step was characterized by only a small specific heat capacity change Δc_p.

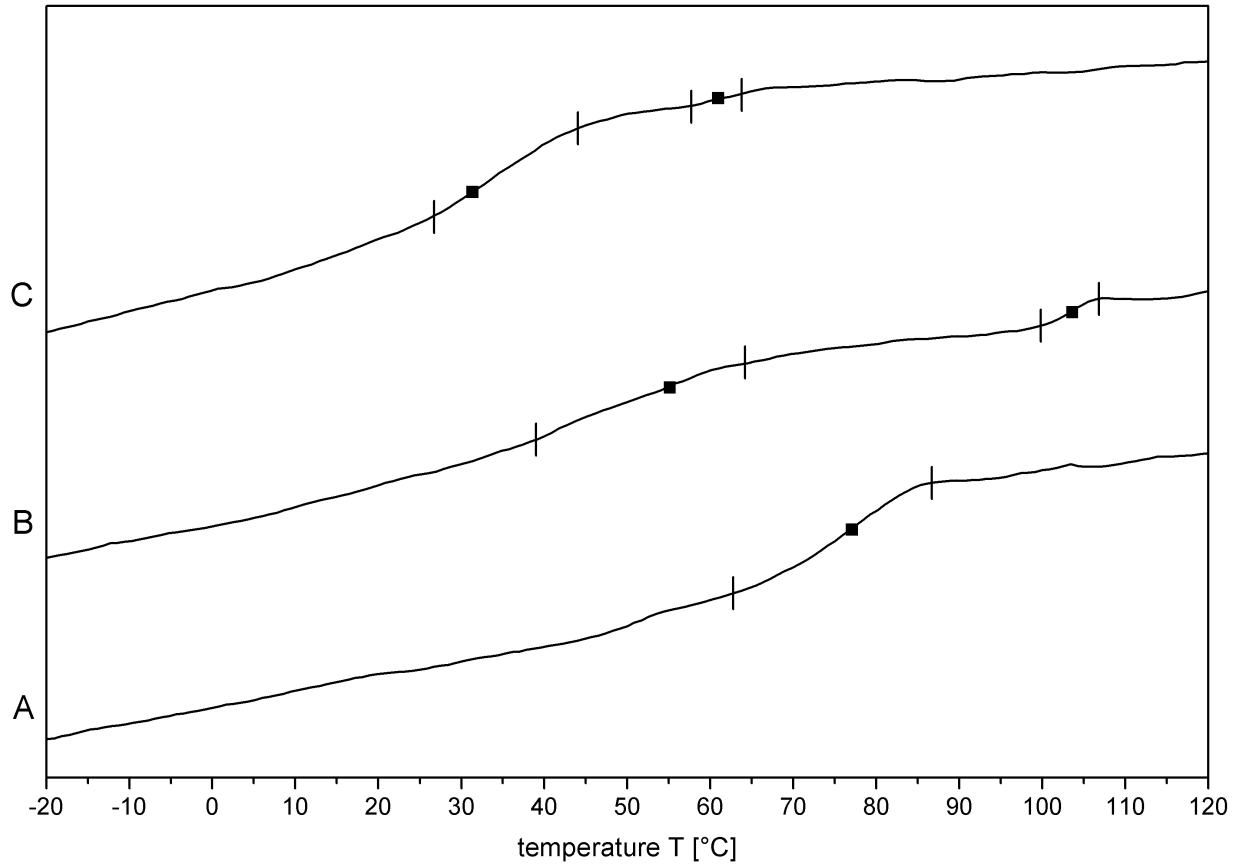

Fig. 10.11.: DSC thermograms of (A) macro initiator V150 P[tBMA] and block copolymers (B) V151 $P[tBMA]_{0.52}$–b–$P[nBMA]_{0.48}$ and (C) V152 $P[tBMA]_{0.47}$–b–$P[BzMA]_{0.53}$ with marked glass transition temperature range ΔT and temperature T_g; second heating runs, heating rate $10\,K \cdot min^{-1}$

The DSC measurements of samples of the to block copolymers were repeated, certainly, with a heating rate of $20\,K \cdot min^{-1}$ to get more distinct glass transition steps. The resulting thermograms did not show obviously better results. The literature values of the T_g of the homopolymers are 107 ℃ for P[tBMA] [90], 20 ℃ for P[nBMA] [91] and 47 ℃ for BzMA [113]. For $P[tBMA]_{0.52}$–b–$P[nBMA]_{0.48}$ the first glass transition step was related to the P[nBMA]–block of the copolymers, but the measured T_g–value is obviously to high. The difference between the measured T_g and the literature values of the P[tBMA]–block was 3.5 ℃. So the measured

values fits in acceptable limits. The two measured T_g–values of P[tBMA]$_{0.47}$–b–P[BzMA]$_{0.53}$ were both distinctly lower than the literature values. Especially the measure value of the P[tBMA]–block was much too low.

The measured glass transition temperatures of the statistical and the gradient copolymers with tBMA– and nBMA–units fitted good to the literature values, see *Sections 3.3.4* and *5.2.5*. The differences between the statistical and the gradient copolymers with tBMA– and BzMA–units were in acceptable ranges, see *Sections 7.2.4* and *8.2.5*.

For the comparison of the thermal behavior of the different types of copolymers the second heating runs of three different copolymers are depicted in *Figure 10.12*. There the different glass transition temperature regions ΔT and the glass transition temperatures T_g are given of a statistical copolymer (A), a gradient copolymer (B) and a block copolymer (C) which all contain tBMA– and nBMA–units and have nearly the same compositions.

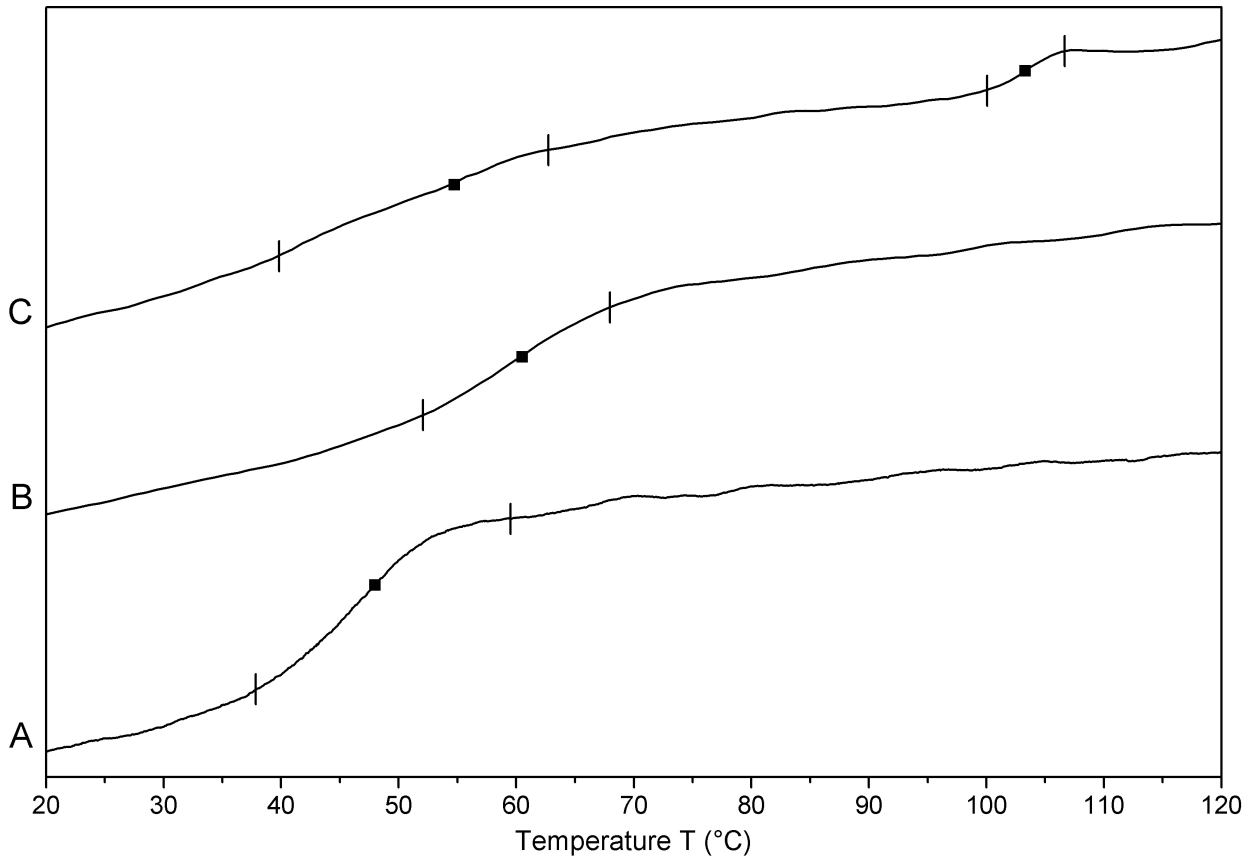

Fig. 10.12.: DSC thermograms of (A) a statistical copolymer P[tBMA$_{0.48}$–co–nBMA$_{0.52}$], (B) a gradient copolymer P[tBMA$_{0.54}$–grad–nBMA$_{0.46}$] and (C) a block copolymers P[tBMA]$_{0.52}$–b–P[nBMA]$_{0.48}$ with marked glass transition temperature range ΔT and temperature T_g; second heating runs, heating rate $10\,K \cdot min^{-1}$

The statistical copolymer P[tBMA$_{0.48}$–co–nBMA$_{0.52}$] and the gradient copolymer P[tBMA$_{0.54}$–grad–nBMA$_{0.46}$] show one glass transition step, the block copolymer two. The glass transition temperature range ΔT of the statistical copolymer is about 20 °C, the one of the gradient

copolymer 15 ℃. The first ΔT of the block copolymer P[tBMA]$_{0.52}$–b–P[nBMA]$_{0.48}$ is about 25 ℃ and the second one about 5 ℃. Even if the ratio of the two monomer–units is nearly the same for the three different copolymers, the thermal behavior did not show the expected behavior, see *Figure 2.12*.

10.3. Summary

A P[tBMA] macroinitiator was synthesized by Atom Transfer Radical Polymerization. The reaction was quenched after a target conversion of 20 % to yield a degree of polymerization of $X_n^{PA} = 35$. The resulting homopolymer was used as macro initiator for the synthesis of two block copolymers, one with P[nBMA] as second block and one with P[BzMA] as second block. The analysis of the ^{1}H–NMR–spectra of the resulting polymers showed that the two blocks of both copolymers were present in nearly the same ratio in the polymer chain. The composition of the first block copolymer was P[tBMA]$_{0.52}$–b–P[nBMA]$_{0.48}$ and the one of the second block copolymer P[tBMA]$_{0.47}$–b–P[BzMA]$_{0.53}$. The elementary analysis of samples of the two block copolymers showed a good agreement between the calculated and measured amount of carbon, hydrogen and oxygen. The samples were free of pollution from solvents. The analysis of the ATR–FTIR–spectra displayed changes of the vibrational bands from the spectrum of the sample of the macro initiator to the spectra of the two block copolymers. The differences were in accordance to the results from the statistical and gradient copolymers before. The differential refractive index of the block copolymers were in the same range than the dn/dc–values of the statistical and the gradient copolymers with the respective monomer–units. The molecular masses of the block–copolymers were two times higher than the molar mass of the macro initiator and hence, fit well to the results of the ^{1}H–NMR analysis. Also the resulting molar masses are in the same range than the ones of the statistical and gradient copolymers before. But the polydispersities of the block copolymers were high, M_w/M_n up to 1.23. Hence, during the polymerization of the second block the control over the synthesis by the ATRP–system was lost. ^{1}H–DOSY–NMR–experiments proofed the lock of non–converted macro initiator in both the samples. The analysis of the DSC–thermogram of the macro initiator gave a glass transition temperature that was obviously lower than the literature values. This was possibly related to the fact that the molar mass of the macro initiator is lower than the values of the polymer in the literature. The thermograms of the block copolymers showed two glass transition steps, one for each block of the copolymers. The second steps had a small specific heat capacity. The glass transition temperatures of the samples of both copolymers differed obviously from the literature values in opposite the results from the statistical and gradient copolymers before. Hence, a comparison of the block copolymers with the relating statistical and gradient copolymers relating to the thermal behavior was not possible.

10.4. Results and Discussion of the Hydrolysis

This section describes the observations on the hydrolysis reaction performed with the AB–di–block copolymers $P[tBMA]_{0.52}$–b–$P[nBMA]_{0.48}$ (V151) and $P[tBMA]_{0.47}$–b–$P[BzMA]_{0.53}$ (V152). Also the results of the analysis of the hydrolysis products are given. The products were compared with the educts. Moreover the two products were compared.

The amount of added MSA depends on the amount of tBMA inside the polymer chains. It was calculated with *Equation 10.4.1* for both block copolymers.

$$V_{MSA} = \frac{m \cdot F_{tBMA} \cdot x \cdot M_{MSA}}{M_{tBMA} \cdot \delta_{MSA}} \tag{10.4.1}$$

with V_{MSA} – Volume of the methanesulfonic acid, m – mass of the polymer, F_{tBMA} – ratio of tBMA in the polymer chain, x – multiplicity factor for the hydrolysis reagent = 2, M_{tBMA} – molar mass of tBMA = 142.2 g · mol^{-1}, M_{MSA} – molar mass of the methanesulfonic acid = 96.11 g · mol^{-1} and δ_{MSA} – density of the methanesulfonic acid = 1.48 g · ml^{-1}

Also the theoretical yields depend on the copolymer composition F_{tBMA}. They were calculated in the same way as in *Section 4.2*, using *Equation 10.4.2*.

$$y_{theo} = \frac{m \cdot F_{tBMA} \cdot M_{MAA}}{M_{tBMA}} + m \cdot (1 - F_{tBMA}) \tag{10.4.2}$$

with y_{theo} – theoretical yield, m – mass of the polymer, F_{tBMA} – ratio of tBMA in the polymer, M_{MAA} – molar mass of MAA = 86.09 g · mol^{-1}, M_{tBMA} – molar mass of tBMA = 142.2 g · mol^{-1}

The results of the two calculations, the needed volumes of methanesulfonic acid and the theoretical yields, as well as the resulting and percentage yields of the two hydrolysis reactions are listed in *Table 10.11*.

Tab. 10.11.: Amount of added MSA and yields of the hydrolysis products V161 and V162

Product	Educt		F_{tBMA}	weighted mass [g]	V_{MSA} [ml]	yield theo [g]	yield actual [g]	yield actual [%]
V161	P[tBMA]–b–P[nBMA]	V151	0.52	0.25	0.11	0.20	0.13	62.02
V162	P[tBMA]–b–P[BzMA]	V152	0.47	0.25	0.10	0.20	0.11	52.34

The reactions proceeded in the same way than the model synthesis in *Section 4.2*. Some minutes after the addition of MSA both reaction mixtures became a dark brown gel. During the second hour the gels liquefied again. The added sodium hydrogen carbonate neutralized the excess of acid after the reaction time. Because a byproduct of this step is a salt, after the precipitation in *n*–pentane a second precipitation in water/ methanol was done. However,

the second precipitations was not only necessary to remove the formed salt. After the first precipitations from *n*–pentane the hydrolysis products were yellow powders, hence a second purification step was needed. After the purification steps the resulting copolymers were obtained in form of white powders. The yields of both hydrolysis were 60 % for experiment V161 and 50 % for experiment V162. Hence, the values of the yield were in the same range than yield of the hydrolysis of the statistical and gradient copolymers before.

The solubility–properties of the hydrolyzed block copolymers V161 and V162 were same as that of the P[nBMA–co–MAA], reported in *Chapter 4* (*Table 4.3*). The structural differences on the polymer chains between the block copolymers, the gradient copolymers and the statistical copolymers had no influence on the solubility. The hydrolyzed AB–di–block copolymers were dissolved in DMSO-d6 for ^{1}H–NMR–spectroscopy. The resulting ^{1}H–NMR–spectra of the two hydrolysis products (black lines) are presented in *Figure 10.14* together with the corresponding ^{1}H–NMR–spectra of the educts (grey lines). The molecular structures of the educts and the products with the numbering of the carbons are shown in *Figure 10.13*.

The changes between the spectra of the educt V151 and the product V161 were distinct. The intensity of the mixed broad peak ranging from 1.3 to 1.45 ppm caused by the signals of the protons 3' and 7' shrank relative to the signals 8' or 9' which remained constant. The reason was the absence of the signal 3' from the protons of the *tert*–butyl group in the product. Additionally the –COOH–signal could be monitored between 12.1 to 12.5 ppm. Also the changes between the spectra of the educt V152 and the corresponding product V162 were obviously. The intensity of the mixed broad peak ranging from 1.22 to 1.54 ppm caused by the signals of the proton 3' shrank relative to the signals 14' from 4.79 to 4.97 ppm, which remained constant. The reason was also the absence of the signal 3' from the protons of the *tert*–butyl group in the products. Further in the spectra of the hydrolysis products the broad –COOH–signal could be monitored between 12.13 to 12.56 ppm. That the signal of the *tert*–butyl–group disappeared nearly completely indicated a total conversion of both educts. In both ^{1}H–NMR–spectra of the products a H_2O signal was present because the DMSO–d_6 was not dry.

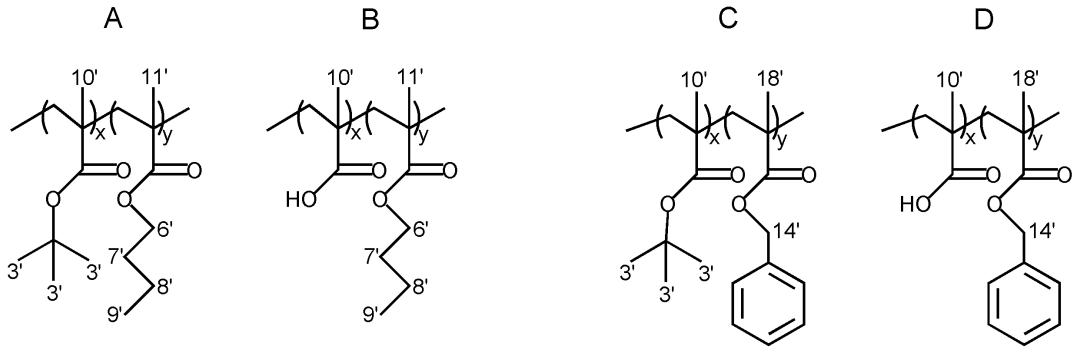

Fig. 10.13.: Molecular structures of (A) educt V151 $P[tBMA]_{0.52}$–b–$P[nBMA]_{0.48}$ and (B) product V161 $P[MAA]_{0.52}$–b–$P[nBMA]_{0.48}$, respectively (C) educt V152 $P[tBMA]_{0.47}$–b–$P[BzMA]_{0.53}$ and (D) product V162 $P[MAA]_{0.47}$–b–$P[BzMA]_{0.53}$ with carbon–atom labels (x + y = 1)

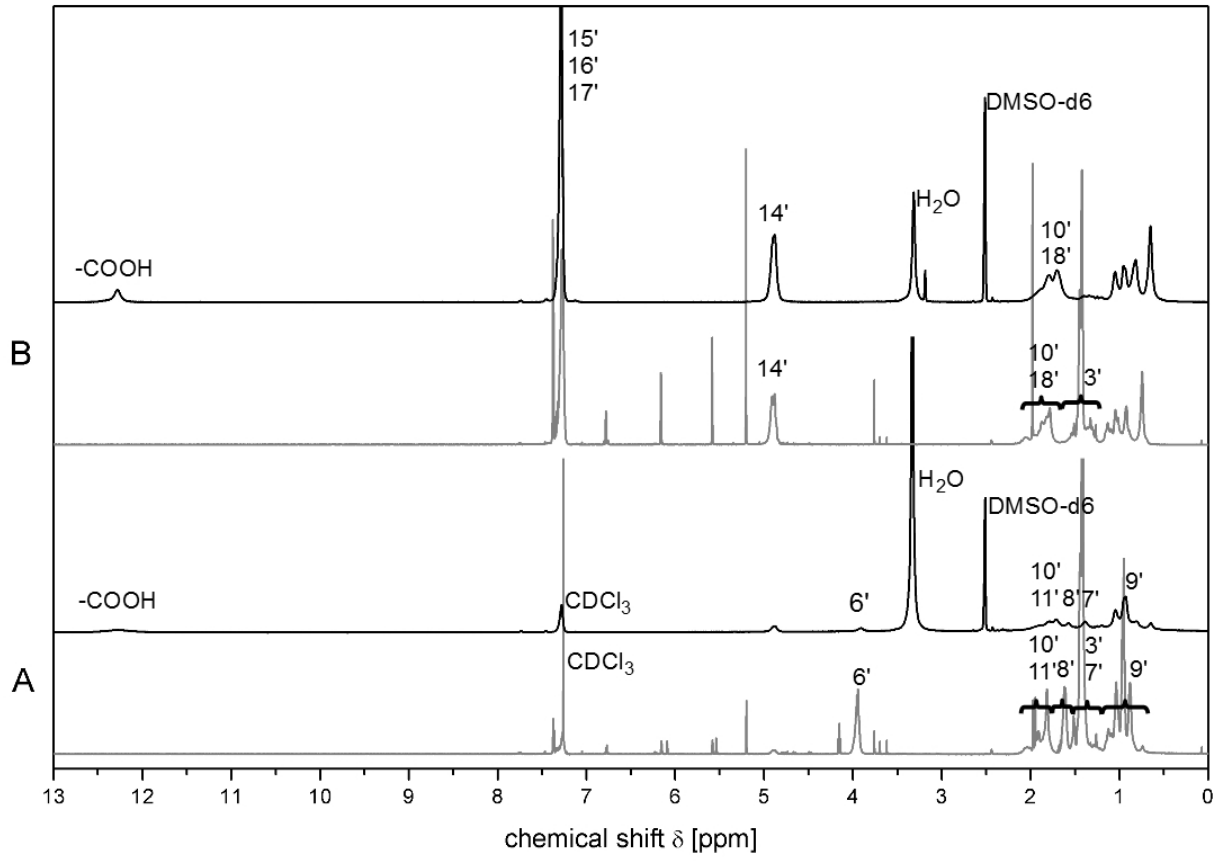

Fig. 10.14.: Comparison of ^{1}H–NMR–spectra of (A) educt V151 $P[tBMA]_{0.52}$–b–$P[nBMA]_{0.48}$ (grey line) and hydrolysis product V161 $P[MAA]_{0.52}$–b–$P[nBMA]_{0.48}$ (black line) and (B) educt V152 $P[tBMA]_{0.47}$–b–$P[BzMA]_{0.53}$ (grey line) and hydrolysis product V162 $P[MAA]_{0.47}$–b–$P[BzMA]_{0.53}$ (black line)

The NMR–analysis is followed by the investigation of the hydrolyzed gradient copolymers by elementary analysis and ATR–FTIR–spectroscopy. The results of the elementary analyzes are listed in *Table 10.12*. The theoretical values were calculated for 100 % conversion of the hydrolysis of the educts.

Tab. 10.12.: Results of the elementary analysis of educts V151 and V152 and hydrolysis–products V161 and V162 with divergence from the set values

Entry	F_{nBMA} F_{BzMA}		C [%]	ΔC	H [%]	ΔH	O [%]	ΔO
V151	0.52	theory	67.57		9.92		22.50	
		is	68.14	0.57	8.97	-0.96	22.89	0.39
V161		theory	62.91		8.78		28.31	
		is	63.60	0.69	8.28	-0.50	28.12	-0.19
V152	0.47	theory	71.89		8.14		19.97	
		is	72.17	0.28	7.49	-0.65	20.34	0.37
V162		theory	69.18		6.91		23.90	
		is	68.56	-0.62	6.60	-0.31	24.85	0.94

The results of the elementary analysis of the two hydrolysis products were slightly different for both block copolymers. For experiment V161 the measured amount of carbon was higher than the calculated amount, also the measured amount of oxygen was higher than the calculated but the difference is lower. The calculated amount of hydrogen was lower than the measured amount. For experiment V162 the measured amounts of carbon and hydrogen are lower than the calculated amounts. The difference for hydrogen is lower than for carbon. The amount of oxygen was higher than the pre–calculated one. But in all cases the differences were justifiable. The results of the elementary analysis showed that the resulting copolymers were clean and dry.

The ATR–FTIR–spectra of the educts (grey lines) and the corresponding product–spectra (black lines) are depicted in *Figure 10.15*. The vibrational bands in the IR–spectra were analyzed in view to changing which were caused by the hydrolysis.

In *Section 10.2.2* bands at 970 cm^{-1}, 850 cm^{-1} and 730 cm^{-1} were introduced that are characteristic of polymer-incorporated *n*–butyl–, *tert*–butyl– and benzyl– units, respectively. The vibrational bands at 970 cm^{-1} of nBu and 730 cm^{-1} of Bz did not change so much but the band at 850 cm^{-1} for tBu differed obviously. The changes of the tBu–band were strong and also influenced the two other bands. Therewith the analysis of peak height and peak area of the bands were not possible anymore. The loss of band intensity at 850 cm^{-1} clearly indicates that the hydrolysis products no longer contained *tert*–butyl–ester side groups. Also the intensity of the bands at 1370 cm^{-1} and 1390 cm^{-1} shrank with the hydrolysis. A third change exhibited the band at 1710 cm^{-1} which is the vibrational bands of ester–C=O-group. In the IR–spectrum of the educts the band was a small singlet. The product–spectra instead had a much broader band at that region. The literature refers 1720 cm^{-1} to ester–C=O vibration and 1700 cm^{-1} belongs to the vibrations of carboxylic acid–C=O groups. [87] Further the range $\tilde{\nu} > 3000\,cm^{-1}$ changed from educt to product in both cases. A broad band ranging from 2350 to 3700 cm^{-1} appeared which could be assigned to the vibrational band of the

carboxylic acid OH–group. All in all the changes in the ATR–FTIR–spectra from the educts to the product–spectra and the differences of the product–spectra among themselves showed that the hydrolysis reactions worked well.

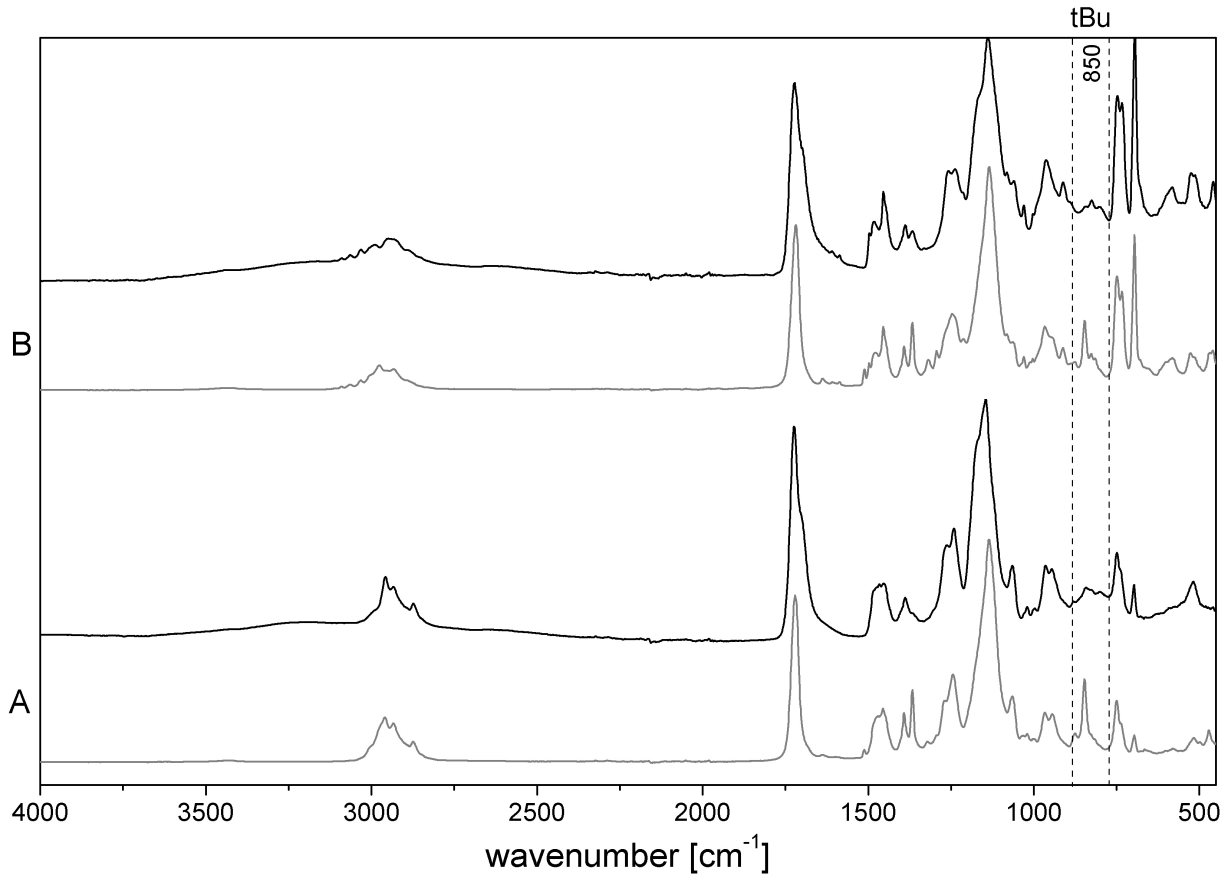

Fig. 10.15.: Comparison of ATR–FTIR–spectra of educts V151 resp. V152 and products V161 resp. V162 (grey line – educt, black line – product); A – V151/V161 = F_{nBMA} = 0.52, B – V151/V161 = F_{BzMA} = 0.47 (Spectra normalized to A_{1134} = 1)

The next type of analysis was the size exclusion chromatography (SEC). As with the hydrolyzed statistical copolymers also the products of V161 and V162 were not soluble in THF. As described in *Section 4.2* about 0.4 mg of the copolymer was mixed with 1 ml THF and two drops of TMSI and the mixture was stirred over night at RT. The copolymer became THF–soluble, because the carboxyl groups were converted into non–polar trimethylsilyl–esters. Since the presence of non–covalent fixed TMSI disturbed the dn/dc determination, only the relative molar mass of the copolymers were calculated from the maximum elution volume of the samples and *Equation 3.3.22* which based on a polystyrene–calibration ("PS–Standard–values"). The resulting elution diagrams of the RI–detector signals are depicted in *Figure 10.16* and the calculated relative molar masses are listed in *Table 10.13*.

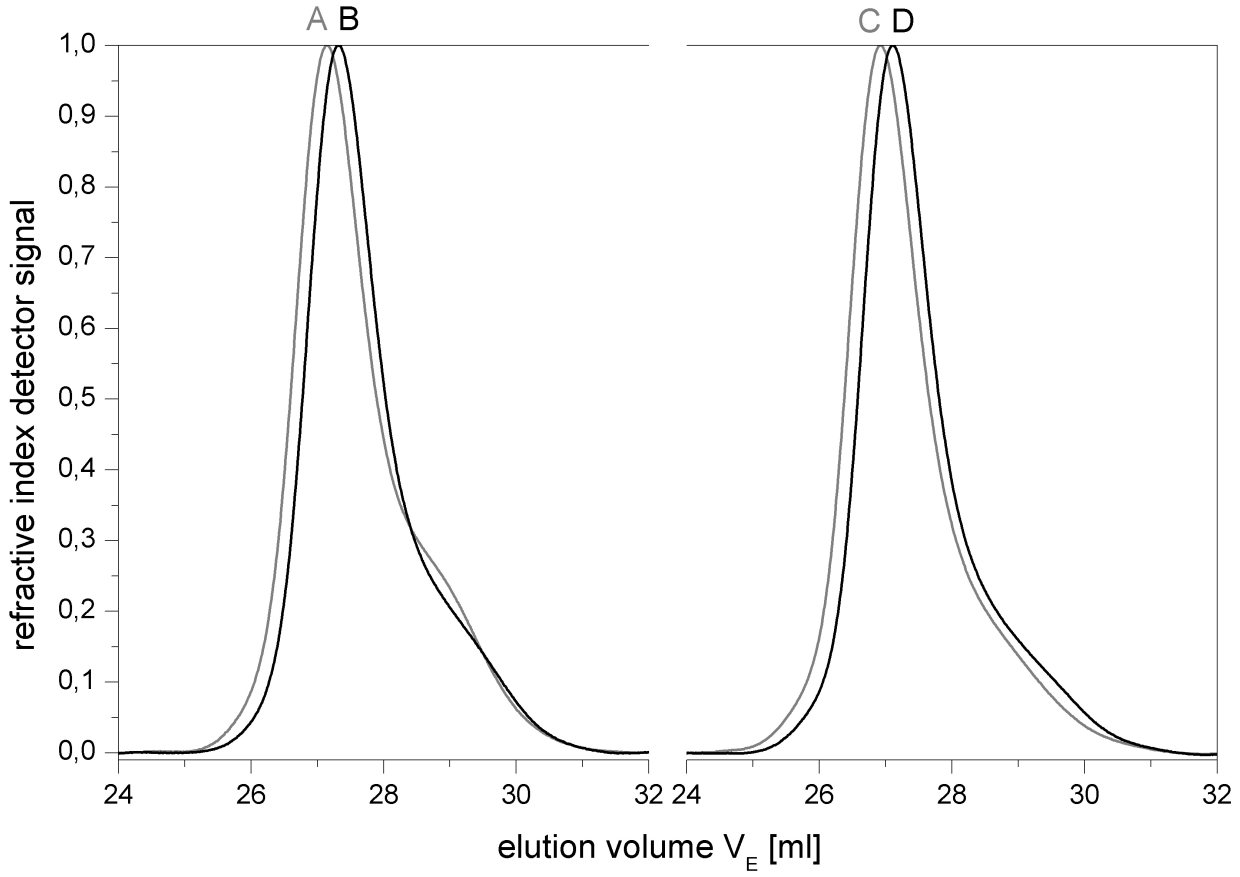

Fig. 10.16.: Comparison of SEC elution diagrams of the educts V151 and V152 as well as the product V161 and V162 (A: educt P[tBMA]$_{0.52}$–b–P[nBMA]$_{0.48}$, V151; B: hydrolysis product P[MAA]$_{0.52}$–b–P[nBMA]$_{0.48}$, V161; C: educt P[tBMA]$_{0.47}$–b–P[BzMA]$_{0.53}$, V152; D: hydrolysis product P[tBMA]$_{0.47}$–b–P[BzMA]$_{0.53}$, V162)

The elution diagrams of both hydrolysis product–samples showed the same tailing than the elution diagrams of the two product–samples. For both experiments the signals of the product–samples shifted towards higher elution volumes, i. e. lower molecular weights. Hence, the molar masses of the products were lower than the educts.

Tab. 10.13.: SEC results of experiments V151, V161, V152 and V162

Entry	F_{nBMA} F_{BzMA}	$V_E{}^a$ [ml]	$M_w{}^b$ [g · mol^{-1}]	ΔM_w [g · mol^{-1}]	[%]
V151	0.52	27.15	23983		
V161		27.32	22037	1946	8.11
V152	0.47	26.92	26933		
V162		27.11	24492	2441	9.06

[a] Peak elution volume
[b] relative values, based on PSS calibration *Eq. 3.3.22*

The reduction of the relative molar masses from the product–samples to the educt–samples lay at 8 to 9 % and so equal for the two hydrolysis reactions. Thereby the resulting relative molar masses were higher than calculated in the forefront. The relative molar mass of the

hydrolyzed block copolymer of experiment V161 should be 19 % lower than the relative molar mass of the educt V151 and the molar mass of product V162 should be 16 % lower than the molar mass of the educt V152. That was caused by the fact that for a relative molecular weight determination only the maximum elution volume is used and this is always higher than the average molar mass of a sample. The relative molar masses of the statistical copolymers and the gradient copolymers that were analyzed before show the same differences between the measured and the expected relative molar masses.

The investigation of the thermal behavior was the next part of analysis. The samples of the hydrolysis products V161 and V162 were heated up for two times from −80 to 200 °C with a cooling run in between (dT/dt = 10 K/min). The samples were not measured up to 300 °C like the samples of *Section 4.2* before because it was worked out that the hydrolyzed polymers will decompose during the DSC–measurement. In *Figure 10.17* the two heating runs and the cooling run of both experiments V161 and V162 are represented.

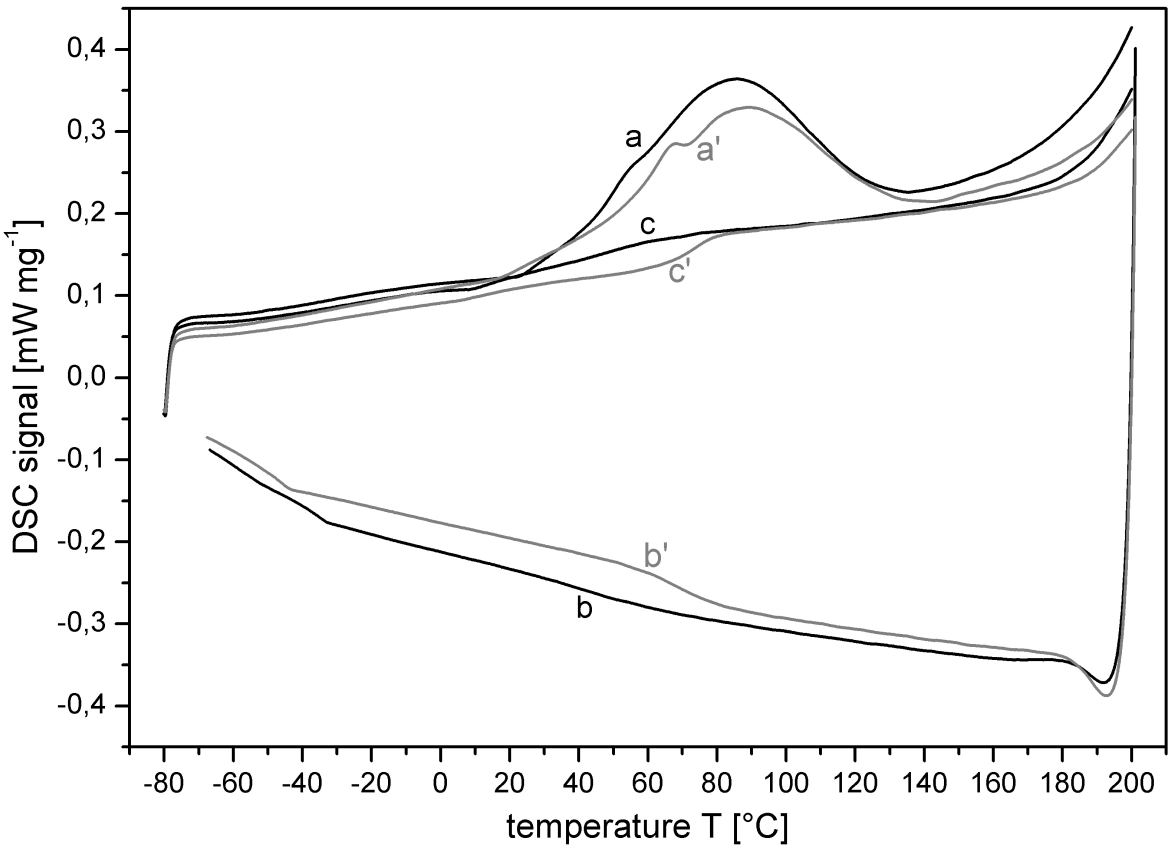

Fig. 10.17.: DSC thermograms of hydrolyzed AB–di–block copolymers V161 (black line) and V162 (grey line); a/a' – first heating run, b/b' – first cooling run, c/c'; second heating runs, heating rate 10 K · min^{-1}

Both thermograms of the first heating run exhibited an endothermic peak in the temperature range from 20 to 140 °C. Then the DSC–signal increased. The second heating run and the cooling run did not show informative peaks or glass transition steps. The DSC–thermograms of P[nBMA–co–MAA], see *Section 4.2*, also shows a similar endothermic peak during the first

heating run. So also the hydrolyzed block copolymers V161 and V162 decomposed during the first heating run. The peak area and peak height of the first heating runs of the thermograms of hydrolyzed copolymers V161 and V162 were determined and the results are listed in *Table 10.14*.

Tab. 10.14.: DSC results of hydrolysis–products of copolymers from experiment V161 and V162

Entry	F_{MAA}	Area $[J \cdot g^{-1}]$	T_{Peak} [℃]	T_{onset} [℃]	T_{offset} [℃]	Width [℃]	Height $[mW \cdot mg^{-1}]$
V111	0.52	60.4	83.2	44.2	117.2	64.2	0.1825
V121	0.47	50.9	85.8	53.8	119.5	63.9	0.1499

The endothermic peaks of the thermograms of the two samples show nearly the same values. So the different functional groups inside the chains of the block copolymers $P[MAA]_{0.52}$–b–$P[nBMA]_{0.48}$ and $P[MAA]_{0.47}$–b–$P[BzMA]_{0.53}$ did not have a strong influence on the decomposition of the hydrolyzed polymers.

10.5. Summary

The *tert*–butyl groups of the AB–di–block copolymer from *tert*–butyl methacrylate and *n*–butyl methacrylate, respectively from *tert*–butyl methacrylate and benzyl methacrylate were hydrolytically cleaved by means of methanesulfonic acid (MSA). The characterization of the hydrolyzed copolymers with ^{1}H–NMR–spectroscopy and elementary analysis showed the absence of *tert*–butyl–groups in the polymer chains, and hence, a total conversion of the hydrolysis. The elementary analysis results agreed decently to the structure of both experiments. The changes in the ATR-FTIR-spectra supported the good results of the ^{1}H–NMR–spectra. The vibrational band of the OH-group occurred and the fingerprint–region change in case of the vibrational bands from the *tert*–butyl–group. The changes were so vigorous that an analysis of the vibrational bands of nBMA– and BzMA–units was not possible. The RI–detector signals of the block copolymers showed the same tailing than the elution diagrams of the two products. The relative molar masses deceased but not as strong as expected. The DSC analysis showed broad endothermic peaks for both copolymers in the same region and the samples did not regenerate after the first heating run. The peak area and the peak height of the endothermic peak were the same for both block copolymers. Both hydrolysis of the AB–di–block copolymers worked well and two amphiphilic AB–di–block copolymers with different composition have successfully be obtained. There was no obvious difference of the hydrolyzed block copolymers to the respective statistical or gradient copolymers which contain the same monomer–units.

11. Synthesis of Gradient Copolymers from Benzyl and tert–Butyl Methacrylate by means of Semibatch Polymerization with Observation by Online IR

This part describes an approach to synthesizes gradient copolymers from benzyl methacrylate and *tert*–butyl methacrylate by means of an automatic, feedback–loop controlled semibatch synthesis, using online infrared–spectroscopy observation to control the monomer feed during the synthesis. The synthesis was a cooperation with the working groups of *Prof. Dr. H.–U. Moritz* from the University of Hamburg. Subsequently the resulting copolymers were hydrolyzed with methanesulfonic acid to obtain functional amphiphilic gradient copolymers which are the aim of this thesis.

11.1. Materials and Methods

Because of the compatibility the copolymers were synthesized with the same materials than in the *Chapters 7* and *8*. Also the hydrolysis were done with the same technique than in *Chapter 9*.

11.1.1. Materials

First are listed the chemicals which were used for the semibatch copolymerization. The treatments of chemicals were the same as detailed in *Section 7.1.1*.

- monomers
  - benzyl methacrylate (BzMA, 98 %, *Alfa Aesar*)
  - *tert*–butyl methacrylate (tBMA, 98 %, *Alfa Aesar*)
- initiator: *para*–toluenesulfonyl chloride (pTSC, 98 %, *Sigma–Aldrich*)
- catalyst: copper(I) chloride (97 %, *Sigma–Aldrich*)

- ligand: N,N,N',N',N"–pentamethyldiethylenetriamine (PMDETA, 99 %, *Sigma-Aldrich*)
- solvent: 2–butanone (MEK, *BDH Prolabo*, chromasol.)

The chemicals which were used for the hydrolysis are listed in the following. They were used as received.

- methanesulfonic acid (MSA, ≤ 99.5 %, *Aldrich*)
- chloroform (99.9 %, *Acros*, extra dry over molecular sieve, stabilized)
- THF (chromasolv, *Aldrich*)
- *n*–pentane (*Aldrich*)

11.1.2. Semibatch Copolymerizations

The experimental setup of the semibatch copolymerization is depicted in *Figure 11.1.*

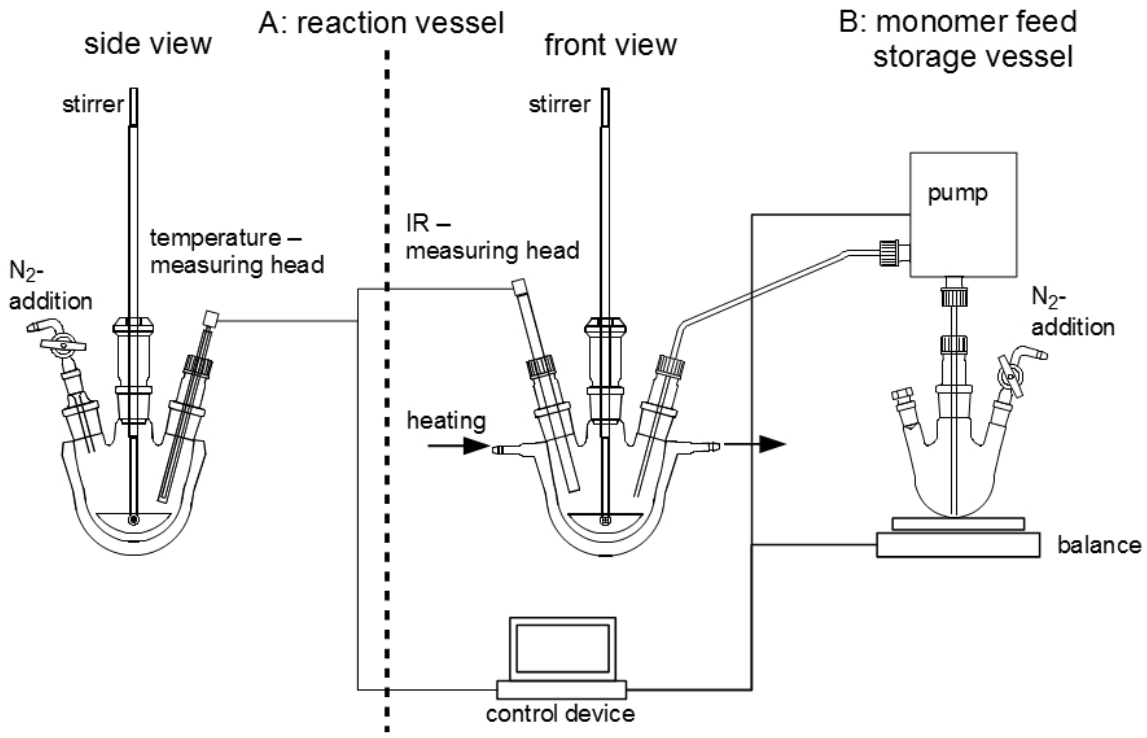

Fig. 11.1.: Experimental setup for semibatch copolymerization with online IR–measuring

In contrast to the semibatch copolymerization of tBMA and BzMA in *Section 8* the total volume of the reaction mixture had to be around 500 ml because of the volume of the reaction vessel. So the amounts of the substances were forty times higher. They are listed in *Table 11.1* for the two semibatch copolymerizations. Both experiments had the same composition and also the preparation of the feed– and the stock–solution were the same. Likewise the work–up of the final solution was the same for both experiments.

The two monomers, respectively the feed– and the stock–solution, were prepared separately. The stock solution, consisting of 1.38 g ($7.22 \cdot 10^{-3}$ mol) pTSC, 89.87 g (0.6320 mol) BzMA, 1.25 g ($7.22 \cdot 10^{-3}$ mol) PMDETA, 0.72 g ($7.22 \cdot 10^{-3}$ mol) CuCl and 89.87 g MEK, was weighted in a round bottom flask. In a second flask (vessel B, *Figure 11.1*) was weighted in the feed solution, with 111.38 g (0.6320 mol) tBMA and 111.38 g MEK. Nitrogen was passed into the solutions under stirring for 30 min to remove the oxygen. The stock solution was transferred into the reaction vessel (vessel A, *Figure 11.1*) under nitrogen counterflow. Into the round bottom flask of feed solution the pump was mounted under nitrogen counterflow and then the pump was connected with the reaction vessel. The stock solution was degassed again by the pass of nitrogen into the solution for 90 sec. Then the stock solution was heated up to 80 °C over 10 min, stirred with 400 rpm over 30 sec, paused for 5 min, stirred with 500 rpm over 6 sec and then paused for 33 min.

V131: After the preparation of the stock– and the feed–solution the injection of the feed–solution was started. In a first phase 5 g feed–solution were injected over 1 min. Then the system paused for calibration over 23 min. Subsequently the feeding was started with $0.3\,\mathrm{g} \cdot \mathrm{min}^{-1}$. The feeding ended when 170 g of feed–solution were added. After the addition the heating was switched off and the solution was stirred with 100 rpm until RT was reached.

V132: After the preparation of the stock– and the feed–solution the program for the dosing control was started. The dosing ended when 170 g of feed–solution were added. After the addition the heating was switched off and the solution was stirred with 100 rpm until RT was reached.

Both final solution were divided into four portions of around 50 g. Each portion was diluted with 100 ml of MEK, filtered over 50 g Al_2O_3 and two-thirds of the solvent was removed by vacuum distillation. The residual mixture of polymer, monomers, initiator components and remaining solvent was slowly dropped into 750 ml of an ice cooled water : methanol (1 : 1 vol : vol) mixture. The precipitated polymer was filtered over a P4 glass filter and dried at 25 °C under vacuum over night.

Tab. 11.1.: Composition of the semibatch copolymerizations of BzMA and tBMA with online IR–measuring

f^0_{tBMA}			n [mol]	m [g]
0.5	Stock	BzMA	0.6320	89.87
		pTSC	$7.22 \cdot 10^{-3}$	1.38
		PMDETA	$7.22 \cdot 10^{-3}$	1.25
		CuCl	$7.22 \cdot 10^{-3}$	0.72
		MEK	1.5444	89.87
	Feed	tBMA	0.6320	111.38
		MEK	2.7907	111.38

Experiment V131 P[BzMA–co–tBMA], linear dosing:

^{1}***H–NMR:*** 1.13–1.30 ppm (broad peak, –C(CH_3)$_3$, P[tBMA]); 1.32 ppm (s, –C(CH_3)$_3$, tBMA); 1.57–1.80 ppm (broad peak, –CH_3, P[tBMA] and P[BzMA]); 1.71 ppm (s, –CH_3, tBMA); 1.79 ppm (s, –CH_3, BzMA); 4.64–4.93 ppm (broad peak, –OCH_2R, P[BzMA]); 5.02 ppm (s, OCH_2R, BzMA); 5.29 ppm (t, CH_2=C–, cis, tBMA); 5.41 ppm (t, CH_2=C–, cis, BzMA); 5.81 ppm (s, CH_2=C–, trans, tBMA); 5.97 ppm (s, CH_2=C–, trans, BzMA); 7.05–7.29 ppm (broad peak, aromatic ring, BzMA and P[BzMA])

EA: 71.84 % C, 7.67 % H, (20.49 % O_{calc})

ATR–FTIR: 3160–2780 cm^{-1} (=CH_2, –CH_2–, –CH_3, aromatic ring); 1722 cm^{-1} (–C=O); 1479 cm^{-1} (–CH_2–, –CH_3); 1455 cm^{-1} (–CH_2–, –CH_3); 1392 cm^{-1}; 1367 cm^{-1} (tBu); 1248 cm^{-1} (tBu); 1134 cm^{-1} (–C–O–C–); 1030 cm^{-1}; 966 cm^{-1} (Bz); 912 cm^{-1}; 876 cm^{-1}; 847 cm^{-1} (tBu); 749 cm^{-1} (Bz); 696 cm^{-1} (Bz); 583 cm^{-1}; 527 cm^{-1}; 459 cm^{-1}

SEC: dn/dc = 0.1177 $ml \cdot g^{-1}$; M_n = 46180 $g \cdot mol^{-1}$; M_w = 55450 $g \cdot mol^{-1}$; M_z = 64590 $g \cdot mol^{-1}$

DSC: T_{onset} = 48.5 °C; T_{midpt} = 55.5 °C; T_g = 57.5 °C; T_{offset} = 63.5 °C; ΔC_p = 0.176 $J \cdot g^{-1} \cdot K^{-1}$

Experiment V132 P[BzMA–co–tBMA], controlled dosing:

^{1}***H–NMR:*** 1.07–1.23 ppm (broad peak, –C(CH_3)$_3$, P[tBMA]); 1.25 ppm (s, –C(CH_3)$_3$, tBMA); 1.49–1.75 ppm (broad peak, –CH_3, P[tBMA] and P[BzMA]); 1.65 ppm (s, –CH_3, tBMA); 1.72 ppm (s, –CH_3, BzMA); 4.60–4.86 ppm (broad peak, –OCH_2R, P[BzMA]); 4.95 ppm (s, OCH_2R, BzMA); 5.23 ppm (t, CH_2=C–, cis, tBMA); 5.35 ppm (t, CH_2=C–, cis, BzMA); 5.75 ppm (s, CH_2=C–, trans, tBMA); 5.90 ppm (s, CH_2=C–, trans, BzMA); 6.99–7.19 ppm (broad peak, aromatic ring, BzMA and P[BzMA])

EA: 71.12 % C, 7.93 % H, (20.95 % O_{calc})

ATR–FTIR: 3160–2785 cm^{-1} (=CH_2, –CH_2–, –CH_3, aromatic ring); 1717 cm^{-1} (–C=O); 1476 cm^{-1} (–CH_2–, –CH_3); 1455 cm^{-1} (–CH_2–, –CH_3); 1392 cm^{-1}; 1367 cm^{-1} (tBu); 1319 cm^{-1}; 1248 cm^{-1} (tBu); 1133 cm^{-1} (–C–O–C–); 1030 cm^{-1}; 967 cm^{-1} (Bz); 912 cm^{-1}; 876 cm^{-1}; 846 cm^{-1} (tBu); 749 cm^{-1} (Bz); 696 cm^{-1} (Bz); 584 cm^{-1}; 528 cm^{-1}; 463 cm^{-1}

SEC: dn/dc = 0.1025 $ml \cdot g^{-1}$; M_n = 53240 $g \cdot mol^{-1}$; M_w = 62470 $g \cdot mol^{-1}$; M_z = 68830 $g \cdot mol^{-1}$

DSC: T_{onset} = 58.0 °C; T_{midpt} = 72.0 °C; T_g = 71.0 °C; T_{offset} = 84.5 °C; ΔC_p = 0.259 $J \cdot g^{-1} \cdot K^{-1}$

11.1.3. Hydrolysis

0.2 g of the copolymer were dissolved in 1.8 g (1.2 ml) $CHCl_3$ and was stirred over night at room temperature. Then the respective amount of MSA, see *Table 11.13*, was added. The mixture was stirred for 2 hours at room temperature. A spatula–spoon of sodium hydrogen carbonate was added and this mixture was stirred for 30 min. Subsequently 5 ml THF were added and the mixture was filtered over a P4 glass filter. Afterward the solution was dropped into 200 ml of ice–cold *n*–pentane. The precipitated polymer was filtered over P4 glass filter and dried at room temperature for two hours. Then the copolymer was re–dissolved in 1 ml THF and the solution was dropped into 200 ml of an ice cooled water : methanol = 1 : 1 vol : vol mixture. The precipitated polymer was filtered over P4 glass filter and dried at room temperature under an oil–pump vacuum over night.

Experiment V141 P[BzMA–co–MAA]:

^{1}***H–NMR:*** 0.53–0.72 ppm (broad peak); 0.73–1.14 ppm (broad peak); 1.56–2.05 ppm (broad peak, $-CH_3$, P[BzMA], P[MAA]); 3.55 ppm (H_2O); 4.76–5.05 ppm (broad peak, $-OCH_2R$, P[BzMA]); 7.19–7.44 ppm (broad peak, aromatic ring, P[BzMA]); 12.03–12.69 ppm (broad peak, –COOH, P[MAA])

EA: 67.55 % C, 6.78 % H, (25.67 % O_{calc})

ATR–FTIR: 3650–2390 cm^{-1} (–COOH); 3115–2790 cm^{-1} ($=CH_2$, $-CH_2-$, $-CH_3$, aromatic ring); 1726 cm^{-1} (–C=O); 1699 cm^{-1} (–C=O); 1483 cm^{-1} ($-CH_2-$, $-CH_3$); 1455 cm^{-1} ($-CH_2-$, $-CH_3$); 1389 cm^{-1}; 1368 cm^{-1}; 1257 cm^{-1}; 1149 cm^{-1} (–C–O–C–); 1030 cm^{-1}; 964 cm^{-1} (Bz); 912 cm^{-1}; 825 cm^{-1}; 801 cm^{-1}; 750 cm^{-1} (Bz); 697 cm^{-1} (Bz); 586 cm^{-1}; 526 cm^{-1}; 460 cm^{-1}

Experiment V142 P[BzMA–co–MAA]:

^{1}***H–NMR:*** 0.57–0.71 ppm (broad peak); 0.73–1.16 ppm (broad peak); 1.57–2.01 ppm (broad peak, $-CH_3$, P[BzMA], P[MAA]); 3.39 ppm (H_2O); 4.79–5.04 ppm (broad peak, $-OCH_2R$, P[BzMA]); 7.21–7.43 ppm (broad peak, aromatic ring, P[BzMA]); 12.11–12.53 ppm (broad peak, –COOH, P[MAA])

EA: 66.44 % C, 7.23 % H, (26.33 % O_{calc})

ATR–FTIR: 3710–2370 cm^{-1} (–COOH); 3320–2790 cm^{-1} ($=CH_2$, $-CH_2-$, $-CH_3$, aromatic ring); 1725 cm^{-1} (–C=O); 1609 cm^{-1} (–C=O); 1484 cm^{-1} ($-CH_2-$, $-CH_3$); 1455 cm^{-1} ($-CH_2-$, $-CH_3$); 1388 cm^{-1}; 1367 cm^{-1}; 1258 cm^{-1}; 1239 cm^{-1}; 1143 cm^{-1} (–C–O–C–); 1030 cm^{-1}; 964 cm^{-1} (Bz); 912 cm^{-1}; 826 cm^{-1}; 802 cm^{-1}; 750 cm^{-1} (Bz); 696 cm^{-1} (Bz); 586 cm^{-1}; 527 cm^{-1}; 459 cm^{-1}

11.1.4. Characterization

All characterization–methods were the same as with the batch copolymers of *Chapter 3*. The used methods were:

- ^{1}H–NMR spectroscopy
- elementary analysis
- ATR–FTIR–spectroscopy
- size exclusion chromatography
- differential scanning calorimetry

The same instruments under the same conditions were used for the investigation of the resulting copolymers.

Online FTIR–measurement

The online FTIR–measurements were performed with a Mettler Toledo ReactIR 15. The device was controlled with the software iC–IR. The measurement–range was 2800 to 650 cm^{-1} and the measurement–interval was 120 sec.

11.2. Results and Discussion of the Semibatch Copolymerization

The subsequent paragraph describes the evaluations of the ATR–FTIR–spectra resulting from the online–measurements and the analysis of the two resulting copolymers P[tBMA–co–BzMA] from the semibatch polymerizations and also their discussion. The resulting copolymers were analyzed with the same methods as the statistical copolymers P[BzMA–co–tBMA] and the gradient copolymers P[tBMA–co–BzMA] before and under the same conditions (cf. *Section 3.2*). Thereby the resulting copolymers P[tBMA–co–BzMA] can be compared with the gradient copolymer P[tBMA–grad–BzMA] $GP_{0.43}$, see *Chapter 8*.

11.2.1. Online ATR–FTIR–Measurement

For the investigation of the polymer solution with online–IR the IR–spectra of the starting components were needed. The complete analyzed measuring range of the two monomers BzMA and tBMA and the solvent MEK are depicted in *Figure 11.2*. In *Figure 11.3* the finger print region with the two analyzed vibrational bands of the three compounds are detailed.

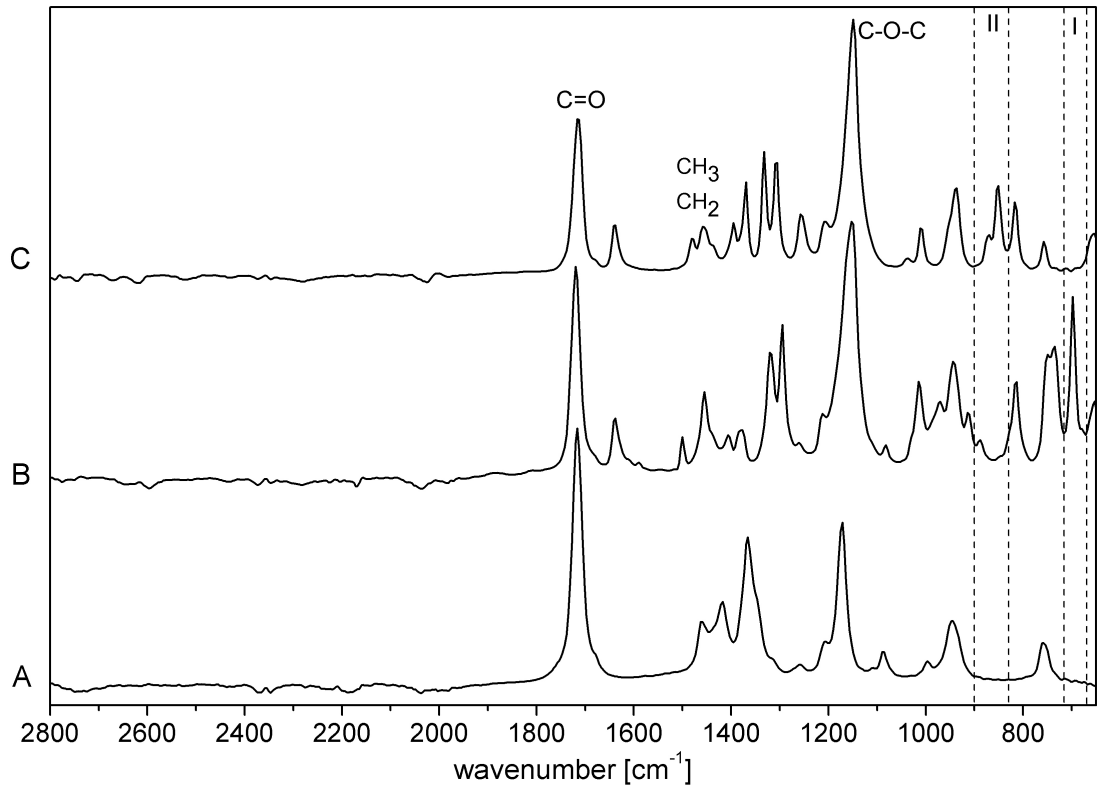

Fig. 11.2.: ATR–FTIR–spectra of (A) 2–butanone, (B) benzyl methacrylate and (C) *tert*–butyl methacrylate with marked analyzed vibrational bands

Overall the IR–spectrum from 650 to 2800 cm^{-1} was observed but only two bands in the finger print region from 650 to 900 cm^{-1} were investigated particularly. Between 2800 cm^{-1} and 1050 cm^{-1} the IR–spectra of the monomers and the solvent were relatively equal. The

vibrational band of C=O was located at 1717 cm^{-1} in the spectra of the two monomers and also in the spectrum of the solvent. For $–CH_2–$ and $–CH_3$ the vibrational band were found at 1485 cm^{-1} and 1456 cm^{-1} in the spectra of the monomers and at 1459 cm^{-1} in the spectrum of the solvent. The vibrational band for C–O–C was located at 1150 cm^{-1} in the monomer spectra and at 1173 cm^{-1} in the solvent spectrum.

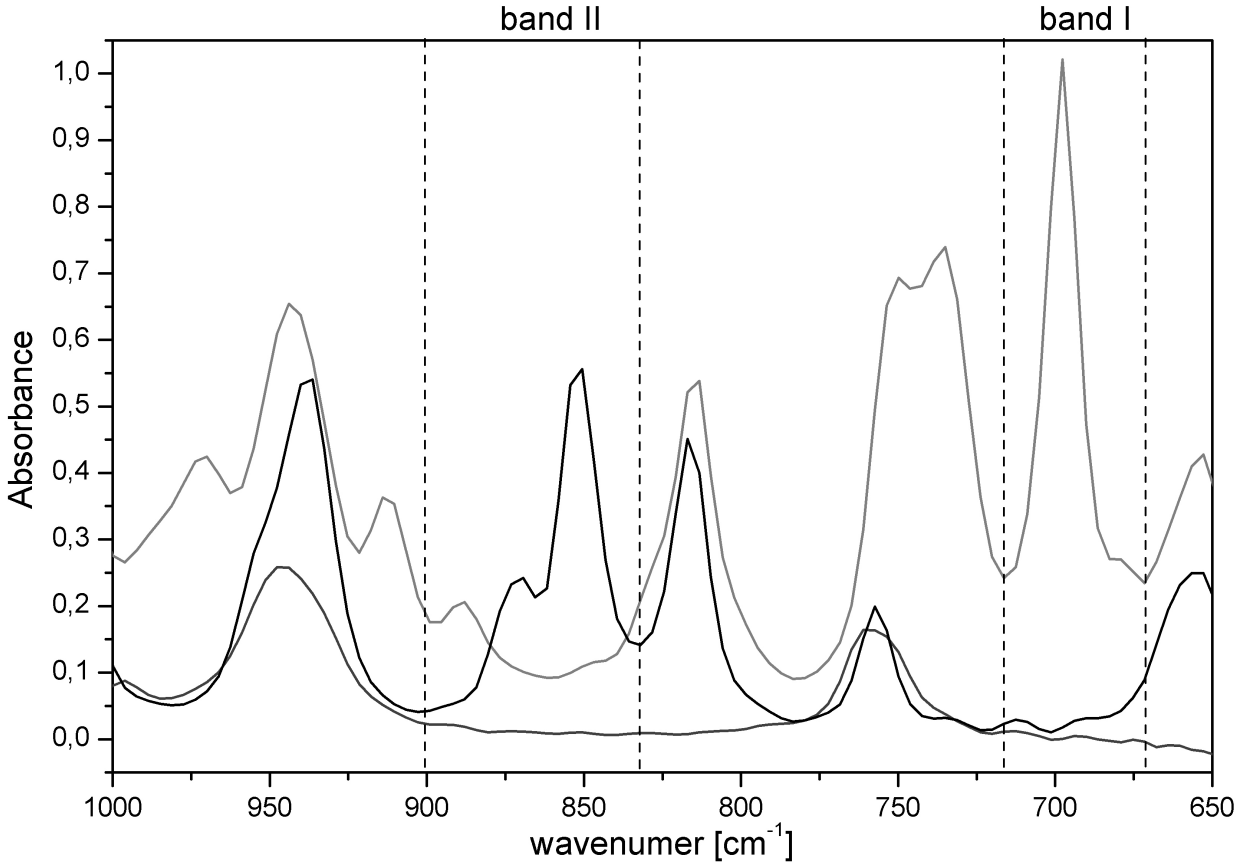

Fig. 11.3.: Section of ATR–FTIR–spectra of 2–butanone (dark grey line), benzyl methacrylate (black line) and *tert*–butyl (grey line) methacrylate with marked analyzed vibrational bands

Between 1050 and 650 cm^{-1}, the lower part of the fingerprint region, the spectra of the monomers among themselves and the solvent varied obviously. For each monomer a vibrational band which is specific for the substance had been searched. The bands at 700 cm^{-1} is characteristic for benzyl methacrylate (*band I*) and the band at 850 cm^{-1} for *tert*–butyl methacrylate (*band II*). These bands were observed by ATR–FTIR–spectroscopy during the semibatch copolymerizations. The changing of the vibrational bands represented the conversion of the two monomers. During experiment V131 the feed–solution was injected without consideration the changing of the vibrational bands linear with 0.3 $g \cdot min^{-1}$. During experiment V132 *band I* was observed and the increase of *band I* was recalculated into the decrease of the monomer BzMA in the stock–solution. The polymerized BzMA was refilled with tBMA by injection of the feed–solution.

In the *Figure 11.4* the fingerprint region of the ATR–FTIR–spectra 1 (0.9 min), 50 (114.3 min), 100 (214.9 min), 150 (314.4 min), 200 (421.1 min), 250 (514.9 min), 300 (620.2 min) and 350 (714.5 min) of experiment V131 are depicted. The two analyzed vibrational bands are marked with dashed lines. In *Figure 11.5* the analyzed section with the vibrational bands was represented more detailed.

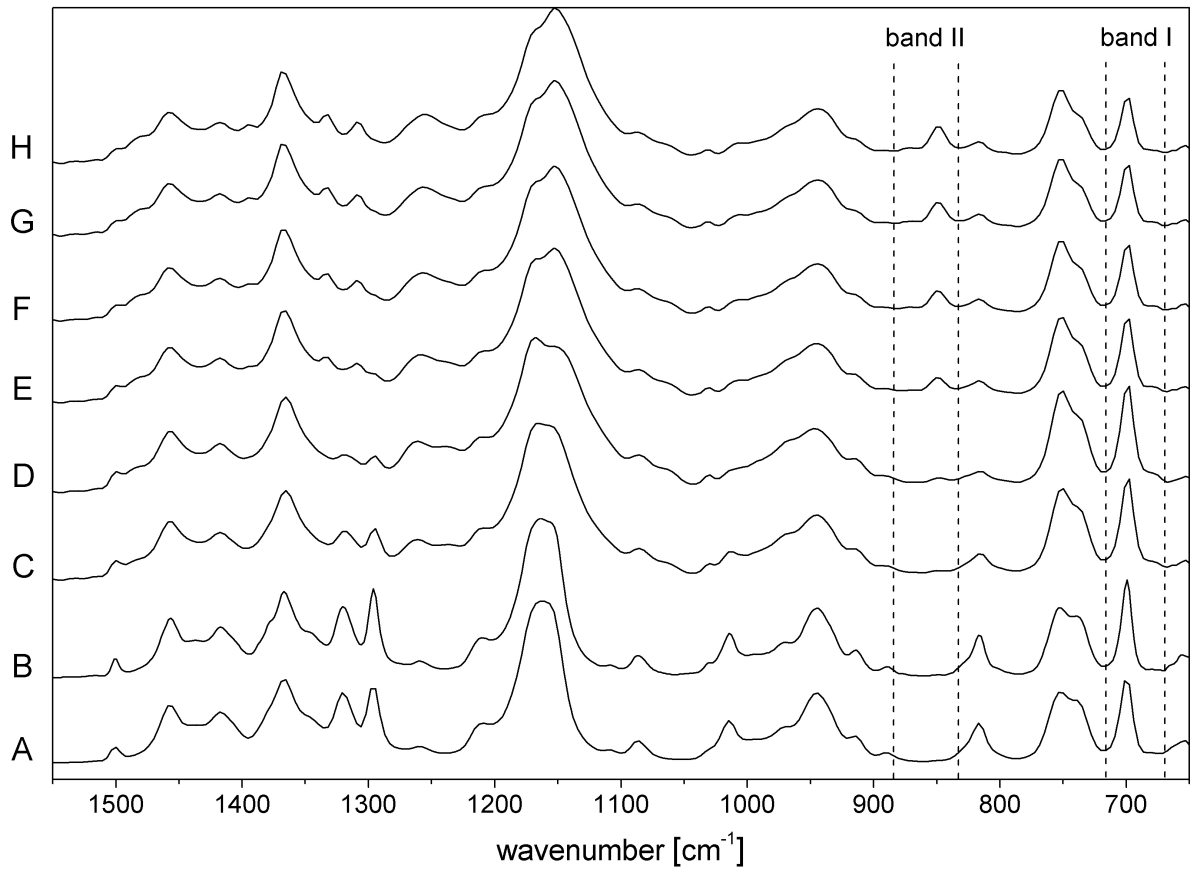

Fig. 11.4.: Finger print region of ATR–FTIR–spectra of samples of experiment V131; A – 0.9 min, B – 114.3 min, C – 214.9 min, D – 314.4 min, E – 421.1 min, F – 514.9 min, G – 620.2 min and H – 714.5 min of reaction time

The different IR–spectra showed changes only in the lower fingerprint region between 650 to 900 cm^{-1}. The four vibrational bands at 700 cm^{-1}, 750 cm^{-1}, 816 cm^{-1} and 850 cm^{-1} changed obviously. *Band II* at 850 cm^{-1} increased and the band at 816 cm^{-1} decreased during the polymerization. The changes of the band at 700 cm^{-1} and *band I* at 750 cm^{-1} were less obvious.

The detailed *Figure 11.5* shows that only the differences of *band II* were considerable. The differences of *band I* were indistinct because the baseline of the band varied between the different spectra. Therefore the peak area and the peak height of the two vibrational bands were determined. The values are listed in *Table 11.2* and depicted in *Figure 11.6*.

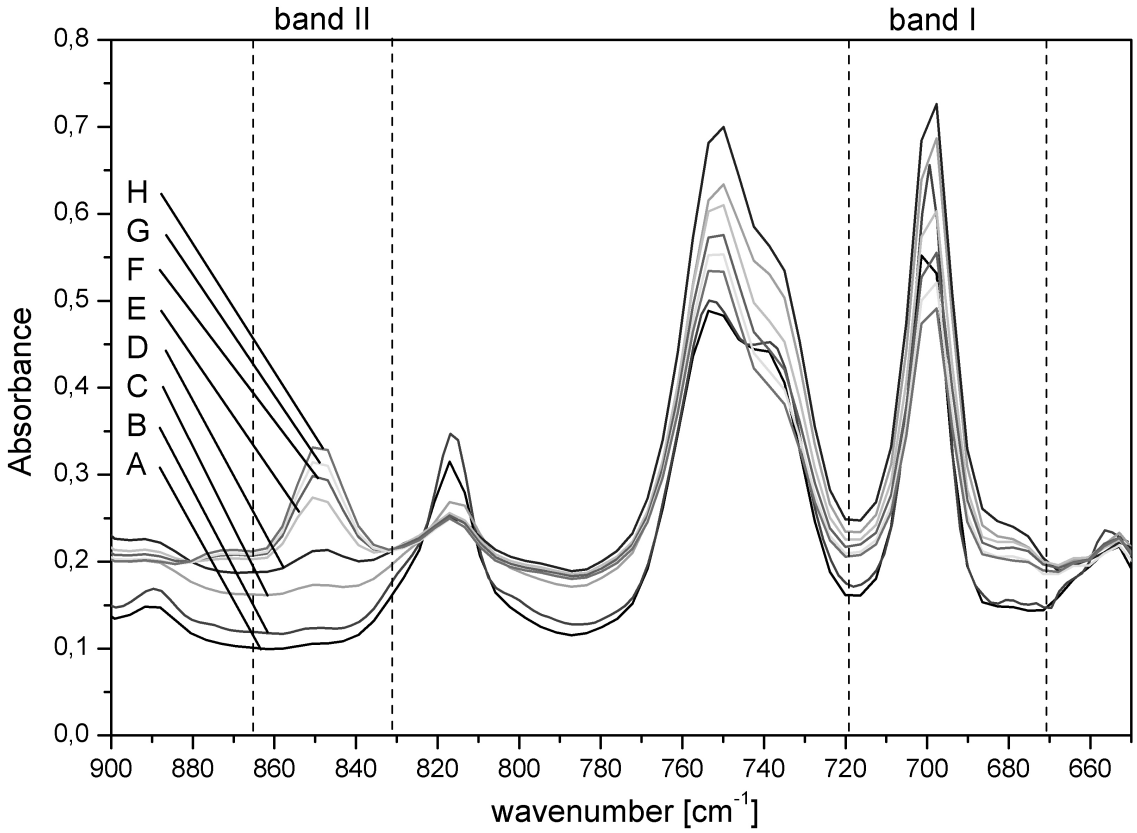

Fig. 11.5.: Section of ATR–FTIR–spectra of samples taken during experiment V131; A – 0.9 min, B – 114.3 min, C – 214.9 min, D – 314.4 min, E – 421.1 min, F – 514.9 min, G – 620.2 min and H – 714.5 min of reaction time

Tab. 11.2.: Peak area and peak height of the analyzed ATR–FTIR–bands the samples taken during experiment V131

Spectrum No.	time [min]	*band I* peak height	*band I* peak area [cm^{-1}]	*band II* peak height	*band II* peak area [cm^{-1}]
001	0.9	5.04	0.41	−0.87	0.02
050	114.3	6.37	0.48	−0.49	0.01
100	214.9	7.16	0.51	−0.15	0.01
150	314.4	5.30	0.40	0.90	0.07
200	421.1	4.73	0.35	1.32	0.09
250	514.9	4.37	0.33	1.64	0.11
300	620.2	3.91	0.30	1.97	0.13
350	714.5	4.16	0.31	2.14	0.14

It was not possible to calculate the conversion of the monomers or the composition of the copolymer during the reaction. First it was not possible to separate the monomer–spectra from the polymer–spectrum. So the ratios of PBzMA and PtBMA in *band I* and *band II* could not be determined. Second it was not possible to determine the actual amount of added feed–solution. The values of the peak areas and the peak heights showed inexplicable runs during the polymerization time for both vibrational bands.

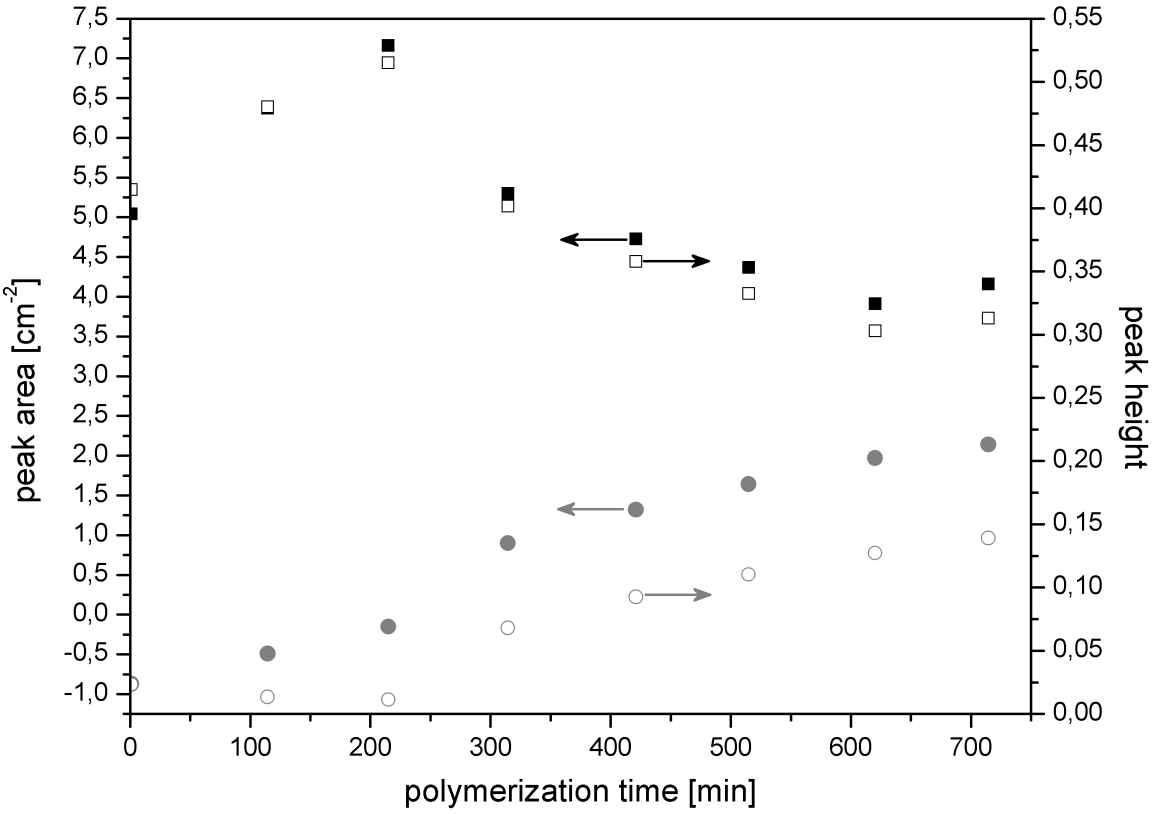

Fig. 11.6.: Plot of peak area (■,●) and peak height (□, ○) of *band I* (black squares) and *band II* (grey circles) of experiment V131

In the *Figure 11.7* the fingerprint region of the ATR–FTIR–spectra 1 (1.4 min), 50 (99.4 min), 100 (199.4 min), 150 (299.4 min), 200 (399.4 min), 250 (499.4 min), 300 (599.4 min) and 350 (699.4 min) of experiment V132 are depicted. The two analyzed vibrational bands are marked with dashed lines. In *Figure 11.8* the analyzed section with the vibrational bands are represented more detailed. The vibrational bands changed in the same way as the IR–spectra of experiment V131 in the lower fingerprint region. The four vibrational bands at 700 cm^{-1}, 750 cm^{-1}, 816 cm^{-1} and 850 cm^{-1} changed distinctly. *Band II* at 850 cm^{-1} increased and the band at 816 cm^{-1} decreased during the polymerization. The changes of the band at 700 cm^{-1} and *band I* at 750 cm^{-1} were less obvious. The detailed *Figure 11.8* shows the same development of the IR–spectra than the IR–spectra of experiment V131. Only the differences of *band II* were considerable. The differences of *band I* were indistinct because the baseline of the band varied between the different spectra. Also here the peak area and the peak height of the two vibrational bands were determined. The values are listed in *Table 11.3* and depict in *Figure 11.9*. Even here it was impossible to calculate the conversion of the monomers or the composition of the copolymer during the reaction. First it was not possible to divide the monomer–spectra from the polymer–spectrum. So the ratios of PBzMA and PtBMA in *band I* and *band II* could not be determined. Second it was not possible to determine the actual amount of added feed–solution. The values of the peak areas and the peak heights show inexplicable runs during the polymerization time for both vibrational bands.

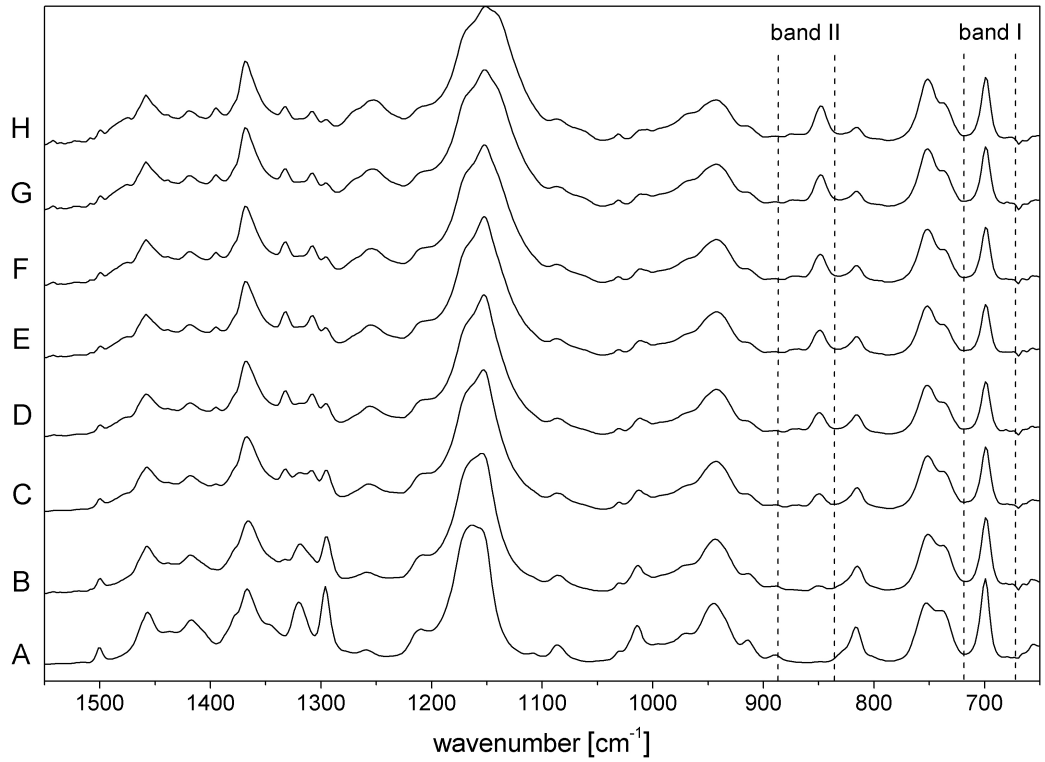

Fig. 11.7.: Finger print region of ATR–FTIR–spectra of samples of experiment V132; A – 1.4 min, B – 99.4 min, C – 199.4 min, D – 299.4 min, E – 399.4 min, F – 499.4 min, G – 599.4 min and H – 699.4 min of reaction time

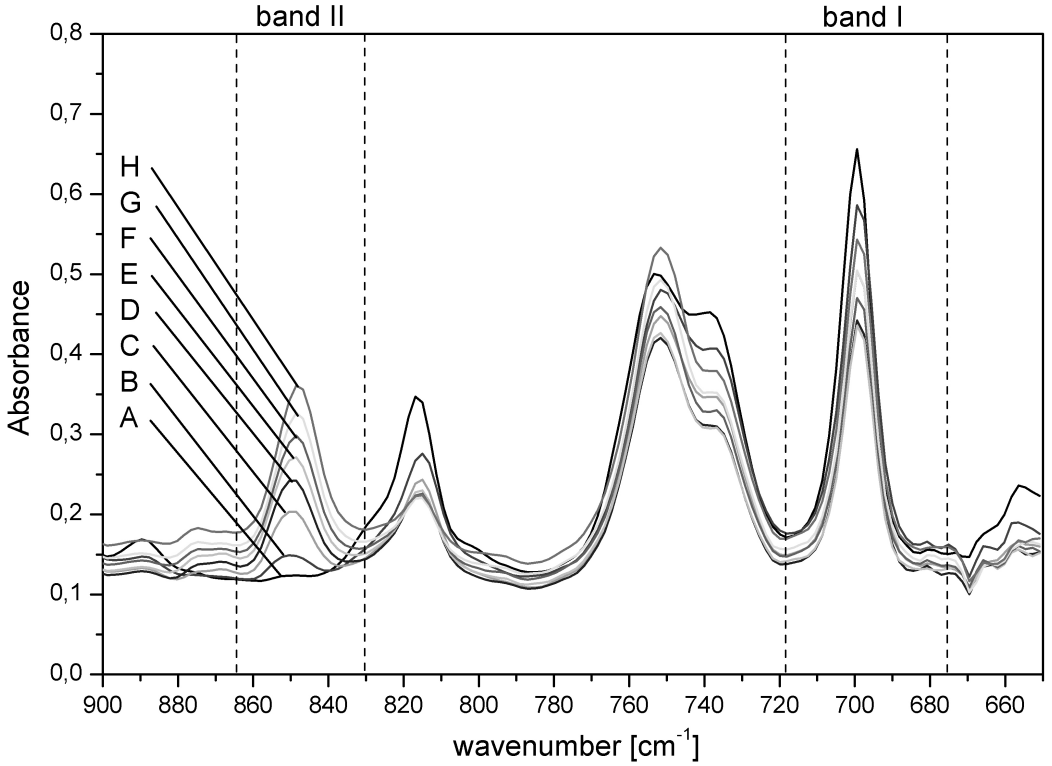

Fig. 11.8.: Section of ATR–FTIR–spectra of samples taken during experiment V132; A – 1.4 min, B – 99.4 min, C – 199.4 min, D – 299.4 min, E – 399.4 min, F – 499.4 min, G – 599.4 min and H – 699.4 min of reaction time

Tab. 11.3.: Peak area and peak height of the analyzed ATR–FTIR–bands the samples taken during experiment V132

Spectrum No.	time [min]	*band I* peak height	*band I* peak area [cm^{-1}]	*band II* peak height	*band II* peak area [cm^{-1}]
001	1.4	5.21	0.50	−1.60	0.01
050	99.4	4.50	0.42	−0.80	0.01
100	199.4	3.85	0.37	0.56	0.07
150	299.4	3.22	0.31	1.38	0.11
200	399.4	3.12	0.30	1.79	0.13
250	499.4	3.47	0.34	2.05	0.15
300	599.4	3.77	0.36	2.32	0.17
350	699.4	4.09	0.39	2.63	0.19

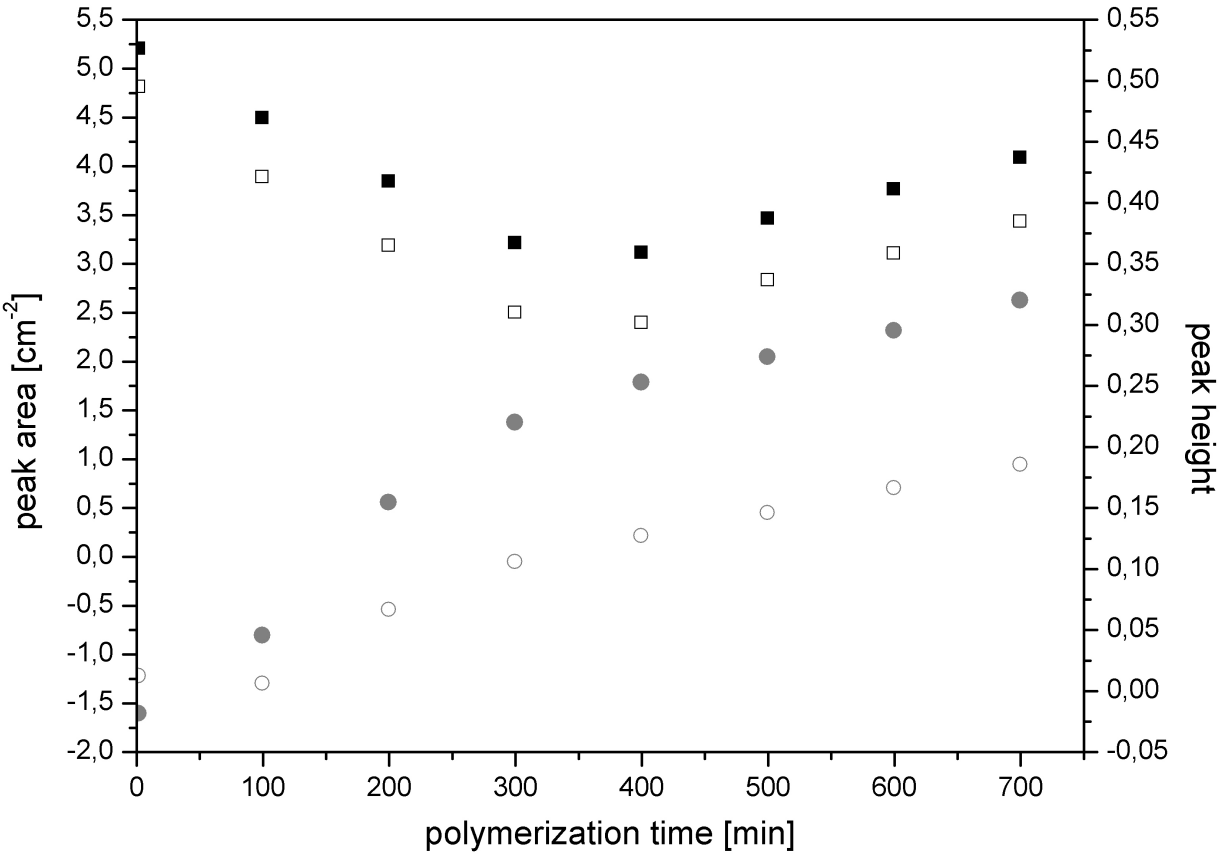

Fig. 11.9.: Plot of peak area (■,●) and peak height (□, ○) of *band I* (black squares) and *band II* (grey circles) of experiment V132

However, the precipitated copolymers of the experiments V131 and V132 were analyzed in the same way as the statistical copolymers P[tBMA–co–BzMA] of *Section 7* and the gradient copolymer P[tBMA–grad–BzMA] *Section 8*.

11.2.2. Structural Analysis

The molecular structures of the monomers tBMA and BzMA and the resulting copolymer as well as the numbering of these carbons are shown in *Figure 11.10*.

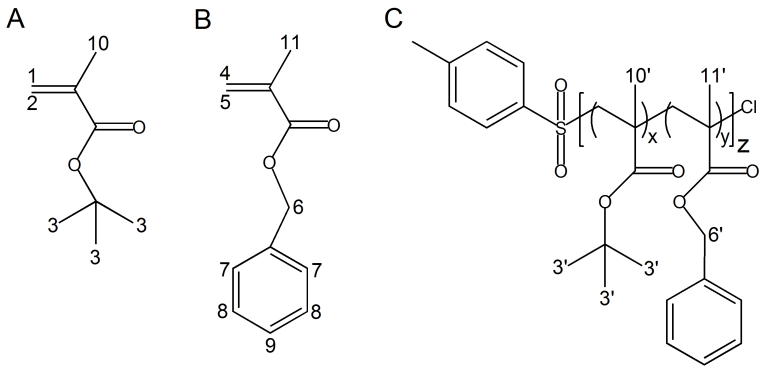

Fig. 11.10.: Molecular structures of the monomers (A) tBMA and (B) BzMA and (C) the copolymer P[tBMA–grad–BzMA] with carbon–atom labels (z = x + y = 1)

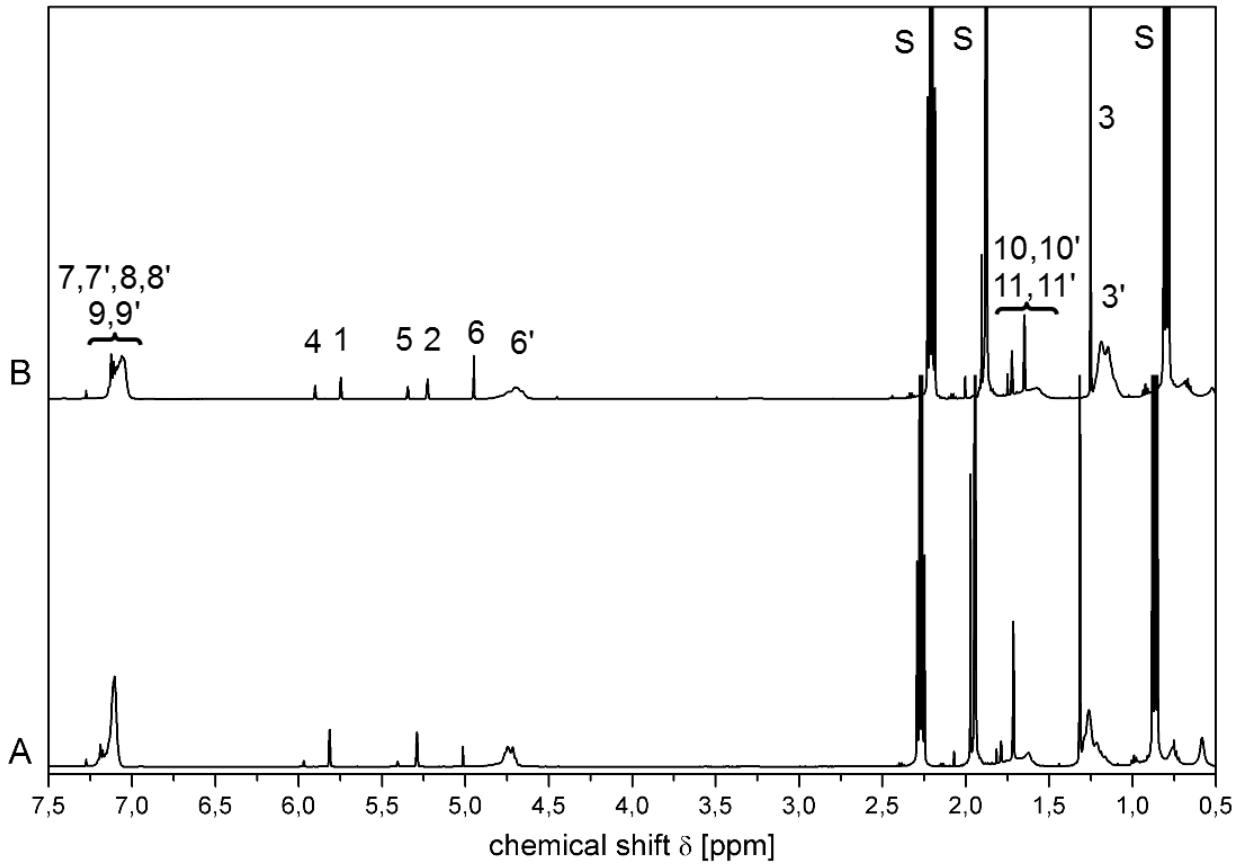

Fig. 11.11.: ^{1}H–NMR–spectra of (A) experiment V131 (P[tBMA$_{0.37}$–co–BzMA$_{0.63}$]) and (B) V132 (P[tBMA$_{0.51}$–co–BzMA$_{0.49}$])

The *Figure 11.11* shows the ^{1}H–NMR–spectra of the resulting copolymers from the experiments (A) V131 P[tBMA$_{0.37}$–co–BzMA$_{0.63}$] and (B) V132 P[tBMA$_{0.51}$–co–BzMA$_{0.49}$]. In both spectra the signals of the monomers together with polymer–signals mixed up with the signals

of the solvent MEK. The signals at 0.96 ppm (t), 2.06 ppm (s) and 2.38 ppm (q) represented the solvent. For the monomer tBMA a singlet at 5.9 ppm ($=CH_2^{cis}$, 1), a triplet at 5.3 ppm ($=CH_2^{trans}$, 2), a singlet at 1.8 ppm ($-CH_3$, 10) of the methacrylate part of the monomer and a singlet at 1.4 ppm of the *tert*–butyl group (3) were found. The BzMA as monomer showed a singlet at 6.1 ppm and a triplet at 5.5 ppm for the vinyl–group (4 and 5) and a singlet at 1.8 ppm for the methyl–group (12) of the methacrylate group. The benzyl–unit exhibited a singlet of the benzylic methylene–group (6) at 5.2 ppm and a broad multiplet was caused the aromatic ring protons (7, 8, 9) between 7.5 to 7.2 ppm. The polymer is represented in the spectra by broad peaks from 7.5 to 7.2 ppm for the aromatic ring protons (7', 8', 9'), at 4.75 to 5.05 ppm ($-OCH_2R$, 6') and at 1.25 to 1.4 ppm a signal caused by the *tert*–butyl group (3') inside the polymer chain. The signals of the aromatic ring of monomer and polymer (7, 8, 9, 7', 8', 9') overlapped. From the ratios of the integrals A of the signals 3' and 6' the compositions of the copolymers were calculated. They are listed in *Table 11.4*.

Tab. 11.4.: Integrals of experiment V131 and V132

entry	A6	A6'	A3	A3'	composition
V131	2.00	31.39	66.19	84.15	P[$tBMA_{0.37}$–co–$BzMA_{0.63}$]
V132	2.00	10.90	17.04	51.31	P[$tBMA_{0.51}$–co–$BzMA_{0.49}$]

The two spectra showed slight differences at the signals of the polymer components. The signal of the monomer parts and the polymer components were set in proportion to the signals of the solvent. The signal of the aromatic ring (7, 8, 9 and 7', 8', 9') was stronger in the spectra of experiment V131 than in the spectra of experiment V132. The same was one view for the signals of the benzylic methylene–group of the polymer (6'). The reason was a higher amount of BzMA inside the polymer chain of copolymer V131 than in polymer chain V132. At reverse, the signal of the *tert*–butyl group of the polymer (3') was stronger in the spectra of experiment V132 than in the one of experiment V131, because of the higher amount of tBMA in the copolymer V132 in comparison to copolymer V131. The calculations of the compositions of the two copolymers, see *Table 11.4*, from the integrals of the signals lead to the same results.

The different kinds of injection methods led to copolymers with a different composition. The continuous linear injection of tBMA during experiment V131 resulted in a copolymer with one third tBMA and two thirds BzMA inside the polymer chain. The IR–controlled injection resulted in a copolymer with 50 % tBMA and 50 % BzMA what was the intended composition.

The purity and also the composition of the resulting copolymers were analyzed by means of elementary analysis. The results of the measurements and the differences between the theoretical and the analysis results are listed in *Table 11.5*.

Tab. 11.5.: Results of the elementary analysis of the experiments V131 and V132

entry	F_{tBMA}		C [%]	ΔC	H [%]	ΔH	O [%]	ΔO
V131	0.37	theory	72.60		7.85		19.56	
		is	71.84	-0.76	7.67	-0.18	20.49	0.94
V132	0.51	theory	71.60		8.26		20.14	
		is	71.12	-0.48	7.93	-0.33	20.95	1.34

The element compositions of the resulting copolymers from the experiments V131 P[$tBMA_{0.37}$–co–$BzMA_{0.63}$] and V132 P[$tBMA_{0.51}$–co–$BzMA_{0.49}$] were similar to the other copolymers from tBMA and BzMA, the statistical copolymers (cf. *Tables 7.7* and *7.8*) and the gradient copolymer (cf. *Table 8.7*). Hence, also this polymerizations gave consistent results. Moreover, the differences between the theoretical compositions and the measured values were small, indicating that the samples were free of pollution.

As well as for the statistical copolymers from *Chapter 7* also for these copolymers the data from elementary analysis were used to calculated the composition of the polymers. The fittings of the calibration curves from the amount of carbon and hydrogen, see *Section 7.2.2*, Figure 7.13, were adapted for the calculations. That was necessary because the equations were established for the amount of BzMA inside the polymer–chain F_{BzMA} and the composition of the gradient copolymers was described by the amount of tBMA inside the polymer–chain F_{tBMA}. So for the determination of the compositions from the amount of carbon *Equation 11.2.1* was used and for the determination from the amount of hydrogen *Equation 11.2.2*.

$$F_{tBMA} = 1 - \frac{C - 0.6757}{0.0741} \tag{11.2.1}$$

$$F_{tBMA} = 1 - \frac{H - 0.0992}{0.0306} \tag{11.2.2}$$

The results of the calculations are given in *Table 11.6*.

Tab. 11.6.: Compositions of copolymers of experiment V131 and V132 resulting from ^{1}H–NMR–analysis and elementary analysis

time [min]	F^{NMR}_{tBMA} [a]	$F^{EA,C}_{tBMA}$ [b]	ΔF^{C}_{tBMA} [c]	$F^{EA,H}_{tBMA}$ [d]	ΔF^{H}_{tBMA} [c]
V131	0.37	0.42	0.05	0.26	-0.11
V132	0.51	0.52	0.01	0.35	-0.16

[a] calculated from ^{1}H–NMR–spectra
[b] calculated from *Eq. 8.2.24*
[c] $\Delta F^{x}_{tBMA} = F^{EA,x}_{tBMA} - F^{NMR}_{tBMA}$
[d] calculated from *Eq. 8.2.25*

Both compositions that were calculated from the amount of carbon $F^{EA,C}_{tBMA}$ as well as from the amount of hydrogen $F^{EA,H}_{tBMA}$ differed obviously from the compositions which were determined from the ^{1}H–NMR–spectra of the precipitated copolymers. The differences between the values and the NMR–measurements could not be caused by a solvent like water because the compositions calculated from the hydrogen amount were to low and the ^{1}H–NMR–spectra did not show the presence of residual solvents. Also the presence of monomers in the sample could falsify the measures amount but even they were not monitored in the NMR–spectra in higher rates. An other possible problem could be that the samples were inhomogeneous. For a NMR–measurement 10 mg of the copolymer was used, for an EA–measurement only 2.5 mg. So the problem of an inhomogeneous substance will be increase at the elementary analysis. But the resulting copolymers were apparently consistent. A fourth possibility is that the pollution happened during the measurement itself. The measurement of standards in periodical intervals should avoid that.

Subsequently the two precipitated copolymers of experiments V131 P[$tBMA_{0.37}$–co–$BzMA_{0.63}$] and V132 P[$tBMA_{0.51}$–co–$BzMA_{0.49}$] were investigated with ATR–FTIR–spectroscopy. The same two IR–vibrational bands that were analyzed in the spectra of the statistical copolymers of experiments V81 to V89, see *Section 7.2.2*, and the the gradient copolymer V101, see *Section 8.2.3*, were investigated in view to the peak height and peak area.

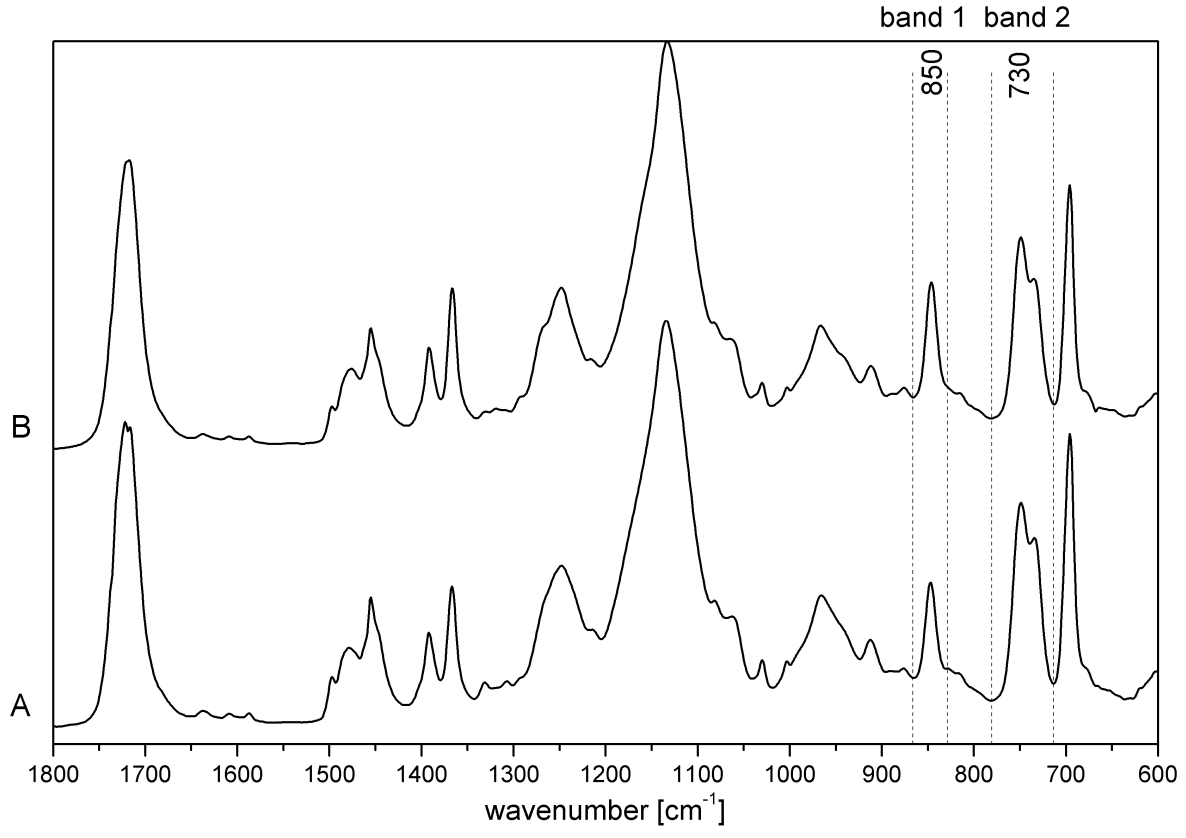

Fig. 11.12.: Finger print region of ATR–FTIR–spectra of (A) experiment V131 P[$tBMA_{0.37}$–co–$BzMA_{0.63}$] and (B) V132 P[$tBMA_{0.51}$–co–$BzMA_{0.49}$] (Spectra normalized to $A_{1134} = 1$)

Band 1 at 850 cm^{-1} is specific for the *tert*–butyl–group, and *band 2* at 730 cm^{-1} is caused by the benzyl–group. In *Figure 11.12* the fingerprint region of the ATR–FTIR–spectra of the two experiments are given.

There was no obvious difference between the two ATR–FTIR–spectra of the two precipitated copolymers of experiment V131 P[$tBMA_{0.37}$–co–$BzMA_{0.63}$] and V132 P[$tBMA_{0.51}$–co–$BzMA_{0.49}$]. In *Figure 11.13* an extended section of the spectra from 700 to 900 cm^{-1} is shown that contained the two analyzed vibrational bands. The values of the analyzed band are summarized in *Table 11.7*.

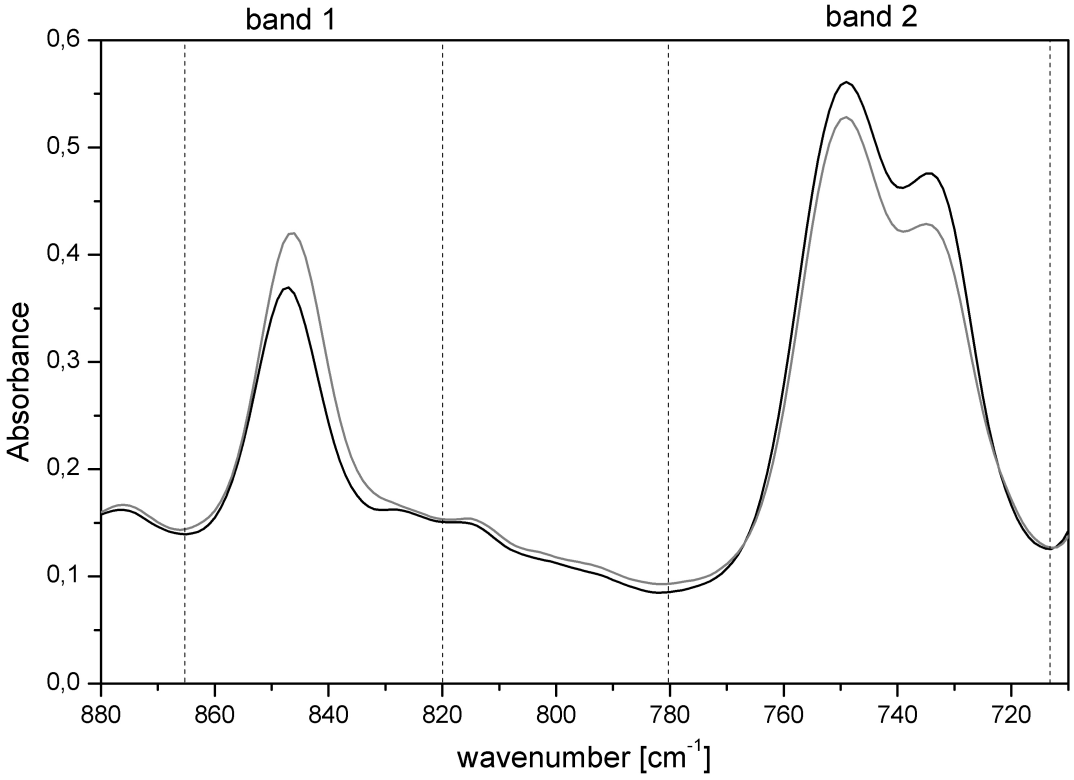

Fig. 11.13.: Section of ATR–FTIR–spectra of experiment V131 P[$tBMA_{0.37}$–co–$BzMA_{0.63}$], black line, and V132 P[$tBMA_{0.51}$–co–$BzMA_{0.49}$], grey line) (Spectra normalized to $A_{1134} = 1$)

Tab. 11.7.: Peak area and peak height of the analyzed ATR–FTIR–bands of experiment V131 and V132

		band 1		*band 2*	
Entry	F_{tBMA}	peak area [cm^{-1}]	peak height	peak area [cm^{-1}]	peak height
V131	0.37	4.91	0.242	13.54	0.457
V132	0.51	5.64	0.289	12.03	0.420

Band 1 at 850 cm^{-1} was higher in the spectra of the sample of experiment V132 $F_{tBMA} = 0.51$ and *band 2* at 730 cm^{-1} was lower. Because *band 1* is the vibrational band of the *tert*–butyl–group and *band 2* the one of the benzyl–group the values of the peak area and the peak height

reflected the results of the calculations of the compositions from the ^{1}H–NMR–spectra of the resulting copolymers which showed a higher amount of tBMA inside the polymer chain of the sample of V132 F_{tBMA} = 0.51 than in the polymer chain of the sample of V131 F_{tBMA} = 0.37.

11.2.3. Molecular Weight Characterization

The obtained copolymers of the semibatch copolymerizations with online IR–measurement were analyzed with size exclusion chromatography. *Figures 11.14* and *11.15* depict the RI– and the 90°–MALS– detector signals of the elution–diagrams of copolymers from experiments V131 P[$tBMA_{0.37}$–co–$BzMA_{0.63}$] and V132 P[$tBMA_{0.51}$–co–$BzMA_{0.49}$].

The RI–detector–signals were bimodal for the samples of both experiments. Hence, there was not the same good control over reactions with the experimental setup of the semibatch copolymerization with online–IR measurements, see *Figure 11.1*, than with the semibatch copolymerization without direct measurements, see *Figure 5.1*. One possible reason for the loss of control could be a slight amount of oxygen during the reaction, because the experimental setup of this reaction was not as tight as the experimental setup for the copolymerizations without online measurements. A second problem was that the copolymer could be precipitated not until three days after the actual synthesis. The reaction mixture was cooled during that days but this is an obvious difference to the procedure of the experiments in *Chapter 7* and *8*.

In a first step, for the investigation of the SEC–data, the signals of the refractive–index detector were analyzed with the calibration curve arising from polystyrene standards, that was used in *Section 3.3.3, Figure 3.15*, in view to the relative molar masses of the copolymers. The values of the maximum elution volume and the calculated relative molar masses of the samples of the two polymers are listed in *Table 11.10*. The elution volumes V_E of the two samples just differed in 0.03 ml. So also the calculated relative molar masses were nearly the same.

The next step was the determination of the differential refractive index increments dn/dc of the resulting copolymer because these values are necessary for the calculation of the absolute molar mass of the polymers from light scattering data. This was done the same way as described with the statistical copolymers of experiment V81 to V89 in THF at 25 °C, cf. *Section 7.2.3*. The measured differential refractive index increments of the copolymers are summarized in *Table 11.8*. The dn/dc–values of the two copolymers resulting from the semibatch copolymerization with online IR–measurement were in the same region than the dn/dc–values of the statistical copolymers in *Section 7.2.3*. Moreover, also these copolymers had a higher dn/dc–values with a higher amount of BzMA inside the polymer chain like the statistical copolymers, see *Table 7.12*.

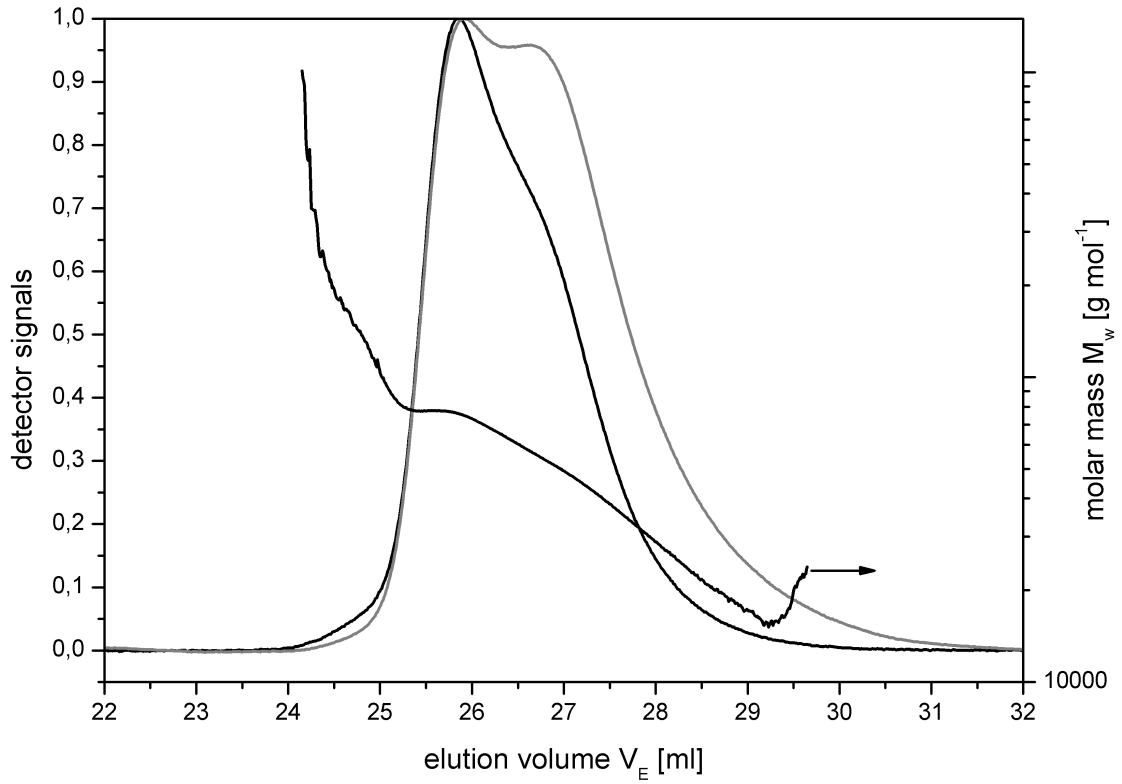

Fig. 11.14.: SEC elution diagrams and molar masses of copolymer V131 P[tBMA$_{0.37}$–co–BzMA$_{0.63}$]; black curve – light scattering signal, grey curve – refractive index signal

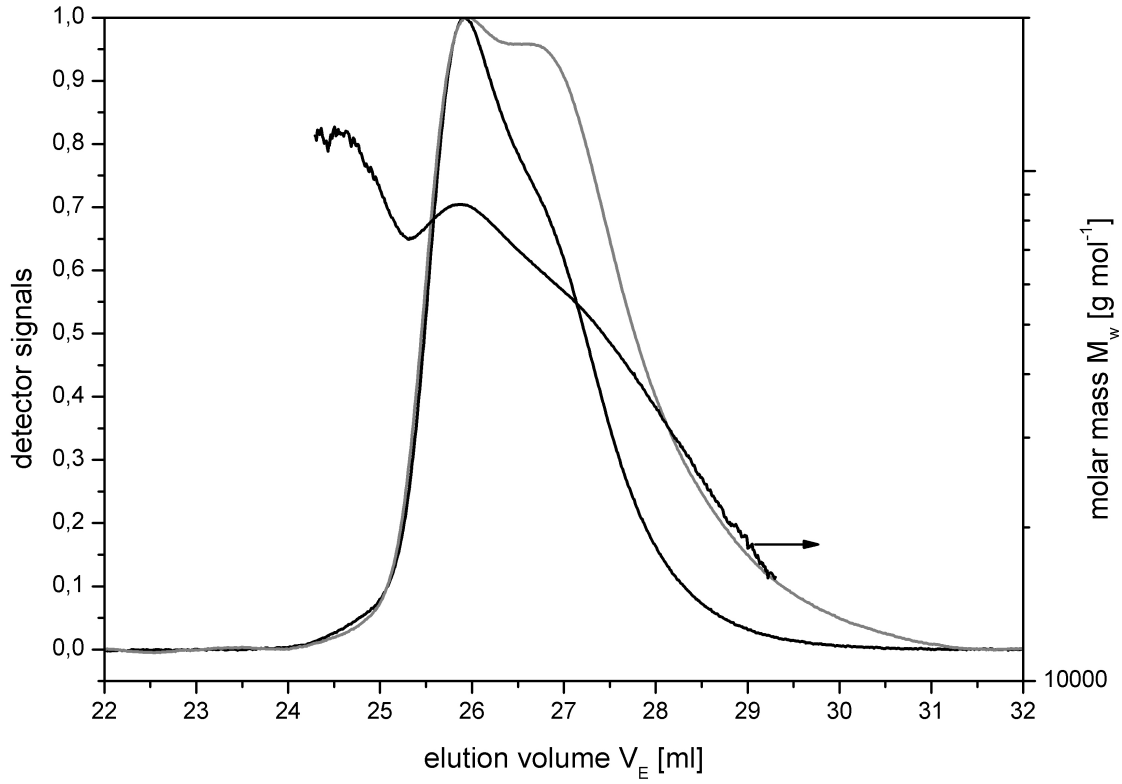

Fig. 11.15.: SEC elution diagrams and molar masses of copolymer V132 P[tBMA$_{0.51}$–co–BzMA$_{0.49}$]; black curve – light scattering signal, grey curve – refractive index signal

Tab. 11.8.: Differential refractive index increment dn/dc of copolymers V131 and V132

Entry	F_{BzMA}	dn/dc $[ml \cdot g^{-1}]$
V131	0.63	0.1177 ± 0.0018
V132	0.49	0.1025 ± 0.0023

From the angle dependence of the scattered light intensity and the known dn/dc–value of the absolute molecular weight of a fraction at a given elution volume can be derived, see *Section 2.4*. The calculated molecular weights are also shown in *Figures 11.14* and *11.15* (right axis). Since the RI–signal is proportional to the weight fraction of the eluted polymer, the complete molecular weight distribution (MWD) of the measured polymer can be obtained and with this the molecular weight averages and the polydispersity indices can be calculated. The obtained values are detailed in *Table 11.9*.

Tab. 11.9.: SEC results of V131 and V132

entry	F_{BzMA}	M_n $[g \cdot mol^{-1}]$	M_w $[g \cdot mol^{-1}]$	M_z $[g \cdot mol^{-1}]$	M_w/M_n	M_z/M_n
V131	0.37	46180 ±462	55450 ±277	64590 ±1292	1.201 ±0.012	1.399 ±0.028
V132	0.51	53240 ±532	62470 ±312	68830 ±688	1.173 ±0.012	1.293 ±0.013

The resulting molar masses of experiments V132 P[$tBMA_{0.51}$–co–$BzMA_{0.49}$] were higher than the ones of V131 P[$tBMA_{0.37}$–co–$BzMA_{0.63}$]. The molar mass of copolymer V132 was higher because of the higher amount of BzMA inside the polymer chain. That the amount of BzMA influenced the resulting molar mass was seen at the statistical copolymers of of *Series F*, see *Table 7.13*. With the increase of BzMA inside the copolymer and with constant reaction time the resulting molar mass also increased. The polydispersities of V132 were lower than the ones of V131. Hence, the control over the reaction V132 was better when the feeding was depended on the conversion of the stock–monomer. The sample of both experiments led to molar masses that were higher than the resulting molar mass of the gradient copolymer V101, cf. *Table 8.12*. The total reaction time of the experiments was equal but the precipitation of the copolymers was done three days of the actual synthesis as told before. So the difference of the synthesis–setup and the cooled storage of the reaction–mixture could influence the results of the SEC–analysis.

Tab. 11.10.: Comparison of relative* and absolute molar masses of of the copolymer of experiment V131 P[$tBMA_{0.37}$–co–$BzMA_{0.63}$] and V132 P[$tBMA_{0.51}$–co–$BzMA_{0.49}$]

entry	F_{tBMA}	V_E [ml]	relative M* $[g \cdot mol^{-1}]$	absolute M $[g \cdot mol^{-1}]$	ΔM $[g \cdot mol^{-1}]$	[%]
V131	0.37	25.92	44862	53330	-1318	2.85
V132	0.51	25.95	44164	46180	-9076	17.09

* calibrated against PS–Standard

The difference between the relative molar masses, calculated from the elution volume V_E and the PS–standard calibration curve differed obviously. The relative molar masses are higher than the absolute molar masses which were calculated from the MALS–detector signals and the dn/dc–values of the copolymers. That is because for the determination of the relative molar mass only the maximum elution volume of the RI–curve is used, that means only one point of the whole measurement. The absolute molar mass is determined from the complete database of the measurement and displays the molecular weight distribution of the whole sample.

11.2.4. Thermal Behavior

The next kind of analysis was the differential scanning calorimetry. Here the thermal behavior of the copolymers was analyzed mainly to determine the dependence of the glass transition temperature T_g on the copolymer composition. The samples of the precipitated copolymers of the two experiments V131 and V132 were analyzed in the same way and the same temperature range as the statistical copolymers of *Series F* (cf. *Section 7.2.4*) and the gradient copolymer V101 (cf. *Section 8.2.5*). The samples of the experiments V131 and V132 were measured with the following temperature program:

- precooling: RT to −50 °C
- standby for 20 min
- 1. heating: −50 to 200 °C
- 1. cooling: 200 to −50 °C
- 2. heating: −50 to 200 °C
- postcooling: 200 °C to RT

In *Figure 11.16* the thermograms of the samples of copolymers V131 (black lines) and V132 (grey lines) are depicted with both heating runs and the cooling run between. Both thermograms looked nearly similar. The first heating runs showed a glass transition overlaid by a relaxation peak between 15 °C and 70 °C. The second heating runs showed a glass transition step nearly in the same range as the peak of the first runs. Only the second heating runs of both samples were analyzed with respect to T_{onset}, T_{offset}, T_g, T_{midpt}, ΔT and Δc_p. [89] The analysis followed the description in *Section 3.3.4*. The complete results of the analysis of the second heating runs from the samples of experiments V131 and V132 are listed in *Table 11.11*.

The thermograms of the second heating runs of the two samples of experiments (A) V131 P[$tBMA_{0.37}$–co–$BzMA_{0.63}$] and (B) V132 P[$tBMA_{0.51}$–co–$BzMA_{0.49}$] are depicted in *Figure 11.17*.

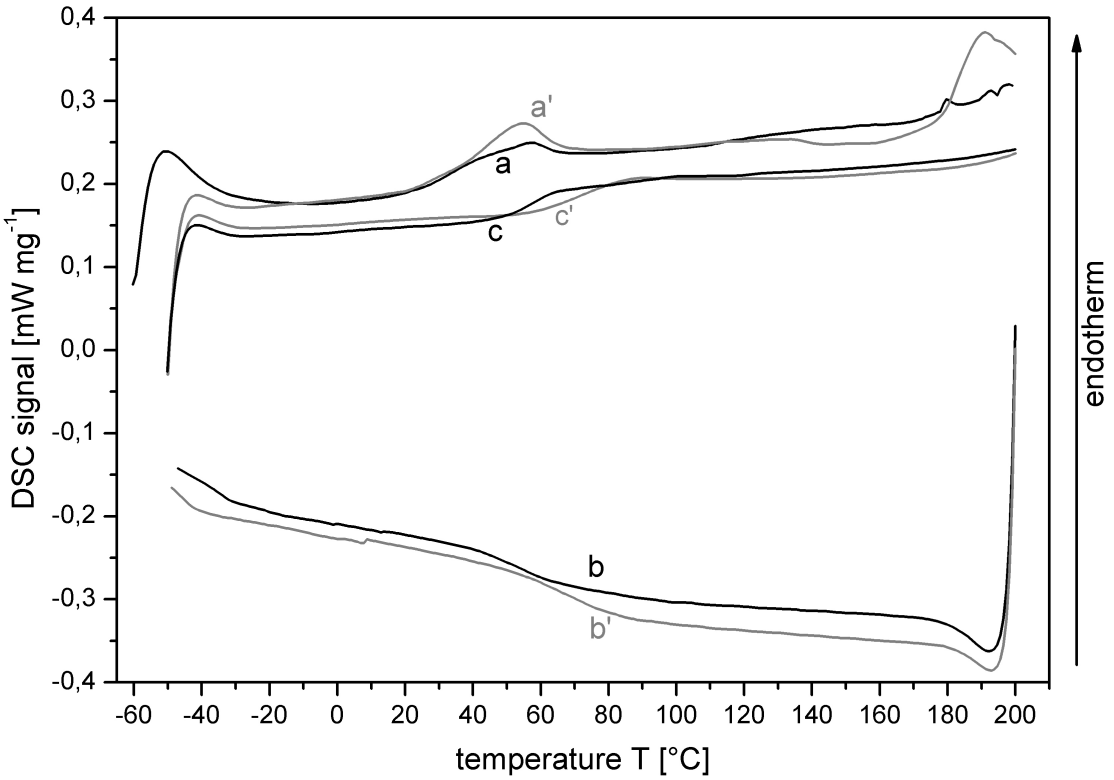

Fig. 11.16.: DSC thermogram of copolymer V131 (P[tBMA$_{0.37}$–co–BzMA$_{0.63}$], black line) and V132 (P[tBMA$_{0.51}$–co–BzMA$_{0.49}$], grey line); a/a' – first heating run, b/b' – first cooling run, c/c' – second heating run; heating rate 10 K · min^{-1}

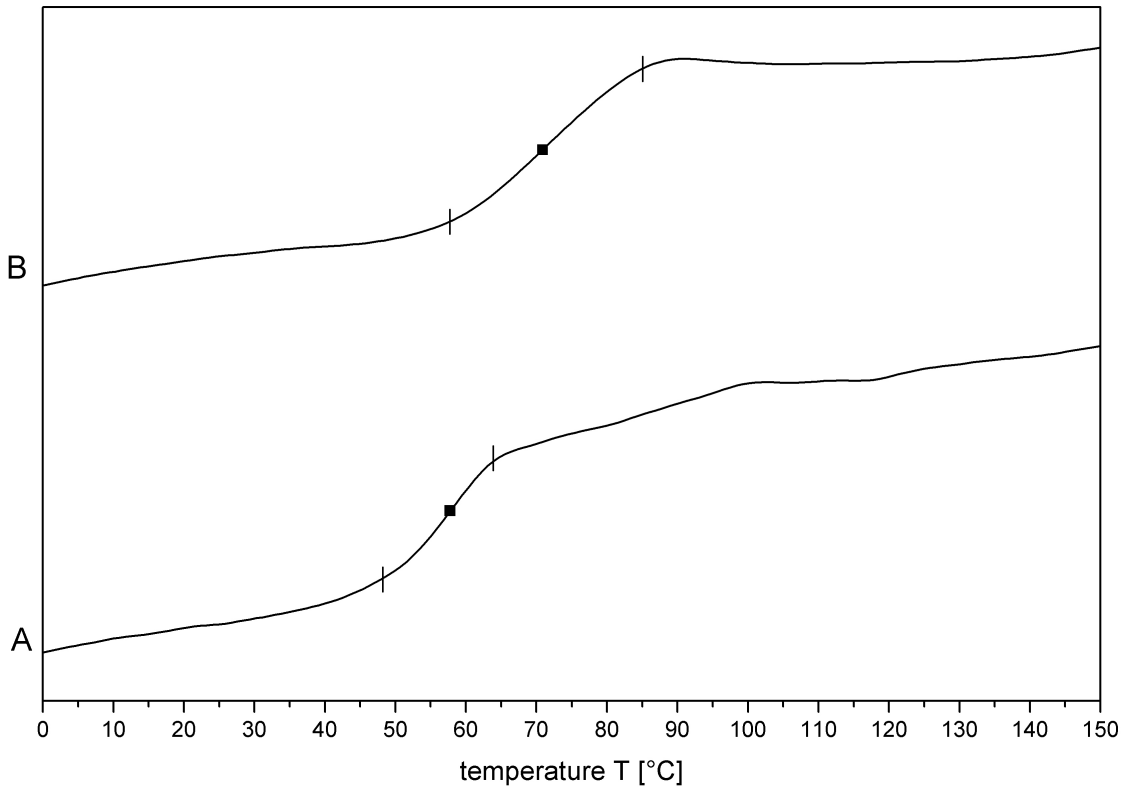

Fig. 11.17.: DSC thermograms of (A) V131 P[tBMA$_{0.37}$–co–BzMA$_{0.63}$] and (B) V132 P[tBMA$_{0.51}$–co–BzMA$_{0.49}$] with marked glass transition temperature range T$_{onset}$, T$_{offset}$ and glass transition temperature T$_g$;second heating runs, heating rate 10 K · min^{-1}

Tab. 11.11.: DSC results of V131 and V132

entry	F_{tBMA}	T_{onset} [℃]	T_{midpt} [℃]	T_g [℃]	T_{offset} [℃]	ΔT [℃]	Δc_p $[J \cdot g^{-1} \cdot K^{-1}]$
V131	0.37	48.5	55.5	57.5	63.5	15.0	0.176
V132	0.51	58.0	72.0	71.0	84.5	26.5	0.259

The limits of the glass transition range ΔT, T_{onset} and T_{offset}, are marked there, as well as the glass transition temperature T_g. There is a clear dependence between the thermal behavior of the sample and the composition of the sample of the copolymer. The sample of copolymer V131 had a lower amount of tBMA inside the polymer chain and so T_{onset} (48.5 ℃) and also the glass transition temperature T_g (57.5 ℃) were lower than the ones of the sample of copolymer V132 (T_{onset} = 58.0 ℃; T_g = 71.0 ℃). Also the glass transition temperature range ΔT was smaller at the sample of copolymer V131. Therefore, composition and structure of the copolymers has an influence on the thermal behavior of them.

For statistical copolymers the glass transition temperature can be described fairly with the *Fox–Equation* (cf. *Section 7.2.4*). But there was a difference of 10 ℃ between the calculated and measured values. So the *Fox–Equation* was just an approximation. However, this analysis was also applied to the copolymers resulting from the semibatch polymerization with online IR–measurements V131 and V132, using *Equation 11.2.3*. The results of the calculations are listed in *Table 11.12*.

$$\frac{1}{T_g} = \frac{F_{tBMA}}{T_{g,tBMA}} + \frac{F_{BzMA}}{T_{g,BzMA}} \tag{11.2.3}$$

with $T_{g,tBMA}$ = 107 ℃ [90] and $T_{g,nBMA}$ = 47 ℃ [113]

Tab. 11.12.: Theoretical and measured glass transition temperature of experiments V131 and V132

entry	F_{tBMA}	F_{nBMA} [a]	$T_g(Fox)$ [b] [℃]	T_g(DSC) [c] [℃]	ΔT_g [d] [℃]
V131	0.37	0.63	59.3	57.5	−1.8
V132	0.51	0.49	65.8	71.0	5.2

[a] $F_{BzMA} = 1 - F_{tBMA}$; [b] calculated with *Eq. 8.2.28*
[c] measured with DSC; [d] $\Delta T_g = T_g(DSC) - T_g(Fox)$

The differences between the glass transition temperature which were measured by DSC and the ones calculated with *Equation 11.2.3* were not as high as they was for the statistical copolymers (cf. *Table 7.17*) and also for the gradient copolymer which was synthesized without online measurements (cf. *Table 8.15*). So here the *Fox–Equation* fits good to the resulting copolymers.

11.3. Results and Discussion of the Hydrolysis

This section describes the observations on the hydrolysis reaction performed with the two copolymer V131 and V132. Also the results of the analysis of the hydrolysis products are given. The products were compared with the educts. Further the differences between the two hydrolyzed copolymer were investigated. The product of the hydrolysis of copolymer V131 was numbered V141 and the product of the hydrolysis of copolymer V132 respectively V142.

The amount of added MSA depends on the amount of tBMA inside the polymer chain. It was calculated with *Equation 11.3.1* for both copolymers with benzyl methacrylate and *tert*–butyl methacrylate.

$$V_{MSA} = \frac{m \cdot F_{tBMA} \cdot x \cdot M_{MSA}}{M_{tBMA} \cdot \delta_{MSA}} \tag{11.3.1}$$

with V_{MSA} – Volume of the methanesulfonic acid, m – mass of the polymer, F_{tBMA} – ratio of tBMA in the polymer chain, x – multiplicity factor for the hydrolysis reagent, M_{tBMA} – molar mass of tBMA = $142.2\,g \cdot mol^{-1}$, M_{MSA} – molar mass of the methanesulfonic acid = $96.11\,g \cdot mol^{-1}$ and δ_{MSA} – density of the methanesulfonic acid = $1.48\,g \cdot ml^{-1}$

Also the theoretical yields depend on the copolymer composition F_{tBMA}. They were calculated in the same way as in *Section 4.2* with *Equation 11.3.2*.

$$y_{theo} = \frac{m \cdot F_{tBMA} \cdot M_{MAA}}{M_{tBMA}} + m \cdot (1 - F_{tBMA}) \tag{11.3.2}$$

with y_{theo} – theoretical yield, m – mass of the polymer, F_{tBMA} – ratio of tBMA in the polymer, M_{MAA} – molar mass of MAA = $86.09\,g \cdot mol^{-1}$, M_{tBMA} – molar mass of tBMA = $142.2\,g \cdot mol^{-1}$

The results of the two calculations, the needed volumes of methanesulfonic acid and the theoretical yields, as well as the resulting and percentage yields of the two hydrolysis reactions are listed in *Table 11.13*.

Tab. 11.13.: Amount of added MSA and yields of hydrolysis products of V141 and V142

Educt	F_{tBMA}	V_{MSA}	yield		
			theoretical	actual	
		[ml]	[g]	[g]	[%]
V141	0.37	0.07	0.17	0.10	60.48
V142	0.51	0.09	0.16	0.11	70.33

The reactions proceeded in the same way than the model synthesis in *Section 4.2*. Some minutes after the addition of MSA the mixture of both experiments became a light brown gel. During the second hour the gels liquefied again. The added sodium hydrogen carbonate

neutralized the excess of acid after the reaction time. The byproduct of the neutralization is a salt and because of this after the precipitation in pentane a second precipitation in water/ methanol was done. However, the second precipitations was not only necessary to remove the formed salt. After the first precipitations from *n*–pentane the hydrolysis products were brown light powder, hence a second purification step was needed. After the purification steps the resulting copolymers were obtained in form of white powders. The yield of experiment V142 was with 70.33 % better than the yield of experiment V141 with 60.48 %.

The solubility–properties of these hydrolysis products were same as before of the P[nBMA–co–MAA], see *Table 4.3*. So the hydrolyzed copolymers V141 and V142 were dissolved in DMSO-d6 for ^{1}H–NMR–spectroscopy as well. The resulting ^{1}H–NMR–spectra of the two hydrolysis products (B) are represented in *Figure 11.19* together with the corresponding ^{1}H–NMR–spectra of the educts (A). The molecular structures of the educts and the carbons with the numbering of the protons are shown in *Figure 11.18*.

The changes between the spectra of the educts and the products were distinct and for both hydrolysis the changes were the same. The intensity of the mixed broad peak ranging from 1.25 to 1.55 ppm caused by the signals of the proton 3' shrank relative to the signals 6' from 4.8 to 5.1 ppm, which remained constant. The reason was the absence of the signal 3' from the protons of the *tert*–butyl group in the products. In the spectra of the hydrolysis products the broad –COOH–signal could be monitored between 12.0 to 12.75 ppm. In the ^{1}H–NMR–spectra of the products additionally a H_2O signal was present because the DMSO–d_6 was not dry. That the signal of the *tert*–butyl–group disappeared nearly completely indicated a total conversion of both educts.

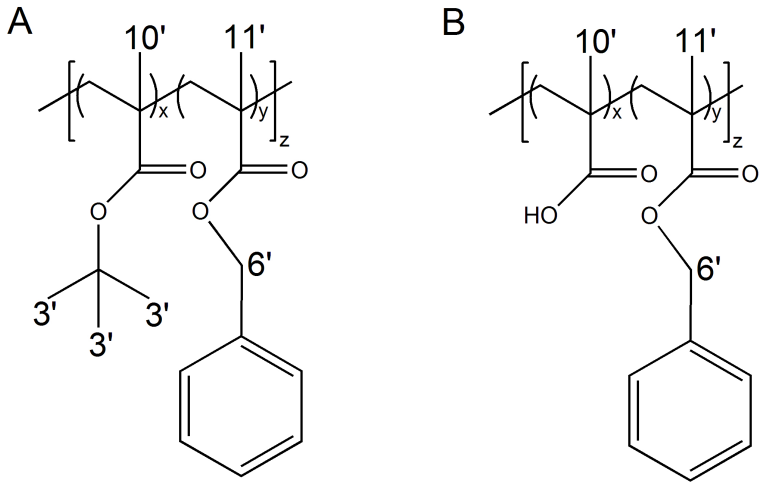

Fig. 11.18.: Molecular structures of educt V131 resp. V132 and product V141 resp. V142 with carbon–atom labels; A – educt P[tBMA$_x$–co–BzMA$_y$] and B – product P[MAA$_x$–co–BzMA$_y$]; (z = x + y = 1)

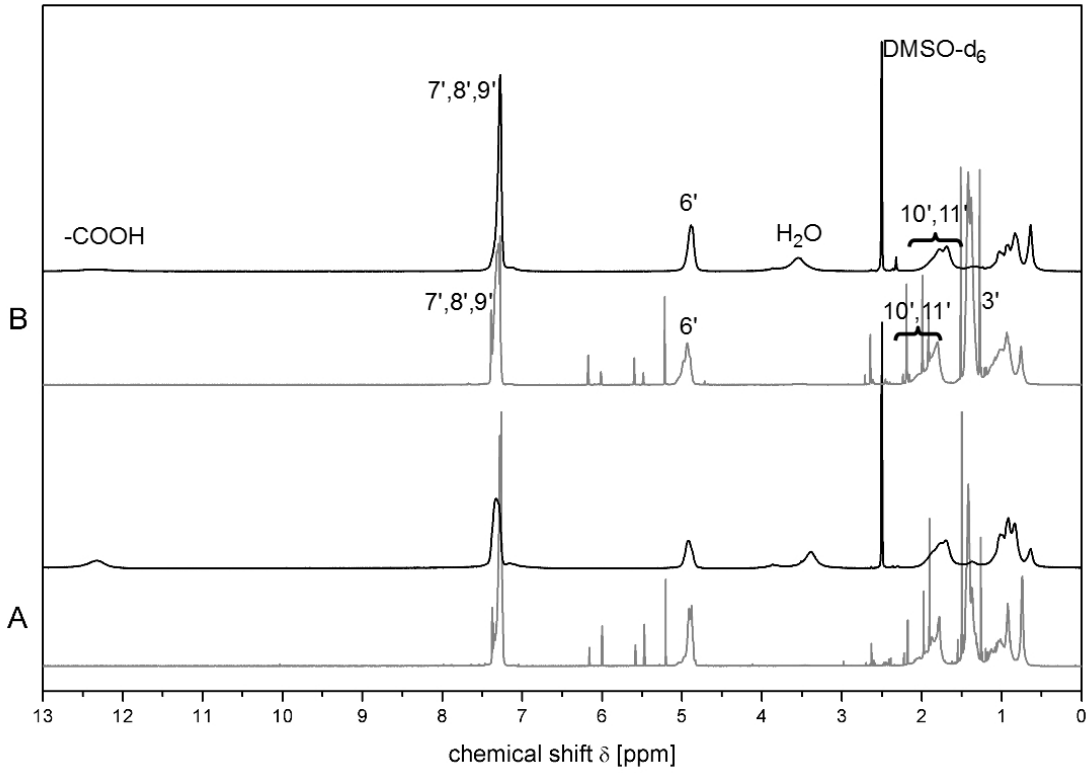

Fig. 11.19.: Comparison of ^{1}H–NMR–spectra of educts V131 resp. V132 and products V141 resp. V142 (grey line – educt, black line – product); A – V131/V141 = F_{BzMA} = 0.63, B – V132/V142 = F_{BzMA} = 0.49

The ^{1}H–NMR–analysis was followed by the investigation of the hydrolyzed gradient copolymers by elementary analysis and ATR–FTIR–spectroscopy. The results of the elementary analyzes are listed in *Table 11.14*. The theoretical values were calculated for 100 % conversion of the hydrolysis of the educts.

Tab. 11.14.: Results of the elementary analysis of the experiments V141 and V142

entry	F_{BzMA}		C [%]	ΔC	H [%]	ΔH	O [%]	ΔO
V131	0.63	theory	72.60		7.85		19.56	
		is	71.84	-0.76	7.67	-0.18	20.49	0.94
V141		theory	70.70		6.90		25.68	
		is	67.55	-3.15	6.78	-0.13	25.67	0.81
V132	0.49	theory	71.60		8.26		20.14	
		is	71.12	-0.48	7.93	-0.33	20.95	0.81
V142		theory	68.52		6.92		24.57	
		is	66.44	-2.08	7.23	0.31	26.33	1.76

The results for the two products were slightly different. Both samples of the hydrolyzed copolymers had a lack of carbon and an excess of oxygen. The sample of experiment V141 had small lack of hydrogen and the sample of V142 a small excess. But in both cases the differences were justifiable. The results of the elementary analysis showed that the resulting

copolymers were clean and dry.

In a next step from the amount of carbon and hydrogen that were measured by the elementary analysis the compositions of the copolymers was calculated like it was done for the educts. For the calculations different calibration curves were needed with the amounts of carbon and hydrogen of homopolymers PMAA and PBzMA as basis. These calibration curves are depicted in *Figure 9.4* and the resulting linear equations are given in *Equations 11.3.3* and *11.3.4*.

$$C = 0.7498 - 0.1917 \cdot F_{MAA} \tag{11.3.3}$$

$$H = 0.0686 + 0.0017 \cdot F_{MAA} \tag{11.3.4}$$

The equations were recalculated to the composition and with the amounts of carbon, respectively hydrogen, taken from elementary analysis the compositions were calculated. The results are listed in *Table 11.15*.

Tab. 11.15.: Compositions of copolymers of experiment V141 and V142 resulting from ^{1}H–NMR–analysis and elementary analysis

entry	$F^{NMR}_{MAA}{}^{a}$	$F^{EA,C}_{MAA}{}^{b}$	$\Delta F^{C}_{MAA}{}^{c}$	$F^{EA,H}_{MAA}{}^{d}$	$\Delta F^{H}_{MAA}{}^{c}$
V141	0.37	0.39	0.02	−0.50	0.16
V142	0.51	0.45	−0.06	2.17	1.66

[a] calculated from ^{1}H–NMR–spectra; [b] calculated from *Eq. 9.2.3*
[c] $\Delta F^{x}_{MAA} = F^{EA,x}_{MAA} - F^{NMR}_{MAA}$; [d] calculated from *Eq. 9.2.4*

The compositions $F^{EA,H}_{tBMA}$ calculated by elementary analysis differed obviously from the compositions which were determined from the ^{1}H–NMR–spectra of the precipitated copolymers for hydrogen. However, the compositions $F^{EA,C}_{tBMA}$ calculated from the amount of carbon fitted well with the compositions determined from the ^{1}H–NMR–spectra. The differences could be caused by various problems. But the ^{1}H–NMR–spectra did not show the presence of residual solvents, hence, that was not the reason for the deviations. Also the presence of monomers in the sample could falsify the measured amounts but even they were not monitored in the ^{1}H–NMR–spectra. Another possible problem could be that the samples were inhomogeneous. For a NMR–measurement 10 mg of the copolymer was used, for an EA–measurement only 2.5 mg. So the problem of an inhomogeneous substance will be increase at the elementary analysis. But the resulting copolymers were apparently consistent. A fourth possibility is that the pollution happened during the measurement itself. The measurement of standards in periodical intervals should avoid that.

The second part of the structure analysis was the ATR–FTIR–spectroscopy. The resulting spectra of the hydrolyzed copolymers (black lines) are depicted in *Figure 11.20* together with the educts (grey lines). In both spectra the vibrational bands that were analyzed before are

marked to show the differences between the educts and the products.

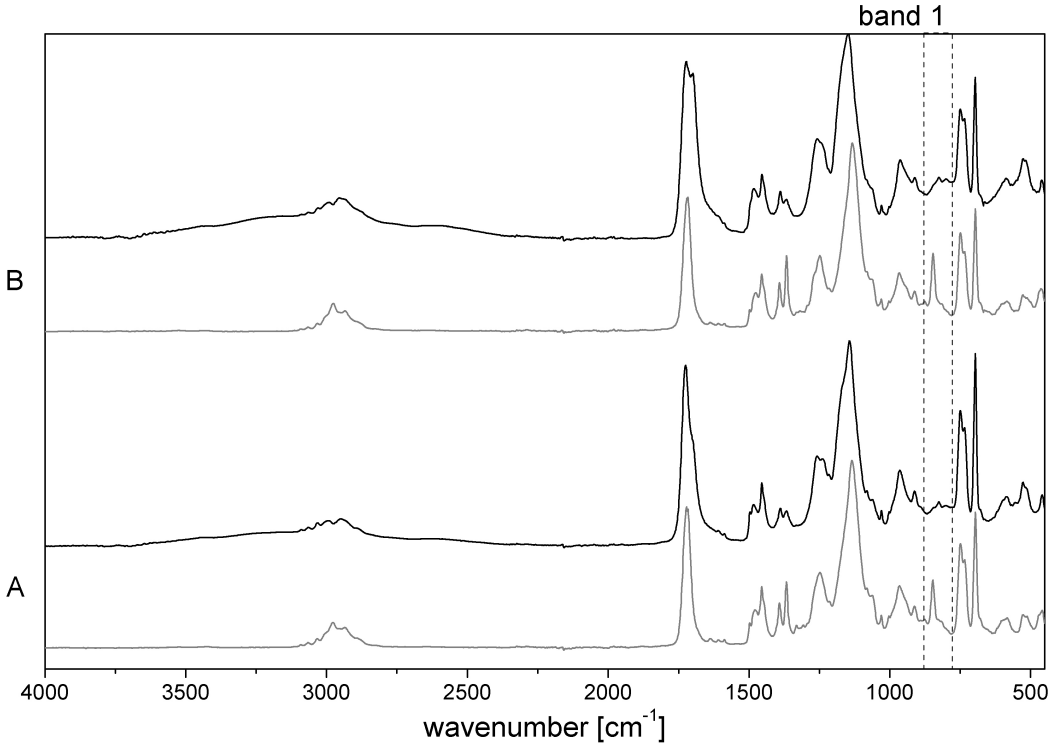

Fig. 11.20.: Comparison of ATR–FTIR–spectra of educts V131 resp. V132 and products V141 resp. V142 (grey line – educt, black line – product); A – V131/V141=F_{BzMA} = 0.63, B – V132/V142=F_{BzMA} = 0.49 (Spectra normalized to A_{1134} = 1)

In *section 7.2.2* two bands at 850 cm^{-1} and 730 cm^{-1} were introduced that are characteristic for polymer-incorporated tBMA and BzMA units, respectively. *Band 2* at 730 cm^{-1} for BzMA did not change so much but *band 1* at 850 cm^{-1} for tBMA differed obviously. The changes of *band 1* were so strong and influenced also *band 2* that the analysis of peak height and peak area of both bands was not possible anymore. The loss of band intensity at 850 cm^{-1} clearly indicates that the hydrolysis products no longer contained tBMA–ester side groups. Also the bands at 1370 cm^{-1} and 1390 cm^{-1} shrank with the hydrolysis. A third change exhibited the band at 1710 cm^{-1} which is the vibrational bands of ester–C=O–group. In the IR–spectrum of the educts the band was a small singlet. The product–spectra instead had a broader doublet at that region. The double band exhibited maxima at 1720 cm^{-1} and 1700 cm^{-1}. The literature refers 1720 cm^{-1} to ester–C=O vibration, while 1700 cm^{-1} belong to the vibrations of carboxylic acid–C=O groups. [87] Further the range $\tilde{\nu} > 3000\,cm^{-1}$ changed from educt to product in both cases. A broad band ranging from 2350 to 3700 cm^{-1} appeared which could be assigned to the vibrational band of the carboxylic acid OH–group. All in all the changes in the ATR–FTIR–spectra from the educts to the products and the differences of the products among themselves showed that the hydrolysis reactions worked well. The changes were the same as for the gradient copolymer resulting from the hydrolyzed copolymers in *Chapter 9*.

The next analysis was the size exclusion chromatography (SEC). As with the hydrolyzed

statistical copolymers also the products of V141 and V142 were not soluble in THF. As described in *Section 4.2* about 0.4 mg of the copolymer was mixed with 1 ml THF and two drops of TMSI and the mixture was stirred over night at RT. The copolymer became THF–soluble, because the carboxyl groups were converted into non–polar trimethylsilyl–esters. Since the presence of non–covalent fixed TMSI disturbed the dn/dc determination, only the relative molar mass of the copolymers were calculated from the maximum elution volume of the samples and *Equation 3.3.22* which based on a a polystyrene–calibration ("PS–Standard–values"). The resulting elution diagrams of the RI–detector signals are depicted in *Figure 11.21* and the calculated relative molar masses are listed in *Table 11.16*.

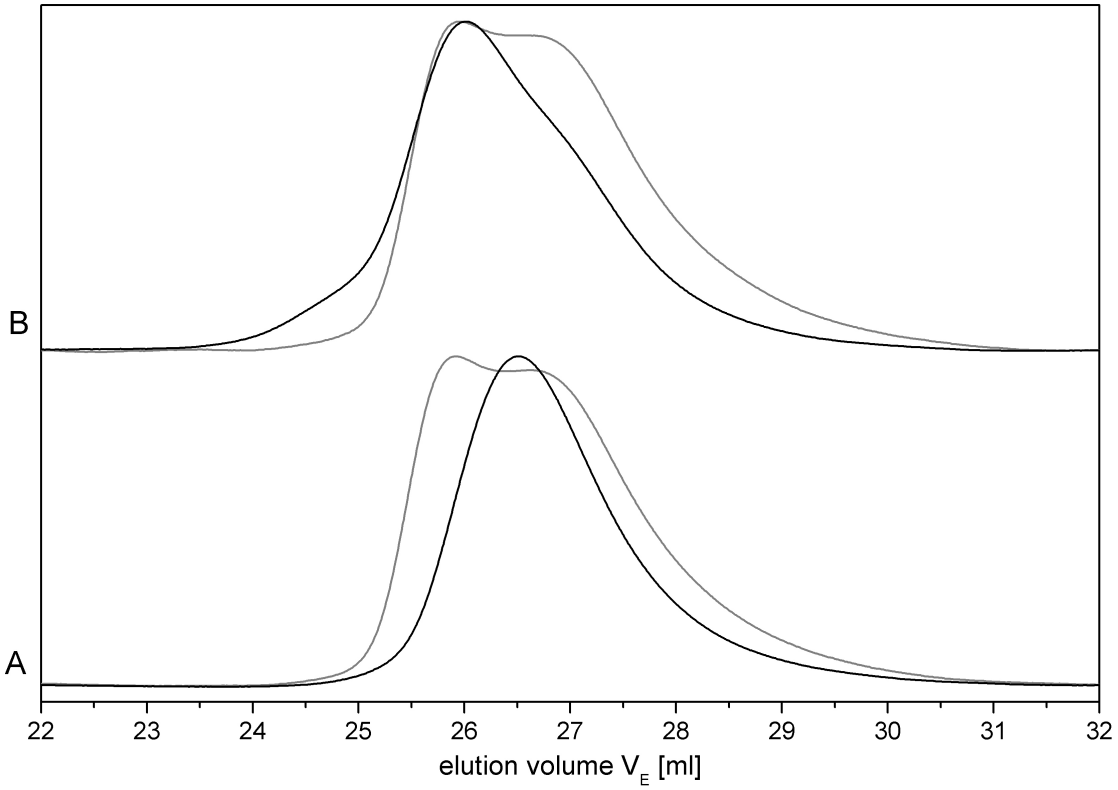

Fig. 11.21.: Comparison of SEC elution diagrams of educts V131 resp. V132 and products V141 resp. V142 (grey line – educt, black line – product); A – V131/V141 = F_{BzMA} = 0.63, B – V132/V142 = F_{BzMA} = 0.49

Tab. 11.16.: SEC results of products of educts V131/V132 and products V141/V142

Entry	F_{BzMA}	V_E[a] [ml]	M [b] [g · mol^{-1}]	ΔM [g · mol^{-1}]	[%]
V131	0.63	25.92	44862		
V141		26.52	33010	11852	26.42
V132	0.49	25.95	44164		
V142		26.01	42815	1349	3.05

[a] Peak elution volume

[b] relative values, based on PSS calibration *Eq. 3.3.22*

The shape of the RI–detector signals changed from the samples of the educts to the products. The one of the product–signals were not so distinctly bimodal as the one of the educt–signals. For the sample of experiment V141 the peak maximum of the RI–signal shifted to lower molar masses and the shape of the peak became smaller. For the sample of experiment V142 the peak maximum did not shifted obviously but the shape of the educt–signal was much smaller then the shape of the product–signal. That the peak maxima of the product–RI–signals did not shifted obviously explained the results of the calculations of the relative molar mass. The molar mass of the sample V141 was obviously smaller than the relative molar mass of the product sample of copolymer V131. Because for the calculation of the relative molar mass only the peak maximum was used there was no difference between the relative molar mass of the sample of the educt V132 and the product V142. The changes of the RI–signal–shapes were caused by the loss of molar mass from the replacement of the *tert*–butyl–group ($58.12\,\mathrm{g \cdot mol^{-1}}$) to the OH–group ($17.01\,\mathrm{g \cdot mol^{-1}}$).

The investigation of the thermal behavior was the next part of analysis. The samples of the experiments V141 and V142 were heated up two times from −80 to 200 °C with a cooling run in between (dT/dt = 10 K/min). The samples were not measured up to 300 °C because from *Section 4.2* it was known that the hydrolyzed polymer–samples will decomposed. In *Figure 11.22* the two heating runs and the cooling run of both experiments V141 and V142 are represented.

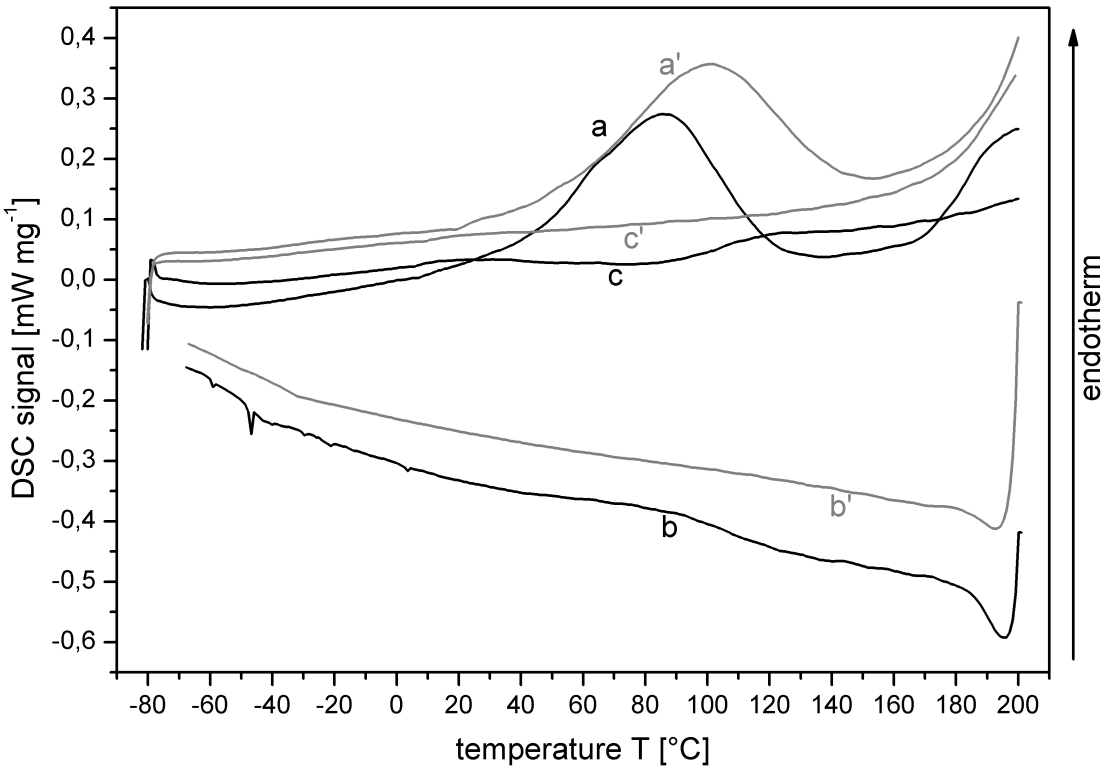

Fig. 11.22.: DSC thermogram of copolymer V141 (P[$MAA_{0.37}$–co–$BzMA_{0.63}$], black line) and V142 (P[$MAA_{0.51}$–co–$BzMA_{0.49}$], grey line); a/a' – first heating run, b/b' – first cooling run, c/c' – second heating run; heating rate 10 $\mathrm{K \cdot min^{-1}}$

Both thermograms of the first heating run exhibited an endothermic peak in the temperature range from 45 to 115 °C for the sample of experiment V141 and in the range from 60 to 135 °C for the sample of experiment V142. Then the DSC–signal increased. The second heating run and the cooling run did not show peaks or glass transition steps. The shape of the curves was the same as at the hydrolysis in *Section 4.2*. So also the hydrolyzed copolymers decomposed during the first heating run. The shape of the endothermic peak and the composition of the copolymer, the peak area and peak height were determined. The results are listed in *Table 11.17*.

Tab. 11.17.: DSC results of hydrolysis–products of copolymers from experiment V141 and V142

Entry	F_{MAA}	Area $[J \cdot g^{-1}]$	T_{Peak} [°C]	T_{onset} [°C]	T_{offset} [°C]	Width [°C]	Height $[mW \cdot mg^{-1}]$
V141	0.37	79.7	85.8	46.6	114.9	58.9	0.2503
V142	0.51	77.8	100.1	62.0	136.9	65.4	0.2234

The peak area and the peak height of copolymer V141 with $F_{MAA} = 0.37$ are higher than the peak area and the peak height of copolymer V142 with $F_{MAA} = 0.51$. The higher amount of MAA inside the polymer chain gave lower values. So the composition of the copolymer influences the thermal behavior.

11.4. Summary

The syntheses of the two copolymers tBMA/BzMA by means of an online ATR–FTIR–spectroscopy measurement controlled automatic process did not yield in evaluable results, because it was not known how many feed–solution was injected at a certain polymerization time. A second problem was that the whole experimental setup was not tight against oxygen. So a partial inhibition of the system during the polymerizations was possible. The resulting IR–spectra showed specific bands for the *tert*–butyl–group and the benzyl group. But it was not possible to distinguish between signals of monomer and polymer, therewith the conversion and the composition of the copolymers during the copolymerizations could not be determined.

However, the resulting precipitated copolymers were analyzed in the same way as the statistical and the gradient copolymers with tBMA and BzMA before. From the integrals of the ^{1}H–NMR–spectra of the resulting products the cumulative compositions of the copolymers were calculated. The copolymer–compositions of experiment V131 is P[$tBMA_{0.37}$–co–$BzMA_{0.63}$] and of V132 P[$tBMA_{0.51}$–co–$BzMA_{0.49}$]. The different kinds of injection methods led to copolymers with a different composition. The continuous linear injection of tBMA during experiment V131 resulted in a copolymer with one third tBMA and two thirds BzMA inside the polymer chain. The IR–controlled injection resulted in a copolymer with 50 % tBMA and 50 % BzMA what was the intended over–all composition. The elementary anal-

ysis of samples of the two copolymers gave only small differences between the theoretical amount of carbon, hydrogen and oxygen to the measured values. So both samples were free of pollution. The values also fit to the data resulting from the analyzes of the statistical and gradient copolymers with tBMA and BzMA. The calculations of the composition of the copolymers from the amount of carbon and hydrogen leaded to results that differed strongly from the compositions which were calculated from the integrals of the ^{1}H–NMR–spectra. The ATR–FTIR–spectra of the two resulting copolymers differed at the investigated vibrational bands at 850 cm^{-1} and 730 cm^{-1} accordingly to the differences of the compositions found by the analysis of the ^{1}H–NMR–spectra. The SEC–analyzes gave bimodal elution diagrams for the samples of both copolymers, that indicated that the control of the polymerizations was lost in both experiments. The DSC–measurements showed the influence of the composition on the thermal behavior. Copolymer V131 has a lower amount of tBMA and so a lower T_{onset} and T_g. The glass transition temperature range ΔT was higher at the sample of copolymer V132. The calculation of the glass transition temperatures by the *Fox–Equation* gave nearly the same values than the measured ones.

The *tert*–butyl groups of the two copolymers resulting from the copolymerizations of BzMA and tBMA with online IR–measurement were hydrolytically cleaved by means of methanesulfonic acid (MSA). The characterization of the hydrolyzed copolymers with ^{1}H–NMR–spectroscopy and elementary analysis showed the absence of *tert*–butyl–groups in the polymer chains, and hence, a total conversion of the hydrolysis. The elementary analysis results agreed decently to the structure of both experiments. A calculation of the monomer molar fraction from the measured contents of carbon or hydrogen leads to values which obviously differed from the compositions resulting from the ^{1}H–NMR–analysis. The changes in the ATR–FTIR–spectra supported the good results of the ^{1}H–NMR–spectroscopy. The vibrational band of the OH-group occurred and the fingerprint–region change in case of the vibrational bands from the *tert*–butyl–group. The changes were so vigorous that an analysis of the vibrational band of BzMA was not possible. The shape of the RI–detector signals changed from educt to product for the samples of both experiments but the maximum elution volumes of both samples did not shifted obviously. So a change of the relative molar mass could not be calculated for both copolymers. The DSC analysis showed broad endothermic peaks for both copolymers in the same region and the samples did not regenerate after the first heating run. That was the same behavior observed for the statistical and the gradient copolymers that contained tBMA and BzMA. The peak height and the peak area of the endothermic peak was different for the samples of the two copolymers. Both hydrolysis of the resulting copolymers worked well and two amphiphilic copolymers with different composition have successfully be obtained.

12. Summary

The purpose of this work was the synthesis of functional amphiphilic gradient copolymers by means of controlled radical polymerizations, more precisely Atom Transfer Radical Polymerization. Two different monomer combinations, *tert*– and *n*–butyl methacrylate and *tert*–butyl and benzyl methacrylate, were copolymerized.

In a first step seven different linear statistical copolymers were synthesized by means of batch polymerization. They were used as comparative material and the analysis of the reaction kinetic yielded the effective rate constants and the copolymerization parameters of the monomers in the particular monomer systems. Furthermore required for gradient polymer syntheses di–block copolymers were synthesized as a second kind of comparative material.

With the results of the kinetic analysis the monomer addition programs for the semibatch polymerizations were calculated to prepare gradient copolymers. Four different gradient copolymers with different compositions of tBMA and nBMA (f_{tBMA} = 0.5, 0.65, 0.75, 0.85) and one gradient copolymer of tBMA and BzMA (f_{tBMA} = 0.5) were synthesized. All semibatch reactions proceeded controlled, i. e. with mostly suppressed termination reactions. The compositions of the resulting copolymers exhibited "double–gradients". The point of change of the compositions were located at 16 %, respectively 11 % of conversion. The effective compositional gradients $\phi = dF_1/dp$ were ϕ = 0.53, 0.46, 0.28, 0.15 and 0.43. A systematic correlation between the thermal behavior of the gradient copolymers and their composition was not found, as opposed to the statistical and the di–block copolymers.

Semibatch synthesis with online infrared–spectroscopy observation to control the monomer feed during the synthesis were used for the polymerization of gradient copolymers. It was not possible to calculate the change of compositions of the polymers because it was not known how much monomer was injected at a certain time of the polymerization. A second problem was that the experimental set–up was not gas–tight. Hence, oxygen led to termination reactions.

Three different kinds of hydrolysis were investigated for the cleavage of the *tert*–butyl groups on the polymer chains. The obtained gradient copolymers were hydrolyzed with methanesulfonic acid to obtain the intended amphiphilic polymer chains. All reactions proceeded with quantitative conversion. Hence, functional amphiphilic copolymers were obtained.

13. Zusammenfassung

Das Ziel der vorliegenden Arbeit war die Synthese von funktionellen amphiphilen Gradienten Copolymeren mittels kontrollierter radikalischer Polymerisation, genauer durch Atom Transfer Radical Polymerization. Zwei verschiedene Monomer–Mischungen wurden untersucht: *tert*– und *n*–Butylmethacrylate und *tert*–Butyl und Benzylmethacrylate.

Im ersten Schritt wurden lineare, statistische Copolymere im Batchverfahren synthetisiert. Zum einen dienten sie als Vergleichsmaterial zu den Gradientencopolymeren und zum zweiten lieferte die Analyse der Reaktionskinetik die effektiven Geschwindigkeitskonstanten und die Copolymerisations–Parameter der Monomere der beiden vorliegenden Monomersysteme (tBMA/nBMA und tBMA/BzMA). Als zweites Vergleichsmaterial wurden Block Copolymere aus den Monomeren hergestellt.

Die Daten aus den Analysen der Batchsynthesen wurden für die Ermittlung der Zudosierungs–Programme für die Semibatchsynthesen der Gradienten Copolymere verwendet. Vier Gradienten Copolymere mit verschiedenen Zusammensetzungen aus tBMA und nBMA ($f_{tBMA} = 0.5$, 0.65, 0.75, 0.85) und ein Gradienten Copolymer aus tBMA und BzMA ($f_{tBMA} = 0.5$) wurden synthetisiert. Alle Semibatchsynthesen verliefen kontrolliert, d. h. unter weitgehender Unterdrückung von Abbruchreaktionen. Die resultierenden Copolymere wiesen alle einen "Doppel–Gradienten" in ihrer Zusammensetzung auf. Die effektive Gradient der Zusammensetzung betrug $\phi = dF_1/dp = 0.53$, 0.46, 0.28, 0.15 und 0.43. Einen systematischen Zusammenhang zwischen dem thermischen Verhalten der Gradienten Copolymere und ihrer Zusammensetzung konnte nicht gefunden werden, anders als bei den statistisch und den Block Copolymere.

Semibatchsynthesen unter kontienuierlicher IR–Messung während der Synthese wurden zur Polymerisation von Gradienten Copolymeren durchgeführt . Es war allerdings nicht möglich die Menge an zudosiertem Monomer zu einem bestimmten Zeitpunkt zu bestimmen, wodurch die Veränderungen in der Zusammensetzung des Polymers nicht ermittelt werden konnten. Des weiteren war die Versuchsapparatur nicht vollständig gasdicht. Der eintretende Sauerstoff führte zu Abbruchreaktionen.

Die erhaltenen Copolymere wurden mittels Methansulfonsäure hydrolysiert um den angestrebten amphiphilen Charakter der Polymerketten zu erhalten. Die Reaktionen liefen alle unter vollständigem Umsatz ab, es wurden saubere, funktionelle amphiphile Copolymere synthetisiert.

A. Feeding–Program of experiment V31

Input

System

```
001   '- Comonomer System Definition File -'
002   't-BuMA / n-BMA, p-TosCl:PMDETA:CuCl, MEK, 80 GrdC'
003   ' '
004   '—- Molar Masses and Densities —-'
005   'MM1 = ', 1.4220d02
006   'rh1 = ', 0.8750d00
007   'MM2 = ', 1.4220d02
008   'rh2 = ', 0.8960d00
009   'MMI = ', 3.6317d02
010   'rhI = ', 0.9950d00
011   'MMS = ', 7.2060d01
012   'rhS = ', 0.8050d00
013   ' '
014   '—- Copolymerisation Parameter —-'
015   'r1 = ', 0.8860d00
016   'r2 = ', 0.4720d00
017   ' '
018   '—- Kinetic Parameter ————-'
019   'nk = ', 2
020   'kf0 = ', 1.0000d00
021   'kf1 = ', 1.4375d-1
022   'kf2 = ', 0.0000d00
023   '————————————————————'
024   EOF
025   'ONLY EDIT 2. line and r1, r2, n, kfi'
```

Dosage

```
001   '— Comonomer Dosage Definition File -'
002   ' g(p) = const. '
003   ' '
004   '— Gradient Definition Parameter —-'
005   'ng = ' 0
006   'gpi = ' -0.10000E+01
007   ' '
008   '— Gamma Definition ————————'
009   'Ga = ' 0.19535E+01
010   ' '
011   '— Alpha1 Definition Parameter ——'
012   'na = ' 0
013   'api = ' 0.00000E+00
014   '— Initial Values ————————-'
015   'p0 = ' 0.00000E+00
016   'pe = ' 0.99000E+00
017   'F10 = ' 0.10000E+01
018   't0 = ' 0.00000E+00
019   '— Integration Control Parameter —-'
020   'ep = ' 0.10000E-12
021   'h1 = ' 0.10000E-09
```

```
022  'hmin= ' 0.10000E-20
023  'hmax= ' 0.10000E-04
024  '— Data Save Control Parameter ——'
025  'Save= ' 1
026  'dpSv= ' 0.10000E-01
027  '————————————————————'
028  EOF
```

Output

GRADDOS1

```
001  0.17486E-09  0.10000E-09  0.10000E+01  0.50000E+00  0.25334E+00  0.00000E+00  0.10000E+01
002  0.17595E-01  0.10001E-01  0.99108E+00  0.50446E+00  0.25383E+00  0.00000E+00  0.99000E+00
003  0.35403E-01  0.20000E-01  0.98203E+00  0.50899E+00  0.25432E+00  0.00000E+00  0.98000E+00
004  0.53428E-01  0.30001E-01  0.97286E+00  0.51357E+00  0.25480E+00  0.00000E+00  0.97000E+00
005  0.71667E-01  0.40000E-01  0.96356E+00  0.51823E+00  0.25527E+00  0.00000E+00  0.96000E+00
006  0.90124E-01  0.50001E-01  0.95413E+00  0.52294E+00  0.25574E+00  0.00000E+00  0.95000E+00
007  0.10880E+00  0.60001E-01  0.94458E+00  0.52772E+00  0.25621E+00  0.00000E+00  0.94000E+00
008  0.12769E+00  0.70000E-01  0.93489E+00  0.53257E+00  0.25667E+00  0.00000E+00  0.93000E+00
009  0.14680E+00  0.80001E-01  0.92508E+00  0.53748E+00  0.25714E+00  0.00000E+00  0.92000E+00
010  0.16612E+00  0.90000E-01  0.91513E+00  0.54245E+00  0.25760E+00  0.00000E+00  0.91000E+00
011  0.18566E+00  0.10000E+00  0.90505E+00  0.54749E+00  0.25807E+00  0.00000E+00  0.90000E+00
012  0.20542E+00  0.11000E+00  0.89485E+00  0.55259E+00  0.25853E+00  0.00000E+00  0.89000E+00
013  0.22539E+00  0.12000E+00  0.88450E+00  0.55776E+00  0.25900E+00  0.00000E+00  0.88000E+00
014  0.24558E+00  0.13000E+00  0.87403E+00  0.56299E+00  0.25946E+00  0.00000E+00  0.87000E+00
015  0.26599E+00  0.14000E+00  0.86343E+00  0.56829E+00  0.25993E+00  0.00000E+00  0.86000E+00
016  0.28661E+00  0.15000E+00  0.85269E+00  0.57366E+00  0.26040E+00  0.00000E+00  0.85000E+00
017  0.30744E+00  0.16000E+00  0.84183E+00  0.57909E+00  0.26087E+00  0.00000E+00  0.84000E+00
018  0.32849E+00  0.17000E+00  0.83084E+00  0.58458E+00  0.26133E+00  0.00000E+00  0.83000E+00
019  0.34975E+00  0.18000E+00  0.81972E+00  0.59014E+00  0.26180E+00  0.00000E+00  0.82000E+00
020  0.37121E+00  0.19000E+00  0.80847E+00  0.59577E+00  0.26226E+00  0.00000E+00  0.81000E+00
021  0.39289E+00  0.20000E+00  0.79710E+00  0.60146E+00  0.26271E+00  0.00000E+00  0.80000E+00
022  0.41478E+00  0.21000E+00  0.78560E+00  0.60721E+00  0.26315E+00  0.00000E+00  0.79000E+00
023  0.43687E+00  0.22000E+00  0.77399E+00  0.61303E+00  0.26359E+00  0.00000E+00  0.78000E+00
024  0.45917E+00  0.23000E+00  0.76225E+00  0.61891E+00  0.26401E+00  0.00000E+00  0.77000E+00
025  0.48167E+00  0.24000E+00  0.75041E+00  0.62486E+00  0.26440E+00  0.00000E+00  0.76000E+00
026  0.50437E+00  0.25000E+00  0.73845E+00  0.63086E+00  0.26478E+00  0.00000E+00  0.75000E+00
027  0.52728E+00  0.26000E+00  0.72639E+00  0.63693E+00  0.26513E+00  0.00000E+00  0.74000E+00
028  0.55038E+00  0.27000E+00  0.71422E+00  0.64306E+00  0.26544E+00  0.00000E+00  0.73000E+00
029  0.57369E+00  0.28000E+00  0.70196E+00  0.64925E+00  0.26571E+00  0.00000E+00  0.72000E+00
030  0.59719E+00  0.29000E+00  0.68960E+00  0.65550E+00  0.26593E+00  0.00000E+00  0.71000E+00
031  0.62089E+00  0.30000E+00  0.67716E+00  0.66180E+00  0.26610E+00  0.00000E+00  0.70000E+00
032  0.64479E+00  0.31000E+00  0.66464E+00  0.66817E+00  0.26619E+00  0.00000E+00  0.69000E+00
033  0.66889E+00  0.32000E+00  0.65204E+00  0.67458E+00  0.26622E+00  0.00000E+00  0.68000E+00
034  0.69318E+00  0.33000E+00  0.63937E+00  0.68105E+00  0.26615E+00  0.00000E+00  0.67000E+00
035  0.71768E+00  0.34000E+00  0.62664E+00  0.68757E+00  0.26599E+00  0.00000E+00  0.66000E+00
036  0.74238E+00  0.35000E+00  0.61386E+00  0.69413E+00  0.26571E+00  0.00000E+00  0.65000E+00
037  0.76728E+00  0.36000E+00  0.60104E+00  0.70074E+00  0.26531E+00  0.00000E+00  0.64000E+00
038  0.79239E+00  0.37000E+00  0.58818E+00  0.70740E+00  0.26476E+00  0.00000E+00  0.63000E+00
039  0.81771E+00  0.38000E+00  0.57529E+00  0.71409E+00  0.26407E+00  0.00000E+00  0.62000E+00
040  0.84324E+00  0.39000E+00  0.56238E+00  0.72083E+00  0.26320E+00  0.00000E+00  0.61000E+00
041  0.86901E+00  0.40000E+00  0.54946E+00  0.72759E+00  0.26215E+00  0.00000E+00  0.60000E+00
042  0.89500E+00  0.41000E+00  0.53654E+00  0.73439E+00  0.26089E+00  0.00000E+00  0.59000E+00
043  0.92123E+00  0.42000E+00  0.52364E+00  0.74122E+00  0.25941E+00  0.00000E+00  0.58000E+00
044  0.94771E+00  0.43000E+00  0.51075E+00  0.74806E+00  0.25770E+00  0.00000E+00  0.57000E+00
045  0.97445E+00  0.44000E+00  0.49789E+00  0.75493E+00  0.25574E+00  0.00000E+00  0.56000E+00
046  0.10015E+01  0.45000E+00  0.48507E+00  0.76181E+00  0.25351E+00  0.00000E+00  0.55000E+00
047  0.10288E+01  0.46000E+00  0.47230E+00  0.76870E+00  0.25100E+00  0.00000E+00  0.54000E+00
048  0.10564E+01  0.47000E+00  0.45959E+00  0.77560E+00  0.24819E+00  0.00000E+00  0.53000E+00
050  0.10844E+01  0.48000E+00  0.44696E+00  0.78249E+00  0.24508E+00  0.00000E+00  0.52000E+00
051  0.11127E+01  0.49000E+00  0.43440E+00  0.78938E+00  0.24166E+00  0.00000E+00  0.51000E+00
052  0.11414E+01  0.50000E+00  0.42193E+00  0.79626E+00  0.23791E+00  0.00000E+00  0.50000E+00
```

053	0.11704E+01	0.51000E+00	0.40956E+00	0.80312E+00	0.23383E+00	0.00000E+00	0.49000E+00
054	0.12000E+01	0.52000E+00	0.39729E+00	0.80996E+00	0.22943E+00	0.00000E+00	0.48000E+00
055	0.12300E+01	0.53000E+00	0.38515E+00	0.81677E+00	0.22470E+00	0.00000E+00	0.47000E+00
056	0.12605E+01	0.54000E+00	0.37313E+00	0.82355E+00	0.21965E+00	0.00000E+00	0.46000E+00
057	0.12915E+01	0.55000E+00	0.36124E+00	0.83029E+00	0.21429E+00	0.00000E+00	0.45000E+00
058	0.13231E+01	0.56000E+00	0.34949E+00	0.83698E+00	0.20862E+00	0.00000E+00	0.44000E+00
059	0.13554E+01	0.57000E+00	0.33789E+00	0.84361E+00	0.20267E+00	0.00000E+00	0.43000E+00
060	0.13884E+01	0.58000E+00	0.32644E+00	0.85019E+00	0.19645E+00	0.00000E+00	0.42000E+00
061	0.14221E+01	0.59000E+00	0.31515E+00	0.85670E+00	0.18998E+00	0.00000E+00	0.41000E+00
062	0.14566E+01	0.60000E+00	0.30402E+00	0.86314E+00	0.18328E+00	0.00000E+00	0.40000E+00
063	0.14919E+01	0.61000E+00	0.29306E+00	0.86950E+00	0.17638E+00	0.00000E+00	0.39000E+00
064	0.15283E+01	0.62000E+00	0.28228E+00	0.87578E+00	0.16932E+00	0.00000E+00	0.38000E+00
065	0.15656E+01	0.63000E+00	0.27167E+00	0.88196E+00	0.16211E+00	0.00000E+00	0.37000E+00
066	0.16040E+01	0.64000E+00	0.26124E+00	0.88805E+00	0.15480E+00	0.00000E+00	0.36000E+00
067	0.16436E+01	0.65000E+00	0.25099E+00	0.89403E+00	0.14740E+00	0.00000E+00	0.35000E+00
068	0.16845E+01	0.66000E+00	0.24093E+00	0.89990E+00	0.13997E+00	0.00000E+00	0.34000E+00
069	0.17267E+01	0.67000E+00	0.23105E+00	0.90566E+00	0.13251E+00	0.00000E+00	0.33000E+00
070	0.17705E+01	0.68000E+00	0.22136E+00	0.91130E+00	0.12508E+00	0.00000E+00	0.32000E+00
071	0.18159E+01	0.69000E+00	0.21186E+00	0.91680E+00	0.11770E+00	0.00000E+00	0.31000E+00
072	0.18630E+01	0.70000E+00	0.20254E+00	0.92218E+00	0.11039E+00	0.00000E+00	0.30000E+00
073	0.19121E+01	0.71000E+00	0.19341E+00	0.92741E+00	0.10319E+00	0.00000E+00	0.29000E+00
074	0.19632E+01	0.72000E+00	0.18447E+00	0.93251E+00	0.96120E-01	0.00000E+00	0.28000E+00
075	0.20166E+01	0.73000E+00	0.17571E+00	0.93745E+00	0.89208E-01	0.00000E+00	0.27000E+00
076	0.20724E+01	0.74000E+00	0.16713E+00	0.94224E+00	0.82475E-01	0.00000E+00	0.26000E+00
077	0.21309E+01	0.75000E+00	0.15873E+00	0.94687E+00	0.75941E-01	0.00000E+00	0.25000E+00
078	0.21923E+01	0.76000E+00	0.15052E+00	0.95134E+00	0.69624E-01	0.00000E+00	0.24000E+00
079	0.22569E+01	0.77000E+00	0.14248E+00	0.95564E+00	0.63541E-01	0.00000E+00	0.23000E+00
080	0.23250E+01	0.78000E+00	0.13462E+00	0.95976E+00	0.57704E-01	0.00000E+00	0.22000E+00
081	0.23970E+01	0.79000E+00	0.12693E+00	0.96371E+00	0.52125E-01	0.00000E+00	0.21000E+00
082	0.24733E+01	0.80000E+00	0.11942E+00	0.96748E+00	0.46815E-01	0.00000E+00	0.20000E+00
083	0.25543E+01	0.81000E+00	0.11206E+00	0.97107E+00	0.41782E-01	0.00000E+00	0.19000E+00
084	0.26406E+01	0.82000E+00	0.10488E+00	0.97447E+00	0.37031E-01	0.00000E+00	0.18000E+00
085	0.27329E+01	0.83000E+00	0.97853E-01	0.97767E+00	0.32567E-01	0.00000E+00	0.17000E+00
086	0.28318E+01	0.84000E+00	0.90987E-01	0.98068E+00	0.28394E-01	0.00000E+00	0.16000E+00
087	0.29383E+01	0.85000E+00	0.84275E-01	0.98349E+00	0.24513E-01	0.00000E+00	0.15000E+00
088	0.30534E+01	0.86000E+00	0.77715E-01	0.98610E+00	0.20926E-01	0.00000E+00	0.14000E+00
089	0.31784E+01	0.87000E+00	0.71304E-01	0.98851E+00	0.17631E-01	0.00000E+00	0.13000E+00
090	0.33151E+01	0.88000E+00	0.65038E-01	0.99070E+00	0.14628E-01	0.00000E+00	0.12000E+00
091	0.34654E+01	0.89000E+00	0.58914E-01	0.99269E+00	0.11914E-01	0.00000E+00	0.11000E+00
092	0.36319E+01	0.90000E+00	0.52929E-01	0.99447E+00	0.94863E-02	0.00000E+00	0.10000E+00
093	0.38182E+01	0.91000E+00	0.47079E-01	0.99603E+00	0.73417E-02	0.00000E+00	0.90001E-01
094	0.40289E+01	0.92000E+00	0.41362E-01	0.99737E+00	0.54758E-02	0.00000E+00	0.80000E-01
095	0.42706E+01	0.93000E+00	0.35773E-01	0.99849E+00	0.38845E-02	0.00000E+00	0.70000E-01
096	0.45529E+01	0.94000E+00	0.30310E-01	0.99939E+00	0.25628E-02	0.00000E+00	0.60001E-01
097	0.48908E+01	0.95000E+00	0.24970E-01	0.10001E+01	0.15057E-02	0.00000E+00	0.50001E-01
098	0.53092E+01	0.96000E+00	0.19749E-01	0.10005E+01	0.70780E-03	0.00000E+00	0.40001E-01
099	0.58551E+01	0.97000E+00	0.14645E-01	0.10007E+01	0.16364E-03	0.00000E+00	0.30001E-01

100 t/kp0 p f1 q dq/dt Alpha1 F1

101

102 GRADPOL.f95 - gfortran version

103 Date: 2013/ 2/12

104 Time: 15:15:36

GRADIENT

001	0.10000E-09	-0.10000E+01
002	0.10001E-01	-0.10000E+01
003	0.20000E-01	-0.10000E+01
004	0.30001E-01	-0.10000E+01
005	0.40000E-01	-0.10000E+01
006	0.50001E-01	-0.10000E+01
007	0.60001E-01	-0.10000E+01
008	0.70000E-01	-0.10000E+01

009	0.80001E-01	-0.10000E+01
010	0.90000E-01	-0.10000E+01
011	0.10000E+00	-0.10000E+01
012	0.11000E+00	-0.10000E+01
013	0.12000E+00	-0.10000E+01
014	0.13000E+00	-0.10000E+01
015	0.14000E+00	-0.10000E+01
016	0.15000E+00	-0.10000E+01
017	0.16000E+00	-0.10000E+01
018	0.17000E+00	-0.10000E+01
019	0.18000E+00	-0.10000E+01
020	0.19000E+00	-0.10000E+01
021	0.20000E+00	-0.10000E+01
022	0.21000E+00	-0.10000E+01
023	0.22000E+00	-0.10000E+01
024	0.23000E+00	-0.10000E+01
025	0.24000E+00	-0.10000E+01
026	0.25000E+00	-0.10000E+01
027	0.26000E+00	-0.10000E+01
028	0.27000E+00	-0.10000E+01
029	0.28000E+00	-0.10000E+01
030	0.29000E+00	-0.10000E+01
031	0.30000E+00	-0.10000E+01
032	0.31000E+00	-0.10000E+01
033	0.32000E+00	-0.10000E+01
034	0.33000E+00	-0.10000E+01
035	0.34000E+00	-0.10000E+01
036	0.35000E+00	-0.10000E+01
037	0.36000E+00	-0.10000E+01
038	0.37000E+00	-0.10000E+01
039	0.38000E+00	-0.10000E+01
040	0.39000E+00	-0.10000E+01
041	0.40000E+00	-0.10000E+01
042	0.41000E+00	-0.10000E+01
043	0.42000E+00	-0.10000E+01
044	0.43000E+00	-0.10000E+01
045	0.44000E+00	-0.10000E+01
046	0.45000E+00	-0.10000E+01
047	0.46000E+00	-0.10000E+01
048	0.47000E+00	-0.10000E+01
049	0.48000E+00	-0.10000E+01
050	0.49000E+00	-0.10000E+01
051	0.50000E+00	-0.10000E+01
052	0.51000E+00	-0.10000E+01
053	0.52000E+00	-0.10000E+01
054	0.53000E+00	-0.10000E+01
055	0.54000E+00	-0.10000E+01
056	0.55000E+00	-0.10000E+01
057	0.56000E+00	-0.10000E+01
058	0.57000E+00	-0.10000E+01
059	0.58000E+00	-0.10000E+01
060	0.59000E+00	-0.10000E+01
061	0.60000E+00	-0.10000E+01
062	0.61000E+00	-0.10000E+01
063	0.62000E+00	-0.10000E+01
064	0.63000E+00	-0.10000E+01
065	0.64000E+00	-0.10000E+01
066	0.65000E+00	-0.10000E+01
067	0.66000E+00	-0.10000E+01
068	0.67000E+00	-0.10000E+01
069	0.68000E+00	-0.10000E+01

```
070   0.69000E+00   -0.10000E+01
071   0.70000E+00   -0.10000E+01
072   0.71000E+00   -0.10000E+01
073   0.72000E+00   -0.10000E+01
074   0.73000E+00   -0.10000E+01
075   0.74000E+00   -0.10000E+01
076   0.75000E+00   -0.10000E+01
077   0.76000E+00   -0.10000E+01
078   0.77000E+00   -0.10000E+01
079   0.78000E+00   -0.10000E+01
080   0.79000E+00   -0.10000E+01
081   0.80000E+00   -0.10000E+01
082   0.81000E+00   -0.10000E+01
083   0.82000E+00   -0.10000E+01
084   0.83000E+00   -0.10000E+01
085   0.84000E+00   -0.10000E+01
086   0.85000E+00   -0.10000E+01
087   0.86000E+00   -0.10000E+01
088   0.87000E+00   -0.10000E+01
089   0.88000E+00   -0.10000E+01
090   0.89000E+00   -0.10000E+01
091   0.90000E+00   -0.10000E+01
092   0.91000E+00   -0.10000E+01
093   0.92000E+00   -0.10000E+01
094   0.93000E+00   -0.10000E+01
095   0.94000E+00   -0.10000E+01
096   0.95000E+00   -0.10000E+01
097   0.96000E+00   -0.10000E+01
098   0.97000E+00   -0.10000E+01
099   p dF1/dp
100
101   GRADPOL.f95 - gfortran version
102   Date: 2013/ 2/12
103   Time: 15:15:36
104   r1 = 0.88600E+00
105   r2 = 0.47200E+00
106   kp(f1)=Sum(af(i)*f1**i): 1.0000000000000000 0.14374999999999999 0.0000000000000000 0.0000000000000000
```

Program

```
001   107.94478,    1.750397
002   109.25153,    1.753782
003   110.58282,    1.757168
004   111.89571,    1.760484
005   113.23313,    1.763732
006   114.57669,    1.766979
007   115.88957,    1.770227
008   117.23926,    1.773405
009   118.52761,    1.776652
010   119.87730,    1.779830
011   121.22699,    1.783078
012   122.51534,    1.786256
013   123.86503,    1.789503
014   125.21472,    1.792682
015   126.50307,    1.795929
016   127.79141,    1.799176
017   129.14110,    1.802424
018   130.42945,    1.805602
019   131.65644,    1.808849
020   133.00613,    1.812028
021   134.29448,    1.815137
```

022 135.52147, 1.818177
023 136.80982, 1.821217
024 138.03681, 1.824119
025 139.26380, 1.826814
026 140.55215, 1.829439
027 141.71779, 1.831857
028 143.00613, 1.833999
029 144.17178, 1.835865
030 145.39877, 1.837385
031 146.62577, 1.838559
032 147.85276, 1.839181
033 149.01840, 1.839388
034 150.30675, 1.838905
035 151.53374, 1.837799
036 152.76074, 1.835865
037 154.04908, 1.833101
038 155.33742, 1.829301
039 156.62577, 1.824533
040 158.09816, 1.818522
041 159.44785, 1.811268
042 160.92025, 1.802562
043 162.45399, 1.792336
044 164.04908, 1.780521
045 165.95092, 1.766979
046 167.48466, 1.751571
047 169.32515, 1.734229
048 171.77914, 1.714814
049 173.61963, 1.693326
050 176.07362, 1.669696
051 177.91411, 1.643787
052 181.59509, 1.615597
053 184.04908, 1.585196
054 187.11656, 1.552515
055 190.18405, 1.517623
056 193.86503, 1.480590
057 198.15951, 1.441414
058 202.45399, 1.400304
059 206.74847, 1.357328
060 211.65644, 1.312625
061 216.56442, 1.266333
062 223.31288, 1.218659
063 228.83436, 1.169879
064 235.58282, 1.120063
065 242.94479, 1.069556
066 250.92025, 1.018428
067 258.89571, 0.967092
068 268.71166, 0.915549
069 278.52761, 0.864213
070 288.95706, 0.813222
071 301.22699, 0.762715
072 313.49693, 0.712969
073 327.60736, 0.664120
074 342.33129, 0.616363
075 358.89571, 0.569843
076 376.68712, 0.524698
077 396.31902, 0.481052
078 417.79141, 0.439023
079 441.71779, 0.398693
080 468.09816, 0.360146
081 496.93252, 0.323458
082 529.44785, 0.288684
083 566.25767, 0.255858

```
084   606.74847,     0.225015
085   653.37423,     0.196182
086   706.13497,     0.169367
087   766.87117,     0.144584
088   838.65031,     0.121818
089   922.08589,     0.101069
090   1021.47239,    0.082317
091   1142.94479,    0.065543
092   1292.63804,    0.050726
093   1482.82209,    0.037834
094   1731.90184,    0.026839
095   2073.00613,    0.017707
096   2566.87117,    0.010403
097   3349.07975,    0.004890
```

RECIPE00

```
001   GRADIENT POLYMER RECIPE FILE:
002
003   Program: GRADMAKE.F95
004   Date: 2013/ 2/12
005   Time: 15:14:56
006
007   Gradient Structure:
008   Start Composition F1(X= 0) = 1.0000
009   Final Composition F1(X=Xe) = 0.0000
010   Gradient g = dF10/dp = ******
011   Final Deg. of Polymn. Xe = 175.
012
013   t-BuMA / n-BMA, p-TosCl:PMDETA:CuCl, MEK, 80 GrdC
014   Monomer 1: Density = 0.8750 g/cm^3, M = 142.200 g/mol
015   Monomer 2: Density = 0.8960 g/cm^3, M = 142.200 g/mol
016   Initiator: Density = 0.9950 g/cm^3, M = 363.170 g/mol
017   Solvent : Density = 0.8050 g/cm^3, M = 72.060 g/mol
018
019   Stock Solution:
020   Monomer 1: 0.89870E+01 g, V = 0.10271E+02 cm^3
021   Monomer 2: 0.00000E+00 g, V = 0.00000E+00 cm^3
022   Initiator: 0.26231E+00 g, V = 0.26363E+00 cm^3
023   Solvent : 0.89870E+01 g, V = 0.11164E+02 cm^3
024   Volume of Stock Solution, V0 = 0.21698E+02 cm^3
025
026   Feed Solution:
027   Monomer 2: 0.89870E+01 g, V = 0.10030E+02 cm^3
028   Solvent : 0.89870E+01 g, V = 0.11164E+02 cm^3
029   Volume of Feed Solution, V0 = 0.21194E+02 cm^3
030
031
032   n10 [mol] = 0.06320
033   n20 [mol] = 0.00000
034   n2add [mol] = 0.06320
035   ne,in [mol] = 0.12640
036   VStock [cm3] = 21.69846
037   Vadd [cm3] = 21.19411
038
039   C* = nin,e / V0 [mol/L] = 5.82527
040   Cadd = nadd / Vadd [mol/L] = 2.98195
041   Cfin = nin,e / Vtot [mol/L] = 2.94688
042
043
044   Initial Monomer Content q0 = 0.50000
045   Gamma = C*/Cadd = 1.95351
046   EOF
```

tau-dqdtau

001	0.17486E-09	0.25334E+00
002	0.17595E-01	0.25383E+00
003	0.35403E-01	0.25432E+00
004	0.53428E-01	0.25480E+00
005	0.71667E-01	0.25527E+00
006	0.90124E-01	0.25574E+00
007	0.10880E+00	0.25621E+00
008	0.12769E+00	0.25667E+00
009	0.14680E+00	0.25714E+00
010	0.16612E+00	0.25760E+00
011	0.18566E+00	0.25807E+00
012	0.20542E+00	0.25853E+00
013	0.22539E+00	0.25900E+00
014	0.24558E+00	0.25946E+00
015	0.26599E+00	0.25993E+00
016	0.28661E+00	0.26040E+00
017	0.30744E+00	0.26087E+00
018	0.32849E+00	0.26133E+00
019	0.34975E+00	0.26180E+00
020	0.37121E+00	0.26226E+00
021	0.39289E+00	0.26271E+00
022	0.41478E+00	0.26315E+00
023	0.43687E+00	0.26359E+00
024	0.45917E+00	0.26401E+00
025	0.48167E+00	0.26440E+00
026	0.50437E+00	0.26478E+00
027	0.52728E+00	0.26513E+00
028	0.55038E+00	0.26544E+00
029	0.57369E+00	0.26571E+00
030	0.59719E+00	0.26593E+00
031	0.62089E+00	0.26610E+00
032	0.64479E+00	0.26619E+00
033	0.66889E+00	0.26622E+00
034	0.69318E+00	0.26615E+00
035	0.71768E+00	0.26599E+00
036	0.74238E+00	0.26571E+00
037	0.76728E+00	0.26531E+00
038	0.79239E+00	0.26476E+00
039	0.81771E+00	0.26407E+00
040	0.84324E+00	0.26320E+00
041	0.86901E+00	0.26215E+00
042	0.89500E+00	0.26089E+00
043	0.92123E+00	0.25941E+00
044	0.94771E+00	0.25770E+00
045	0.97445E+00	0.25574E+00
046	0.10015E+01	0.25351E+00
047	0.10288E+01	0.25100E+00
048	0.10564E+01	0.24819E+00
049	0.10844E+01	0.24508E+00
050	0.11127E+01	0.24166E+00
051	0.11414E+01	0.23791E+00
052	0.11704E+01	0.23383E+00
053	0.12000E+01	0.22943E+00
054	0.12300E+01	0.22470E+00
055	0.12605E+01	0.21965E+00
056	0.12915E+01	0.21429E+00
057	0.13231E+01	0.20862E+00
058	0.13554E+01	0.20267E+00
059	0.13884E+01	0.19645E+00

060	0.14221E+01	0.18998E+00
061	0.14566E+01	0.18328E+00
062	0.14919E+01	0.17638E+00
063	0.15283E+01	0.16932E+00
064	0.15656E+01	0.16211E+00
065	0.16040E+01	0.15480E+00
066	0.16436E+01	0.14740E+00
067	0.16845E+01	0.13997E+00
068	0.17267E+01	0.13251E+00
069	0.17705E+01	0.12508E+00
070	0.18159E+01	0.11770E+00
071	0.18630E+01	0.11039E+00
072	0.19121E+01	0.10319E+00
073	0.19632E+01	0.96120E-01
074	0.20166E+01	0.89208E-01
075	0.20724E+01	0.82475E-01
076	0.21309E+01	0.75941E-01
077	0.21923E+01	0.69624E-01
078	0.22569E+01	0.63541E-01
079	0.23250E+01	0.57704E-01
080	0.23970E+01	0.52125E-01
081	0.24733E+01	0.46815E-01
082	0.25543E+01	0.41782E-01
083	0.26406E+01	0.37031E-01
084	0.27329E+01	0.32567E-01
085	0.28318E+01	0.28394E-01
086	0.29383E+01	0.24513E-01
087	0.30534E+01	0.20926E-01
088	0.31784E+01	0.17631E-01
089	0.33151E+01	0.14628E-01
090	0.34654E+01	0.11914E-01
091	0.36319E+01	0.94863E-02
092	0.38182E+01	0.73417E-02
093	0.40289E+01	0.54758E-02
094	0.42706E+01	0.38845E-02
095	0.45529E+01	0.25628E-02
096	0.48908E+01	0.15057E-02
097	0.53092E+01	0.70780E-03
098	0.58551E+01	0.16364E-03

t-dVdt

001	10593.25153,	0.915549
002	10861.96319,	0.864213
003	11140.49080,	0.813222
004	11429.44785,	0.762715
005	11730.67485,	0.712969
006	12044.17178,	0.664120
007	12371.77914,	0.616363
008	12714.11043,	0.569843
009	13073.00613,	0.524698
010	13449.69325,	0.481052
011	13846.01227,	0.439023
012	14263.80368,	0.398693
013	14705.52147,	0.360146
014	15173.61963,	0.323458
015	15670.55215,	0.288684
016	16200.00000,	0.255858
017	16766.25767,	0.225015
018	17373.00613,	0.196182
019	18026.38037,	0.169367
020	18732.51534,	0.144584

```
021   19499.38650,    0.121818
022   20338.03681,    0.101069
023   21260.12270,    0.082317
024   22281.59509,    0.065543
025   23424.53988,    0.050726
026   24717.17791,    0.037834
027   26200.00000,    0.026839
028   27931.90184,    0.017707
029   30004.90798,    0.010403
030   32571.77914,    0.004890
031   t [s] dV/dt [uL/s]
032
033   GRADMAKE.f95 - gfortran version
034   Date: 2013/ 2/12
035   Time: 15:15:36
036   r1 = 0.88600E+00
037   r2 = 0.47200E+00
038   kp(f1)=Sum(af(i)*f1**i): 1.0000000000000000 0.14374999999999999 0.0000000000000000 0.0000000000000000
```

B. Feeding–Program of experiment V32

Output

Program

001 83.40483, 2.070719
002 83.76074, 2.068232
003 84.60123, 2.065399
004 85.44785, 2.062359
005 86.29448, 2.059181
006 87.15337, 2.055726
007 88.01840, 2.052064
008 88.86503, 2.048195
009 89.81595, 2.044119
010 90.67485, 2.039835
011 91.53374, 2.035275
012 92.45399, 2.030507
013 93.43558, 2.025533
014 94.29448, 2.020282
015 95.27607, 2.014754
016 96.13497, 2.008950
017 97.17791, 2.002939
018 98.09816, 1.996583
019 99.14110, 1.989950
020 100.06135, 1.983040
021 101.10429, 1.975786
022 102.08589, 1.968185
023 103.12883, 1.960309
024 104.17178, 1.952018
025 105.21472, 1.943312
026 106.25767, 1.934261
027 107.42331, 1.924795
028 108.46626, 1.914915
029 109.63190, 1.904551
030 110.73620, 1.893703
031 111.96319, 1.882372
032 113.06748, 1.870557
033 114.35583, 1.858189
034 115.58282, 1.845200
035 116.80982, 1.831657
036 118.15951, 1.817493
037 119.44785, 1.802707
038 120.79755, 1.787161
039 122.20859, 1.770994
040 123.68098, 1.753997
041 125.15337, 1.736240
042 126.62577, 1.717723
043 128.28221, 1.698308
044 129.87730, 1.678064
045 131.53374, 1.656921
046 133.37423, 1.634811
047 135.15337, 1.611734
048 136.99387, 1.587621

049	139.07975,	1.562540
050	141.10429,	1.536354
051	143.25153,	1.509062
052	145.52147,	1.480734
053	147.91411,	1.451231
054	150.36810,	1.420623
055	153.06748,	1.388840
056	155.58282,	1.355883
057	158.89571,	1.321751
058	161.96319,	1.286513
059	165.03067,	1.250101
060	168.71166,	1.212514
061	172.39264,	1.173891
062	176.68712,	1.134163
063	180.36810,	1.093398
064	185.27607,	1.051666
065	189.57055,	1.008966
066	195.09202,	0.965507
067	201.22699,	0.921218
068	206.74847,	0.876238
069	212.88344,	0.830706
070	220.85890,	0.784690
071	227.60736,	0.738398
072	236.19632,	0.691829
073	245.39877,	0.645177
074	255.21472,	0.598609
075	265.64417,	0.552268
076	277.30061,	0.506314
077	290.79755,	0.460913
078	304.29448,	0.416237
079	320.85890,	0.372474
080	338.03681,	0.329802
081	357.66871,	0.288401
082	380.36810,	0.248459
083	404.29448,	0.210160
084	432.51534,	0.173693
085	465.03067,	0.139236
086	501.84049,	0.106984
087	544.17178,	0.077101
088	595.09202,	0.049775
089	653.98773,	0.025173

RECIPE00

```
001  GRADIENT POLYMER RECIPE FILE:
002
003  Program: GRADMAKE.F95
004  Date: 2012/ 8/28
005  Time: 15:28:15
006
007  Gradient Structure:
008  Start Composition F1(X= 0) = 1.0000
009  Final Composition F1(X=Xe) = 0.3000
010  Gradient g = dF10/dp = -.7000
011  Final Deg. of Polymn. Xe = 175.
012
013  t-BuMA / n-BMA, p-TosCl:PMDETA:CuCl, MEK, 80 GrdC
014  Monomer 1: Density = 0.8750 g/cm^3, M = 142.200 g/mol
015  Monomer 2: Density = 0.8960 g/cm^3, M = 142.200 g/mol
016  Initiator: Density = 0.9950 g/cm^3, M = 363.170 g/mol
017  Solvent : Density = 0.8050 g/cm^3, M = 72.060 g/mol
018
019  Stock Solution:
020  Monomer 1: 0.11683E+02 g, V = 0.13352E+02 cm^3
021  Monomer 2: 0.00000E+00 g, V = 0.00000E+00 cm^3
022  Initiator: 0.26231E+00 g, V = 0.26363E+00 cm^3
023  Solvent : 0.11683E+02 g, V = 0.14513E+02 cm^3
024  Volume of Stock Solution, V0 = 0.28129E+02 cm^3
025
026
027  Feed Solution:
028  Monomer 2: 0.62910E+01 g, V = 0.70212E+01 cm^3
029  Solvent : 0.62909E+01 g, V = 0.78148E+01 cm^3
030  Volume of Feed Solution, V0 = 0.14836E+02 cm^3
031
032
033  n10 [mol] = 0.08216
034  n20 [mol] = 0.00000
035  n2add [mol] = 0.04424
036  ne,in [mol] = 0.12640
037  VStock [cm3] = 28.12915
038  Vadd [cm3] = 14.83594
039
040  C* = nin,e / V0 [mol/L] = 4.49358
041  Cadd = nadd / Vadd [mol/L] = 2.98196
042  Cfin = nin,e / Vtot [mol/L] = 2.94194
043
044
045  Initial Monomer Content q0 = 0.65000
046  Gamma = C*/Cadd = 1.50692
047  EOF
```

C. Feeding–Program of experiment V33

Output

Program

001	72.26373,	1.969221
002	72.54601,	1.958857
003	73.24540,	1.948078
004	73.95092,	1.937092
005	74.66871,	1.925830
006	75.39264,	1.914292
007	76.14110,	1.902477
008	76.88957,	1.890386
009	77.66258,	1.878018
010	78.40491,	1.865305
011	79.26380,	1.852384
012	80.00000,	1.839118
013	80.85890,	1.825576
014	81.71779,	1.811758
015	82.51534,	1.797594
016	83.43558,	1.783153
017	84.29448,	1.768367
018	85.21472,	1.753305
019	86.13497,	1.737897
020	87.05521,	1.722144
021	88.03681,	1.706114
022	88.95706,	1.689670
023	90.06135,	1.672950
024	90.98160,	1.655815
025	92.14724,	1.638403
026	93.12883,	1.620577
027	94.29448,	1.602406
028	95.39877,	1.583889
029	96.56442,	1.565026
030	97.73006,	1.545749
031	98.95706,	1.526058
032	100.24540,	1.506021
033	101.53374,	1.485639
034	102.82209,	1.464842
035	104.23313,	1.443630
036	105.64417,	1.422004
037	107.05521,	1.400032
038	108.58896,	1.377646
039	110.12270,	1.354845
040	111.71779,	1.331699
041	113.37423,	1.308069
042	115.15337,	1.284094
043	116.87117,	1.259704
044	118.71166,	1.234900
045	120.61350,	1.209681
046	122.63804,	1.184116
047	124.66258,	1.158138
048	126.80982,	1.131744

049	129.07975,	1.105005
050	131.34969,	1.077920
051	133.80368,	1.050491
052	136.38037,	1.022646
053	139.01840,	0.994525
054	141.77914,	0.965990
055	144.72393,	0.937247
056	147.79141,	0.908159
057	150.98160,	0.878794
058	154.35583,	0.849223
059	157.97546,	0.819374
060	161.90184,	0.789388
061	165.64417,	0.759125
062	169.93865,	0.728793
063	174.23313,	0.698323
064	178.52761,	0.667791
065	184.04908,	0.637204
066	189.57055,	0.606616
067	195.09202,	0.576063
068	201.22699,	0.545593
069	207.36196,	0.515254
070	214.72393,	0.485095
071	222.08589,	0.455171
072	230.06135,	0.425537
073	238.65031,	0.396242
074	247.85276,	0.367354
075	258.89571,	0.338929
076	269.32515,	0.311043
077	281.59509,	0.283751
078	295.09202,	0.257123
079	309.20245,	0.231241
080	325.76687,	0.206160
081	343.55828,	0.181970
082	363.19018,	0.158734
083	385.88957,	0.136535
084	411.04294,	0.115441
085	439.87730,	0.095542
086	472.39264,	0.076907
087	509.81595,	0.059617
088	554.60123,	0.043748
089	605.52147,	0.029377
090	668.09816,	0.016580

RECIPE00

```
001  GRADIENT POLYMER RECIPE FILE:
002
003  Program: GRADMAKE.F95
004  Date: 2012/ 8/28
005  Time: 15:30:34
006
007  Gradient Structure:
008  Start Composition F1(X= 0) = 1.0000
009  Final Composition F1(X=Xe) = 0.5000
010  Gradient g = dF10/dp = -.5000
011  Final Deg. of Polymn. Xe = 175.
012
013  t-BuMA / n-BMA, p-TosCl:PMDETA:CuCl, MEK, 80 GrdC
014  Monomer 1: Density = 0.8750 g/cm^3, M = 142.200 g/mol
015  Monomer 2: Density = 0.8960 g/cm^3, M = 142.200 g/mol
016  Initiator: Density = 0.9950 g/cm^3, M = 363.170 g/mol
017  Solvent : Density = 0.8050 g/cm^3, M = 72.060 g/mol
018
019  Stock Solution:
020  Monomer 1: 0.13481E+02 g, V = 0.15406E+02 cm^3
021  Monomer 2: 0.00000E+00 g, V = 0.00000E+00 cm^3
022  Initiator: 0.26231E+00 g, V = 0.26363E+00 cm^3
023  Solvent : 0.13481E+02 g, V = 0.16746E+02 cm^3
024  Volume of Stock Solution, V0 = 0.32416E+02 cm^3
025
026
027  Feed Solution:
028  Monomer 2: 0.44935E+01 g, V = 0.50151E+01 cm^3
029  Solvent : 0.44935E+01 g, V = 0.55820E+01 cm^3
030  Volume of Feed Solution, V0 = 0.10597E+02 cm^3
031
032
033  n10 [mol] = 0.09480
034  n20 [mol] = 0.00000
035  n2add [mol] = 0.03160
036  ne,in [mol] = 0.12640
037  VStock [cm3] = 32.41612
038  Vadd [cm3] = 10.59709
039
040  C* = nin,e / V0 [mol/L] = 3.89931
041  Cadd = nadd / Vadd [mol/L] = 2.98196
042  Cfin = nin,e / Vtot [mol/L] = 2.93864
043
044
045  Initial Monomer Content q0 = 0.75000
046  Gamma = C*/Cadd = 1.30763
047  EOF
```

D. Feeding–Program of experiment V34

Output

Program

001	63.76681 ,	1.517628
002	64.01227 ,	1.502151
003	64.62577 ,	1.486467
004	65.26380 ,	1.470645
005	65.90798 ,	1.454684
006	66.56442 ,	1.438586
007	67.23313 ,	1.422349
008	67.91411 ,	1.405974
009	68.61350 ,	1.389460
010	69.34969 ,	1.372809
011	70.06135 ,	1.356019
012	70.79755 ,	1.339161
013	71.53374 ,	1.322095
014	72.33129 ,	1.304960
015	73.19018 ,	1.287686
016	73.92638 ,	1.270275
017	74.78528 ,	1.252794
018	75.64417 ,	1.235107
019	76.50307 ,	1.217350
020	77.42331 ,	1.199524
021	78.34356 ,	1.181490
022	79.32515 ,	1.163388
023	80.24540 ,	1.145217
024	81.22699 ,	1.126907
025	82.26994 ,	1.108459
026	83.31288 ,	1.089942
027	84.35583 ,	1.071356
028	85.52147 ,	1.052701
029	86.62577 ,	1.033908
030	87.79141 ,	1.015045
031	89.01840 ,	0.996045
032	90.24540 ,	0.977044
033	91.53374 ,	0.957975
034	92.82209 ,	0.938767
035	94.23313 ,	0.919559
036	95.64417 ,	0.900282
037	97.05521 ,	0.880936
038	98.52761 ,	0.861521
039	100.12270 ,	0.842106
040	101.71779 ,	0.822690
041	103.37423 ,	0.803137
042	105.09202 ,	0.783653
043	106.80982 ,	0.764100
044	108.71166 ,	0.744615
045	110.61350 ,	0.725062
046	112.63804 ,	0.705509
047	114.66258 ,	0.686004
048	116.80982 ,	0.666513

049 119.01840 , 0.647049
050 121.34969 , 0.627627
051 123.80368 , 0.608253
052 126.25767 , 0.588935
053 128.95706 , 0.569686
054 131.71779 , 0.550512
055 134.60123 , 0.531429
056 137.54601 , 0.512449
057 140.79755 , 0.493580
058 144.04908 , 0.474828
059 147.54601 , 0.456207
060 151.22699 , 0.437739
061 155.09202 , 0.419422
062 159.07975 , 0.401285
063 163.19018 , 0.383328
064 168.09816 , 0.365564
065 173.00613 , 0.348015
066 177.91411 , 0.330693
067 182.82209 , 0.313613
068 188.95706 , 0.296789
069 195.09202 , 0.280234
070 201.84049 , 0.263970
071 208.58896 , 0.248009
072 216.56442 , 0.232360
073 223.92638 , 0.217056
074 233.12883 , 0.202097
075 242.33129 , 0.187512
076 252.14724 , 0.173313
077 263.80368 , 0.159522
078 275.46012 , 0.146152
079 288.95706 , 0.133225
080 303.06748 , 0.120761
081 319.63190 , 0.108773
082 337.42331 , 0.097283
083 357.05521 , 0.086318
084 379.75460 , 0.075885
085 404.29448 , 0.066009
086 433.74233 , 0.056712
087 466.87117 , 0.048010
088 505.52147 , 0.039925
089 550.30675 , 0.032477
090 604.90798 , 0.025685
091 669.93865 , 0.019570
092 751.53374 , 0.014152
093 853.37423 , 0.009449
094 988.95706 , 0.005484

RECIPE00

```
001  GRADIENT POLYMER RECIPE FILE:
002
003  Program: GRADMAKE.F95
004  Date: 2012/ 8/28
005  Time: 15:32:35
006
007  Gradient Structure:
008  Start Composition F1(X= 0) = 1.0000
009  Final Composition F1(X=Xe) = 0.7000
010  Gradient g = dF10/dp = -.3000
011  Final Deg. of Polymn. Xe = 175.
012
013  t-BuMA / n-BMA, p-TosCl:PMDETA:CuCl, MEK, 80 GrdC
014  Monomer 1: Density = 0.8750 g/cm^3, M = 142.200 g/mol
015  Monomer 2: Density = 0.8960 g/cm^3, M = 142.200 g/mol
016  Initiator: Density = 0.9950 g/cm^3, M = 363.170 g/mol
017  Solvent : Density = 0.8050 g/cm^3, M = 72.060 g/mol
018
019  Stock Solution:
020  Monomer 1: 0.15278E+02 g, V = 0.17461E+02 cm^3
021  Monomer 2: 0.00000E+00 g, V = 0.00000E+00 cm^3
022  Initiator: 0.26231E+00 g, V = 0.26363E+00 cm^3
023  Solvent : 0.15278E+02 g, V = 0.18979E+02 cm^3
024  Volume of Stock Solution, V0 = 0.36703E+02 cm^3
025
026
027  Feed Solution:
028  Monomer 2: 0.26961E+01 g, V = 0.30091E+01 cm^3
029  Solvent : 0.26961E+01 g, V = 0.33492E+01 cm^3
030  Volume of Feed Solution, V0 = 0.63583E+01 cm^3
031
032
033  n10 [mol] = 0.10744
034  n20 [mol] = 0.00000
035  n2add [mol] = 0.01896
036  ne,in [mol] = 0.12640
037  VStock [cm3] = 36.70308
038  Vadd [cm3] = 6.35825
039
040  C* = nin,e / V0 [mol/L] = 3.44386
041  Cadd = nadd / Vadd [mol/L] = 2.98196
042  Cfin = nin,e / Vtot [mol/L] = 2.93535
043
044
045  Initial Monomer Content q0 = 0.85000
046  Gamma = C*/Cadd = 1.15490
047  EOF
```

E. Feeding–Program of experiment V101

Input

System

```
001  - Comonomer System Definition File -'
002  t-BMA(1) / BzMA(2), p-TosCl:PMDETA:CuCl, MEK, 80 GrdC'
003  '
004  —- Molar Masses and Densities —-'
005  MM1 = ', 1.4220d02
006  rh1 = ', 0.8750d00
007  MM2 = ', 1.7220d02
008  rh2 = ', 1.0400d00
009  MMI = ', 3.6317d02
010  rhI = ', 0.9950d00
011  MMS = ', 7.2060d01
012  rhS = ', 0.8050d00
013  '
014  —- Copolymerisation Parameter —-'
015  r1 = ', 2.0550d00
016  r2 = ', 0.5170d00
017  '
018  —- Kinetic Parameter ————-'
019  nk = ', 2
020  kf0 = ', 1.0000d00
021  kf1 = ',-4.0424d-1
022  kf2 = ', 0.0000d00
023  ————————————————————'
024  EOF
025  ONLY EDIT 2. line and r1, r2, n, kfi'
```

Dosage

```
001  — Comonomer Dosage Definition File -'
002  g(p) = const. '
003  '
004  — Gradient Definition Parameter —-'
005  ng = ' 0
006  gpi = ' -0.10000E+01
007  '
008  — Gamma Definition ————————'
009  Ga = ' 0.22397E+01
010  '
011  — Alpha1 Definition Parameter ——'
012  na = ' 0
013  api = ' 0.00000E+00
014  — Initial Values ————————-'
015  p0 = ' 0.00000E+00
016  pe = ' 0.99000E+00
017  F10 = ' 0.10000E+01
018  t0 = ' 0.00000E+00
019  — Integration Control Parameter —-'
020  ep = ' 0.10000E-12
021  h1 = ' 0.10000E-09
```

```
022   hmin= ' 0.10000E-20
023   hmax= ' 0.10000E-04
024   — Data Save Control Parameter ——'
025   Save= ' 1
026   dpSv= ' 0.10000E-01
027   — Error Handling Flags ————-'
028   ErrT: tau¡0 ' 0
029   Errf1: 0¿f1¡1' 0
030   ErrTs: tau*¿0' 0
031   Errq: q0¿q¡1' 0
032   ————————————————————'
033   EOF
```

Output

Program

```
001   177.17657 ,    2.798505
002   174.80600 ,    2.805362
003   172.62677 ,    2.809202
004   170.61763 ,    2.810117
005   168.81046 ,    2.808105
006   167.16275 ,    2.803442
007   165.67450 ,    2.795945
008   164.34570 ,    2.785887
009   163.12321 ,    2.773269
010   162.06017 ,    2.758183
011   161.15659 ,    2.740719
012   160.35931 ,    2.720969
013   159.66833 ,    2.699025
014   159.08366 ,    2.674978
015   158.71160 ,    2.648920
016   158.33953 ,    2.620941
017   158.07377 ,    2.591134
018   158.02062 ,    2.559498
019   158.02062 ,    2.526307
020   158.07377 ,    2.491654
021   158.28638 ,    2.455446
022   158.55214 ,    2.417867
023   158.97736 ,    2.379099
024   159.45572 ,    2.339143
025   160.04040 ,    2.298089
026   160.78452 ,    2.256030
027   161.47550 ,    2.213056
028   162.43223 ,    2.169351
029   163.38897 ,    2.124823
030   164.45200 ,    2.079746
031   165.67450 ,    2.034121
032   166.95014 ,    1.987947
033   168.43840 ,    1.941407
034   169.55459 ,    1.894502
035   171.68066 ,    1.847322
036   173.27522 ,    1.800051
037   174.86978 ,    1.752597
038   176.99585 ,    1.705052
039   178.59041 ,    1.657598
040   181.24801 ,    1.610235
041   183.37408 ,    1.562964
042   186.03168 ,    1.515876
043   188.15775 ,    1.469062
044   191.34687 ,    1.422522
045   194.00446 ,    1.376348
```

046 197.19358 , 1.330540
047 199.85117 , 1.285189
048 203.57181 , 1.240295
049 207.29244 , 1.195859
050 210.48156 , 1.152062
051 214.73371 , 1.108814
052 218.45434 , 1.066206
053 223.23801 , 1.024238
054 227.49017 , 0.983001
055 232.27384 , 0.942405
056 237.05751 , 0.902586
057 242.90422 , 0.863498
058 248.21941 , 0.825178
059 253.53460 , 0.787663
060 260.44435 , 0.750952
061 266.82258 , 0.715074
062 273.73233 , 0.680027
063 281.17359 , 0.645850
064 288.61486 , 0.612522
065 297.11917 , 0.580081
066 305.62347 , 0.548519
067 315.19082 , 0.517852
068 325.28968 , 0.488081
069 335.92006 , 0.459216
070 347.08196 , 0.431255
071 358.77538 , 0.404209
072 372.59488 , 0.378068
073 385.88285 , 0.352842
074 401.29691 , 0.328530
075 417.77400 , 0.305123
076 435.31413 , 0.282630
077 454.44881 , 0.261043
078 475.70958 , 0.240369
079 498.56490 , 0.220592
080 523.54630 , 0.201711
081 551.71681 , 0.183717
082 582.54491 , 0.166619
083 617.09365 , 0.150399
084 655.36303 , 0.135047
085 699.47911 , 0.120564
086 749.44190 , 0.106950
087 806.84597 , 0.094186
088 872.75433 , 0.082260
089 951.41916 , 0.071175
090 1044.43500 , 0.060918
091 1157.11704 , 0.051481
092 1296.37504 , 0.042854
093 1473.37089 , 0.035028
094 1704.58169 , 0.027995
095 2020.83555 , 0.021747
096 2479.00500 , 0.016272
097 3202.40247 , 0.011564
098 4520.03827 , 0.007618
099 7705.43213 , 0.004440

RECIPE00

```
001  GRADIENT POLYMER RECIPE FILE:
002
003  Program: GRADMAKE.F95
004  Date: 2013/ 2/12
005  Time: 13:42:24
006
007  Gradient Structure:
008  Start Composition F1(X= 0) = 1.0000
009  Final Composition F1(X=Xe) = 0.0000
010  Gradient g = dF10/dp = ******
011  Final Deg. of Polymn. Xe = 175.
012
013  t-BMA(1) / BzMA(2), p-TosCl:PMDETA:CuCl, MEK, 80 GrdC
014  Monomer 1: Density = 0.8750 g/cm^3, M = 142.200 g/mol
015  Monomer 2: Density = 1.0400 g/cm^3, M = 172.200 g/mol
016  Initiator: Density = 0.9950 g/cm^3, M = 363.170 g/mol
017  Solvent : Density = 0.8050 g/cm^3, M = 72.060 g/mol
018
019  Stock Solution:
020  Monomer 1: 0.89870E+01 g, V = 0.10271E+02 cm^3
021  Monomer 2: 0.00000E+00 g, V = 0.00000E+00 cm^3
022  Initiator: 0.26231E+00 g, V = 0.26363E+00 cm^3
023  Solvent : 0.89870E+01 g, V = 0.11164E+02 cm^3
024  Volume of Stock Solution, V0 = 0.21698E+02 cm^3
025
026
027  Feed Solution:
028  Monomer 2: 0.10883E+02 g, V = 0.10464E+02 cm^3
029  Solvent : 0.11137E+02 g, V = 0.13835E+02 cm^3
030  Volume of Feed Solution, V0 = 0.24299E+02 cm^3
031
032
033  n10 [mol] = 0.06320
034  n20 [mol] = 0.00000
035  n2add [mol] = 0.06320
036  ne,in [mol] = 0.12640
037  VStock [cm3] = 21.69846
038  Vadd [cm3] = 24.29932
039
040  C* = nin,e / V0 [mol/L] = 5.82527
041  Cadd = nadd / Vadd [mol/L] = 2.60088
042  Cfin = nin,e / Vtot [mol/L] = 2.74795
043
044
045  Initial Monomer Content q0 = 0.50000
046  Gamma = C*/Cadd = 2.23973
047  EOF
```

Bibliography

[1] H. Staudinger. Die Chemie der hochmolekularen organischen Stoffe im Sinn der Kekuléschen Strukturlehre. *Berichte der Deutschen Chemischen Gesellschaft*, 59:3019–3043, 1926.

[2] G. Schwedt. *Plastisch, elastisch, fantastisch – Ohne Kunststoffe geht es nicht.* Wiley-VCH, 2013.

[3] G. Odian. *Principles of Polymerization.* Wiley-Interscience, 4th edition, 2004.

[4] T. Otsu and M. Yoshida. Role of initiator–transfer agent–terminator (iniferter) in radical polymerizations: Polymer design by organic disulfides as iniferters. *Makromol. Chem. Rapid Commun.*, 3:127–132, 1982.

[5] M. Szwarc. 'Living' polymers. *Nature*, 178:1168–1167, 1956.

[6] O. W. Webster. Living polymerization methods. *Science*, 251:887–893, 1991.

[7] H. Fischer. The persistent radical effect in "living" radical polymerization. *Macromolecules*, 30(19):5666–5672, 1997.

[8] K. Matyjaszewski. Controlled radical polymerization. *Current opinion in solid state & materials science*, 1:769–776, 1996.

[9] M. Kato, M. Kamigaito, M. Sawamoto, and T. Higashimura. Polymerization of methyl methacrylate with carbon tetrachlorid/ dichlorotris- (triphenylphosphine) ruthenium(II)/ methylaluminum bis(2,6–di-tert–butylphenoxide) initiating system: Possibility of living radical polymerization. *Macromolecules*, 25(5):1721–1723, 1995.

[10] J.-S. Wang and K. Matyjaszewski. Controlled/ "living" radical polymerization, atom transfer radical polymerization in the presence of transition–metal complexes. *J. Am. Chem. Soc.*, 117(20):5614–5615, 1995.

[11] G. Riess, J. Kohler, C. Tournut, and A. Branderet. Über die Verträglichkeit von Copolymer mit den entsprechenden Homopolymeren. *Makromol. Chem.*, 101:58–73, 1967.

[12] J. Noolandi and K. M. Hong. Interfacial properties of immiscible homopolymer blends in the presence of block copolymers. *Macromolecules*, 15(2):483–492, 1982.

[13] M. Kryszewski. Gradient polymers and copolymers. *Polymers of Advanced Technologies*, 9:244–259, 1998.

[14] K. Matyjaszewski, M. J. Ziegler, S. V. Arehart, D. Greszta, and T. Pakula. Gradient copolymers by atom transfer radical polymerization. *J. Phys. Org. Chem.*, 13:775–786, 2000.

[15] U. Beginn. Gradient copolymers. *Colloid Polym. Sci.*, 286:1465–1474, 2008.

[16] K. Matyjaszewski and J. Xia. Atom Transfer Radical Polymerization. *Chem. Rev.*, 101:2921–2990, 2001.

[17] H.-G. Elias, editor. *Makromoleküle – Chemische Struktur und Synthesen*, volume 1. Wiley-VCH, 6th edition, 1999.

[18] B. Tieke. *Makromolekulare Chemie*. Wiley-VCH, 2nd edition, 2005.

[19] P. C. Hiemenz and T. P. Lodge. *Polymer Chemistry*. CRC Press, 2nd edition, 2007.

[20] F. R. Mayo and F. M. Lewis. Copolymerization I. A basis for comparing the behavior of monomer in copolymerization; the copolymerization of styrene and methyl methacrylate. *J. Am. Chem. Soc.*, 66(9):1594–1599, 1944.

[21] F. T. Wall. The structures of copolymers II. *J. Am. Chem. Soc.*, 66(12):2050–2057, 1944.

[22] F. S. Bates. Polymer–polymer phase behavior. *Science*, 251:898–905, 1991.

[23] P. J. Flory. *Principles of Polymer Chemistry*. Cornell University Press, 1953.

[24] D. J. Meier. Theory of block copolymers. I. domain formation in A–B block copolymers. *J. Polym. Sci., Part C: Polym. Symp.*, 26:81–98, 1969.

[25] E. Helfand. Block copolymer theory. III. Statistical mechanics of the microdomain structure. *Macromolecules*, 8(4):552–556, 1975.

[26] E. Helfand and Z. R. Wassermann. Block copolymer theory. 4. Narrow interphase approximation. *Macromolecules*, 9(6):879–888, 1976.

[27] E. Helfand and Z. R. Wassermann. Block copolymer theory. 5. Spherical domains. *Macromolecules*, 11(5):960–966, 1978.

[28] E. Helfand and Z. R. Wassermann. Block copolymer theory. 6. Cylindrical domains. *Macromolecules*, 13(4):994–998, 1980.

[29] L. Leibler. Theory of microphase separation in block copolymers. *Macromolecules*, 13:1602–1617, 1980.

[30] G. H. Fredrickson and E. Helfand. Fluctuation effects in the theory of microphase separation in block copolymers. *J. Chem. Phys.*, 87:697–705, 1987.

[31] M. W. Matsen and F. S. Bates. Unifying weak– and strong– segregation block copolymer theories. *Macromolecules*, 29(4):1091–1098, 1996.

[32] D. A. Hajduk, P. E. Harper, and S. M. Gruner. The Gyroid: A new equilibrium morphology in weakly segregated diblock copolymers. *Macromolecules*, 27(15):4063–4075, 1994.

[33] M. D. Lefebvre, M. O. de la Cruz, and K. R. Shull. Phase segregation in gradient copolymer melts. *Macromolecules*, 38(4):1037–1040, 2004.

[34] R. Jiang, Q. Jin, B. Li, D. Ding, R. A. Wickham, and A.-C. Shi. Phase behavior of gradient copolymers. *Macromolecules*, 41(14):5457–5465, 2008.

[35] M. M. Mok, C. J. Ellison, and J. M. Torkelson. Effect of gradient sequencing on copolymer order–disorder transitions: Phase behavior of styrene/n–butyl acrylate block and gradient copolymers. *Macromolecules*, 44(15):6220–6226, 2011.

[36] H. F. Mark et. al., editor. *Encyclopedia of Polymer Science and Engineering*, volume 2. Wiley-Interscience, 1985.

[37] G. Sauvet and P. Sigwalt. Carbcationic polymerization: General aspects and initiation. In G. Allen et. al., editor, *Comprehensive Polymer Science*, volume 3, chapter 39, pages 579–619. Pergaman Press, 1989.

[38] M. Fontanille. Carbanionic polymerization: General aspects and initiation. In G. Allen et. al., editor, *Comprehensive Polymer Science*, volume 3, chapter 25, pages 365–387. Pergaman Press, 1989.

[39] G. Moad, J. Chiefari, R. T. Mayadunne, C. L. Moad, A. Postma, E. Rizzardo, and S. H. Thang. Initiating free radical polymerization. *Macromol. Symp.*, 182:65–80, 2002.

[40] G. Oster and N.-L. Yang. Photopolymerization of vinyl monomers. *Chem. Rev.*, 68(2):125–151, 1968.

[41] K. Matyjaszewski and T. P. Davis, editors. *Handbook of Radical Polymerization*. Wiley-Interscience, 2002.

[42] C. J. Hawker, A. W. Bosman, and E. Harth. New polymer synthesis by nitroxide mediated living radical polymerizations. *J. Am. Chem. Soc.*, 101:3661–3688, 2001.

[43] Y. K. Chong, T. P. T. Le, G. Moad, E. Rizzardo, and S. H. Thang. A more versatile route to block copolymers and other polymers of complex architecture by living radical polymerization: The RAFT process. *Macromolecules*, 32:2071–2074, 1999.

[44] K. Matyjaszewski. Macromolecular engineering by controlled/ living ionic and radical polymerization. *Macromol. Symp.*, 174:51–67, 2001.

[45] T. E. Patten and K. Matyjaszewski. Atom transfer radical polymerization and the synthesis of polymeric materials. *Advanced Materials*, 10(12):901–915, 1998.

[46] K. Matyjaszewski, M. Wei, J. Xia, and N. E. McDermott. Controlled/"living" radical polymerization of styrene and methyl methacrylate catalyzed by iron complexes. *Macromolecules*, 30(26):8161–8164, 1997.

[47] T. Nishikawa, M. Kamigaito, and M. Sawamoto. Living radical polymerization in water and alcohols: Suspension polymerization of methyl methacrylate with $RuCl_2(PPh_3)_3$ complex. *Macromolecules*, 32(7):2204–2209, 1999.

[48] S. G. Gaynor, J. Qiu, and K. Matyjaszewski. Controlled/"living" radical polymerization applied to water-borne systems. *Macromolecules*, 31(17):5951–5954, 1998.

[49] J. Qiu, S. G. Gaynor, and K. Matyjaszewski. Emulsion polymerization of n–butyl methacrylate by reverse atom transfer radical polymerization. *Macromolecules*, 32(9):2872–2875, 1999.

[50] J. Xia, T. Johnson, S. G. Gaynor, K. Matyjaszewski, and J. DeSimone. Atom transfer radical polymerization in supercritical carbon dioxide. *Macromolecules*, 32(15):4802–4805, 1999.

[51] K. Matyjaszewski, Y. Nakagawa, and C. B. Jasieczek. Polymerization of n–butyl acrylate by atom transfer radical polymerization. Remarkable effect of ethylene carbonate and other solvents. *Macromolecules*, 31(5):1535–1541, 1998.

[52] K. Matyjaszewski, T. E. Patten, and J. Xia. Controlled/"living" radical polymerization. kinetics of the homogeneous atom transfer radical polymerization of styrene. *J. Am. Chem. Soc.*, 119(4):674–680, 1997.

[53] K. Matyjaszewski, K. Davis, T. E. Patten, and M. Wei. Observation and analysis of a slow termination process in the atom transfer radical polymerization of styrene. *Tetrahedron*, 53(45):15321–15329, 1997.

[54] S. Pascual, B. Coutin, M. Tard, A. Polton, and J.-P. Vairon. Homogeneous atom transfer radical polymerization of styrene initiated by 1–chloro–1–phenylethane/copper(I) chloride/bipyridine in the presence of dimethylformamide. *Macromolecules*, 32(5):1432–1437, 1999.

[55] V. Percec, B. Barboiu, A. Neumann, J. C. Ronda, and M. Zhao. Metal–catalyzed "living" radical polymerization of styrene initiated with arenesulfonyl chlorides. From heterogeneous to homogeneous catalysis. *Macromolecules*, 29(10):3665–3668, 1996.

[56] J.-L. Wang, T. Grimaud, and K. Matyjaszewski. Kinetic study of the homogeneous atom transfer radical polymerization of methyl methacrylate. *Macromolecules*, 30(21):6507–6512, 1997.

[57] A. T. Levy, M. M. Olmstead, and T. E. Patten. Synthesis, characterization, and polymerization activity of [bis(4,4'–bis(neophyldimethylsilylmethyl)–2,2'–bipyridyl)copper(i)]$^{+}$CuBr$_2^{-}$– and implications for copper(I) catalyst structures in atom transfer radical polymerization. *Inorg. Chem.*, 39(8):1628–1634, 2000.

[58] K. A. Davis, H.-K. Paik, and K. Matyjaszewski. Kinetic investigation of the Atom Transfer Radical Polymerization of methyl acrylate. *Macromolecules*, 32(6):1767–1776, 1999.

[59] K. Matyjaszewski, J.-L. Wang., T. Grimaud, and D. A. Shipp. Controlled/"living" atom transfer radical polymerization of methyl methacrylate using various initiator systems. *Macromolecules*, 31(5):1527–1534, 1998.

[60] H. Zhang, V. Marin, M. W. M. Fijten, and U. S. Schubert. High–throughput experimentation in atom transfer radical polymerization: A general approach towards a directed design and understanding of optimal catalytic systems. *J. Polym. Sci., Part A: Polym. Chem.*, 42(8):1876–1885, 2004.

[61] P. A. Gurr, M. F. Mills, G. G. Qiao, and D. H. Solomon. Initiator efficiency in ATRP: the tosyl chloride/ CuBr/ PMDETA system. *Polymer*, 46(7):2097–2104, 2005.

[62] S. Karanam, H. Goossens, B. Kluperman, and P. Lemstra. "Controlled" synthesis and characterization of model methyl methacrylate/ tert-butyl methacrylate triblock copolymers via ATRP. *Macromolecules*, 36(9):3051–3060, 2003.

[63] C. Schmitz. *Micellar Properties and Application of Amphiphilic Linear Block Copolymers with Different Microstructure but Same Molecular Weight.* PhD thesis, RWTH Aachen, Juli 2009.

[64] K. R. Shull, E. J. Kramer, G. Hadziioannou, and W. Tangs. Segregation of block copolymers to interfaces between immiscible homopolymers. *Macromolecules*, 23(22):4780–4787, 1990.

[65] D. Horn. Angewandte Polymerforschung – Ein Kapitel der supermolekularen Forschung. In *Polymere – Neue Strategien in der Polymerforschung*, pages 20–33. BASF, 1995.

[66] C. L. H. Wong, J. Kim, C. B. Roth, and J. M. Torkelson. Comparison of critical micelle concentrations of gradient copolymer and block copolymer in homopolymer: Novel characterization by intrinsic fluorescence. *Macromolecules*, 40(16):5631–5633, 2007.

[67] J. Kim, K. Gray, H. Zhou, S. T. Nguyen, and J. M. Torkelson. Polymer blend compatibilization by gradient copolymer addition during melt processing: Stabilization of dispersed phase to static coarsening. *Macromolecules*, 38(4):1037–1040, 2005.

[68] L. H. Sperling and J. J. Fay. Factors which affect the glass transition and damping capability of polymers. *Polym. Adv. Technol.*, 2(1):49–56, 1991.

[69] M. L. Williams, R. F. Landel, and J. D. Ferry. The temperature dependence of relaxation mechanisms in amorphous polymers and other glass–forming liquids. *J. Am. Chem. Soc.*, 77(14):3701–3707, 1955.

[70] L. Dagdug and L. S. Garcia-Colin. Generalization of the Williams–Landel–Ferry–Equation. *Physica A*, 250(1-4):133–141, 1998.

[71] T. G. Fox and P. J. Flory. Second–order transition temperatures and related properties of polystryrene. I. Influence of molecular weight. *J. Appl. Phys.*, 21:581–591, 1950.

[72] D. J. Hourston and I. D. Hughes. Polymeric systems for acoustic damping. I. Poly(vinyl chloride)–segmented polyether ester blends. *J. Appl. Polym. Sci.*, 21(11):3099–3109, 1977.

[73] C. L. H. Wong, J. Kim, and J. M. Torkelson. Breadth of glass transition temperature in styrene/acrylic acid block, random, and gradient copolymers: Unusual sequence distribution effects. *J. Polym. Sci., Part B: Polym. Phys.*, 45(20):2842–2849, 2007.

[74] J. H. Gibbs and E. A. DiMarzio. Nature of the glass transition and the glassy state. *J. Chem. Phys.*, 28(3):373/383, 1958.

[75] M. K. Gray, H. Zhou, S. T. Nguyen, and J. M. Torkelson. Synthesis and glass transition behavior of high molecular weight styrene/4–acetoxystyene and styrene/4–hydroxystyrene gradient copolymers made via nitroxide-mediated controlled radical polymerization. *Macromolecules*, 37(15):5586–5595, 2004.

[76] M. M. Mok, J. Kim, and J. M. Torkelson. Gradient copolymers with broad glass transition temperature regions: Design of purely interphase compositions for daming applications. *J. Polym. Sci., Part B: Polym. Phys.*, 46:48–56, 2008.

[77] F. R. S. Lord Rayleigh. X. On the electromagnetic theory of light. *Philos. Mag.*, 12(73):81–101, 1881.

[78] F. R. S. Lord Rayleigh. XXXIV. On the transmission of light through an atmosphere containing small partparti in suspension, and on the origin of the blue sky. *Philos. Mag.*, 47(287):375–384, 1899.

[79] M. D. Lechner, K. Gehrke, and E.H. Nordmeier. *Makromolekulare Chemie*. Birkhaeuser, 3rd, 2003.

[80] J. M. G. Cowie and V. Arrighi. *Polymers: Chemistry and Physics of Modern Materials*. CRC Press, 3rd, 2008.

[81] P. Debye. Light scattering on solutions. *J. Appl. Phys.*, 15:338–342, 1944.

[82] P. Debye. Molecular–weight determination by light scattering. *J. Phys. Coll. Chem.*, 51(1):18–32, 1947.

[83] D. R. Burfield and R. H. Smithers. Desiccant efficiency in solvent drying. 3. Dipolar aprotic solvents. *J. Org. Chem.*, 43(20):3966–3968, 1978.

[84] J. Österlöf. Copper compound of acetylene. *Acta Chem. Scand.*, 04:374–386, 1950.

[85] E. Pretsch, P. Bühlmann, C. Affolter, and M. Badertscher. *Spektroskopische Daten zur Strukturaufklärung organischer Verbindungen*. Springer, 4th edition, 2001.

[86] T. Alfrey and G. Goldfinger. The mechanism of copolymerization. *J. Chem. Phys.*, 12(6):205–209, 1944.

[87] B. H. Stuart. *Infrared Spectroscopy: Fundamentals and Applications*. Wiley-Interscience, 2004.

[88] A. R. Copper. Determination of molecular weight. In *Chemical Analysis – A Series of Monographs on Analytical Chemistry and its Applications*, volume 103. Wiley-Interscience, J. D. Winefordener and I. M. Kolthoff edition, 1989.

[89] G. W. H. Höhne, W-F. Hemminger, and H.-J. Flammersheim. *Different Scanning Calorimetry*. Springer, 2nd edition, 2003.

[90] S. Krause, J. J. Gormley, N. Roman, J. A. Shetter, and W. H. Watanabe. Glass temperatures of some acrylic polymers. *J. Polym. Sci., Part A: Polym. Chem.*, 3:3573–3586, 1965.

[91] S. A. Stern, U. M. Vakil, and G. R. Mauze. The solution and transport of gases in poly(n–butyl methacrylate) in the glass transition regions. I. Absorption–desorption measurements. *J. Polym. Sci., Part B: Polym. Phys.*, 27:405–429, 1989.

[92] T. W. Green and P. G. M. Wuts. *Protective Groups in Organic Synthesis*. Wiley, 2nd edition, 1991.

[93] D. Boles Bryan, R. F. Hall, K. G. Holden, W. F. Huffmann, and J. G. Gleason. Nuclear analogs of beta-lactam antibiotics. 2. The total synthesis of 8-oxo-4-thia-1-azabicyclo[4.2.0]oct-2-ene-2-carboxylic acids. *J. Am. Chem. Soc.*, 99(7):2353–2355, 1977.

[94] Z. Gu, Y. Yuan, J. He, M. Zhang, and P. Ni. Facile approach for DNA encapsulation in functional polyion complex for triggered intracellular gene delivery: Design, synthesis and mechanism. *Langmuir*, 25(9):5199–5208, 2009.

[95] H. Lu, L. Fan, Q-Liu, J. Wei, T. Ren, and J. Du. Preparation of water–dispersible silver–decorated polymer vesicles and micelles with exellent antibacterial efficacy. *Polym. Chem.*, 3:2217–2227, 2012.

[96] Q. Ma and L. Wooley. The preparation of t–butyl acrylate and methyl acrylate and styrene block copolymers by atom transfer radical polymerization: Precursors to amphiphilic and hydrophilic block copolymers and conversion to complex nanostructured materials. *J. Polym. Sci., Part A: Polym. Chem.*, 38:4805–4820, 2000.

[97] S. McSheehy, I. Yang, and Z. Mester. Selenmethionine extraction from selenized yeast: An LC–MS study of the acid hydrolysis of a synthetic selenopeptide. *Microchim. Acta*, 155:373–377, 2006.

[98] R. J. Simpson, M. R. Neuberger, and T. Y. Liu. Complete amino acid analysis of proteines from a single hydrolysate. *J. Biol. Chem.*, 251(7):1936–1940, 1976.

[99] K. Wrobel, S. S. Kannamkumarath, K. Wrobel, and J. A. Caruso. Hydrolysis of proteines with methanesulfonic acid from improved HPLC-ICP-MS determination of selenomethionine in yeast and nuts. *Anal. Bioanal. Chem.*, 375:133–138, 2003.

[100] Ph. Dubois, Y. S. Yu, Ph. Teyssié, and R. Jérôme. New polybutadiene–based thermoplastic elastomers: Synthesis, morphology and mechanical properties. *Rubber Chem. Technol.*, 70(5):714–726, 1997.

[101] K. R. M. Vidts, B. Dervaux, and F. E. Du Prez. Block, block gradient and random copolymers of 2–ethylhexyl acrylate and acrylic acid by atom transfer radical polymerization. *Polymer*, 47:6028–6037, 2006.

[102] G. T. Gavranovic, M. M. Smith, W. Jeong, A. Y. Wong, R. M. Waymouth, and G. G. Fuller. Effects of temperature and chemical modification on polymer langmuir films. *J. Phys. Chem. B*, 110:22285–22290, 2006.

[103] T.-L. Ho and G. A. Olah. Spaltung von Estern und Ethern mit Iodtrimethylsilan. *Angewandte Chemie*, 88(24):847, 1976.

[104] M. E. Jung and M. A. Lyster. Quantitative dealkylation of alkyl esters via treatment with trimethylsilyl iodide. A new method for ester hydrolysis. *J. Am. Chem. Soc.*, 99(3):968–969, 1977.

[105] G. A. Olah and C. Narang. Iodotrimethylsilane – A versaile synthetic reagent. *Tetrahedron*, 38(15):2225–2277, 1982.

[106] D. R. Lide, editor. *CRC Handbock of Chemistry and Physics*. CRC Press, 89th edition, 2008-2009.

[107] U. Beginn. Monomer addition programs to generate constant gradient block copolymers. *Polymer*, 47:6880–6894, 2006.

[108] K. Matyjaszewski and T. P. Davis, editors. *Handbock of Radical Polymerization*. Wiley-Interscience, 2002.

[109] S. Medel, J. M. Garcia, L. Garrido, I. Quijada-Garrido, and R. Paris. Thermo- and pH-responsive gradient and block copolymers based on 2–(2–methoxyethoxy)ethyl methacrylate synthesized via atom transfer radical polymerization and the formation of thermoresponsive surfaces. *J. Polym. Sci., Part A: Polym. Chem.*, 49(3):690–700, 2011.

[110] B.-S. Kim, H.-K. Lee, S. Jeong, J.-O. Lee, and H.-J. Paik. Amphiphilic gradient copolymer of [poly(ethylene glycol) methyl ether] methacrylate and styrene via atom transfer radical polymerization. *Macromol. Res.*, 19(12):1257–1263, 2011.

[111] P. H. M. Van Steenberge, D. R. D. Hooge, Y. W. Mingjiang Zhong, M.-F. Reyniers, D. Konkolewicz, K. Matyjaszewski, and G. B. Marin. Linear gradient quality of ATRP copolymers. *Macromolecules*, 45:8519–8531, 2012.

[112] L. A. Wood. Glass transition temperatures of copolymers. *J. Polym. Sci., Part A: Polym. Chem.*, 28(117):319–330, 1958.

[113] M. I. Munoz, L. Gargallo, and D. Radic. Effect of the side chain structure on the glass transition temperature. part 4: Molecular weight dependence of Tg on chalcogenides containing poly(methacrylates). *Thermochimica Acta*, 146:137–147, 1989.

List of Figures

List of Tables

List of Abbreviations

^{1}H–NMR	proton nuclear magnetic resonance spectroscopy
^{13}C–NMR	carbon nuclear magnetic resonance spectroscopy
A	area of NMR–Integral
a	alternating
ATR	attenuated total reflectance
ATRP	atom transfer radical polymerization
b	block
BMA	butyl methacrylate
Bz	benzyl
BzMA	benzyl methacrylate
CoPo	copolymer
CMC	critical micelle concentration
CRP	controlled radical polymerization
D	dilution
DMSO	dimethyl sulfoxide
dn/dc	differential refractive index increment
DOSY–NMR	diffusion ordered NMR spectroscopy
DSC	differential scanning calorimetry
EA	elementary analysis
FRP	free radical polymerization
FT	fourier transform
F	copolymer composition

f	monomer composition
grad	gradient
GPC	gel permeation chromatography
IR	infra red
k(eff)	effective rate constant
LS	light scattering
MA	methacrlate
MAA	methacrylic acid
MALS	multi angle light scattering
MEHQ	4–methoxyphenol
MEK	methyl ethyl ketone or 2-butanone
MSA	methanesulfonic acid
MWD	molecular weight distribution
n	molar mass
nBMA	*n*–butyl methacrylate
nBu	*n*–butyl
n. m.	not measured
NMP	nitroxide mediate polymerization
NMR	nuclear magnetic resonance
obdd	ordered bicontinuous double diamond
p	conversion
PA	peak area
PBzMA	poly–benzyl methacrylate
PDI	polydispersity index
PH	peak height
PI	polyisoprene

PMDETA	N,N,N',N',N"–pentamethyldiethylenetriamin
PnBMA	poly–*n*–butly methacrylate
PS	polystyrene
PSS	polystyrene standard
PtBMA	poly–*tert*–butly methacrylate
PTFE	polytetrafluoroethylene
pTSC	*para*–toluenesulfonyl chloride
RAFT	reversible addition fragmentation transfer polymerization
RI	refractive index
RP	radical polymerization
q	total monomer addition function
SEC	size exclusion chromatography
s	statistic
SSL	strong segregation limit
t	time
T	temperature
tBMA	*tert*–butyl methacrylate
tBu	*tert*–butyl
TFA	trifluoroacetic acid
Tg	glass transition temperature
THF	tetrahydrofuran
TMS	trimethylsilyl
TMSI	trimethylsilyl iodide
TOA	thermo optical analysis
V	volume
vol	volume
WSL	weak segregation limit